



**SURVIVABILITY - SUSTAINABILITY - MOBILITY
SCIENCE AND TECHNOLOGY
SOLDIER SYSTEM INTEGRATION**



**TECHNICAL REPORT
NATICK/TR-97/009**

AD _____

DISPLAY SIMULATION AND ANALYSIS: TWO-PRIMARY COLOR AND ALTERNATIVE GRAY SCALE DISTRIBUTION

**By
Henry Franklin
and
William Reinhart**

**Honeywell, Inc.
Phoenix, AZ 85027-1111**

February 1997

FINAL REPORT

June 1994 - August 1995

Approved for Public Release; Distribution Unlimited

**Prepared for
UNITED STATES ARMY SOLDIER SYSTEMS COMMAND
NATICK RESEARCH, DEVELOPMENT AND ENGINEERING CENTER
NATICK, MASSACHUSETTS 01760-5015
ADVANCED SYSTEMS CONCEPTS DIRECTORATE**

19970319 195

DTIC QUALITY INSPECTED 4

DISCLAIMERS

The findings contained in this report are not to be construed as an official Department of the Army position unless so designated by other authorized documents.

Citation of trade names in this report does not constitute an official endorsement or approval of the use of such items.

DESTRUCTION NOTICE

For Classified Documents:

Follow the procedures in DoD 5200.22-M, Industrial Security Manual, Section II-19 or DoD 5200.1-R, Information Security Program Regulation, Chapter IX.

For Unclassified/Limited Distribution Documents:

Destroy by any method that prevents disclosure of contents or reconstruction of the document.

REPORT DOCUMENTATION PAGE

*Form Approved
OMB No. 0704-0188*

Public reporting burden for this collection of information is estimated to average 1 hour per response, including the time for reviewing instructions, searching existing data sources, gathering and maintaining the data needed, and completing and reviewing the collection of information. Send comments regarding this burden estimate or any other aspect of this collection of information, including suggestions for reducing this burden, to Washington Headquarters Services, Directorate for Information Operations and Reports, 1215 Jefferson Davis Highway, Suite 1204, Arlington, VA 22202-4302, and to the Office of Management and Budget, Paperwork Reduction Project (0704-0188), Washington, DC 20503.

1. AGENCY USE ONLY (Leave blank)	2. REPORT DATE	3. REPORT TYPE AND DATES COVERED	
	February 1997	FINAL	June 1994 - August 1995
4. TITLE AND SUBTITLE		5. FUNDING NUMBERS	
DISPLAY SIMULATION AND ANALYSIS: TWO-PRIMARY COLOR AND ALTERNATIVE GRAY SCALE DISTRIBUTION		DAAK60-94-C-0042 6T-6T06 4H20 63739E S19129 CC: 42510KFG10000 2581	
6. AUTHOR(S)		8. PERFORMING ORGANIZATION REPORT NUMBER	
Henry Franklin and William Reinhart			
7. PERFORMING ORGANIZATION NAME(S) AND ADDRESS(ES)		8. PERFORMING ORGANIZATION REPORT NUMBER	
Honeywell, Inc. Honeywell Technology Center 21111 N. 19th Ave. Phoenix, AZ 85027-1111			
9. SPONSORING/MONITORING AGENCY NAME(S) AND ADDRESS(ES)		10. SPONSORING / MONITORING AGENCY REPORT NUMBER	
Defense Advanced Research Projects Agency Electronics Technology Office (E.C.Urban) 3701 North Fairfax Drive Arlington, VA 22203-1714		NATICK/TR-97/009	
11. SUPPLEMENTARY NOTES Monitors: U.S. Army Soldier Systems Command, Natick Research, Development and Engineering Center(Henry Girolamo), Natick, MA 01760, and U.S. Air Force Armstrong Laboratory, Wright-Patterson AFB, (David Post) Dayton, OH 43433			
12a. DISTRIBUTION/AVAILABILITY STATEMENT		12b. DISTRIBUTION CODE	
Approved for Public Release; Distribution Unlimited			
13. ABSTRACT (Maximum 200 words)			
<p>Two areas of display innovation have been identified which will promote the development of helmet or head-mounted displays (HMDs) that are both small and inexpensive, while delivering high performance and reliability at the same time. These innovations involve the use of two-primary color displays and alternative gray scale control. Two-primary color displays offer the advantage of significant reductions in cost and complexity for applications such as aircraft helmet-mounted sights and field process control monitors where the display requirements call for greater than monochrome, yet less than full, color, especially for subtractive color displays. Alternative gray scale control offers the potential for reduction of perceptual artifacts such as luminance and color banding, especially in displays with relatively limited numbers of gray scale levels. This report describes five principal tasks completed by Honeywell in the simulation and analysis of two-primary color display and alternative gray scale concepts: Display Requirement Analysis; System Configuration Concepts; Test Cell Fabrication and Evaluation; Display Analysis; and Simulation Development and Evaluation. The report also includes suggestions for additional future research.</p>			
14. SUBJECT TERMS		15. NUMBER OF PAGES	
DISPLAY REQUIREMENTS HELMET MOUNTED DISPLAYS HEAD MOUNTED DISPLAYS		HIGH PERFORMANCE RELIABILITY COST REDUCTION	
		GRAY SCALE IMAGERY	
		474	
16. PRICE CODE			
17. SECURITY CLASSIFICATION OF REPORT		18. SECURITY CLASSIFICATION OF THIS PAGE	
UNCLASSIFIED		UNCLASSIFIED	
19. SECURITY CLASSIFICATION OF ABSTRACT		20. LIMITATION OF ABSTRACT	
UNCLASSIFIED		SAR	

TABLE OF CONTENTS

1 DISPLAY REQUIREMENTS ANALYSIS	1
1.1 Considerations for Two-Primary Color	2
1.2 Considerations for Alternative Gray Scale Control	6
1.3 Review of HMD Applications.....	9
1.4 Preliminary Display Requirements.....	22
2 SYSTEM CONFIGURATION CONCEPTS	46
2.1 Major Image Source Options for HMS+	49
2.2 Major Color Approaches for HMS+	51
2.3 Gray Scale Approaches.....	52
2.4 Additional System Considerations.....	56
3 TEST CELL FABRICATION AND EVALUATION	74
3.1 Test Cell Fabrication and Evaluation.....	74
3.2 High Resolution Aperture Test Cell Design.....	74
3.3 Stack Test Methods	75
3.4 Stack #1 Configuration and Results.....	78
3.5 Stack #2 Configuration and Results.....	91
3.6 Stack #3 Configuration and Results.....	104
3.7 Stack #4 Configuration and Results.....	123
3.8 Stack #5 Configuration & Results	136
3.9 Stack #6 Configuration and Results.....	177
3.10 Summary of Stack Test Data	191

TABLE OF CONTENTS (continued)

4 DISPLAY ANALYSIS	192
4.1 Electronic System Analysis.....	192
4.2 Analysis of Display Manufacturability .	196
4.3 Luminance Capability Analysis.....	217
5 SIMULATION DEVELOPMENT AND EVALUATION	224
5.1 Overview	224
5.2 Evaluation 1	253
5.3 Evaluation 2	268
5.4 Evaluation 3	291
5.5 Evaluation 4	308
5.6 Evaluation 5	322
5.7 Evaluation 6	350
5.8 Evaluation 7	372
5.9 Evaluation 8	387
5.10 Evaluation 9	399
5.11 Evaluation 10	417
5.12 Simulation Summary (Evaluations 1 Through 10).....	426
6 RECOMMENDATIONS.....	431
6.1 Major Program Findings	431
6.2 Suggestions for Future Work.....	432

TABLE OF CONTENTS (continued)

7 APPENDIX	435
8 BIBLIOGRAPHY	445
9 DISTRIBUTION LIST	449

LIST OF FIGURES

Figure 1-1. Hypothetical AHMS weapons targeting display.....	13
Figure 1-2. TDC 3000 Area Alarm Summary Display.....	16
Figure 1-3. Hypothetical process schematic display for the Field Process Control Monitor (FPCM).....	17
Figure 1-4. Possible image format for Registered Noninvasive Medical Imager (RNMI).....	19
Figure 2-1. Sony Display Panel with 1.3 in. x 1.0 in. Active Display Area.....	54
Figure 2-2. Block diagram of overall system	56
Figure 2-3. Full Frame of 1280 x 1024 video.....	58
Figure 2-4. Magnification about the vertical blank period.....	59
Figure 2-5. Horizontal line from the 1280 x 1024 image data source	60
Figure 2-6. Expansion about the Horizontal blank period of the input video.....	61
Figure 2-7. Inverted analog waveforms needed to drive the 640 x 480 continuous gray scale flat panel, precursor to the 1280 x 1024.....	63
Figure 2-8. Timing required for the 640 x 480 continuous gray scale flat panel, precursor to the 1280 x 1024.....	64
Figure 2-9. Schematic of interface unit comprised of local and remote interface units.....	68
Figure 3-1. Two-Primary Color Directional Light Measurement Setup.....	76
Figure 3-2. Two-Primary Color Expanded View of Stack #1 (MCD Configuration)	78
Figure 3-3. Stack #1 - Filtered Power vs. Wavelength (Xenon Lamp).....	81
Figure 3-4. Stack #1 - Filtered Power vs. Wavelength (Xenon Lamp).....	82
Figure 3-5. Stack #1 - Transmission vs. Wavelength (Xenon Lamp).....	83
Figure 3-6. Stack #1 - Filtered Transmission vs. Wavelength (Xenon Lamp).....	84
Figure 3-7. Stack #1- Filtered Transmission (calculated filters) vs. Wavelength (Xenon Lamp).....	85
Figure 3-8. Stack #1 - Contrast Ratio vs. Wavelength (Xenon Lamp).....	86

LIST OF FIGURES (continued)

Figure 3-9. Xenon Lamp Characteristics - Power vs. Wavelength.....	87
Figure 3-10. Filtered Power vs. Wavelength (Tri-band lamp #69).....	88
Figure 3-11. Stack #1 - Filtered Power (calculated filters) vs. Wavelength (Tri-band Lamp #69).....	89
Figure 3-12. Tri-band Lamp Characteristics - Power vs. Wavelength.....	90
Figure 3-13. Two-Primary Color Expanded View of Stack #2 (Notch Polarizer Configuration).....	91
Figure 3-14. Stack #2 - Filtered Power vs. Wavelength (Xenon Lamp).....	94
Figure 3-15. Stack #2 - Filtered Power (calculated filters) vs. Wavelength (Xenon Lamp).....	95
Figure 3-16. Stack #2 - Transmission vs. Wavelength (Xenon Lamp).....	96
Figure 3-17. Stack #2 - Filtered Transmission vs. Wavelength (Xenon Lamp).....	97
Figure 3-18. Stack #2 - Filtered Transmission (calculated filters) vs. Wavelength (Xenon Lamp).....	98
Figure 3-19. Stack #2 - Contrast Ratio vs. Wavelength (Xenon Lamp).....	99
Figure 3-20. Xenon Lamp Characteristics - Power vs. Wavelength.....	100
Figure 3-21. Stack #2 - Filtered Power vs. Wavelength (Tri-band Lamp #69).....	101
Figure 3-22. Stack #2 - Filtered Power (calculated filters) vs. Wavelength (Tri-band Lamp #69).....	102
Figure 3-23. Tri-band Lamp Characteristics - Power vs. Wavelength.....	103
Figure 3-24. Two-Primary Color Expanded View of Stack #3 (Hybrid).....	104
Figure 3-25. Stack #3 - Filtered Power vs. Wavelength (Xenon Lamp).....	107
Figure 3-26. Stack #3 - Filtered Power (calculated filters) vs. Wavelength (Xenon Lamp).....	108
Figure 3-27. Stack #3 Transmission vs. Wavelength (Xenon Lamp).....	109
Figure 3-28. Stack #3 - Filtered Transmission vs. Wavelength (Xenon Lamp).....	110
Figure 3-29. Stack #3 - Filtered Transmission (calculated filters) vs. Wavelength (Xenon Lamp).....	111
Figure 3-30. Stack #3 - Contrast Ratio vs. Wavelength (Xenon Lamp).....	112

LIST OF FIGURES (continued)

Figure 3-31. Xenon Lamp Characteristics - Power vs. Wavelength	113
Figure 3-32. Stack #3 - Filtered Power vs. Wavelength (Tri-band Lamp #69).....	114
Figure 3-33. Stack #3 - Filtered Power (calculated filters) vs. Wavelength (Tri-band Lamp #69).....	115
Figure 3-34. Tri-Band Lamp Characteristics - Power vs. Wavelength.....	116
Figure 3-35. Stack #3 - Gray Scale: Voltage vs. Transmission vs. Wavelength (Red) (Xenon Lamp).....	117
Figure 3-36. Stack #3 - Gray Scale: Voltage vs. Power vs. Wavelength (Red) (Xenon Lamp).....	118
Figure 3-37. Stack #3 - Gray Scale: Voltage vs. Transmission vs. Wavelength (Green) (Xenon Lamp).....	119
Figure 3-38. Stack #3 - Gray Scale: Voltage vs. Power vs. Wavelength (Green) (Xenon Lamp).....	120
Figure 3-39. Stack #3 - Gray Scale: Voltage vs. Transmission vs. Wavelength (Xenon Lamp).....	121
Figure 3-40. Stack #3 - Gray Scale: Voltage vs. Power vs. Wavelength (Xenon Lamp)	122
Figure 3-41. Two-Primary color Expanded View of Stack #4 (Hybrid #2).....	123
Figure 3-42. Stack #4 - Filtered Power vs. Wavelength (Xenon Lamp)	126
Figure 3-43. Filtered Power (calculated filters) vs. Wavelength (Xenon Lamp).....	127
Figure 3-44. Stack #4 - Transmission vs. Wavelength (Xenon Lamp).....	128
Figure 3-45. Stack #4 - Filtered Transmission vs. Wavelength (Xenon Lamp).....	129
Figure 3-46. Stack #4 - Filtered Transmission (calculated filters) vs. Wavelength (Xenon Lamp).....	130
Figure 3-47. Stack #4 - Contrast Ratio vs. Wavelength (Xenon Lamp)	131
Figure 3-48. Xenon Lamp Characteristics - Power vs. Wavelength	132
Figure 3-49. Stack #4 - Filtered Power vs. Wavelength (Tri-band Lamp #69).....	133
Figure 3-50. Stack #4 - Filtered Power (calculated filters) vs. Wavelength (Tri-band Lamp #69).....	134
Figure 3-51. Tri-band Lamp Characteristics - Power vs. Wavelength.....	135
Figure 3-52. Two Primary-Color Expanded View of Stack #5.....	137

LIST OF FIGURES (continued)

Figure 3-53. Stack #5 - Filtered Power vs. Wavelength (Xenon Lamp).....	140
Figure 3-54. Stack #5 - Filtered Power (calculated filters) vs. Wavelength (Xenon Lamp).....	141
Figure 3-55. Stack #5 - Transmission vs. Wavelength (Xenon Lamp).....	142
Figure 3-56. Stack #5 - Filtered Transmission vs. Wavelength (Xenon Lamp).....	143
Figure 3-57. Stack #5 - Filtered Transmission vs. Wavelength (Xenon Lamp).....	144
Figure 3-58. Stack #5 - Contrast Ratio vs. Wavelength (Xenon Lamp).....	145
Figure 3-59. Xenon Lamp Characteristics - Power vs. Wavelength.....	146
Figure 3-60. Stack #5 - Filtered Power vs Wavelength (Tri-band Lamp #69).....	147
Figure 3-61. Stack #5 - Filtered Power vs. Wavelength (Tri-band Lamp #69).....	148
Figure 3-62. Tri-band Lamp Characteristics - Power vs. Wavelength.....	149
Figure 3-63. Optical Effects Test Device.....	152
Figure 3-64. Diffractive spreading, 32% aperture	155
Figure 3-65. Diffractive spreading, 48% aperture	156
Figure 3-66. Diffractive spreading, 73% aperture	157
Figure 3-67. Diffractive spreading, 92% aperture	158
Figure 3-68. Diffractive spreading, 67% aperture	159
Figure 3-69. Diffractive spreading, 90% aperture	160
Figure 3-70. Effective Edge Profile, Rear Cell Image.....	161
Figure 3-71. Relative intensities, rear cell image features.....	162
Figure 3-72. Setup for characterization of Moiré effects.....	165
Figure 3-73. Far-field Moiré patterns as seen with stacked AMLCD light valves	166
Figure 3-74. Moiré intensity profile, 32% aperture ratio and 24 micron pitch.....	167

LIST OF FIGURES (continued)

Figure 3-75. Moiré intensity profile, 48% aperture ratio and 24 micron pitch.....	168
Figure 3-76. Moiré intensity profile, 73% aperture ratio and 24 micron pitch.....	169
Figure 3-77. Moiré intensity profile, 92% aperture ratio and 24 micron pitch.....	170
Figure 3-78. Moiré intensity profile, 67% aperture ratio and 20 micron pitch.....	171
Figure 3-79. Moiré intensity profile, 90% aperture ratio and 20 micron pitch.....	172
Figure 3-80. Estimated non-uniformity due to Moiré artifacts—assumes moderate corrective measures and 73% aperture ratio.....	173
Figure 3-81. Estimated non-uniformity due to Moiré artifacts—assumes moderate corrective measures and 48% aperture ratio	174
Figure 3-82. Measured and predicted transmittances of optical effects test device regions, 24 micron pitch.....	176
Figure 3-83. Two-Primary Color Expanded View of Stack #6 (Active Matrix).....	177
Figure 3-84. Stack #6 - Filtered Power vs. Wavelength (Xenon Lamp).....	180
Figure 3-85. Stack #6 - Filtered Power (calculated filters) vs. Wavelength (Xenon Lamp).....	181
Figure 3-86. Stack #6 - Transmission vs. Wavelength (Xenon Lamp).....	182
Figure 3-87. Stack #6 - Filtered Transmission vs. Wavelength (Xenon Lamp).....	183
Figure 3-88. Stack #6 - Filtered Transmission (calculated filters) vs. Wavelength (Xenon Lamp).....	184
Figure 3-89. Stack #6 - Contrast Ratio vs. Wavelength (Xenon Lamp)	185
Figure 3-90. Xenon Lamp Characteristics - Power vs. Wavelength	186
Figure 3-91. Stack #6 - Filtered Power vs. Wavelength (Tri-band Lamp #69).....	187
Figure 3-92. Stack #6 - Filtered Power (calculated filters) vs. Wavelength (Tri-band Lamp #69).....	188
Figure 3-93. Tri-band Lamp Characteristics - Power vs. Wavelength.....	189
Figure 4-1. AMLCD Manufacturing System Flowchart for Scenario #1.....	201
Figure 4-2. AMLCD Manufacturing System Flowchart for Scenario #2.....	202
Figure 4-3. AMLCD Manufacturing System Flowchart for Scenario #4.....	204

LIST OF FIGURES (continued)

Figure 4-4. Substrate size versus processing tolerance.....	215
Figure 4-5. Simplified optical collimating configuration.....	219
Figure 5-1. General AMLCD Simulation and Evaluation Process.....	225
Figure 5-2. Image Processing Steps Incorporated in Simulation Software.....	228
Figure 5-3. Simulation Model of Additive Color AMLCD (40%).....	229
Figure 5-4. Simulation Model of Subtractive Color AMLCD (40%).....	230
Figure 5-5. Simulation Model of Subtractive Color AMLCD (50%).....	231
Figure 5-6. Simulation Model of Subtractive Color AMLCD (60%).....	232
Figure 5-7. Simulation Model of Subtractive Color AMLCD (70%).....	233
Figure 5-8. Simulation Model of Subtractive Color AMLCD (80%).....	234
Figure 5-9. Evaluation Software Used to Control Simulation Image Presentation	236
Figure 5-10. Original Image of Flight Guidance, Reference, and Targeting Symbols.....	239
Figure 5-11. Original FLIR Truck Image.....	240
Figure 5-12. Original FLIR Tank Image.....	241
Figure 5-13. Construction of Standard Image for Symbol Images Used in Evaluations 1, 7, 8 and 10.....	242
Figure 5-14. Construction of Standard Image for FLIR Truck Images Used in Evaluations 2 through 6 and 9.....	243
Figure 5-15. Construction of Standard Image for FLIR Tank Images Used in Evaluations 2 through 6.....	244
Figure 5-16. Binocular Visual Acuity of Evaluation Participants.....	249
Figure 5-17. Serial Image Comparison Procedure Used in Evaluations 1 through 4.....	251
Figure 5-18. Simultaneous Image Comparison Procedure Used in Evaluations 5 Through 10.....	252
Figure 5-19. Original Image from which Cloud and Blue Sky Backgrounds Were Extracted in Evaluations 1, 2, and 3.....	255
Figure 5-20. Luminance Contrast for Symbol Images in Evaluation 1, Ranging from 1.3 (a) to 50 (b).....	256

LIST OF FIGURES (continued)

Figure 5-21. Gray Scale Levels for Symbol Images in Evaluation 1, Ranging from 4 levels (a) to 32 levels (b).....	257
Figure 5-22. Gray Scale Distribution Exponents for Symbol Images in Evaluation 1, Ranging from 0.3 (a) to 1.0 (b).....	258
Figure 5-23. Contrast and Aliasing Rating Scales Used in Evaluations 1 and 2.....	260
Figure 5-24. Mean Contrast Rating as a Function of Luminance Contrast (Evaluation 1, Symbols).....	264
Figure 5-25. Mean Aliasing Rating as a Function of Luminance Contrast (Evaluation 1, Symbols).....	265
Figure 5-26. Mean Aliasing Rating as a Function of Gray Scale Level (Evaluation 1, Symbols).....	266
Figure 5-27. Mean Aliasing Rating as a Function of Luminance Contrast by Gray Scale Exponent (Evaluation 1, Symbols).....	267
Figure 5-28. Luminance Contrast for FLIR Truck Images in Evaluation 2, Ranging from 1.3 (a) to 10 (b).....	270
Figure 5-29. Luminance Contrast for FLIR Tank Images in Evaluation 2, Ranging from 1.3 (a) to 5 (b).....	271
Figure 5-30. Gray Scale Levels for FLIR Truck Images in Evaluations 2, 3, and 4, Ranging from 8 (a) to 64 Levels (b).....	272
Figure 5-31. Gray Scale Levels for FLIR Tank Images in Evaluations 2, 3, and 4, Ranging from 8 (a) to 64 Levels (b).....	273
Figure 5-32. Gray Scale Distribution Exponents for FLIR Truck Images in Evaluations 2, 3, and 4, Ranging from 0.3 (a) to 1.0 (b).....	274
Figure 5-33. Gray Scale Distribution Exponents for FLIR Tank Images in Evaluations 2, 3, and 4, Ranging from 0.3 (a) to 1.0 (b).....	275
Figure 5-34. Mean Contrast Rating as a Function of Luminance Contrast (Evaluation 2, Truck)	281
Figure 5-35. Mean Contrast Rating as a Function of Luminance Contrast (Evaluation 2, Tank).....	282
Figure 5-36. Mean Aliasing Rating as a Function of Gray Scale Level (Evaluation 2, Truck).....	283
Figure 5-37. Mean Aliasing Rating as a Function of Gray Scale Level (Evaluation 2, Tank).....	284
Figure 5-38. Mean Contrast Rating as a Function of Gray Scale Exponent (Evaluation 2, Truck).....	285
Figure 5-39. Mean Contrast Rating as a Function of Gray Scale Exponent (Evaluation 2, Tank).....	286
Figure 5-40. Mean Contrast Rating as a Function of Gray Scale Exponent by Luminance Contrast (Evaluation 2, Truck).....	287
Figure 5-41. Mean Aliasing Rating as a Function of Gray Scale Exponent by Luminance Contrast (Evaluation 2, Truck).....	288
Figure 5-42. Mean Aliasing Rating as a Function of Gray Scale Level by Luminance Contrast (Evaluation 2, Truck).....	289

LIST OF FIGURES (continued)

Figure 5-43. Mean Aliasing Rating as a Function of Gray Scale Level by Gray Scale Exponent (Evaluation 2, Truck)	290
Figure 5-44. Aperture Ratio Variable for FLIR Truck Images in Evaluations 3 and 4	293
Figure 5-45. Aperture Ratio for FLIR Tank Images in Evaluations 3 and 4.....	294
Figure 5-46. Line Visibility and Image Quality Rating Scales Used in Evaluations 3 Through 10	296
Figure 5-47. Mean Line Visibility Rating as a Function of Aperture Ratio (Evaluation 3, Truck)	300
Figure 5-48. Mean Line Visibility Rating as a Function of Aperture Ratio (Evaluation 3, Tank)	301
Figure 5-49. Mean Image Quality Rating as a Function of Gray Scale Level (Evaluation 3, Truck).....	302
Figure 5-50. Mean Image Quality Rating as a Function of Gray Scale Level (Evaluation 3, Tank).....	303
Figure 5-51. Mean Image Quality Rating as a Function of Gray Scale Exponent (Evaluation 3, Truck).....	304
Figure 5-52. Mean Image Quality Rating as a Function of Gray Scale Exponent (Evaluation 3, Tank).....	305
Figure 5-53. Mean Image Quality Rating as a Function of Gray Scale Level by Gray Scale Exponent (Evaluation 3, Truck)	306
Figure 5-54. Mean Image Quality Rating as a Function of Gray Scale Level by Gray Scale Exponent (Evaluation 3, Tank)	307
Figure 5-55. Mean Line Visibility Rating as a Function of Aperture Ratio (Evaluation 4, Truck).....	314
Figure 5-56. Mean Line Visibility Rating as a Function of Aperture Ratio (Evaluation 4, Tank)	315
Figure 5-57. Mean Image Quality Rating as a Function of Gray Scale Level (Evaluation 4, Truck)	316
Figure 5-58. Mean Image Quality Rating as a Function of Gray Scale Level (Evaluation 4, Tank).....	317
Figure 5-59. Mean Image Quality Rating as a Function of Gray Scale Exponent (Evaluation 4, Truck)	318
Figure 5-60. Mean Image Quality Rating as a Function of Gray Scale Exponent (Evaluation 4, Tank).....	319
Figure 5-61. Mean Image Quality Rating as a Function of Gray Scale Level by Gray Scale Exponent (Evaluation 4, Truck)	320
Figure 5-62. Mean Image Quality Rating as a Function of Gray Scale Level by Gray Scale Exponent (Evaluation 4, Tank)	321
Figure 5-63. Convolution Kernel Applied to Red Layer of Subtractive Color Images in Evaluations 5 Through 10 (40% AR).	325
Figure 5-64. Convolution Kernel Applied to Red Layer of Subtractive Color Images in Evaluations 5 through 10 (70% AR).....	326

LIST OF FIGURES (continued)

Figure 5-65. Additive Color Image Source (40% AR) Modeled in Evaluations 5, 6, and 9 for FLIR Truck Images.....	327
Figure 5-66. Additive Color Image Source (40% AR) Modeled in Evaluations 5, 6, and 9 for FLIR Tank Images.....	328
Figure 5-67. Subtractive Color Image Source (40% AR) Modeled in Evaluations 5, 6, and 9 for FLIR Truck Images.....	329
Figure 5-68. Subtractive Color Image Source (40% AR) Modeled in Evaluations 5, 6, and 9 for FLIR Tank Images.....	330
Figure 5-69. Subtractive Color Image Source (70% AR) Modeled in Evaluations 5, 6, and 9 for FLIR Truck Images.....	331
Figure 5-70. Subtractive Color Image Source (70% AR) Modeled in Evaluations 5, 6, and 9 for FLIR Tank Images.....	332
Figure 5-71. Sharpness Rating Scale Used in Evaluations 5, 6, and 9.....	334
Figure 5-72. Mean Line Visibility Rating as a Function of Resolution (Evaluation 5, Truck).....	338
Figure 5-73. Mean Line Visibility Rating as a Function of Resolution (Evaluation 5, Tank).....	339
Figure 5-74. Mean Image Quality Rating as a Function of Image Color (Evaluation 5, Truck).....	340
Figure 5-75. Mean Line Visibility Rating as a Function of Image Source (Evaluation 5, Truck).....	341
Figure 5-76. Mean Line Visibility Rating as a Function of Image Source (Evaluation 5, Tank).....	342
Figure 5-77. Mean Sharpness Rating as a Function of Image Source (Evaluation 5, Truck).....	343
Figure 5-78. Mean Line Visibility Rating as a Function of Image Source (Evaluation 5, Tank).....	344
Figure 5-79. Mean Image Quality Rating as a Function of Image Source (Evaluation 5, Truck).....	345
Figure 5-80. Mean Image Quality Rating as a Function of Image Source (Evaluation 5, Tank).....	346
Figure 5-81. Mean Sharpness Rating as a Function of Image Color by Image Source (Evaluation 5, Tank).....	347
Figure 5-82. Mean Image Quality Rating as a Function of Image Color by Image Source (Evaluation 5, Tank).....	348
Figure 5-83. Mean Line Visibility Rating as a Function of Resolution by Image Source (Evaluation 5, Tank).....	349
Figure 5-84. Mean Line Visibility Rating as a Function of Resolution (Evaluation 6, Truck).....	358
Figure 5-85. Mean Line Visibility Rating as a Function of Resolution (Evaluation 6, Tank).....	359
Figure 5-86. Mean Line Visibility Rating as a Function of Image Color (Evaluation 6, Tank).....	360

LIST OF FIGURES (continued)

Figure 5-87. Mean Image Quality Rating as a Function of Image Color (Evaluation 6, Truck).....	361
Figure 5-88. Mean Line Visibility Rating as a Function of Image Source (Evaluation 6, Truck)	362
Figure 5-89. Mean Line Visibility Rating as a Function of Image Source (Evaluation 6, Tank).....	363
Figure 5-90. Mean Image Quality Rating as a Function of Image Source (Evaluation 6, Truck)	364
Figure 5-91. Mean Image Quality Rating as a Function of Image Source (Evaluation 6, Tank).....	365
Figure 5-92. Mean Line Visibility Rating as a Function of Image Color by Image Source (Evaluation 6, Tank).....	366
Figure 5-93. Mean Sharpness Rating as a Function of Image Color by Image Source (Evaluation 6, Truck).....	367
Figure 5-94. Mean Sharpness Rating as a Function of Image Color by Image Source (Evaluation 6, Tank).....	368
Figure 5-95. Mean Image Quality Rating as a Function of Image Color by Image Source (Evaluation 6, Truck).....	369
Figure 5-96. Mean Image Quality Rating as a Function of Image Color by Image Source (Evaluation 6, Tank).....	370
Figure 5-97. Mean Line Visibility Rating as a Function of Resolution by Image Source (Evaluation 6, Truck)	371
Figure 5-98. Additive Color Image Source (40% AR) Modeled in Evaluations 7, 8, and 10 for Symbol Images.....	374
Figure 5-99. Subtractive Color Image Source (40% AR) Modeled in Evaluations 7, 8, and 10 for Symbol Images	375
Figure 5-100. Subtractive Color Image Source (70% AR) Modeled in Evaluations 7, 8, and 10 for FLIR Symbol Images.....	376
Figure 5-101. Mean Line Visibility Rating as a Function of Resolution (Evaluation 7, Symbol).....	381
Figure 5-102. Mean Image Quality Rating as a Function of Resolution (Evaluation 7, Symbol).....	382
Figure 5-103. Mean Image Quality Rating as a Function of Image Color (Evaluation 7, Symbol)	383
Figure 5-104. Mean Line Visibility Rating as a Function of Image Source (Evaluation 7, Symbol)	384
Figure 5-105. Mean Image Quality Rating as a Function of Image Source (Evaluation 7, Symbol)	385
Figure 5-106. Mean Image Quality Rating as a Function of Image Color by Image Source (Evaluation 7, Symbol)	386
Figure 5-107. Mean Line Visibility Rating as a Function of Resolution (Evaluation 8, Symbol).....	393
Figure 5-108. Mean Image Quality Rating as a Function of Resolution (Evaluation 8, Symbol)	394

LIST OF FIGURES (continued)

Figure 5-109. Mean Image Quality Rating as a Function of Image Color (Evaluation 8, Symbol)	395
Figure 5-110. Mean Line Visibility Rating as a Function of Image Source (Evaluation 8, Symbol)	396
Figure 5-111. Mean Image Quality Rating as a Function of Image Source (Evaluation 8, Symbol)	397
Figure 5-112. Mean Image Quality Rating as a Function of Image Color by Image Source (Evaluation 8, Symbol)	398
Figure 5-113. Modification of Standard Image in Evaluation 9 for FLIR Truck Images	401
Figure 5-114. Modification of Standard Image in Evaluation 9 for FLIR Tank Images	402
Figure 5-115. Mean Line Visibility Rating as a Function of Resolution and Standard Image (Evaluation 9, Truck)	405
Figure 5-116. Mean Line Visibility Rating as a Function of Resolution and Standard Image (Evaluation 9, Tank)	406
Figure 5-117. Mean Sharpness Rating as a Function of Resolution and Standard Image (Evaluation 9, Truck)	407
Figure 5-118. Mean Sharpness Rating as a Function of Resolution and Standard Image (Evaluation 9, Tank)	408
Figure 5-119. Mean Image Quality Rating as a Function of Resolution and Standard Image (Evaluation 9, Truck)	409
Figure 5-120. Mean Image Quality Rating as a Function of Resolution and Standard Image (Evaluation 9, Tank)	410
Figure 5-121. Mean Line Visibility Rating as a Function of Image Source and Standard Image (Evaluation 9, Truck)	411
Figure 5-122. Mean Line Visibility Rating as a Function of Image Source and Standard Image (Evaluation 9, Tank)	412
Figure 5-123. Mean Sharpness Rating as a Function of Image Source and Standard Image (Evaluation 9, Truck)	413
Figure 5-124. Mean Sharpness Rating as a Function of Image Source and Standard Image (Evaluation 9, Tank)	414
Figure 5-125. Mean Image Quality Rating as a Function of Image Source and Standard Image (Evaluation 9, Truck)	415
Figure 5-126. Mean Image Quality Rating as a Function of Image Source and Standard Image (Evaluation 9, Tank)	416
Figure 5-127. Modification of Standard Image in Evaluation 10 for Symbol Images	419
Figure 5-128. Mean Line Visibility Rating as a Function of Resolution and Standard Image (Evaluation 10, Symbol)	422
Figure 5-129. Mean Image Quality Rating as a function of Resolution and Standard Image (Evaluation 10, Symbol)	423

LIST OF FIGURES (continued)

Figure 5-130. Mean Line Visibility Rating as a Function of Image Source and Standard Image (Evaluation 10, Symbol)..... 424

Figure 5-131. Mean Image Quality Rating as a Function of Image Source and Standard Image (Evaluation 10, Symbol)..... 425

LIST OF TABLES

Table 1-1. Representative classes of future HMD applications.....	10
Table 1-2. Characteristics assumed for three HMD applications.....	20
Table 1-3. Preliminary display requirements for three HMD applications.....	23
Table 1-4. Rationale for preliminary display requirements.....	37
Table 2-1. Major preliminary requirements for HMS+.....	47
Table 2-2. Compatibility of image source technologies with respect to HMS+ preliminary requirements.....	50
Table 2-3. Power dissipation differences.....	55
Table 3-1. Test Cells, Summary of Key Results (see accompanying data for further details)	77
Table 3-2. Stack #1 Directional Illumination Measured With Xenon Lamp and Reynard Filters.....	79
Table 3-3. Stack #1 Directional Illumination Measured With Xenon Lamp and Calculated Filters (Y cutoff < 500 nm, IR cutoff > 650 nm)	80
Table 3-4. Stack #2 Directional Illumination Measured With Xenon Lamp and Reynard Filters.....	92
Table 3-5. Stack #2 Directional Illumination Measured With Xenon Lamp and Calculated Filters (Y cutoff < 500 nm, IR cutoff > 650 nm)	93
Table 3-6. Stack #3 (Hybrid #1) Directional Illumination Measured With Xenon Lamp and Reynard Filters.....	105
Table 3-7. Stack #3 Directional Illumination Measured With Xenon Lamp and Calculated Filters (Y cutoff < 500 nm, IR cutoff > 650 nm)	106
Table 3-8. Stack #4 Directional Illumination Measured With Xenon Lamp & Reynard Filters.....	124
Table 3-9. Stack #4 Directional Illumination Measured With Xenon Lamp and Calculated Filters (Y cutoff < 500 nm, IR cutoff > 650 nm)	125
Table 3-10. Stack #5 Directional Illumination Measured With Xenon Lamp and Reynard Filters.....	138

LIST OF TABLES (continued)

Table 3-11. Stack #5 Directional Illumination Measured With Xenon Lamp and Calculated Filters (Y cutoff < 500 nm, IR cutoff > 650 nm)	139
Table 3-12. Stack #6 Directional Illumination Measured With Xenon Lamp and Reynard Filters.....	178
Table 3-13. Stack #6 Directional Illumination Measured With Xenon Lamp and Calculated Filters (Y cutoff < 500 nm, IR cutoff > 650 nm)	179
Table 3-14. Stack Test Data Summary, Xenon Lamp and Reynard Filters.....	190
Table 3-15. Stack Test Data Summary, Xenon Lamp and Calculated Filters.....	191
Table 5-1. Illustrated and actual pixel mask luminance coefficients	235
Table 5-2. Summary of Evaluation Designs (Evaluations 1 - 10).....	247
Table 5-3. Design variables for Evaluation 1.....	254
Table 5-4. ANOVA summary table for Evaluation 1	261
Table 5-5. Preliminary conclusions based on Evaluation 1 results.....	262
Table 5-6. Design variables for Evaluation 2.....	269
Table 5-7. ANOVA summary table for Evaluation 2	277
Table 5-8. Preliminary conclusions based on Evaluation 2 results	279
Table 5-9. Design variables for Evaluation 3.....	292
Table 5-10. ANOVA Summary Table for Evaluation 3	297
Table 5-11. Preliminary conclusions based on Evaluation 3 results	298
Table 5-12. Design variables for Evaluation 4.....	309
Table 5-13. ANOVA summary table for Evaluation 4	311
Table 5-14. Preliminary conclusions based on Evaluation 4 results	312
Table 5-15. Mean rating differences between Evaluations 3 and 4	313

LIST OF TABLES (continued)

Table 5-16. Design variables for Evaluation 5.....	324
Table 5-17. ANOVA summary table for Evaluation 5.....	335
Table 5-18. Preliminary conclusions based on Evaluation 5 results.....	337
Table 5-19. Design variables for Evaluation 6.....	351
Table 5-20. ANOVA summary table for Evaluation 6.....	353
Table 5-21. Preliminary conclusions based on Evaluation 6 results.....	355
Table 5-22. Mean rating differences between Evaluations 5 and 6.....	357
Table 5-23. Design variables for Evaluation 7.....	373
Table 5-24. ANOVA summary table for Evaluation 7.....	378
Table 5-25. Preliminary conclusions based on Evaluation 7 results.....	379
Table 5-26. Design variables for Evaluation 8.....	388
Table 5-27. ANOVA summary table for Evaluation 8.....	390
Table 5-28. Preliminary conclusions based on Evaluation 8 results.....	391
Table 5-29. Mean rating differences between Evaluations 7 and 8.....	392
Table 5-30. Design variables for Evaluation 9.....	400
Table 5-31. Design variables for Evaluation 10.....	418
Table 5-32. Summary of conclusions from Evaluations 1 through 10.....	426

PREFACE AND ACKNOWLEDGEMENTS

The work described in this report was performed by the Honeywell Technology Center, under contract to the U.S. Army Natick RDEC, during the period of June, 1994 through August, 1995. The Honeywell contract number is DAAK60-94-C-0042. Mr. Henry Girolamo (U.S. Army Natick RDEC) and Dr. David Post (U.S. Air Force Armstrong Laboratory) served as contract monitors. Dave Galyardt (Boeing) generously donated his time and talent in providing the raw FLIR imagery used in many of the simulations reported here. The contributions of all these individuals to the concepts and results described in this report are gratefully acknowledged.

EXECUTIVE SUMMARY

Honeywell has identified two areas of display innovation which will promote the development of helmet or head mounted displays (HMDs) that are both small and inexpensive while at the same time delivering high performance and high reliability. These innovations concern the use of two-primary color displays and alternative gray scale control. Two-primary displays offer the advantages of significant reductions in cost and complexity for applications such as aircraft helmet mounted sights and field process control monitors where the display requirements call for greater than monochrome yet less than full color, especially for subtractive color displays. Alternative gray scale control offers the potential for reduction of perceptual artifacts such as luminance and color banding, especially in displays with relatively limited numbers of gray scale levels. This report describes the five principal tasks completed by Honeywell in the simulation and analysis of two-primary color display and alternative gray scale concepts.

Display Requirements Analysis

In this section, we present general considerations for two-primary color and alternative gray scale control, as well as preliminary display requirements for three representative applications. Preliminary display requirements for these applications are accompanied by a table outlining the rationale for the required parameter values.

System Configuration Concepts

The application of aircraft helmet mounted sight (HMS+, specifically) was selected for further system concept development in this section. Baseline configurations for two-primary image sources and color approaches are compared with the preliminary display requirements. Gray scale approaches as well as other system considerations such as interconnect, driver architecture, packaging, and electronics are also presented.

Test Cell Fabrication and Evaluation

In order to evaluate pixel aperture, as well as color gamut and luminance performance, very high resolution metallized patterns were processed for the light valve LCD test cells. Procedures and tests results of the single-pixel LCD test cells (two-primary color stacks) are provided. Results led to identification of an exceptional test stack configuration that was used on the Sony 1068 by 480 two-primary color AMLCD stacks.

Display Analysis

The results of examining and developing gray scale driver approaches are presented. Strategies are discussed on ways to achieve the lowest possible cost and the highest possible image quality for various gray scale approaches. We found that integrated analog drive systems meet this objective.

Another objective of this section was the analysis of display manufacturability. The cost of manufacturing two-primary color image sources was analyzed and compared to three-primary color image sources. The most effective cost solution combines drivers fabricated at silicon foundries with pixel arrays fabricated separately. These tested, yielded components are connected using flip-chip on glass bonding methods.

Simulation Development and Evaluation

A general simulation method and the results of ten human factors simulation evaluations are presented in this section. The simulations addressed a wide range of HMS+ design parameters including luminance contrast, gray scale levels and distribution, resolution, color method, and aperture ratio. The simulation results indicate the use of a red-green subtractive color AMLCD stack with high (>70%) aperture ratio will yield superior image quality to alternative image sources. Additional image quality improvements could be realized by increasing the resolution above the baseline resolution of 22 pix/deg (by reducing display FOV). Making use of yellow/orange in addition to red and green could also prove beneficial.

Recommendations

This final section of the report contains a summary of the major program results, as well as suggestions for additional future research.

1 DISPLAY REQUIREMENTS ANALYSIS

While alternative gray scale control technologies may be applied across a wide gamut of display applications, not all HMD applications require gray scale. Similarly, two-primary color concepts will only provide advantage for those display applications which require a color gamut beyond that provided by monochrome displays, but not the full gamut provided by most contemporary color displays incorporating three-color primaries. It is therefore important to carefully examine application-specific requirements for these technologies.

In this section, we present background assumptions and preliminary display requirements for selected applications using two-primary color and alternative gray scale control. The background material includes a general discussion of considerations for two-primary color systems and alternative gray scale control, including generally expected benefits as well as unique constraints. Next, we give an overview of future HMD applications and their suitability for two-primary and alternative gray scale control technologies.

Finally, we provide a more detailed description of three representative HMD application areas, including assumed characteristics of the display systems, environments, and imagery. Each of the applications is included in a detailed table of preliminary display requirements, including definitions of parameters. The preliminary requirements are accompanied by a table outlining the rationale for the given parameter values.

1.1 Considerations for Two-Primary Color

Two-primary color concepts offer the advantages of significant reductions in cost and complexity for HMDs. The following discussion identifies some of the specific benefits anticipated for two-primary color displays. However, several perceptual phenomenon exist that may influence the effective presentation of primary color pairs, especially where highly saturated primary colors are displayed. These phenomenon are also discussed below (see Walraven, 1992; 1985 and Murch, 1984 for more detail).

1.1.1 Two-Primary Transmission Gains

It has been estimated that the transmission gain for a two-primary subtractive color display is at least two to four times that of a full color (3 primary) display. The initial gain is at least a factor of two by accounting for one less aperture cell (assuming a typical active matrix aperture ratio of 50%). This gain can be factored again by as much as 1.4 due to elimination of blue notch overlap. Another factor could arise for possible increased luminance efficiency of lamp design.

Two-primary transmission gains may also be expected for field-sequential color display (e.g., Melzer and Moffitt, 1992a; 1992b; and Wei and Kalmanash, 1989). A conventional CRT-based full-color display using field-sequential color uses a monochrome CRT with a series of three color polarizers with two LC coils between them. By modulating the polarization of light in coordination with the refresh of the CRT, a full-color image is produced over the period of time required to refresh the CRT three times. By reducing the requirement from three to two color primaries, field-sequential displays can be simplified by removing one of the LC cells and one of the polarizers.

1.1.2 Manufacturability Gains

The use of two rather than three color primaries is expected to have a significant impact on manufacturing yield and cost. Such knowledge of the incremental cost associated with the addition of a third display layer in a subtractive color stack is expected to play a deciding factor in the selection of the most appropriate application-specific display configuration.

1.1.3 Selection of Color Primaries

Most two-primary display concepts assume the use of green and red primaries. For example, Kaiser's KROMA LC shutter and monochrome CRT developed for head-down display in the F/A-18 cockpit uses red and green primaries, with the combined primaries presenting yellow (e.g., Sweetman, 1988a; 1988b). Blue is selected as the missing primary for a number of reasons, some physical and others perceptual in nature. The most common physical reason is the difficulty in producing efficient blue phosphors; that is, phosphors that show a good ratio of emitted light energy relative to the amount of energy required to excite the phosphor. A good example of a phosphor-limited red-yellow-green EL display was reported by Tsurumaki et. al. (1991). The most common perceptual reason is that the human visual system is relatively insensitive to blue light. Even designers of full color displays often limit their use of blue. For example, most aircraft EFIS displays use a cyan primary rather than saturated blue. Some exceptions to the use of red-green two-primary displays do exist. For example, Kaiser demonstrated a display which uses red and cyan. The selection of cyan was calculated to allow the display of white with the use of both primaries (Melzer and Moffitt, 1992a; 1992b). In addition, Young (1990) proposed and simulated an opponent color display using a brightness (black-white) channel and a single red-blue channel.

1.1.4 Expected Color Gamut for Two-Primary Color

The most elementary color gamut one might expect from a red-green two-primary color display with no usable gray scale is described by four colors: black (background) red; green; and yellow/orange (the amount of yellow or orange is dependent on the relative luminance mix and chromaticities of the red and green primaries). Adding gray scale to the display will allow more colors to be addressed. However, the total number of addressable colors in the two-primary color display is reduced geometrically with the removal of one primary. For example, for a three-primary display capable of displaying 8 gray levels per color channel, the number of displayable colors is reduced from 512 to 64 for a comparable two-primary color display. The achievable color gamut can be predicted theoretically using conventional chromaticity diagrams by drawing a straight line connecting the two primary coordinates. The colors (with the exception of the background color) are those colors that have coordinates falling on this line. It is possible that the use of unconventional primaries (e.g., opponent-process displays) could yield wider perceived color gamuts than is achievable with a conventional red-green approach.

1.1.5 Helmholtz-Kohlrausch Effect

Two displays of equal luminance but varied chrominance will not appear to an observer as equally bright displays. Stated another way, brightness perception varies as a function of chromatic as well as achromatic contrast (see, for example, Calhoun and Post, 1990). This effect exists, despite the use of a correction in the Luminance scale for the spectral sensitivity of the human visual system. Murch (1984) documented this effect by asking observers to match the brightness of colored CRT images to a white image. By recording the luminance of colored and white images after they had been matched in brightness, he was able to document the magnitude of the luminance differences. Green images that were only 71% of the luminance of the white image appeared equally bright to the white image; luminances were only 49% and 27% those of the white image for equally bright red and blue images, respectively. Two-primary color displays that are balanced for equal primary luminance, therefore, are not likely to be equally bright. Correction equations can be used to better approximate equal brightness based on the luminance of colored images (e.g., Calhoun and Post, 1990) but the most accurate approach to balancing two-primary brightness (assuming a balanced brightness is desired) is likely to require empirical measurement of display brightness through subjective evaluation by observers. In high-ambient environments, equal brightness of see-through display colors may be less important than maintaining adequate luminance contrast of display imagery with the background.

1.1.6 Color Vision Deficiencies

Approximately 8% of males and less than 1% of females have a significant degree of deficiency in their color vision. Most commonly, this deficiency is manifested as a difficulty (but not a complete inability) in discriminating reds and greens. In a smaller number of cases (protanopic and deutanopic dichromats, about 25% of the color-deficient population), there is a complete lack of red or green cones in the eyes, and red-green confusions are even more likely (images are seen as varying in degrees of yellowness or blueness). Color deficient individuals may also lack blue cones (tritanopic dichromats) or be completely without color vision (monochromats). Although redundant information coding (e.g., position, shape) can be used to compensate for some color confusions, the reduced color gamut of a two-primary display will limit the degrees of freedom available for accentuating color differences for color-deficient observers. For example, by varying images in luminance as well as the relative contribution of blue, deuteranopes are better able to make red-green discriminations. The ability to modulate blue light in this way will be lacking in a red-green two-primary display.

1.1.7 Chromatic Aberration of the Eye

The lens of the eye images light at different focal lengths, contingent on the color of the light. Perceptually, this effect usually manifests itself as a slight blurring of long and short wavelength components (red and blue) of an image. However, in instances where adjacent, saturated primary colors are presented, the eye may experience some variance in accommodation. Chromatic aberration can be a problem for two-primary and full-color displays where separated primaries are used in the absence of any intermediate color mixing. The impact of chromatic aberration on viewer discomfort is likely to be small, except in cases where extremely saturated images are presented for extended periods of time.

1.1.8 Chromostereopsis

The small misalignment (5 degrees) of the foveal axis and the optical axis of the eye leads to a slight prismatic deviation. The chromatic dispersion that results is generally not noticeable. However, because the effect is mirror-imaged from left-eye to right-eye, a binocular disparity can be produced which results in a stereoscopic (3-D) separation of image colors. Chromostereopsis is generally only noticeable when adjacent, saturated primary colors are presented to an observer, and the effect is most evident with increased color saturation and separation of primaries. Chromostereopsis is generally uncomfortable and should be avoided. Chromostereopsis is a potential problem for two-primary and full-color displays, especially if separated primaries are used in absence of any intermediate color mixing.

1.1.9 Fluttering Hearts Phenomenon

When saturated red images presented on a green (or blue) background (or vice versa) are moved perpendicular to the line of sight, the foreground may appear to become detached from the background and move with an independent motion. The effect is most likely to be visible at low luminance levels, where highly saturated colors are involved, and when peripheral vision is involved. In theory, a two-primary or full-color display incorporating dynamic imagery could be susceptible to a related effect, although the use of photopic luminance levels and relatively narrow fields of view should mitigate the likelihood of this phenomenon manifesting itself.

1.2 Considerations for Alternative Gray Scale Control

Alternative gray scale approaches such as nonlinear digital gray scale distribution and temporal multiplexing offer the potential for reduction of perceptual artifacts such as luminance and color banding, as well as reduced complexity and cost. The following topics should be considered in the selection of gray scale approaches.

1.2.1 Color Vision Deficiencies

As noted above, a significant portion of the population suffers some degree of color deficiency. Red-deficient individuals (protans) are also sensitive to (red light) (Walraven, 1992) and may require larger changes in luminance per gray scale step to discern luminance differences than a color-normal individual (for images using red light).

1.2.2 Nonlinear Relationship of Luminance to Brightness

Luminance is a measurable photometric attribute of a display, while brightness is a perceptual analog to luminance measured over a broad area with properties governed by the human visual system. In addition to the chromatic contribution to brightness noted above, it is well known that brightness for any given monochrome image is not linearly related to luminance. Rather, brightness is best expressed as a power function of luminance, commonly recognized to have a cube-root or square-root relationship. The consequence of the nonlinearity of the luminance-brightness relationship is that linearly spaced gray steps on a display may be perceptually inefficient, especially for low cost driver systems that have a paucity of available gray levels. Gray steps at the high end of the linear luminance range appear to be very finely separated, while gray steps at the low end of the luminance range appear to be very coarsely distributed. A similar but inverse relationship is typical for display drive voltage and display luminance, where larger changes in drive voltage are typically necessary to effect equal changes in display luminance at the low end of the luminance range relative to the high end. The slope of the log/log plot of display drive voltage and display luminance is referred to as the display's gamma. Similarly, the slope of the log/log plot of display luminance and perceived brightness could be referred to as the gamma of the human visual system. It may be necessary to account for both types of gamma functions in order to realize the most economical implementation of display gray scale.

1.2.3 Application-Specific Imagery

Gray scale requirements for high image quality vary significantly as a function of the imagery being displayed. For example, as few as 8 levels of gray scale per color channel, spaced in even luminance steps, may be sufficient for anti-aliasing of binary symbology for electronic flight instrument system (EFIS) displays. By contrast, Honeywell has demonstrated that image quality benefits can be realized by using as many as 32 linear levels of gray scale per color channel for endoscopic surgical HMD applications using low contrast video imagery with a preponderance of red tones. Generally speaking, though, 64 to 256 gray levels are in common use in the video and graphics communities. As a rule of thumb, the human eye is capable of discriminating about 40 to 50 gray levels. With fewer gray levels than this, iso-luminance contours (banding) can become evident. The fewer the number of gray levels, the more evident the iso-luminance contours become.

The hierarchy of gray scale influence on image quality of general video may be cast into the following qualitative descriptions:

- With 2 gray levels, the general video image is coarse and difficult to interpret;
- With 4 gray levels, the image is clearly “posteriorized” or digitized in appearance and still difficult to interpret. The general scene content may be recognizable at this point but not easily so;
- With 8 gray levels, the scene content is recognizable but quite artificial looking. Iso-luminance contours are still prominently evident;
- With 16 gray levels, the spacing of the contours is much finer, leading to an almost analog and natural appearance, provided that the video signal is carefully adjusted to span the dynamic range of the available gray shades;
- With 32 grays, the scene can look quite natural. The luminance profiles of many scenes that commonly occur in the world can be adjusted to span the available range of grays and provide an artifact free image. But, images having clusters of energy pocketed in varying concentrations over the range of lights and darks can cause this methodology to fail, especially for real time systems;

- With 64 levels, the iso-contouring is much reduced; natural looking images are the norm with this many grays available. However, a good strategy must be invoked to carefully distribute the luminance values of the intended scene over the available range. Automatic gain control methods suitable for real time processing are widely practiced. Still, little margin for error exists;
- With 256 or more grays, there is enough headroom for managing the general image. Sufficient margin exists to handle images that do have luminance clusters distributed in various areas over the viewing field.

Gray scale requirements for specialized applications such as radiological diagnosis may be higher still, with some gray scale displays incorporating in excess of 1024 gray shades. These are needed to discern fine-featured and subtle patterns.

Many of the technologies in use today that are commonly constrained to a limited gray scale count are limited by the driver technology itself and not the physics of the display medium. For example, in the case of liquid crystal displays, the liquid crystal electro-optic curve is completely analog. It may be feasible to couple analog drive mechanisms to the display without sacrificing high performance and low cost objectives.

1.3 Review of HMD Applications

For the purposes of this report, the term HMD is used interchangeably to refer to either helmet mounted or head mounted displays. Where required, the more specific terms are used. While *helmet mounted* denotes integration of the display system into a helmet designed for use in a hazardous environment (e.g., military cockpit, chemical plant, manufacturing floor), *head mounted* denotes the use of a light-weight display mounting system without any special hardening requirements (e.g., a head band). Table 1-1 contains a review of several generic helmet and head mounted display applications envisioned for future use. The table is not meant to be exhaustive, but rather illustrative of a range of HMD applications. The applications represent a variety of military as well as commercial domains, and they are intended to be generically representative of a class of use. The application classes vary as to their likely need for image transparency and dual image sources, as well as the likelihood they will benefit from the two-primary color and alternative gray scale technologies addressed in this research. Where opaque displays are indicated, it is assumed that the display would not occlude the complete field of view. That is, some degree of natural vision would be retained by the occluded eye through a look-over, -under, or -around capability (none of the applications reviewed represent immersive virtual reality uses; all require interaction with an environment beyond the display). In addition, most opaque HMD applications could benefit from the provision of a mechanism to allow rapid movement of the display to a location outside of the primary field of view in the event of an unforeseen event such as display failure.

Table 1-1. Representative classes of future HMD applications.

Application	Mode	Purpose	Imagery	Color Requirement	Gray Scale Requir.
Aircraft Helmet Mounted Sight	Transparent, monocular	Overlay of weapons targeting and flight reference data over pilot's forward view through the aircraft canopy.	Alphanumerics, Line and filled symbols, FLIR	Limited color for separation of symbols and state designation.	Yes (required for FLIR, possibly for anti-aliasing of symbology).
Image Guided Assembly	Transparent, monocular	Overlay of manufacturing data such as wiring schematics over components on the shop floor.	Alphanumerics, Line and filled symbols, shaded figures.	Full color preferred.	Yes.
Endoscopic Imaging	Opaque, binocular	Display of internal sensor information (e.g., laparoscopy) for minimally invasive surgical procedures.	TV video, augmented by line and filled symbols, alphanumerics.	Full color preferred.	Yes.
Registered Noninvasive Medical Imaging	Transparent, binocular	Overlay of medical imagery such as MRI, CT, and ultrasound over the external view of the body for diagnostic examination and treatment.	Sensor video, augmented by line and filled symbology, alphanumerics.	Limited color for separation of video from symbols and state designation.	Yes (likely to have high gray scale requirement for feature discrimination).
Field Process Control Monitor	Opaque, monocular	Access to distributed process control while at remote plant location.	Alphanumerics, Line and filled symbols, shaded figures, TV video.	Limited color for separation of symbols and state designation.	Yes (necessary for shaded figures and eventually sensor video).
Field Emergency Medical Display	Opaque, monocular	Access to emergency medical procedures and patient information for field treatment.	Alphanumerics, Line and filled symbols, shaded figures.	Limited color for separation of symbols and state designation.	Yes.
Combat Vehicle Crew Display	Transparent, binocular	Display of weapons management and vehicle state data for ground combat vehicle crew.	Filled areas, line symbology, alphanumerics, filled objects.	Full color preferred.	Yes.
Portable Infantry Display	Transparent, monocular	Provide enhanced vision and tactical information to individual combat soldiers.	Sensor video, alphanumerics, Line and filled symbols.	Limited color for separation of video from symbols and state designation.	Yes.

Three representative applications from Table 1-1 are described in greater detail below. The three applications were selected to represent diverse modes of use and imagery. In addition, the applications represent both military and commercial domains. Assumptions regarding display system characteristics, environmental characteristics, and image characteristics for these three applications are summarized in Table 1-2.

1.3.1 Aircraft Helmet-Mounted Sight (AHMS)

Weapons targeting information in U.S. Air Force fighter/attack fixed-wing aircraft is commonly presented on a glare-shield mounted head up display (HUD) incorporating a monochrome (green) CRT image source. Typical HUDs for this application offer a total binocular FOV of approximately 16×12 deg, although contemporary holographic HUDs offer FOVs in excess of 30 deg. Head down CRTs are also used for target identification and weapon delivery. The imagery displayed includes stroke flight guidance (e.g., terrain following cues) and flight reference (e.g., pitch ladder) information, stroke targeting symbology, and Forward Looking Infrared (FLIR). To target a weapon (e.g., a missile), the pilot must align the boresight of his or her aircraft with the intended target to visually capture the target within the FOV of the HUD. The targeting FLIR is then slewed to capture the target. Such aircraft maneuvering and manual slewing adds time and complexity to the pilot's response during typically time-critical engagements. A more time efficient and simpler (from the pilot's perspective) means to cue aircraft weapon systems to targets is the aircraft helmet mounted sight (AHMS).

The term AHMS generically refers to monocular, transparent displays of weapon targeting information. A contemporary example of the AHMS currently in development is the VCATS (Visually-Coupled Acquisition and Targeting System) HMD, which will present monochromatic line symbology via a miniature helmet mounted CRT. For weapon targeting, VCATS will display a targeting reticle which is overlaid on the pilot's forward scene. The position and orientation of the pilot's helmet will be tracked, allowing the pilot to use head position to aim weapon systems. This ability to visually cue missile position has been demonstrated in simulations (e.g., Sweetman, 1988) to provide a survivability advantage to pilots when engaged in WVR (within visual range) combat. While the Israeli Air Force has been flying HMS-equipped F-15s and F-16s for at least 5 years (Hewish et. al., 1991), the first successful U.S. demonstration of an HMS-guided firing of an off-boresight missile was completed only this year, using a Honeywell helmet-mounted sight (Hughes, 1994).

A likely next-generation of the VCATS will be the HMS+ (read "HMS PLUSS" (Polychromatic Link Using Solid State). The HMS+ is intended for use in fast jets carrying High Off-Boresight Angle (HOBA) missiles and will likely be integrated with a standard Air Force HGU-55/P helmet. Like the HUD and VCATS systems preceding it, the HMS+ is intended for both day and night use, and in addition to air-to-air and air-to-ground weapons targeting the HMS+ may also be used for display of flight guidance and reference information and FLIR (Figure 1-1). The FLIR to be used with HMS+ is LANTIRN (Low Altitude Navigation and Targeting Infrared System for Night). (See Jones, 1991; Kelly and Spear, 1986; Brahney, 1985; and Lerner, 1985 for reviews of LANTIRN FLIR). Brightness of the LANTIRN FLIR image is proportional to the temperature of the objects being imaged, although a reverse video mode is available to present hot objects as dark rather than light. In navigational mode, LANTIRN FLIR covers a sensor FOV of 28 deg (horizontal) x 21 deg (vertical). In targeting mode, FLIR sensors housed in a targeting pod, separate from FLIR sensors in the navigation pod, are used. The FLIR FOV in the targeting mode is reduced to either 5.97 x 5.98 deg or 1.69 x 1.69 deg to present a zoomed image of the target area to the pilot. An array of 180 sensor elements is interleaved to provide a 360 line FLIR image via an RS-170 video interface to the display (640 x 480 pixels).

The display system requirements for HMS+ differ from VCATS in several important ways. While VCATS will use a CRT, the HMS+ image source must be "solid state" and low voltage (assumed to be a matrix-addressed flat panel display). In addition, while VCATS images will be monochrome, HMS+ will incorporate a limited color gamut for perceptual segregation of symbols as well as segregation of symbols from FLIR images. Because of the requirements for high luminance in daylight use and low helmet mounted weight, the light source for the HMS+ will likely be mounted remotely in the cockpit, with light piped to the helmet via fiber optics.

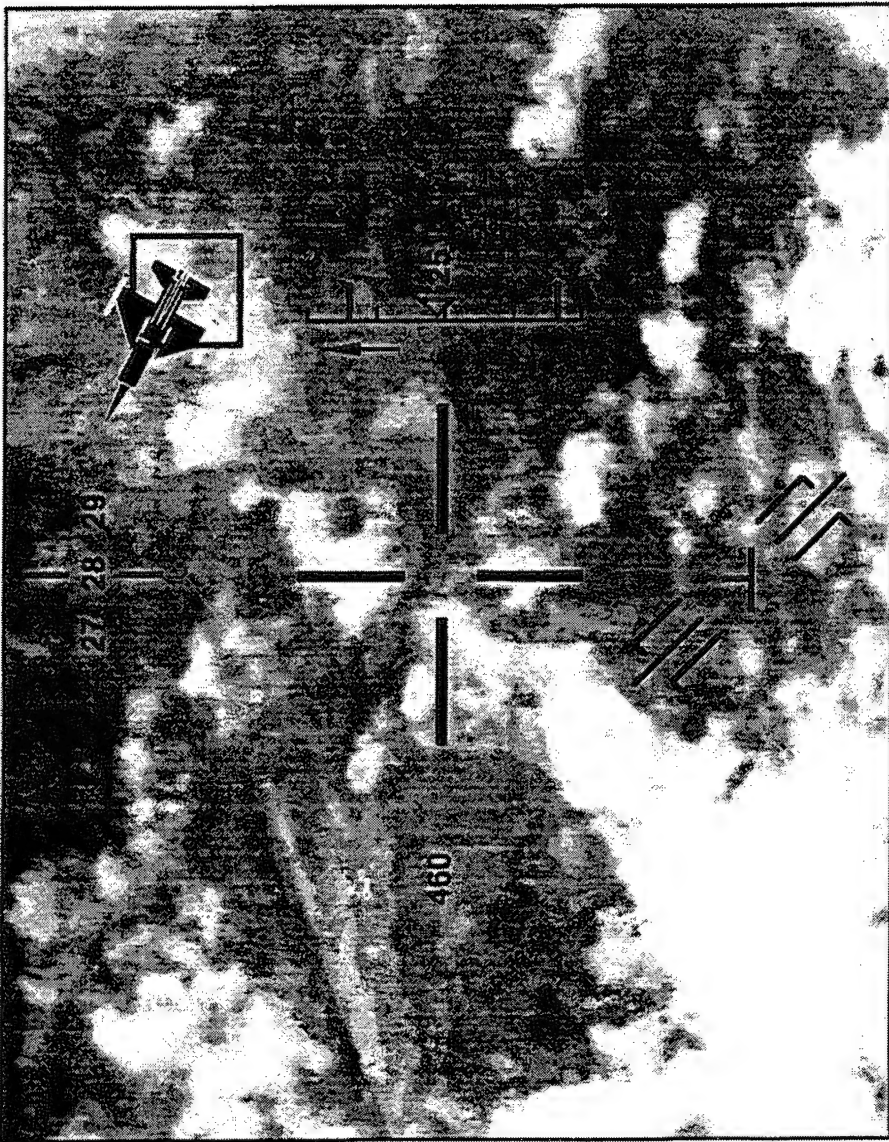


Figure I-1. Hypothetical AHMS weapons targeting display.
Flight reference and guidance symbology and FLIR are superimposed on the pilot's view through the aircraft canopy.

Many requirements exist to qualify the HMS+ as suitable for use in the fighter cockpit. For example, optical alignment of the HMS+ assembly with respect to individual users will be critical, since registration accuracy of the sight with the outside visual scene will contribute to overall accuracy of sensor or weapons aiming. Registration may also be disrupted by turbulence-induced head vibration; electronic image stabilization may be required. The helmet must be ejection compatible and the optics must be stable in high-G flight. The system must be safe for ground egress in an explosive vapor environment. Cabling must be flexible so as not to inhibit head motion, lightweight to avoid excessive head-supported weight, and must provide quick disconnect for rapid egress and ejection. Many additional requirements not listed here also exist.

1.3.2 Field Process Control Monitor (FPCM)

Just as the HMS+ exemplifies a promising military two-primary color HMD application, a good example of a U.S. commercial business which stands to benefit from advances in HMD technology is the petrochemical industry. Most refineries and petrochemical plants rely on distributed control systems (DCSs) to set and maintain desired process conditions (like temperature, pressure, flow rate, etc.) in different parts of the plant. As long as deviations such as changes in the quality of raw materials feeding into the process, variations in throughput, and degradation of equipment performance occur within a limited range, a DCS will automatically bring the plant back to the desired operating state. Beyond this range, however, it is the responsibility of the human operations staff to manually intervene. The coordinated response of the operations staff is typically interfaced with the DCS via a display screen with touchscreen and dedicated keyboard. When a process value goes beyond its desired operating limits, the DCS is configured to warn the operators of these conditions through messages, alarms and horns. An example of an alarm summary display for Honeywell's TDC 3000 is shown in Figure 1-2. Process schematics (Figure 1-3) are also used for information display and control, and are custom built at individual sites.

Operators are expected to manually intervene and correct any abnormal situations based on information obtained from the DCS. Unfortunately, members of the operations team (e.g., field operators, instrument technicians) may be located at sites remote from the control room with no direct access to DCS information. Currently, these personnel must crosscheck local sensor information with the DCS through control room operators via radio and telephone. Such communications, coming from multiple field personnel, are distracting to control room personnel. In addition, field access to information is delayed and lacking in visual representation. A more satisfactory solution would be to provide field personnel with remote DCS links through a helmet (hard hat) mounted display. Alternately, the display could be mounted to a light-weight head

band to allow use of the display in areas of the plant not requiring a hard hat. The display need not be transparent since overlay with the outside world is not necessary in the most fundamental implementation of this concept; indeed, significant luminance contrast advantages will accrue from using an opaque display. Similarly, a monocular display would be more advantageous than a biocular or binocular display, because field personnel must have at least one eye unobstructed to visually navigate in the complex and hazardous plant environment.

The FPCM would communicate with the DCS in a wireless mode, relying on high-speed digital radio communication and battery power. Although power would be a major issue here, this configuration would afford field personnel the maximum flexibility in access to the DCS at arbitrary locations. Alternately, an option could be provided for use of the unit via conventional cable links. Communication with the control room or other plant locations, currently accomplished through portable radios or dedicated telephone lines, could be integrated with the FPCM. Navigation through the DCS displays could be accomplished by voice, or by providing a portable membrane keyboard.

One pitfall associated with the use of a monocular, opaque HMD is the potential for binocular rivalry and visual distraction, especially at times when the user is attending to the outside visual scene rather than the HMD image. To mediate this problem, the FPCM should be mounted in such a way as to allow easily moving the display out of the primary field of view during periods of nonuse or emergency.

The imagery to be displayed would include standard and future DCS imagery of the types depicted in Figure 1-2 and Figure 1-3. Such imagery would enhance the operational effectiveness of field personnel by making direct visual representations of the plant state immediately available to them as they coordinate their field operations with control room personnel. In addition to process control, the FPCM could also be used for coordination of maintenance activity, retrieval of process history data, and training of operations personnel. Although contemporary DCS displays incorporate full color CRT monitors, more often than not the use of the full color gamut adds clutter to the display and reduces the contrast and visibility of text and symbols. A limited color gamut which includes red, yellow, and green should be sufficient to capture the most common industry standards for color usage and color meaning while at the same time allowing the construction of a higher-resolution, lighter-weight, and lower-cost HMD than would be possible with a full color display. Video window inserts for television or other sensor information could be incorporated in next generation incarnations of this display. However, like transparency, it is unlikely that video would be used in initial FPCM models.

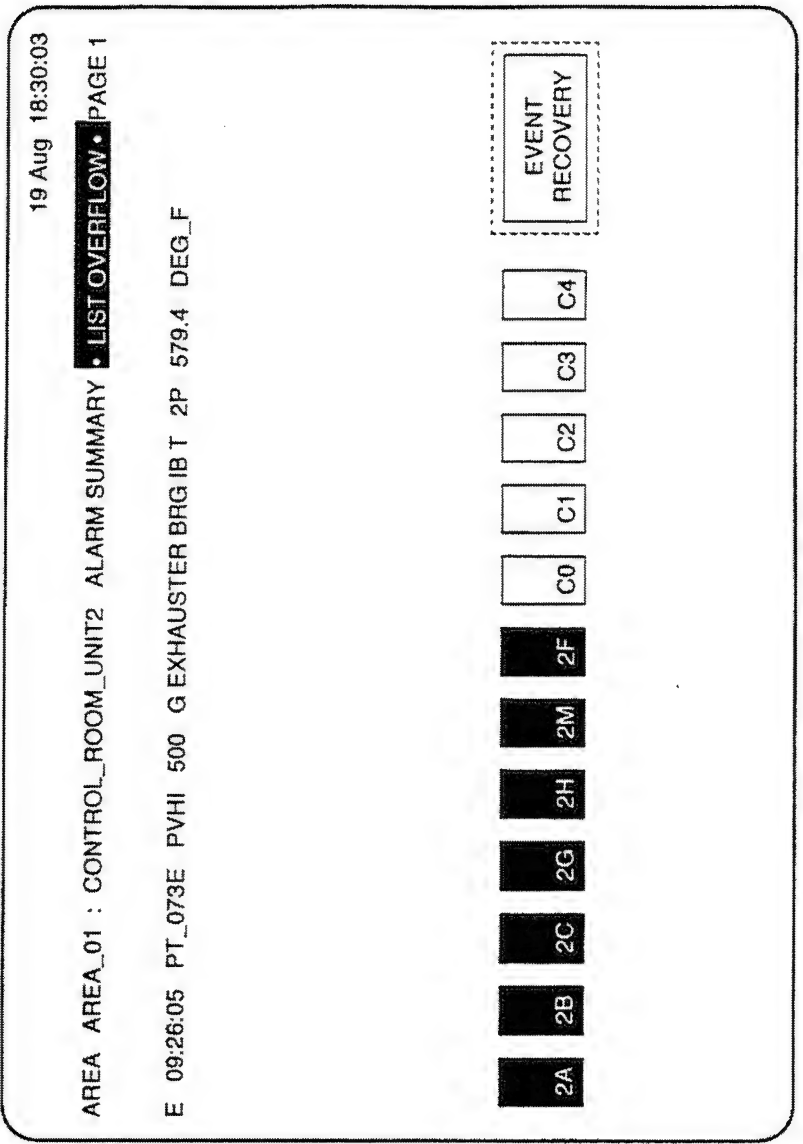


Figure 1-2. TDC 3000 Area Alarm Summary Display.

This and many other displays are serially or simultaneously viewed for DCS interaction via one or more console mounted CRTs.

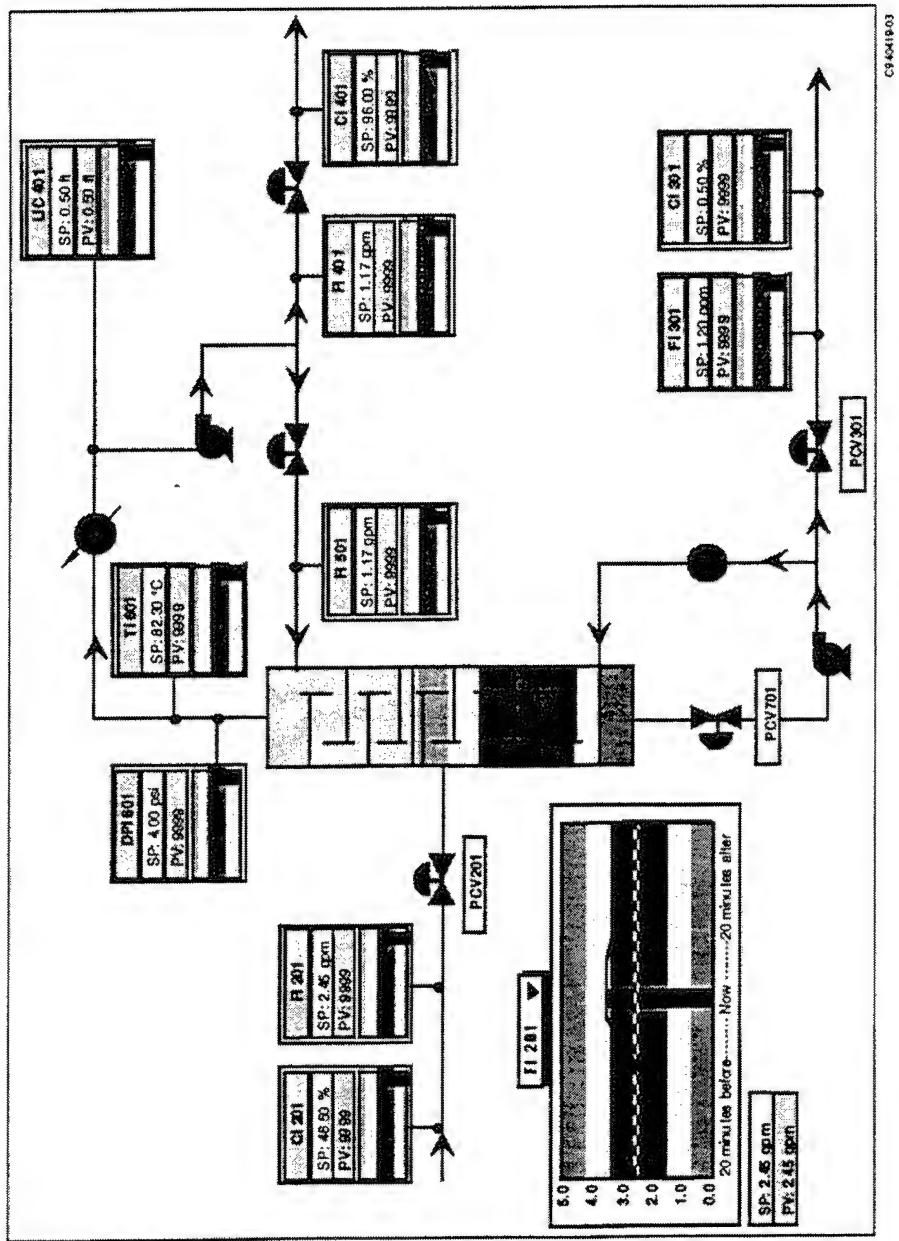


Figure 1-3. Hypothetical process schematic display for the Field Process Control Monitor (FPCM).

This schematic illustrates the operating state of a distillation column in a petrochemical process. The schematic depicts integrated trending functions not typically used in contemporary DCS displays, but envisioned for future DCS use.

1.3.3 Registered Noninvasive Medical Imager (RNMI)

One widely discussed commercial HMD application concerns the display of diagnostic medical imagery. Various contemporary medical imaging technologies (e.g., Computed Radiography (CR), Computed Tomography (CT), Magnetic Resonance Imaging (MRI), ultrasound, fluoroscopy, angiography, etc.) are routinely used to reveal hidden anatomical features of the body without the use of invasive procedures (e.g., exploratory endoscopy). The current use of such noninvasive diagnostic medical imaging is limited in effectiveness and ease of use by the inability of medical practitioners to precisely register 2D imagery on the patient's 3D body. Currently, such registration must be made in approximate reference to gross anatomical landmarks. That is, the general location and orientation of the imagery with respect to the patient's body is approximated by visually scanning the imagery for prominent organs or skeletal features and then mentally overlaying the imaged body features on the patient's physical body. In addition to registration, interpretation of the 2D imagery with respect to the 3D body requires extensive training.

An alternative approach is to display diagnostic imagery on a transparent, head mounted display (Figure 1-4). A head tracker coordinated with sensor and body position would allow precise, real-time registration of sensor imagery with the patient's body. A limited prototype of a similar system concept is described and was demonstrated by Bajura et al. (1992) at the University of North Carolina.

Unlike endoscopic applications which require full color for adequate identification of tissue pathology and internal anatomical landmarks, a limited color gamut should suffice for the RNMI because current diagnostic imagery is typically gray scale or pseudo-colored rather than photorealistic. Contemporary digital CRT display systems for medical imagery range from 8 to 12 bits of gray scale (monochrome) with between 60 to 80 fL of luminance being common. Image formats range from 512×512 to over $2K \times 2K$ pixels. Requirements for some imagery such as ultrasound are likely to be sensor-limited and therefore will not drive display performance. On the other hand, displays of radiographic film require high end display performance to present image quality approximating that of the original film.

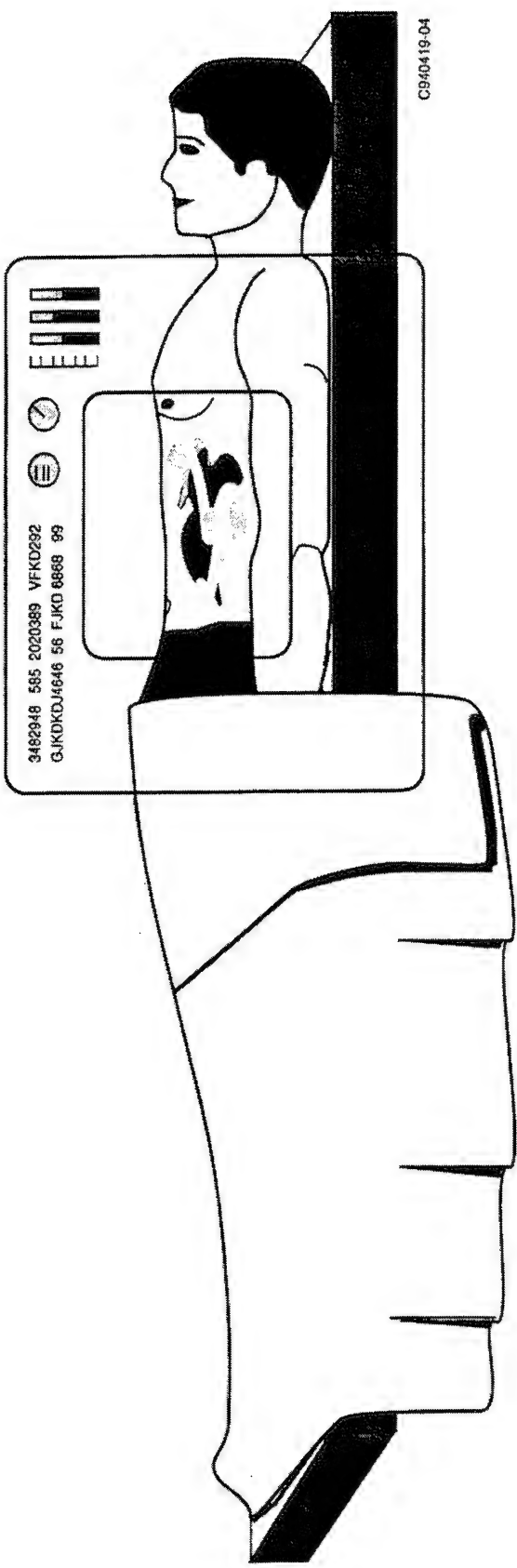


Figure 1-4. Possible image format for Registered Noninvasive Medical Imager (RNMI).

The outer frame represents the limits of the display FOV, while the inner frame represents a variable sized display window for sensor video (e.g., CT, MRI, ultrasound). Health monitoring and patient identification and status information is presented graphically and textually.

Table 1-2. Characteristics assumed for three HMD applications.

Attribute	Aircraft Helmet Mounted Sight (AHMS)	Field Process Control Monitor (FPCM)	Registered Noninvasive Medical Imager (RNMI)
Display System Characteristics	Solid State, Matrix Addressable	Solid State, Matrix Addressable	Solid State, Matrix Addressable
Image Source (Type)	Monocular (1)	Monocular (1)	Binocular (2)
Image Source (Number)	Lightweight, flexible cable.	Lightweight, flexible cable.	Lightweight, flexible cable.
Interconnect	Head-mounted preferred; remote mounting acceptable if size, weight, or safety prohibit head mounting.	Head-mounted preferred; remote mounting acceptable if size, weight, or safety prohibit head mounting.	Head-mounted preferred; remote mounting acceptable if size, weight, or safety prohibit head mounting.
Light Source	Minimal shock during normal use and doffing of head mounting. Moderate shock if dropped or if head collides with cockpit canopy or other structure.	Negligible shock during normal use. Minimal shock during doffing of head mounting. Moderate shock if dropped or if head collides with environmental protrusion.	Negligible shock during normal use. Minimal shock during doffing of head mounting. Moderate shock if dropped if head band.
Mechanical Shock	Integrated with standard HCU-55/P flight helmet.	Integrated with industrial hard hat. Alternatively, mounted with a light-weight head band. Display should move out of FOV during periods of noise or emergency.	Integrated with industrial hard hat.
Packaging	Compatible with available aircraft power supply, low voltage preferred for safety.	Battery operated for portability, low voltage preferred for safety, low wattage preferred for battery life.	Transformer compatible with standard 110 V, 60 Hz power, low voltage preferred for safety.
Power	Transparent	Opaque (with look-around capability and flexible display position)	Transparent
Transparency	Must meet limits of ejection safety, helmet comfort and stability.	Limited by comfort for extended wearing.	Limited by comfort for extended wearing.
Weight			
Environmental Characteristics	Sustained accelerations as great as those experienced in normal military jet flight due to takeoff, turbulence, high-G maneuvers, and landing.	Minimal, brief acceleration due to head motion.	Minimal, brief acceleration due to head motion.
Acceleration	5% to 95% RH	5% to 95% RH	5% to 60% RH
Humidity (Operating)	5% to 95% RH	5% to 95% RH	5% to 95% RH
Humidity (Storage)			

Table 1-2. Characteristics assumed for three HMD applications (continued).

Attribute	Aircraft Helmet Mounted Sight (AHMS)	Field Process Control Monitor (FPCM)	Registered Noninvasive Medical Imager (RNMI)
Illumination (Ambient)	Direct and reflected sunlight shafting through aircraft canopy. Ambient (outside of cockpit) assumed to vary from dark to 10,000 fc, with direct glare sources as high as 10,000 fL (windscreens transmittance not yet factored in).	Industrial overhead fluorescent lighting for interior use. Direct and reflected sunlight and sunlight shafting outdoors. Ambient indoors of 500 fc maximum, with direct glare sources as high as 500 fL. Ambient of outdoors assumed to vary from dark to 8,000 fc, with direct glare sources as high as 8,000 fL.	Well-controlled, specialized lighting. Diffuse, indoor lighting, dimmed to 10 fc. Reflected light as high as 10 fL.
Temperature (Operating)	5 to 35 deg C	-15 to 40 deg C	15 to 27 deg C
Temperature (Storage)	-40 to 55 deg C	-40 to 55 deg C	-40 to 55 deg C
Vibration	Whole body vibration from random turbulence, especially from 2-10 Hz, may disrupt head stability (Wells and Haas, 1992).	Negligible vibration during normal use.	Negligible vibration during normal use.
Image Characteristics			
Alphanumeric	Yes	Yes	Yes
Dynamic	Yes	Yes	Yes
Filled or Shaded Graphics	No	Yes	Yes
Line Symbols	Yes	Yes	Yes
Sensor Video	Yes	No (possibility for future)	Yes

1.4 Preliminary Display Requirements

Table 1-3 is a summary of preliminary display requirements for the three previously described HMD applications. The preliminary requirements apply to the HMD system as a whole, not just the image source(s). For example, MTF requirements for transparent displays apply to the quality of superimposed imagery as well as the visibility of the forward scene. Preliminary requirements are those values which are likely to yield the most satisfactory display system performance from the user's perspective. Complex tradeoffs among the many display parameters outlined here must be made in any display system design. Consequently, it is expected that no system design will be able to meet all preliminary requirements as presented in Table 1-3. Similarly, as system concepts are developed, improvements to display system performance may be realized by modifying the preliminary requirements.

A definition is provided for each parameter in Table 1-3, and recommended values are given. The rationale used for selection of recommended values is given in Table 1-4. These display system requirements were developed assuming the display system, environmental, and image characteristics described in Table 1-2. The requirements were derived from human performance data and prior experience with display system development.

For the purposes of these preliminary requirements, the following definitions apply:

- *Color Element:* The smallest addressable area of the display image. Individual color elements may vary in luminance but are limited to a single dominant wavelength, except in cases where color elements are equivalent to pixels (e.g., monochrome displays, subtractive color displays, projection displays using optical combination of multiple image sources, time-multiplexed color displays).
- *Pixel:* A combination of one or more color elements sufficient to display any color within the color gamut of the display system. As noted in the definition of color element, color elements are in some circumstances equivalent to pixels.

All preliminary display requirements should be met over the full operating environmental range of the display, over the full usable life of the display.

Table 1-3. Preliminary display requirements for three HMD applications.

Display Parameter	Definition	Aircraft Helmet Mounted Sight (AHMS)	Field Process Control Monitor (FPCM)	Registered Noninvasive Medical Imager (RNMI)	Comments
Active Noise Reduction	The use of adaptive filtering of sensor imagery to increase the signal to noise ratio in the displayed image.	TBD	Not required.	TBD	May be required for image sources such as FLIR.
Anti-aliasing	The use of gray scale to increase apparent positional accuracy and resolution for binary symbol definitions. Generally specified in terms of the number of gray shades and some measure of positional quantization allowed over the instantaneous field of view of the display.	8 gray levels, positions symbol to 1 part in 4096 over the height and width of the display.	Not Required	Not Required	Anti-aliasing generally facilitates the legibility of symbolic display where resolution is lower than the limits of human vision, especially where dynamic symbology is used.
Aspect Ratio (Display Image) (Ratio)	The ratio of the width of the display image to the height of the display image. Perceptually, the apparent shape of the display image as viewed from the center of the exit pupil.	Rectangular, 4:3	Rectangular, 4:3	Rectangular, 16:9	$4:3 = 1.33:1$ and assumes 640×480 or 1024×768 . $16:9 = 1.78:1$ and assumes 1920×1080 .
Aspect Ratio (Pixel) (Ratio)	The ratio of the width of a pixel to the height of a pixel. Perceptually, the apparent shape of a pixel.	1:1 color pixel aspect ratio	1:1 color pixel aspect ratio	1:1 color pixel aspect ratio	A delta-triad pixel arrangement with square color elements has also been demonstrated to offer satisfactory image quality.
Astigmatism (Oblique) (Diopters)	A form of optical aberration in which objects located off the optical axis are imaged with differing orientations, depending on the imaging distance. Perceptually, astigmatic display optics require the observer to shift accommodation to bring image features of differing orientation into focus. Unfocused image components will appear blurred.	See MTF.	See MTF.	See MTF.	Oblique astigmatism is assumed to be reflected in the requirement for MTF.
Automatic Brightness Control	Automatic control of display luminance using measured values of the ambient and the forward scene luminances.	Both manual and automatic brightness controls required.	Manual brightness control required.	Manual brightness control required. In addition, automatic brightness control is preferred.	Location and FOV of sensor with impact effectiveness of automatic control.

Table 1-3. Preliminary display requirements for three HMD applications (continued).

Display Parameter	Definition	Aircraft Helmet Mounted Sight (AHMS)	Field Process Control Monitor (FPCM)	Registered NonInvasive Medical Imager (RNMI)	Comments
Automatic Contrast Control	Automatic control of display contrast using measured values of the ambient and the forward scene luminances.	Both manual and automatic contrast controls required.	Manual contrast control required.	Manual contrast control required. In addition, automatic contrast control is preferred.	Location and FOV of sensor will impact effectiveness of automatic control.
Automatic Image Stabilization.	The automatic compensation for image plane movement due to shock and vibration.	Not required, but preferred.	Not required	Not required, but preferred.	
Built In Test	The inclusion of functionality to test the display system. For example, the ability to call up gray scale test patterns.	Both automatic and initiated BIT required.	Initiated BIT required.	Initiated BIT required.	
Centrifuge (Gravities)	The minimum gravity (g) loading the HMD may be subjected to in a centrifuge and still provide a stable optical mounting platform.	-9g to +9g.	No requirement.	No requirement.	
Chromatic Aberration (Diopters)	A form of optical aberration in which objects of different colors have different image distances. Perceptually, display optics with chromatic aberration require the observer to shift accommodation to bring image features of different colors into focus. Unfocused image components will appear blurred.	See MTF.	See MTF.	See MTF.	Chromatic aberration is assumed to be reflected in the requirement for MTF.
Color Element Failures (Percent total)	The loss of addressability of individual color elements or clusters of color elements. Color elements may fail either on or off.	Maximum of 0.25% total failed red and green color elements.	Maximum of 0.25% total failed red and green color elements.	Maximum of 0.25% total failed red and green color elements.	For biocular or binocular displays, element cluster restrictions apply to each image source used.

Table 1-3. Preliminary display requirements for three HMD applications (continued).

Display Parameter	Definition	Aircraft Helmet Mounted Sight (AHMS)	Field Process Control Monitor (FPCM)	Noninvasive Medical Imager (RNMI)	Comments
Color Gamut (Maximum gamut and uniformity) (u' , v')	The identification of each color primary (red and green) within the CIE 1976 uniform color space (UCS) when displaying the maximum luminance and the uniformity of these primaries across the display FOV. Large-area chromatic uniformity refers to the absence of unintended chromatic differences as measured from the center of the exit pupil and an edge of the exit pupil. Small area chromatic uniformity refers to the absence of unintended color differences within 0.5 degrees of the image FOV.	red .469 .522 green .127 .560 blue no blue primary	red .469 .522 green .127 .560 blue no blue primary	red .469 .522 green .127 .560 blue no blue primary	These UCS coordinates serve as an example of a commercial, avionic-grade CRT primary flight display. The uniformity requirement also applies to unintended variation in color between or among binocular image fields or image tiles. Also, see prior discussion in text regarding considerations for use of two-primary color displays.
Coma (TBD)	A form of optical aberration in which points viewed off the optical axis appear elongated. Coma contributes to image blur.	See MTF.	See MTF.	See MTF.	Coma is assumed to be reflected in the requirement for MTF.
Decompression (Rapid)	The ability of the HMD to withstand rapid decompression without loss of display function or risk of injury to the wearer.	Required	Not required.	Not required.	
Dimming Range (Ratio)	The ratio of the max and the min output luminances through which the display system must traverse in a smooth and continuous manner to provide dimming control of the display.	$\geq 2000:1$ Preferred is 6000:1 No loss of grayscale steps throughout dimming range.	$\geq 1500:1$ No loss of grayscale steps throughout dimming range.	$\geq 250:1$ No loss of grayscale steps throughout dimming range.	Dimming range will impact control of image transparency and visual adaptation for night vision.
Divergence (Degrees)	The presence of disparities between binocular or biocular images in the vertical direction due to vertical misregistration between fields.	Not applicable	Not applicable	≤ 0.08 degrees.	

Table 1-3. Preliminary display requirements for three HMD applications (continued).

Display Parameter	Definition	Aircraft Helmet Mounted Sight (AHMS)	Field Process Control Monitor (FPCM)	Registered Noninvasive Medical Imager (RNMI)	Comments
Distortion (Percent)	A form of optical aberration. The net percent of unintended variation in the position of an image element with respect to an ideal image. Perceptually, the degree to which optical aberrations such as pin cushion or barrel distortion are present in the image.	Maximum of 5% distortion over the total FOV.	Maximum of 5% distortion over the total FOV.	Maximum of 5% distortion over the total, binocular FOV.	The insertion of the dithering noise can be done explicitly or implicitly by the display system. Implicit noise addition can include noise from sensors.
Dithering	The insertion of image noise (e.g., Robert's noise) to enhance perceived image quality. The amount of noise power per unit time over the span of the display is typically related to the degree of quantization in the luminance signal during the process of digitization, e.g. + 1/2 lsb.	TBD	TBD	TBD	The insertion of the dithering noise can be done explicitly or implicitly by the display system. Implicit noise addition can include noise from sensors.
Don/Doff Time	The amount of time required to don or doff the HMD.	Time should be minimized (TBD). Assistance should not be required.	Time should be minimized. Assistance should not be required.	Time should be minimized. Assistance may be required if performing sterile procedure.	Time should be minimized. Assistance may be required if performing sterile procedure.
Drift (Percent, Hours)	The extent to which display characteristics such as image registration, relative image position, and chromaticity vary over a 24-hour period.	Maximum color gamut drift is 20% of the maximum deviation over 24 hours. Maximum drift in registration accuracy is 20% of the maximum deviation over 24 hours.	Maximum color gamut drift is 20% of the maximum deviation over 24 hours. Maximum drift in registration accuracy is 20% of the maximum deviation over 24 hours.	Maximum color gamut drift is 20% of the maximum deviation over 24 hours. Maximum dipvergence drift is 20% of the maximum over 24 hours. Maximum drift in registration accuracy is 20% of the maximum deviation over 24 hours.	Where drift is anticipated, controls should be provided for calibration. Stereoscopic displays may be especially sensitive to drift if the two stereoscopic fields are differentially affected.
Dwell Time (Micro-seconds)	The time required to change a pixel from its minimum luminance to its maximum luminance.	Dwell time should be minimized to meet the requirements for total number of pixels and refresh rate.	Dwell time should be minimized to meet the requirements for total number of pixels and refresh rate.	Dwell time should be minimized to meet the requirements for total number of pixels and refresh rate.	Dwell time should be minimized to meet the requirements for total number of pixels and refresh rate.

Table 1-3. Preliminary display requirements for three HMD applications (continued).

Display Parameter	Definition	Aircraft Helmet Mounted Sight (AHMS)	Field Process Control Monitor (FPCM)	Noninvasive Medical Imager (RNMI)	Comments
Electro-magnetic Interference (EMI)	Any functional or quality interference associated with electromagnetic emissions, including static electricity and lightning. EMI may be transmitted from within one display component to another, from outside of the display system to the display, or from the display to a system outside of the display.	The display system should incorporate appropriate shielding, bonding, filtering, grounding, and/or circuit design to ensure no EMI effects.	The display system should incorporate appropriate shielding, bonding, filtering, grounding, and/or circuit design to ensure no EMI effects.	The display system should incorporate appropriate shielding, bonding, filtering, grounding, and/or circuit design to ensure no EMI effects.	
Exit Pupil (mm)	The size of the aperture through which an unvignetted image is visible from the design eye relief.	≥ 17 mm	≥ 10 mm	≥ 10 mm	Vignetting refers to the occlusion of peripheral image points.
Explosive Atmosphere	The system must comply with safety standards IAW MIL-STD-810. The HMD must operate normally in explosive atmospheres without posing risk of explosion.	Required.	Required.	Required.	
Eye Relief (mm)	The minimum physical distance between the nearest optical element and the eye of the display observer.	≥ 25 mm	≥ 30 mm	≥ 30 mm	Large eye reliefs may require smaller exit pupils.
Field Curvature (Diopters)	A form of optical aberration in which the image of a flat object does not lie in a plane, with object points falling off optical axis showing the aberration. Perceptually, the presence of variations in the accommodation distance where none should occur.	Maximum of ± 0.25 diopters over the total FOV.	Maximum of ± 0.25 diopters over the total FOV.	Maximum of ± 0.25 diopters over the total binocular FOV.	
Field of View (Degrees)	The angular subtense, horizontally and vertically, of the image that is visible from the center of the exit pupil.	Monocular: 28 deg (horizontal) $\times 21$ deg (vertical)	Monocular: 32 deg (horizontal) $\times 24$ deg (vertical)	Binocular (full overlap): 48 deg (horizontal) $\times 27$ deg (vertical)	

Table 1-3. Preliminary display requirements for three HMD applications (continued).

Display Parameter	Definition	Aircraft Helmet Mounted Sight (AHMMS)	Field Process Control Monitor (FPCM)	Noninvasive Medical Imager (RNMI)	Comments
Field Rate (Hertz)	The number of times within a one-second interval that all display pixels in a single time-multiplexed field may be addressed. For time-multiplexed displays, a single frame is the sum of all constituent fields (see <i>Frame Rate</i>). Time multiplexing includes conventional interleaving techniques as well as time-multiplexed color.	Minimum of the frame rate multiplied by the total number of fields.	Minimum of the frame rate multiplied by the total number of fields.	Minimum of the frame rate multiplied by the total number of fields.	Time-multiplexed color displays will typically have one field corresponding to each color primary. Perceptually, field rate is a strong determiner to whether flicker may be perceived in the display.
Flicker (Subjective)	The visible and unintended modulation of large area display luminance as a function of time, usually due to inadequate frame rate or short image persistence.	The display should be "flicker free."	The display should be "flicker free."	The display should be "flicker free."	Flicker thresholds vary as a function of the age of the observer, as well as display parameters such as ambient and display illumination and display FOV. Display refresh rate may interact with some indoor lighting frequencies to form visible beats.
Frame Rate (Hertz)	The number of times within a one-second interval that all display pixels may be addressed. For time-multiplexed displays, a single frame is the sum of all constituent fields (see <i>Field Rate</i>). Time multiplexing includes conventional interleaving techniques as well as time-multiplexed color.	60 Hz. 90 Hz preferred.	60 Hz.	≥60 Hz.	Perceptually, frame rate is a strong determiner of whether flicker may be perceived in the display. AHMS should be a multiple of 30 Hz (LA-NIRN FLIR).
Gray Scale (Shades of gray per color primary) (Total)	The number of discretely addressable luminance levels for each color primary.	≥64 linearly distributed shades of gray per color channel, where the first luminance step is equal to the background luminance No grayscale loss throughout dimming range.	≥16 linearly distributed shades of gray per color channel, where the first luminance step is equal to the background luminance	≥64 linearly distributed shades of gray per color channel, where the first luminance step is equal to the background luminance	If gray shades are nonlinearly distributed, the minimum requirement may change. Analog gray scale, if possible, may be preferred.

Table 1-3. Preliminary display requirements for three HMD applications (continued).

Display Parameter	Definition	Aircraft Helmet Mounted Sight (AHMS)	Field Process Control Monitor (FPCM)	Registered Imager (RNI)	Comments
Gray Scale Distribution of Luminance)	The algorithm describing the distribution of available gray scale levels over the luminance range of the display.	Minimum of linear. Alternate for consideration is: Luminance _n = $[(L_{\max}^{1/3} - L_{\min}^{1/3}) * n / (\text{steps} - 1) + L_{\min}^{1/3}]^3$, where n = 0 to (steps - 1), steps is the number of gray scale levels incorporated in the gray scale, and L _{max} and L _{min} define the maximum and minimum display luminance.	Minimum of linear. Alternate for consideration is: Luminance _n = $[(L_{\max}^{1/3} - L_{\min}^{1/3}) * n / (\text{steps} - 1) + L_{\min}^{1/3}]^3$, where n = 0 to (steps - 1), steps is the number of gray scale levels incorporated in the gray scale, and L _{max} and L _{min} define the maximum and minimum display luminance.	Minimum of linear. Alternate for consideration is: Luminance _n = $[(L_{\max}^{1/3} - L_{\min}^{1/3}) * n / (\text{steps} - 1) + L_{\min}^{1/3}]^3$, where n = 0 to (steps - 1), steps is the number of gray scale levels incorporated in the gray scale, and L _{max} and L _{min} define the maximum and minimum display luminance.	Applies to digital display systems only. Equation from McCartney (1992). Advantages of nonlinear gray scale distributions are image dependent.
Hanging Harness	The degree to which the HMD interferes with post-ejection bailout procedures.	No interference, as per LAW TO-14D1-2-1.	Not required.	Not required.	
Head Tracking	The use of magnetic, optical, or acoustic head tracking to allow image registration with the forward scene.	Required.	Not required.	Required.	
Humidity (Operating) (RH)	The range of ambient relative humidity over which the display is expected to operate normally.	5% to 95% RH	5% to 95% RH	5% to 60% RH	
Humidity (Storage) (RH)	The range of ambient relative humidity over which the display is expected to be stored without damage.	5% to 95% RH	5% to 95% RH	5% to 95% RH	
Image Distance (cm)	The distance from the eye to the plane of visual accommodation.	Collimated to infinity.	30-40 cm, user adjustable.	30-60 cm, head tracked.	
Image Enhancement	The general use of display algorithms to optimize distribution of image components over the dynamic range of the display.	TBD	Not required.	TBD	Cited in HMS+ Industry Briefing.

Table 1-3. Preliminary display requirements for three HMD applications (continued).

Display Parameter	Definition	Aircraft Helmet Mounted Sight (AHMS)	Field Process Control Monitor (FPCM)	Noninvasive Medical Imager (RNMI)	Comments
Image Masking and Priority Assignment	The prioritization of visual information where multiple sources of imagery are overlaid. Priority may be designated through contrast enhancement techniques such as haloing or by excluding the writing of conflicting visual information within specified zones on the display.	Required.	Not required	Required.	Haloing is most significant when symbology must be easily distinguishable with respect to random fields of video or the forward scene in a transparent display as frequently is the case with symbology overlays.
Image Persistence (Milli-seconds)	The extent to which a pixel remains active after no longer being addressed or after being commanded to turn off. Image persistence is usually a brief (milliseconds) phenomenon which is a factor in display luminance, flicker, and crosstalk.	Maximum of the inverse of the frame rate. For time-multiplexed displays, maximum should be less than the inverse of the field rate, the exact amount to be determined empirically. Minimum for all displays to be determined by compliance with the luminance and flicker requirements.	Maximum of the inverse of the frame rate. For time-multiplexed displays, maximum should be less than the inverse of the field rate, the exact amount to be determined empirically. Minimum for all displays to be determined by compliance with the luminance and flicker requirements.	Maximum of the inverse of the frame rate. For time-multiplexed displays, maximum should be less than the inverse of the field rate, the exact amount to be determined empirically. Minimum for all displays to be determined by compliance with the luminance and flicker requirements.	Image persistence interacts with field rate in determining crosstalk in time-multiplexed displays. May be a problem for video-rate LCDs.
Image Retention (No Units)	The visible presence of an image or portion of an image while the display is not active. Image retention is a lasting phenomenon (minutes, hours, or days) with no desirable contribution to display system performance.	No visible image retention should be observed over the usable life of the display.	No visible image retention should be observed over the usable life of the display.	TBD	No visible image retention should be observed over the usable life of the display.
Impact/Penetration Interconnect (No units)	TBD	Compliant with IAW G-OAV-3-102	TBD	Flexible, light-weight cable; quick disconnect.	Flexible, light-weight cable; quick disconnect.

Table 1-3. Preliminary display requirements for three HMD applications (continued).

Display Parameter	Definition	Aircraft Helmet Mounted Sight (AHMS)	Field Process Control Monitor (FPCM)	Noninvasive Medical Imager (RNMI)	Comments
Interlacing (Spatial) (Ratio)	The conservation of display system bandwidth by addressing only a subset of total display pixels during each display refresh cycle. Each subset of pixels addressed comprises a field, with the combined fields in time forming a frame. Interlacing is described by the ratio of fields to frames.	1:1	1:1	1:1	Values given here assume interlacing in the classic sense as opposed to interlacing of time-multiplexed color fields.
Jitter (Degrees/Second)	The combined vertical and horizontal angular excursion of an image pixel across the display FOV over a one-second period of time due to instability within the display system. Perceptually, the movement of the image or portions of the image with respect to stationary elements of the display system.	≤0.01 degrees per second.	≤0.01 degrees per second.	≤0.01 degrees per second.	Although jitter is often associated with raster displays, matrix-addressed displays may exhibit a similar phenomenon due to noise in the video signal, especially where multiple signals are combined.
Line Failures (Percent)	The loss of addressability of a complete row or column of pixels. Lines may fail either on or off.	No line failures are allowable.	No line failures are allowable.	No line failures are allowable.	
Luminance (Foot Lamberts (fL))	The total amount of light integrated over a fixed angular portion of the image.	≥7,500 fL red, ≥7,500 fL green at the image source, 5,625 fL to 8,125 fL each after display optics (including any combined light).	1,000 fL red, 1,000 fL green at the image source, 750 fL each after display optics (including any combined light).	700 fL red, 700 fL green at the image source, 527 fL each after display optics (including any combined light)	Equal brightness of primaries will require unequal luminance weightings.
Luminance Asymmetry (Percent)	The percent difference in luminance between stereoscopic image fields or tilted images when the desired value is identical.	≤10%.	≤10%.	≤10%.	
Luminance Contrast (Contrast Ratio)	The most common method of expressing display luminance contrast in the display industry.	≥100:1 at the image source; 3:1 to 50:1 combined.	≥50:1	≥100:1 at the image source; 40:1 combined.	See rationale for discussion of grayscale requirements relative to luminance contrast.

Table 1-3. Preliminary display requirements for three HMD applications (continued).

Display Parameter	Definition	Aircraft Helmet Mounted Sight (AHMS)	Field Monitor (FPCM)	Registered Noninvasive Medical Imager (RNMI)	Comments
Luminance Half-Life (Hours)	The time required for the maximum luminance of the display to be reduced to below 50% of the initial value over the life of the display.	≥ 1000 hours.	≥ 1000 hours.	≥ 1000 hours.	
Luminance Non-uniformity (Percent)	The percent of unintended variation in luminance between two areas across the display FOV. Large-area luminance nonuniformity refers to unintended luminance differences between that measured from the center of the exit pupil and an edge of the exit pupil. Small-area nonuniformity refers to unintended luminance differences within a 0.5 degree area of the display FOV.	$\leq 20\%$ for large-area nonuniformity. $\leq 10\%$ for small-area nonuniformity.	$\leq 20\%$ for large-area nonuniformity, $\leq 10\%$ for small-area nonuniformity.	$\leq 20\%$ for large-area nonuniformity. $\leq 10\%$ for small-area nonuniformity.	
Mean Time Between Failures (MTBF) (Hours)	The mean consecutive hours of operation before which the display system is expected to operate without loss of function.	≥ 10000	≥ 5000	≥ 5000	Relates to the criticality level of the system.
Modulation Transfer Factor (at display resolution) (MTF)	The minimum modulation transmittance of the display optics at the maximum display resolution. Perceptually, the extent to which the display optics faithfully represent image sharpness.	≥ 0.3 at the display resolution.	≥ 0.3 at the display resolution.	≥ 0.3 at the display resolution.	

Table 1-3. Preliminary display requirements for three HMD applications (continued).

Display Parameter	Definition	Aircraft Helmet Mounted Sight (AHMS)	Field Process Control Monitor (FPCM)	Noninvasive Medical Imager (RNMI)	Comments
Packaging (No Units)	The mechanical design of the display system packaging and the means by which the packaged display system is secured to the head.	Integration with HGU-55/P helmet (size Large) prefabricated, but novel helmet design is allowed. Must be consistent with ejection safety, weight, and center of gravity requirements. Must not physically interfere with other cockpit controls or displays or prevent rapid emergency egress.	Modular integration with plain hard hat, with option of removing hard hat. Consistent with weight and center of gravity requirements. Must not physically interfere with operation of other controls or displays.	Lightweight, adjustable head band or harness. Consistent with weight and center of gravity requirements. Must not physically interfere with operation of other controls or displays.	
Parachute Deployment	The degree to which the HMD interferes with the deployment of a parachute.	Required. HMD must remain intact and can't cause injury nor interfere with chute deployment, such as riser interference.	Not required.	Not required.	
Personal Equipment Compatibility	The personal equipment with which the HMD must be compatible (i.e., must not interfere with comfort, function, or with don/doff of equipment)	Standard flight suit; WAMRS; I.PU-9/P; MBU-12/P and 20/P Oxygen mask; Standard flight gloves; Anti-g suit; Torso harness.	Eye glasses; Hearing protectors.	Eye glasses; Surgical cap; Surgical mask.	
Pixel Count (Total)	Total number of addressable display pixels in both the horizontal and vertical dimensions.	640 (horizontal) x 480 (vertical)	1024 (horizontal) x 768 (vertical)	1920 (horizontal) x 1080 (vertical)	
Power (HMD) (Watts)	The total power requirements for the display system, excluding remote components such as graphics processors.	≤ 100 Watts	Watts TBD based on battery life and heat.	Watts TBD based on heat.	
Refresh Rate (Hertz)	A nonspecific term used interchangeably for either Field Rate or Frame Rate.	See <i>Field Rate</i> and <i>Frame Rate</i> .	See <i>Field Rate</i> and <i>Frame Rate</i> .	See <i>Field Rate</i> and <i>Frame Rate</i> .	

Table 1-3. Preliminary display requirements for three HMD applications (continued).

Display Parameter	Definition	Aircraft Helmet Mounted Sight (AHMS)	Field Process Control Monitor (FPCM)	Noninvasive Medical Imager (RNMI)	Comments
Registration Accuracy (Degrees)	Maximum allowable angular deviation of correspondence between the display image and the real-world forward scene due to optical considerations in the display system.	Maximum deviation of 0.4 deg. Does not include external sources of misregistration (e.g., canopy distortions).	Not applicable.	Maximum deviation of 2.0 deg. Provide manual calibration controls to eliminate visible misregistration.	
Registration Control	The provision of manual and/or automatic means to control the correspondence between the display image and the real-world forward scene.	Both manual and automatic registration control required.	Not required.	Both manual and automatic registration control required.	
Resolution (Pixels /Degree)	The total number of pixels subtended within one degree at the observer's eye in both the horizontal and vertical directions.	23 pixels/deg (horizontal) x 23 pixels/deg (vertical).	32 pixels/deg (horizontal) x 32 pixels/deg (vertical).	40 pixels/deg (horizontal) x 40 pixels/deg (vertical).	
Smearing (Subjective)	The apparent blur of display elements between refresh cycles when displaying object motion. Smearing is caused either by mismatches between image persistence and refresh rate or mismatches between update rate and refresh rate.	Smearing should not be observable when moving symbology is displayed.	Smearing should not be observable when moving symbology is displayed.	Smearing should not be observable when moving symbology is displayed.	See <i>image persistence, dwell time, refresh rate, and update rate.</i>
Sound Attenuation	The degree to which the HMD provides hearing protection from ambient sounds.	Required per IAW MIL-F-38268C and ANSI S1.2.6	HMD must provide hearing protection equivalent to existing means used or must allow integrated use with existing means.	No requirement.	
Speech Intelligibility	The degree to which the system must not adversely affect communication capability.	Required	Required	Required	
Spherical Aberration (Diopters)	A form of optical aberration in which focal length varies as a function of object distance from the optical axis. Perceptually, the presence of blur at the edges of the image.	See <i>MTF</i> .	See <i>MTF</i> .	See <i>MTF</i> .	Spherical aberration is assumed to be reflected in the requirement for <i>MTF</i> .
Stability (No Units)	See <i>Drift</i> .	See <i>Drift</i>	See <i>Drift</i>	See <i>Drift</i>	

Table 1-3. Preliminary display requirements for three HMD applications (continued).

Display Parameter	Definition	Aircraft Helmet Mounted Sight (AHMS)	Field Process Control Monitor (FPCM)	Registered Noninvasive Medical Imager (RNMI)	Comments
Symbol Rendering Speed (Degrees per Second)	The speed with which symbology can be rendered on the display in a stroke fashion.	$\geq 279 \text{ deg/s}$	No requirement.	No requirement.	Matrix-addressed displays may display symbology in a stroke-like fashion when generating anti-aliased symbology (e.g., Beamformer). This parameter will determine the upper bound of symbolic information content on the display when symbols are rendered in this way.
Temperature (External) (Degrees)	The maximum temperature of any external (unprotected) surface of the display system.	External surfaces intended to be touched during normal operation should not exceed 35 deg C. External surfaces which may be inadvertently touched during display system operation should not exceed 50 deg C.	External surfaces intended to be touched during normal operation should not exceed 35 deg C. External surfaces which may be inadvertently touched during display system operation should not exceed 50 deg C.	External surfaces intended to be touched during normal operation should not exceed 35 deg C. External surfaces which may be inadvertently touched during display system operation should not exceed 50 deg C.	External surfaces intended to be touched during normal operation should not exceed 35 deg C.
Temperature (Operating) (Degrees)	The range of ambient temperature over which the display is expected to operate normally.	5 to 35 deg C	-15 to 40 deg C	-15 to 27 deg C	
Temperature (Storage) (Degrees)	The range of ambient temperature over which the display is expected to be stored without damage.	-40 to 55 deg C	-40 to 55 deg C	-40 to 55 deg C	
Transparency (See-Through) (Percent)	The transparency of the HMD optics to the forward scene; the percent contribution of luminance from the forward scene, through the display optics, to the luminance of the image.	$\geq 40\%$ Preferred is variable transparency.	0% (no transparency)	$\geq 40\%$ Preferred is variable transparency.	Active control of the forward luminance is likely to provide optimal human performance and will lower the amount of power required of the system to provide adequate contrast.

Table 1-3. Preliminary display requirements for three HMD applications (continued).

Display Parameter	Definition	Aircraft Helmet Mounted Sight (AHMS)	Field Process Control Monitor (FPCM)	Noninvasive Medical Imager (RNMI)	Comments
Transport Delay (milliseconds)	The time it takes an image signal to move from the input of the system to where the signal can be seen by the observer.	≤ 50 milliseconds for high priority crosshair symbol	≤ 100 milliseconds	≤ 100 milliseconds	
Update Rate (Hertz)	The number of times within a one-second interval that changes in the source of the display signal (e.g., sensor, graphic generator) are provided to the display system.	Display update rate should match the display frame rate.	Display update rate should match the display frame rate.	Display update rate should match the display frame rate.	
Video and Graphics Standard (No units)	RS-170 VGA	No video XVGA	HDTV	May require scan conversion.	Standard interface for video and for graphics implies the presence of a scan converter and/or multi-sync capability.
Voltage (Volts)	Electrical potential expressed in Volts. Voltage of components with potential for electrical contact with the body.	≤ 10 volts DC ≤ 9 volts AC	≤ 70 volts DC ≤ 9 volts AC	≤ 70 volts DC ≤ 9 volts AC	
Volume (HMD) (Inches)	The physical dimensions of the display components to be worn on the head.	Consistent with packaging, center of gravity, and weight requirements.	Consistent with packaging, center of gravity, and weight requirements.	Consistent with packaging, center of gravity, and weight requirements.	
Volume (Remote) (Inches)	The physical dimensions of all remote system components (not to be worn on the head).	Consistent with cockpit constraints.	Consistent with individual portability (e.g., belt-mounted).	Consistent with portable track or cart mounting.	
Weight (HMD) (Pounds)	The total weight of the helmet or head mounting and display, including all components to be worn on the head.	≤ 4.5 lbs	≤ 1.5 lbs	≤ 1.0 lbs	
Weight (Remote) (Pounds)	The total weight of all remote system components, excluding any components to be worn on the head.	Consistent with cockpit constraints.	Consistent with individual portability (e.g., belt-mounted).	Consistent with portable track or cart mounting.	
Windblast	The ability of the HMD to withstand windblast forces and remain structurally intact and cause no injury to personnel.	Required up to 600 KEAS	Not required.	Not required.	

Table 1-4. Rationale for preliminary display requirements.

Display Parameter	Rationale for Selected Values
Active Noise Reduction	TBD
Anti-aliasing	AHMS requirement based on likelihood of visible symbol aliasing (and subsequent reduction in image quality) at required resolution. FPCM image quality will benefit from the higher required resolution, and aliasing is less critical for this application. Aliasing is not expected to be a significant problem for RNMI imagery at the required resolution.
Aspect Ratio (Display Image) (Ratio)	Based on requirements for total pixel count and a square color pixel aspect ratio.
Aspect Ratio (Pixel) (Ratio)	Based on Burnette (1976), cited in Decker et. al., (1987), p. 44. Using a 5x7 character matrix on a simulated matrix-addressed display, Burnette (1976) demonstrated superior reading speed, search time, and low reading errors for square, monochrome pixels versus vertically rectangular and horizontally rectangular pixels. A delta-triad arrangement (additive color) with square pixels has also been demonstrated to offer satisfactory image quality.
Astigmatism (Oblique) (Diopters)	Astigmatism contributes to image blur and is reflected in the requirement for MTF. See <i>MTF</i> .
Automatic Brightness Control	Manual control required for all applications to accommodate individual preferences. Automatic control required for AHMS due to transparency and the extreme range in luminance of forward scene and ambient.
Automatic Contrast Control	Manual control required for all applications to accommodate individual preferences. Automatic control required for AHMS due to transparency and the extreme range in luminance of forward scene and ambient.
Centrifuge	AHMS requirement is preliminary Armstrong Laboratory target for HMS+ Program.
Chromatic Aberration (Diopters)	Chromatic aberration contributes to image blur and is reflected in the requirement for MTF. See <i>MTF</i> .
Color Element Failures (Percent total)	Decker et. al., 1987 and Lloyd et. al. 1991 presented performance data that indicate that random monochrome cell failures below 0.5% will not affect search accuracy or speed of reading, regardless of failure polarity. No data are known to exist regarding tolerance to element failures in color displays. However, related Honeywell display programs (i.e., MEDS, B/77) have addressed color element failures. To allow for image quality effects, the maximum allowable element failures for red and green elements was taken to be 50% below the performance criteria from Decker and Lloyd. Cluster tolerances are derived from target values in the MEDS program.

Table 1-4. Rationale for preliminary display requirements (continued).

Display Parameter	Rationale for Selected Values
Color Gamut (Maximum gamut and uniformity) (u' , v')	Primary color coordinates are based on the actual color gamut of the 757/767 cockpit CRTs. The target color gamut for the B777 LCD is more constrained, especially with regards to red, but may represent a more readily obtainable gamut for LCD-based display systems. The uniformity requirement is based on target values from the MEDS program.
Coma (TBD)	Coma contributes to image blur and is reflected in the requirement for MTF. See <i>MTF</i> .
Decompression (Rapid)	AHMS requirement is preliminary Armstrong Laboratory target for HMS+ Program.
Dimming Range (Ratio)	AHMS requirement is based on approximate dimming range of B-777 DU. Preferred dimming range is based on estimated range required to reduce luminance (after optics) of single primary to below 1 fL for night vision. FPCM requirement is based on range required to reduce luminance (after optics) of single optics) of single primary to 1 fL for night vision. RNMI requirement is based on range required to reduce luminance (after optics) of single primary to below 50% of expected forward scene luminance (after optics) to control superimposed image transparency.
Divergence (Degrees)	Stereoscopic viewing is particularly sensitive to vertical disparities existing between left and right images. Vertical disparities are often the result of using a convergent stereo camera geometry, a rotational stereoscopic transformation algorithm, or misaligned display optics. Vertical misregistrations as small as 19 arcminutes may produce immediate eye strain, while diplopia (double images) will occur at 45 arcminutes of divergence. Sensitivity to divergence will increase as a function of time, so lower thresholds should be designed to. For example, divergence thresholds as low as 5 arcminutes have been reported. Furthermore, smaller amounts of divergence may degrade stereoscopic image quality without producing eye strain. Diplopia in stereoscopic displays may be minimized through careful control of factors such as field curvature and distortion.
Distortion (Percent)	Based on typical distortion tolerance allowed in Honeywell optical designs.
Dithering	TBD
Don/Doff Time	AHMS requirement is preliminary Armstrong Laboratory target for HMS+ Program.
Drift (Percent, Hours)	A 20% maximum drift over 24 hours ensures that no parameter may drift out of the required range in less than 5 days. Specification of drift requirements for image registration and divergence ensures control of image position.
Dwell Time (Micro-seconds)	Large dwell times will limit the total number of pixels and the refresh rate.
Electro-magnetic Interference (EMI)	AHMS requirement is preliminary Armstrong Laboratory target for HMS+ Program.
Exit Pupil (mm)	AHMS requirement is preliminary Armstrong Laboratory target for HMS+ Program. A large exit pupil may be required to compensate for helmet instability in flight. Requirements for FPCM and RNMI are based on a need for a larger eye relief (to accommodate eyeglasses) and the assumption that HMD stability in these nonvehicular applications will be relatively high.

Table 1-4. Rationale for preliminary display requirements (continued).

Display Parameter	Rationale for Selected Values
Explosive Atmosphere	AHMS requirement is preliminary Armstrong Laboratory target for HMS+ Program. FPCM requirement is based on likely operation near petrochemical vapors. RNMI requirement is based on hospital standards regarding use of Oxygen.
Eye Relief (mm)	Based on estimate of comfortable eye relief without eyeglasses (AHMS) and with eye glasses (FPCM and RNMI). Eye relief should be minimized within limits of comfort and safety to allow greater exit pupil size.
Field Curvature (Diopters)	Based on typical field curvature tolerance allowed in Honeywell optical designs.
Field of View (Degrees)	AHMS requirement is preliminary Armstrong Laboratory target for HMS+ Program. This FOV matches LANLIRN FLIR FOV in navigational mode. FPCM and RNMI requirements derived by dividing total pixels by resolution. RNMI requirement assumes the use of a subset of the total display FOV for display of a sensor insert, with the balance used for presentation of computer-generated imagery such as alphanumeric information. Generally, FOV of the sensor display should correspond to sensor FOV.
Field Rate (Hertz)	In order to satisfy the minimum requirements for frame rate, time-multiplexed displays (including conventionally-interlaced displays) must use field rates faster than the frame rate by a factor of the number of fields composing each frame. As an example, contemporary field-sequential stereoscopic CRTs incorporating 120 Hz stereoscopic field rates (60 Hz frame rate) have been demonstrated to offer "flicker free" performance. Standard procedures exist (e.g., ANSI/HFS 100-1988) for empirical evaluation of subjective flicker in direct view displays; these procedures may be modified for HMD testing.
Flicker (Subjective)	While flicker has generally not been shown to be associated with specific performance decrements, the presence of flicker is acknowledged to be a distraction and, in general, detracts from overall subjective image quality. Related display design parameters which will influence flicker include frame and field rate, image persistence, FOV, and luminance. Standard procedures exist (e.g., ANSI/HFS 100-1988) for empirical evaluation of subjective flicker in direct view displays; these procedures may be modified for HMD testing.
Frame Rate (Hertz)	AHMS requirement is preliminary Armstrong Laboratory target for HMS+ Program. Generally, a 60 Hz frame rate is sufficiently high to produce a flickerless CRT workstation display (typically 10-20 fL). However, as display luminance and FOV increases, corresponding increases are also seen in the critical flicker frequency. Data from Kelly (Boff and Lincoln, 1988, p. 170) suggests that flicker may be visible in high luminance displays (>100 fL) at frame rates greater than 70 Hz, given a sufficiently wide FOV. Requirement for FPCM is for conformity with anticipated DCS video standard. Requirement for RNMI is estimated minimum for flicker-free display.
Gray Scale (Shades of gray per color primary) (Total)	AHMS requirement is preliminary Armstrong Laboratory target for HMS+ Program. FPCM requirement is based on Honeywell human performance data (Reinhart, 1992; Silverstein et. al., 1989) and experience with the B-777 program. RNMI requirement is based on estimate of gray scale resolution required for interpretation of diagnostic medical imagery (excluding X-ray). Experience both at Honeywell and elsewhere suggests that gray scale requirements are highly sensitive to resolution, luminance contrast, application algorithm, and figure of merit. The use of a power function to distribute gray scale may modify this requirement.

Table 1-4. Rationale for preliminary display requirements (continued).

Display Parameter	Rationale for Selected Values
Gray Scale (Distribution of Luminance)	Minimum requirement is to insure smoothly varied gray scale. Alternate is a distribution in the form of a power function, because is well known that the perceptual dimension of brightness is not linearly related to luminance (e.g., brightness = luminance ^a , where $0 < a < 1$). Although values recommended for the exponent in this Stevens' power function of luminance (e.g., Carter, 1993), values of 0.3 to 0.5 appear to be typical. Although a factor of the square root of 2 is a frequently used guideline for separation of gray scale levels (e.g., Rash et al., 1990; Farrell and Booth, 1984), this factor tends to exaggerate separation of gray scale levels at all but the lowest levels. A power function of the general form $\Delta L = L^{1/3}$, where ΔL is the minimum change in luminance from the gray scale step with luminance L , provides a more perceptually even distribution of luminance. In either case, it should be noted that the visual threshold to gray scale changes (as measured in controlled laboratory conditions) is likely to be smaller than is suggested by the separation given by these functions. The consequence of the nonlinearity of the luminance-brightness relationship is that linearly spaced gray steps on a display are perceptually inefficient, with gray steps at the high end of the luminance range appearing to be very fine and gray steps at the low end of the luminance range appearing to be very coarse.
Haloing (Priority Masking)	TBD
Hanging Harness	AHMS requirement based on preliminary Armstrong Laboratory target for HMS+ Program.
Head Tracking	AHMS requirement based on assumed requirement for head-slaved weapons and sensor cueing. RNMI requirement based on need for registration of imagery with patient's body.
Humidity (Operating) (RH)	Based on estimates of ambient humidity range during normal operation, indoor and/or outdoor as appropriate per application.
Humidity (Storage) (RH)	Based on estimates of ambient humidity range during storage, indoor and/or outdoor as appropriate per application.
Image Distance (cm)	Collimation to infinity is necessary for AHMS to allow registration of targeting imagery on the forward scene. For FPCM and RNMI, accommodation distances as close as 30 cm would be minimally tolerable for comfortable accommodation (ANSI (HFS 100-1988)). User adjustability is required for FPCM to allow for individual differences in comfortable focus distance. Image distance should be tied to a head tracker for the medical HMD to allow automatic registration of the image with the patient's body.
Image Enhancement	AHMS requirement based on preliminary Armstrong Laboratory target for HMS+ Program.
Image Masking and Priority Assignment	Based on assumed need for visual preservation of application-critical elements of the display (e.g., attitude indication for AHMS). A priority overlay symbology such as haloing is required for the two applications calling for transparency (AHMS and RNMI) to preserve the visibility of overlay symbology with respect to the forward scene.

Table 1-4. Rationale for preliminary display requirements (continued).

Display Parameter	Rationale for Selected Values
Image Persistence (Milli-seconds)	To avoid smearing of images, no visual evidence of a display image should remain on the display longer than one frame cycle after the image has been commanded to be removed or the display is no longer being addressed. Image persistence should be based on field rate for time-multiplexed color displays to minimize crosstalk. Selection of minimum persistence should allow compliance with display luminance, display flicker, and crosstalk requirements.
Image Retention (No. Units)	Retained images can reduce display contrast and introduce visual artifacts in images currently displayed.
Impact/Penetration	AHMS requirement is preliminary Armstrong Laboratory target for HMS+ Program.
Interconnect (No. units)	Preliminary Armstrong Laboratory target for HMS+ Program. Flexible, light-weight cabling is needed for head mobility and reduced head-supported weight for all three applications. Quick disconnect for AHMS is needed for selection compatibility.
Interlacing (Ratio)	AHMS requirement is preliminary Armstrong Laboratory target for HMS+ Program. Noninterlaced (1:1) FPCM and RNMI displays are desirable to avoid trading off flicker for resolution.
Jitter (Degrees/Second)	Requirement is derived from the maximum ANSI (HFS 100-1988) jitter for workstation displays.
Line Failures (Percent)	Decker et. al., 1987 and Lloyd et. al. 1991 presented performance data that indicate random monochrome line failures below 0.5% will not affect search accuracy or speed of reading, regardless of failure polarity. No data are known to exist regarding tolerance to line failures in color displays. However, line failures are likely to degrade subjective image quality and may lead to inadvertent errors in displayed color. A randomly occurring line failure could also interfere with display legibility if it is coincident with small characters or symbols. Related Honeywell display programs (i.e., MEDS, B777) have target values of zero line failures for these reasons.
Luminance (Foot Lambert (fL))	AHMS image source luminance is preliminary Armstrong Laboratory target for HMS+ Program. Luminance combined is based on requirements for <i>Luminance Contrast</i> for AHMS and RNMI. Luminance for FPCM is based on expected adaptation range of nondisplay eye, which is likely to include outdoor use in daylight. Luminance requirement for AHMS is in approximate agreement Sauerborn's (1992) estimate of approximately 6,000 fL required for daylight visibility of a monochrome HMD, the differences largely attributable to differing assumptions in optical transmittance.
Luminance Asymmetry (Percent)	Honeywell laboratory investigations have been conducted to determine the effects of binocular HMD asymmetries on helicopter pilot performance (e.g., Lipper, 1990). Luminance imbalances as small as 15% will be detectable by pilots.

Table 1-4. Rationale for preliminary display requirements (continued).

Display Parameter	Rationale for Selected Values
Luminance Contrast (Contrast Ratio)	<p>Although there appears to be little performance benefit associated with high image source contrast ratios ($>3:5:1$) for binary workstation displays, a higher luminance contrast will be required in order to achieve meaningful separation of gray scale levels, especially for transparent HMDs. Post et al. (1994) describe an equation for predicting HMD luminance contrast: $C = (T_d L_{\max} + L_s T_c T_s)/(T_d L_{\min} + L_s T_c T_s)$, where C is the predicted HMD contrast ratio, T_d and T_s are the transmittance of the HMD optics for the display and forward scene, respectively, T_c is the transmittance of the aircraft canopy, L_s is the luminance of the forward scene, and L_{\min} and L_{\max} represent the luminance range of the display. Post et al. assume the following constants: $T_d = 0.75$, $T_s = 0.40$, $T_c = 0.625$ (F-16 canopy), and $L_s(\max) = 10,000 \text{ fL}$. The Armstrong Laboratory (AL) baseline luminance requirement for HMS+ is $L_{\max} = 15,000 \text{ fL}$, and L_{\min} can be derived to be 150 fL (from the image source luminance contrast requirement of 100:1). The AL baseline color requirement for HMS+ calls for equal primary luminances (red = $7,500 \text{ fL}$, green = $7,500 \text{ fL}$) and for primaries to be used separately (no use of yellow). Therefore, the effective L_{\max} should be reduced to $7,500 \text{ fL}$. Using the equation above, it can be seen that the maximum value of C will be 50:1 assuming night flight ($L_s = 0$). The minimum value of C (assuming $L_s = 10,000 \text{ fL}$) will be 3:1. It is important to note from these calculations that display grayscale will be unusable during worst case daylight flight. For the FPCM, the term of $L_s T_c T_s$ can be dropped from the above equation, since the HMD is not transparent and no canopy or windscreen exists. Consequently, T_d may also be removed as a factor in determining opaque luminance contrast. Not accounting for stray ambient light incident on the display, the FPCM luminance contrast is therefore equivalent to L_{\max}/L_{\min}.</p> <p>For the RNMI requirement, $L_s(\max)$ is assumed to be 10 fL (well-controlled dim indoor lighting). Transparency does apply, so all terms from the above equation must be retained. The luminance requirement for RNMI is $L_{\max} = 1,400 \text{ fL}$, and L_{\min} can be derived to be 14 fL (from the image source luminance contrast requirement of 100:1). Furthermore, the baseline color requirement for RNMI calls for equal primary luminances (red = 700 fL, green = 700 fL) and for primaries to be used separately (no use of yellow). Therefore, the effective L_{\max} should be reduced to 700 fL.</p> <p>Using the equation above, it can be seen that the anticipated value of C is 40:1.</p>
Luminance Half-Life (Hours)	Based on estimate of tolerance to interruptions for servicing the display. For comparison, a typical LCD cold cathode fluorescent backlight has a luminance half-life of approximately 10,000 hours.
Luminance Non-uniformity (Percent)	Maximum ANSI (HFS 100-1988) large and small area luminance variations for workstation displays are 50%. However, more conservative values were derived from the transmittance uniformity target in the MEDS program (20% and 10%).
Mean Time Between Failures (MTBF) (Hours)	Based on estimate of application criticality.
Modulation Transfer Factor (at display resolution) (MTF)	This general expression of optical quality is assumed to encompass optical aberrations such as coma, spherical aberration, chromatic aberration, and astigmatism. A modulation transfer factor of 0.3 at the limiting resolution of the display has been used by Honeywell to represent the threshold ability of observers to see luminance modulation. In theory, however, a more complete characterization of usable display modulation is obtained by comparing a complete modulation transfer function with an observer contrast threshold function.

Table 1-4. Rationale for preliminary display requirements (continued).

Display Parameter	Rationale for Selected Values
Packaging (No Units)	AHMS requirement based on preliminary Armstrong Laboratory target for HMS+ Program. Process control and medical HMD requirements based on concepts discussions with commercial display vendors from industrial and medical sectors.
Parachute Deployment	AHMS requirement based on preliminary Armstrong Laboratory target for HMS+ Program.
Personal Equipment Compatibility	AHMS requirement based on preliminary Armstrong Laboratory target for HMS+ Program.
Pixel Count (Total)	AHMS requirement based on preliminary Armstrong Laboratory target for HMS+ Program. AHMS requirement to display LAN/TIRN FLIR (RS-170 interface) indicates a 640 x 480 format. FPCM requirement reflects anticipated trends in DCS display formats (commonality is required). RNMI requirement assumes panoramic HD/TV format will allow central display of high resolution images, with side displays of computer-generated imagery (aphanumeric, data graphs, etc.).
Power (HMD) (Watts)	AHMS requirement is preliminary Armstrong Laboratory target for HMS+ Program. Low voltage requirement based on safety for head mounting.
Refresh Rate (Hertz)	See <i>Field Rate and Frame Rate</i> .
Registration Accuracy (Degrees)	AHMS requirement based on the approximate display accuracy achievable in precision-mounted HMDs (e.g., Wood, 1991, p. 349). Other sources of registration error include sensor, canopy, and installation. Wells and Haas (1992) estimate the canopy-induced deviation in the F-16 could be as great as 0.4 deg. No registration is required for the FPCM. The RNMI requirement assumes that the imagery will be used for noninvasive diagnostic procedures rather than surgical interventions. Consequently, using manual controls to remove visible misregistration should provide sufficient registration accuracy.
Registration Control	AHMS and RNMI requirement based on the assumption that drift may occur in registration accuracy, and that initial and periodic calibration will be required.
Resolution (Pixels /Degree)	AHMS requirement calculated by dividing total pixels by FOV. FPCM requirement derived from Honeywell display simulations [32 linear gray scale levels, stereoscopic viewing, subtractive color, 40 fL max white, 40:1 CR, and 70% aperture ratio] which demonstrated excellent image quality for video images at as low as 32 pixels/degree. RNMI requirement assumes higher resolution will be required for interpretation of diagnostic medical imagery (MRI, CAT, ultrasound). Note that for additive color displays, the number of rows or columns of color elements must be converted to pixels to obtain resolution approximately equivalent to subtractive color displays. This conversion is required because in the full-color case, three color elements are required to represent each additive color pixel, whereas in the subtractive color case, each color element is equivalent to a pixel. For example, for a delta triad arrangement of three color primaries, the number of rows and columns of color elements may be multiplied by $1/\sqrt{3}$ (approximately 0.577) to estimate an equivalent number of subtractive color pixels. The equivalent image quality of additive and subtractive color displays with equal resolutions calculated in this fashion is only estimated and should be tested. Note also that aperture ratio will have a significant impact on required resolution due to the effect of aperture ratio on the visibility of row and column spacing in the image.
Smearing (Subjective)	Smearing degrades image quality and the effective display system MTF for moving objects. Smearing can be a significant problem with LCDs, especially at low temperatures.
Sound Attenuation	AHMS requirement based on preliminary Armstrong Laboratory target for HMS+ Program.

Table 1-4. Rationale for preliminary display requirements (continued).

Display Parameter	Rationale for Selected Values
Speech Intelligibility	AHMS requirement based on preliminary Armstrong Laboratory target for HMS+ Program.
Spherical Aberration (Diopters)	Spherical aberration contributes to image blur and is reflected in the requirement for MTF. See <i>MTF</i> .
Stability (No Units)	See <i>Drift</i> .
Symbol Rendering Speed (Degrees per Second)	AHMS requirement based on stroke writing speed for Head Guidance System HUD symbology. Matrix-addressed displays may display symbology in a stroke-like fashion when generating anti-aliased symbology (e.g., Transformer). The speed with which symbology can be rendered on the display will determine the upper bound of symbolic information content on the display.
Temperature (External) (Degrees)	Based on recommendations for maximum external display unit temperatures found in ANSI/HFSS 100-1988.
Temperature (Operating) (Degrees)	Based on estimate of ambient temperature range during normal operation.
Temperature (Storage) (Degrees)	Based on estimate of ambient temperature range during storage and transportation.
Transparency (See-Through) (Percent)	AHMS and RNMI requirement based on typical HMD transparency to forward scene. Although it might be assumed that the highest possible transparency is desired, high transparencies will drive up image source luminance requirements for daylight use in order to achieve desired luminance contrast. Ideally, a variable transparency should be used for active contrast enhancement. No transparency is required (or desired) for the FPCM, although a related application of this display concept could include transparency for visual overlay of sensor data on process hardware.
Transport Delay (milli-seconds)	TBD
Update Rate (Hertz)	The effects of mismatches between update rate and refresh rate on moving objects will depend on the velocity and duration of movement (Lindholm, 1992). For very short durations and steady eye fixations, jerky movement will be seen. For longer durations and smooth pursuit eye movement, images will appear blurred and have reduced contrast, the magnitude depending on the extent of the mismatch. A similar but separate perceptual phenomenon is <i>smearing</i> .
Video and Graphics Standard (No units)	AHMS requirement based on preliminary Armstrong Laboratory target for HMS+ Program. Based on compatibility with LANTIRN FLIR, RNMI may require scan conversion to allow a wide variety of sensor sources.

Table 1-4. Rationale for preliminary display requirements (continued).

Display Parameter	Rationale for Selected Values
Voltage (Volts)	Armstrong Laboratory target for HMS+ Program is for low voltage relative to CRTs. Required values are based on 50% of maximum nonfatal voltages given in Hammer (1989).
Volume (HMD) (Inches)	No special volume constraints exist; provide the display system volume is consistent with packaging, center of gravity, and weight requirements.
Volume (Remote) (Inches)	AHMS and RNMI requirements have latitude for variation without directly impacting usability. FPCM requirements require further study.
Windblast	AHMS requirement based on preliminary Armstrong Laboratory target for HMS+ Program.
Weight (HMD) (Pounds)	Requirement for AHMS is derived from Perry and Green's data presented at HMS+ Program industry briefing. Value is upper limit of estimated ejection-safe weight. The same value is suggested by Wells and Haas (1992). By comparison, the U.S. Army (Honeywell) Integrated Helmet and Display Sighting System (IHADSS) has a head-supported weight of 4.0 pounds Rash et al., 1990). Requirements for FPCM and RNMI are estimates of maximum comfortable weight, allowing a higher weight budget for FPCM (hard hat).
Weight (Remote) (Pounds)	AHMS and RNMI requirements have latitude for variation without directly impacting usability. FPCM requirements require further study.

2 SYSTEM CONFIGURATION CONCEPTS

In this section, we present system configuration concepts for the Armstrong Laboratory (AL) HMS+ Program, an HMD program which is representative of the next-generation aircraft helmet mounted sight. Table 2-1 (p. 47) recaps the major preliminary requirements for HMS+. The preliminary development schedule for HMS+ calls for delivery in October, 1997 and initial flight safety tests in January, 1998. The baseline system cost is unspecified, although low cost is a program objective.

The display concepts presented in this section include image source options, major two-primary color approaches, gray scale approaches, and additional system considerations for the HMS+. These concepts form the basis of the subsequent program tasks of test cell fabrication and evaluation, display analysis, and simulation development and evaluation.

Table 2-1. Major preliminary requirements for HMS+.

Parameter	Preliminary Requirement	Rationale/Comment
Color	Red and green primaries, no yellow required.	Preliminary AL target for HMS+ Program.
Dimming Range (Ratio)	$\geq 2000:1$ Preferred is 6000:1 No loss of grayscale steps throughout dimming range.	Minimum requirement based on approximate dimming range of B-777 DU. Preferred dimming range is based on estimated range required to reduce luminance (after optics) of single primary to below 1 fL for night vision.
Eye Relief	≥ 25 mm	Based on estimate of comfortable eye relief without eyeglasses. Eye relief should be minimized within limits of comfort and safety to allow greater exit pupil size. Preliminary AL target for HMS+ Program. A large exit pupil may be required to compensate for helmet instability in flight.
Exit Pupil	≥ 17 mm	Preliminary AL target for HMS+ Program. This FOV matches LANTRN FLIR FOV in navigational mode.
Field of View	Monocular: 28 deg (horizontal) \times 21 deg (vertical)	Preliminary AL target for HMS+ Program. Flicker may still be visible in high luminance displays (>100 fL) at frame rates greater than 70 Hz, given a sufficiently wide FOV.
Frame Rate	60 Hz, 90 Hz preferred.	Preliminary AL target for HMS+ Program. Based on need to display FLIR images. The use of a power function to distribute gray scale, for example, may lead to more economical use of gray scale and may allow fewer discrete steps. Alternatively, an analog approach should be considered.
Gray Shades	≥ 64 linearly distributed shades of gray per color channel, where the first luminance step is equal to the background luminance. No grayscale loss over full dimming range.	Collimation to infinity is necessary to allow registration of targeting imagery on the forward scene.
Image Distance	Collimated to infinity.	Preliminary AL target for HMS+ Program. Flexible, light weight cabling is needed for head mobility and reduced head-supported weight. Quick disconnect is needed for ejection compatibility.
Interconnect	$\leq 5/16$ inch (OD) cable; flexible, light weight cable; quick disconnect.	Preliminary AL target for HMS+ Program. A noninterlaced (1:1) display is desirable to avoid aliasing effects associated with sampling the 2:1 interlaced FLIR.
Interlacing	1:1 (no interlacing)	Preliminary AL target for HMS+ Program. Based on equation for predicting HMD luminance contrast found in Post et al. (in press). Requirement for AHMS is in approximate agreement Sauerborn's (1992) estimate of approximately 6,000 fL required for daylight visibility of a monochrome HMD, the differences largely attributable to differing assumptions in optical transmittance.
Luminance	$\geq 7,500$ fL red, $\geq 7,500$ fL green at the image source, 5,625 fL to 8,125 fL each after display optics (including combined light).	Based on equation for predicting HMD luminance contrast found in Post et al. (in press) and assumptions regarding forward scene luminance and optical transmittance found in the same paper.
Luminance Contrast	$\geq 100:1$ at the image source; 3:1 to 50:1 combined.	This general expression of optical quality is assumed to encompass optical aberrations such as coma, spherical aberration, chromatic aberration, and astigmatism. A modulation transfer factor of 0.3 at the limiting resolution of the display has been used at Honeywell to represent the threshold ability of observers to see luminance modulation.
MTF	≥ 0.3 at the display resolution.	Preliminary AL target for HMS+ Program.
Packaging	HGU-55/P helmet (Large) preferred.	Preliminary AL target for HMS+ Program. Requirement to display LANTRN FLIR (RS-170 interface) indicates a 640 \times 480 format.
Pixel Count	640 (horizontal) \times 480 (vertical)	

Table 2-1. Major preliminary requirements for HMS+ (continued).

Parameter	Preliminary Requirement	Rationale/Comment
Power (HMD)	≤ 100 Watts, low voltage	Preliminary AL target for HMS+ Program. Low voltage requirement based on safety for head mounting.
Video and Graphics Standard	RS-170 VGA	Preliminary AL target for HMS+ Program. Based on compatibility with LAN/TIRN FLIR.
Voltage (volts)	≤ 70 volts DC ≤ 9 volts AC	AL target for HMS+ Program is for low voltage relative to CRTs. Required values are based on 50% of maximum nonfatal voltages given in Hammer (1989).
Weight (total helmet)	≤ 4.5 lbs	Preliminary AL target for HMS+ Program. Derived from Perry and Buhman data presented at HMS+ Program industry briefing. Value is upper limit of estimated ejection-safe weight. The same value is suggested by Wells and Haas (1992). Weight of IHADSS is 4.0 lbs (Rash et al., 1990).

2.1 Major Image Source Options for HMS+

General image source technologies for the HMS+ are reviewed in Table 2-2 (p. 50). The approaches are reviewed with respect to their ability to meet the preliminary display requirements as well as demonstrated and reasonable anticipated development of the technology within the required time frame. Insufficient luminance limits the suitability of most emissive display technologies, suggesting a light valve approach. Active contrast enhancement approaches may eventually reduce the display luminance requirements for daylight see-through display applications, but the enabling technologies for active contrast enhancement have not yet been sufficiently demonstrated.

A color projection approach using two side-by-side image sources is possible using either a DMD or TN AMLCD, but this approach may be too bulky. The best match with program requirements appears to be a TN AMLCD light valve, used in either a spatially integrated additive color or subtractive color mode. The additive mode offers the simplicity of a single image source, while the subtractive color mode offers the advantage that each color element is capable of displaying the full color gamut of the display. The likely color approaches for these image source options are reviewed in the text following Table 2-2.

Table 2-2. Compatibility of image source technologies with respect to HMS+ preliminary requirements.

Technology	Compatible	Rationale (primary)
Additive color emissive		
CRT	No	Insufficient luminance
Electroluminescent	No	Insufficient luminance
Field Emission Display	No	Insufficient luminance
Laser (scanned)	No	Scanner volume, laser availability.
Light emitting diode (scanned array)	No	Insufficient luminance
Light emitting diode (2-D array)	No	Thermal considerations, development risk
Plasma	No	Insufficient luminance
Vacuum Fluorescent	No	Insufficient luminance
Additive color light valves		
Digital Micromirror Device	Fair	Uncertainty regarding size and weight in required configuration. Although it may be possible to use side-by-side or a split array for two-color projection, it may be difficult to meet FOV and exit pupil requirements without an unacceptably bulky system.
TN AMLCD light valve, combined additive color	Fair	Uncertainty regarding size and weight in required configuration. Although it may be possible to use side-by-side or a split array for two-color projection, it may be difficult to meet FOV and exit pupil requirements without an unacceptably bulky system.
TN AMLCD light valve, two-color mosaic filter	Good	High efficiency system possible.
Other light valve technologies	No	Includes numerous other LCD modes, PLZT, and others. Generally lower performance and higher risk than TN AMLCD.
Time sequential color light valve systems (e.g. DMD)	No	Risk of temporal artifacts with current technology limitations.
Subtractive color light valves		
TN AMLCD light valve, subtractive color	Good	High efficiency system possible. Potentially most compact approach, resolution advantage.
Other subtractive light valve technologies	No	Generally lower performance and higher risk than TN AMLCD.

2.2 Major Color Approaches for HMS+

2.2.1 One Image Source, Spatial Additive

The use of a single image source in a spatial additive fashion is the most common approach used to achieve multiple colors in electronic displays. The area of the image source is divided into color elements corresponding to the primary colors of the display. Red and green are the most common and likely color primaries to use, as was discussed in the previous section. The color elements are formed using either color filters, phosphors, or a combination of the two, and may be formed with different shapes (square, rectangular) and different groupings (diagonal, vertical, or horizontal stripes). A two-primary display yields either red or green at the color elements, and red, green, or yellow/orange pixels (the combination of red and green primaries will yield a color somewhere between yellow and orange, depending on the relative luminance mix and the chromaticities of the red and green primaries). In addition, black will be available when no light is transmitted. A square pixel (rectangular color element) is likely indicated for a two-primary additive color display.

2.2.2 Two Image Sources, Spatial Subtractive

By stacking two image sources with cyan and magenta polarizers, a subtractive color display can be fabricated with twice the number of pixels per active area of a comparable display using the spatial additive approach. The red-green version of the two-primary subtractive display requires removing blue from the backlight, because no means exists to modulate blue in this design. The first image source and polarizer pass red light and selectively pass green light, while the second image source and polarizer are used to modulate red light. Because the blue will have been eliminated at the light source, green and red polarizers could also be substituted for the cyan and magenta polarizers. (Red polarizers are believed to be available which yield superior performance to magenta polarizers, but green polarizer availability and performance is limited). Red, green, yellow, and black are available at each color element location. Although two (stacked) image sources are required to achieve a color gamut comparable to the spatial additive approach, for a fixed number of pixels the color elements may be larger.

2.3 Gray Scale Approaches

2.3.1 Low-Power Analog Gray Scale

It has long been recognized by the aerospace flat panel displays industry that a precision gray scale driver is needed. The precision driver should be capable of providing high quality graphics as well as displaying the continuous range of grays needed for showing high quality video. Below are two excellent candidates for meeting these objectives and those of the Two-Primary Color program. Both are integrated driver technologies that make the drive electronics extremely small. Both are analog drive methods that provide as much gray scale drive flexibility as needed. One, that from Kopin, is based on a crystalline silicon technology whose characteristics over temperature are excellent. The other, that from Sony, is based on a polycrystalline silicon technology. Newer and somewhat riskier over temperature, it has the advantage that it is embodied in a low power drive configuration. Which of the two is preferred for a given application or a range of applications will depend on more detailed performance and cost requirements. Both indicate a drive system of trivial cost (dollars, size and weight) and excellent performance is available to the two-primary color derivative products.

2.3.2 Kopin Integrated Analog Drive

The Kopin 640 x 480 monochrome AMLCD display with integrated analog drivers was measured in terms of power dissipation and general image quality. Power has been a long-standing obstacle for successful implementation of analog drive. What we measured is that approximately 500 μ w of power are dissipated by each of the 640 column drivers across the panel. This brings the total for each panel to 320 mw. Power as a function of image content (amount of darks, grays and brights) was also evaluated. Image gray scale content was found to be a negligible contributor, that is, the power remained constant regardless of what was shown.

The total power of the column drive used in a two panel two-primary color display will be in the neighborhood of about a half a watt (0.64 W), assuming a Kopin 640 x 480 display is used. This low amount of power plus the fact that the driver is analog means two-primary color implementation is feasible.

To measure image quality, a difficult but representative image was selected. An EFIS image was displayed on the panel. An EFIS image tends to be more challenging than many video images because of the high contrast and the need for excellent background uniformity. The resultant image quality, informally evaluated, appeared to be acceptable though formal acceptance/rejection criteria remain to be established.

The significance of these two data points was that the driver technology as it exists in the Kopin Smart Slide product appears to be adequate for the two-primary color implementations envisioned now.

2.3.3 Sony Integrated Analog Drive

The suitability of the Sony 1068 x 480 AMLC display for the target applications was measured in terms of image quality and power dissipation. The Sony display includes ITO electrodes and a representative aperture (40% - same as Kopin units).

The gray scale drive was found to be analog and suitable for displaying video as well as symbology. The image was of high quality showing no evidence of iso-contrast contouring and no observable noise.

In testing the power dissipation, one display was measured under three conditions, black, 50 % full white (checkerboard) and white. The average power dissipation under these conditions was found to be 133.9 mw. This compares favorably with the 320-mw figure of the lower resolution Kopin Smart Slide tested. On a per column basis the Sony power dissipation is more efficient. The Sony design dissipates only 125 μ w/column versus the Kopin 500 μ w/column, which is about four times more efficient.

At a resolution of 640 columns, the Sony design would dissipate only about 80 mw per panel and 161 mw for the column drive of a two panel two-primary color display system. This means the Sony design uses 480 mw less power than the Kopin design, which has the advantage of reducing the amount of heat dissipated at the user's head.

For a 1068 column system the Kopin design, if not changed, would dissipate 1.068 W for a two-panel system. In this case the Sony design would dissipate only about one-fourth the power and would eliminate 800 mw from the vicinity of the head. This may be substantial.

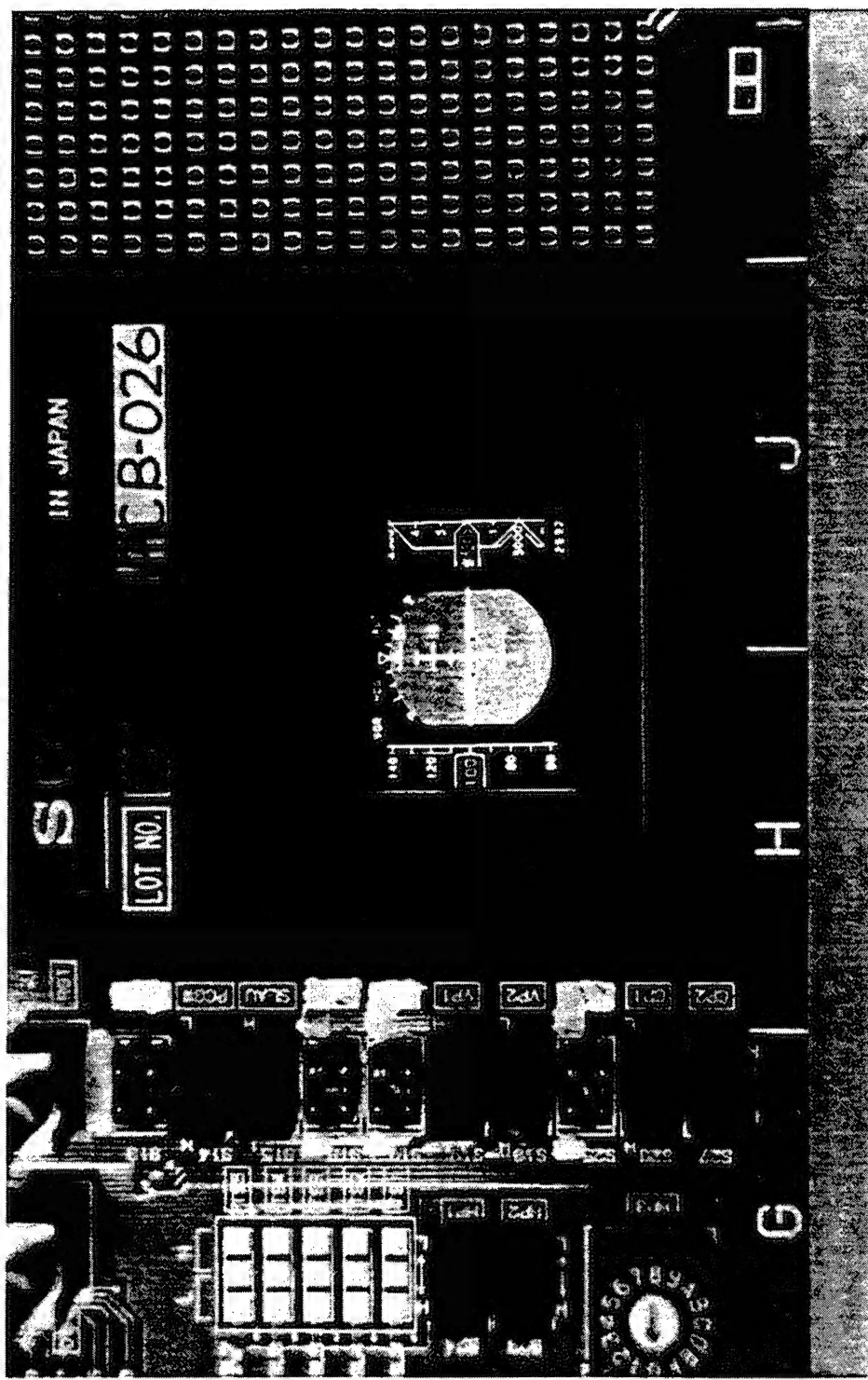


Figure 2-1. Sony Display Panel with 1.3 in. x 1.0 in. Active Display Area.

Comparison: Sony – Kopin Power Dissipation

Table 2-3 below summarizes the power dissipation differences between the two analog integrated driver designs tested. The first column shows the number of horizontal pixels of each flat panel under test. The second column shows the power measured for the entire panel and the third shows the power at each column driver output. This is the total divided by the number of horizontal pixels. The next two columns under the heading Monocular Two-Primary Color Display show the power that would be dissipated by each of the designs if they were configured for the same horizontal pixel count, 640 in one case and 1280 in the other. Two panels are assumed to be used in the monocular configuration. These values are doubled in the binocular two-primary display. The Sony flat panel analog gray scale implementation would save about 1.9 W in a 1280 pixel wide binocular two primary color display.

Table 2-3. Power dissipation differences.

Integrated Analog Column Drivers						
Number of Columns	per Panel	per Column	per Monocular Two-Primary Color Display		per Binocular Two-Primary Color Display	
			640 wide	1280 wide	640 wide	1280 wide
Kopin	640	320	0.50	640	1280	2560
Sony	1068	134	0.125	161	321	642

Either of the two display types, Kopin or Sony, is suitable for two-primary color and derivative applications from a power and analog gray scale perspective. The data above indicate the Sony has positive benefits with respect to power. These benefits become more attractive as the application migrates toward higher resolution and binocular requirements.

2.4 Additional System Considerations

2.4.1 Electronic Interface - Image Data Source to Two-Primary Color Display



Figure 2-2. Block diagram of overall system

Figure 2-2 above illustrates the signal stream from the image source to two-primary color display system. The job of the interface circuitry is to convert the image signals from the image source into a form compatible with the specific requirements of the two-primary color display. An additional function of the interface unit is to supply power to the two-primary color display.

The interface function can be divided into two parts: 1) the remote interface which may be mounted nearby the data image sources and in a remote cabinet or bay; and 2) the local interface which is mounted at the site of the two-primary color application. The remote interface is typically not constrained as significantly in size, weight and power as the local interface unit, which in some applications may be battery powered and need to be extremely small and light weight.

Remote Interface Unit

The power of the a typical remote interface is estimated to be in the range of 10 to 20 W. The size is expected to be in the $3 \times 6 \times 8$ inch range. Only one card comprising analog and digital circuitry is expected to be required, based on prior designs used to drive 640×480 flat panel

displays. In addition to this card, a commercial off-the-shelf power supply and power signal conditioner may be required. The signal conditioner may be a re-implementation of that which Honeywell used to drive the Kopin 640 x 480 flat panel displays.

Local Interface Unit

The local interface unit will need to be optimized for small size, low power and light weight. Something in the range of 2 W or less is desired and feasible, provided careful partitioning of remote and local functions is accomplished. It is likely that micro-electronic technologies will be mandatory. Additionally, customization of the link from the remote to the local interface will need to be done but with little to no sacrifice of generality. The local unit should be capable of displaying video and graphics, either separately or simultaneously. Graphics overlay and image merging may best be done at the site of the remote interface unit, though the requirements specific to any given application would need to be considered. The design philosophy of minimizing the electronic content in the local interface unit but without sacrificing generality, a philosophy which may not reflect today's known requirements, is expected to lead to a broader user base and thus to lower cost.

The Output of the Image Source can span the range of signal types from custom protocol for showing symbolic formats to VGA and SVGA formats to RS-170 standard TV formats and higher resolution video formats seen in workstation (1280 x 1024) and HDTV formats. The images can be symbolic to pictorial and combinations in between. Combinations require image merging functionality. Image merging would typically be handled by the remote interface unit.

What is detailed below is at the high end of standard video formats. It is an RS-343 compatible signal that results in an active imaging area of 1280 x 1024 pixels, suitable for high quality video images and graphics or symbolic images. The two-primary color interface units, in combination, must accommodate this signal or a signal like it. Presumably, as was stated above, the best location for interfacing with this standard set of signals is at the Remote Interface Unit. It can handle a wider variety of input standards and video overlay requirements.

Figure 2-3 shows a full frame of the 1280 x 1024 video. The frame lasts approximately 16.66 msec as can be seen by examining the spacing between the rising edges of the two vertical sync pulses. Note that the sampling frequency used to obtain Figure 2-3 introduced some artifacts, including the attenuation of the full depth of the horizontal sync pulses.

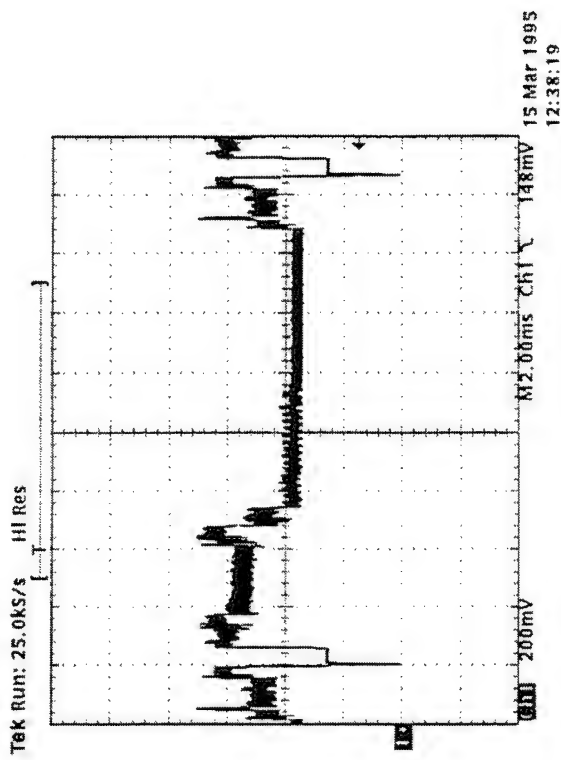


Figure 2-3. Full Frame of 1280 x 1024 video

Figure 2-4 zooms in on the vertical blank period. It shows that the top of the image shown on a display screen occurs 35 horizontal sync pulses after the rising edge of the vertical sync pulse. This implies a strict timing alignment on the interface circuitry. It must ensure that the first row of active video sampled from the image data source corresponds with the first row to be shown on each of the three flat panels.

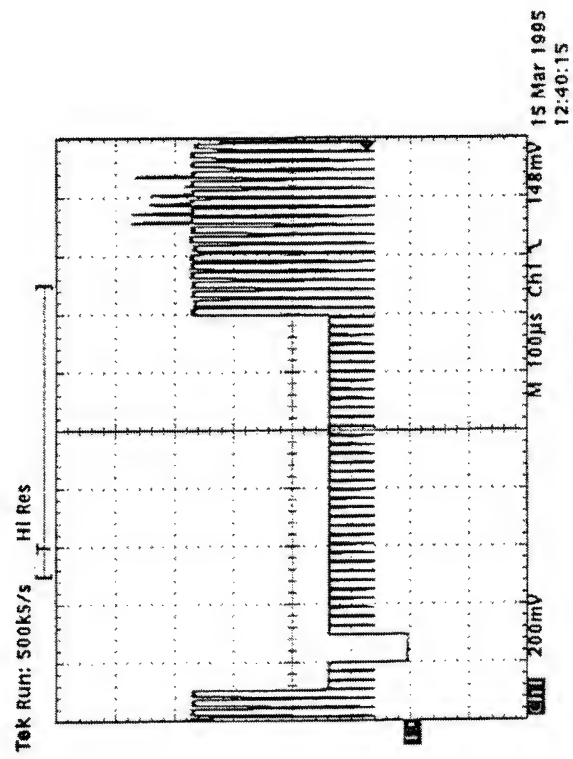


Figure 2-4. Magnification about the vertical blank period.

Figure 2-5 details the horizontal period in the high resolution 1280×1024 video signal. The active period and the blanking period are shown. In a manner similar to that required to vertically align the picture, the interface must time the sampling and readout of the video to the flat panel displays in such a manner that the video registers with the left and the right edges of each flat panel display.

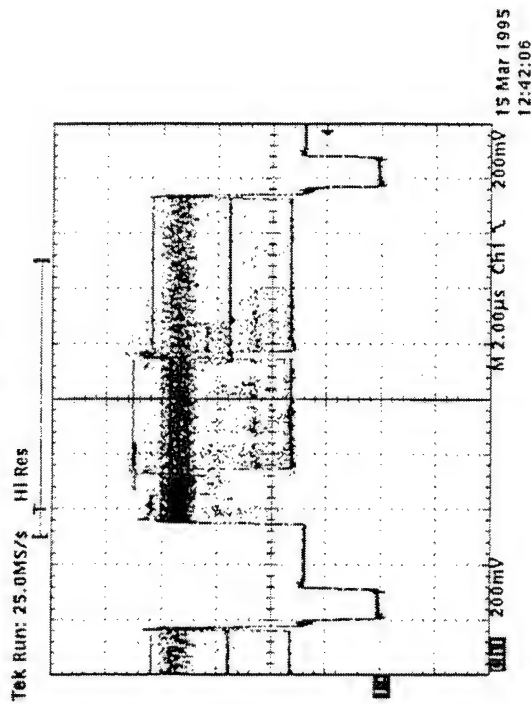


Figure 2-5. Horizontal line from the 1280 x 1024 image data source

Figure 2-6 details the start of the left edge and the right edges of the image with respect to the horizontal sync pulse. The timing shown was taken from an 1280 X 1024 image data source Crimson Elan located at the Honeywell facility. The timing from various models of 1280 x 1024 image sources may be sufficiently stable and precise and may imply further that a phase lock loop may not be necessary in the Interface Units to ensure that the left- right and top-bottom edges of the video match up well with the flat panel displays embedded in the two-primary color application. If this is the case, the interface system can be timed as a precise and, for the most part, open loop system, not requiring an extensive amount of feedback. In practice, we recommend that some small amount of feedback is inserted to ensure that signals are sampled properly. As will be discussed in greater detail below, the Interface can circumvent the need for much higher sampling frequencies because the phasing of the video information may be known a priori. In the cases measured, the left edge of the video begins 2.32 usec after the rising edge of the horizontal sync pulse. The right edge of the screen begins 160 nsec before the falling edge of the horizontal sync pulse which also corresponds with 1.32 usec before the rising edge of the same sync pulse.

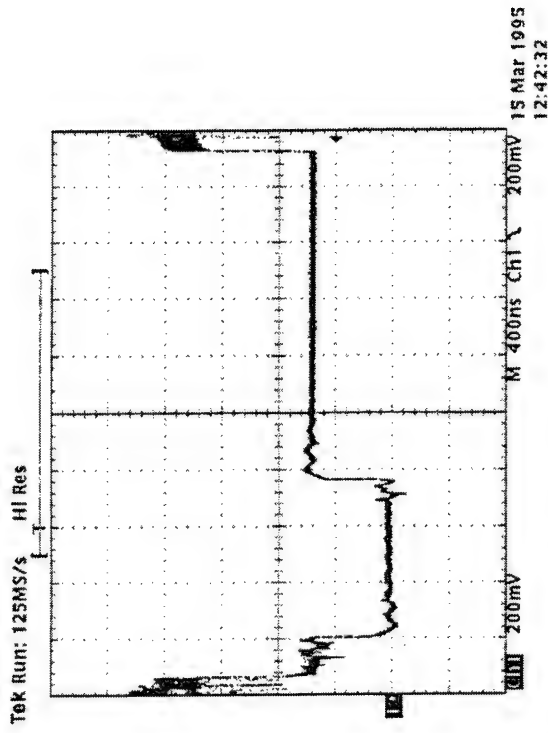


Figure 2-6. Expansion about the Horizontal blank period of the input video.

Taken together, these four images illustrate the timing required in the state machine - controller of the remote interface unit to maintain the proper sizing and placement of the high resolution image within the field of each flat panel. The four figures show the top-bottom and the right-left temporal alignment. They imply when the A/D conversion process should start and stop and where the alignment signals the flat panel needs should be placed as well.

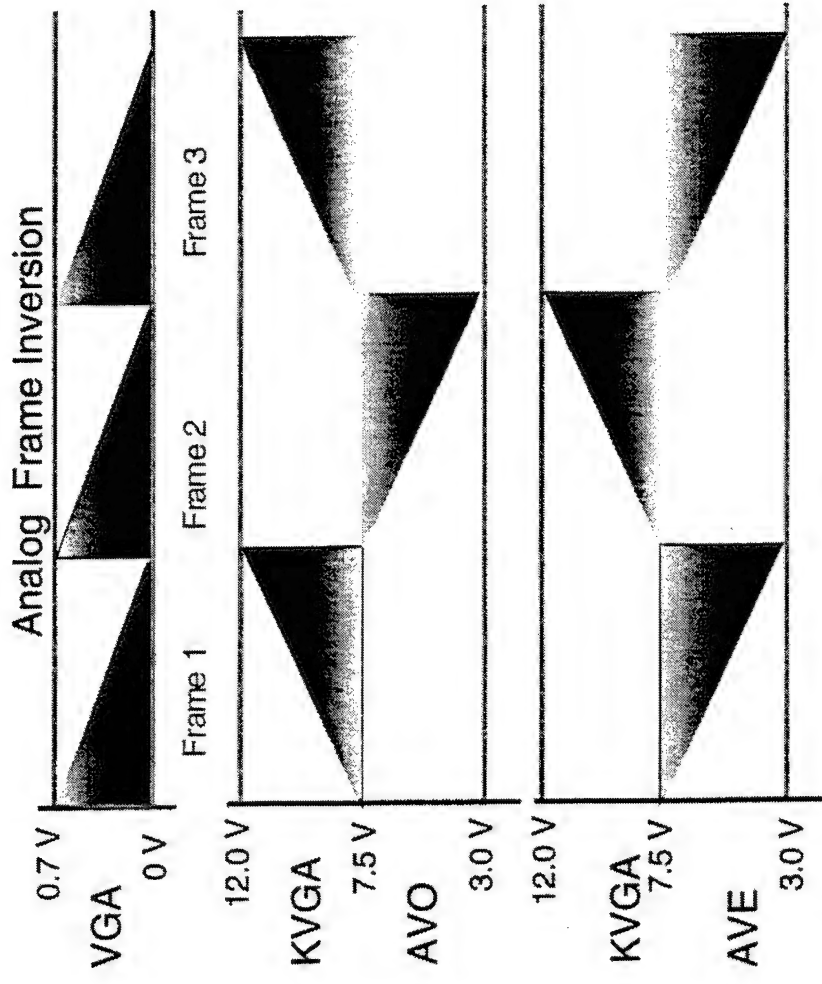
Interface to the Kopin Flat Panel

Figure 2-7 and Figure 2-8 indicate the output requirements of the interface circuitry required by the Kopin display system. This is representative of the interface used in the 64Q, as well as the newer 1280 and 2560 designs. Given the inputs specified above, the interface unit must provide signals similar to those shown below. The exact nature of the signals is being determined by the vendor at the time of writing of this report and

so are unavailable. However, the vendor stated that the continuous gray scale integrated driver used on the 640×480 product is the basis for the higher resolution unit in all major respects except one: 16 channels of analog input are required versus the one channel of the lower resolution unit. This is required to ensure that the video timing signals, the driver and all the support circuitry can operate at significantly more manageable frequencies. Instead of injecting the analog video into the flat panel drive chain at 107 MHz, only 6.7 MHz is required. Thus, the input 1280 pixels must be absorbed by the Interface Unit and re-partitioned or scan-converted into 16 sub-segments that all get read out simultaneously and written to each flat panel column drive system. Of course the signals must be converted from digital form to analog form first, as indicated by Figure 2-7 below and must be inverted with respect to the common voltage level, 8 volts, in order to prevent flicker and preclude damaging electro-plating action on the flat panel pixel electrodes.

Level shifting circuitry is included in the driver to bring the RS-343 signal levels through the A/D and the D/A processes to conform with the detailed signal requirements of the panels. Gamma correction is assumed to take place in the 1280×1024 image data source. There the gamma correction function relating input-output non-linear relationships is encoded in a Look-up-table, typically included in the video digital to analog converter (DAC). This of course assumes that the image seen at the 1280×1024 image data source is not necessarily of optimal quality when shown simultaneously on the two-primary color display.

As an option, gamma correction capability can be inserted directly into the remote interface unit. But this entails additional expense. A gray shade look-up-table (LUT) is required for each color. Additionally, a PC and PC interface (or equivalent) is needed to load the LUT.



VGA is the standard VGA analog input. Typically 3 analog signals are provided representing Red, Green and Blue. For monochrome RGB the following proportions are added:

$$\text{MONO} = 30\% \text{ Red} + 59\% \text{ Green} + 11\% \text{ Blue}$$

AVO & AVE show voltages applied to the panel with frame inversion to prevent flicker.

Figure 2-7. Inverted analog waveforms needed to drive the 640 x 480 continuous gray scale flat panel, precursor to the 1280 x 1024.

KVGA LIQUID CRYSTAL DISPLAY MODULE

Product No: 800-0005-00

Specification No. 835-0001

Timing Charts

Note:
TS = Setup Time
TH = Hold Time

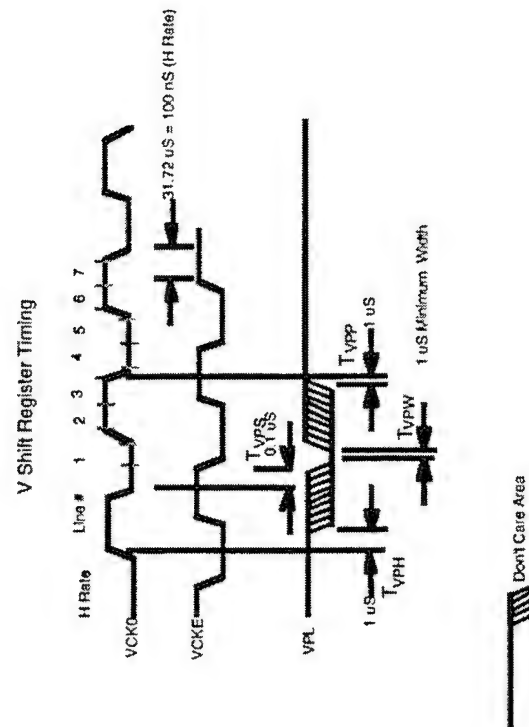
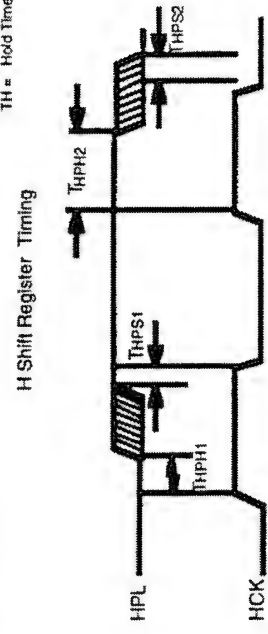


Figure 2-8. Timing required for the 640 x 480 continuous gray scale flat panel, precursor to the 1280 x 1024.

Details of the Interface Circuitry

The 1280 x 1024 output of the 1280 x 1024 image data source may be conveniently available in analog form in RS-343 RGB (red, green and blue) signal format. All three lines carry the synchronization signals (see Figure 2-3 through Figure 2-6). The G (green) line is the one typically used in decoders/monitors to derive all the synchronization information. The sync signals are composited with the video, that is, the vertical and horizontal timing signals are encoded together along with the RGB signals. The composited information must be separated and routed through the interface circuitry to the two-primary color display to create the final image.

The horizontal sync is used not only to time the beginning and ending of each row read-out but also to establish the pixel clock. 1280 clocks are required during the 11.94 usec active row time meaning that the analog to digital converter on each of the three RGB lines is must sustain a clock period of 9.3 nsec, corresponding to a 107 MHz sampling frequency. Note that selecting this as the sampling frequency requires that the driving clock be in precise phase alignment with the 1280 X 1024 image data source image generator pixel clock, otherwise the sampling cycle could straddle two pixels resulting in a smeared version of the input image. It is required only that the sampling period fall sufficiently within the timing bin of the source pixel. Other than a one-time adjustment (tapping the correct point via a jumper in the clock generation chain), no other sampling alignment is required.

The interface is inserted into the analog video stream of the 1280 X 1024 image data source output. This may be effected by a T-type stub, which appears to the user as a standard loop through connection. The line receiver shown in Figure 2-9, buffers the incoming signal and converts it from a differential signal into a single-ended signal. Immediately following that, the signal is routed for sync separation and A/D conversion. Conversion to digital form as soon as possible is required to minimize noise injection. The digital form is required because the signal must be reformatted into 16 channels to drive the 16 integrated column drivers, embedded on each of the three flat panels, one for each of the primary colors.

The horizontal sync is used to derive the pixel clock using a phase lock loop or equivalent. Because of the precision and repeatability from unit to unit in the 1280 X 1024 image data source product line (assumed from a sampling of two units and an understanding of how easy this level of precision is to obtain from standard crystal clock sources and digital circuitry), the phase lock loop will be implemented as a simple

multiplexer-delay line and counter; it will pick the delayed crystal driven clock edge closest to the middle of the pixel bin. The middle of the pixel bin is derived from the rising edge of the horizontal sync pulse in accordance with Figure 2-6.

The timing and control state machine provides the overall coordination between the 1280×1024 image data source and the flat panels. Its purpose is to ensure the top-bottom and left-right edges of the input image fall within the corresponding areas of each flat panel.

The 1 to 16 channel scan converter is a Ping-Pong arrangement of memory. The memory is 1280 pixels long by 8 bits deep. The Ping-Pong arrangement is needed so that an input line can be stored while a previously read line can be read out in 16 segments, thus providing the flat panel with the lower rate video needed to refresh the integrated column drivers.

The timing and control state machine is also tasked with running the row by row refresh of each flat panel. One significant difference between the standard 640×480 panel and the higher resolution 1280×1024 panel is the row drive. The high resolution unit allows non-sequential row activation, needed to support the "falling raster" color video option.

The polarity D/A converters are derived from existing circuits developed by Honeywell to drive a 1280×1024 flat panel display. Brightness and contrast controls are included. Brightness and contrast can be implemented in a number of ways. Potentiometers can be used to alter the DC offset and peak to peak values of the AC video signal. Alternatively, the look-up-table used to do the gamma correction can be used. Variations between these two approaches (analog intensive versus digital intensive) are possible.

The driving factor as to which or what mixture of both is chosen depends in large part on where the controls for adjusting the brightness and contrast are located. If they are to be on the head set, then a compact analog approach (potentiometers) is recommended. No digital controller will be needed on the head to update look up tables there. However, alternatives exist here, too. Noting that the number and type of digital components needed to implement the digital contrast and brightness is modest, it is feasible to stay compact. All the functions could be embedded in one IC.

If the brightness and contrast controls (knobs, rocker switches, sliders...) are on the local interface unit or on a flight deck surface or some equivalent, then implementing the contrast and brightness adjustments at the control units (local or remote) or at the image data sources may be more appropriate. Because the gamma correction function is implemented using a look-up-table (typically located at the image data source or at the remote interface unit), which allows the input output relationships to be arbitrarily adjusted, the contrast and brightness functions can be embedded along with the gamma correction functions and temperature correction functions.

These two approaches capture a wide range of possibilities, allowing the controls for brightness and contrast to be placed almost anywhere, including on the pilot's head assembly, person or some support structure on the vehicle. Adjustments, thereafter, will be made using the 1280 X 1024 image data source look up tables, most often used for effecting gamma correction.

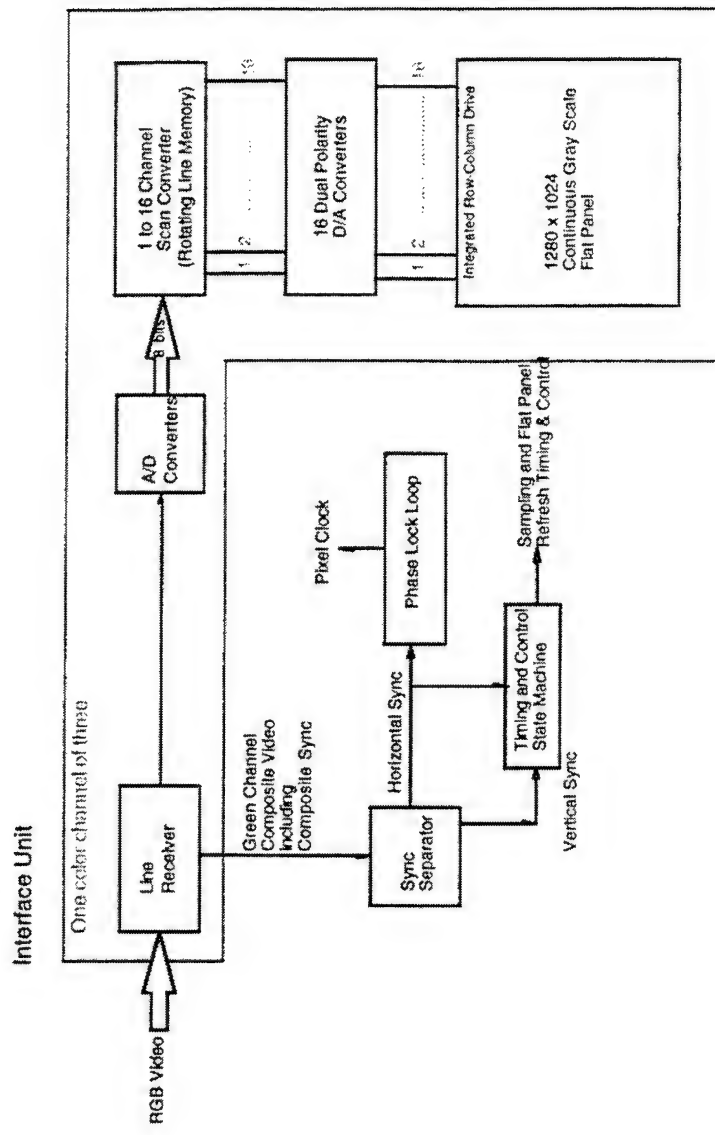


Figure 2-9. Schematic of interface unit comprised of local and remote interface units.

2.4.2 Fiber Optic Interface to the Two-Primary Color Display

It is clear that a fiber optic (FO) interface from the image data source to the head mounted display is desirable for a number of reasons including light weight and immunity to electro-magnetic interference. A fiber optic interface also has the potential for transmitting very high bandwidth, high definition video.

Accordingly, we conducted a technology assessment to determine the suitability of fiber optics for the two-primary color display target applications. What became evident was that the fiber optic interface presents a medium risk interface. The diameters of the links discussed below are all in the 0.1 inch range. Regarding size, weight and physical robustness, all the approaches below result in implementations that are a small fraction of the size, weight and physical robustness of the total link. The total link is dominated by the light pipe that will furnish the backlight energy to the head-mounted display. At about 0.1 inches in diameter for the electrical conduit and at about 0.5 inches for the light pipe, the relative size, weight and physical attributes are proportional to the area. This ratio shows that the light pipe is 25 times bigger than the signal conduit.

Boeing 777 Fiber Optic Interface for EFIS Formats

A FO interface was investigated for use on the Boeing 777 program in 1989-1990. The interface was designed, built and demonstrated. It performed well, transporting compressed EFIS images over a 100 MHz channel with no signs of technical artifacts of any kind. Of the 100 MHz available, only about 20 MHz was needed to transmit the symbolic imagery.

However, one issue was life cycle cost. Analyses done then indicated that a downselect to a coaxial transmission line was favored for maintenance-cost reasons.

Since then, developments are ongoing which are expected to eliminate the maintenance cost issue. One new design (please see program description below) eliminates the major risk area in the interface scheme; the FO connector is gone. This means the concerns regarding special FO repair training, special tools, special test equipment, tedious end to end fiber cable splicing, etc. are eliminated. The FO is permanently mounted at either end to a small electro-optic printed circuit board that has a small electrical connector attached. It is this standard electrical connector through which the interface and mechanical coupling will occur.

We also identified an effort (please see program description below) which merges high bandwidth video signals into a small bundle of 10 optical fibers, of which two carry control and clock signals and the rest carry data. Whether this scheme is necessary for the target applications of this project depends on what the final resolution of the image source will be and on whether or not video of medium or high bandwidth is to

be transported. It is possible for example that the requirements provide relief on the bandwidth requirement which would imply fewer fibers are needed. This implies a potential cost saving. Each of the fibers alone is capable of sustaining about 1 GHz of bandwidth. This means that even very high resolution images will be supported by relatively low technical risk technology being built in the laboratory now and ready for demonstration by about mid-96.

Fiber and Microcoax Blend, an Attractive Two-Primary Color Display Link

Elements in the two-primary color display require electrical power. One approach to getting the power to the head area is to use electrical conductive signal lines that have at least two purposes. One is to conduct the DC voltages needed to power the integrated circuits and other components. The other is to conduct control and clock lines and perhaps some of the image content, too. Below is a brief description of the state of the art for a preferred approach, a blend of the benefits of micro-coax (u-coax) and fiber optic transmission media. These data are taken from ongoing research projects that target commercialization and thus low cost two-primary color display applications.

Power: Currently we are estimating a 2x reduction in power at low speeds to a 3/4x reduction at high speeds in an ongoing R&D program. The reduction at high speed is impeded somewhat by the need for differential PECL drivers potentially being required with u-coax at high speeds. Note that power as a function of distance is a more sensitive factor for u-coax versus standard video coax.

Weight: A 2x reduction in weight is estimated as follows. In a separate R&D project, Honeywell is working with Northern Lights Cable which has a 12 fiber encased product. We are modifying it to be more weight efficient among other things. For a 40" length of cable the weights are:

Fiber	612-IN-CB-XXX	65.76 grams
Coax	RG-174	132.11 grams qty. 11

Many applications including HMDs require distributed power and grounds. Accordingly, 3 u-coax lines alongside the signal carrying parallel fiber optic lines are recommended for carrying power and grounds.

Here we are assuming that the central member in the 12 element can be replaced with 3 u-coax lines and the outside jacket replaced with a light polyurethane coating. We are also assuming that the additional weight of the 3 u-coax will be offset by the replacement of the central fiber member(s). Thus, 3 u-coax lines will serve as the central member about which the remaining fiber optic lines will be twisted.

Bandwidth-Distance: For two-primary color display purposes, the fiber bandwidth length is not a driving issue. Rather, the issue is one again of cost especially if one were to replace all the fiber elements with a low cost u-coax. Unfortunately, about 5-10 Gbps will be required for very high resolution displays and computer systems. Unfortunately, at these rates, implementations that rely on u-coax as a high speed signal pathway for runs of over 30' are not currently cost effective.

In a separate program, we have a 30' link running at 800 Mbps. It is encoded to a 1-Gbps channel. To reach this distance, we were forced to use a very high quality and relatively expensive u-coax cable. The cost was \$500 for the two lines in test. If the u-coax were to replace all 8 fiber lines, then the cost would be in the neighborhood of \$2000 and possibly more. A full up u-coax transmission line system like this would provide 8Gbps and be limited to about 30' applications. From our initial tests of u-coax under the CVCHMD program, Honeywell found considerable S/N rolloff above 1 Gbps using 20'-30' lengths of u-coax.

AGM Program - Developing Low-Cost, Versatile Fiber Optic Links for HMDs

Goal: Develop a link with 10 optical channels delivering imagery to a head mounted display. Eight data channels will transmit data at 300 Mbps per channel, resulting in a total bandwidth of 2.4 Gbps aggregate data rate. The minimum will be with 200 Mbps per channel. Total link power consumption will be less than 1 W. The size and weight will be less than or equal to that of a standard 15-pin D-subminiature connector. The total cost of the link will be less than \$150. This assumes a commercial demand of 10,000 links per month.

Content of Link: The module will consist of an array of lasers, an array of integrated photodetectors/pre-amp circuits, another array of postamplifiers, an array of laser drivers, and mux and demux chips. Thus, about 4-6 integrated circuit die will be needed. The approach is to downconvert convert 40 electrical lines into 8-10 optical lines. There will be no optical connector-just an electrical connector. This implies that

the cable will be an active cable; it will have power, which is desirable because the two-primary color display will require power as well so no additional costs are implied.

Note regarding conduction of power across the link: In two-primary color applications, where the head mounted display is to be powered by a remote and local interface unit set, the power may need to be transmitted by an electrical wire connecting the stream of signal carrying components. Alternatively, each unit can carry its own power. To highlight the distinction between the two approaches, it is possible to embed the power in the jacket and central conductors of a micro-coax link. The micro-coax then would serve two functions: 1) provide an electrically conductive power pathway; and 2) provide a high integrity, high frequency transmission line. It is also possible to arrange the links so that each unit is supplied with its own power source. This can be done by using another separate conductive power link or by stored power (e.g., a battery) or by environmentally supplied or ambient power (e.g., solar, vibration, motion). In this latter approach, no conductive element is needed on the data link.

Given the current understanding of what is intended for the derivatives of this program, embedding an electrical conductor in the data link is preferred because of simplicity, reliability and cost reasons. Which of the transmission schemes is finally selected will determine whether or not a separate conductor for power will be required.

Status: The project is in the early stages of performance. It will produce working prototypes for testing and evaluation by the end of '96. At that time commercial feasibility and marketing assessments will be made. The most likely manufacturing candidate on the short list of candidates is Micro Switch of Richardson, Texas.

Other High Bandwidth Transmission Link Option: Micro Switch is currently developing a 1-Gbps single-channel link. Prototypes have been built and delivered for demonstrations.

A number of groups and companies have been developing parallel links as demo projects (not real products yet). Honeywell has been involved in one with AT&T, IBM and Martin Marietta (called OETC). The team has built a 32 channel link, with each channel running at 500 Mbps, for

an aggregate bit rate of 16 Gbps (or 2 GBytes). Eight such links have been assembled. In the current phase we (OETC) are building 50-75 additional links, to be finished by the end of 1995. Samples are available to the program to test and evaluate. Motorola is offering a parallel link with 10 fibers and an aggregate bit rate of 1.5 Gbps, but only have sample quantities, and people seem to be having trouble getting their hands on those.

High Speed Plastic Optical Fiber

Program Objective: This two-year program will advance the state of the art in high speed plastic optical fiber (POF). HTIC and Micro Switch will be developing low cost ATM transceiver modules. Packard Hughes Interconnect (a subsidiary of General Motors) will lead the \$5M program and develop a low cost plastic fiber connectors for auto, office and industrial use. Boston Optical Fiber will be developing the manufacturing capability for the high speed plastic fiber. Boeing Aircraft will be demonstrating plastic fiber in the 777 Avionics LAN.

Technology Nugget: Plastic fiber promises performance similar to glass fiber at a cost that is competitive with copper wire. Low cost plastic fiber can compete against copper in bringing 155Mbit/Sec ATM to the desktop.

3 TEST CELL FABRICATION AND EVALUATION

3.1 Test Cell Fabrication and Evaluation

In this section, we present the procedures and results of building five high resolution single-pixel and one active matrix experimental liquid crystal subtractive color (two primary color) stacks. Methods and rationale for stack configurations are based partly on experience gained from prior subtractive color programs. Four two-primary color single pixel stack/polarizer configurations were built and evaluated for luminance, color gamut, transmission and contrast ratio. Two-primary colors evaluated yielded yellow, red, green and black, measured with an ILC LX300 Xenon arc lamp, and an ILC Tri-band metal halide lamp. The results of the measurements led to identification of an exceptional stack/polarizer configuration, which was used to build an active matrix subtractive color stack, using Sony 1068x480 monochrome AMLCDs. Gray scale was evaluated for eight shades (8 voltages), where voltage versus contrast was measured for three scenarios: yellow to black, red to black, and green to black on the best stack configuration (hybrid #1). To achieve optimal tuning to the ILC Tri-band lamp, once characterized, a fifth single pixel two-primary color stack for analyzing diffractive effects was built and evaluated utilizing notch polarizers tuned to tri-band lamp #69.

3.2 High Resolution Aperture Test Cell Design

To enable testing of aperture as well as color gamut / luminance performance, very high resolution metalization patterns were processed on ITO for building display test cells (light valve LCDs). Six test cells were designed into one mask, with each array being 640x480 pixels at 1000 lines per inch. Four cells study various apertures at 24μ pitch (32%, which simulates Kopin, 48%, which simulates the Sony AMLCDs, 73%, which simulates DSRC pixel enhancement, and 92%, which simulates Honeywell's high efficient pixel efforts.) The last two cells analyze diffractive effects of multiple cells, which were analyzed after stacking two light valve LCDs (with an image plane to image plane distance of 0.051 in.). The last two cells analyze diffractive effects of 32%, 48%, 73%, 92% apertures at 24μ and 67% and 90% apertures at 20μ pitch. These are incorporated into six arrays within each of the diffractive effect test cells with designed in artifacts for measuring diffractive effects. The designed in artifacts simulate one pixel "on", surrounded by "off" pixels, as well as one pixel "off", surrounded by "on" pixels. There are also four groups of arrays (2x2, 3x3, 4x4, and 5x5) with pixels "on" surrounded by "off" pixels.

Optical measurements were performed to determine transmission efficiency through single layer apertures only for yield study. The results were as follows:

Designed Aperture Transmission	Processed Aperture Transmission
32.0%	30.8%
48.0%	47.8%
73.0%	73.3%
92.0%	93.5%

3.3 Stack Test Methods

The two light sources used were an ILC LX300 Xenon arc lamp and an ILC Tri-band lamp (#69) with a 1/4 in. fiber optic bundle. A Photo Research PR 703A/PC SpectraRadiometer (photometer) with version 3.1 SpectraView software was used for all measurements. Luminance values are for the display “off” state (yellow), with a filtered backlight (<1% in blue wavelength) and with calculated filter correction, achieved by shifting the measured transmission spectra of the yellow filter -20nm and the cyan filter +50 nm. This yielded a band pass from 500 nm-650 nm, and allowed specification of dielectric filters to be implemented in the system design. Note: Transmission is the ratio of the yellow luminance to the white backlight luminance, and includes the attenuation of the yellow filter as well as the LCD stack attenuation. Contrast ratio is the ratio of yellow to black luminance. Comprehensive measurements were taken of display chrominance performance as a function of applied drive voltage for use in display modeling and control. Gray scale is evaluated for eight shades (8 voltages) with three scenarios: yellow to black, red to black, and green to black on the stack #3 configuration (hybrid #1). Figure 3-1 illustrates the directional light measurement system used to analyze each of the subtractive color light valve LCD stacks. Test results of measurements taken using the Xenon arc lamp and test results of measurements taken using the ILC Tri-band lamp (#69) can be found in Sections 3.3 through 3.10.

Table 3-1 provides a summary of key results for the test cells fabricated. An additional summary of stack test data is included in Section 3.10. Figures 3-35 through 40 represent the test results of the gray scale measurements taken on stack #3 (hybrid #1).

Two-Primary Color Directional Light Measurement Setup

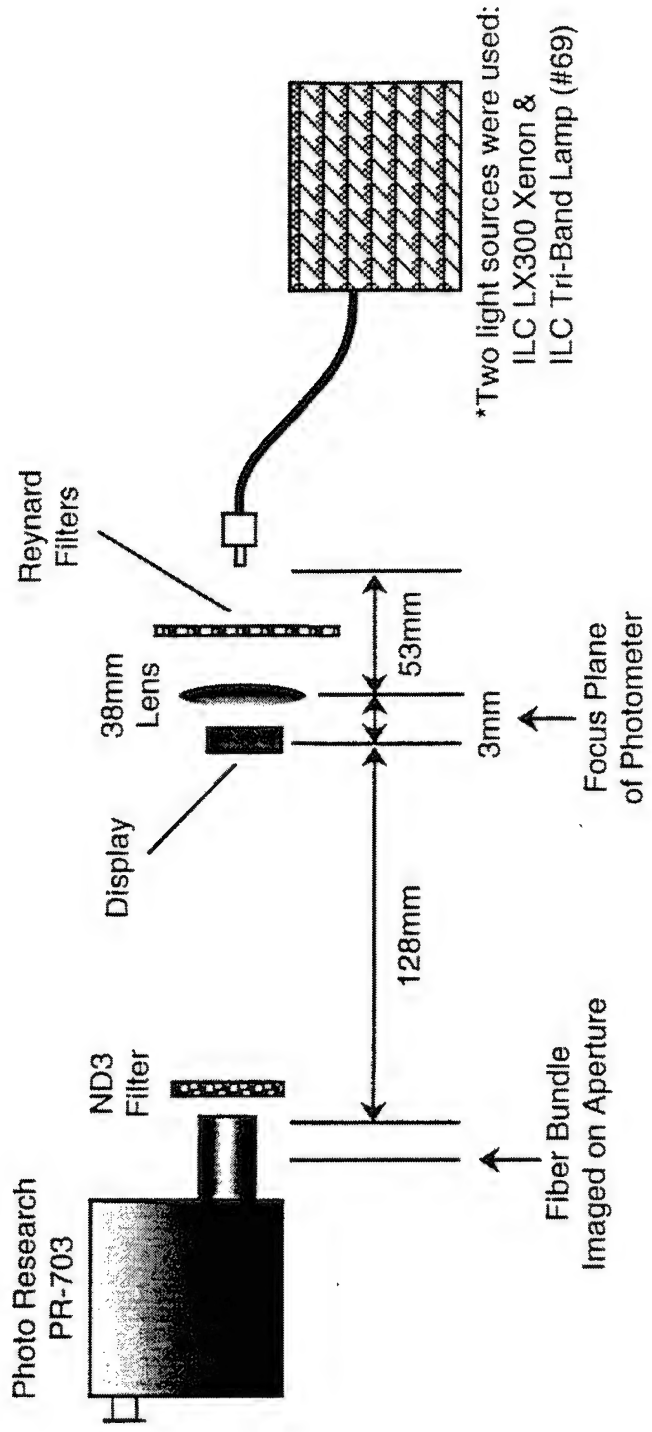


Figure 3-1. Two-Primary Color Directional Light Measurement Setup.

Table 3-1. Test Cells, Summary of Key Results (see accompanying data for further details)

Stack	Description	Selection Scenario	Transmittance (approx.)	Contrast Ratio (approx.)	Comments
#1	"MCD-like" design, uses absorbing polarizers, adapted directly from best "Miniature Color Display" 3-color design. Each layer has 73% aperture mask.	Serves as a baseline, using only absorbing polarizers and prior design. Configuration was optimized assuming a notch filter in the yellow-orange spectral region.	$T_{g,G} = 4.1\%$, $T_{r,R} = 8.2\%$ $T_{g,Y} = 9.5\%$, $T_{r,Y} = 9.0\%$	$CR_{g,G} = 7$, $CR_{r,R} = 20$ $CR_{g,Y} = 16$, $CR_{r,Y} = 23$	Moderate contrast and transmittance High green crosstalk Peaks in spectral contrast ratio miss the R,G lamp peaks
#2	No notch polarizer design, uses cholesteric notch polarizers, adapted directly from "Subtractive Color Using Notch Polarizers" 3-color design. Each layer has 73% aperture mask.	Serves as a baseline, using only cholesteric notch polarizers and prior design. Original configuration was optimized for an anticipated tri-band spectrum with somewhat broad bands.	$T_{g,G} = 12.3\%$, $T_{r,R} = 12.2\%$ $T_{g,Y} = 15.0\%$, $T_{r,Y} = 15.8\%$	$CR_{g,G} = 13$, $CR_{r,R} = 63$ $CR_{g,Y} = 16$, $CR_{r,Y} = 82$	High transmittance, low crosstalk Moderate contrast as measured, but could be higher (perhaps 80:1) with minor adjustment to the polarizer formulation Peak of tri-band lamp slightly offset from peak green contrast
#3	Hybrid #1, combines variety of polarizer types. Each layer has 73% aperture mask.	Optimized for high contrast, even with broad band lamp. Transmittance is sacrificed somewhat for the contrast.	$T_{g,G} = 5.1\%$, $T_{r,R} = 5.8\%$ $T_{g,Y} = 9.1\%$, $T_{r,Y} = 10.3\%$	$CR_{g,G} = 372$, $CR_{r,R} = 181$ $CR_{g,Y} = 663$, $CR_{r,Y} = 324$	Very high contrast, moderate transmittance Moderate crosstalk Could be improved if revised for tuned lamp
#5	Double narrow-band design, uses narrow band hybrid approach. Includes all six aperture mask configurations.	Optimized for maximum transmittance and good contrast for the primary green and red peaks of the tri-band lamp. Assumes other spectral components are removed elsewhere in optical path.	$T_{g,G} = 13.8\%$, $T_{r,R} = 14.4\%$ $T_{g,Y} = 16.4\%$, $T_{r,Y} = 15.1\%$	$CR_{g,G} = 86$, $CR_{r,R} = 120$ $CR_{g,Y} = 102$, $CR_{r,Y} = 126$	High transmittance, high contrast and low crosstalk Suitable lamp and optical designs are required.
#6	Functional AMLCD stack, using two Sony LCX007 AL displays, and the Hybrid #1 polarizer design.	Working subtractive color demonstration stack, optimized primarily for contrast, but with reasonably good transmittance	$T_{g,G} = 1.0\%$, $T_{r,R} = 1.4\%$ $T_{g,Y} = 2.1\%$, $T_{r,Y} = 2.4\%$	$CR_{g,G} = 156$, $CR_{r,R} = 201$ $CR_{g,Y} = 339$, $CR_{r,Y} = 421$	Very high contrast is achieved with either broadband or narrow band light source. CR results shown for this stack were measured with reduced and filtered light levels (AMLCD contrast was observed to be light-sensitive).

Notes:

Transmittances are with respect to: Yellow (pre-filtered) tri-band lamp, White Xenon lamp (T includes attenuation by suitable filters), and the primary G and R peaks of the tri-band lamp.
In the latter case, $T_{a,B}$ indicates the transmittance for the 'a' spectral peak ($a = r, g$) with 'B' driving conditions ($B = R, G, Y$). Spectral peaks are the primary red and green peaks of the tri-band lamp.
 $CR_{a,B}$ indicates the contrast ratio (relative to the black state) for the 'a' spectral peak ($a = r, g$) with 'B' driving conditions ($B = R, G, Y$).

3.4 Stack #1 Configuration and Results

Stack #1 is based on an “MCD-like” configuration, which consists of two 73% aperture light valve LCDs, one magenta dichroic polarizing cell, two red sheet polarizers, two blue sheet polarizers and one cyan sheet polarizer as shown in Figure 3-2. Stack #1 has an image plane to image plane distance of 0.090 in. This configuration was designed prior to the tri-band lamp availability and characterization.

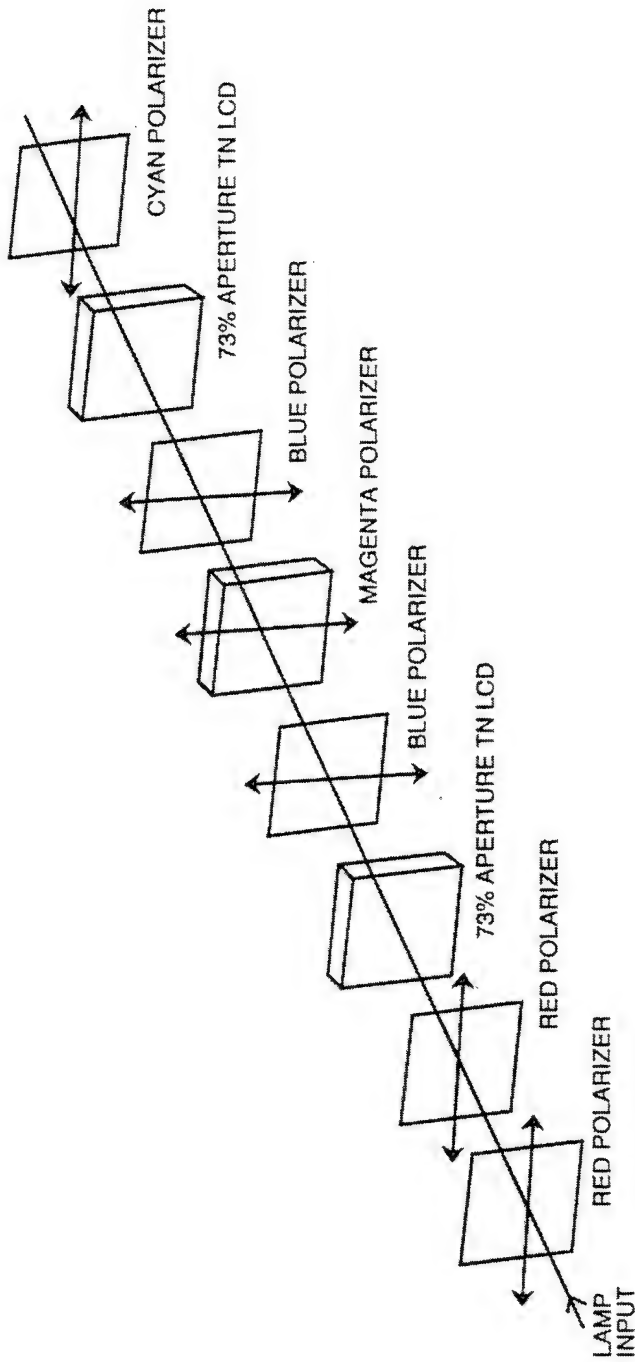


Figure 3-2. Two-Primary Color Expanded View of Stack #1 (MCD Configuration).

The test results of Stack #1 (“MCD-like”) follow.

Table 3-2. Stack #1 Directional Illumination Measured With Xenon Lamp and Reynard Filters

MCD Configuration: Lamp = 8504000 Π; Contrast Ratio = 23.09				
State	Π	u'	v'	
Yellow	519200	0.2197	0.5638	
Red	130600	0.4086	0.5374	
Green	128100	0.1239	0.5749	
Black	22490	0.1819	0.5634	
Filter Location	Backlight Luminance	Stack Transmittance		
In Backlight	6294000	9.0%		
Part of Stack	8504000	6.1%		

MCD Configuration: Lamp = 7750000 Π; Contrast Ratio = 28.34				
State	Π	u'	v'	
Yellow	40760	0.2599	0.5587	
Red	15590	0.4226	0.5355	
Green	10220	0.1258	0.5764	
Black	1438	0.2357	0.5601	
Filter Location	Backlight Luminance	Stack Transmittance		
In Backlight	463100	8.8%		
Part of Stack	775000	5.3%		

Table 3-3. Stack #1 Directional Illumination Measured With Xenon Lamp and Calculated Filters (Y cutoff < 500 nm, IR cutoff > 650 nm)

MCD Configuration: Lamp = 6294000 ΗΙ; Contrast Ratio = 17.79			
State	ΗΙ	u'	v'
Yellow	570400	0.1943	0.5636
Red	127300	0.3860	0.5373
Green	159300	0.1023	0.5695
Black	32070	0.1314	0.5517
Filter Location	Backlight Luminance	Stack Transmittance	
In Backlight	6294000	9.1%	
Part of Stack	8504000	6.7%	
MCD Configuration: Lamp = 583300 ΗΙ; Contrast Ratio = 27.40			
State	ΗΙ	u'	v'
Yellow	48740	0.2333	0.5612
Red	16170	0.4089	0.5368
Green	12140	0.1140	0.5740
Black	1779	0.2073	0.5522
Filter Location	Backlight Luminance	Stack Transmittance	
In Backlight	583300	8.4%	
Part of Stack	775000	6.3%	

Two-Primary Color MCD Type Stack
Filtered Power (Reymard Filters)

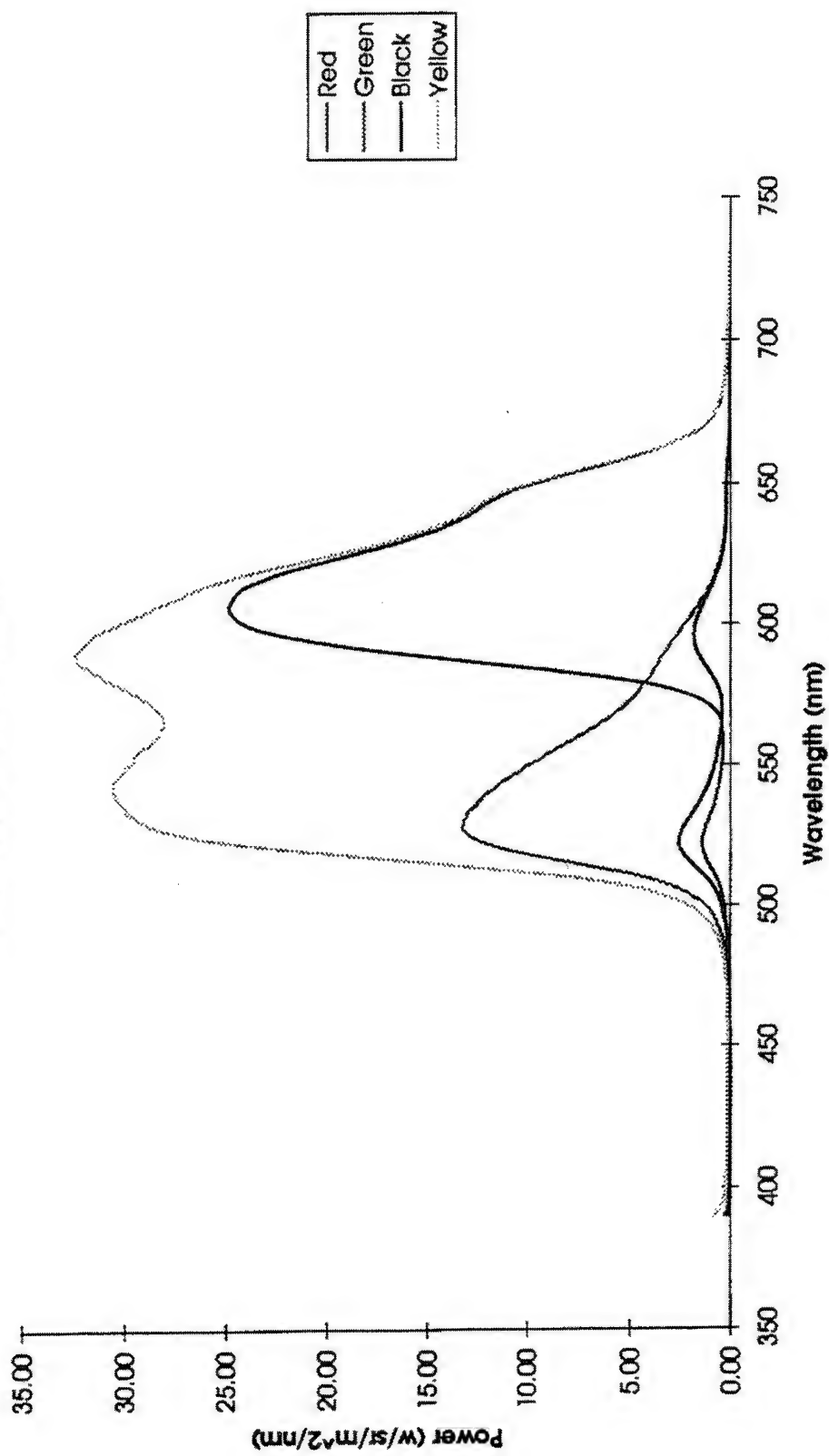


Figure 3-3. Stack #1 - Filtered Power vs. Wavelength (Xenon Lamp).

Two-Primary Color MCD Type Stack
Filtered Power (Calculated Filters)

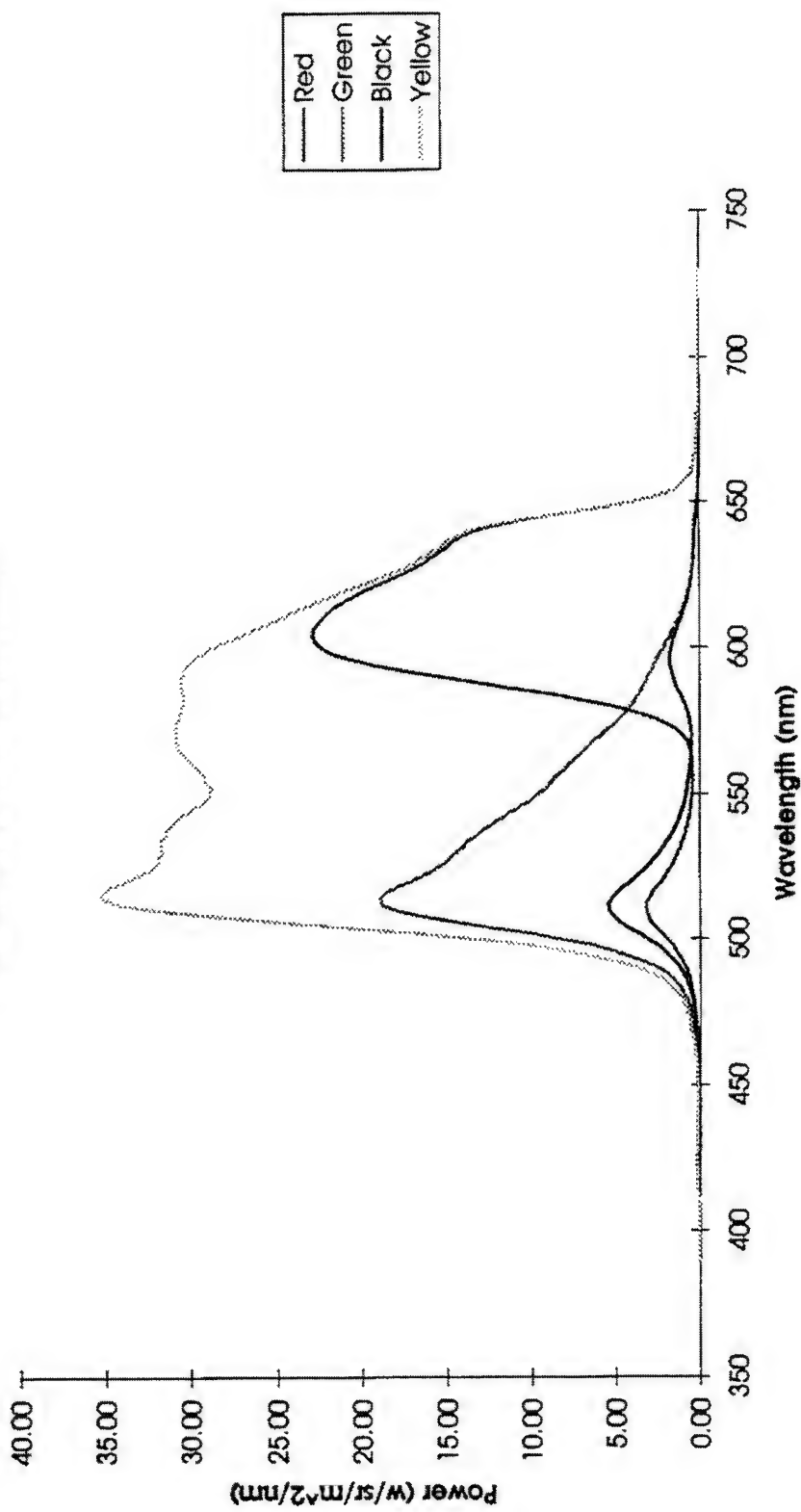


Figure 3-4. Stack #1 - Filtered Power vs. Wavelength (Xenon Lamp)

Two-Primary Color MCD Type Stack

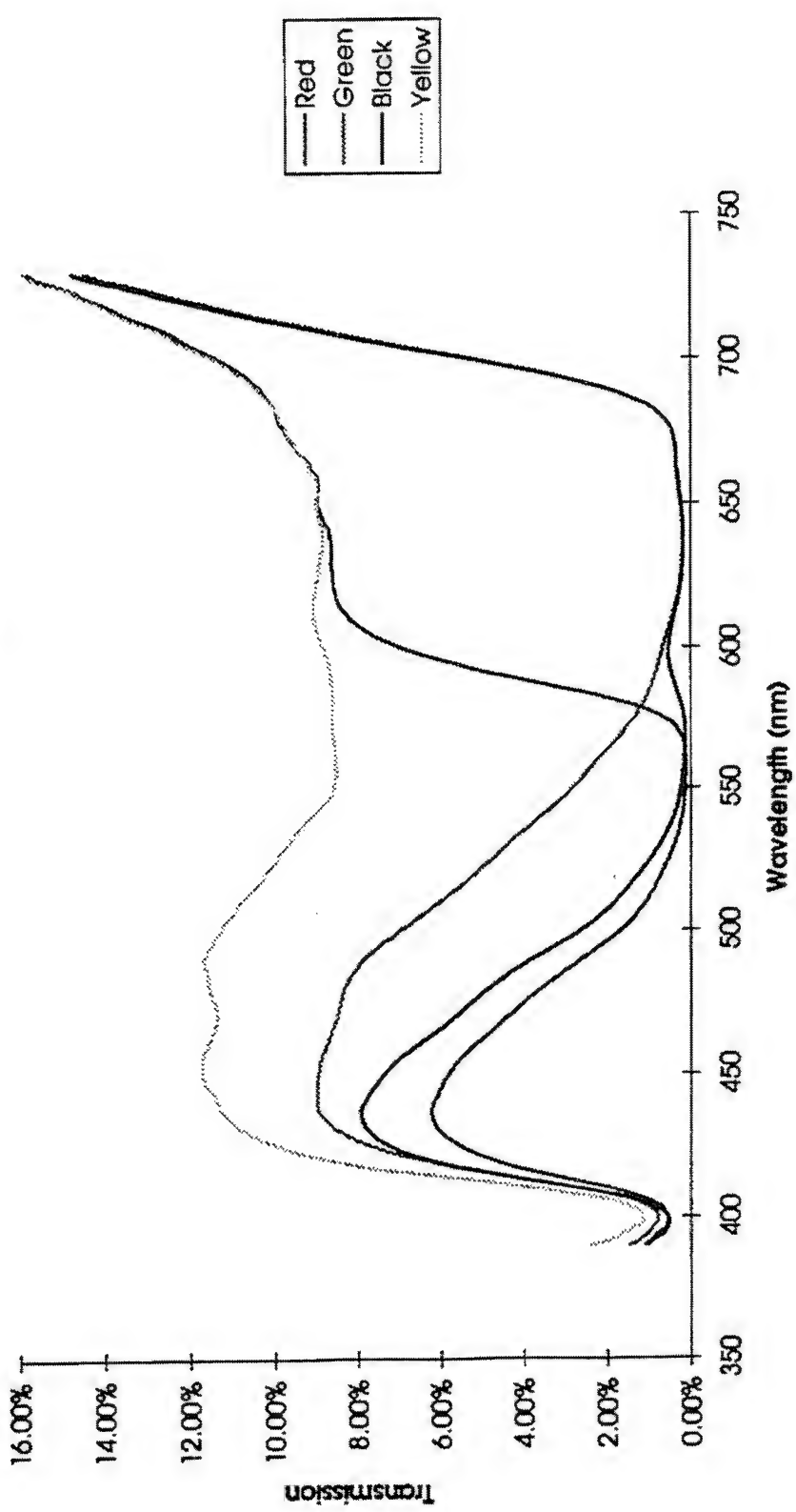


Figure 3-5. Stack #1 - Transmission vs. Wavelength (Xenon Lamp).

Two-Primary Color MCD Type Stack
Filtered Transmission (Reynard Filters)

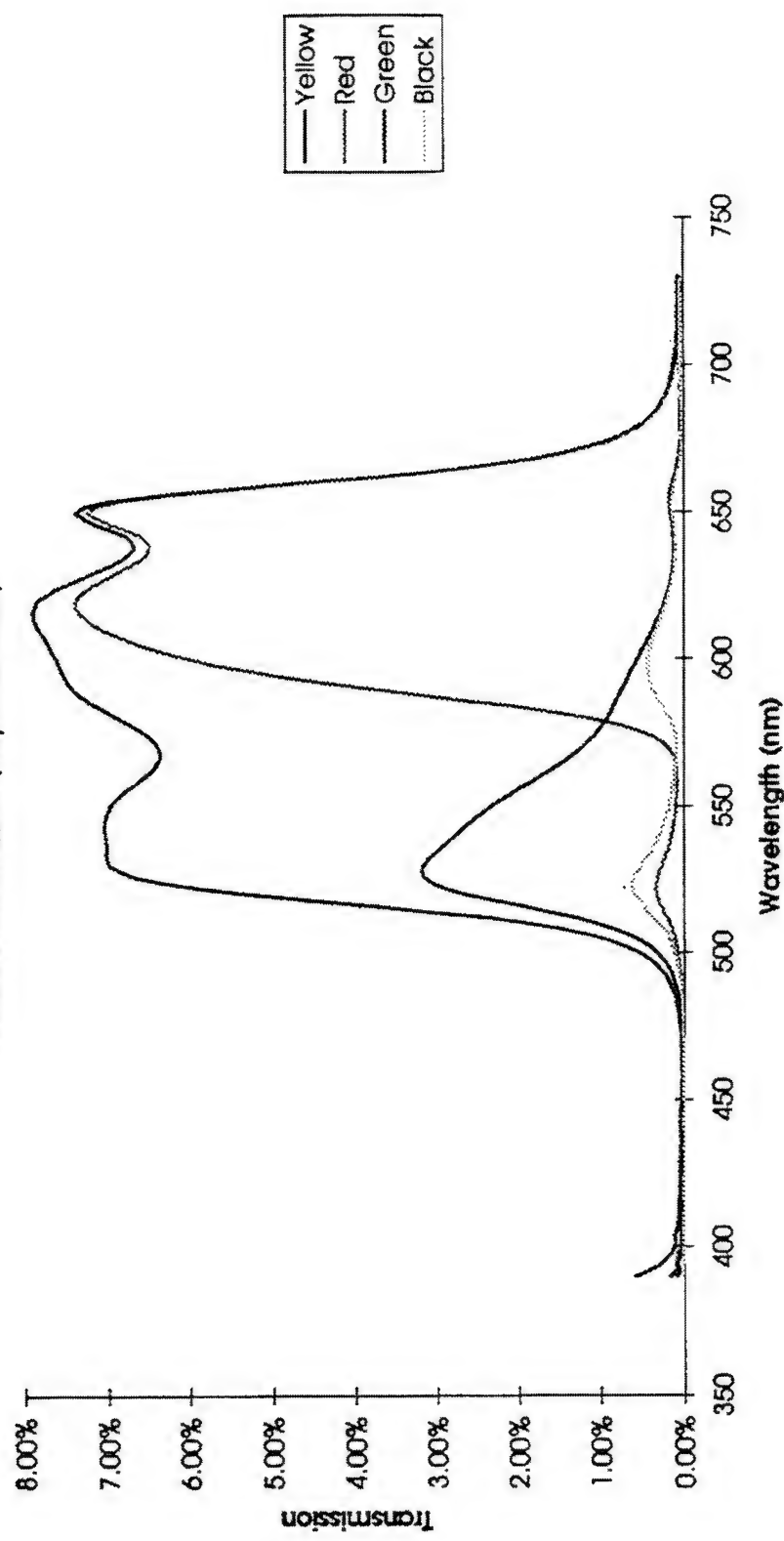


Figure 3-6. Stack #1 - Filtered Transmission vs. Wavelength (Xenon Lamp).

Two-Primary Color MCD Type Stack
Filtered Transmission (Calculated)

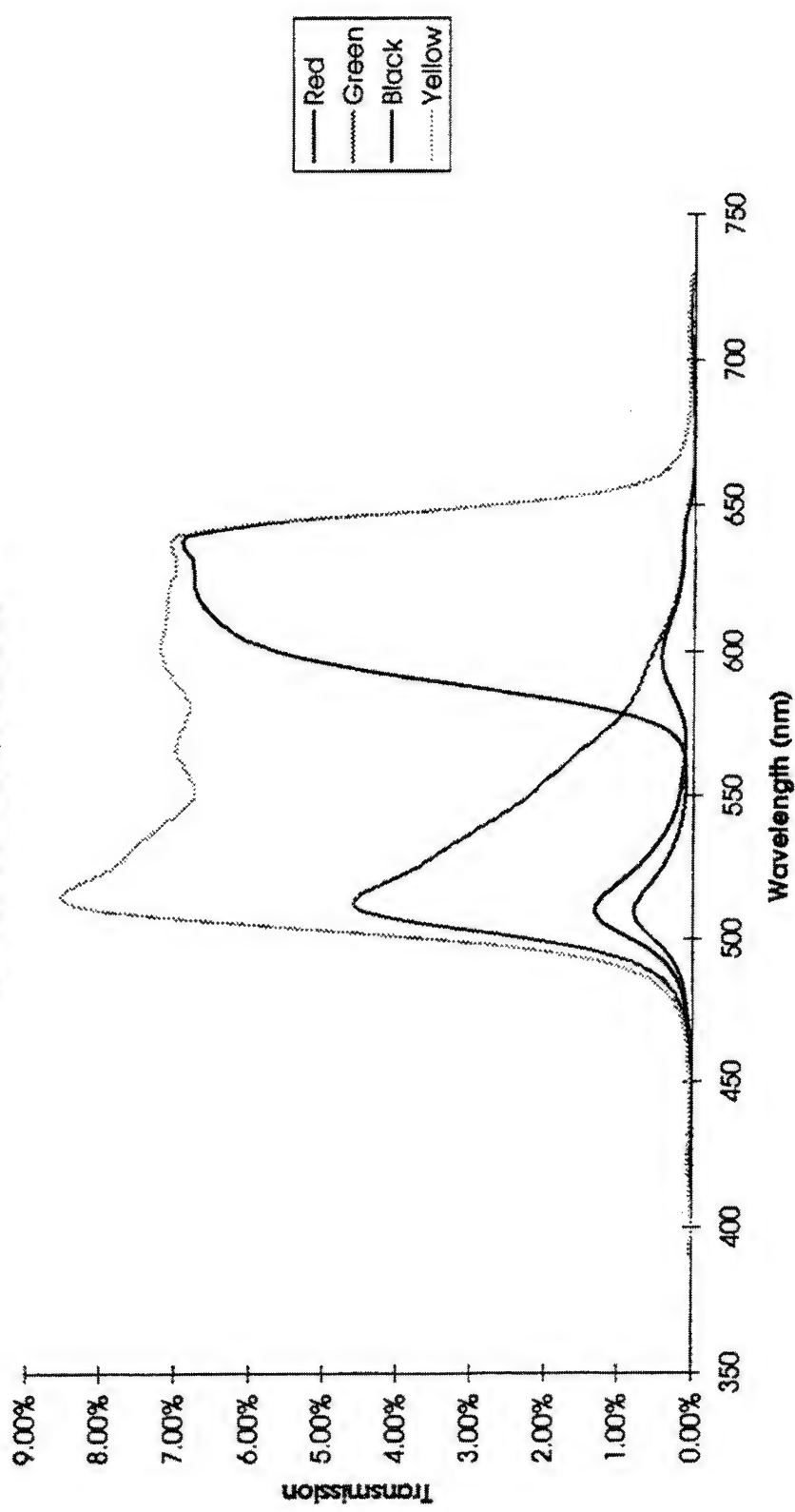


Figure 3-7. Stack #1- Filtered Transmission (calculated filters) vs. Wavelength (Xenon Lamp).

Two-Primary Color MCD Type Stack

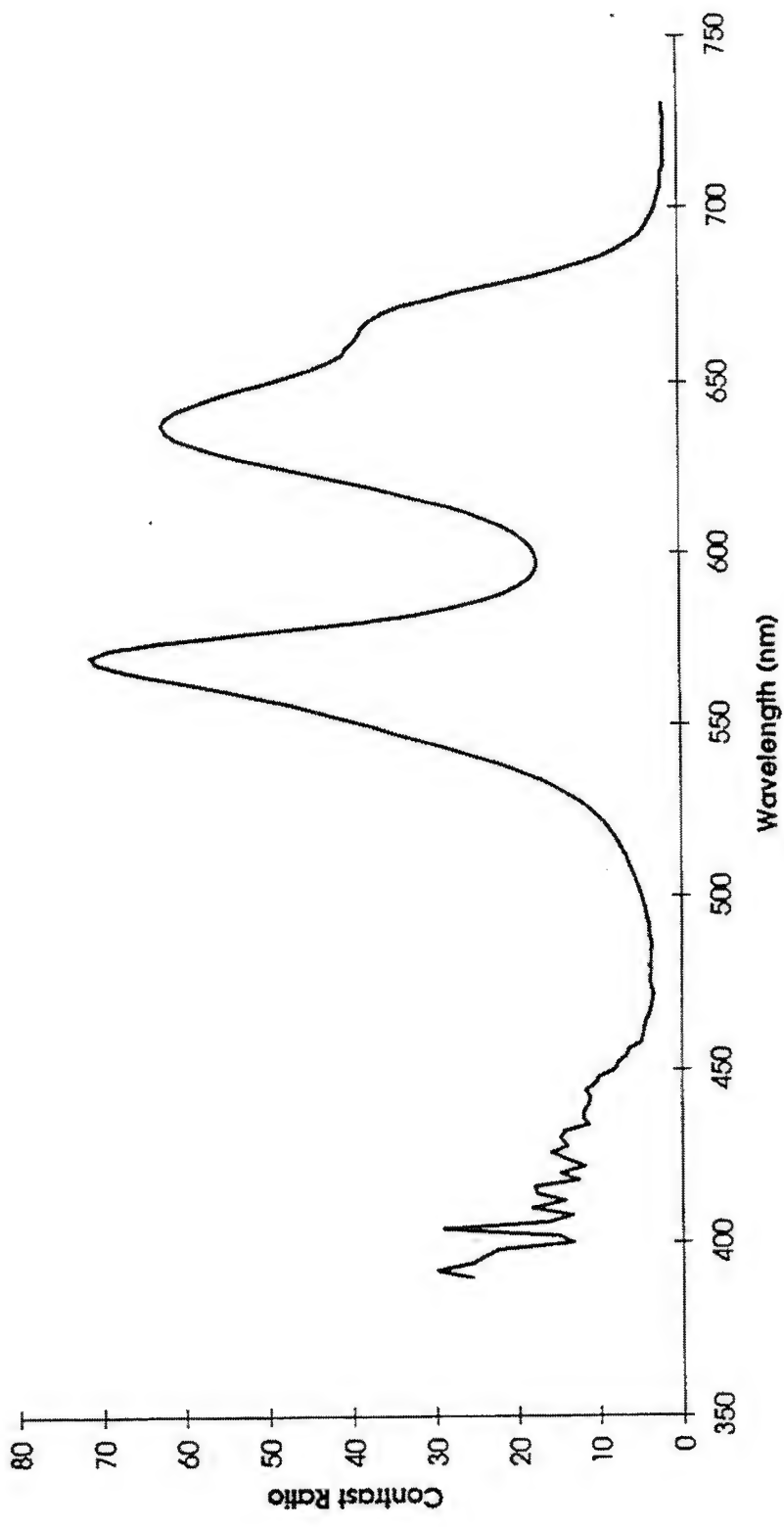


Figure 3-8. Stack #1 - Contrast Ratio vs. Wavelength (Xenon Lamp).

Two-Primary Color MCD Type Stack
Lamp Characteristics

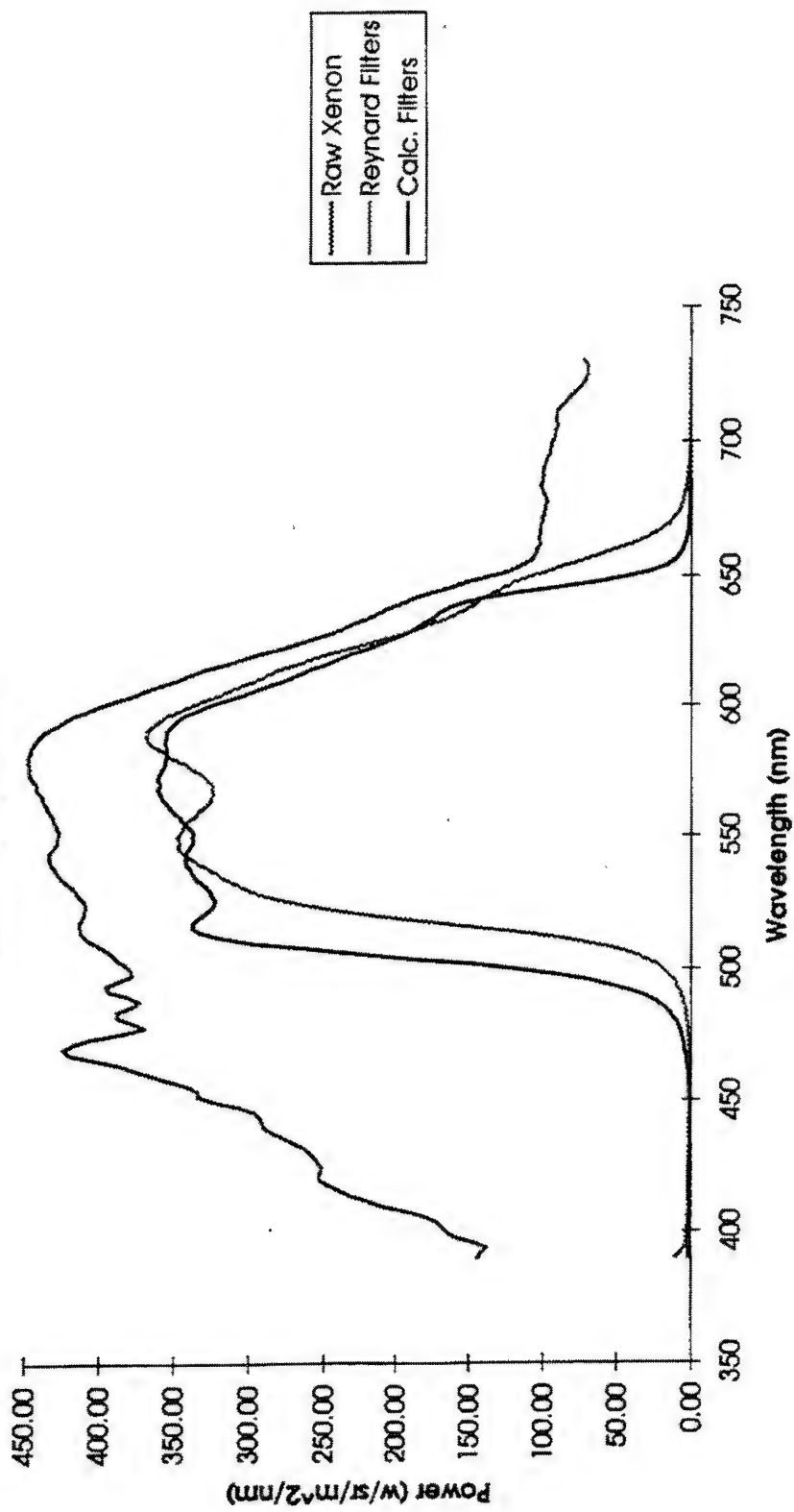


Figure 3-9. Xenon Lamp Characteristics - Power vs. Wavelength.

Two Primary Color MCD Type Stack
Filtered Power (Reynard Filters)

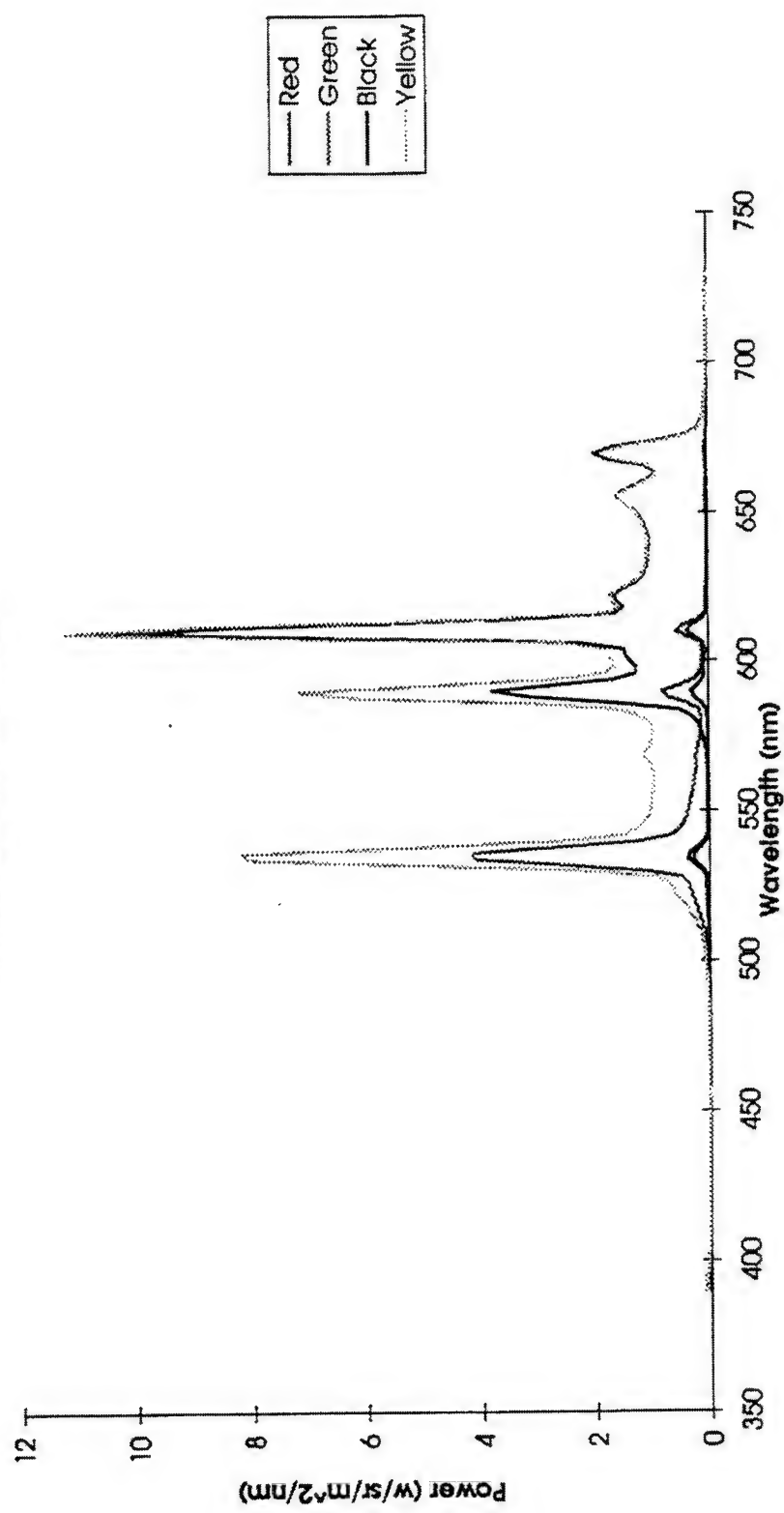


Figure 3-10. Filtered Power vs. Wavelength (Tri-band lamp #69).

Two-Primary Color MCD Type Stack

Filtered Power (Calculated Filters)

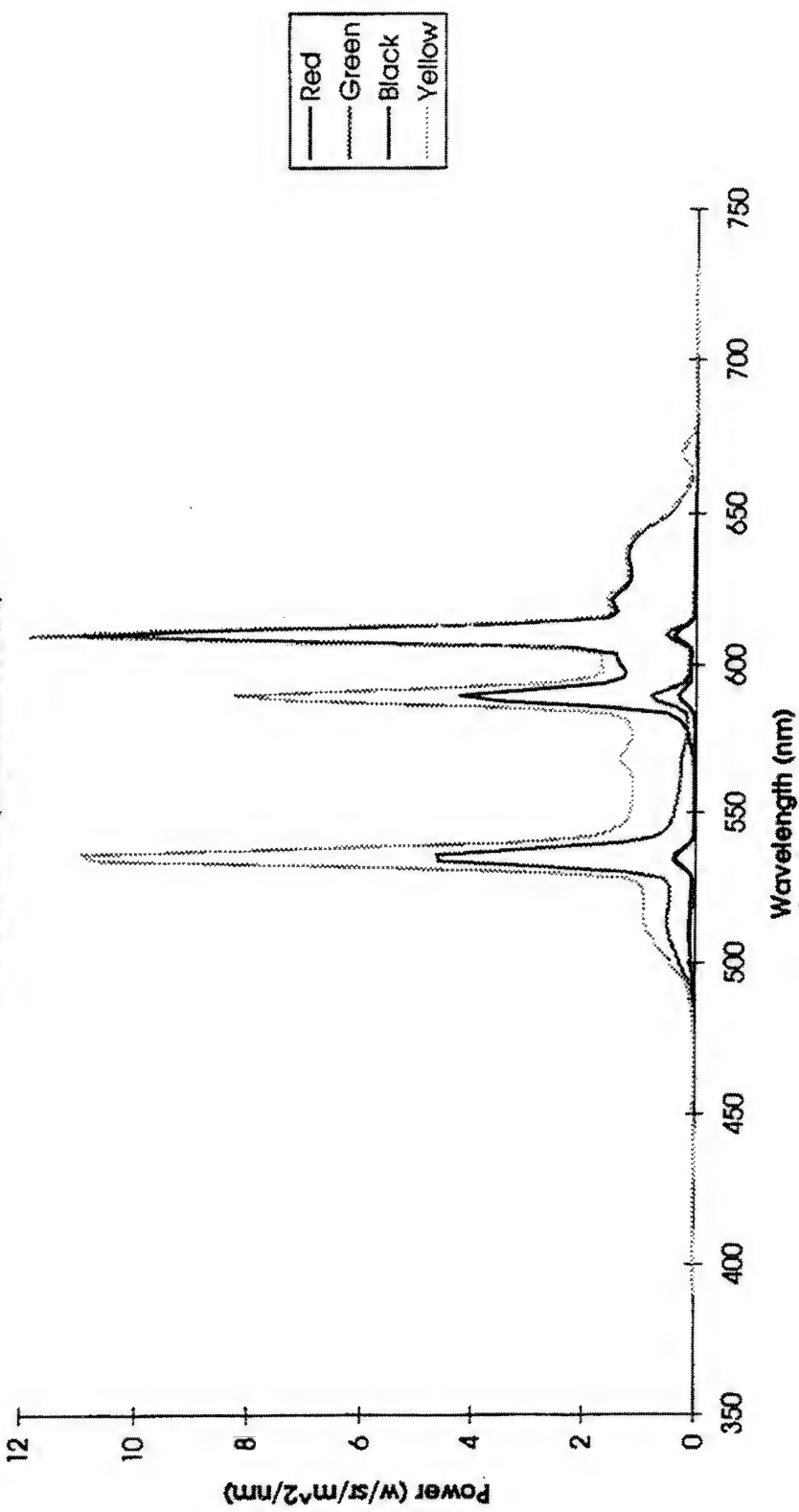


Figure 3-11. Stack #1 - Filtered Power (calculated filters) vs. Wavelength (Tri-band Lamp #69).

Two-Primary Color MCD Type Stack Lamp Characteristics

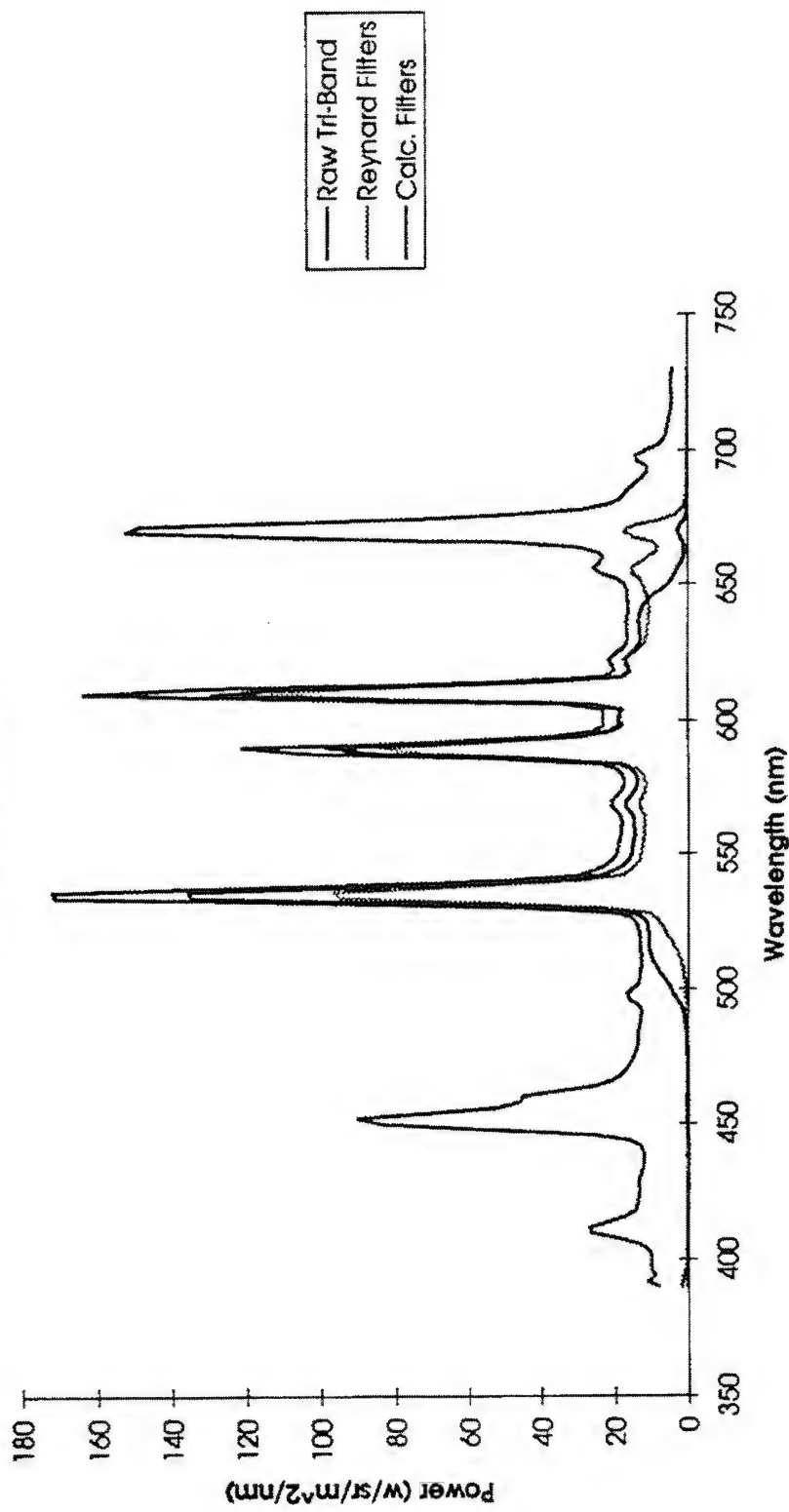


Figure 3-12. Tri-band Lamp Characteristics - Power vs. Wavelength.

3.5 Stack #2 Configuration and Results

Stack #2 is based on a notch polarizer configuration, which consists of two 73% aperture light valve LCD cells, two cyan notch polarizers, two magenta notch polarizers, and four wide-band $\lambda/4$ retarders as shown in Figure 3-13. Stack #2 has an image plane to image plane distance of 0.0866 in. This notch polarizer configuration was designed prior to the tri-band lamp availability and characterization.

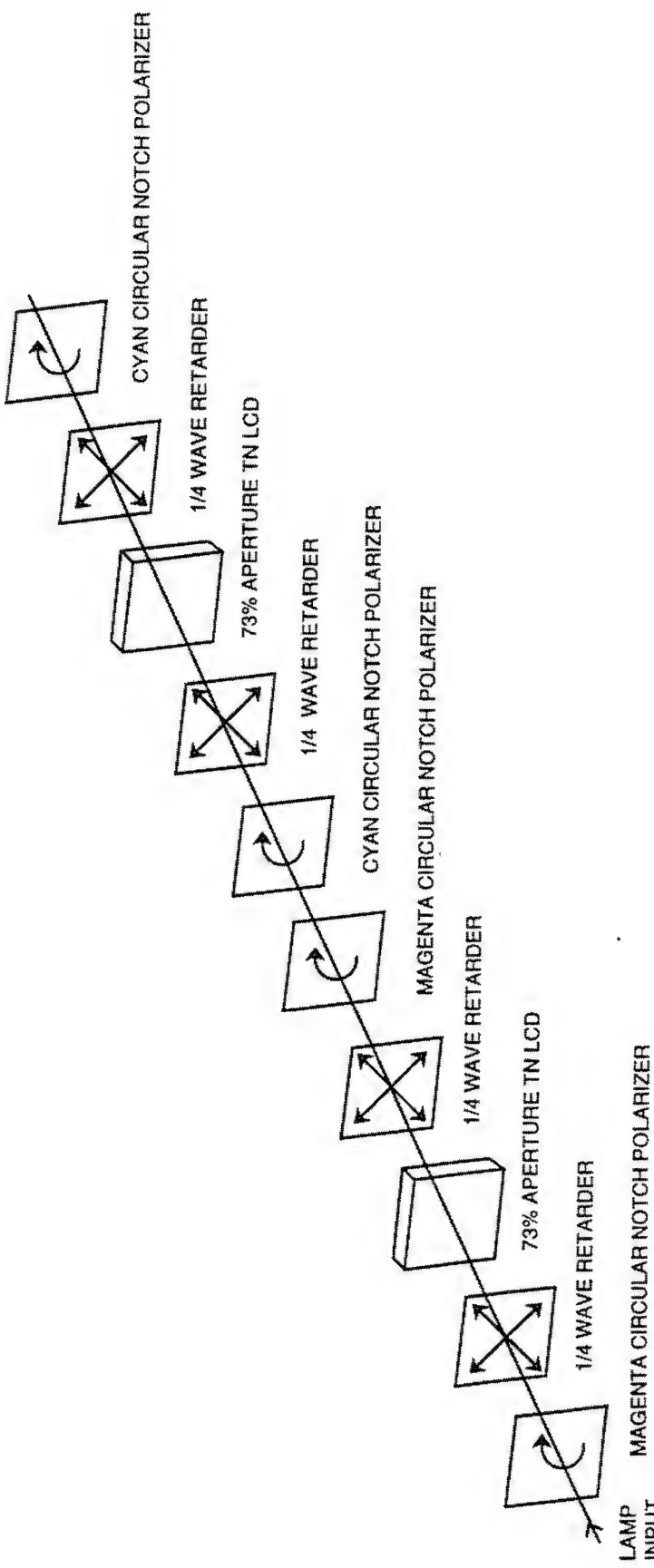


Figure 3-13. Two-Primary Color Expanded View of Stack #2 (Notch Polarizer Configuration).

The test results of Stack #2 (Notch Polarizer) follow.

Table 3-4. Stack #2 Directional Illumination Measured With Xenon Lamp and Reynard Filters

Notch Polarizer Configuration: Lamp = 9757000 fL; Contrast Ratio = 22.90			
State	fL	u'	v'
Yellow	1069000	0.2226	0.5638
Red	216100	0.3946	0.5393
Green	552300	0.1303	0.5671
Black	46690	0.1378	0.5731
Filter Location	Backlight Luminance	Stack Transmittance	
In Backlight	6450000	16.6%	
Part of Stack	9757000	11.0%	
Notch Polarizer Configuration: Lamp = 7329000 fL; Contrast Ratio = 19.01			
State	fL	u'	v'
Yellow	77940	0.2538	0.5597
Red	24140	0.4002	0.5385
Green	32810	0.1124	0.5789
Black	4101	0.1582	0.5716
Filter Location	Backlight Luminance	Stack Transmittance	
In Backlight	477200	16.3%	
Part of Stack	732900	10.6%	

Table 3-5. Stack #2 Directional Illumination Measured With Xenon Lamp and Calculated Filters (Y cutoff < 500 nm, IR cutoff > 650 nm)

Notch Polarizer Configuration: Lamp = 7252000 fL; Contrast Ratio = 23.07				
State	fL	u'	v'	
Yellow	1130000	0.2039	0.5638	
Red	205200	0.3815	0.5363	
Green	622500	0.1173	0.5734	
Black	48990	0.1296	0.5528	
Filter Location	Backlight Luminance	Stack Transmittance		
In Backlight	7252000	15.6%		
Part of Stack	9757000	11.6%		
Notch Polarizer Configuration: Lamp = 552300 fL; Contrast Ratio = 19.74				
State	fL	u'	v'	
Yellow	855340	0.2376	0.5610	
Red	22600	0.3887	0.5388	
Green	37290	0.1055	0.5777	
Black	4333	0.1437	0.5631	
Filter Location	Backlight Luminance	Stack Transmittance		
In Backlight	552300	15.5%		
Part of Stack	732900	11.7%		

Two-Primary Color Notch Polarizer Stack
Filtered Power (Reynard Filters)

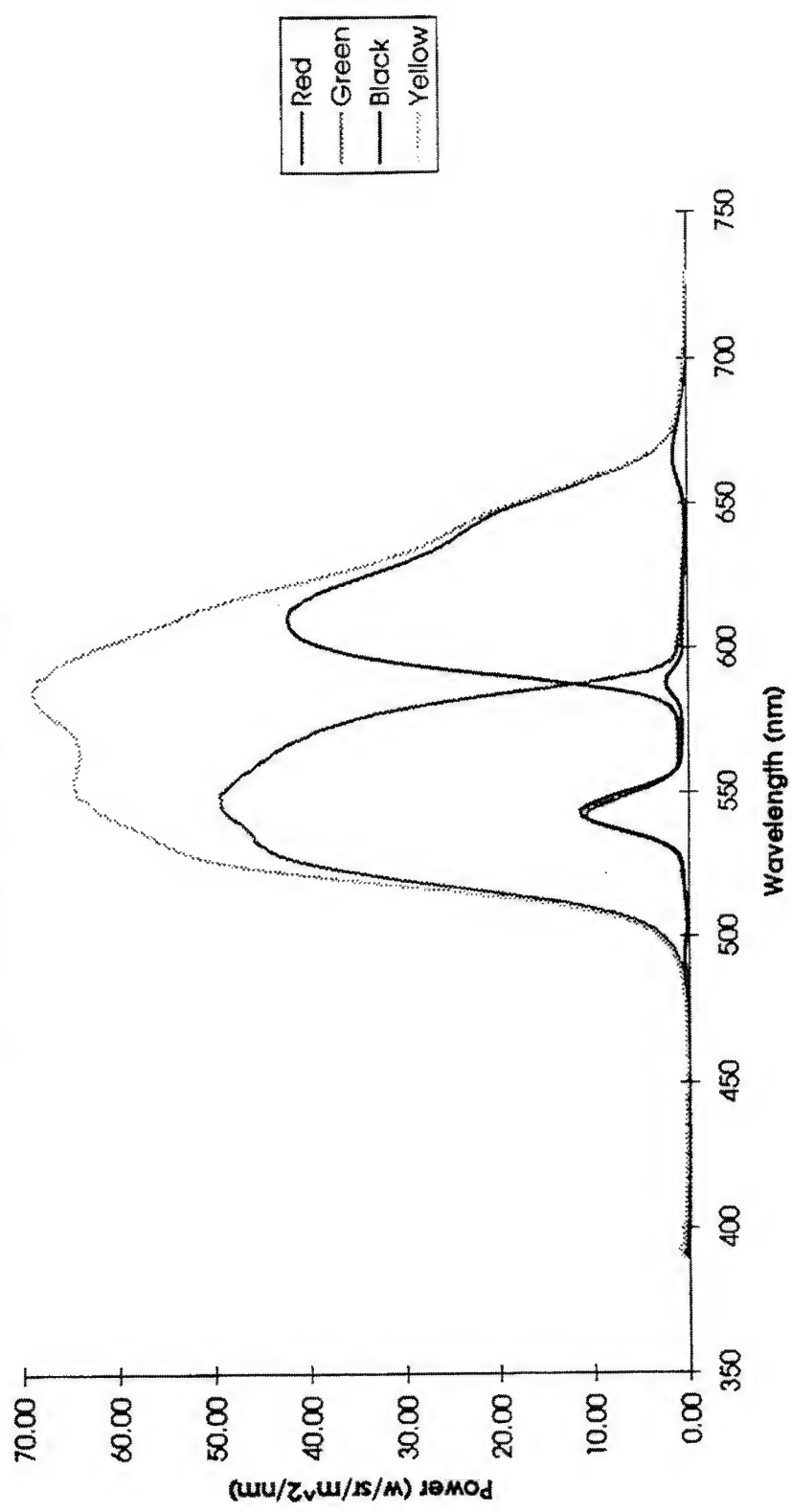


Figure 3-14. Stack #2 - Filtered Power vs. Wavelength (Xenon Lamp).

Two-Primary Color Notch Polarizer Stack

Filtered Power (Calculated Filters)

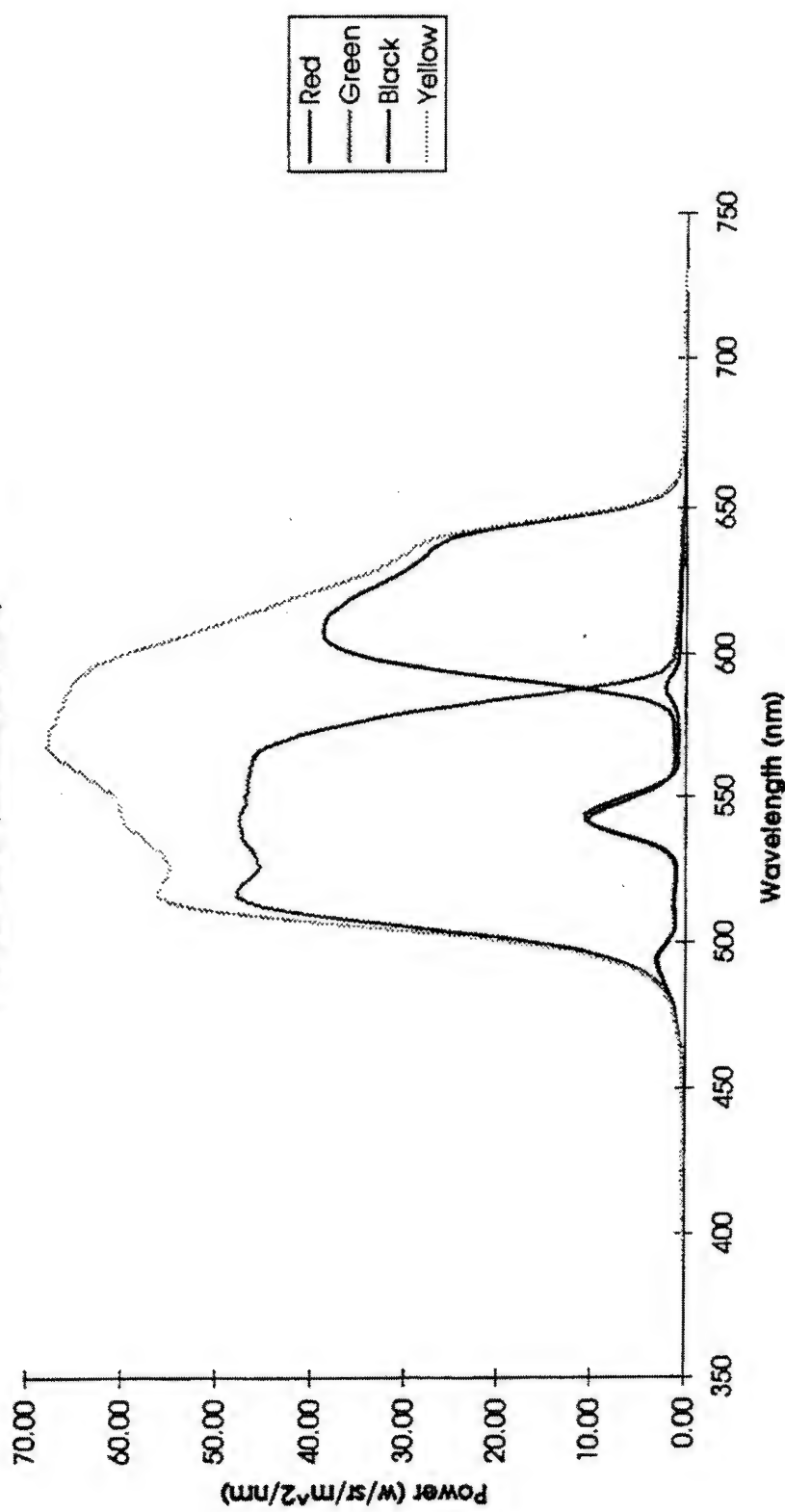


Figure 3-15. Stack #2 - Filtered Power (calculated filters) vs. Wavelength (Xenon Lamp).

Two-Primary Color Notch Polarizer Stack

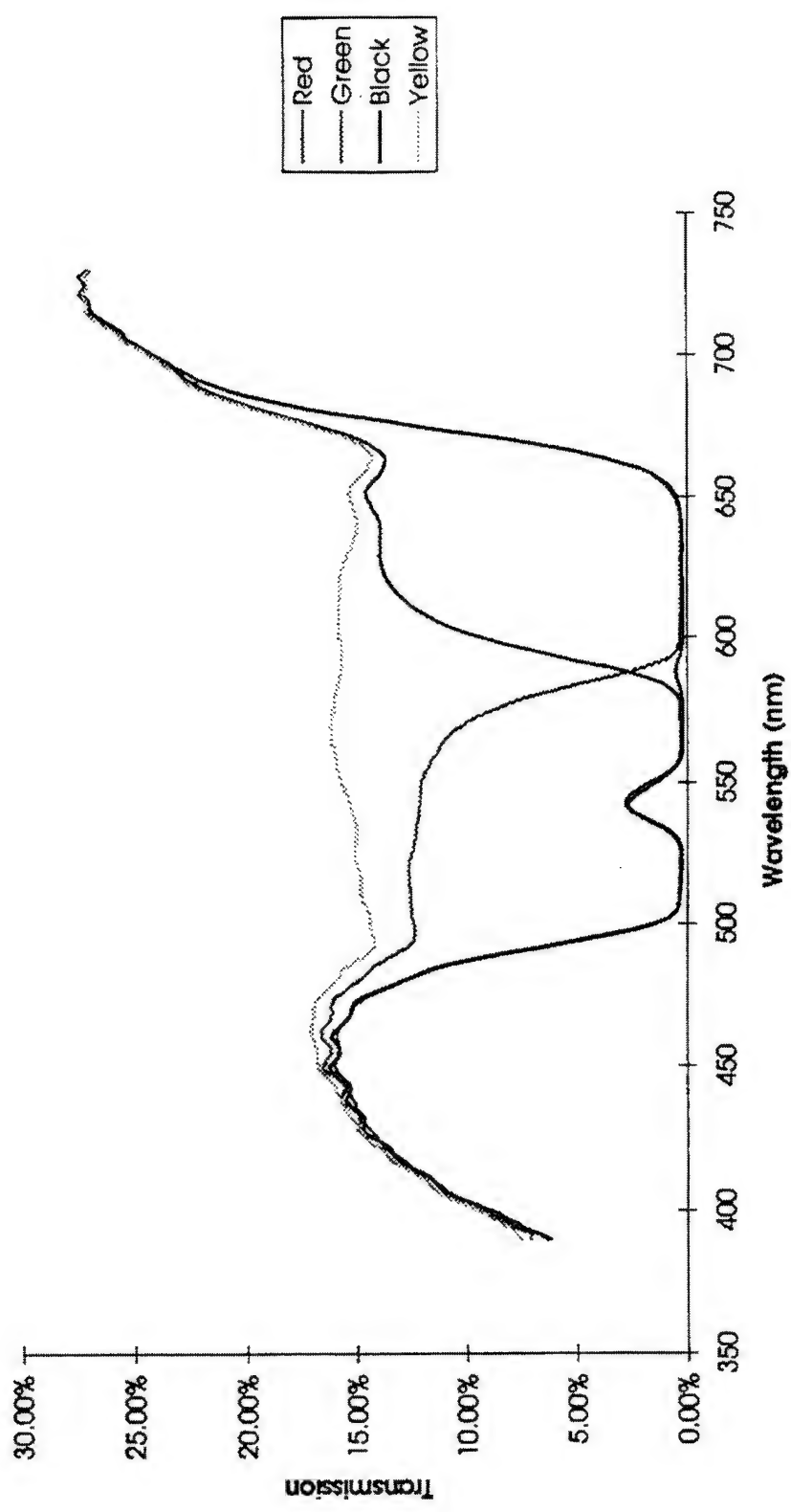


Figure 3-16. Stack #2 - Transmission vs. Wavelength (Xenon Lamp).

Two-Primary Color Notch Polarizer Stack
Filtered Transmission (Reynard Filters)

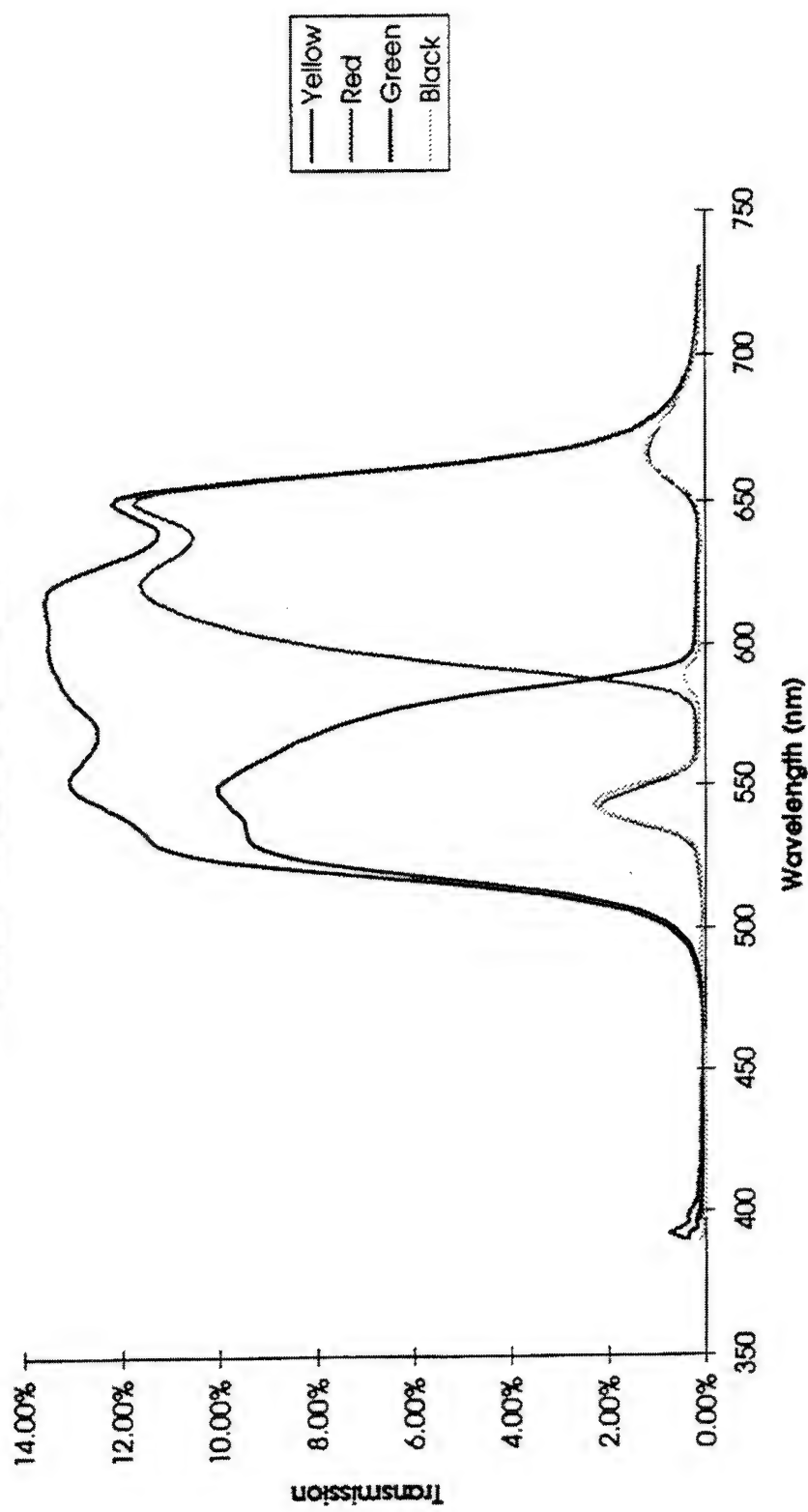


Figure 3-17. Stack #2 - Filtered Transmission vs. Wavelength (Xenon Lamp).

Two-Primary Color Notch Polarizer Stack
Filtered Transmission (Calculated Filters)

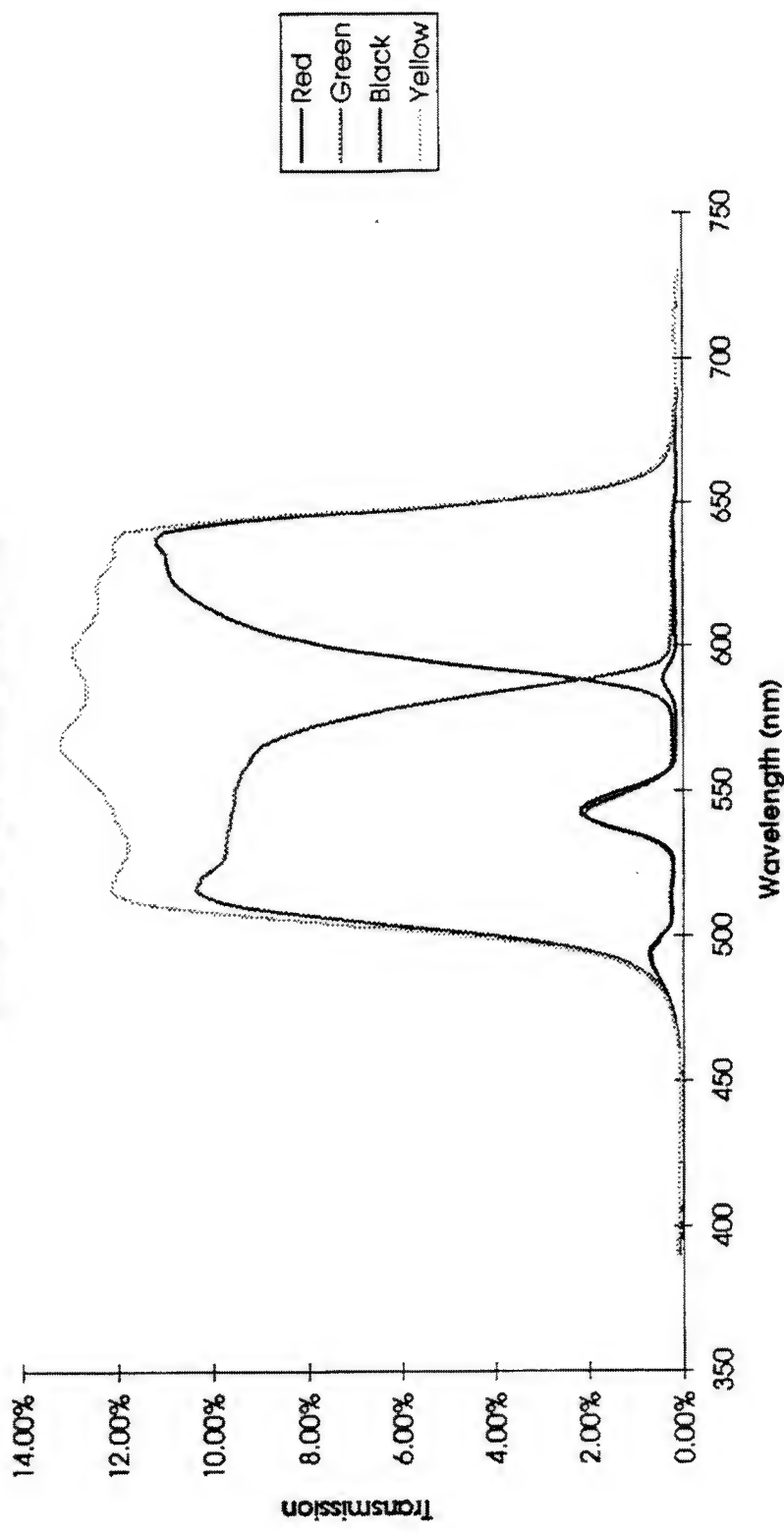


Figure 3-18. Stack #2 - Filtered Transmission (calculated filters) vs. Wavelength (Xenon Lamp).

Two-Primary Color Notch Polarizer Stack

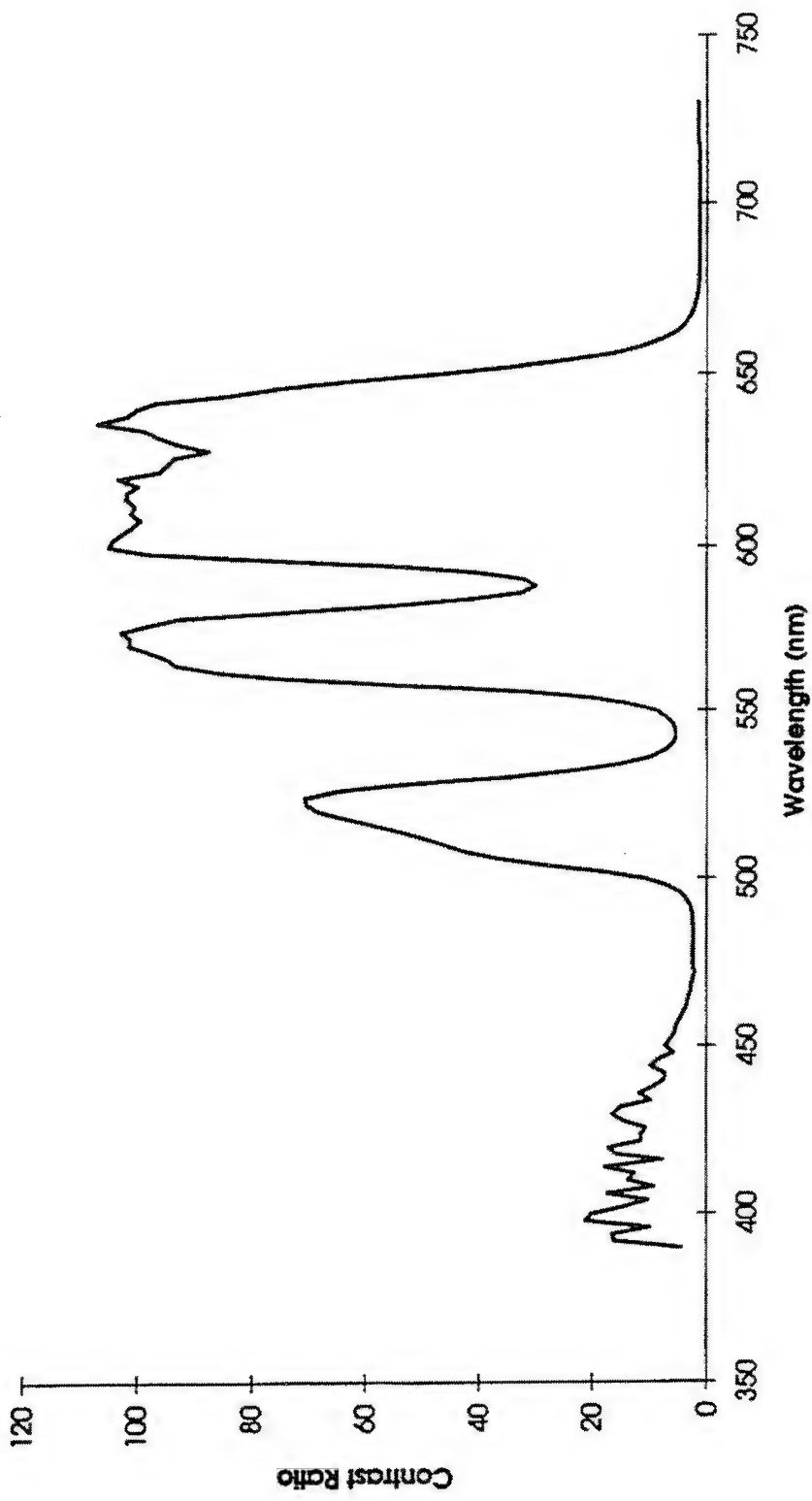


Figure 3-19. Stack #2 - Contrast Ratio vs. Wavelength (Xenon Lamp).

Two-Primary Color Notch Polarizer
Lamp Characteristics

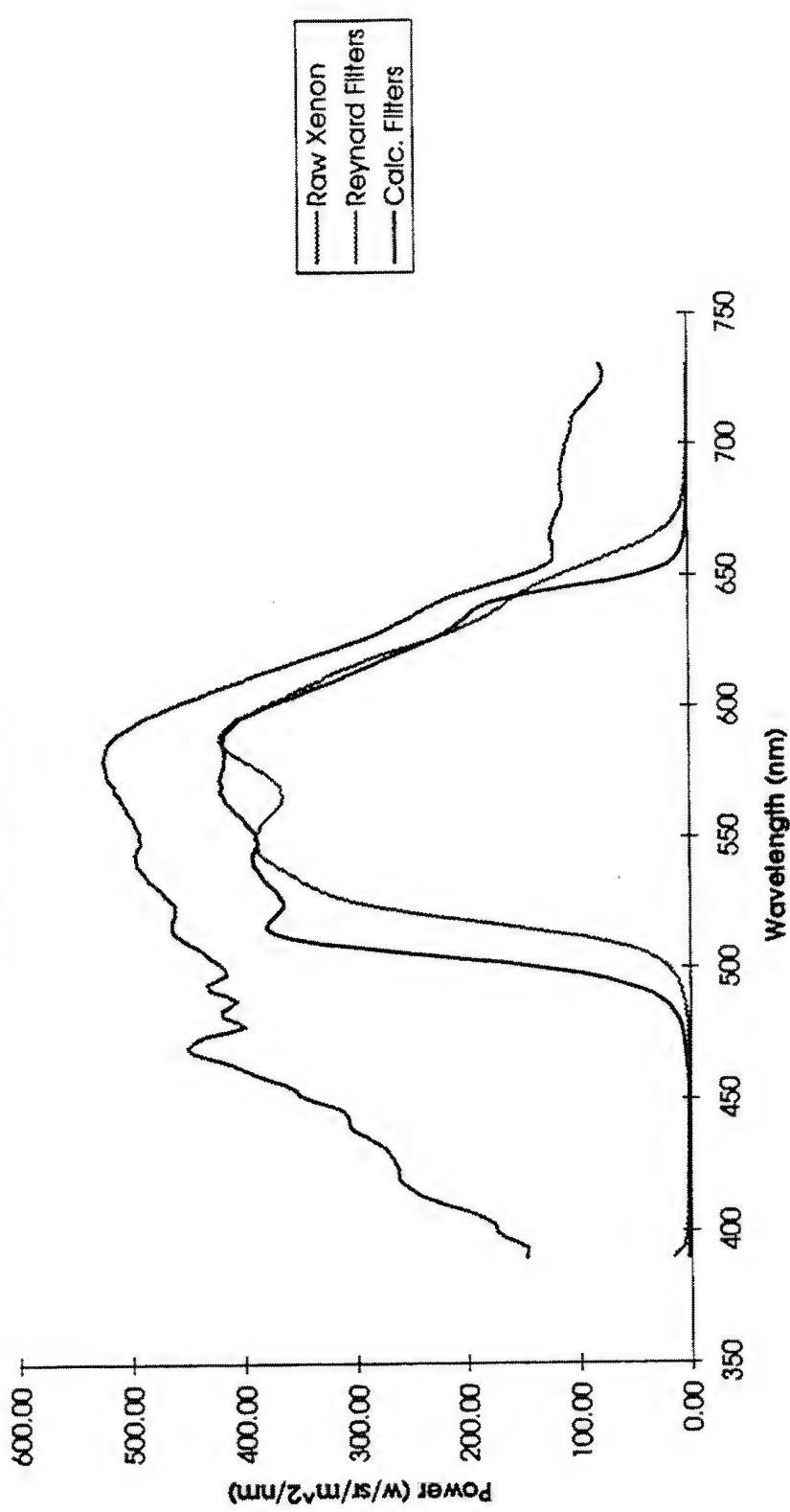


Figure 3-20. Xenon Lamp Characteristics - Power vs. Wavelength.

Two-Primary Color Notch Polarizer Stack

Filtered Power (Raymar Filters)

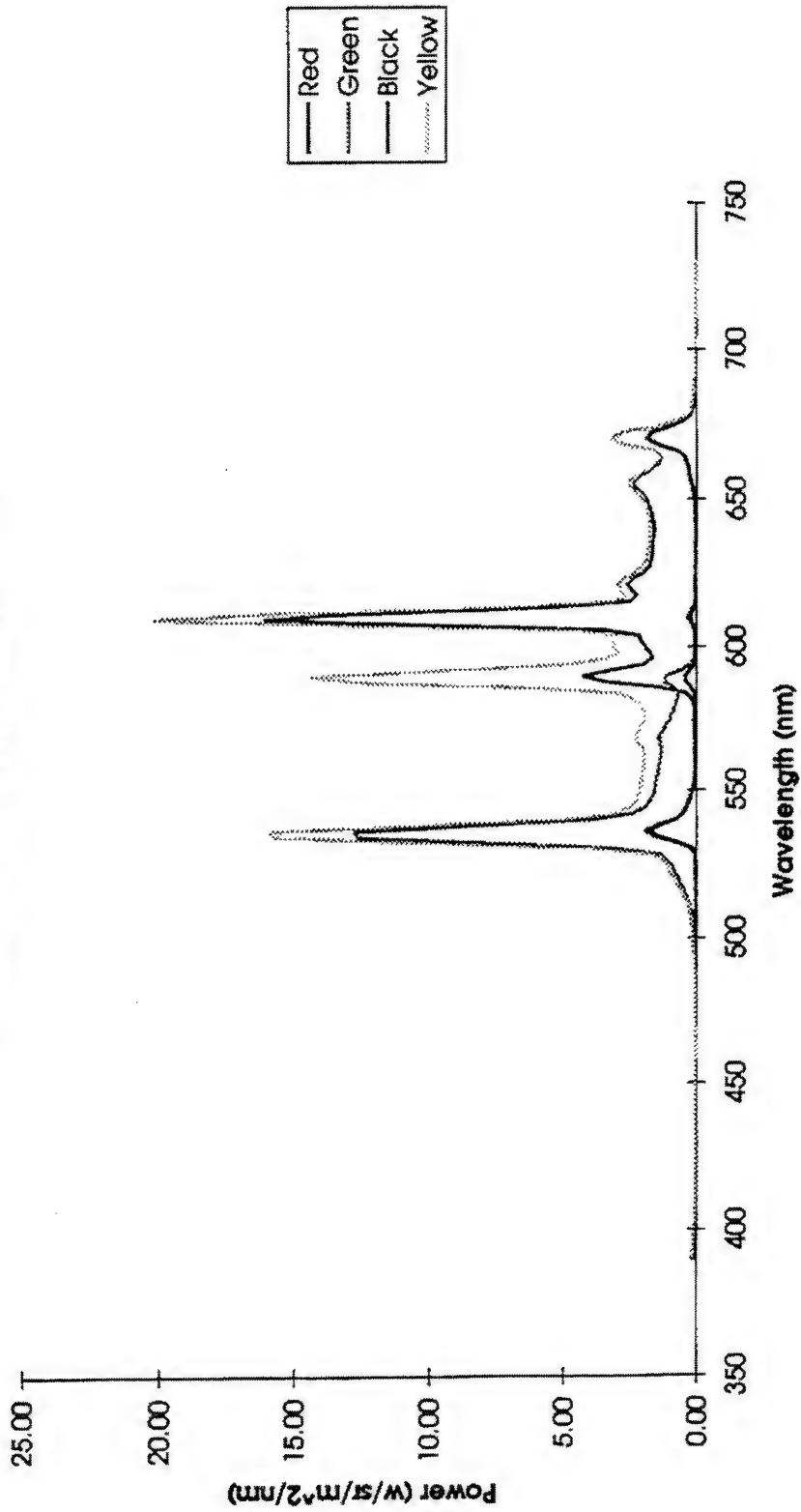


Figure 3-21. Stack #2 - Filtered Power vs. Wavelength (Tri-band Lamp #69).

Two-Primary Color Notch Polarizer Stack
Filtered Power (Calculated Filters)

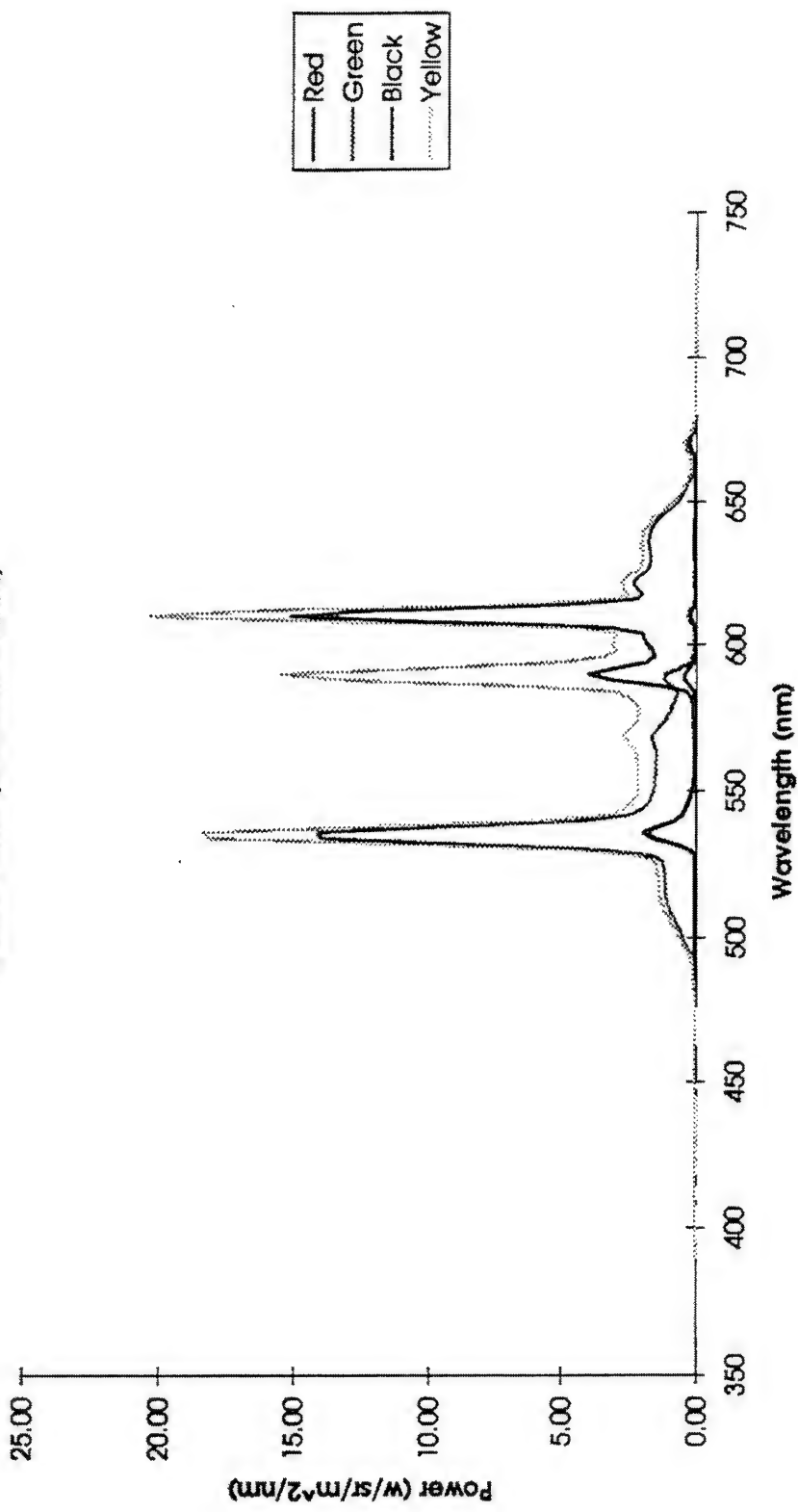


Figure 3-22. Stack #2 - Filtered Power (calculated filters) vs. Wavelength (Tri-band Lamp #69).

Two-Primary Color Notch Polarizer Stack Lamp Characteristics

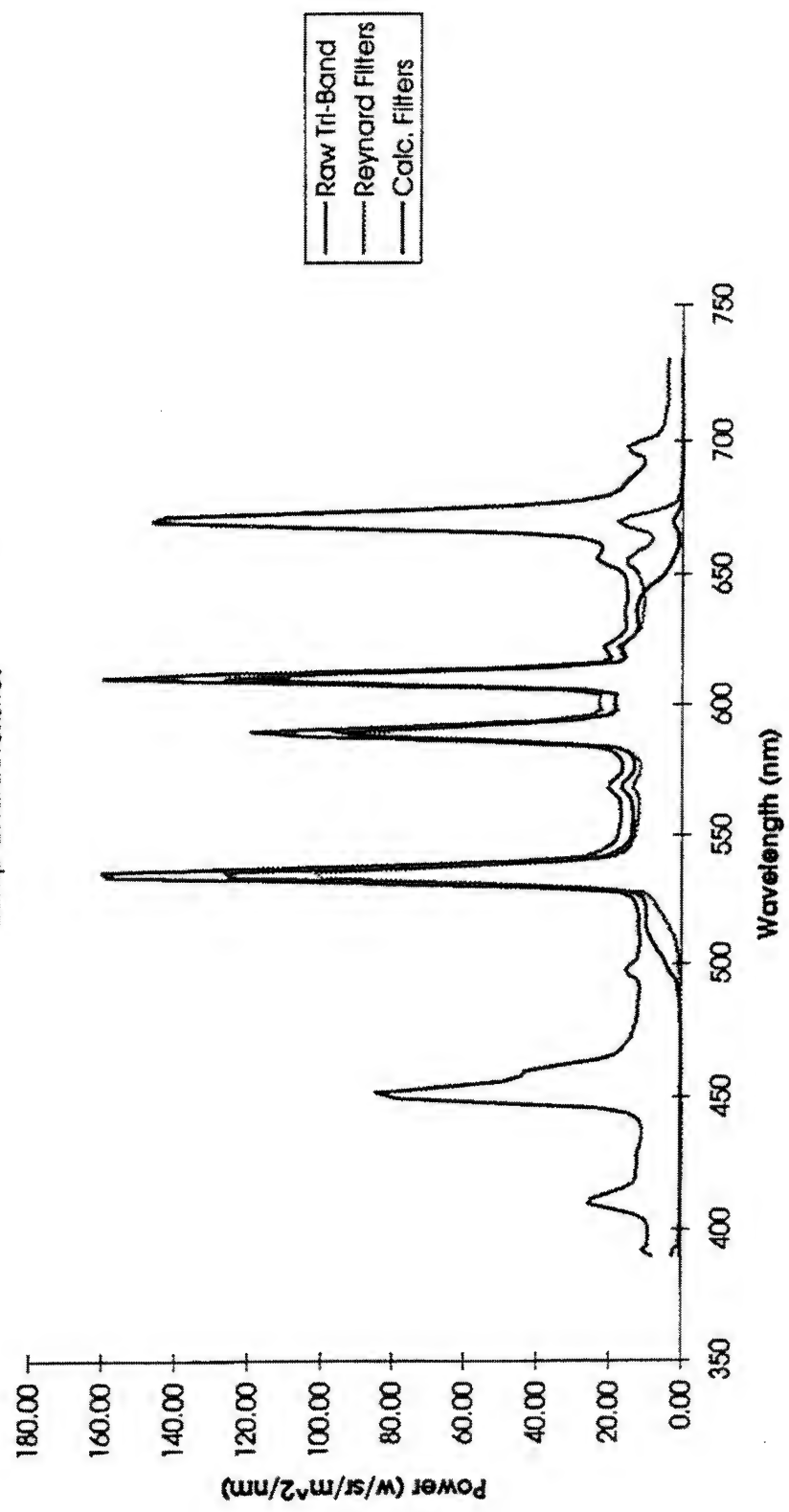


Figure 3-23. Tri-band Lamp Characteristics - Power vs. Wavelength.

3.6 Stack #3 Configuration and Results

Stack #3 is the first of two hybrid designs (hybrid #1), which consists of two 73% aperture light valve LCD cells, one magenta dichroic polarizing cell, two red dichroic sheet polarizers, one neutral density sheet polarizer, one cyan dichroic polarizing cell, and one cyan notch polarizer with two wide-band $\lambda/4$ retarders, as shown in Figure 3-24. Stack #3 has an image plane to image plane distance of 0.051 in.

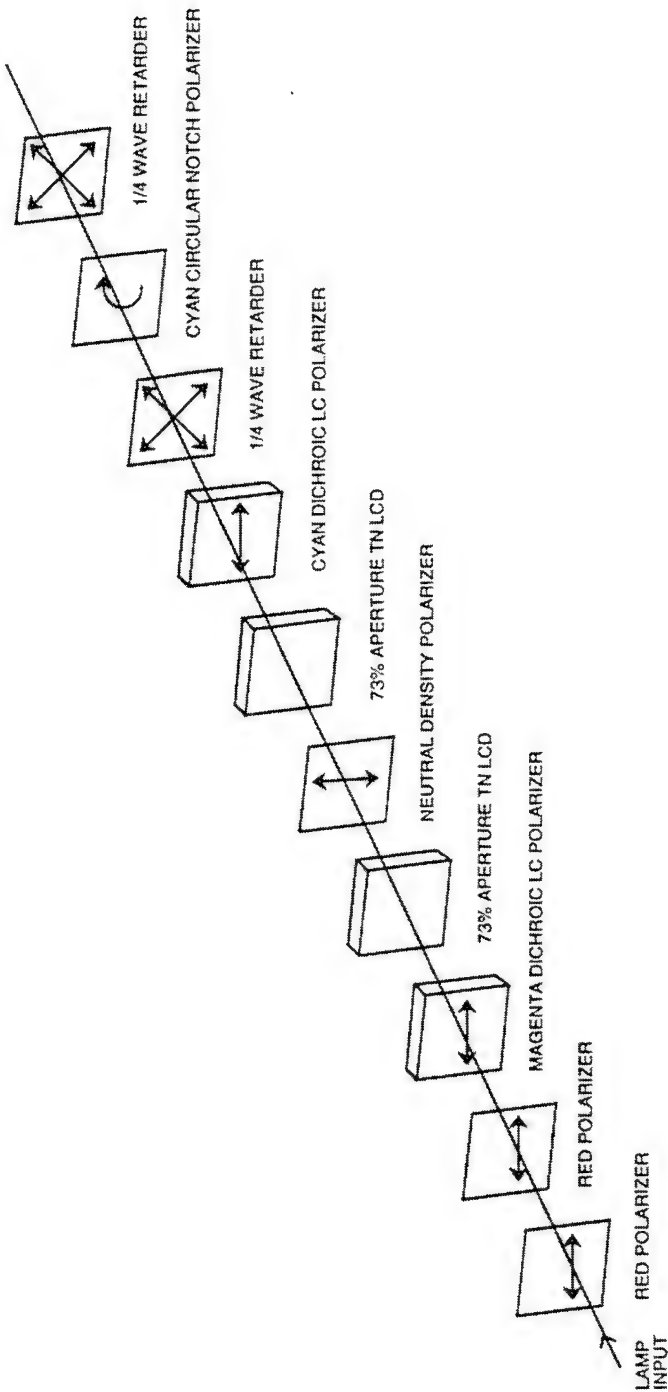


Figure 3-24. Two-Primary Color Expanded View of Stack #3 (Hybrid).

The test results of Stack #3 (Hybrid #1) follow.

Table 3-6. Stack #3 (Hybrid #1) Directional Illumination Measured With Xenon Lamp and Reynard Filters

Hybrid #1 Configuration: Lamp = 9565000 fL ; Contrast Ratio = 459.53				
State	fL	u'	v'	
Yellow	619900	0.2300	0.5628	
Red	83560	0.4704	0.5287	
Green	172500	0.1066	0.5782	
Black	1349	0.2740	0.5556	
Filter Location	Backlight Luminance	Stack Transmittance		
In Backlight	6410000	9.7%		
Part of Stack	9565000	6.5%		
Hybrid #1 Configuration: Lamp = 7255000 fL ; Contrast Ratio = 487.52				
State	fL	u'	v'	
Yellow	57820	0.2609	0.5587	
Red	10750	0.4673	0.5292	
Green	13560	0.0893	0.5815	
Black	118.6	0.2938	0.5530	
Filter Location	Backlight Luminance	Stack Transmittance		
In Backlight	592600	9.8%		
Part of Stack	725900	8.0%		

Table 3-7. Stack #3 Directional Illumination Measured With Xenon Lamp and Calculated Filters (Y cutoff < 500 nm, IR cutoff > 650 nm)

Hybrid #1 Configuration: Lamp = 7109000 FL; Contrast Ratio = 456.26			
State	FL	u'	v'
Yellow	663000	0.2086	0.5634
Red	75960	0.4654	0.5298
Green	204700	0.0913	0.5741
Black	1425	0.2493	0.5502
Filter Location	Backlight Luminance	Stack Transmittance	
In Backlight	7109000	9.3%	
Part of Stack	9565000	6.9%	

Hybrid #1 Configuration: Lamp = 7259000 FL; Contrast Ratio = 487.52			
State	FL	u'	v'
Yellow	533350	0.2454	0.5601
Red	8928	0.4559	0.5313
Green	13360	0.0842	0.5798
Black	225.3	0.2511	0.5549
Filter Location	Backlight Luminance	Stack Transmittance	
In Backlight	547000	9.8%	
Part of Stack	725900	7.4%	

Two-Primary Color Stack #3 = Hybrid #1
Filtered Power (Reynard Filters)

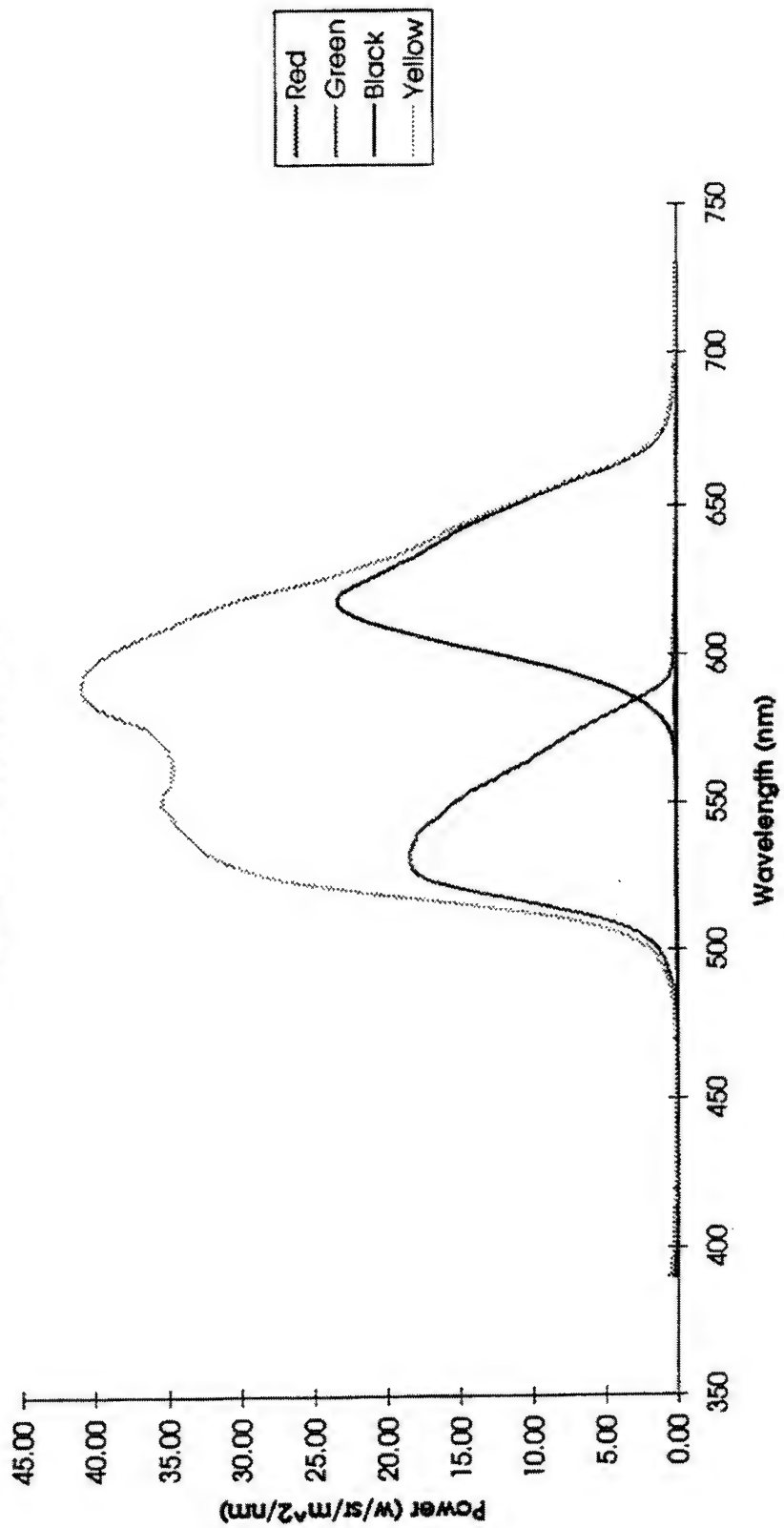


Figure 3-25. Stack #3 - Filtered Power vs. Wavelength (Xenon Lamp).

Two-Primary Color Stack #3 = Hybrid #1
Filtered Power (Calculated Filters)

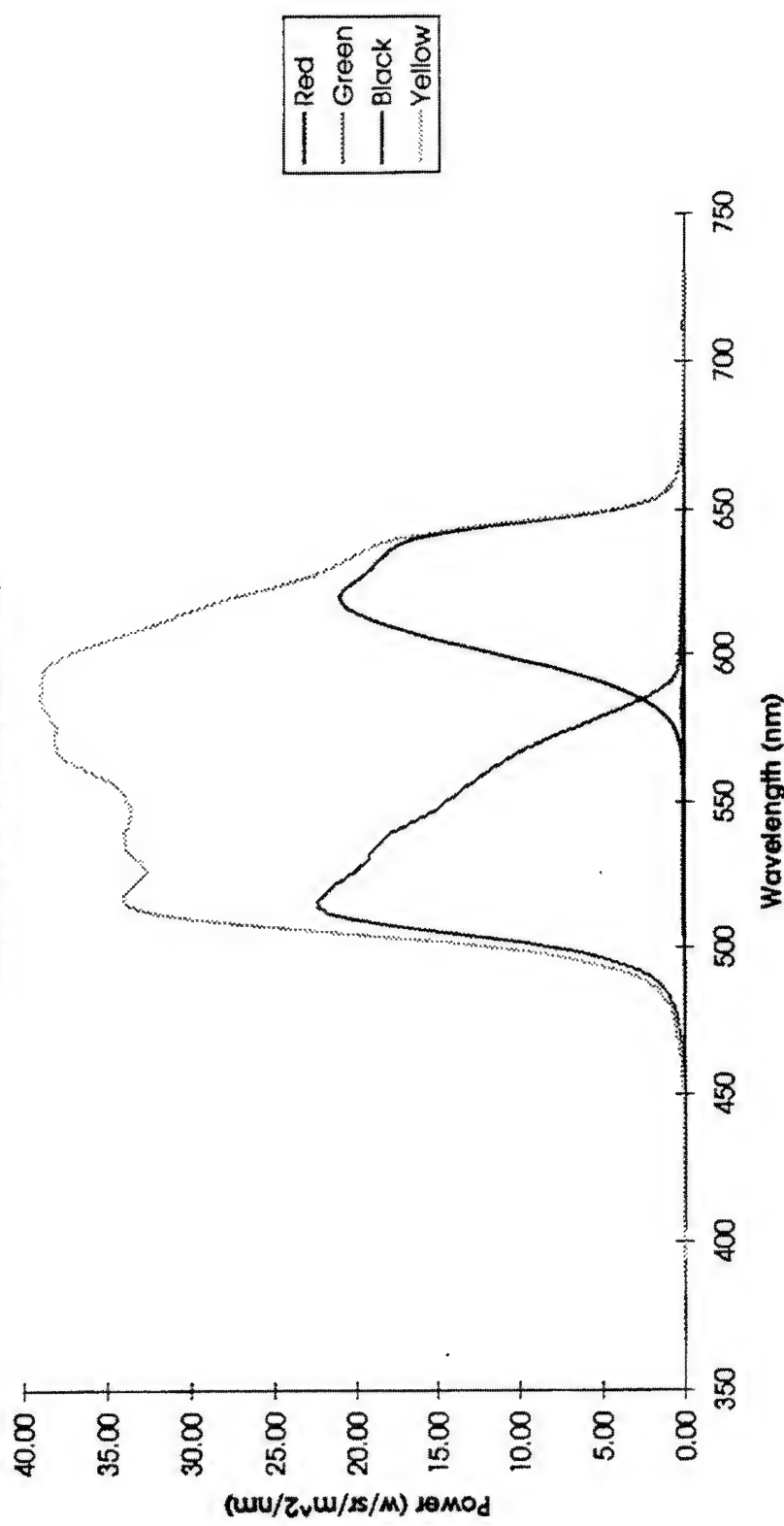


Figure 3-26. Stack #3 - Filtered Power (calculated filters) vs. Wavelength (Xenon Lamp).

Two-Primary Color Stack #3 = Hybrid #1

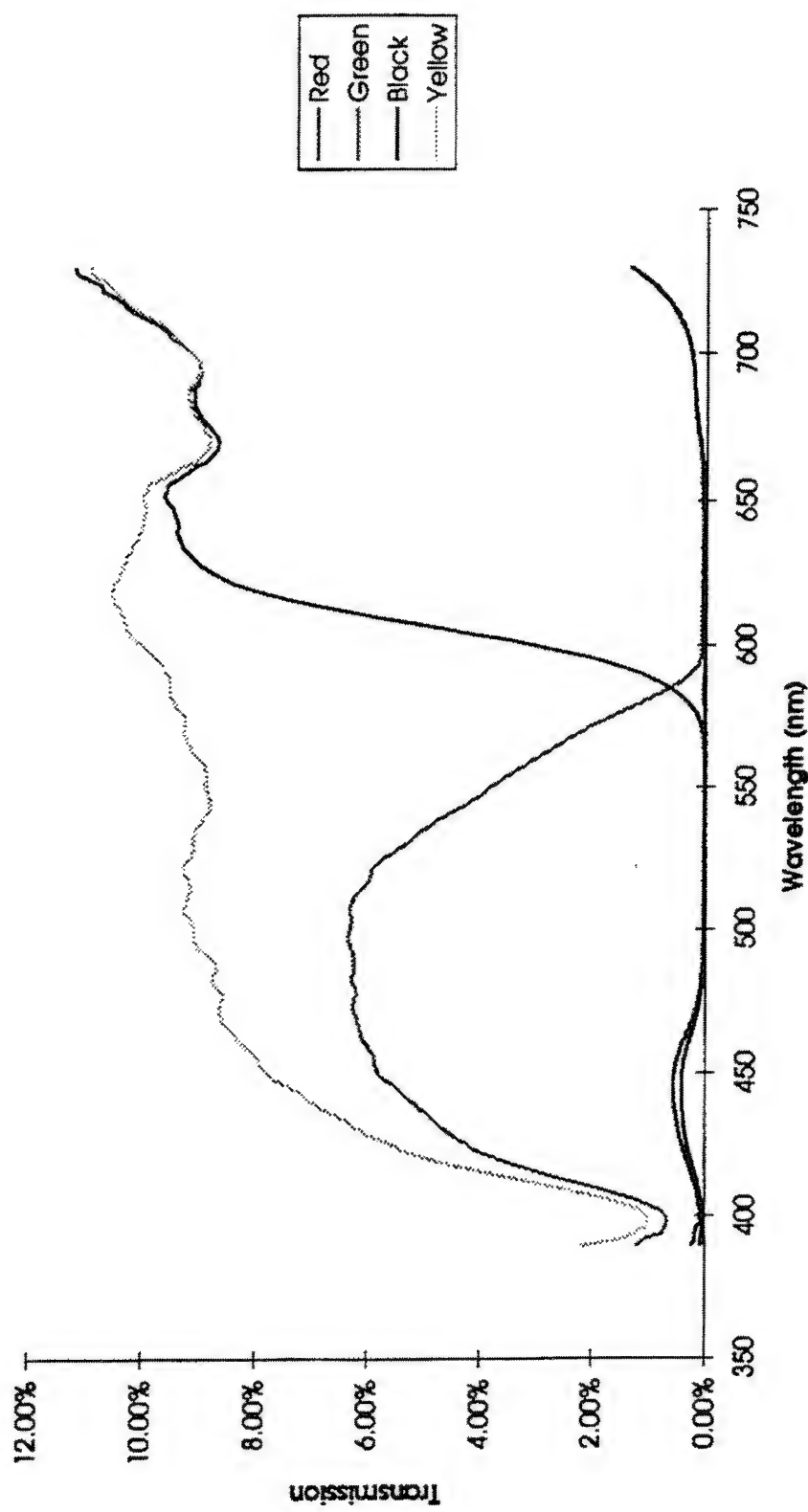


Figure 3-27. Stack #3 Transmission vs. Wavelength (Xenon Lamp).

Two-Primary Color Stack #3 = Hybrid #1
Filtered Transmission (Reynard Filters)

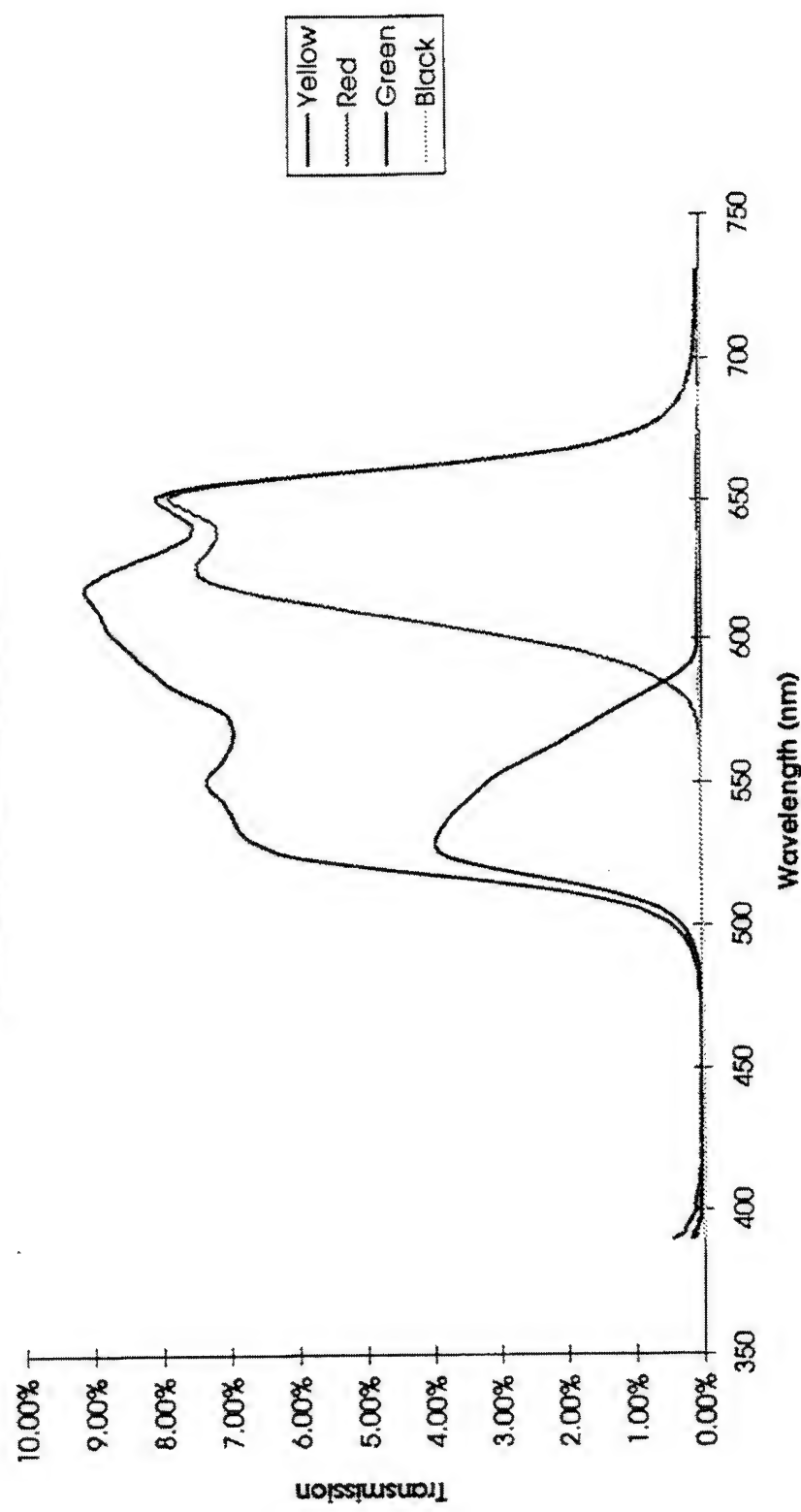


Figure 3-28. Stack #3 - Filtered Transmission vs. Wavelength (Xenon Lamp).

Two-Primary Color Stack #3 = Hybrid #1
Filtered Transmission (Calculated Filters)

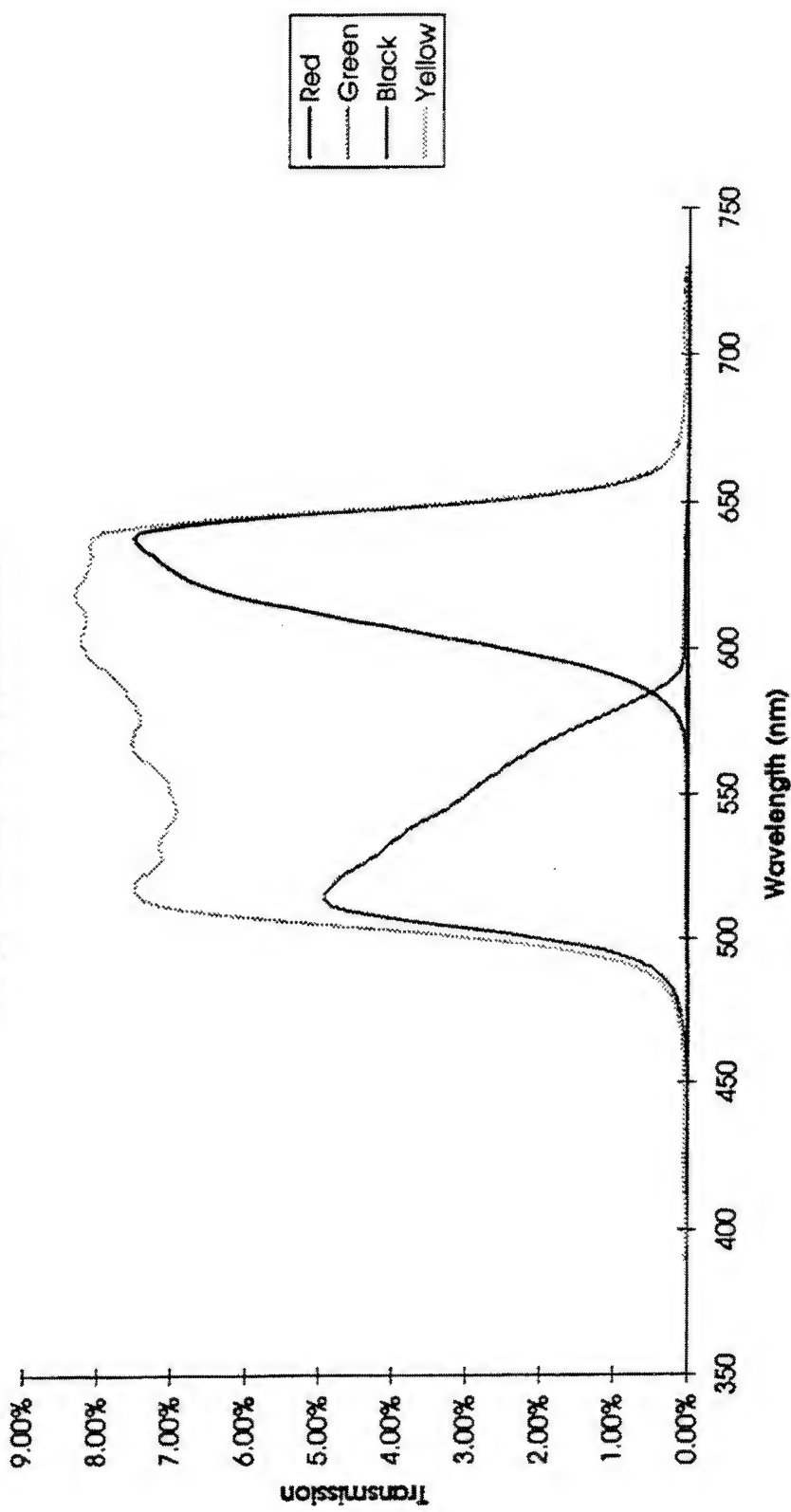


Figure 3-29. Stack #3 - Filtered Transmission (calculated filters) vs. Wavelength (Xenon Lamp).

Two-Primary Color Stack #3 = Hybrid #1

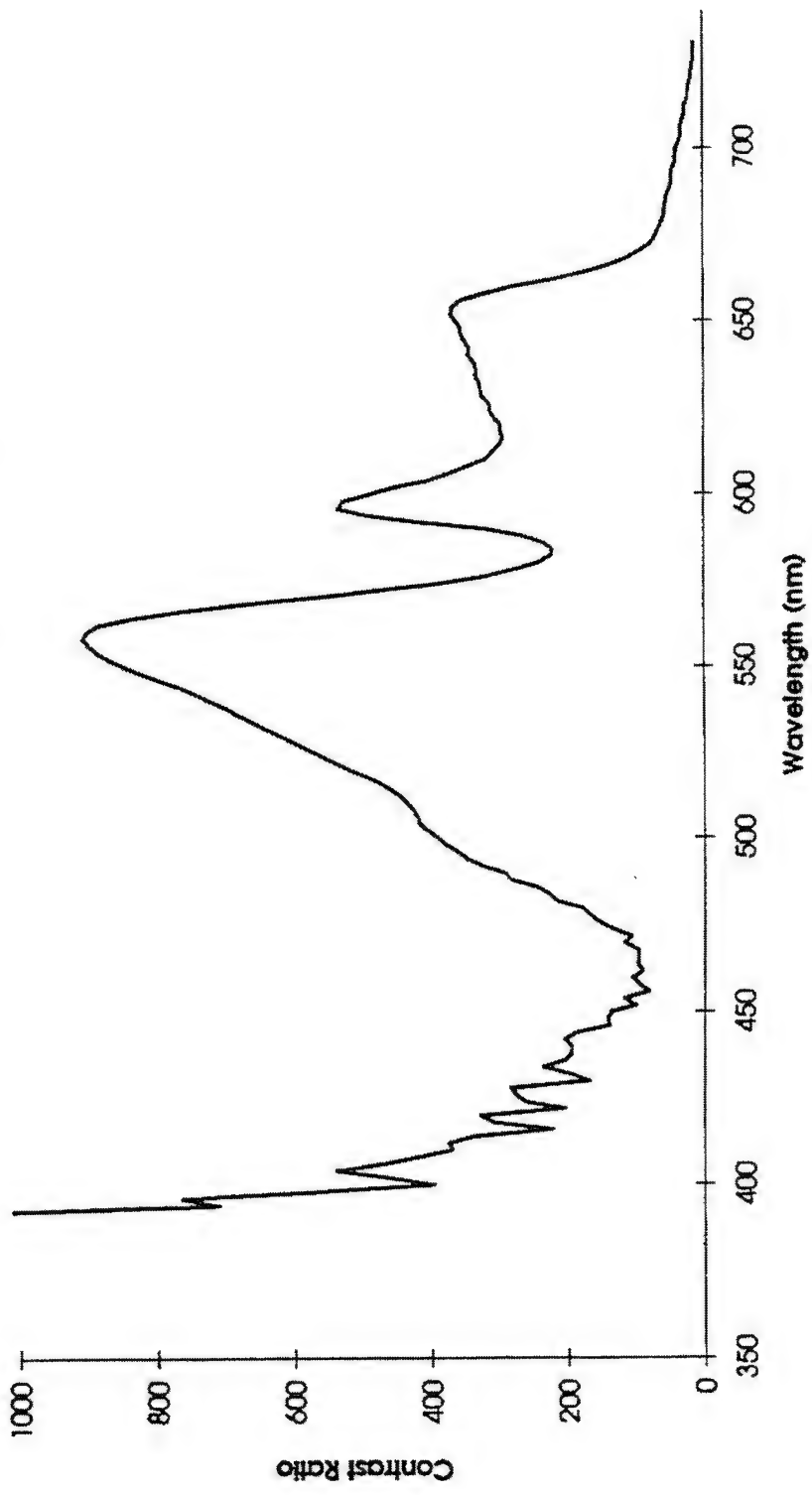


Figure 3-30. Stack #3 - Contrast Ratio vs. Wavelength (Xenon Lamp).

Two-Primary Color Stack #3 = Hybrid #1
Lamp Characteristics

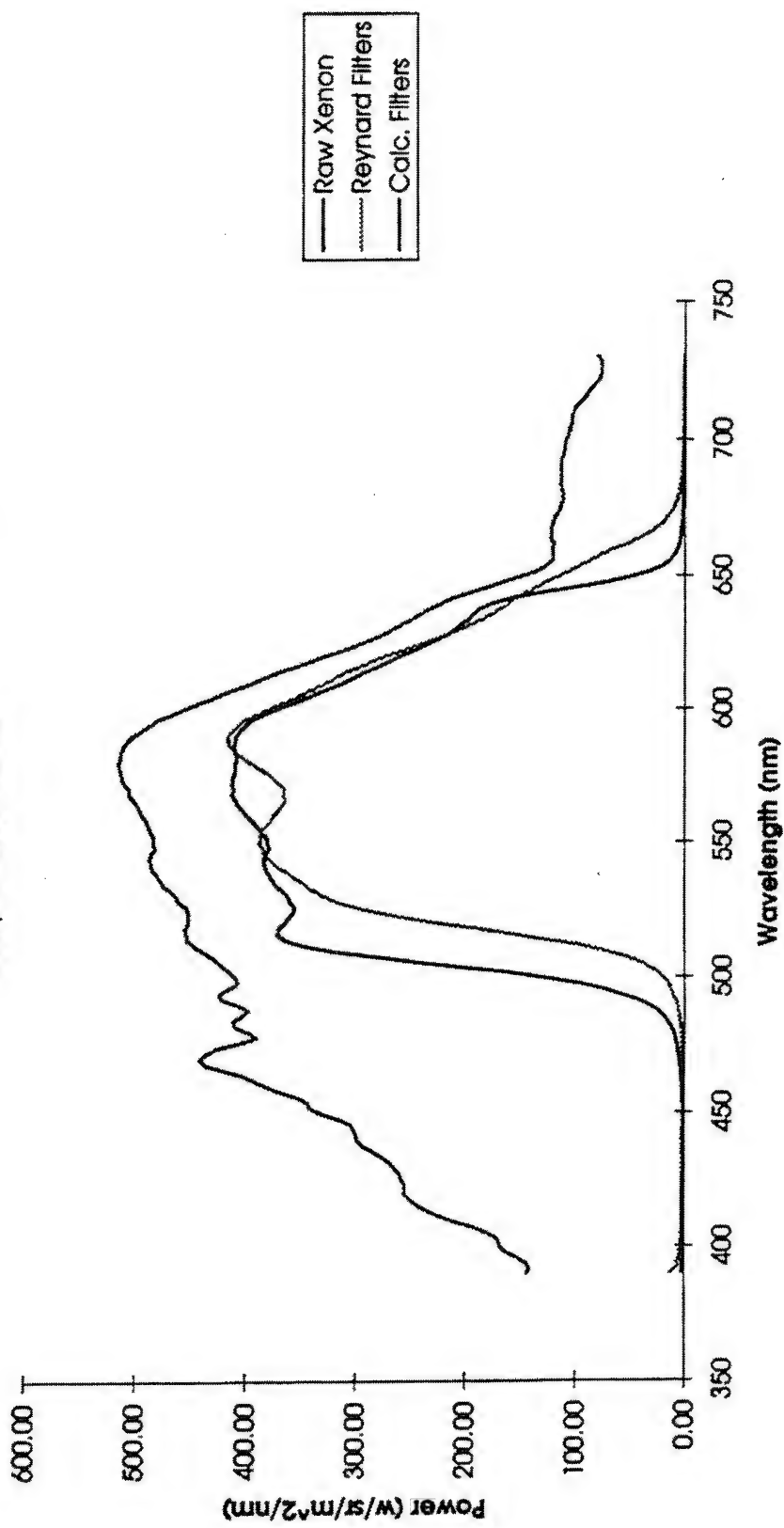


Figure 3-31. Xenon Lamp Characteristics - Power vs. Wavelength

Two-Primary Color Stack #3 = Hybrid #1
Filtered Power (Reynard Filters)

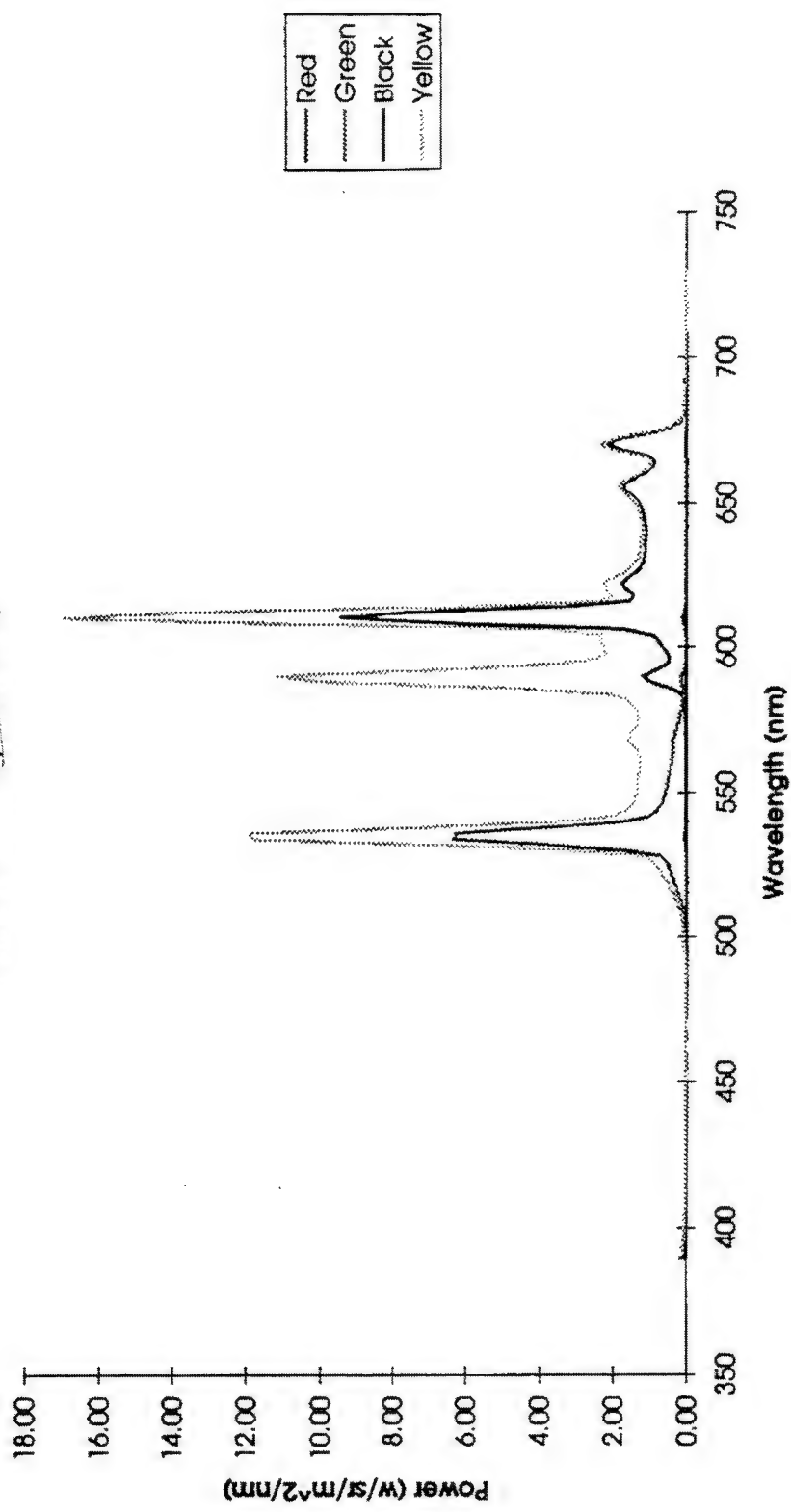


Figure 3-32. Stack #3 - Filtered Power vs. Wavelength (Tri-band Lamp #69)

Two-Primary Color Stack #3 = Hybrid #1

Filtered Power (Calculated Filters)

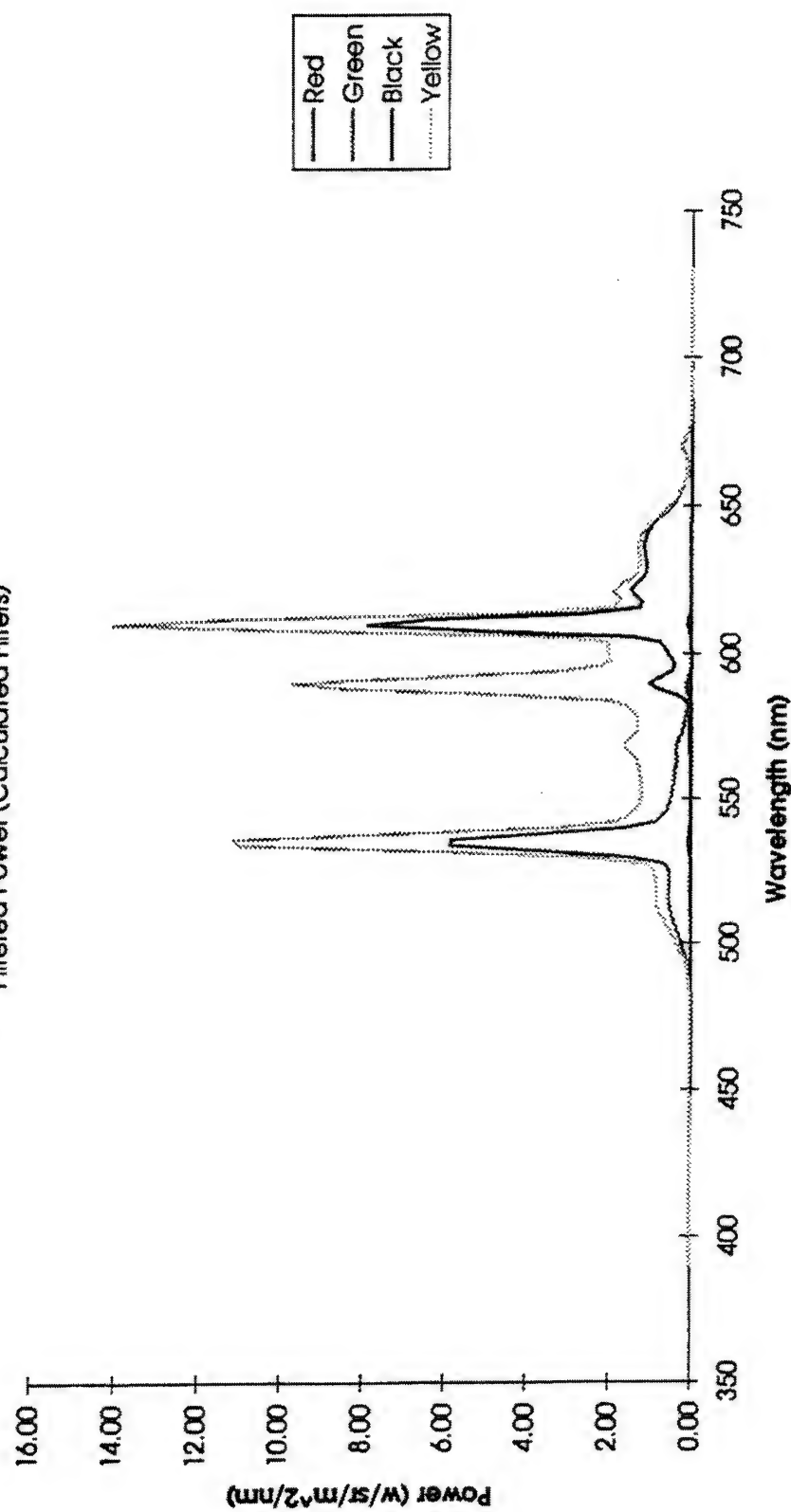


Figure 3-33. Stack #3 - Filtered Power (calculated filters) vs. Wavelength (Tri-band Lamp #69).

Two-Primary Color Stack #3 = Hybrid#1
Lamp Characteristics

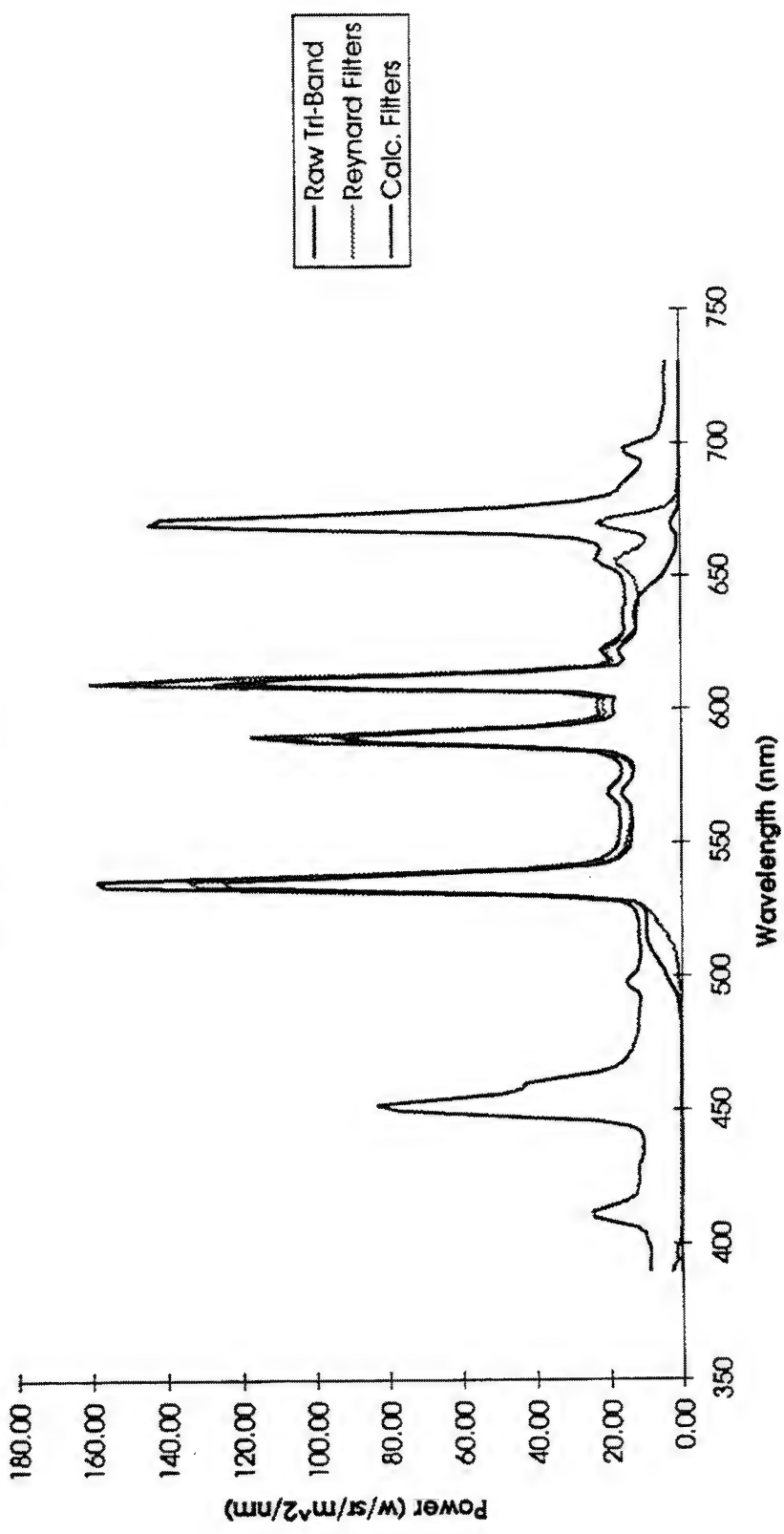


Figure 3-34. Tri-Band Lamp Characteristics - Power vs. Wavelength.

Two-Primary Color Stack #3 = Hybrid #1

Filtered Power (Calculated Filters)

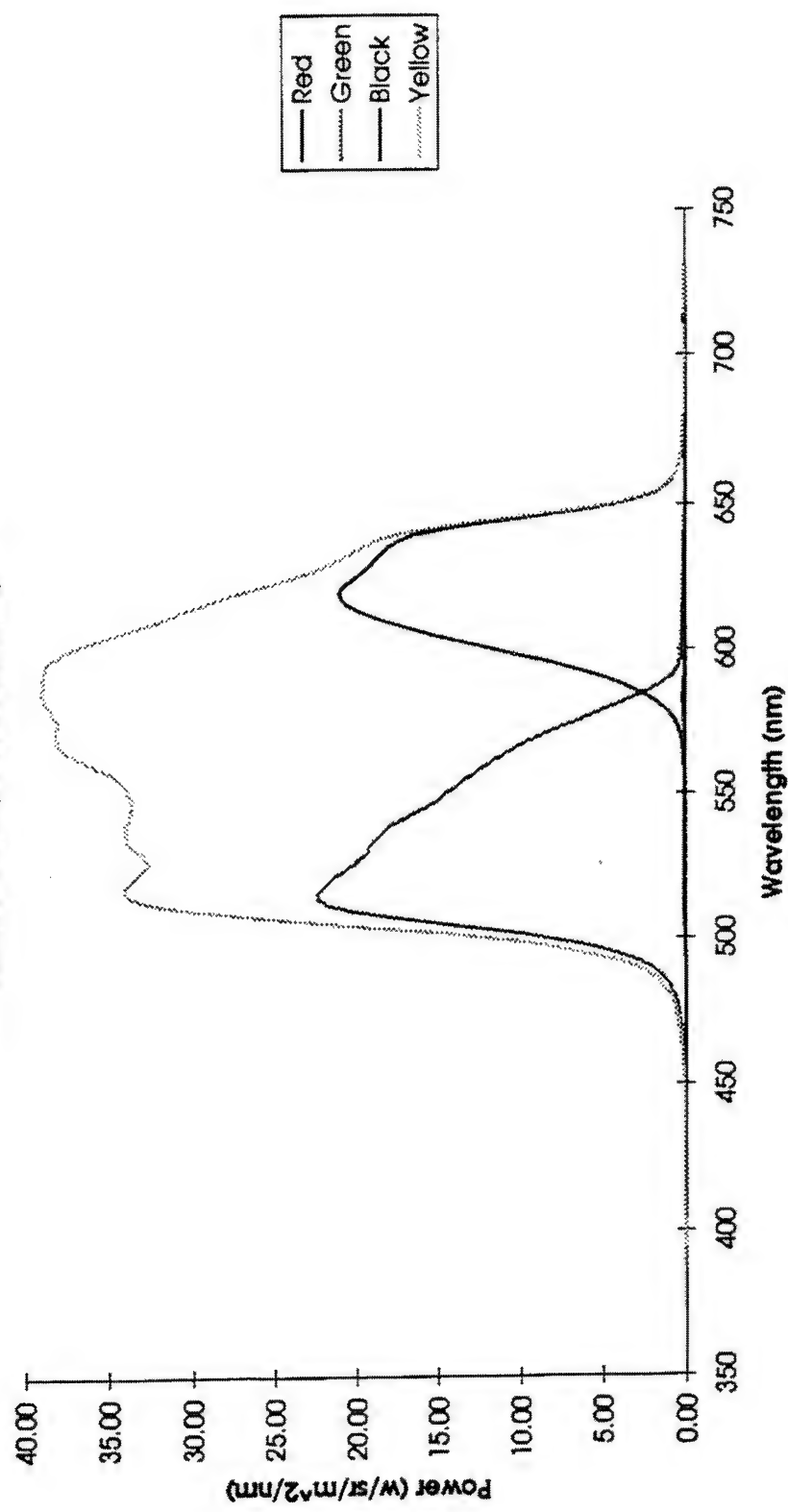


Figure 3-35. Stack #3 - Gray Scale: Voltage vs. Transmission vs. Wavelength (Red) (Xenon Lamp).

Two-Primary Color Stack #3 = Hybrid #1

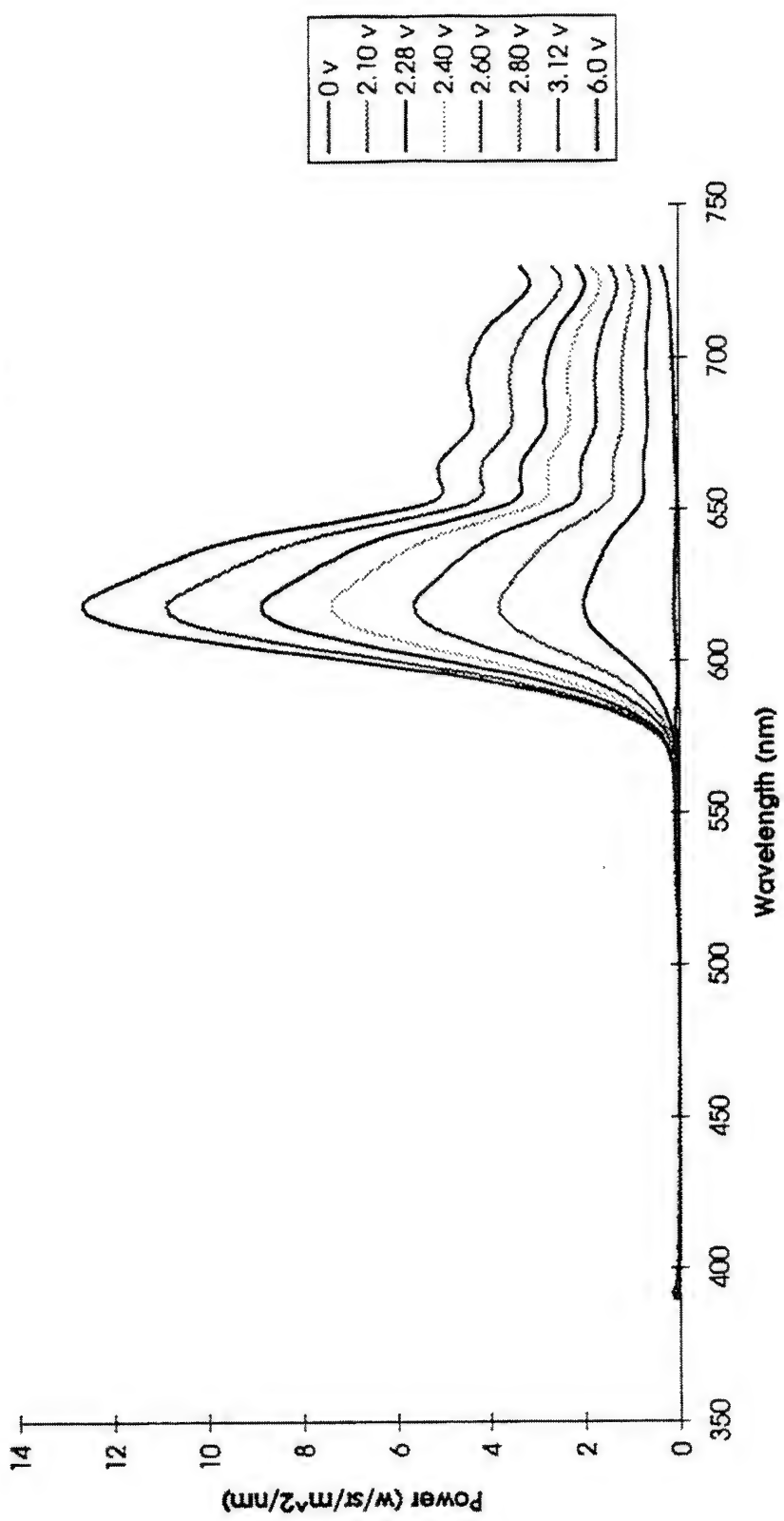


Figure 3-36. Stack #3 - Gray Scale: Voltage vs. Power vs. Wavelength (Red) (Xenon Lamp).

Two-Primary Color Stack #3 = Hybrid #1

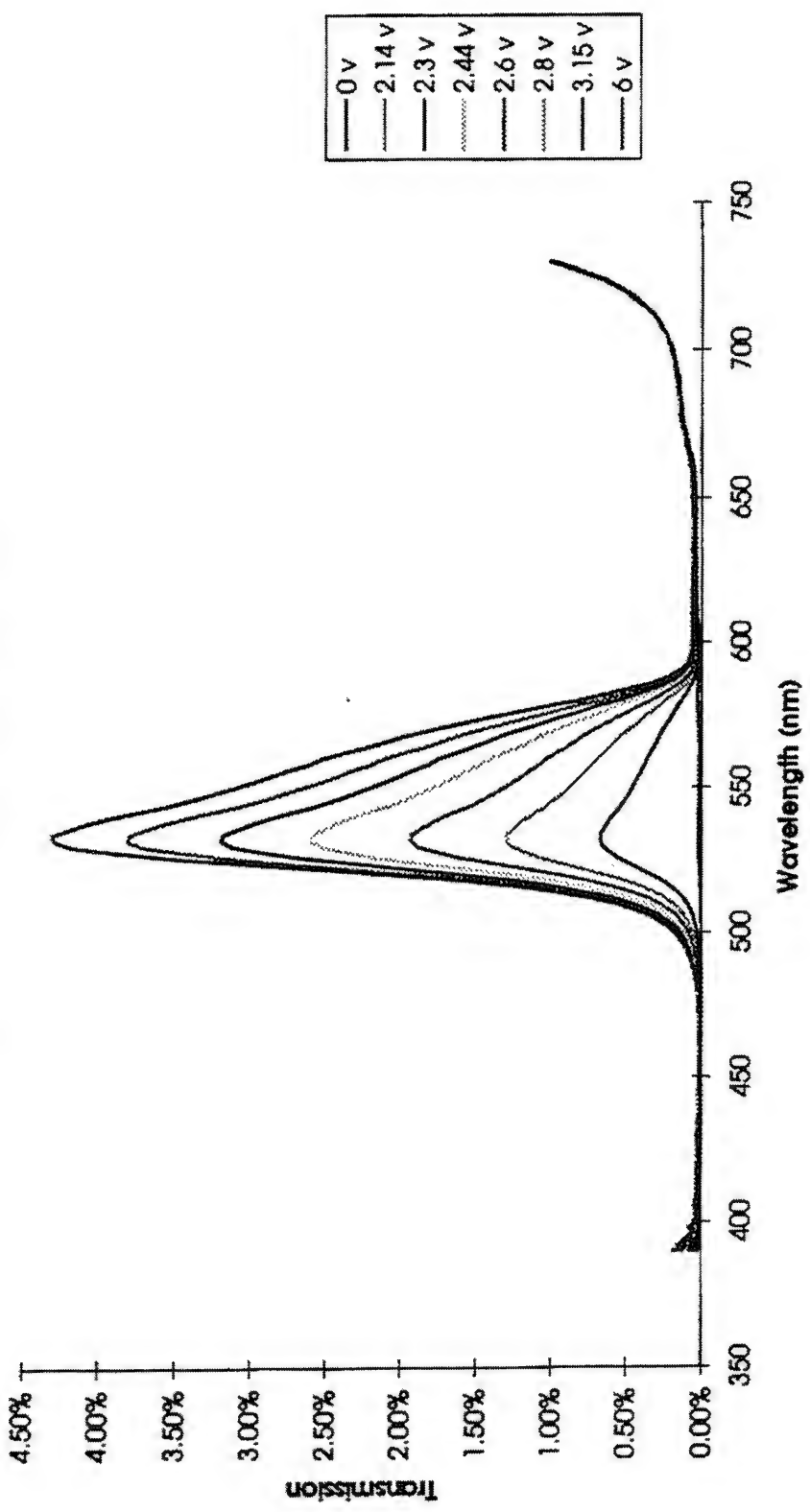


Figure 3-37. Stack #3 - Gray Scale: Voltage vs. Transmission vs. Wavelength (Green) (Xenon Lamp).

Two-Primary Color Stack #3 = Hybrid #1

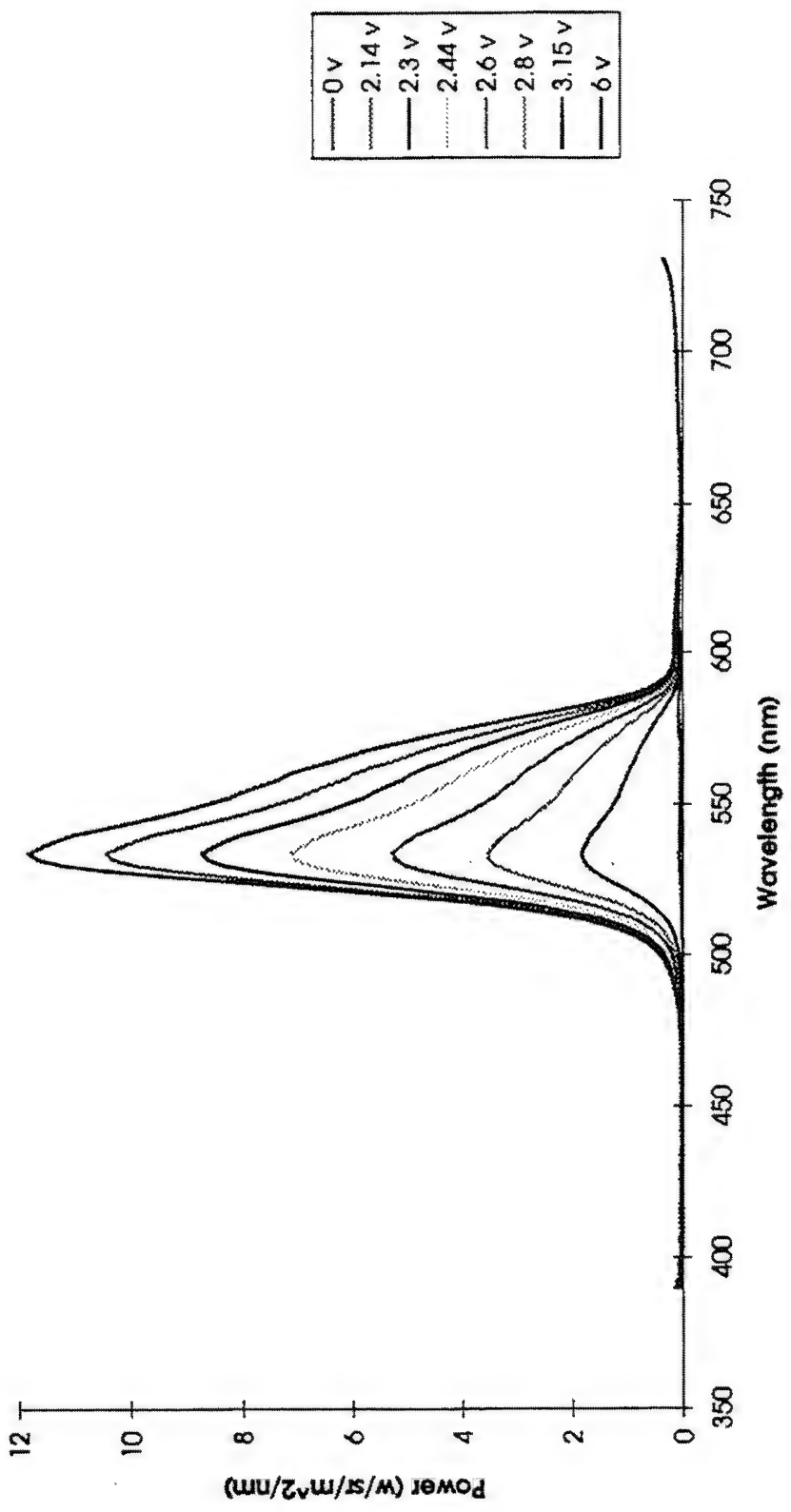


Figure 3-38. Stack #3 - Gray Scale: Voltage vs. Power vs. Wavelength (Green) (Xenon Lamp).

Two-Primary Color Stack #3 = Hybrid #1

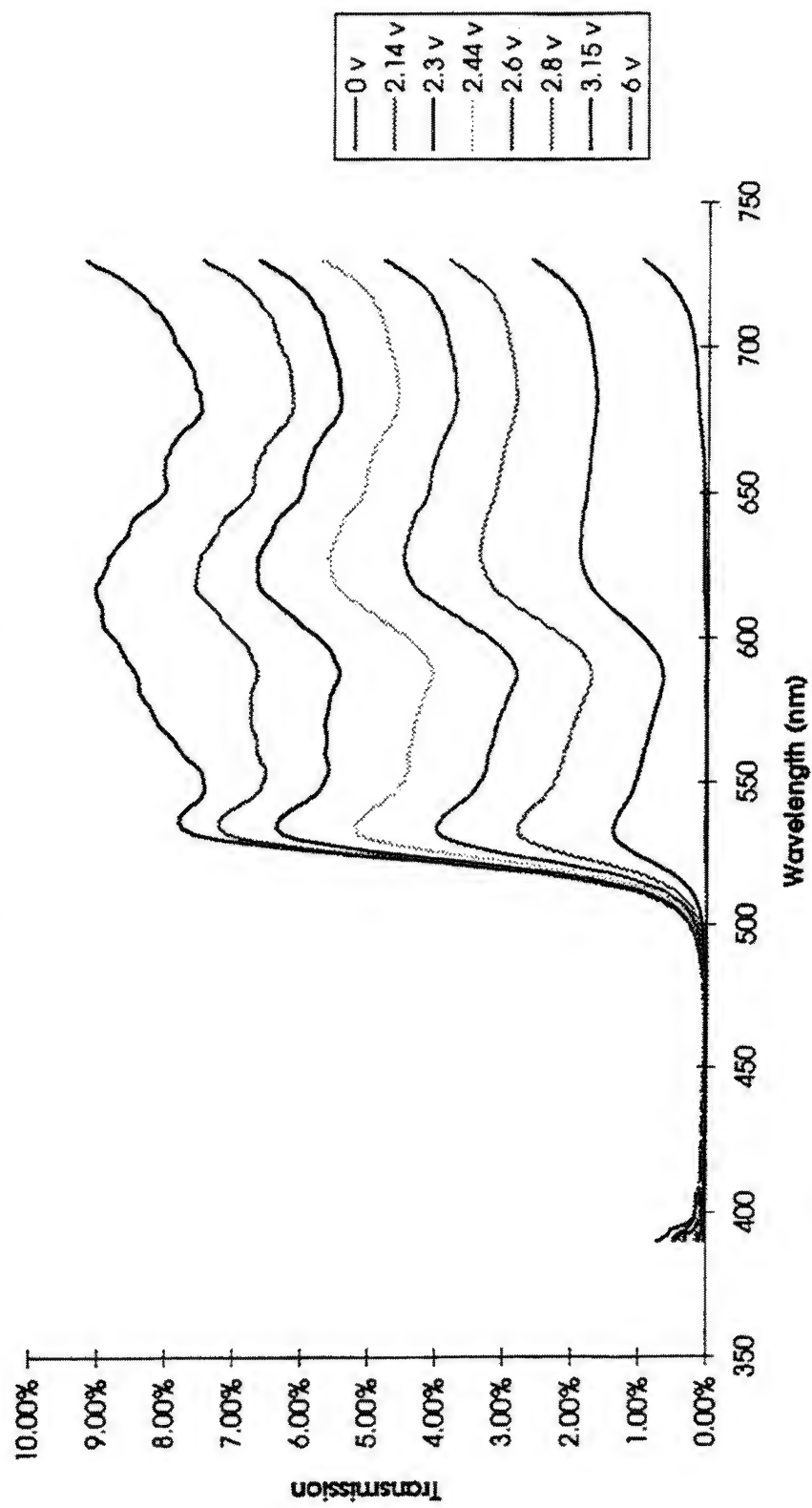


Figure 3-39, Stack #3 - Gray Scale: Voltage vs. Transmission vs. Wavelength (Xenon Lamp).

Two-Primary Color Stack #3 = Hybrid #1

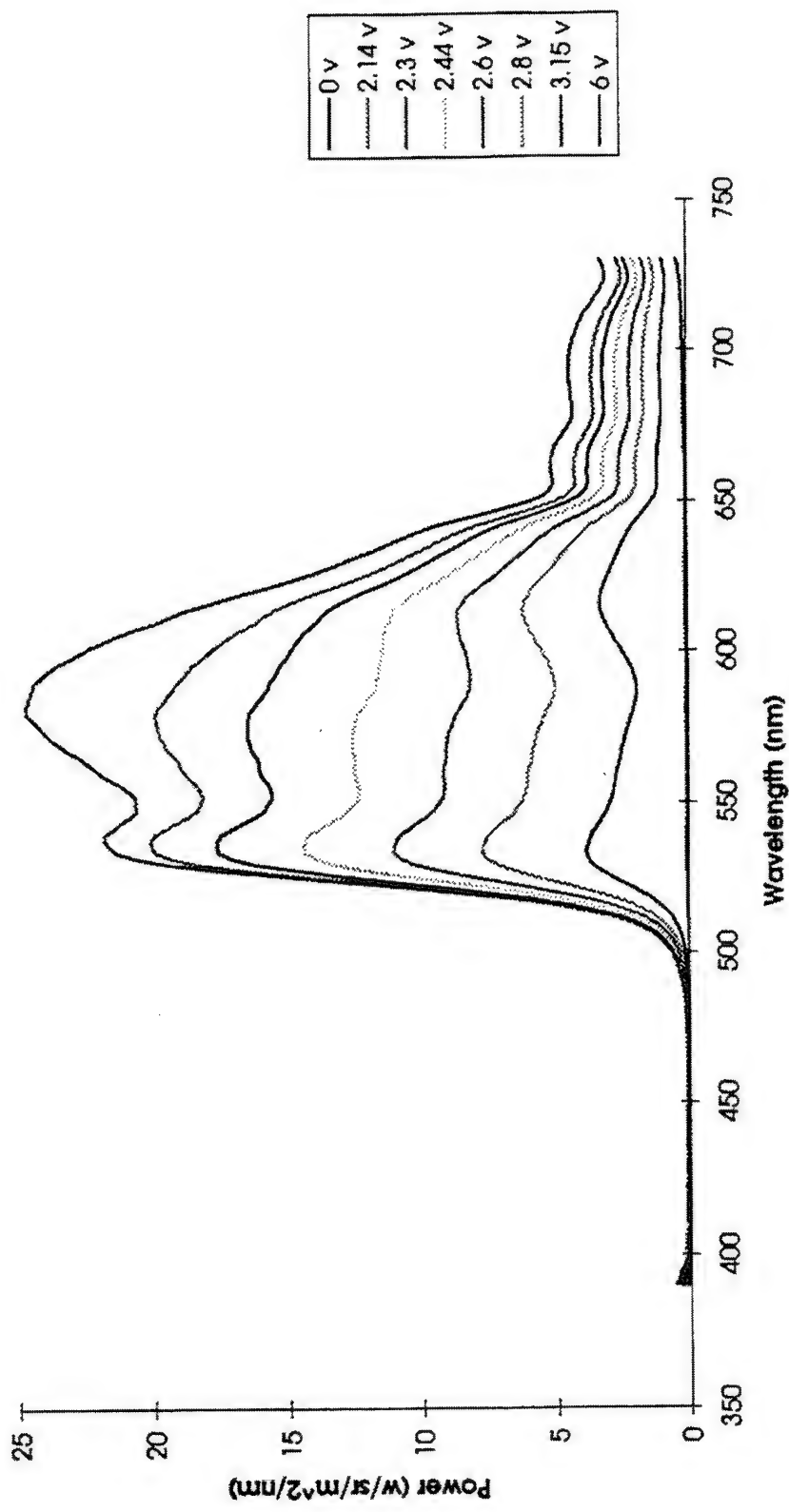


Figure 3-40. Stack #3 - Gray Scale: Voltage vs. Power vs. Wavelength (Xenon Lamp).

3.7 Stack #4 Configuration and Results

Stack #4 is the second of two hybrid designs (hybrid #2), which consists of two 73% aperture light valve LCD cells, two red dichroic sheet polarizers, one neutral density sheet polarizer, and one cyan notch polarizer with two wide-band $\lambda/4$ retarders, as shown in Figure 3-41. Stack #4 has an image plane to image plane distance of 0.051 in.

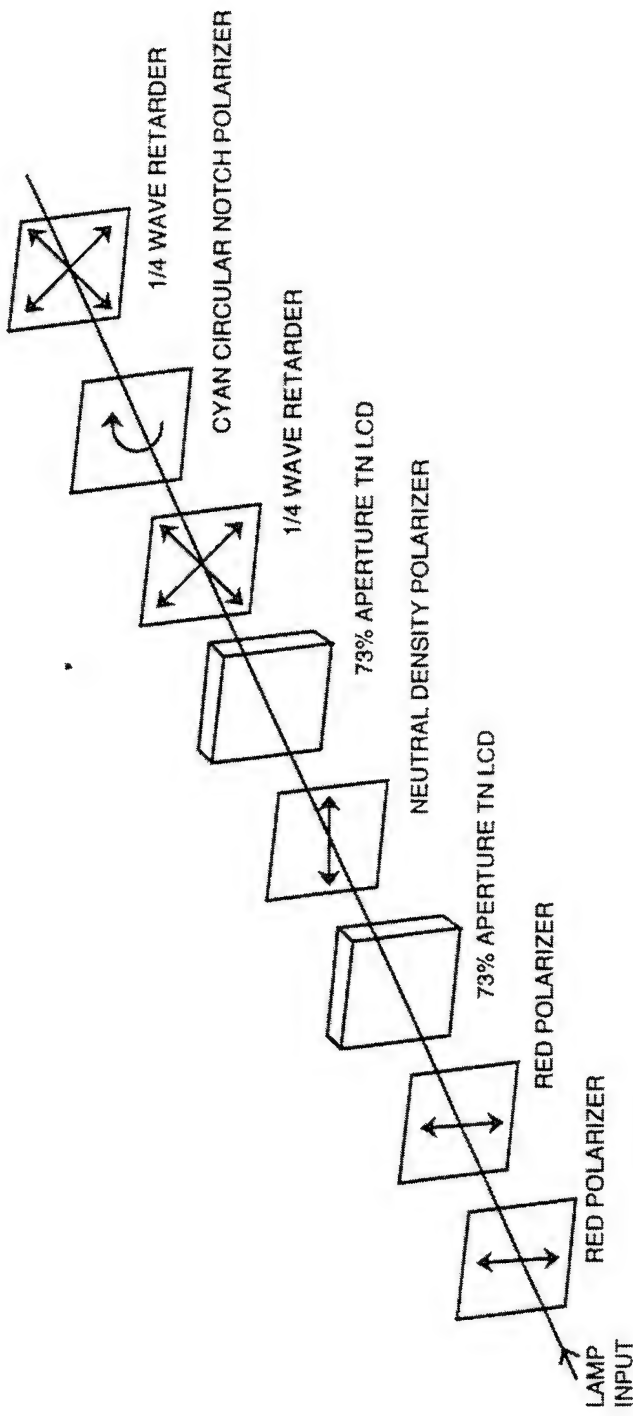


Figure 3-41. Two-Primary color Expanded View of Stack #4 (Hybrid #2).

The test results of stack #4 (hybrid #2) follow.

Table 3-8. Stack #4 Directional Illumination Measured With Xenon Lamp & Reynard Filters

Hybrid #2 Configuration: Lamp = 9493000 fL; Contrast Ratio = 75.39

State	fL	u'	v'
Yellow	880600	0.2305	0.5625
Red	226800	0.4234	0.5360
Green	421800	0.1245	0.5767
Black	11680	0.2938	0.5545
Filter Location	Backlight Luminance	Stack Transmittance	
In Backlight	6361000	13.8%	
Part of Stack	9493000	9.3%	

Hybrid #2 Configuration: Lamp = 784400 fL; Contrast Ratio = 64.72

State	fL	u'	v'
Yellow	79860	0.2530	0.5598
Red	24230	0.4241	0.5354
Green	28660	0.1045	0.5798
Black	1234	0.3524	0.5441
Filter Location	Backlight Luminance	Stack Transmittance	
In Backlight	526900	15.2%	
Part of Stack	784400	10.2%	

Table 3-9. Stack #4 Directional Illumination Measured With Xenon Lamp and Calculated Filters (Y cutoff < 500 nm, IR cutoff > 650 nm)

Hybrid #2 Configuration: Lamp = 7052000 fL; Contrast Ratio = 74.08				
State	fL	u'	v'	
Yellow	943000	0.2088	0.5630	
Red	179400	0.4200	0.5339	
Green	492900	0.1117	0.5738	
Black	12730	0.2822	0.5548	
Filter Location	Backlight Luminance	Stack Transmittance		
In Backlight	7052000	13.4%		
Part of Stack	9493000	9.9%		
Hybrid #2 Configuration: Lamp = 5924000 fL; Contrast Ratio = 75.87				
State	fL	u'	v'	
Yellow	83000	0.2378	0.5611	
Red	23290	0.4202	0.5367	
Green	37700	0.0982	0.5790	
Black	1094	0.3097	0.5508	
Filter Location	Backlight Luminance	Stack Transmittance		
In Backlight	5924000	14.0%		
Part of Stack	784400	10.6%		

Two-Primary Color Stack #4 = Hybrid #2
Filtered Power (Reynard Filters)

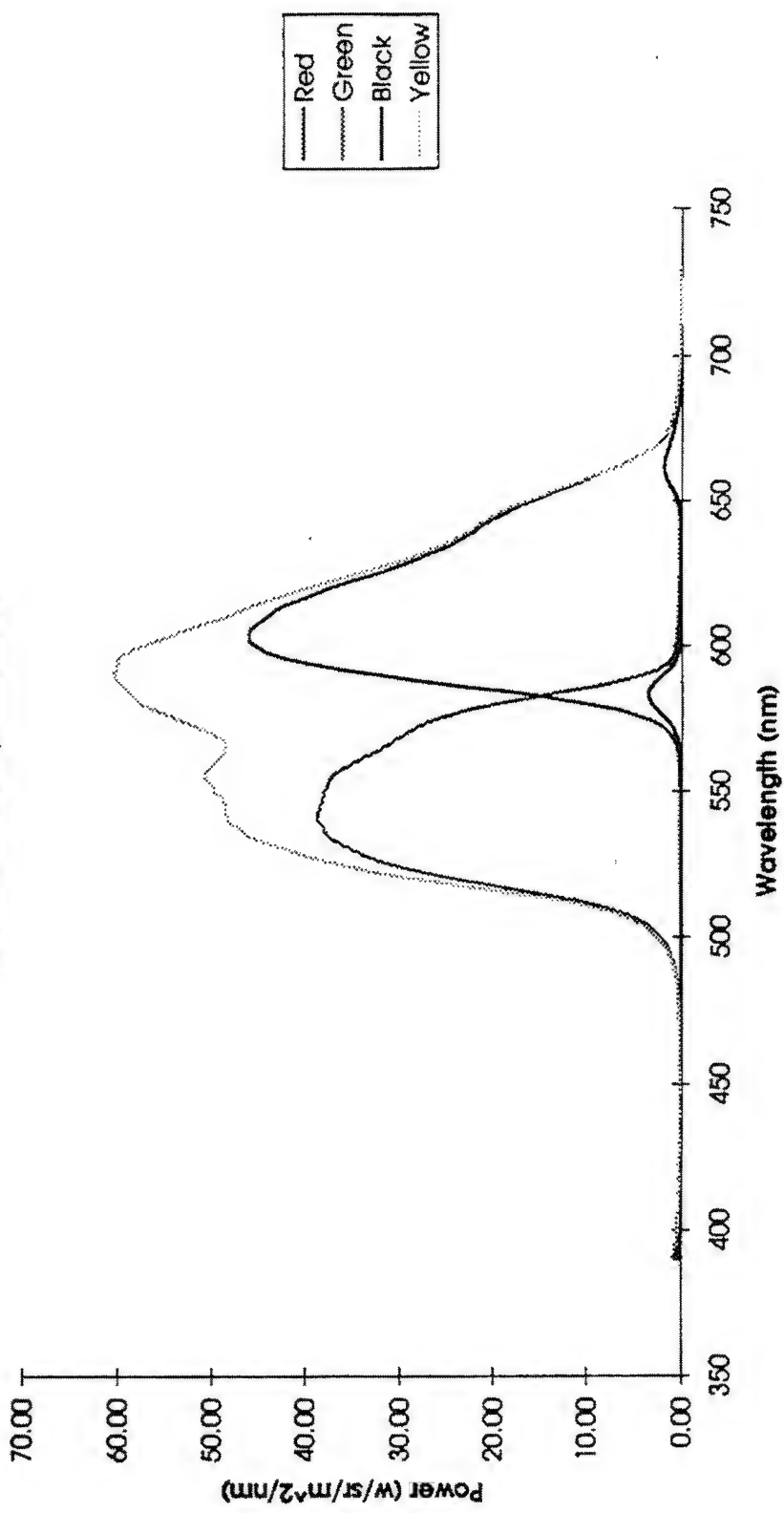


Figure 3-42. Stack #4 - Filtered Power vs. Wavelength (Xenon Lamp).

Two-Primary Color Stack #4 = Hybrid #2
Filtered Power (Calculated Filters)

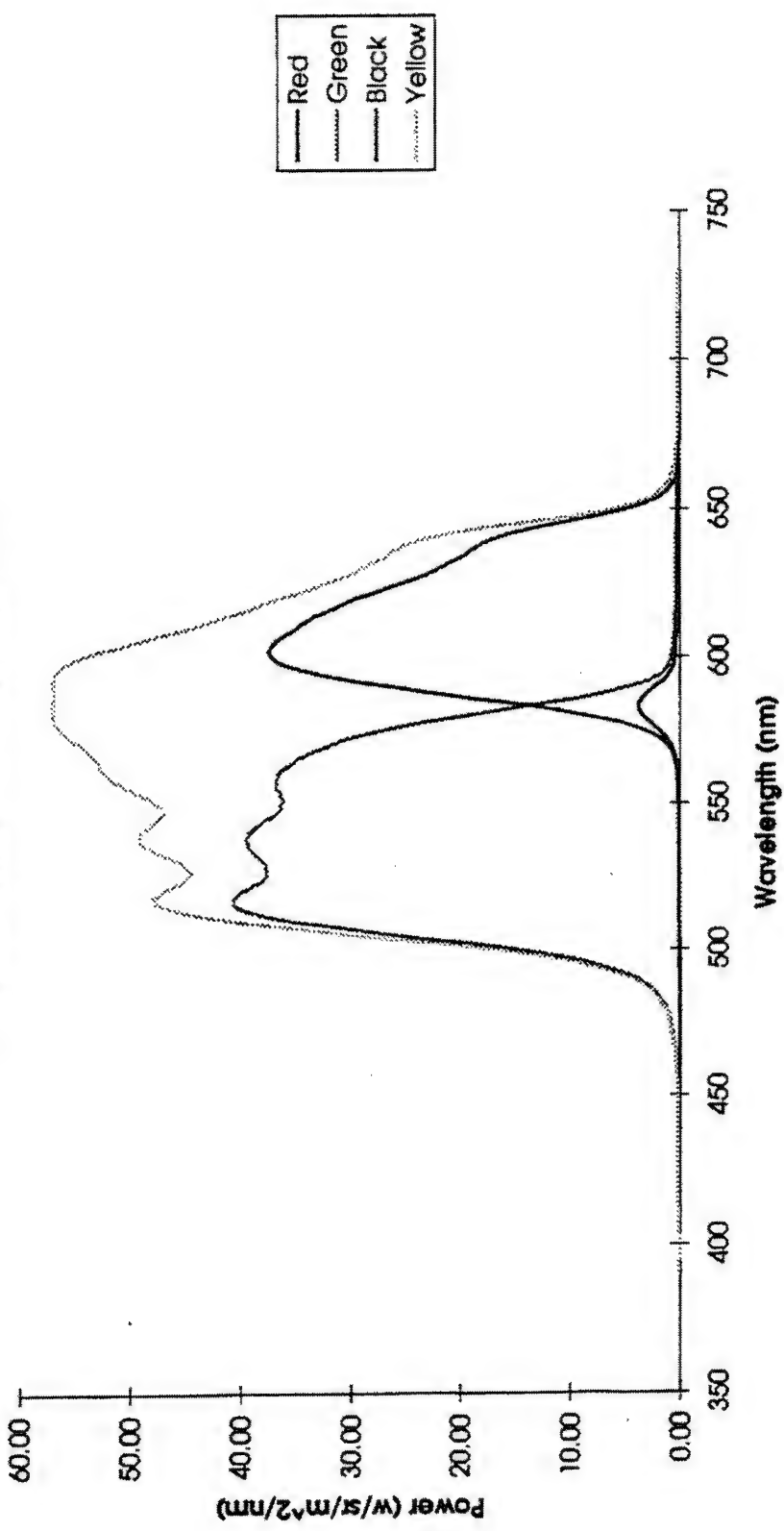


Figure 3-43. Filtered Power (calculated filters) vs. Wavelength (Xenon Lamp).

Two-Primary Color Stack #4 = Hybrid #2

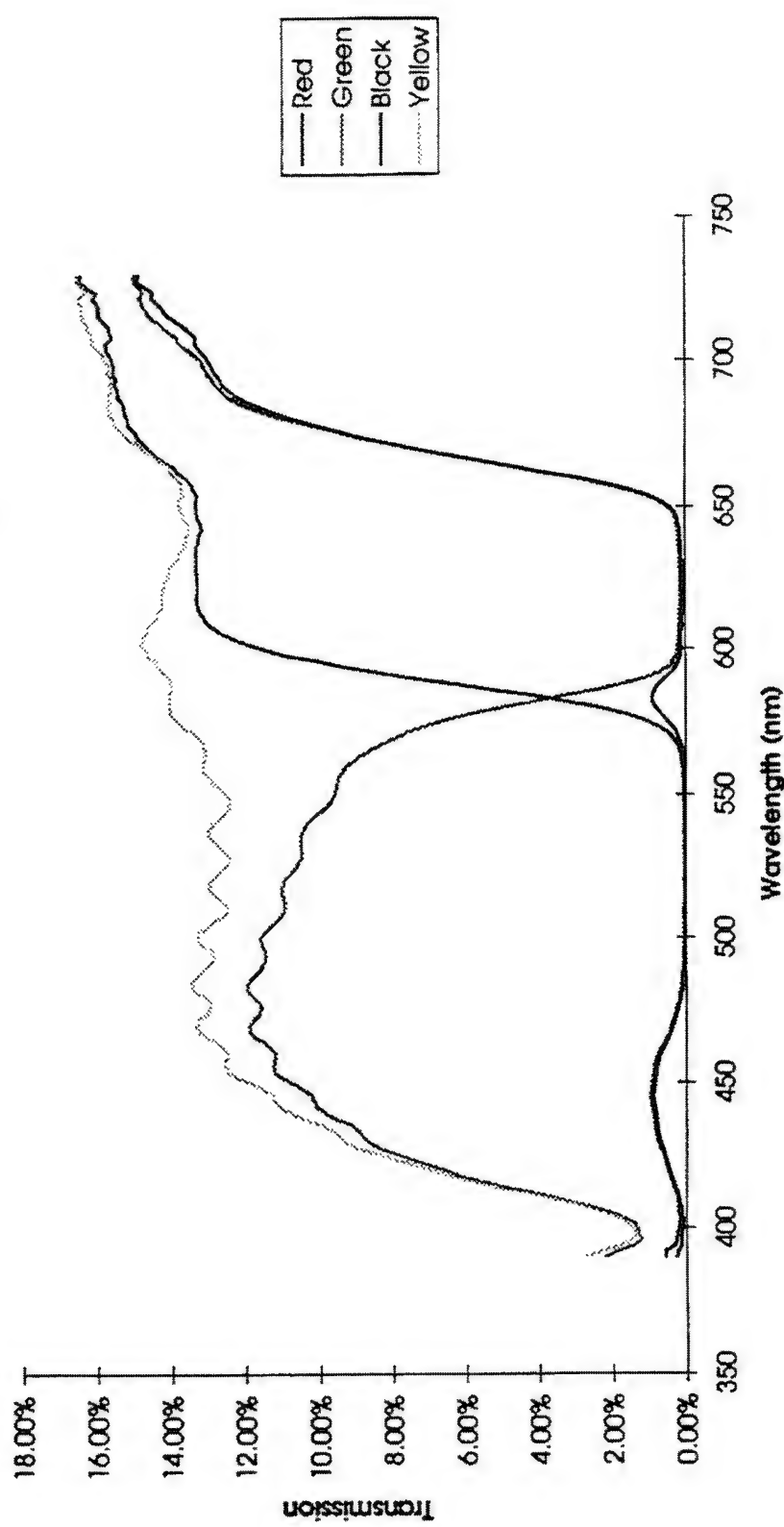


Figure 3-44. Stack #4 - Transmission vs. Wavelength (Xenon Lamp).

Two-Primary Color Stack #4 = Hybrid #2
Filtered Transmission (Reynard Filters)

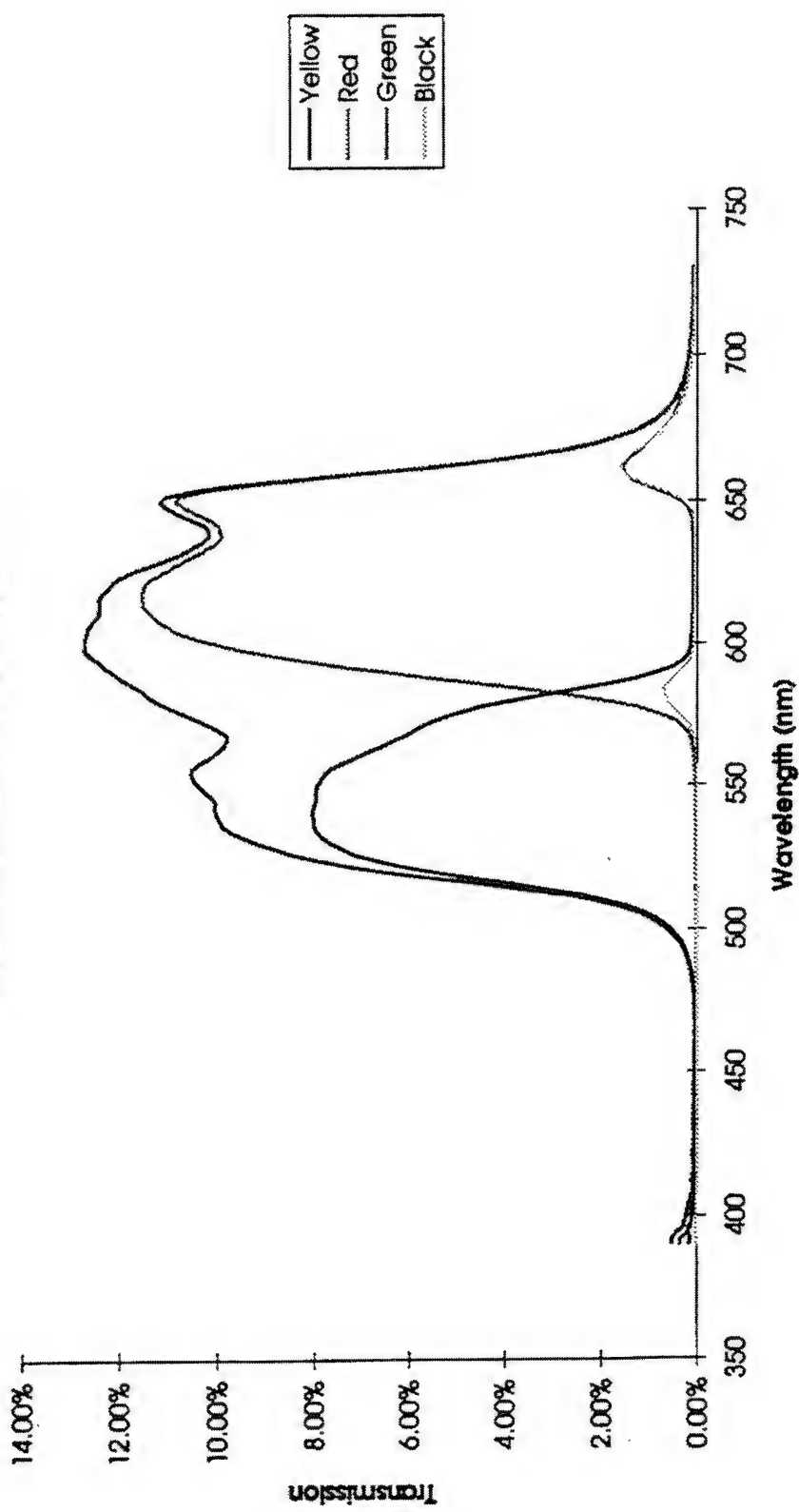


Figure 3-45. Stack #4 - Filtered Transmission vs. Wavelength (Xenon Lamp).

Two-Primary Color Stack #4 = Hybrid #2
Filtered Transmission (Calculated Filters)

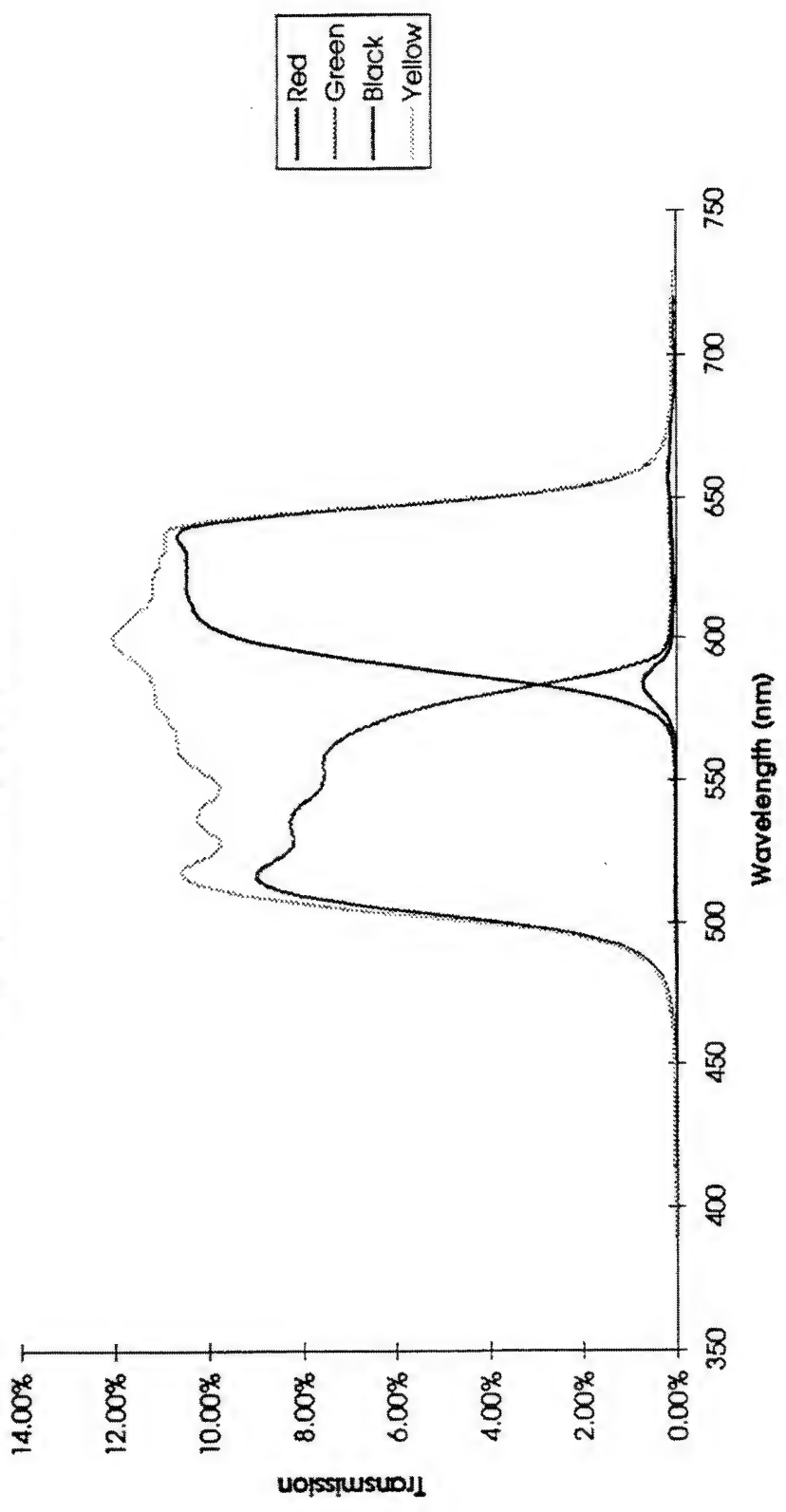


Figure 3-46. Stack #4 - Filtered Transmission (calculated filters) vs. Wavelength (Xenon Lamp).

Two-Primary Color Stack #4 = Hybrid #2

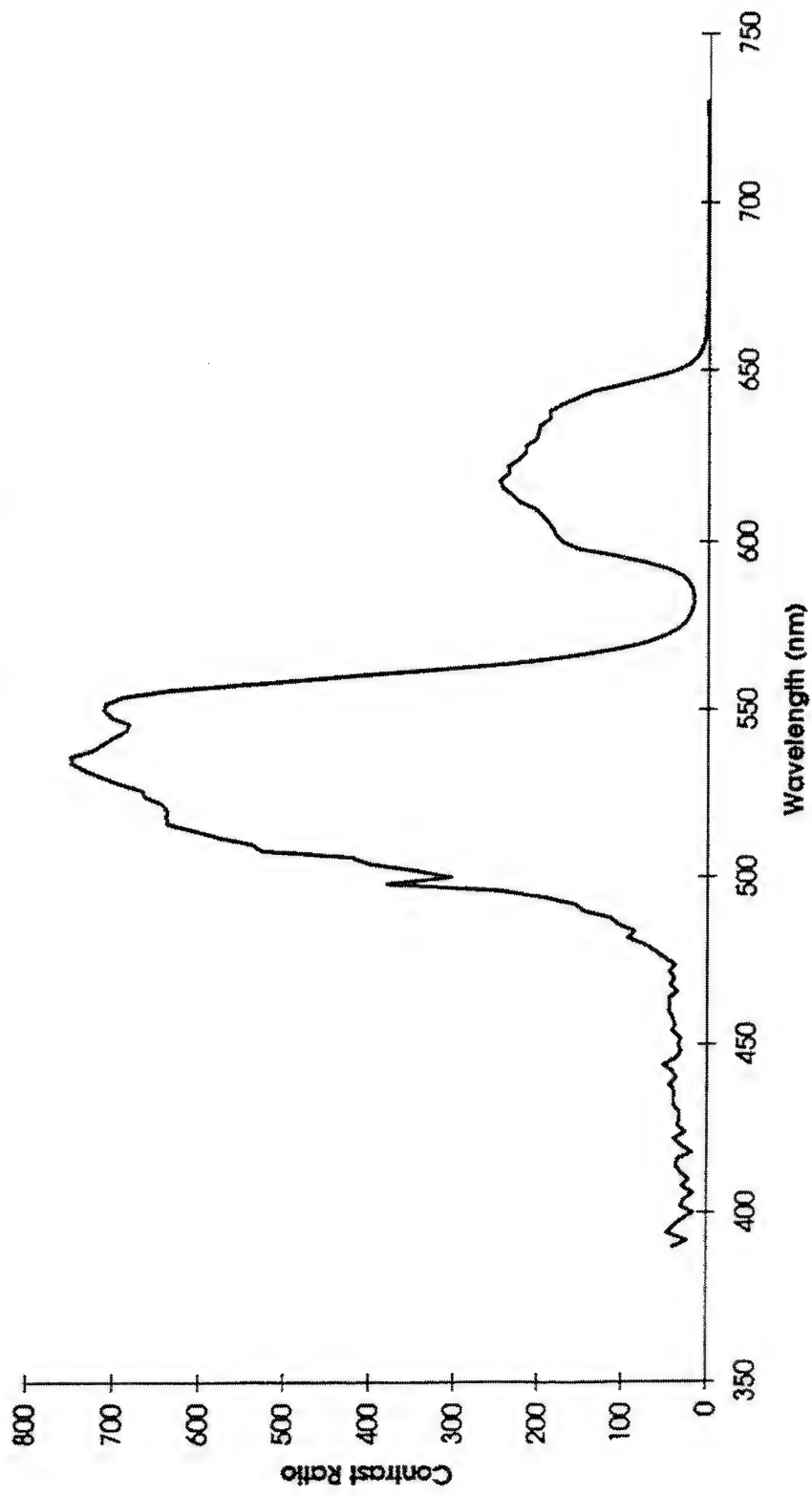


Figure 3-47. Stack #4 - Contrast Ratio vs. Wavelength (Xenon Lamp).

Two-Primary Color Stack #4 = Hybrid #2
Lamp Characteristics

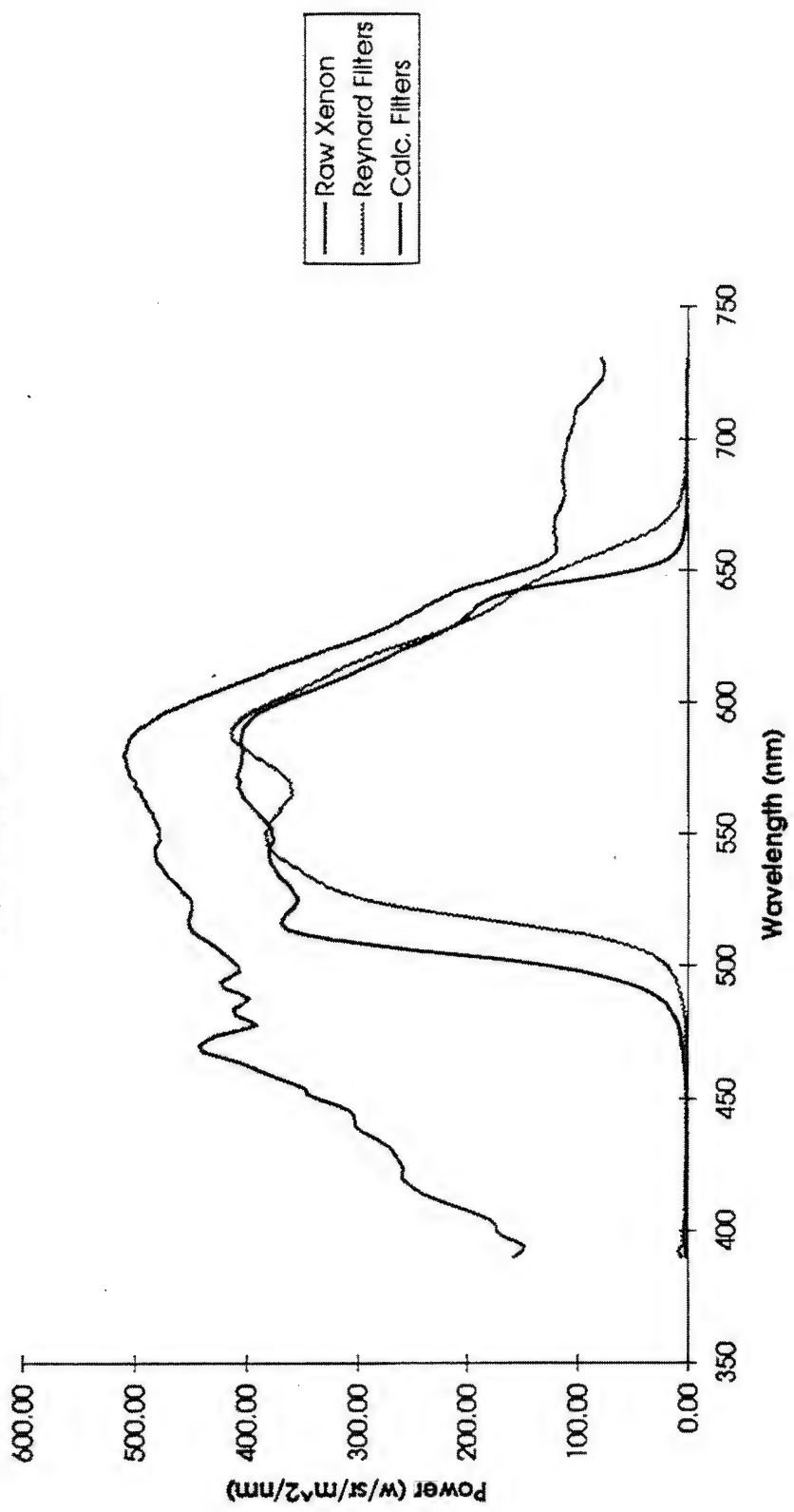


Figure 3-48. Xenon Lamp Characteristics - Power vs. Wavelength.

Two-Primary Color Stack #4 = Hybrid #2
Filtered Power (Reynard Filters)

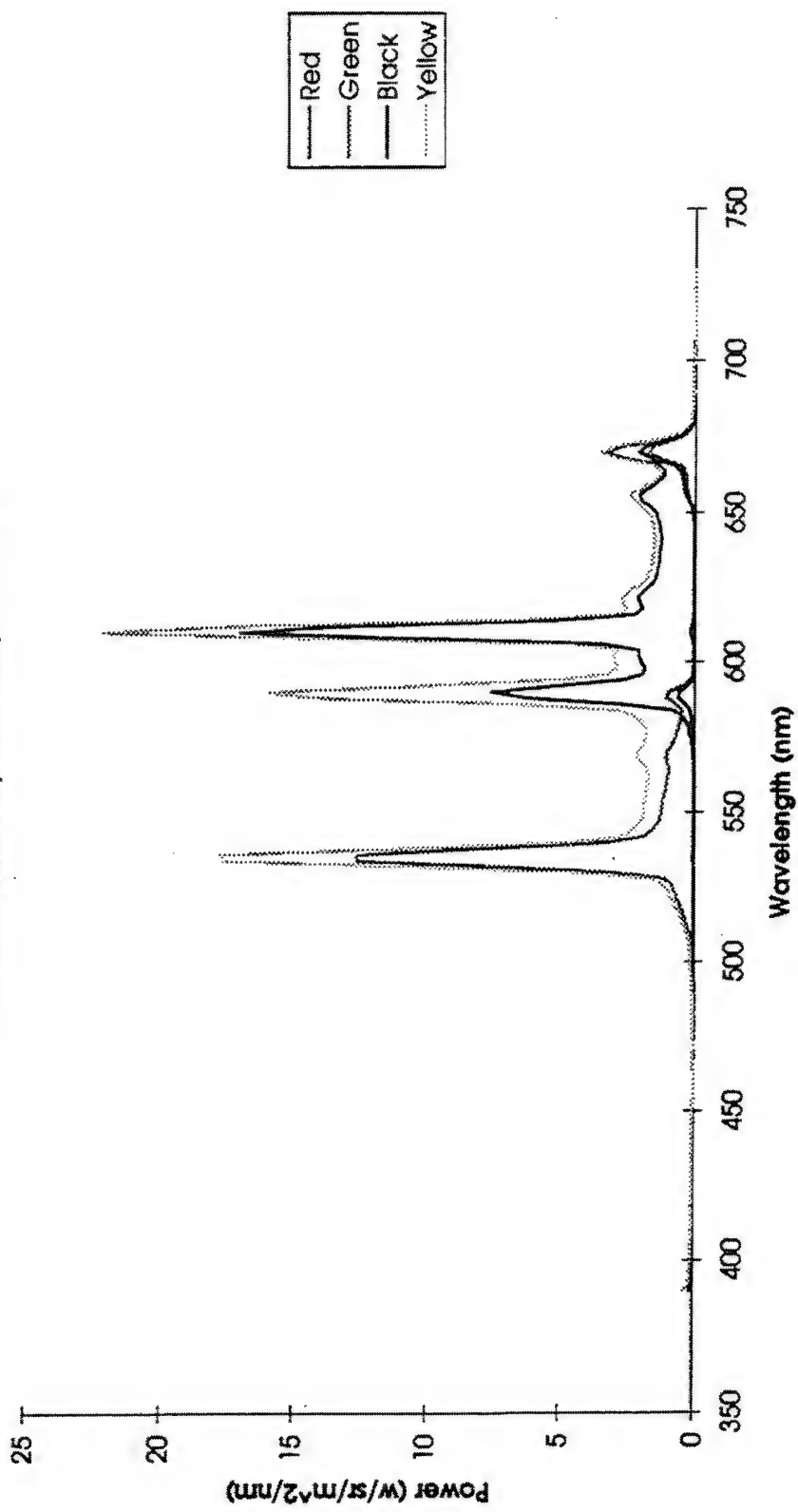


Figure 3-49. Stack #4 - Filtered Power vs. Wavelength (Tri-band Lamp #69).

Two-Primary Color Stack #4 = Hybrid #2
Filtered Power (Calculated Filters)

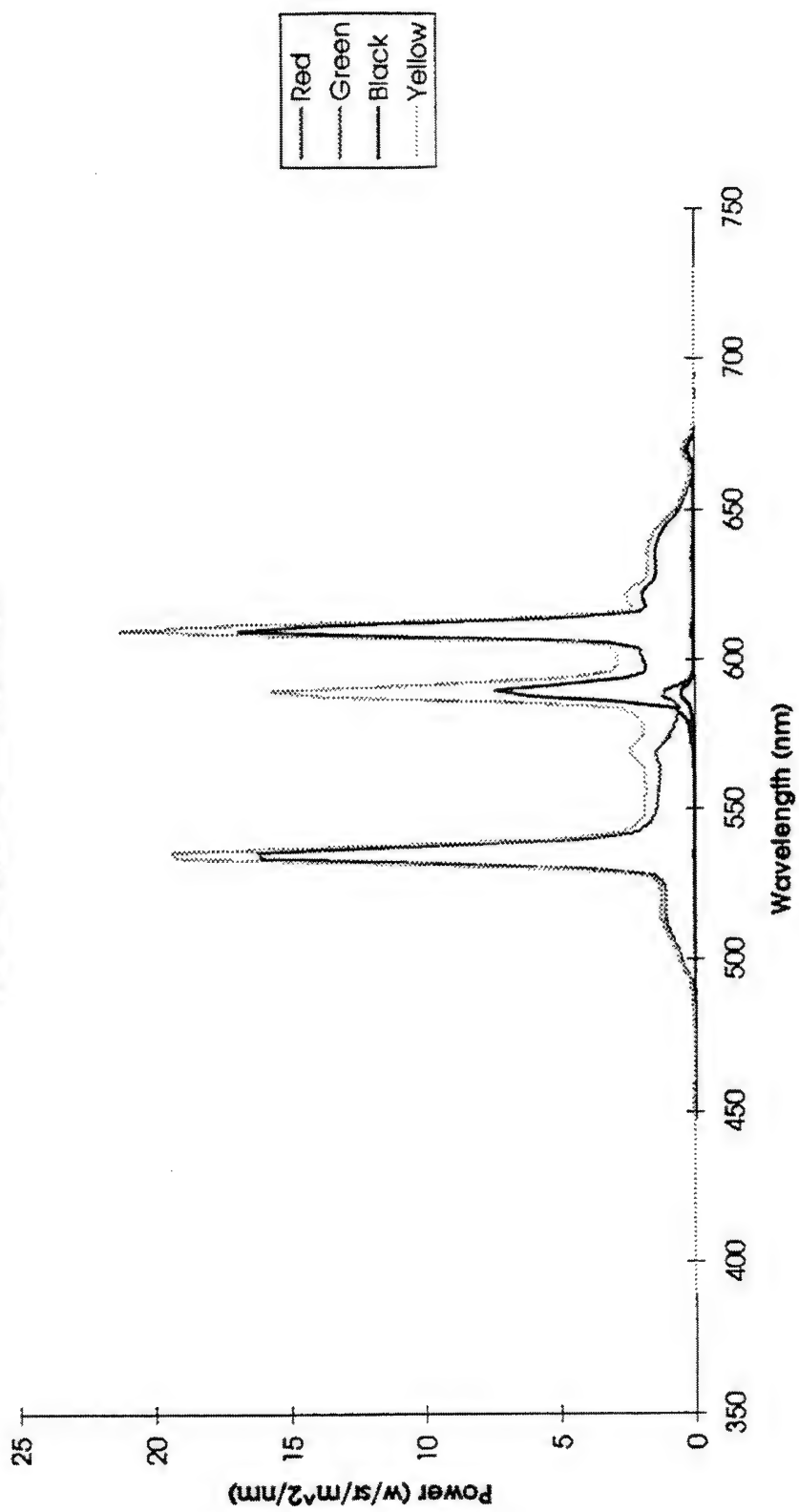


Figure 3-50. Stack #4 - Filtered Power (calculated filters) vs. Wavelength (Tri-band Lamp #69).

Two-Primary Color Stack #4 = Hybrid #2
Lamp Characteristics

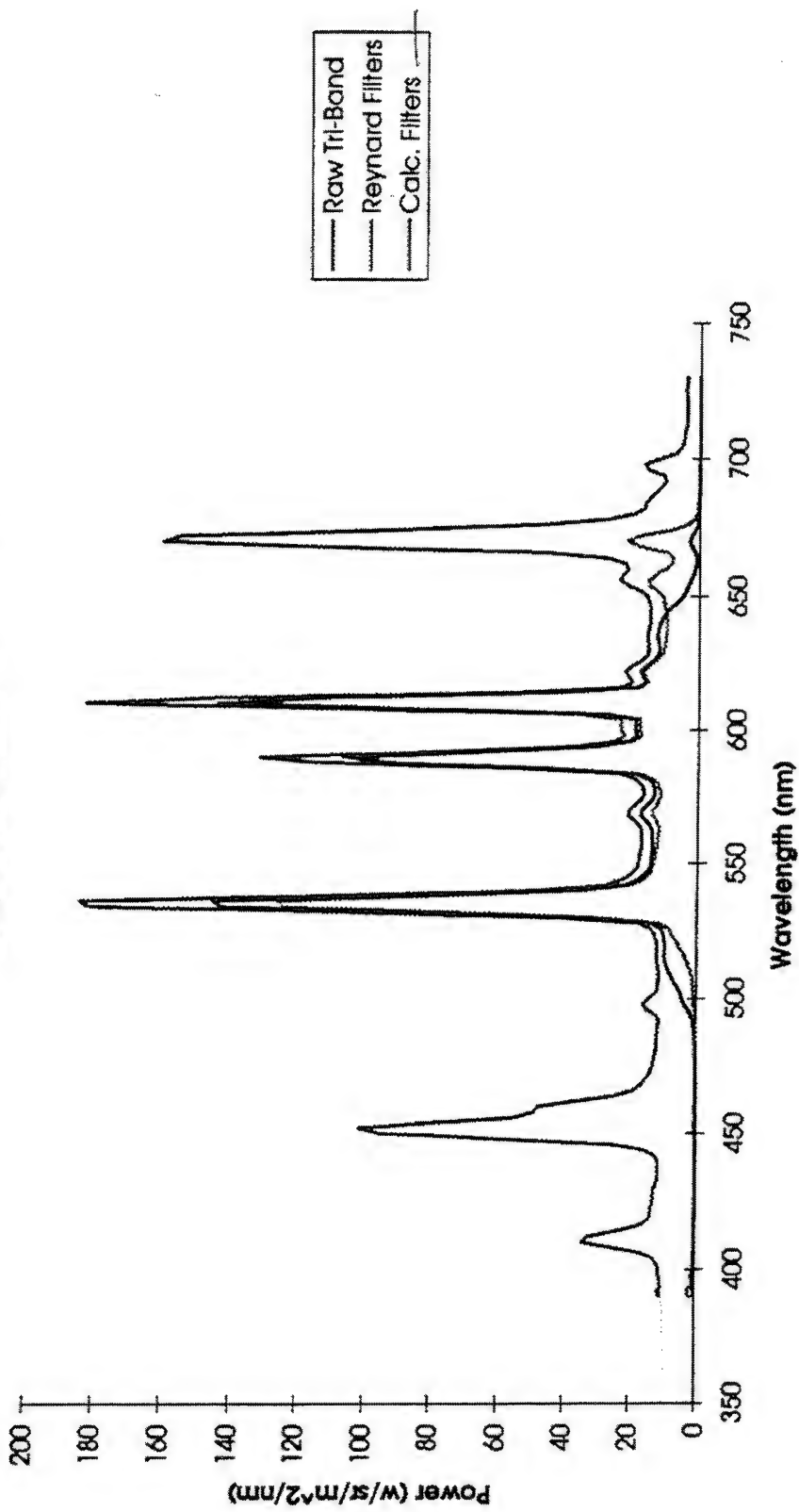


Figure 3-51. Tri-band Lamp Characteristics - Power vs. Wavelength.

3.8 Stack #5 Configuration & Results

Due to the tri-band lamp arrival and characterization, a fifth single pixel two-primary color stack was designed to achieve optimal tuning of the notch polarizers to the ILC Tri-band lamp #69, while allowing analysis of diffraction effects. Stack #5 consists of two varied aperture light valve LCDs, one cyan notch polarizer, one neutral density sheet polarizer, one magenta notch polarizer and two wide-band $\lambda/4$ retarders, as shown in Figure 3-52. Two varied aperture light valve LCD cells with designed in artifacts for measuring diffractive effects are used for Stack #5, allowing analysis of the diffractive effects of the two bonded light valve LCDs before attaching outer polarizers. Diffractive effects are examined for apertures of 32%, 48%, 73%, and 92% at 24 μ pitch as well as 67% and 90% at 20 μ pitch. Stack #5 has an image plane to image plane distance of 0.051 in.

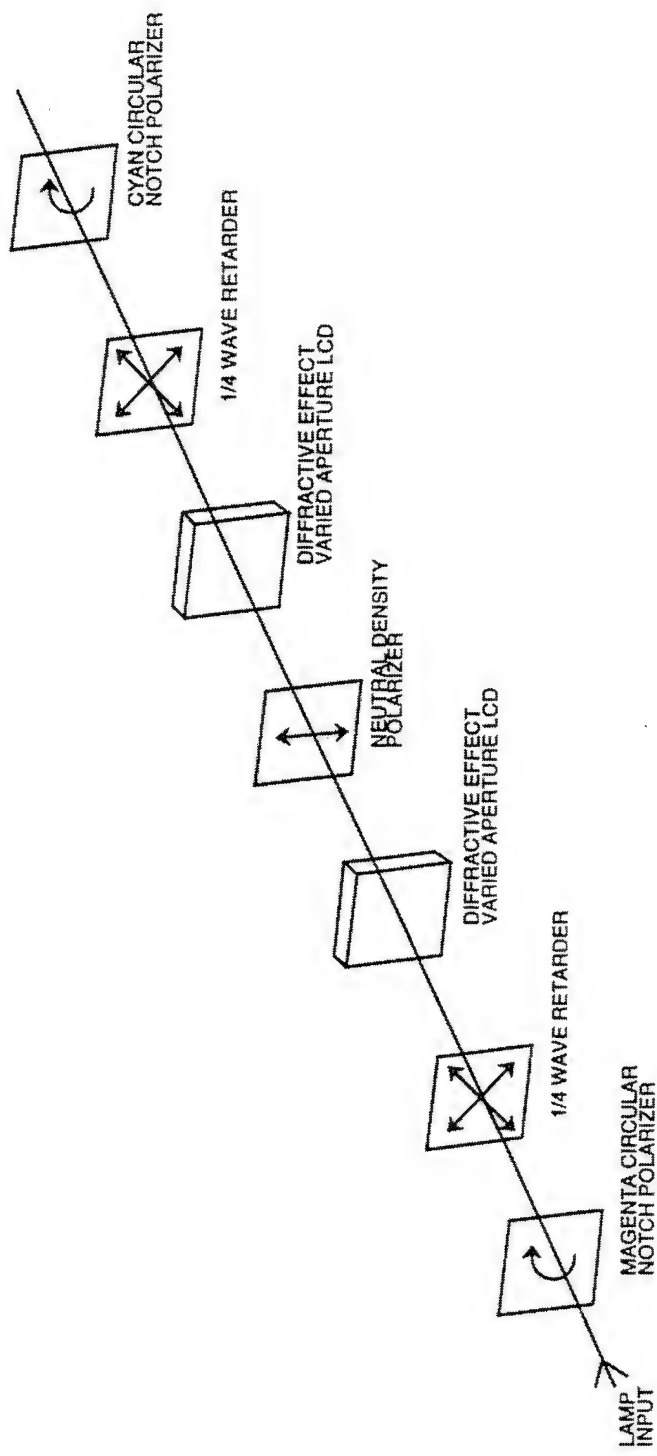


Figure 3-52. Two Primary-Color Expanded View of Stack #5.

The test results of Stack #5 follow.

Table 3-10. Stack #5 Directional Illumination Measured With Xenon Lamp and Reynard Filters

Double Narrow-Band Design Configuration: Lamp = 9311000 fL; Contrast Ratio = 7.03			
State	fL	u'	v'
Yellow	995700	0.2175	0.5644
Red	488100	0.3259	0.5498
Green	524300	0.1162	0.5764
Black	141600	0.2179	0.5641
Filter Location	Backlight Luminance	Stack Transmittance	
In Backlight	6294000	15.8%	
Part of Stack	9311000	10.7%	

Double Narrow-Band Design Configuration: Lamp = 656900 fL; Contrast Ratio = 13.38			
State	fL	u'	v'
Yellow	76680	0.2294	0.5630
Red	36620	0.3686	0.5436
Green	34440	0.1068	0.5795
Black	5732	0.2611	0.5581
Filter Location	Backlight Luminance	Stack Transmittance	
In Backlight	462200	16.6%	
Part of Stack	656900	11.7%	

Table 3-11. Stack #5 Directional Illumination Measured With Xenon Lamp and Calculated Filters (Y cutoff < 560 nm, IR cutoff > 650 nm)

Double Narrow-Band Design Configuration: Lamp = 6904000 FL; Contrast Ratio = 6.53			
State	FL	u'	v'
Yellow	1088000	0.1954	0.5647
Red	501600	0.3052	0.5496
Green	620700	0.1111	0.5738
Black	166500	0.1868	0.5592
Filter Location	Backlight Luminance	Stack Transmittance	
In Backlight	6904000	15.8%	
Part of Stack	9311000	11.7%	

Double Narrow-Band Design Configuration: Lamp = 4958000 FL; Contrast Ratio = 13.29			
State	FL	u'	v'
Yellow	79800	0.2171	0.5639
Red	36990	0.3572	0.5441
Green	37350	0.0985	0.5789
Black	6004	0.2181	0.5555
Filter Location	Backlight Luminance	Stack Transmittance	
In Backlight	4958000	16.1%	
Part of Stack	6556900	12.3%	

Two-Primary Color Stack #5 = Double Narrow Band Design

Filtered Power (Reymard Filters)

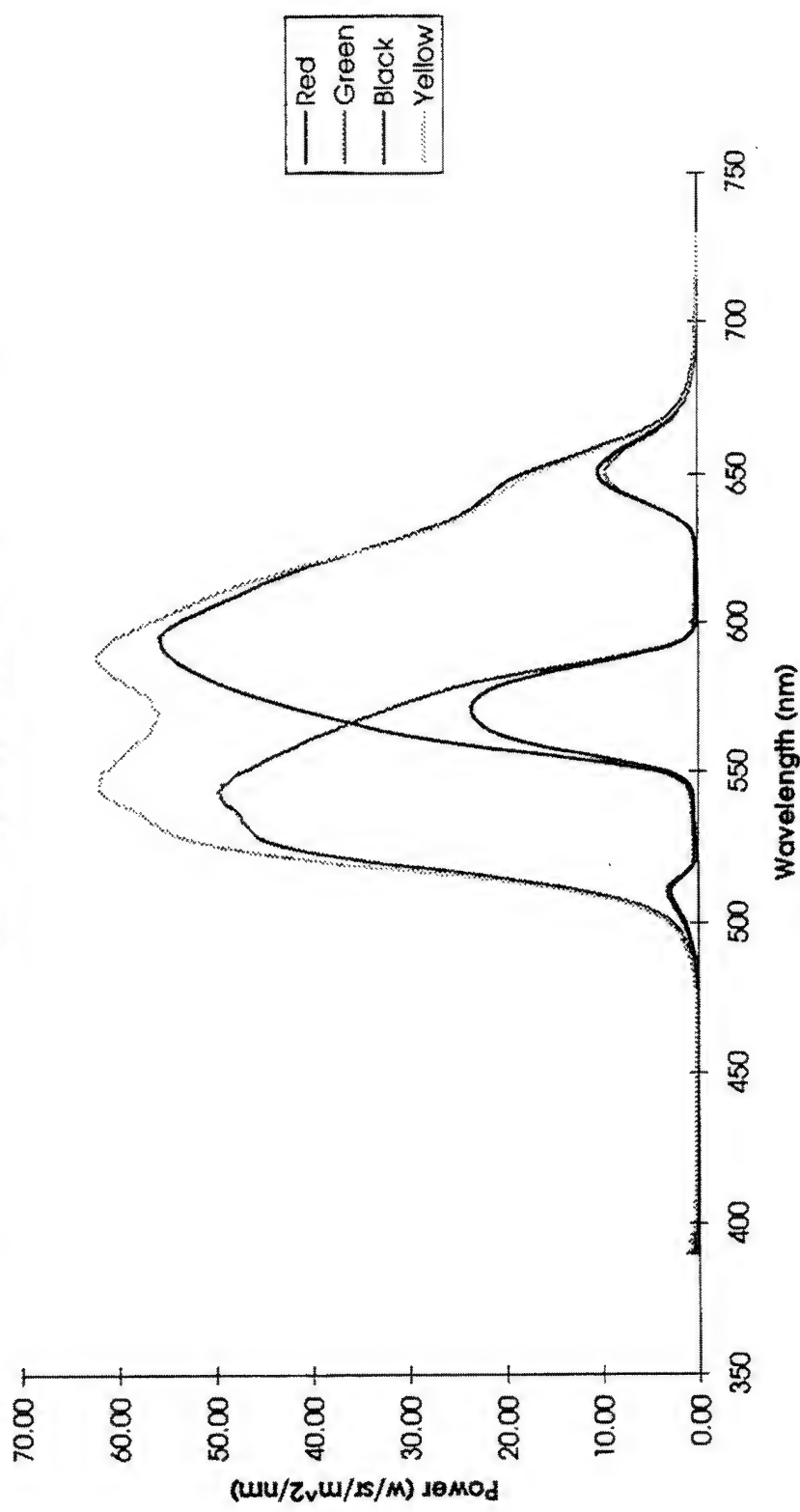


Figure 3-53. Stack #5 - Filtered Power vs. Wavelength (Xenon Lamp).

Two-Primary Color Stack #5 = Double Narrow Band Design

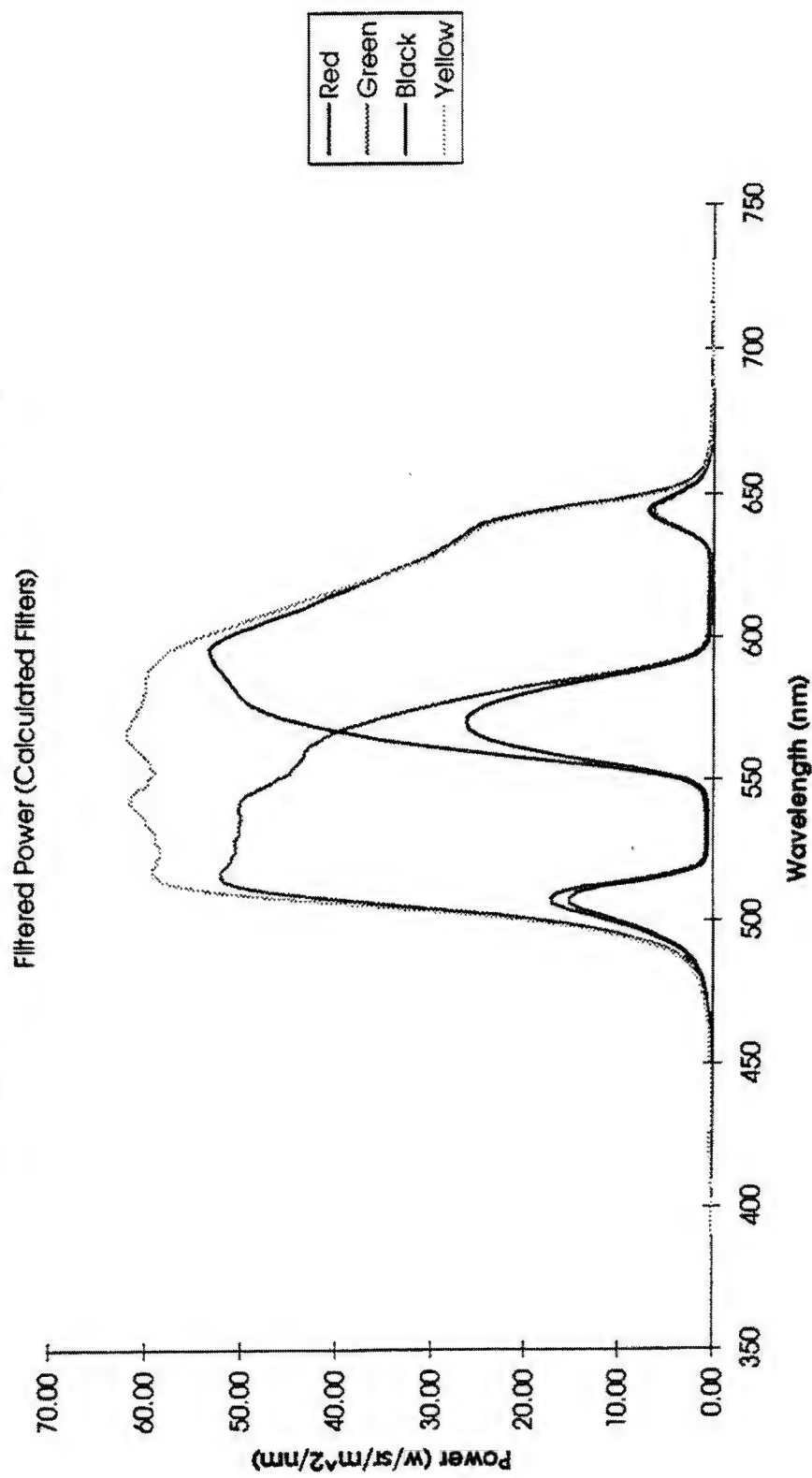


Figure 3-54. Stack #5 - Filtered Power (calculated filters) vs. Wavelength (Xenon Lamp).

Two-Primary Color Stack #5 = Double Narrow Band Design

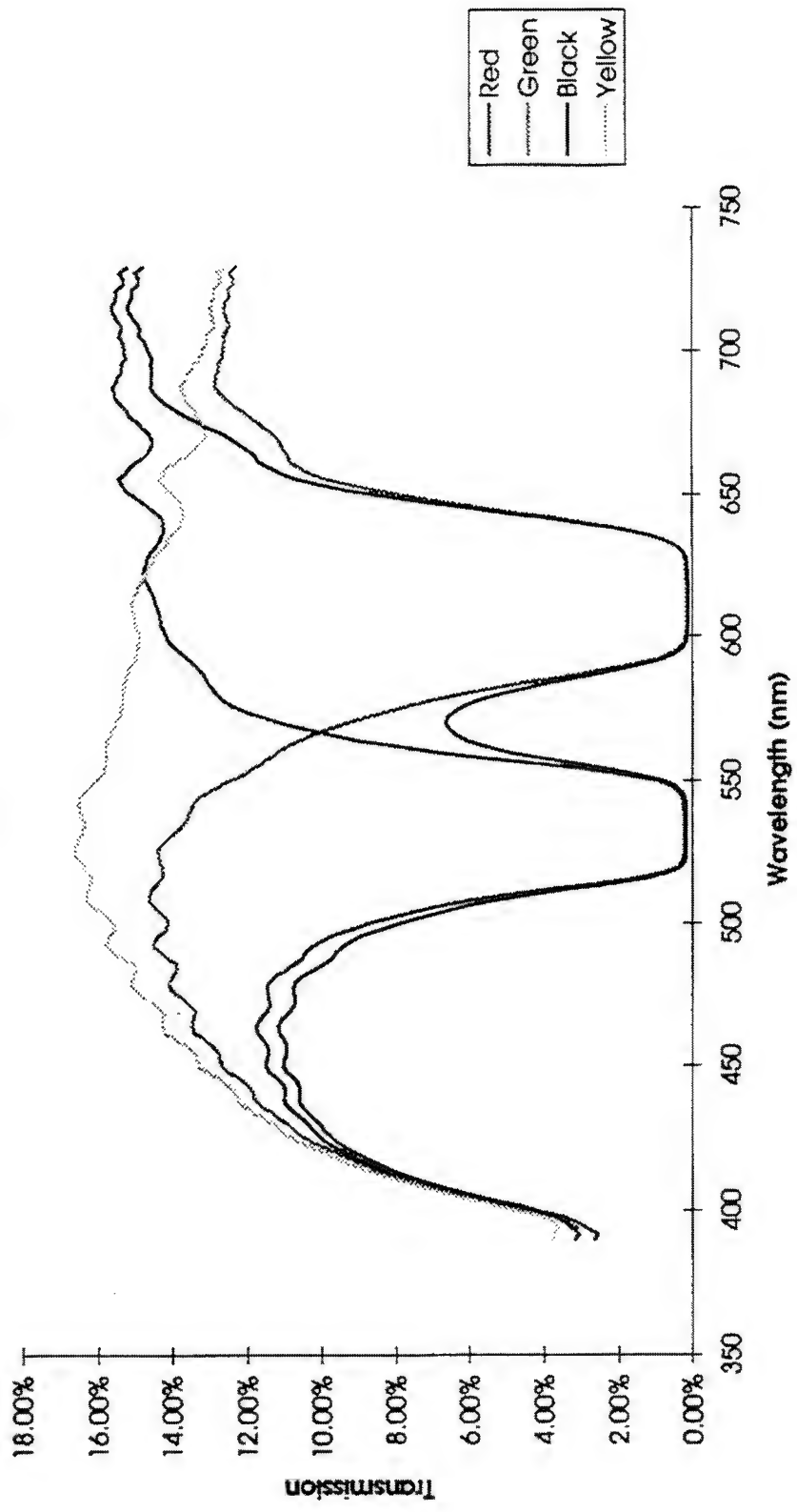


Figure 3-55. Stack #5 - Transmission vs. Wavelength (Xenon Lamp).

Two-Primary Color Stack #5 = Double Narrow Band Design

Filtered Transmission (Reynard Filters)

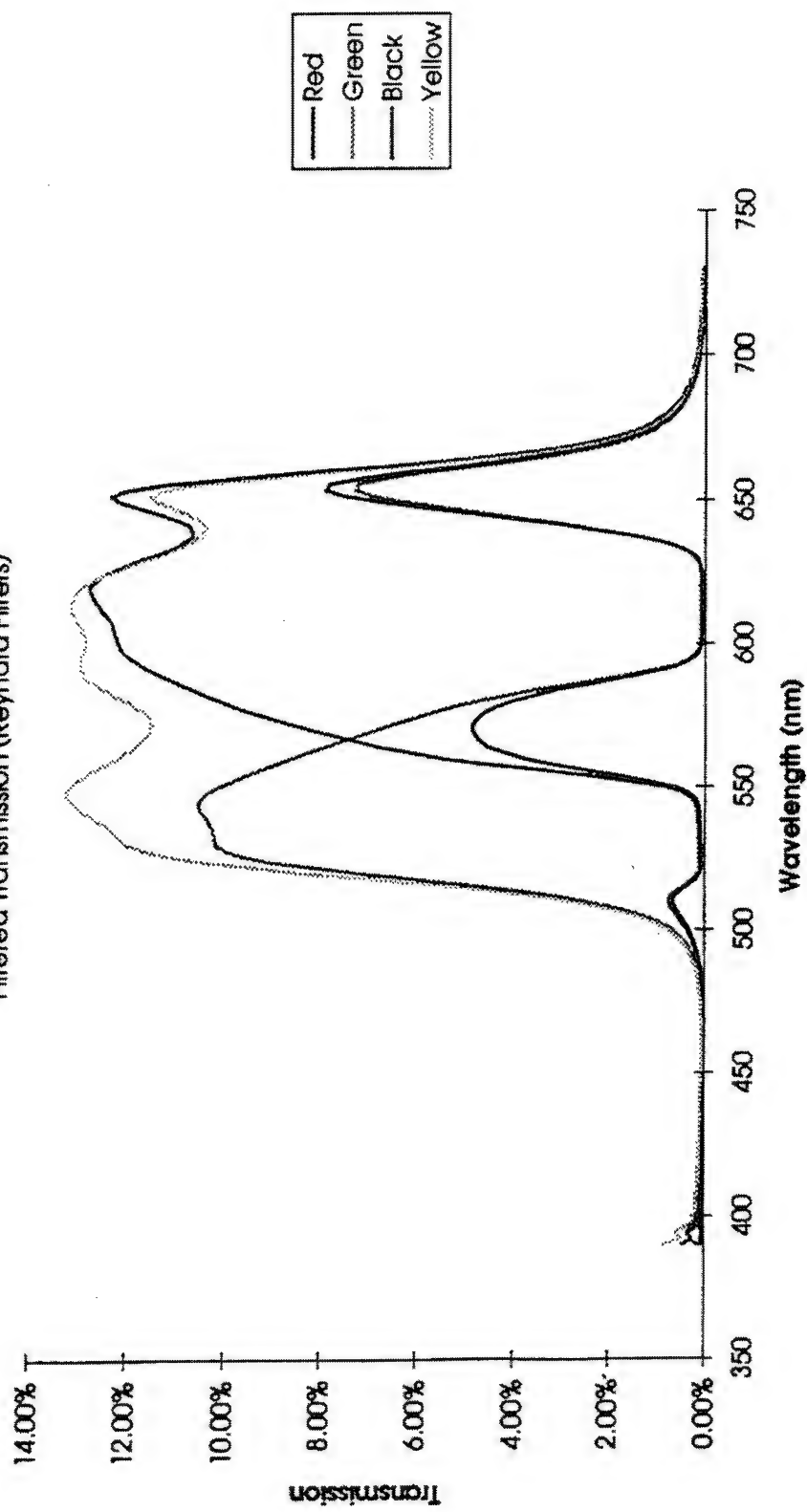


Figure 3-56. Stack #5 - Filtered Transmission vs. Wavelength (Xenon Lamp).

Two-Primary Color Stack #5 = Double Narrow Band Design

Filtered Transmission (Calculated Filters)

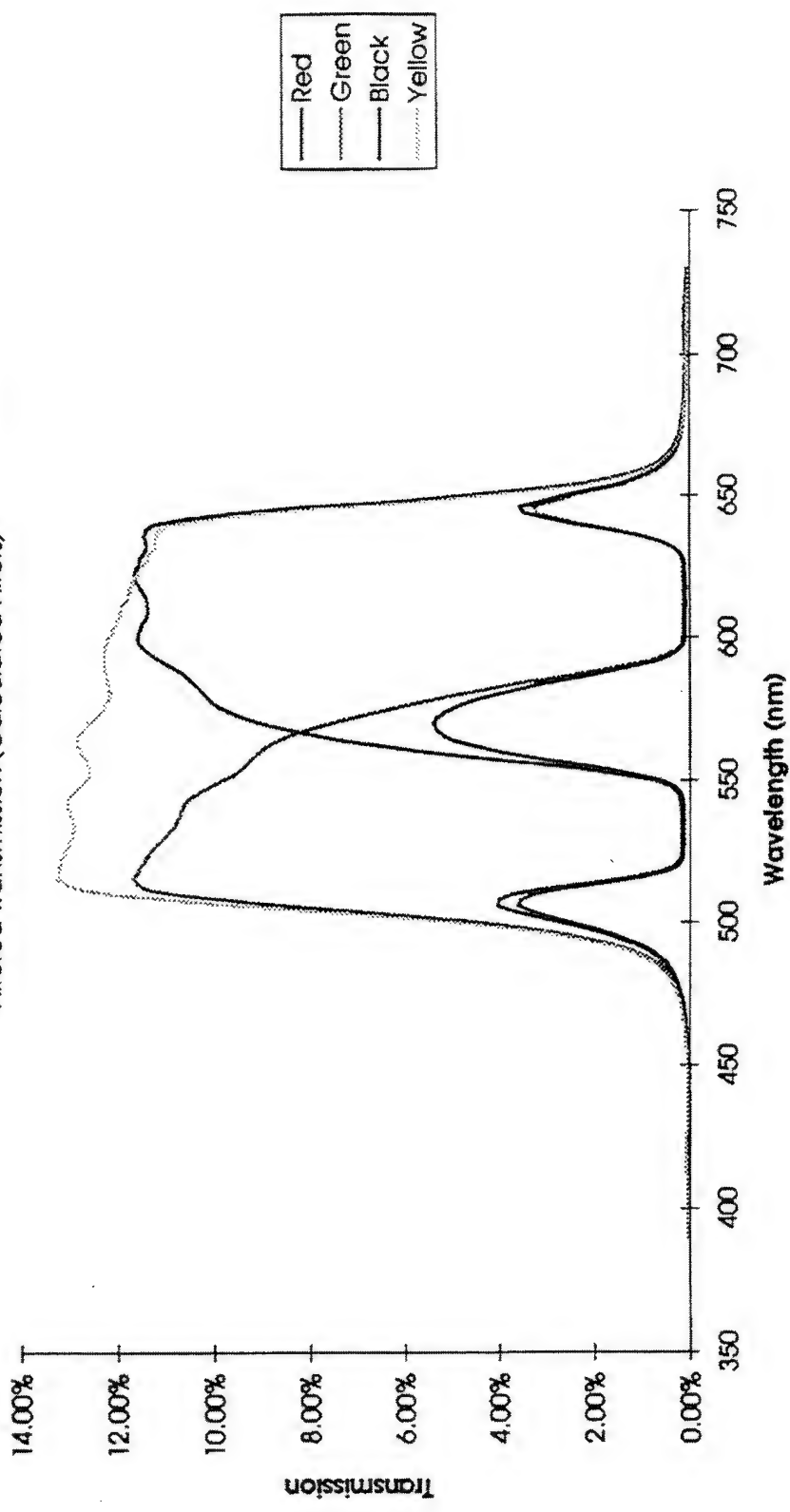


Figure 3-57. Stack #5 - Filtered Transmission vs. Wavelength (Xenon Lamp).

Two-Primary Color Stack #5 = Double Narrow Band Design

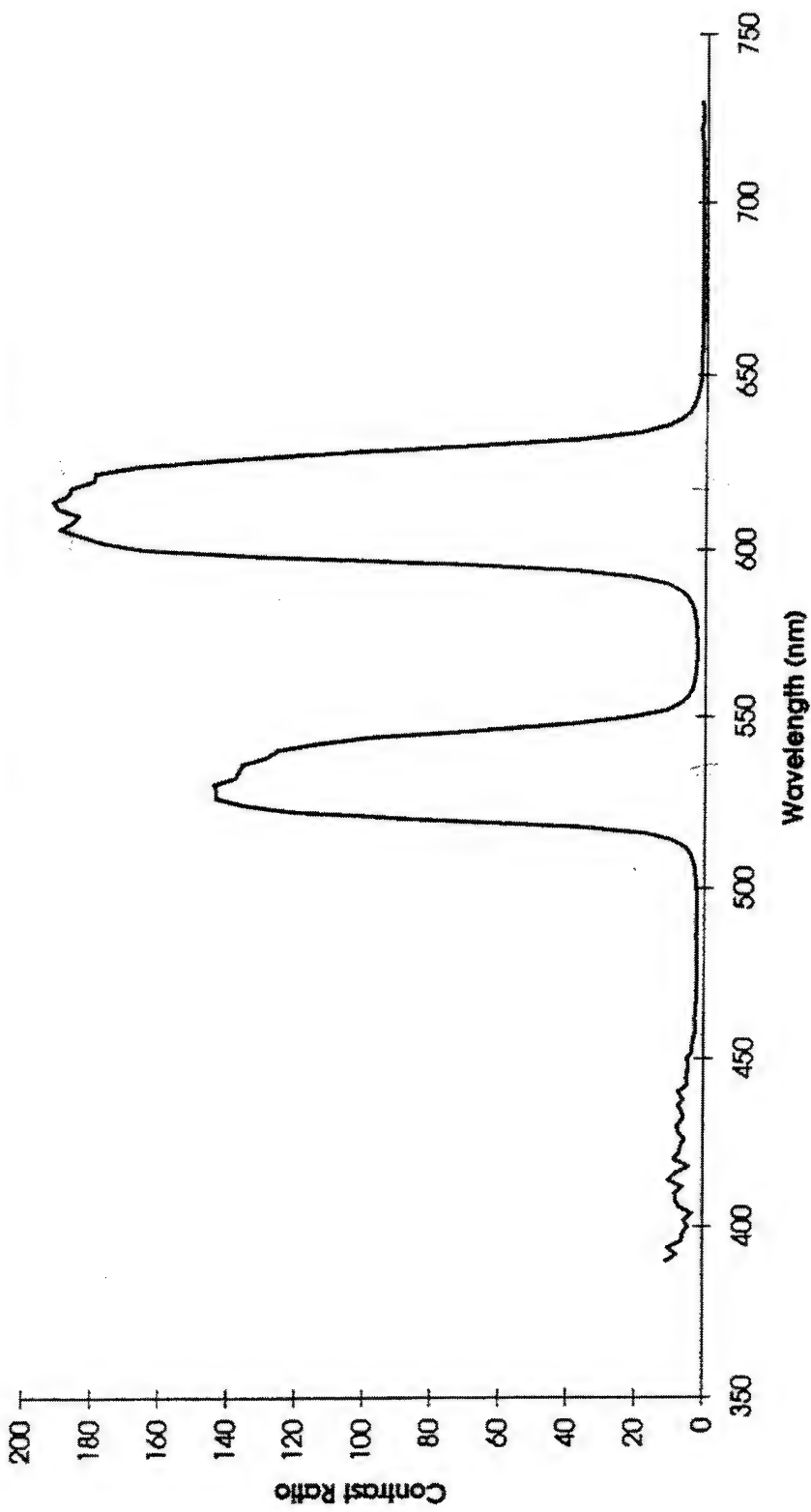


Figure 3-58. Stack #5 - Contrast Ratio vs. Wavelength (Xenon Lamp).

Two-Primary Color Stack #5 = Double Narrow Band Design

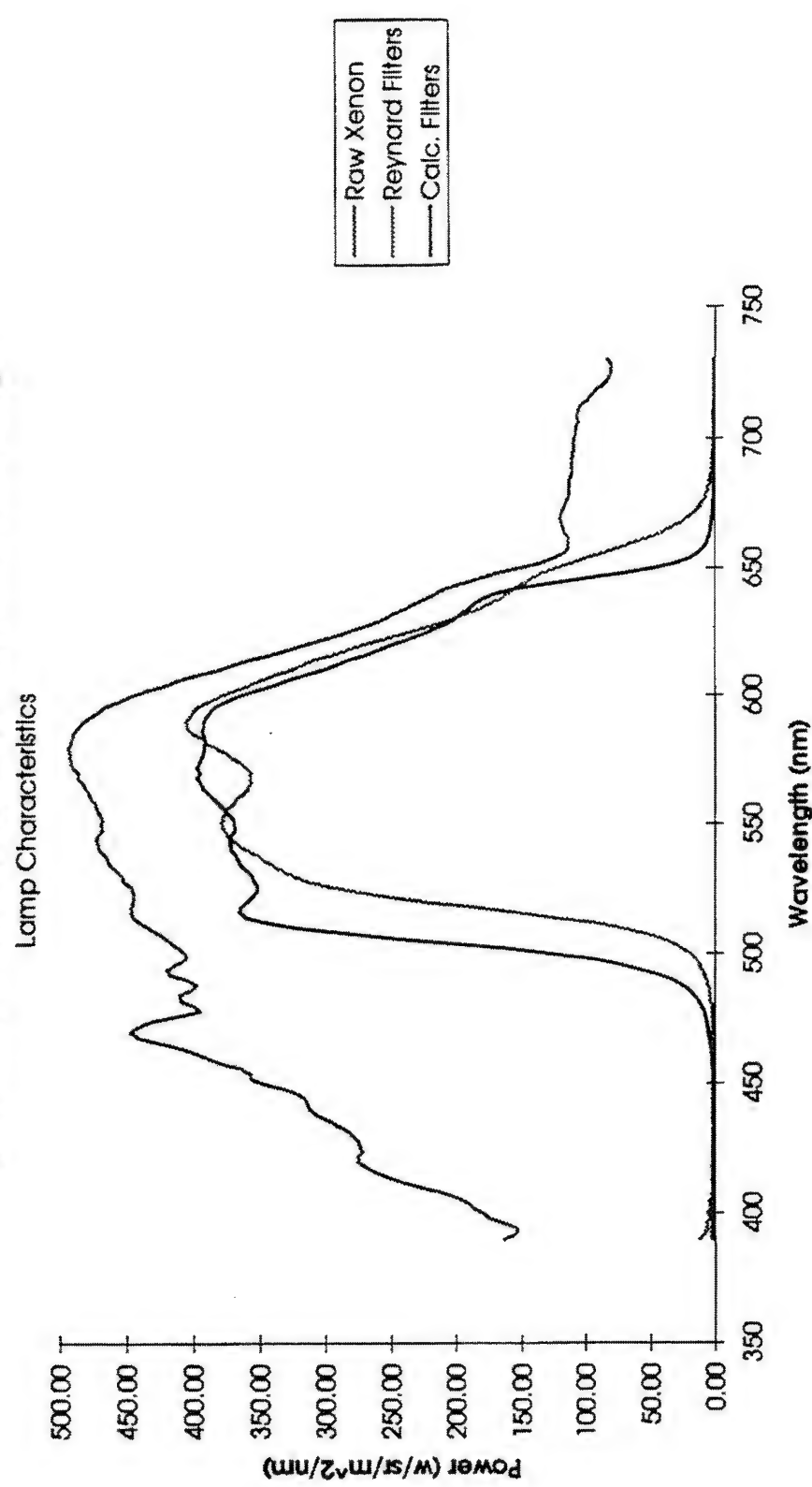


Figure 3-59. Xenon Lamp Characteristics - Power vs. Wavelength.

Two-Primary Color Stack #5 = Double Narrow Band Design

Filtered Power (Reynard Filters)

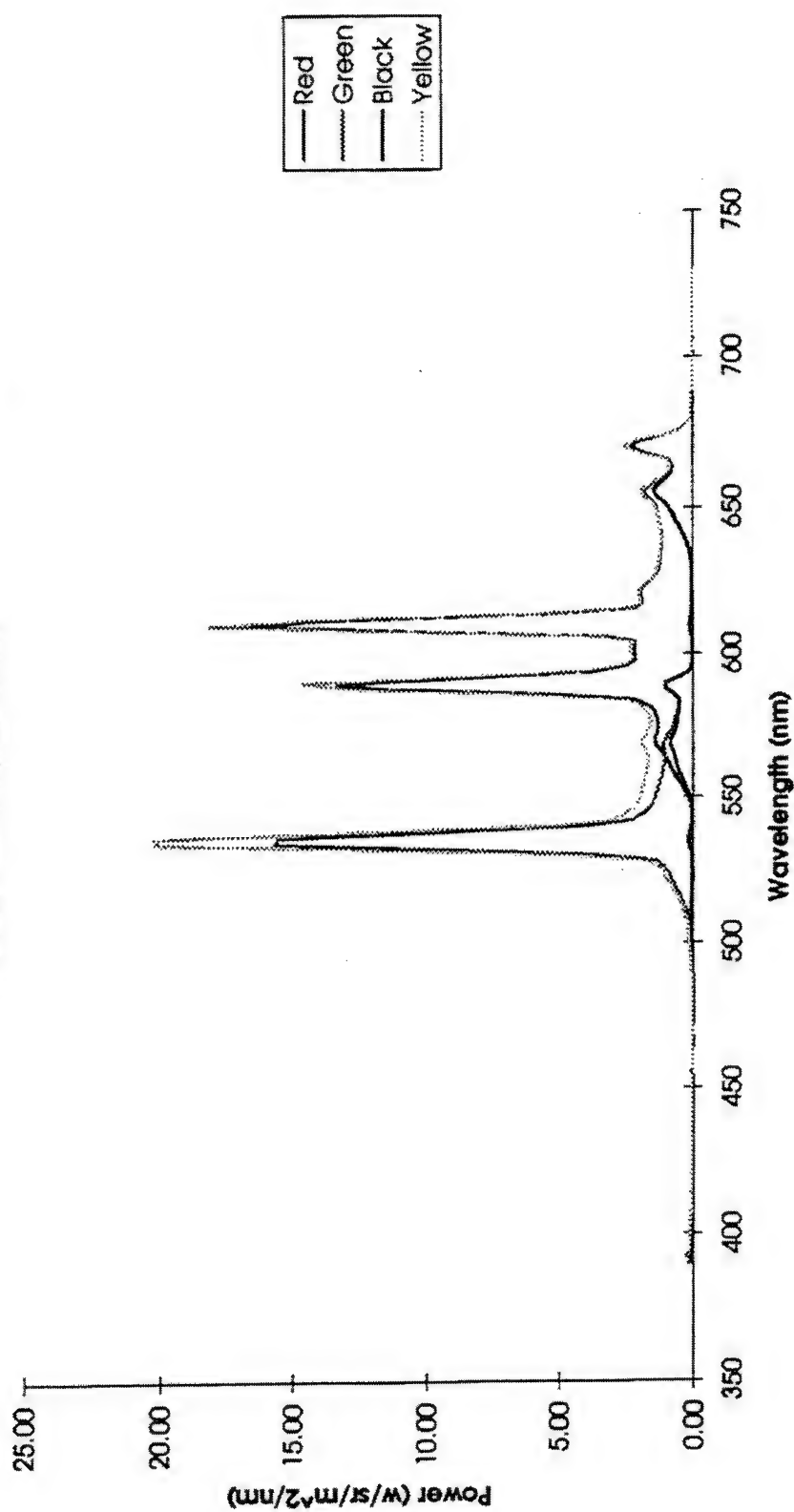


Figure 3-60. Stack #5 - Filtered Power vs Wavelength (Tri-band Lamp #69).

Two-Primary Color Stack #5 = Double Narrow Band Design

Filtered Power (Calculated Filters)

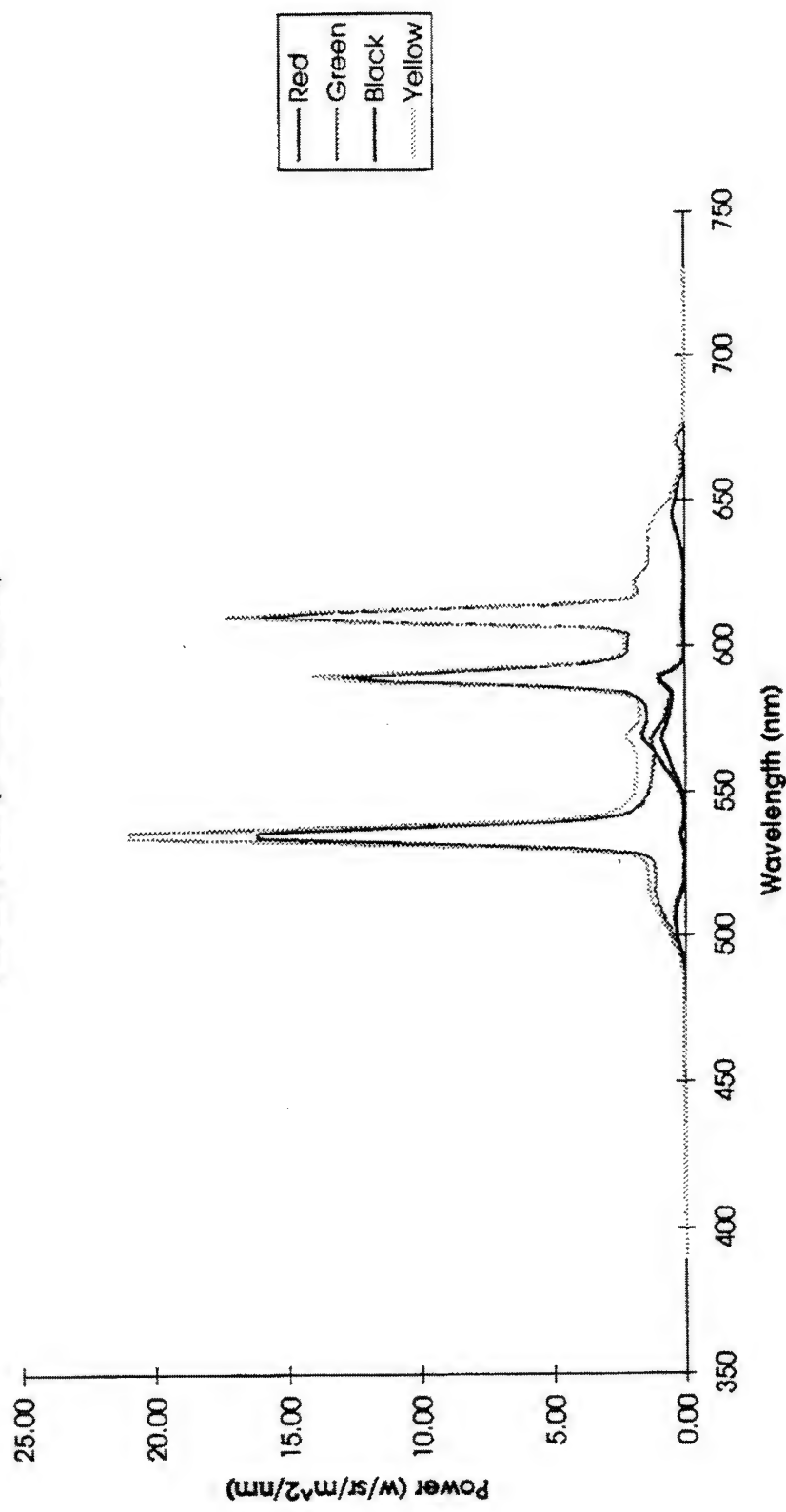


Figure 3-61. Stack #5 - Filtered Power vs. Wavelength (Tri-band Lamp #69).

Two-Primary Color Stack #5 = Double Narrow Band Design

Lamp Characteristics

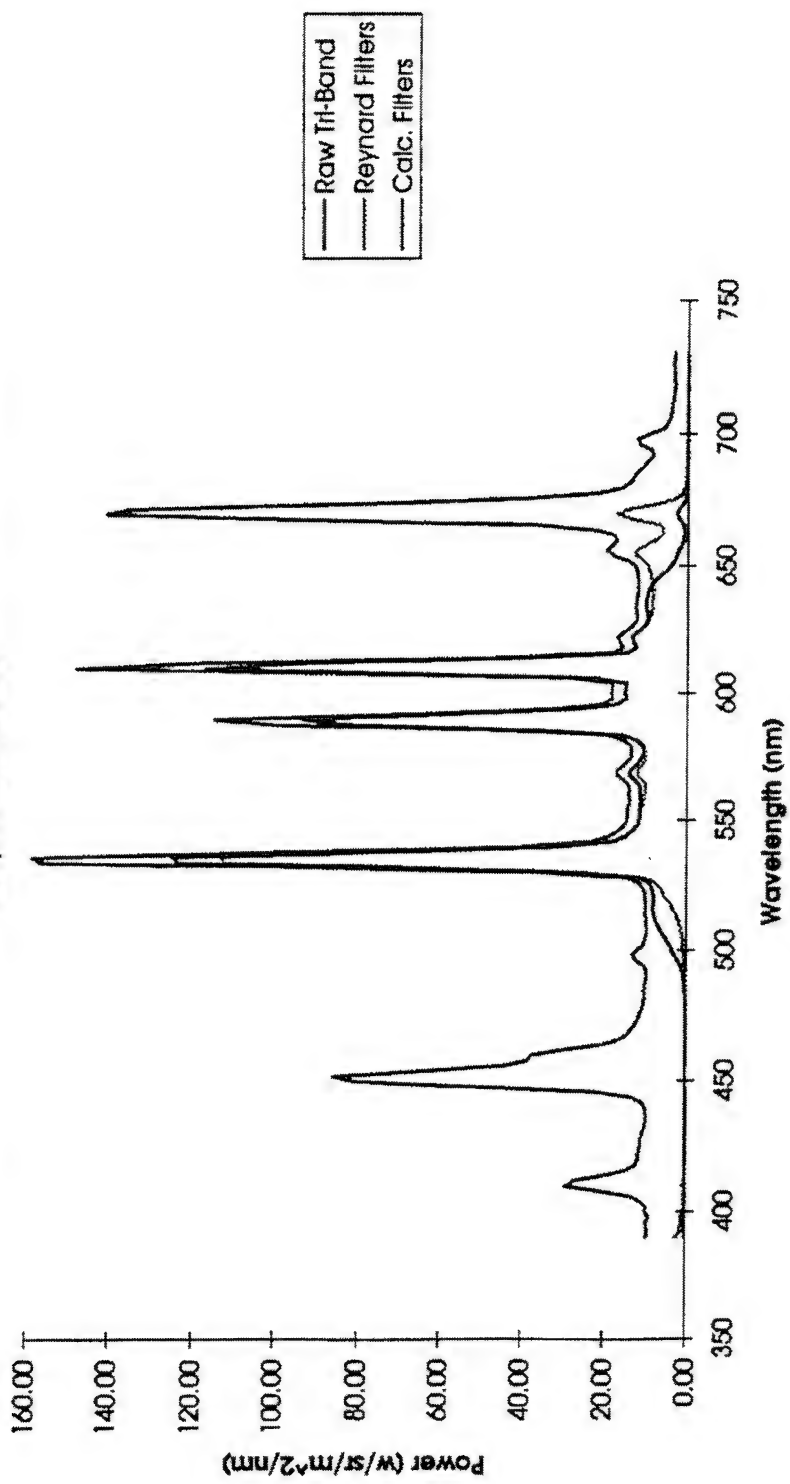


Figure 3-62. Tri-band Lamp Characteristics - Power vs. Wavelength.

3.8.1 Additional Optical Testing of Stack #5

The construction of stack #5 includes several special test patterns which facilitated special testing relevant to subtractive color performance. The optical effects, testing methods and summary of results are provided below.

3.8.2 Special Optical Considerations

While providing high, full-color light valve resolution in a small volume, the use of subtractive color introduces special considerations not normally encountered when utilizing other color methods. The image is formed in separate planes, each modulating a different range of wavelengths. A primary consideration is the merging of the respective light valve images into a single full color image. This is done optically, and can either be done external to the stack or internal to the stack. Each method has advantages and disadvantages. The preferred approach for a given application will depend upon a number of factors, a complete discussion of which is beyond the scope of the present task.

The present task addresses the optical considerations intrinsic to a two layer stack of active matrix liquid crystal light valves, with the assumption that the light valve images will be merged using optics external to the subtractive color stack. The presence of stacked opaque grid structures, with an aperture ratio less than 100%, gives rise to several potential optical issues which must be effectively managed in the design of the imaging system.

- **Diffractive Effects:** The presence of the front aperture array causes diffractive broadening of the light from the pixels in the rear light valve image. The image modulated by the front light valve is not broadened, since there is not aperture array between it and the viewer.
- **Moiré Artifacts:** These are optical aliasing patterns caused by multiplying the grid transmissions of the two light valves. The multiplication generates sum and difference frequencies, with the low frequency visual artifacts (difference frequencies) being given the name of Moiré patterns, similar to the pattern seen when looking through two stacked window screens.

- **Transmittance of Stacked Grids:** The anticipated effect on transmission of stacking multiple aperture arrays can vary depending upon the specific geometry of the structures as well as the optics used.

All of these potential artifacts have been previously modeled, and were characterized under the present program with regard to potential issues for the use of two-primary subtractive color.

3.8.3 Diffractive Effects

The rear light valve in a subtractive color stack must of course be imaged or viewed through the array of apertures which make up the front light valve. Since the two light valves modulate two different spectral bands of light, the image on the front light valve does not affect the visibility of the rear image (with the possible exception of phase effects, which are not considered here). Assuming that the pixel pitch is significantly smaller than the separation between the light valve planes, the effect of the opaque grid structure can be related to a far field diffraction pattern through an aperture. A bundle of parallel rays (such as from a single, "distant" pixel) will be diffracted into a pattern which is determined by the Fourier transform of the aperture array. The Fourier transform of an array of apertures is the product of an array of delta functions and the Fourier transform of an individual aperture.

We thus can expect that a single pixel in the rear image will appear as a central pixel surrounded by a two dimensional series of satellite images, each resembling the shape of the original pixel but having a different intensity. To characterize this spreading, a test device was fabricated. The optical effects test device consists of two single pixel LCD cells, stacked and bonded together with a polarizing film between them. The polarizing film in this test served primarily as a spacer to adjust the light valve to light valve spacing appropriately. White light was used for the evaluation, for simplicity. Each test cell included an opaque metalization pattern, complete with matrix structure and designed-in pixel test patterns (non-dynamic). Six regions were provided in the device, including 32%, 48%, 73% and 92% aperture ratios at 24 micron pitch as well as 67% and 90% apertures at 20 micron pitch. Dark pixels were simulated by filling in the metalization pattern for that pixel (giving it 0% aperture), and light pixels retain the nominal aperture ratio. The test cell arrangement is shown in Figure 3-63.

The patterns allow for measurement of both single pixel and large area performance in both light valve planes. Black squares of varying sizes are also provided on the rear layer.

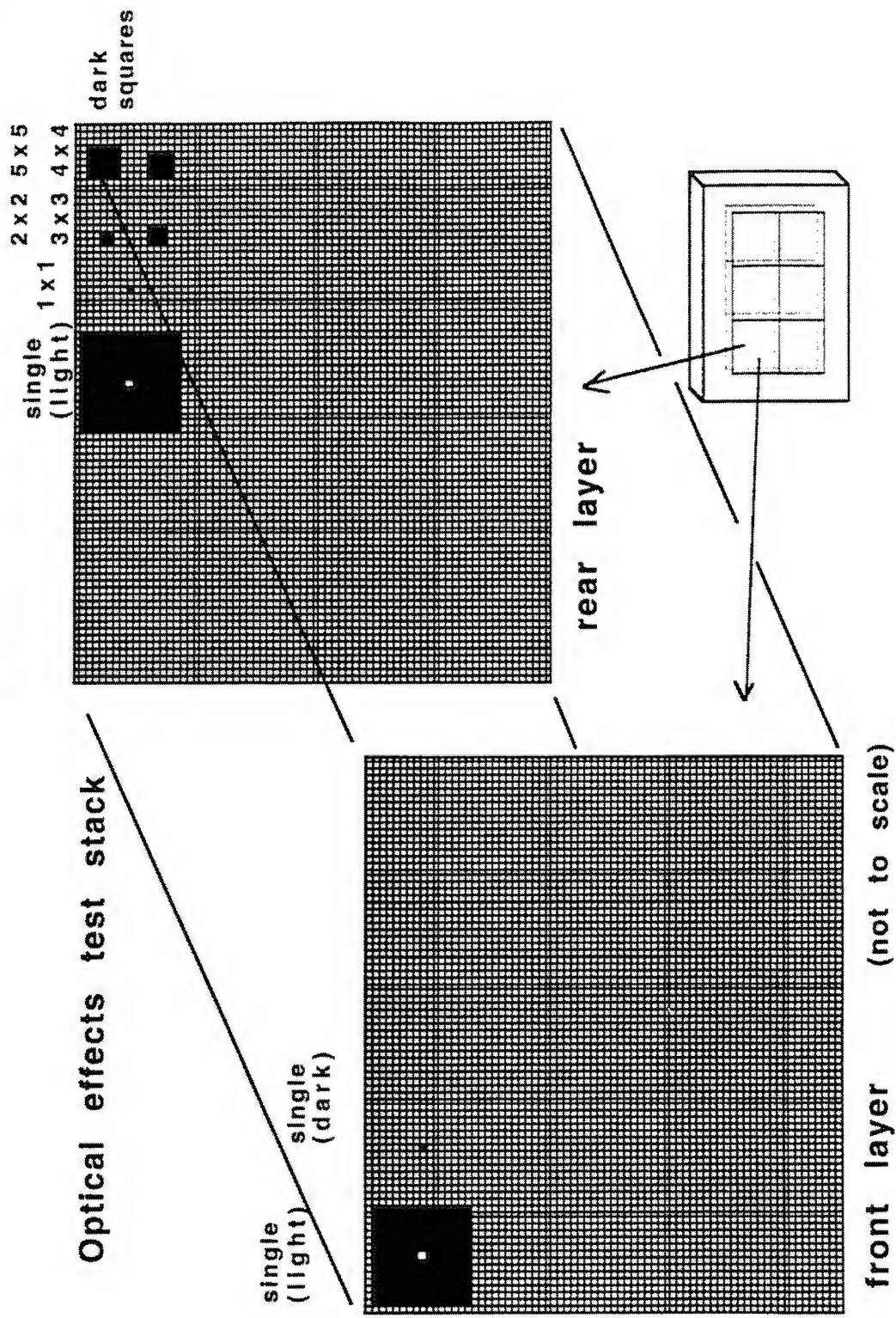


Figure 3-63. Optical Effects Test Device.

The following diffractive tests were run:

- Single light pixel (rear layer) diffraction pattern—intensity in each of the lobes was measured.
- Effective Edge Profile
- Rear layer intensity comparisons, large area light, dark squares of different sizes.

As expected, no diffractive spreading of the front layer was observed.

The rear layer, single pixel diffraction patterns are shown in Figure 3-64 through Figure 3-65, and identified below.

Figure #	aperture ratio (designed)	pixel pitch (microns)	approximate lobe spacing (microns)
Figure 3-64	32 %	24	20
Figure 3-65	48 %	24	20
Figure 3-66	73 %	24	20
Figure 3-67	92 %	24	20
Figure 3-68	67 %	20	26
Figure 3-69	90 %	20	26

The approximate lobe spacing agrees reasonably well with that expected based upon a .051 in. layer to layer separation, and the nominal pixel pitch (within measurement error using a micrometer translation adjustment). In particular, the spacing of the satellite images goes up as the pixel pitch goes down. The design of this mask brackets the pitch (for this nominal separation) at which the lobe spacing is comparable to the pitch. Lobe spacing would also be expected to vary directly with the layer to layer separation.

The referenced figures show, in bar chart form, the relative intensities (measured as luminance, with a white backlight and photometric microscope) of each diffracted pixel image, with each being normalized by the luminance of a white pixel surrounded by other white pixels (i.e., in the center of the pattern shown in Figure 3-63). The x and y axis labels symbolize the order of the peaks, which can be converted to distance using the lobe spacing numbers above. Where no peaks are shown, the intensity of the peaks (if visible) is close to the background black level (although additional power can be found in those low-level peaks).

The diffraction figures agree quite well with what is expected based upon simple far-field diffraction theory. The intensity of the center peak in each case is reduced from the normal, white level by approximately the aperture ratio. As the aperture ratio is increased, the extent and intensity of the side lobes decreases, with a corresponding increase in the primary, center peak. This, in essence, gives the pixel spread function for the rear layer due to the use of the two-layer subtractive color configuration. Of course, other contributions to the total pixel spread function are not included in the figures. These would include the response of the optics and image data source, as well as diffraction and other limitations in the human visual system.

A different representation of the effect of diffraction on the rear image is shown in Figure 3-70. Here, the effective edge profile is seen. For clarity, only the 24 micron pitch data are shown. The 20 micron pitch data behave similarly. The pixel intensity was measured along a line through the large black square (in Figure 3-63), taking care to avoid the light pixel in the center. This shows that the softening of the edge increases as the aperture goes down. In all cases, there is a moderately long but faint tail on the spreading, associated with the crispness of the masked pixel edges.

Yet another picture of the diffractive effects can be seen in Figure 3-71. This chart shows the relative intensity of various patterned features in the rear light valve. In particular, the intensities of small dark dots surrounded by a light background are shown. Again, higher aperture yields higher contrast for very small features. While it is true that the contrast of the small dots is degraded (for example, the small dots in the front light valve would be limited by the LCD contrast ratio), similar degradation of fine detail results from typical collimation optics as well as resolution limiting effects in the eye (e.g., diffraction at the pupil). Hence, this loss of contrast is merely one of many contributions to the modulation transfer function (MTF) of the optical path, and should be taken into account during the design of the system.

To summarize the diffraction studies, no diffractive spreading was expected or observed in imagery on the front light valve layer. The rear layer exhibited diffractive spreading as expected. The degree and extent of the spreading are decreased as the aperture ratio is increased. The extent of the spreading is also related to both the pixel pitch and the layer separation. To minimize the diffractive effects, a high aperture ratio is preferred, and layer separation should kept as small as is practical. Use of a limited aperture ratio is still a valid option, although the resulting pixel spreading should be factored into the overall characterization of the system resolution.

Diffractive Spreading, 32% aperture

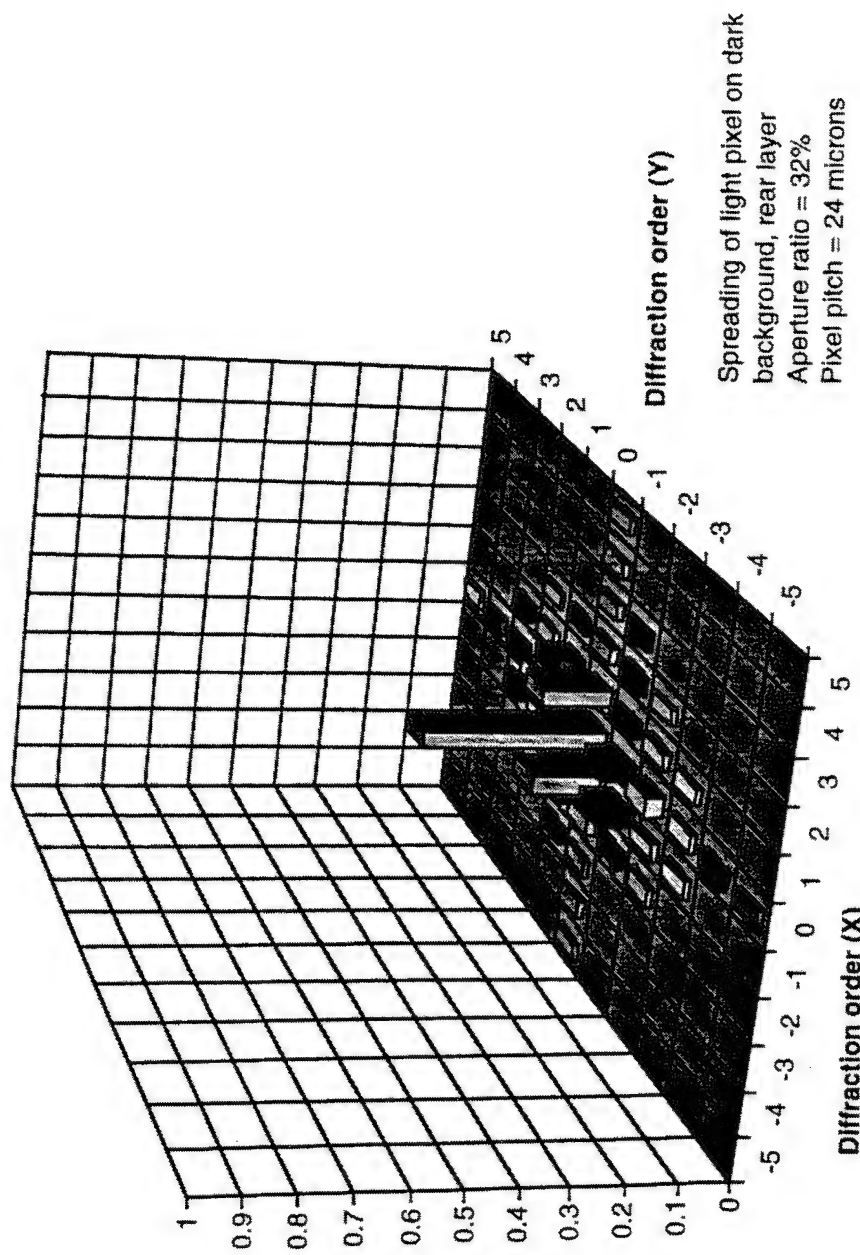


Figure 3-64. Diffractive spreading, 32% aperture.

Diffractive Spreading, 48% aperture

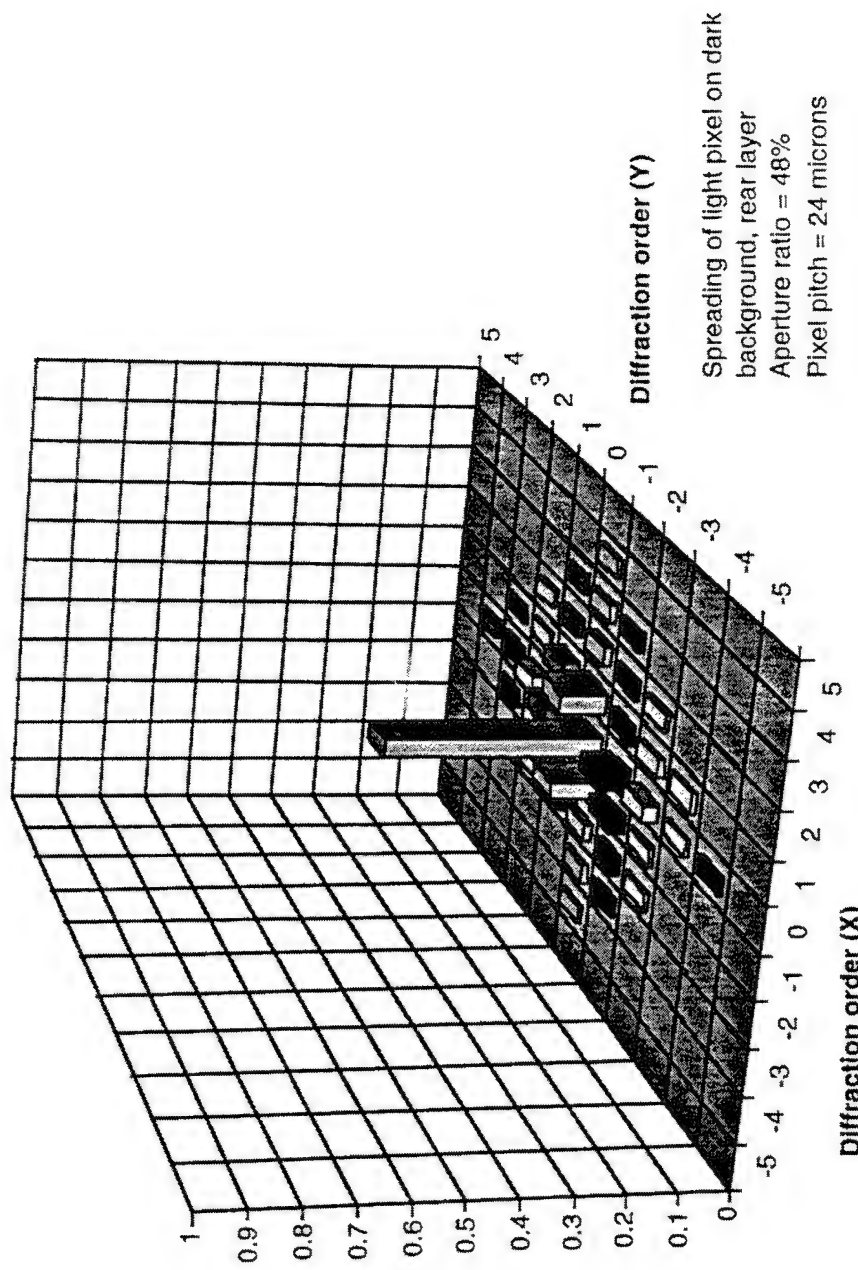


Figure 3-65. Diffractive spreading, 48% aperture.

Diffractive Spreading, 73% aperture

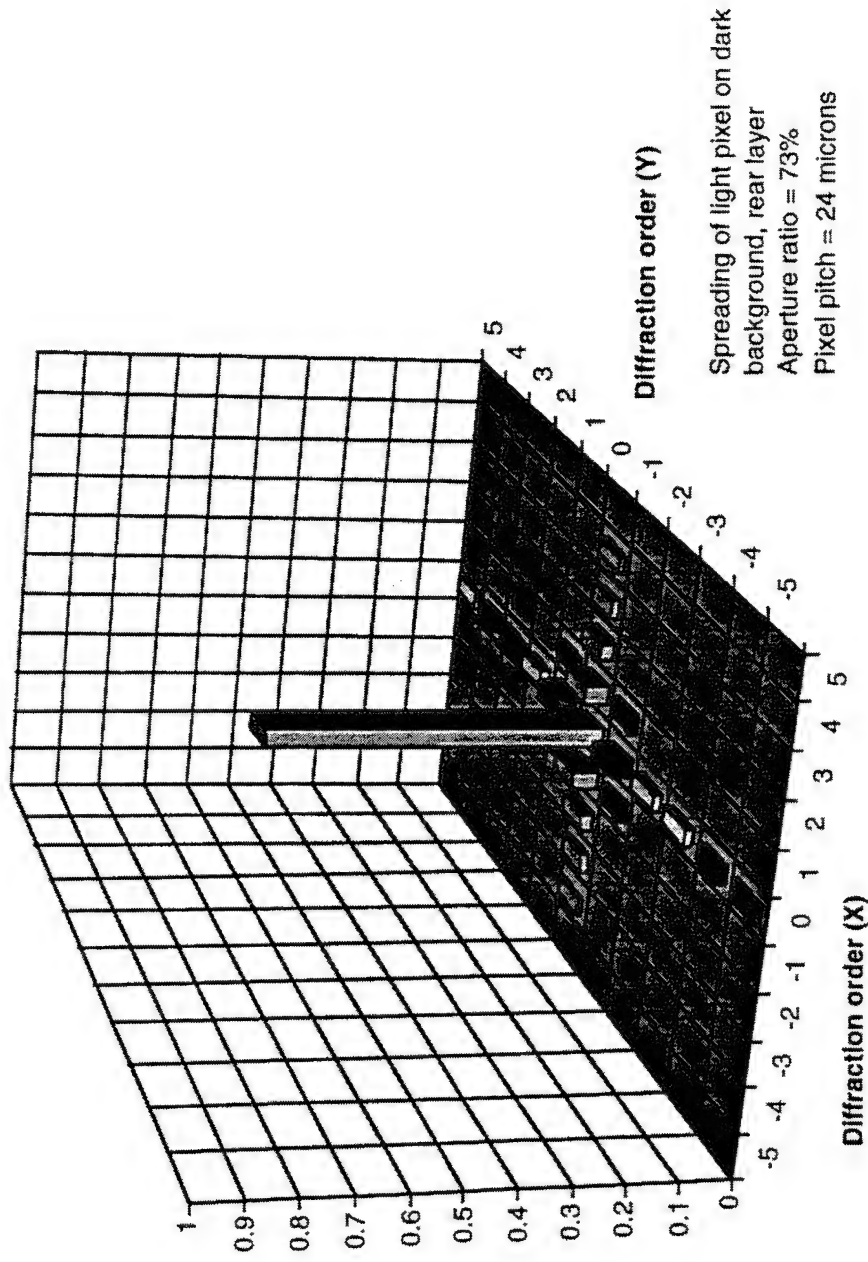


Figure 3-66. Diffractive spreading, 73% aperture.

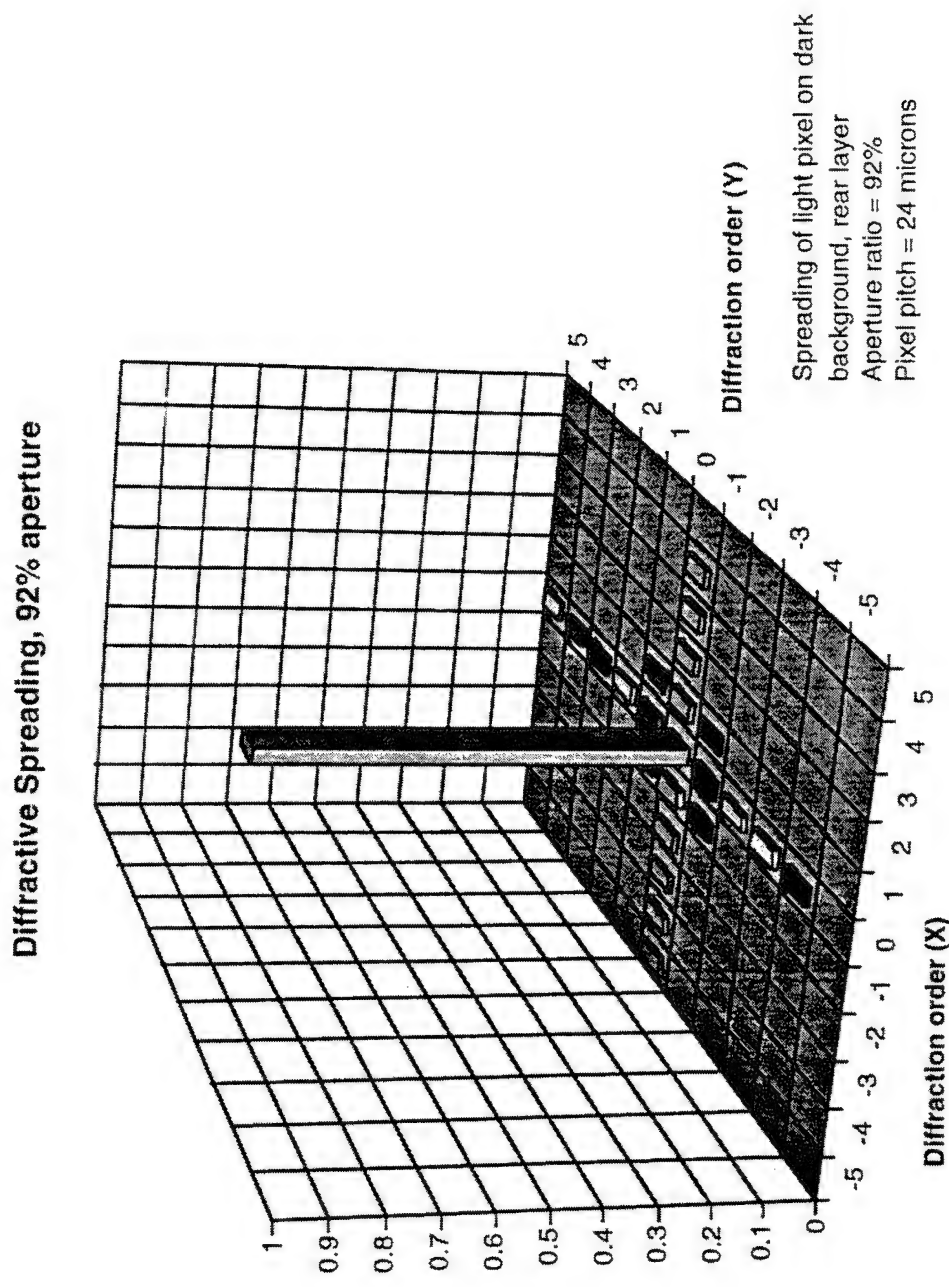


Figure 3-67. Diffractive spreading, 92% aperture.

Diffractive Spreading, 67% aperture

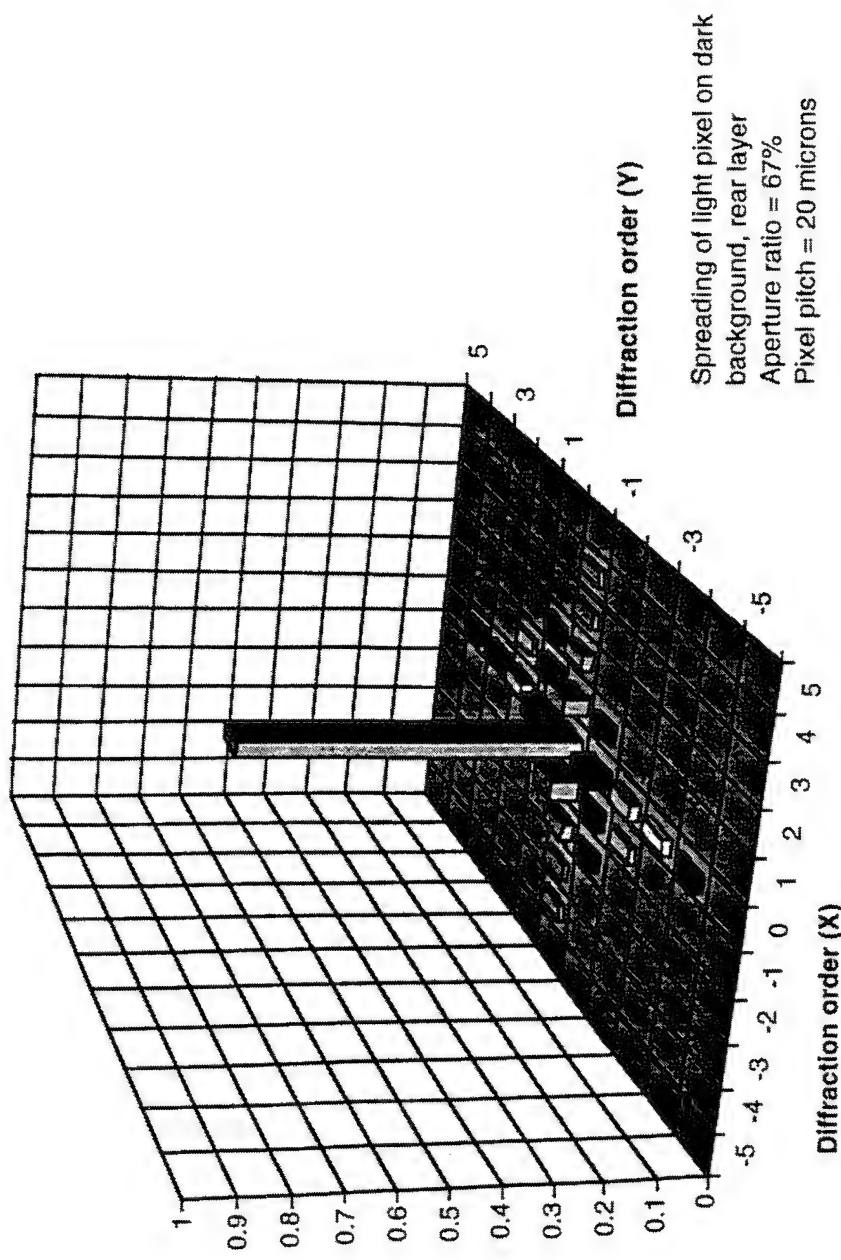


Figure 3-68. Diffractive spreading, 67% aperture.

Diffractive Spreading, 90% aperture

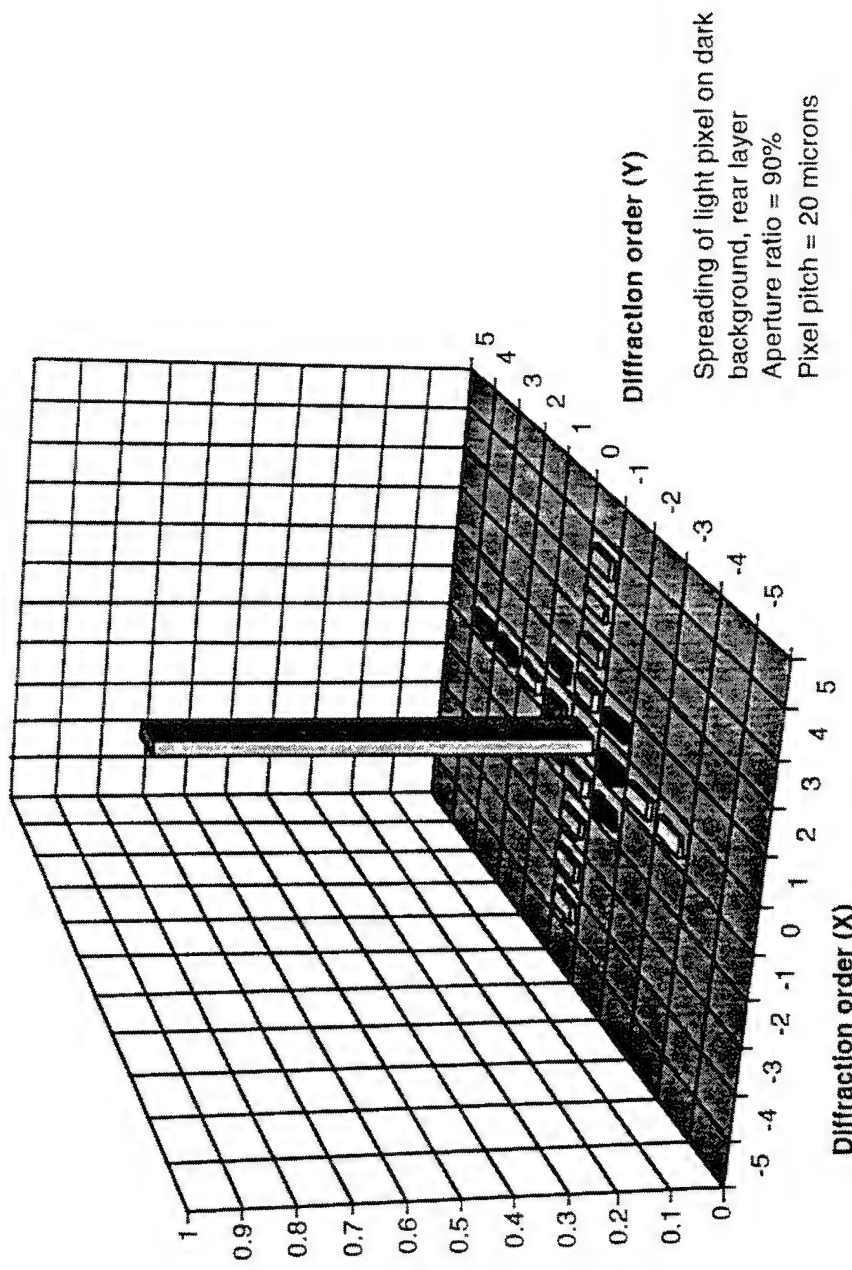


Figure 3-69. Diffractive spreading, 90% aperture.

Effective Edge Profile, Rear Cell Image

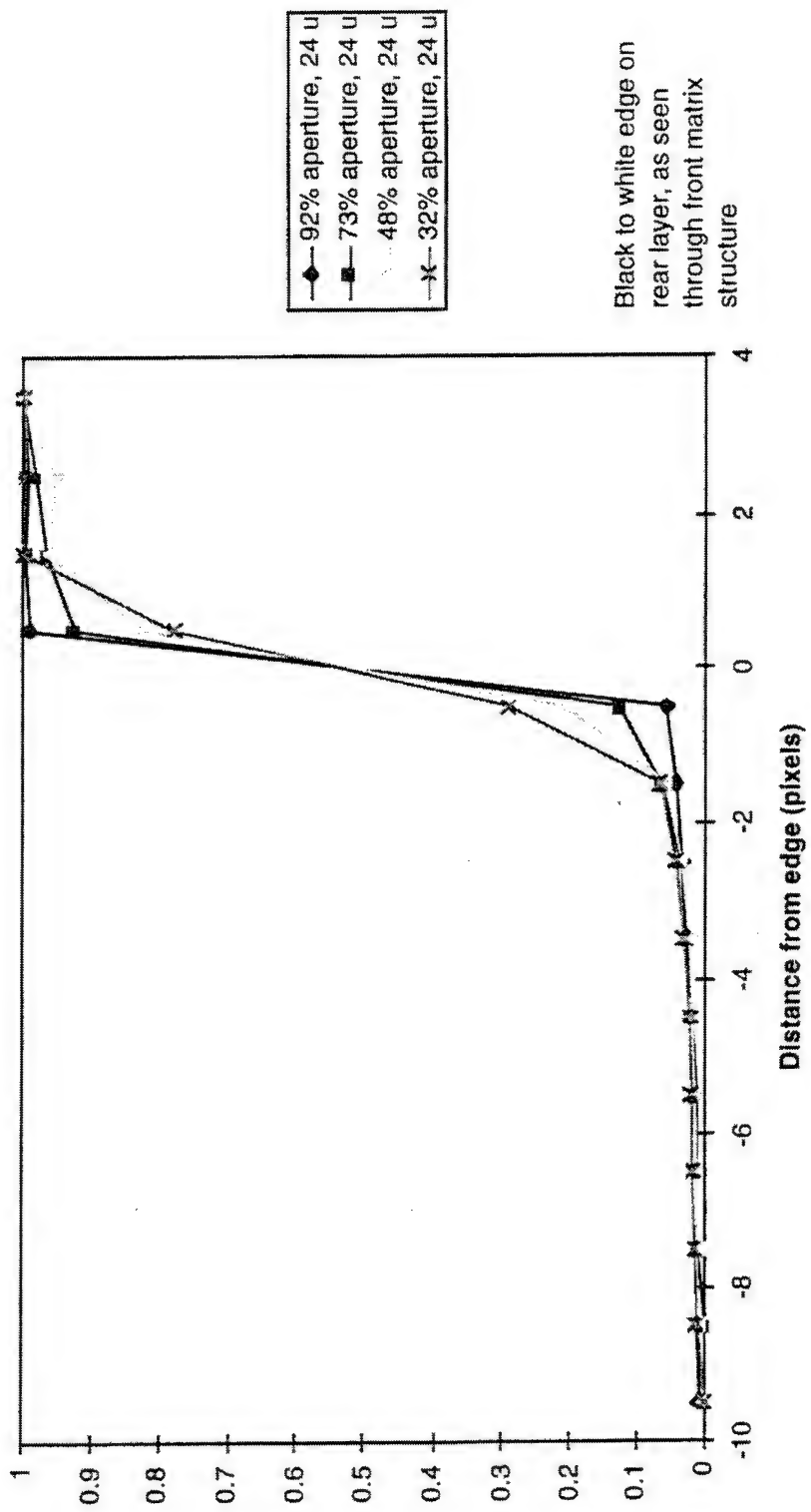


Figure 3-70. Effective Edge Profile, Rear Cell Image.

Relative Intensities, Rear Cell Image features

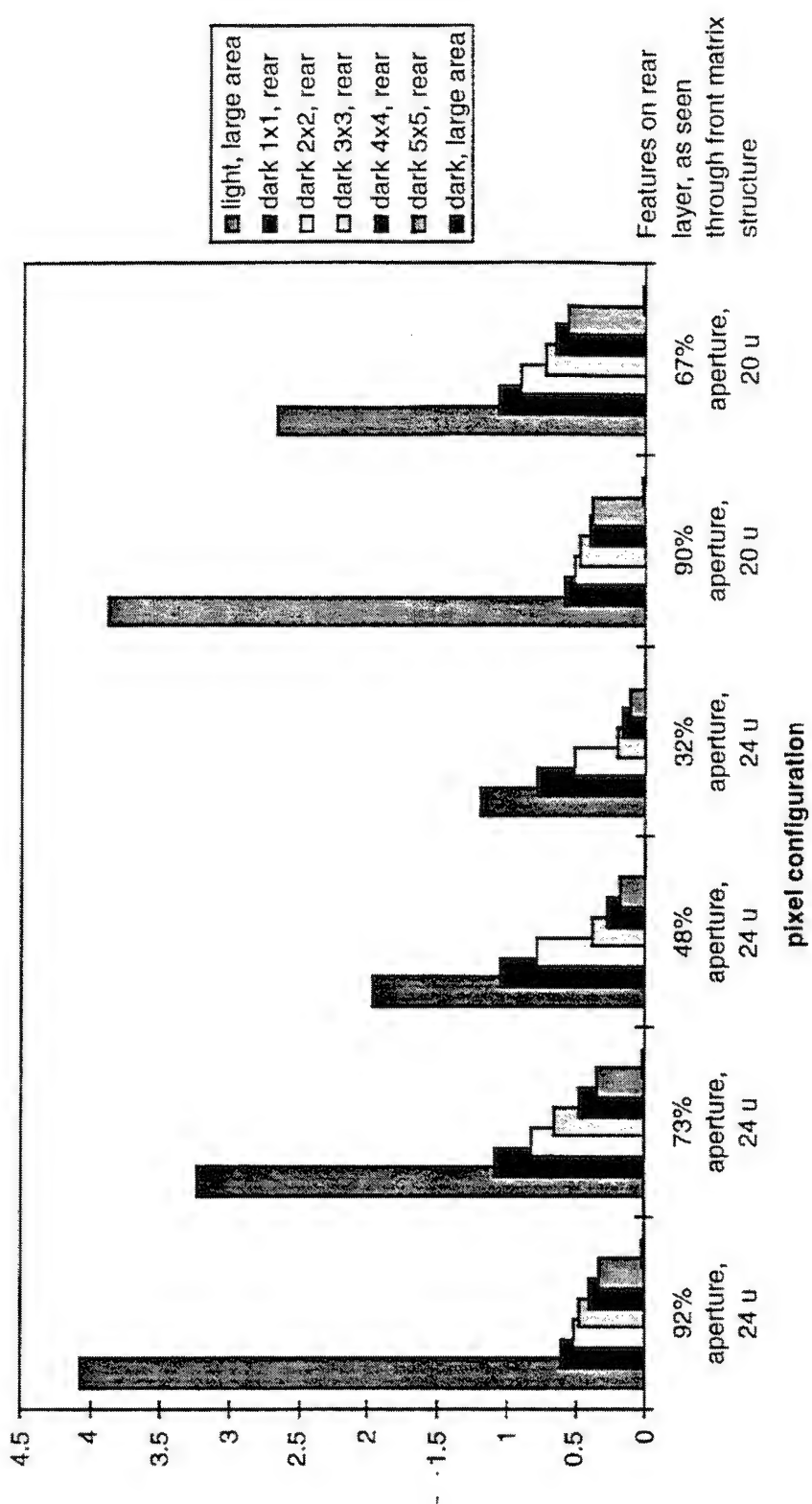


Figure 3-71. Relative intensities, rear cell image features.

3.8.4 Moiré Artifacts

Moiré effects are visual interference, or aliasing patterns which can become visible in subtractive color AMLCD stacks due to the presence of the opaque matrix structures. In the subtractive color devices considered here, the pixel pitch is considerably smaller than the separation between the two layers. This causes the interference pattern to be dependent upon the angle from which the stack is viewed. Assuming that the visual system will average the light received, at the angle of viewing, from all portions of the pixel, the Moiré properties can be analyzed as what can be called “angular aliasing effects.” Viewing a region of spatially uniform luminance at different angles will yield angular variation in the apparent luminance. This is the effect seen when viewing a bare subtractive color light valve stack from across the room.

Artifacts such as these are clearly unacceptable for a useful display. It is a goal of the Two-Primary Color analysis to measure this aliasing, and to verify that it can be managed and will not pose a problem in an HMD system.

The optical effects test device described above was also utilized to characterize the occurrence of Moiré artifacts as a function of aperture ratio. The test setup is shown schematically in Figure 3-72. A uniform (containing only opaque matrix patterns in both subtractive planes) is diffusely backlit and collimated by a lens. The purpose of the lens is to bring the far field (infinity) into focus on the projection screen shown. An aperture is provided near the stack to ensure that only a single aperture configuration is being viewed. The stack is translated to enable viewing of the other patterns. The lens images each unique angle through the stack onto a unique position on the screen. Thus the Moiré pattern is clearly shown on the screen. A CCD camera is used to record the image for display or subsequent analysis.

Sample images from each of the six sections of the test device are shown in Figure 3-73. Moiré is clearly visible at low aperture ratios and becomes progressively less pronounced as the aperture goes up. To better show the relative amplitudes of the aliasing patterns, representative surface plots of the intensity profile are shown in Figures 3-74 through 3-79.

Knowing the angular aliasing characteristics allows the Moiré patterns to be predicted for a given optical design. Several methods can be used to minimize and eliminate the patterns in the system design. While these methods are not reviewed here, Figure 3-80 shows an example of how the

Moiré can be effectively suppressed. The surface plot of Figure 3-80 represents the apparent intensity across the full field of view of a hypothetical, realistic collimated display configuration. This is based upon the 73%, 24 micron scenario. The Moiré artifacts are virtually eliminated. Depending upon the optical design, the period of the ripple can be extended to provide even smoother performance. Figure 3-81 shows a similar estimate, based upon measured Moiré data for the 48%, 24 micron case. Here again, performance can be improved even further. Laboratory mockups using the optical effects test device confirm that the Moiré is virtually eliminated by these methods, and indicates that Moiré is a consideration in the design stage, but can be effectively managed.

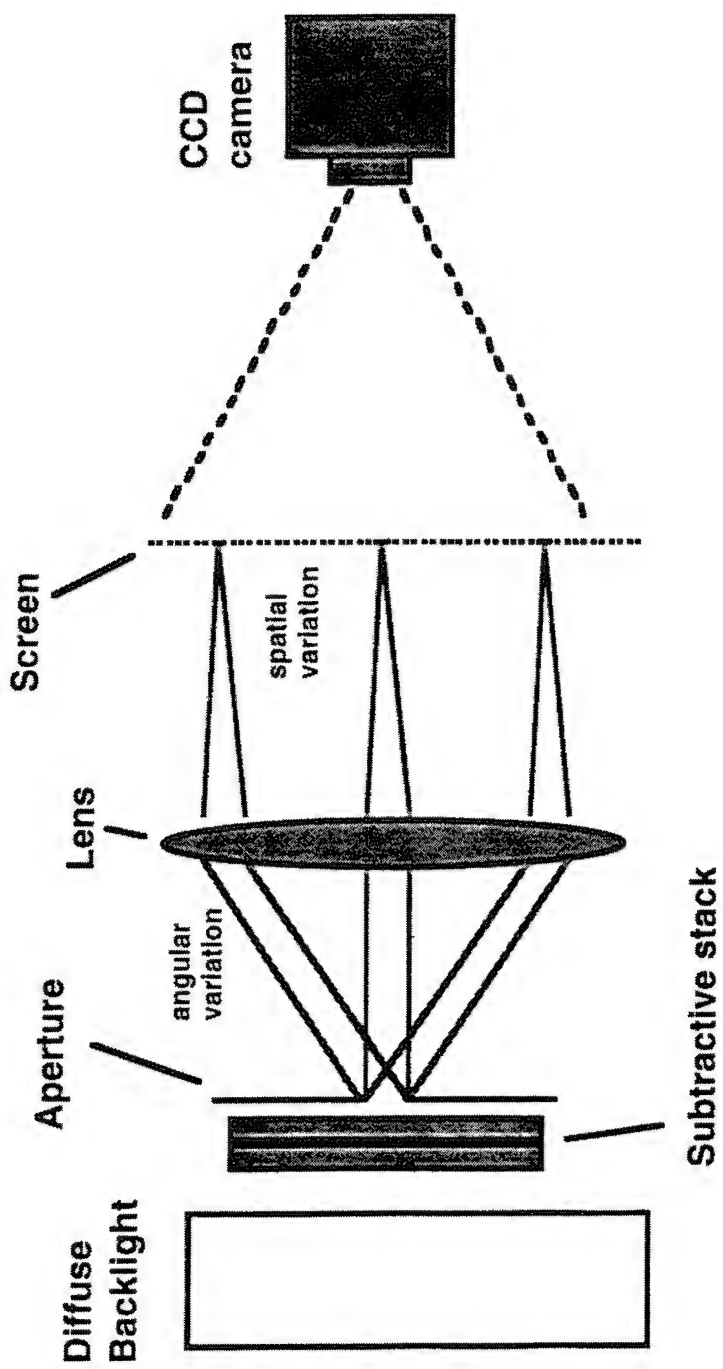
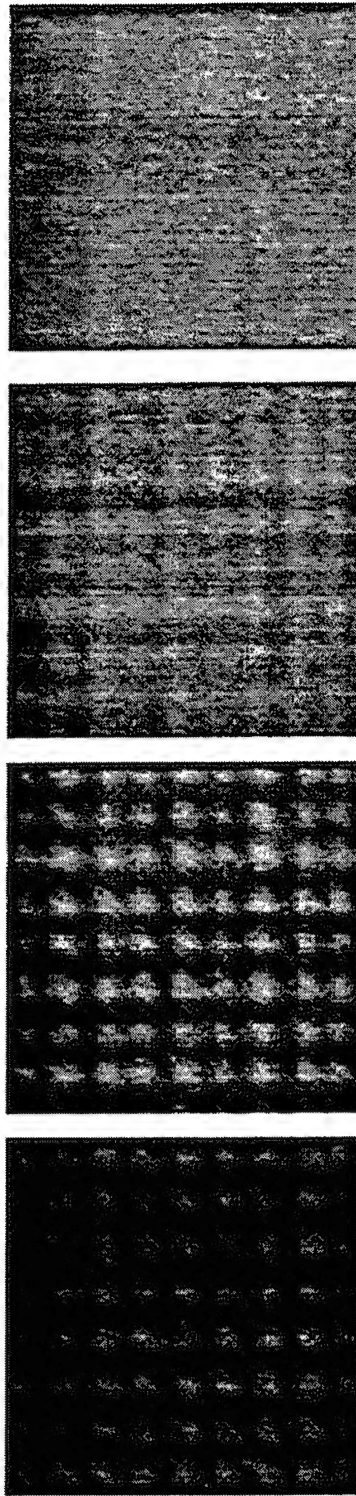
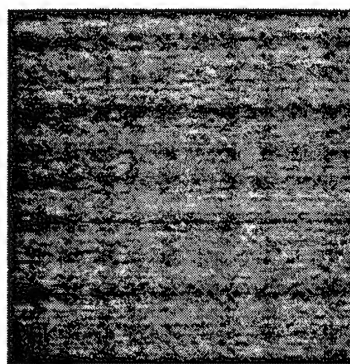
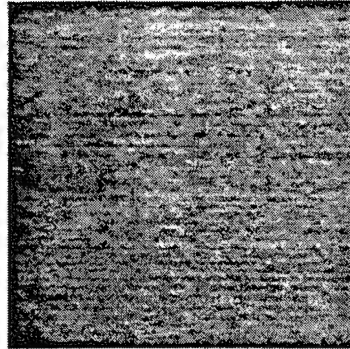


Figure 3-72. Setup for characterization of Moiré effects.



32%, 24u 48%, 24u 73%, 24u 92%, 24u



67%, 20u 90%, 20u

each division equals
approximately
1.15 degrees of angle

Figure 3-73. Far-field Moiré patterns as seen with stacked AMLCD light valves

32%, 24 mic

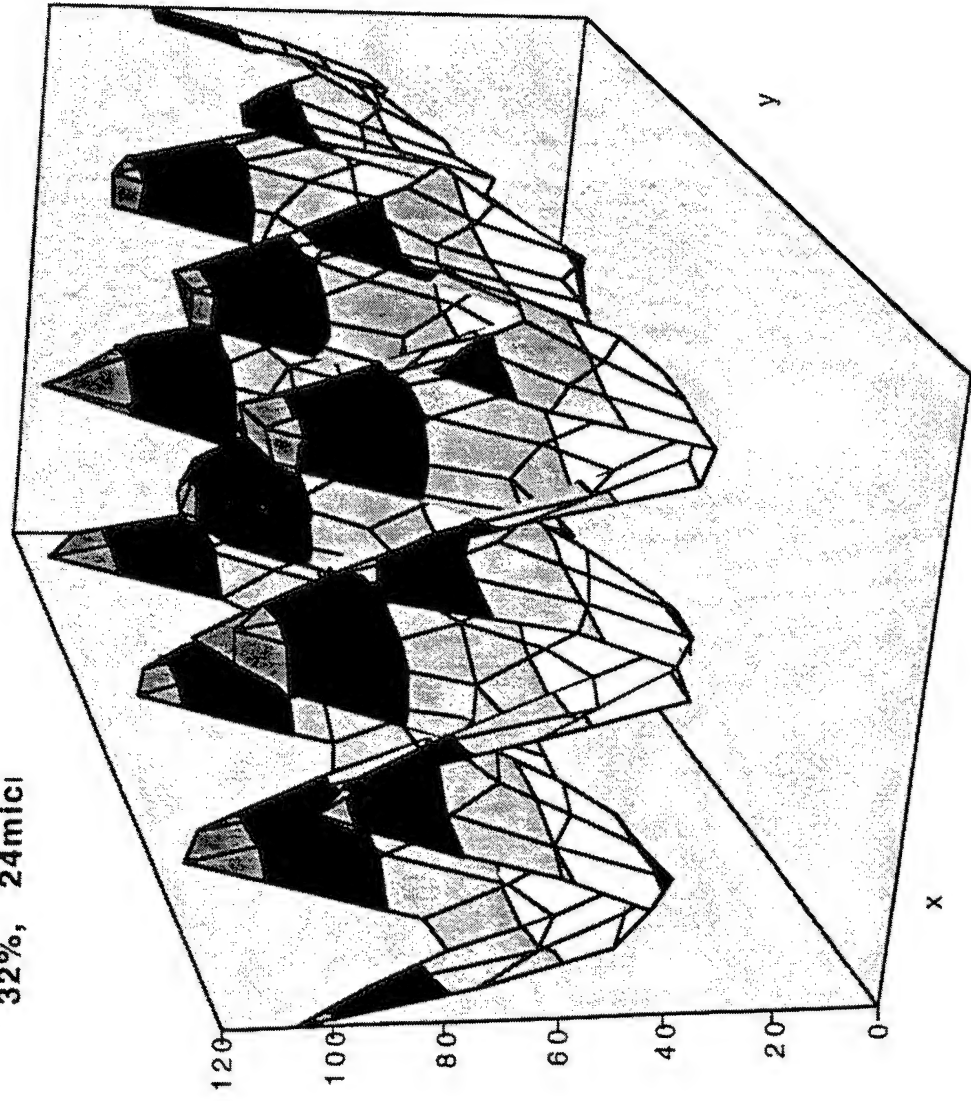


Figure 3-74. Moiré intensity profile, 32% aperture ratio and 24 micron pitch.

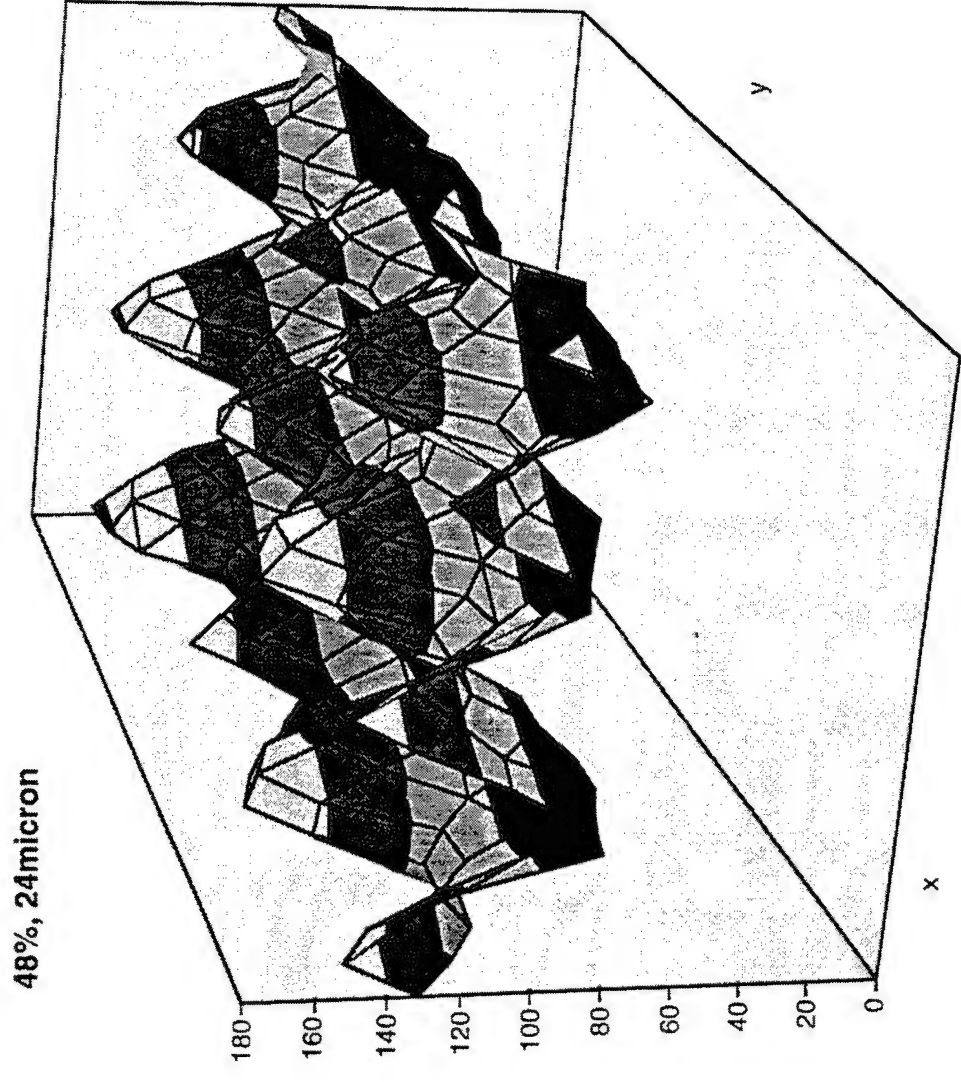


Figure 3-75. Moiré intensity profile, 48% aperture ratio and 24 micron pitch.

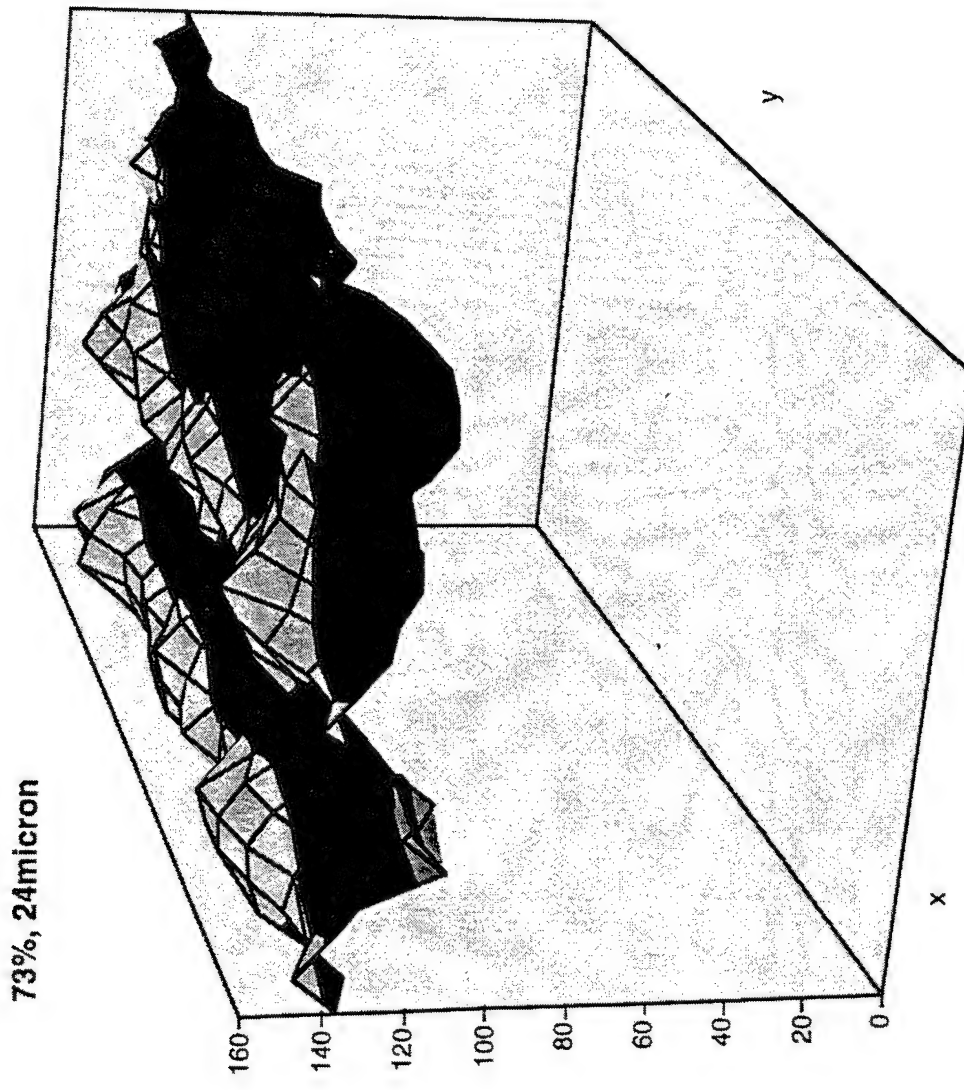


Figure 3-76. Moiré intensity profile, 73% aperture ratio and 24 micron pitch.

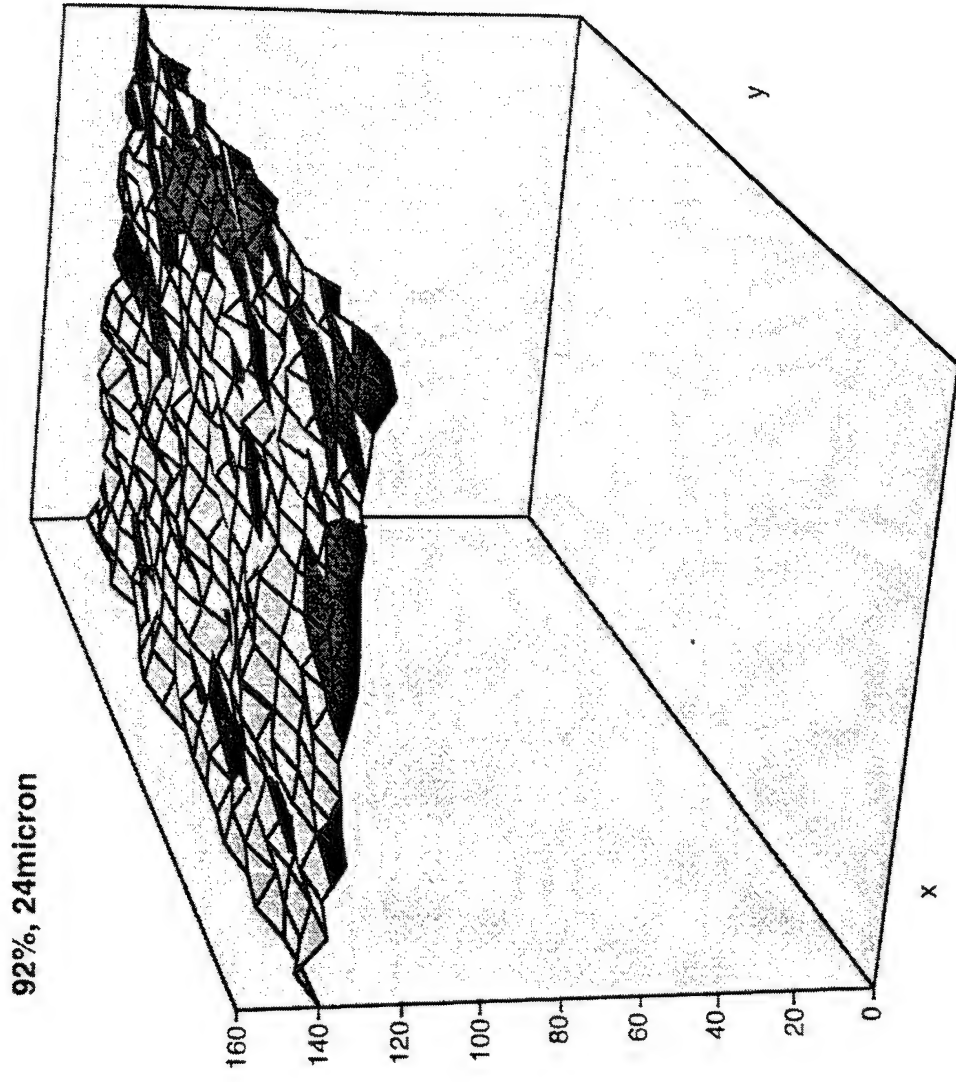


Figure 3-77. Moiré intensity profile, 92% aperture ratio and 24 micron pitch.

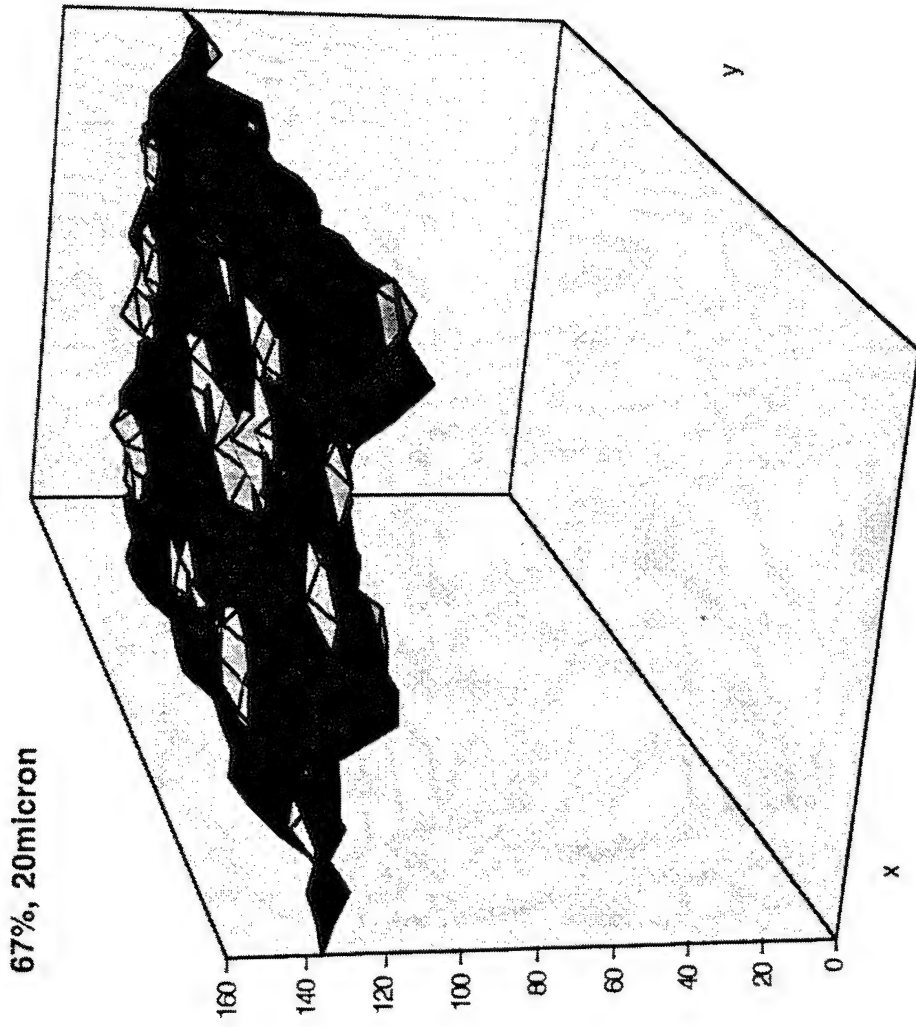


Figure 3-78. Moiré intensity profile, 67% aperture ratio and 20 micron pitch.

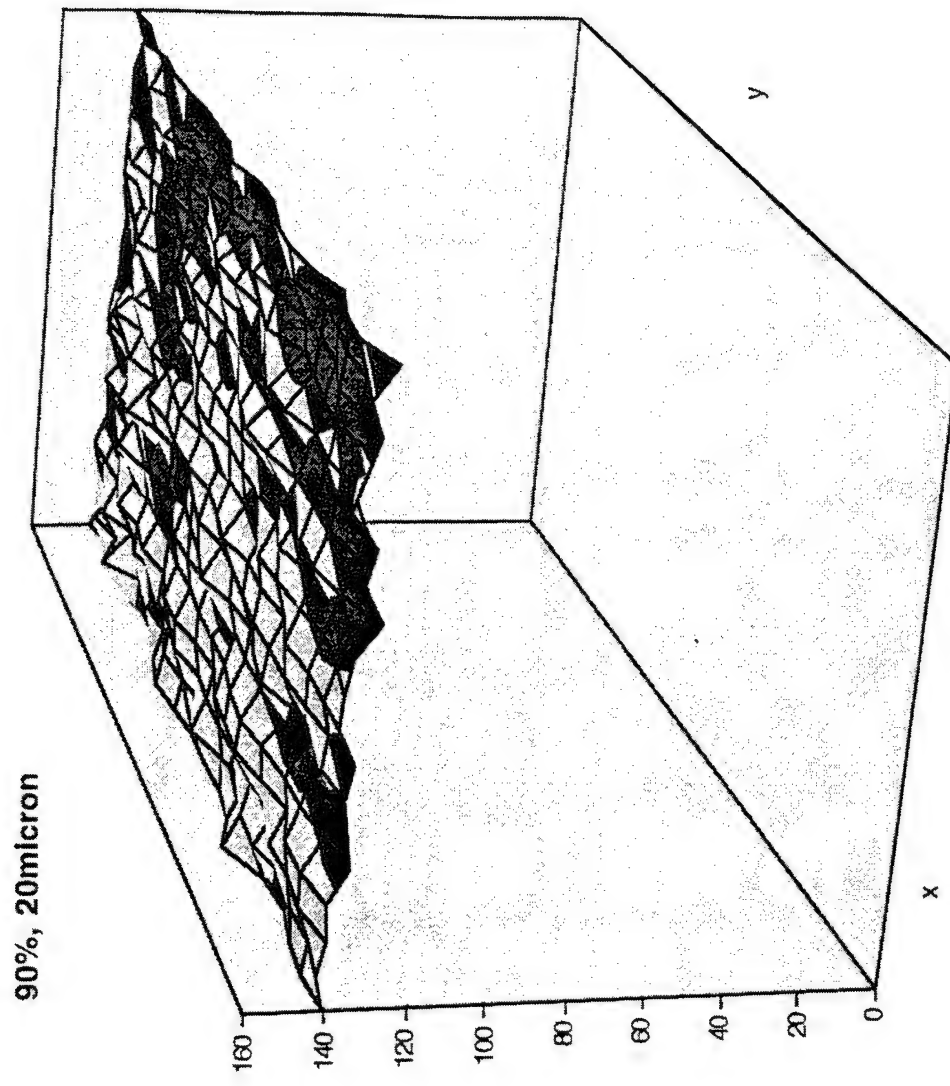


Figure 3-79. Moiré intensity profile, 90% aperture ratio and 20 micron pitch.

**Estimated non-uniformity
due to Moiré artifacts**

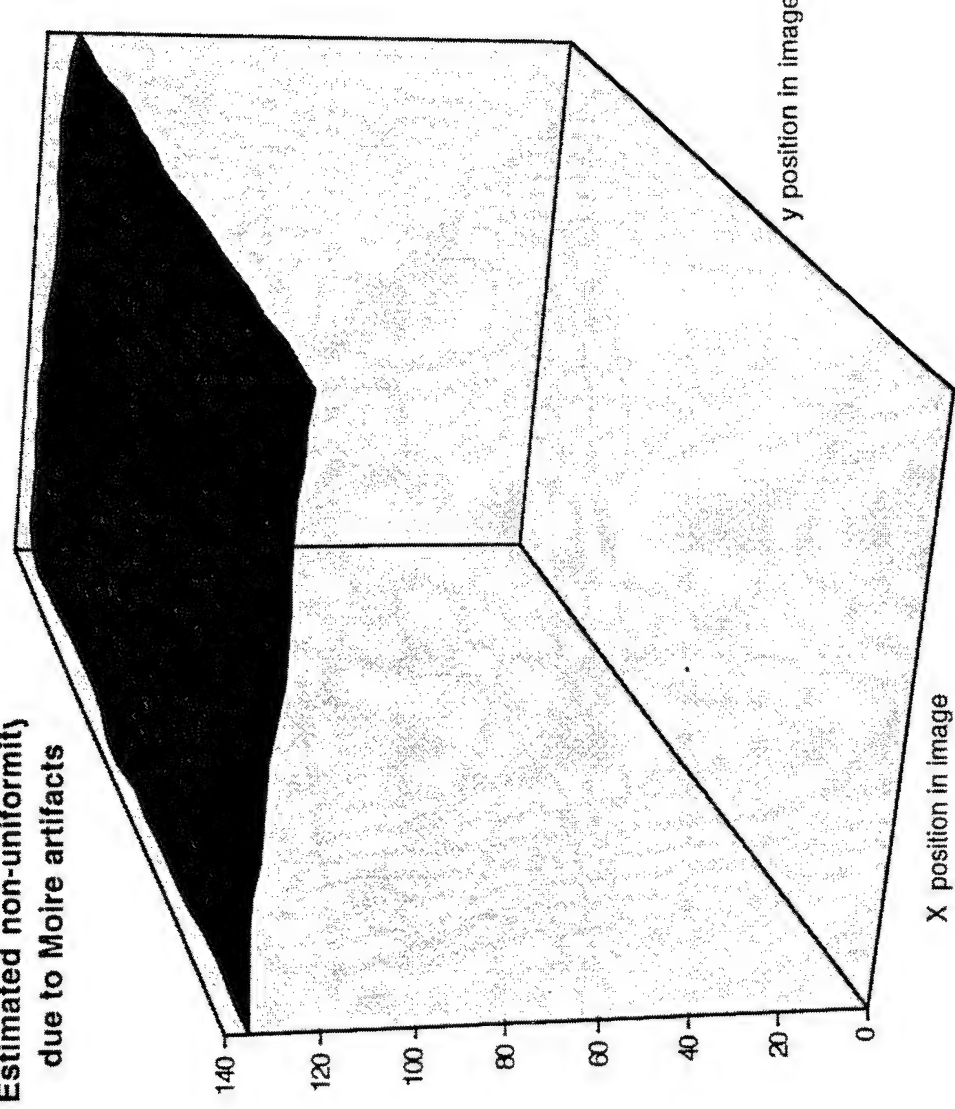


Figure 3-80. Estimated non-uniformity due to Moiré artifacts—assumes moderate corrective measures and 73% aperture ratio.

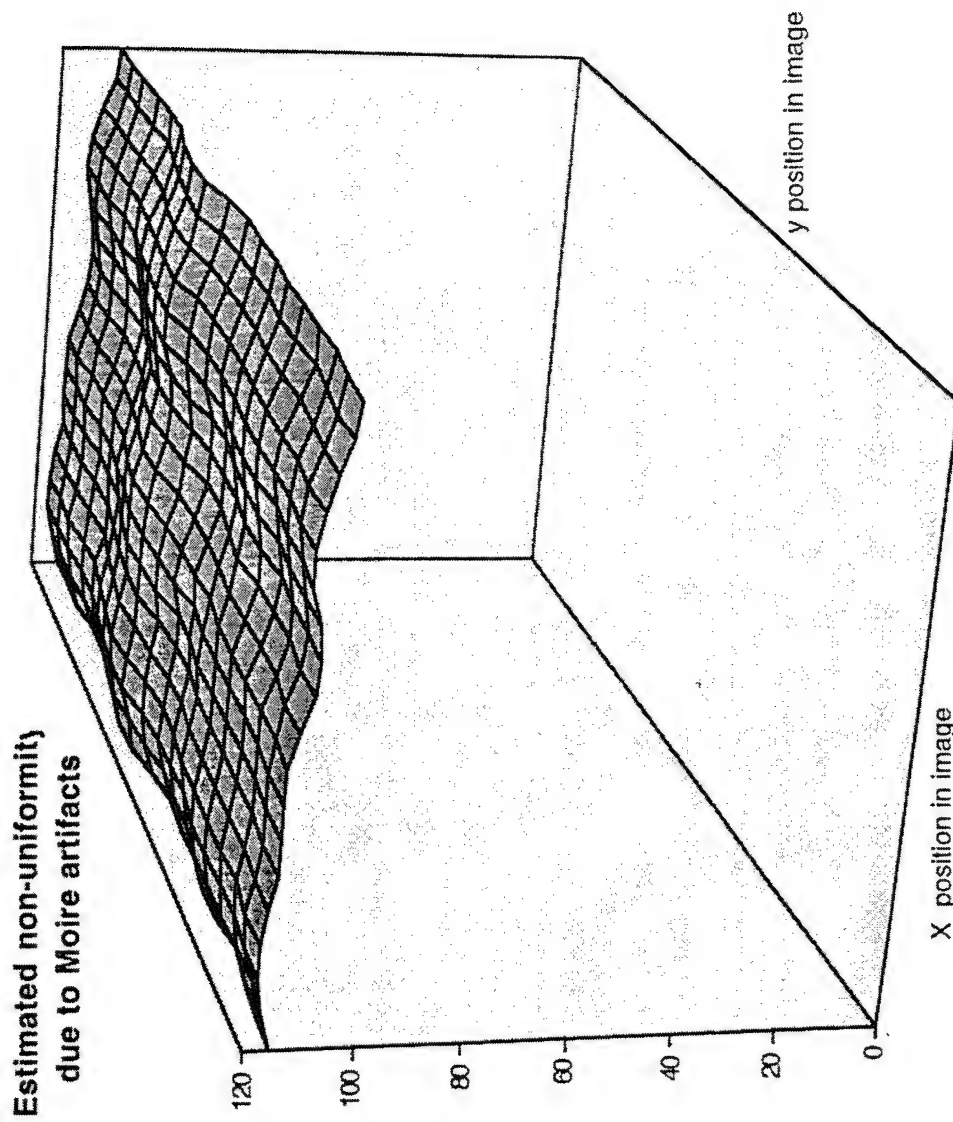


Figure 3-81. Estimated non-uniformity due to Moiré artifacts—assumes moderate corrective measures and 48% aperture ratio.

3.8.5 Transmittance of Stacked Grids

In the subtractive color approach being analyzed here, we have made the assumption that external optics are used to superimpose the separate active layers. For the configuration being considered, modeling predicts that the transmittance of the stack will vary as the product of the aperture ratios in each of the layers. To verify this prediction, the transmittance of the optical effects test device was measured in the individual aperture regions. The transmittance measurement used white (unfiltered) Xenon light and the equipment configuration described in Section 3.3.

The measured results for the 24 micron are shown in Figure 3-82. In addition to the moderately directional light configuration described previously, a second set of measurements were taken using a diffuse backlight. This was achieved by inserting opal glass between the fiber bundle and the lens, in close proximity to the lens. The third set of points represents the anticipated transmittance as predicted by the product of the individual aperture ratios and independently measured transmittances of the substrates, ITO and centrally bonded polarizer (outer polarizers were not used for these measurements). As is evident from the data, the transmittance follows the predicted trend reasonably well. Similar agreement was found with the two 20 micron pitch arrays. The more directional backlight yielded somewhat lower results than the diffuse one. One likely mechanism for this is the spreading of the directional light due to diffractive effects in the aperture arrays.

Transmittance of optical effects test device

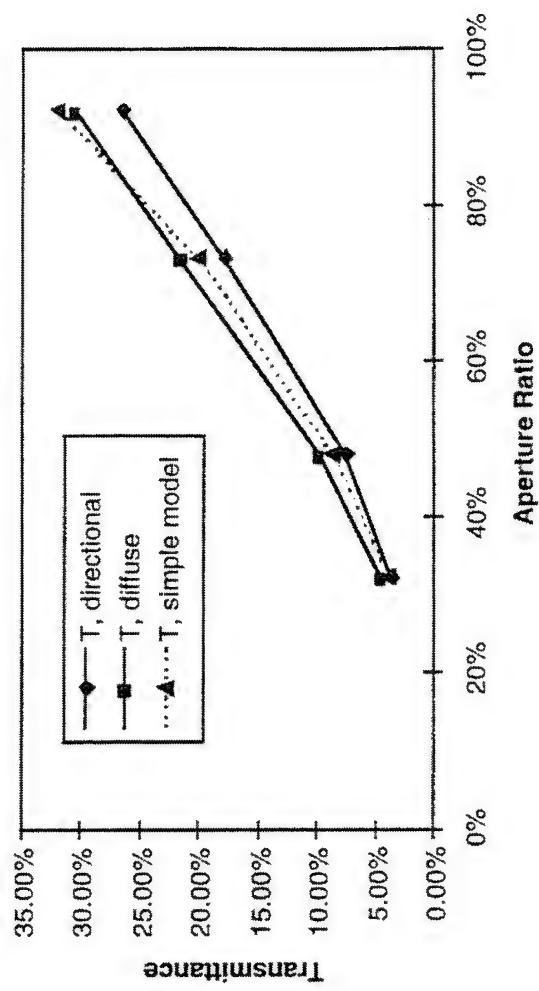


Figure 3-82. Measured and predicted transmittances of optical effects test device regions, 24 micron pitch.

3.9 Stack #6 Configuration and Results

Stack #6 configuration is based on the hybrid #1 design and consists of two Sony LCX007 AL active matrix liquid crystal displays. These AMLCDs have a 1.35 in. diagonal active area of 1068x480 pixels, with a 48% aperture and a 16x9 switchable aspect ratio. They are monochrome displays for implementing into the best resulting stack configuration (hybrid #1) for Two-Primary Color subtractive color displays. Stack #6 has an image plane to image plane distance of 0.093 in.

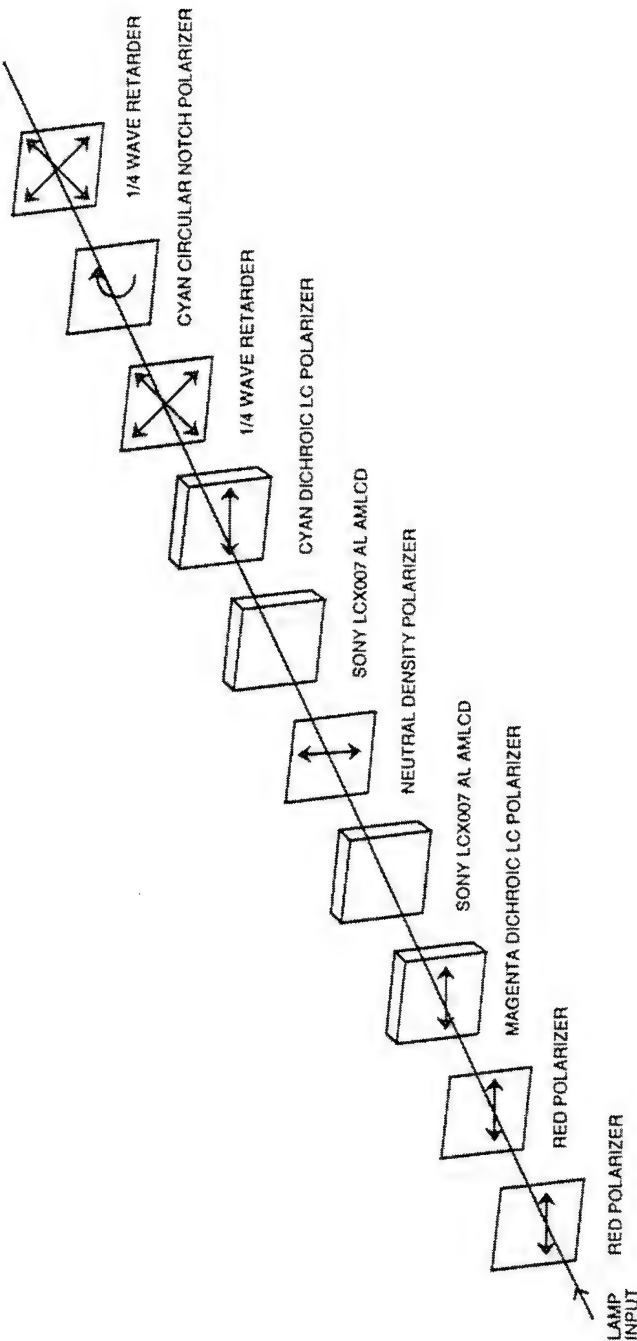


Figure 3-83. Two-Primary Color Expanded View of Stack #6 (Active Matrix).

The test results of stack #6 follow.

Table 3-12. Stack #6 Directional Illumination Measured With Xenon Lamp and Reynard Filters

Sony AMLCD Configuration: Lamp = 3661000 fL; Contrast Ratio = 259.38				
State	fL	u'	v'	
Yellow	51410	0.2280	0.5630	
Red	7143	0.4484	0.5319	
Green	10930	0.0935	0.5790	
Black	198.2	0.1877	0.5666	
Filter Location	Backlight Luminance	Stack Transmittance		
In Backlight	856900	2.20%		
Part of Stack	1279000	1.47%		

Sony AMLCD Configuration: Lamp = 711600 fL; Contrast Ratio = 304.52				
State	fL	u'	v'	
Yellow	11870	0.2486	0.5603	
Red	2197	0.4566	0.5303	
Green	2465	0.0847	0.5820	
Black	38.98	0.2303	0.5618	
Filter Location	Backlight Luminance	Stack Transmittance		
In Backlight	570800	2.08%		
Part of Stack	711600	1.67%		

Table 3-13. Stack #6 Directional Illumination Measured With Xenon Lamp and Calculated Filters (Y cutoff < 500 nm, IR cutoff > 650 nm)

Sony AMLCD Configuration: Lamp = 2700000 fL; Contrast Ratio = 52.16				
State	fL	u'	v'	
Yellow	49680	0.2101	0.5629	
Red	8710	0.3786	0.5410	
Green	11330	0.0832	0.5740	
Black	952.5	0.1004	0.5704	
Filter Location	Backlight Luminance	Stack Transmittance		
In Backlight	856900	2.20%		
Part of Stack	1279000	1.47%		

Sony AMLCD Configuration: Lamp = 535000 fL; Contrast Ratio = 252.71				
State	fL	u'	v'	
Yellow	9924	0.2393	0.5609	
Red	1928	0.4495	0.5322	
Green	2326	0.0797	0.5800	
Black	39.27	0.1930	0.5613	
Filter Location	Backlight Luminance	Stack Transmittance		
In Backlight	535000	1.85%		
Part of Stack	711600	1.39%		

Two-Primary Color Sony Stack
Filtered Power (Reynard Filters)

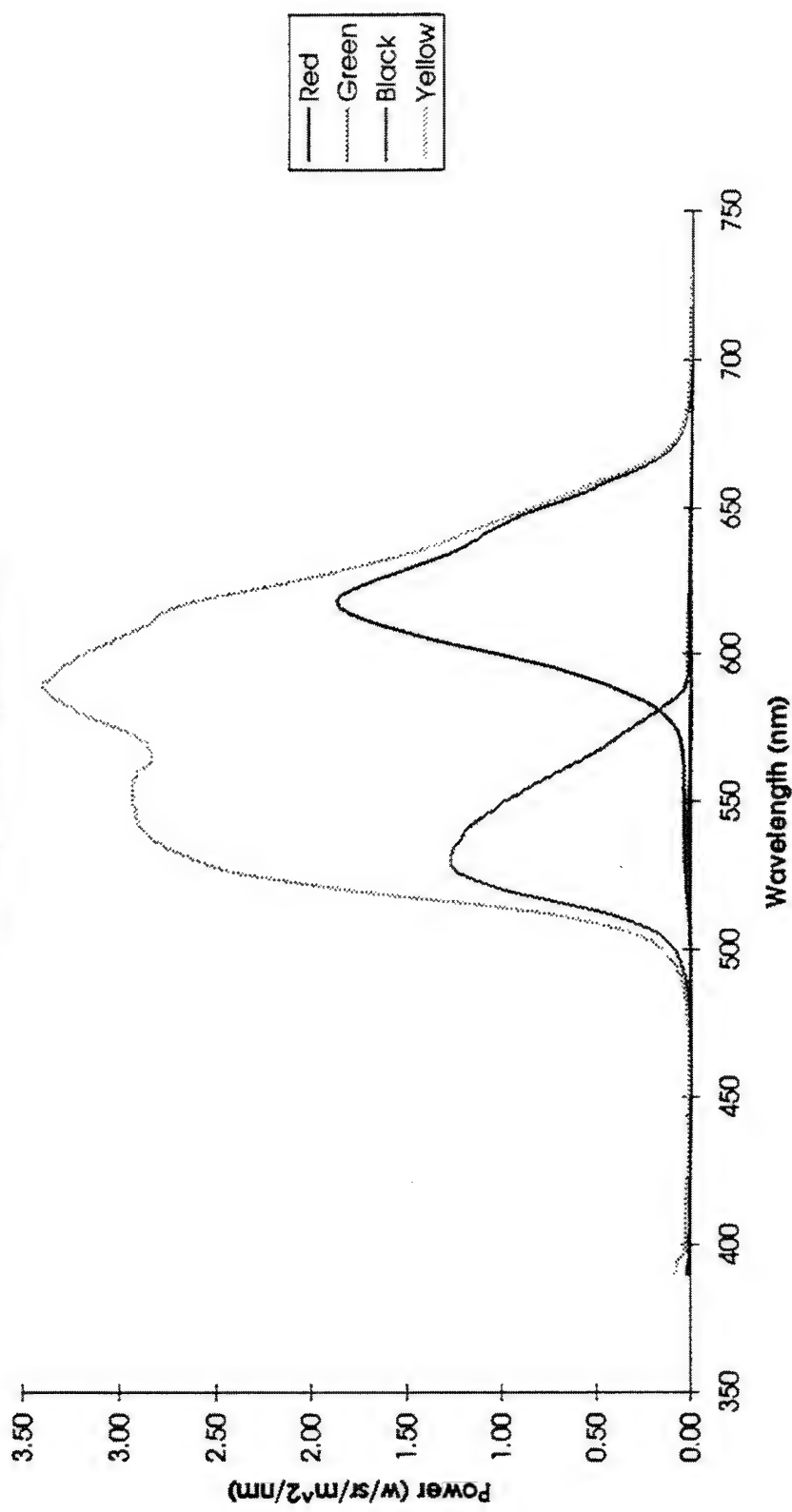


Figure 3-84. Stack #6 - Filtered Power vs. Wavelength (Xenon Lamp).

Two-Primary Color Sony Stack
Filtered Power (calculated filters)

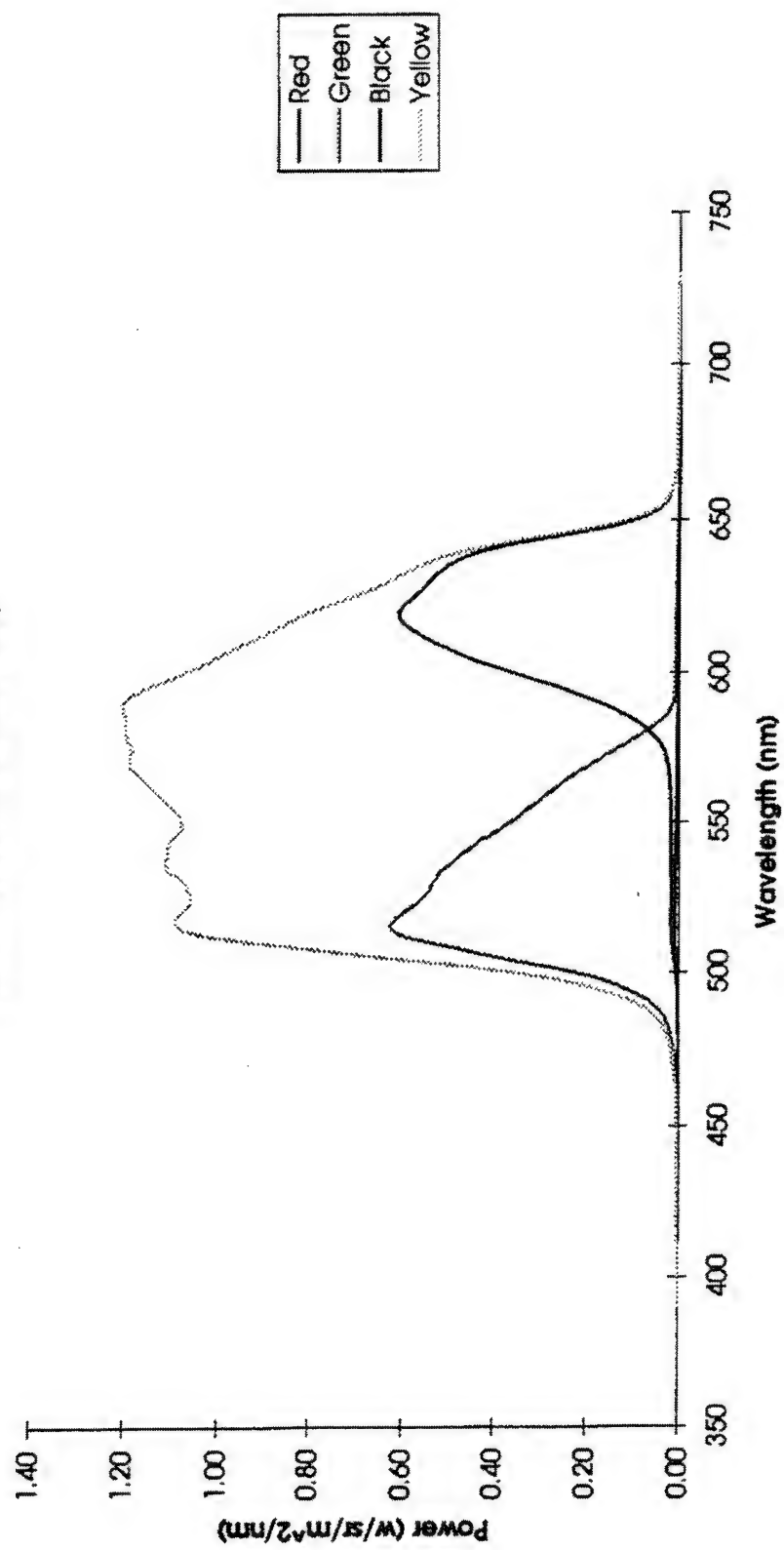


Figure 3-85. Stack #6 - Filtered Power (calculated filters) vs. Wavelength (Xenon Lamp).

Two-Primary Color Sony Stack

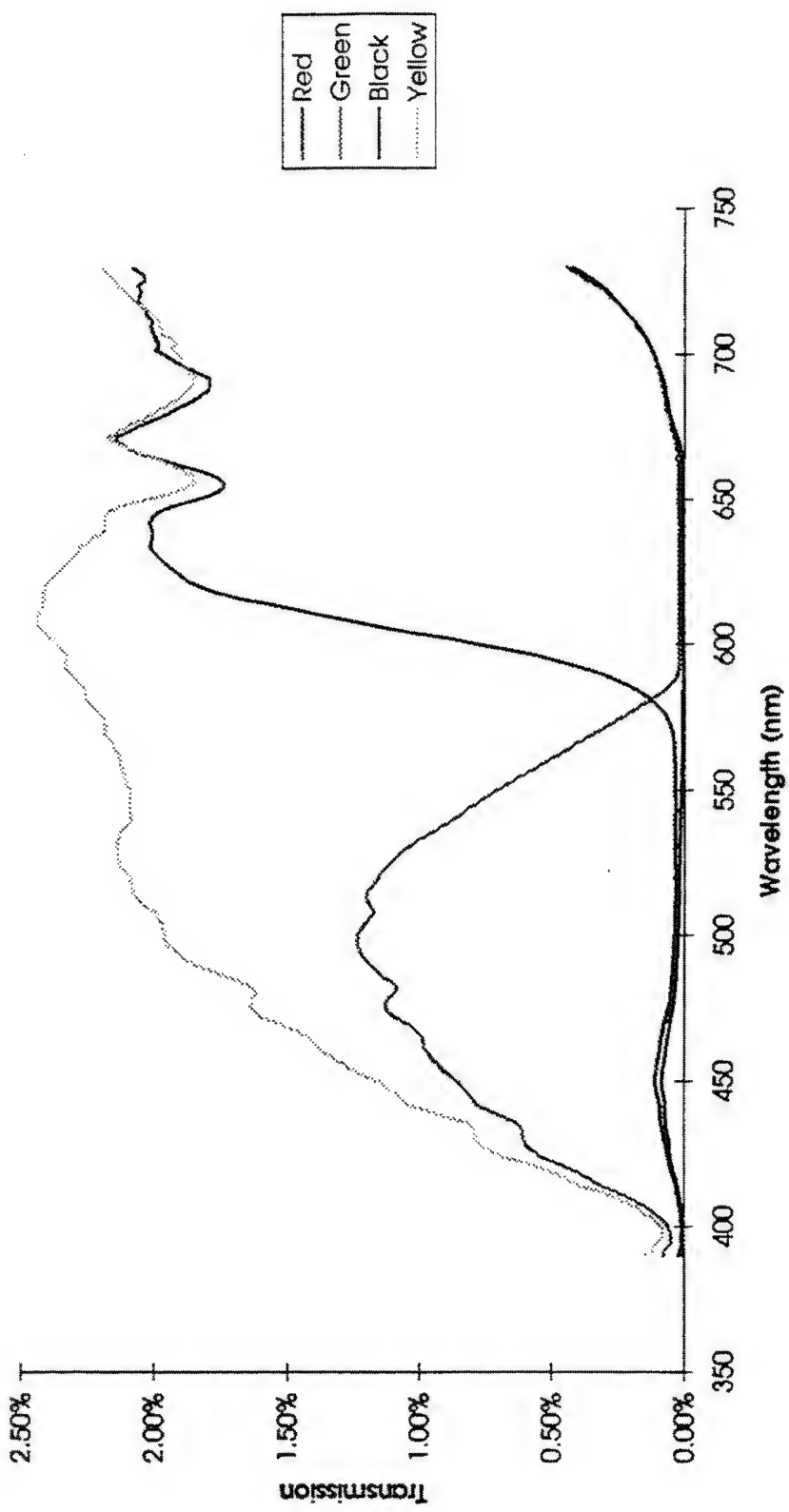


Figure 3-86. Stack #6 - Transmission vs. Wavelength (Xenon Lamp).

Two-Primary Color Sony Stack
Filtered Transmission (Reynard Filters)

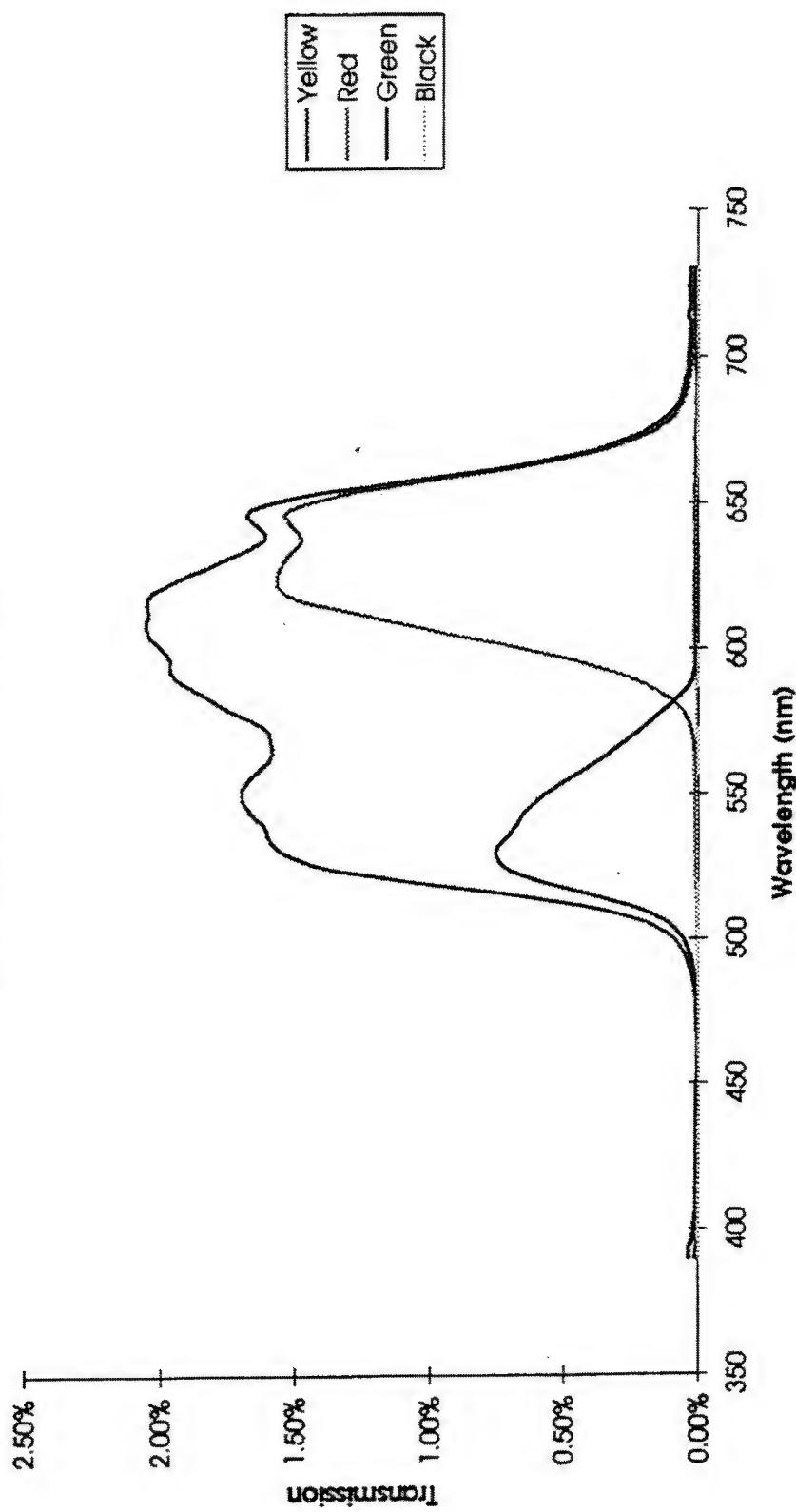


Figure 3-87. Stack #6 - Filtered Transmission vs. Wavelength (Xenon Lamp).

Two-Primary Color Sony Stack
Filtered Transmission (Calculated Filters)

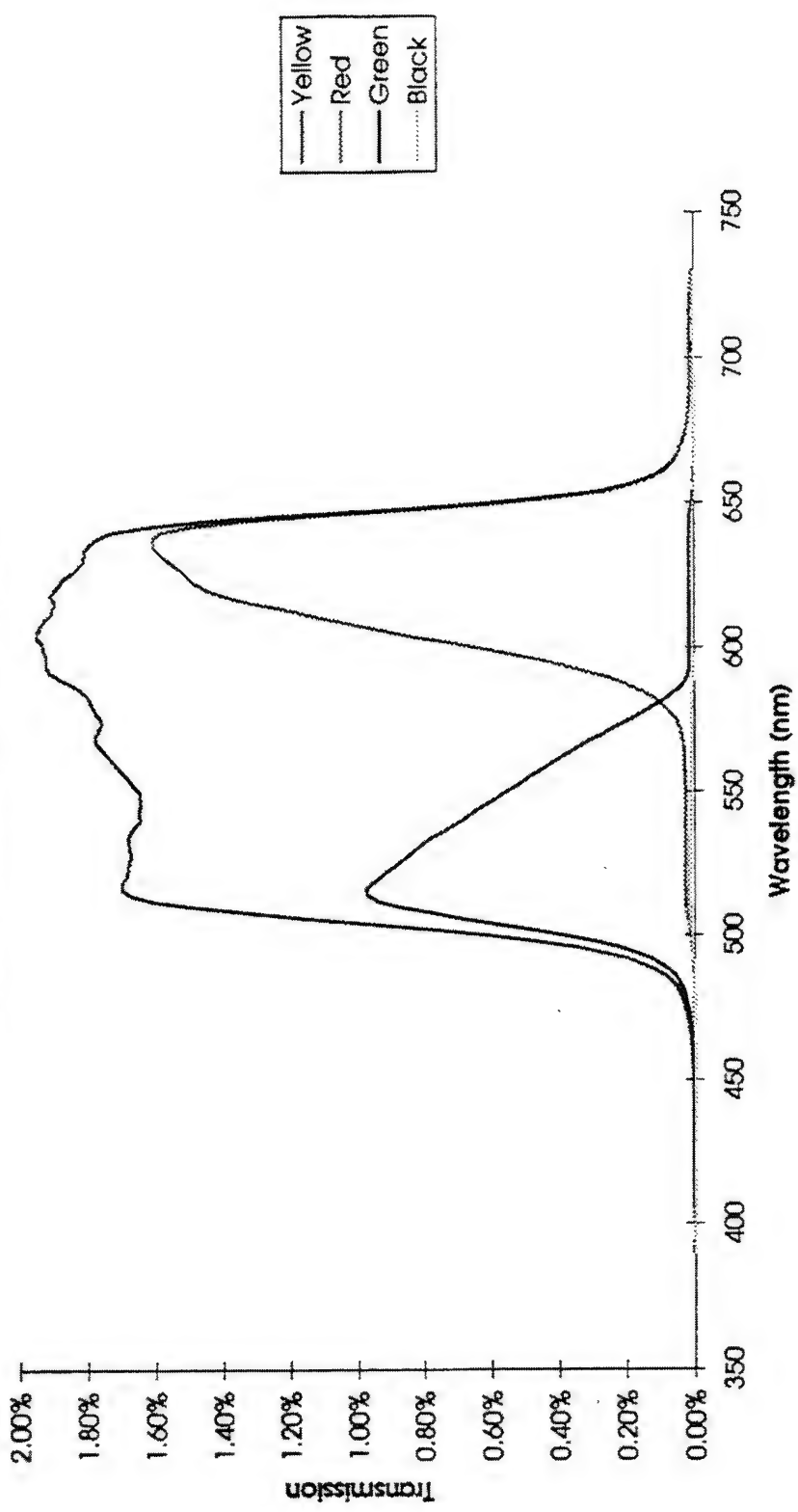


Figure 3-88. Stack #6 - Filtered Transmission (calculated filters) vs. Wavelength (Xenon Lamp).

Two-Primary Color Sony Stack

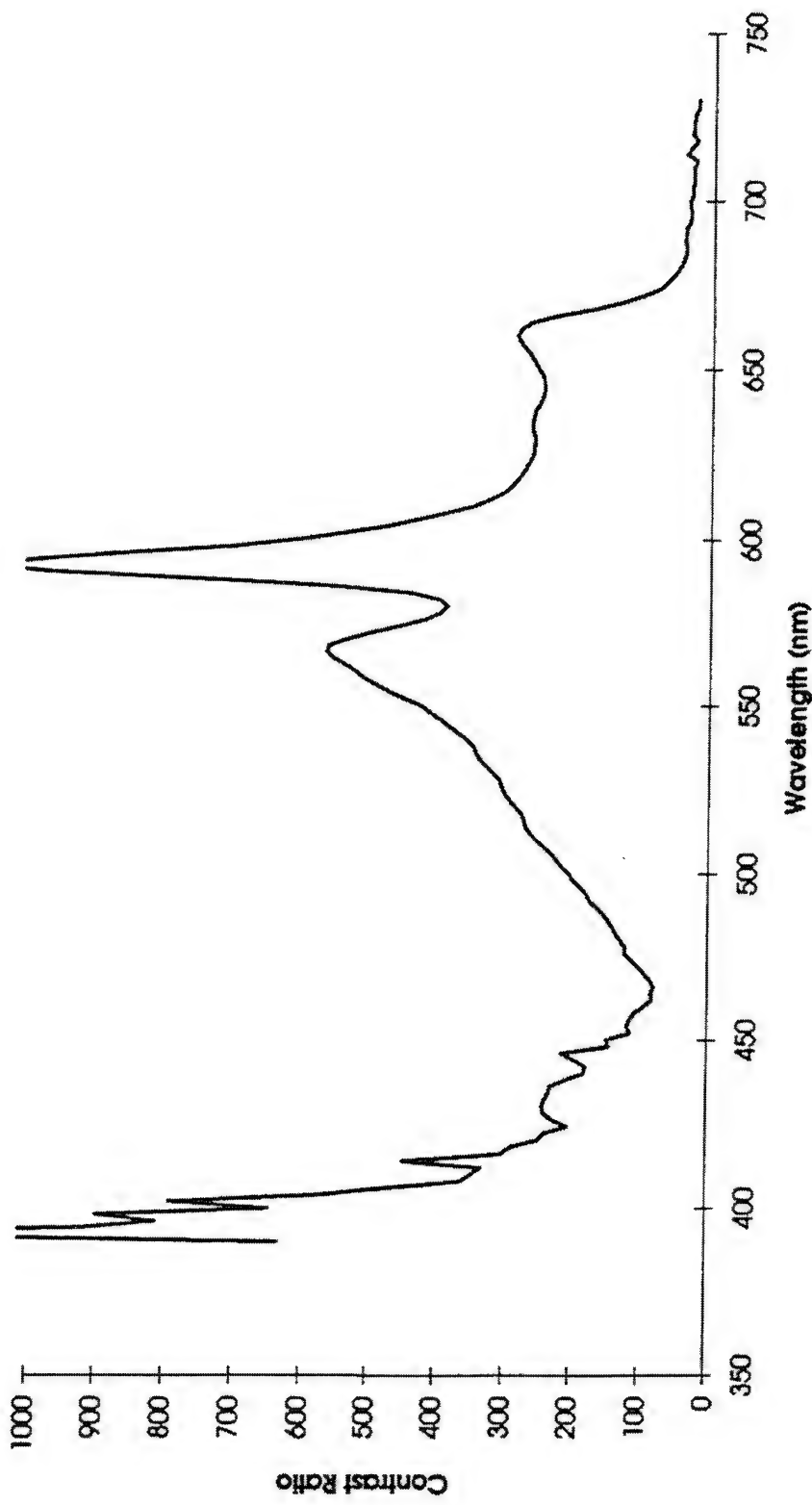


Figure 3-89. Stack #6 - Contrast Ratio vs. Wavelength (Xenon Lamp).

Two-Primary Color Sony Stack
Lamp Characteristics

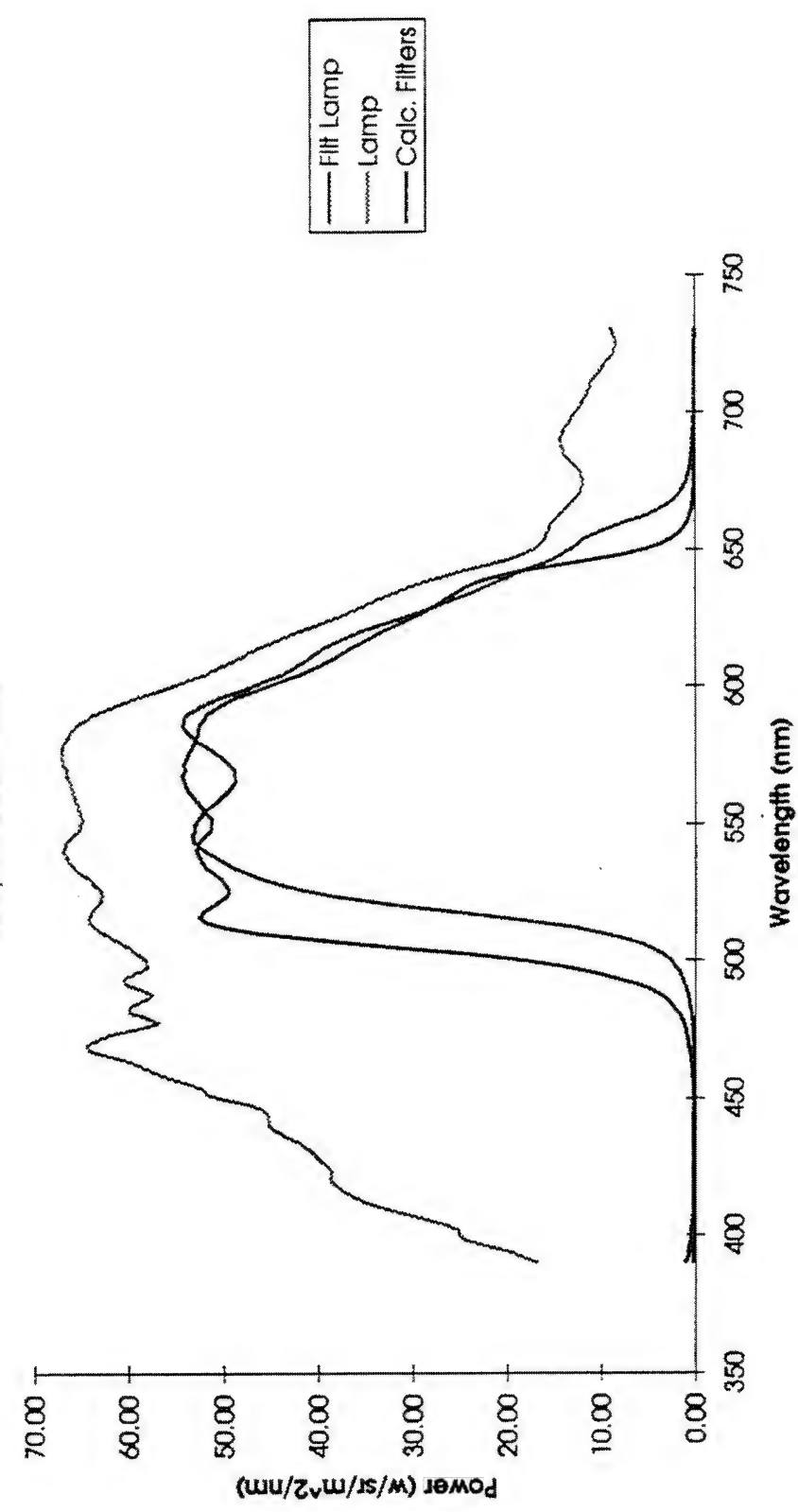


Figure 3-90. Xenon Lamp Characteristics - Power vs. Wavelength.

Two-Primary Color Sony Stack
Filtered Power (Reynard Filters)

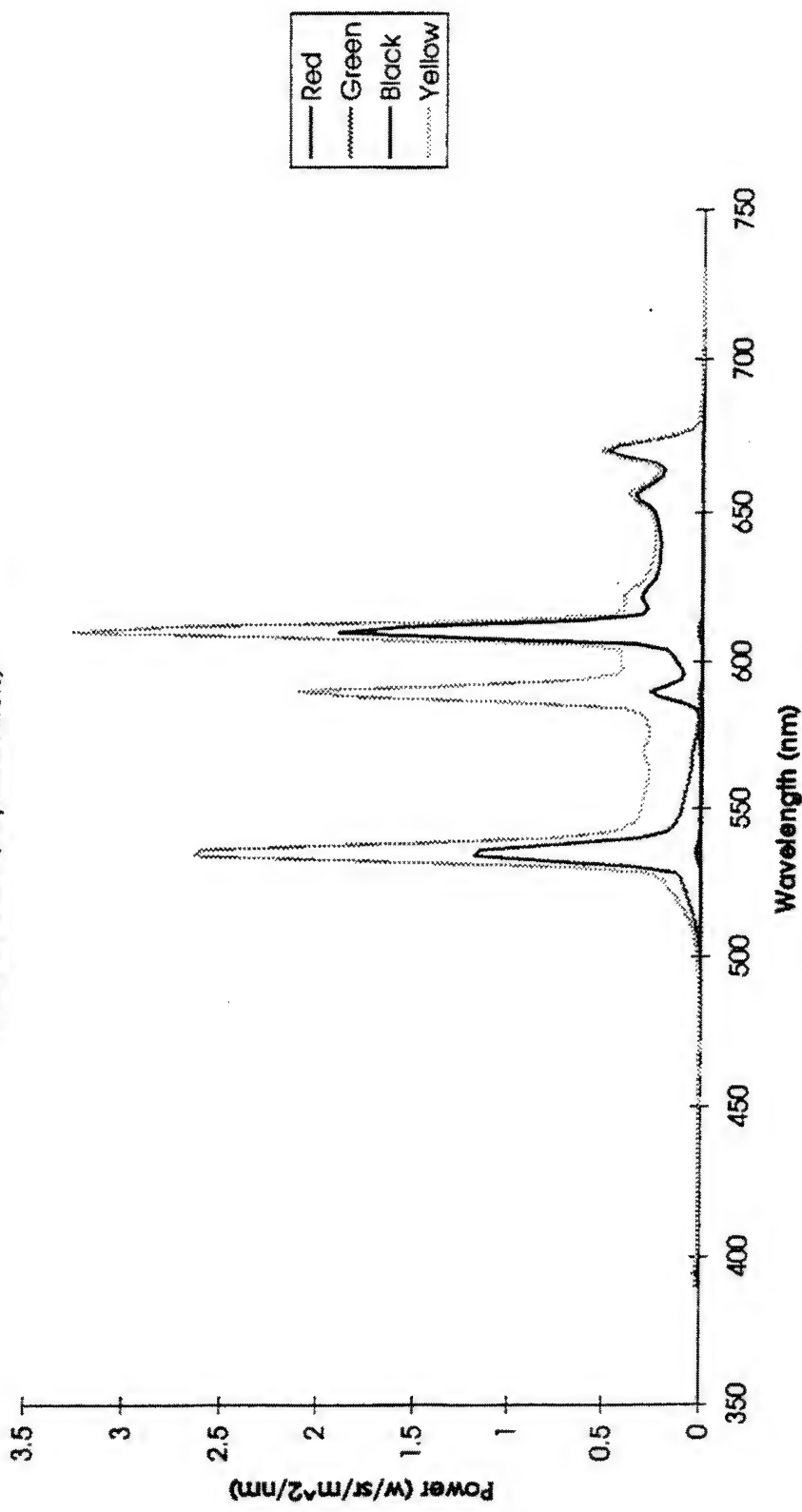


Figure 3-91. Stack #6 - Filtered Power vs. Wavelength (Tri-band Lamp #69).

Two-Primary Color Sony Stack
Filtered Power (Calculated Filters)

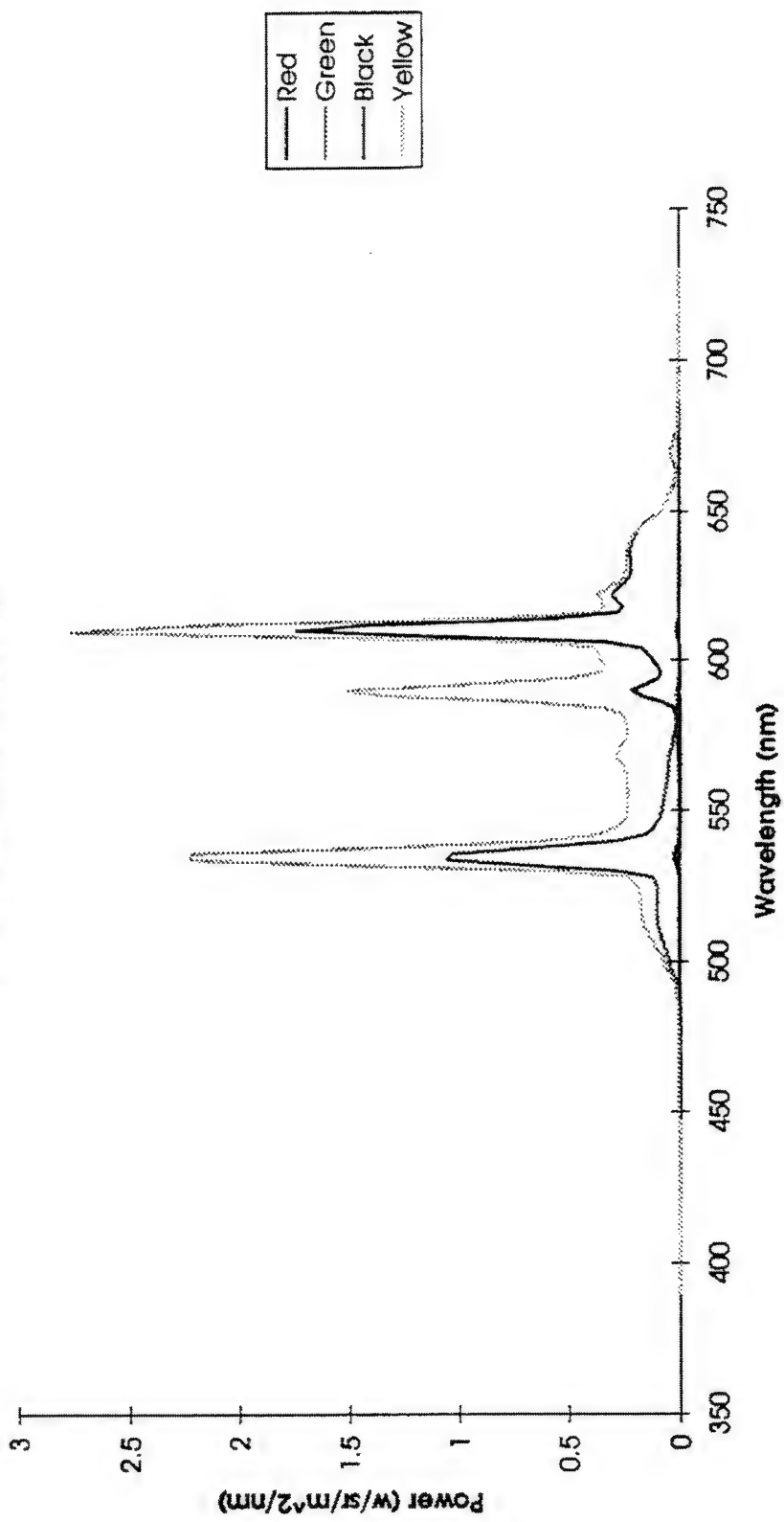


Figure 3-92. Stack #6 - Filtered Power (calculated filters) vs. Wavelength (Tri-band Lamp #69).

Two-Primary Color Sony Stack
Lamp Characteristics

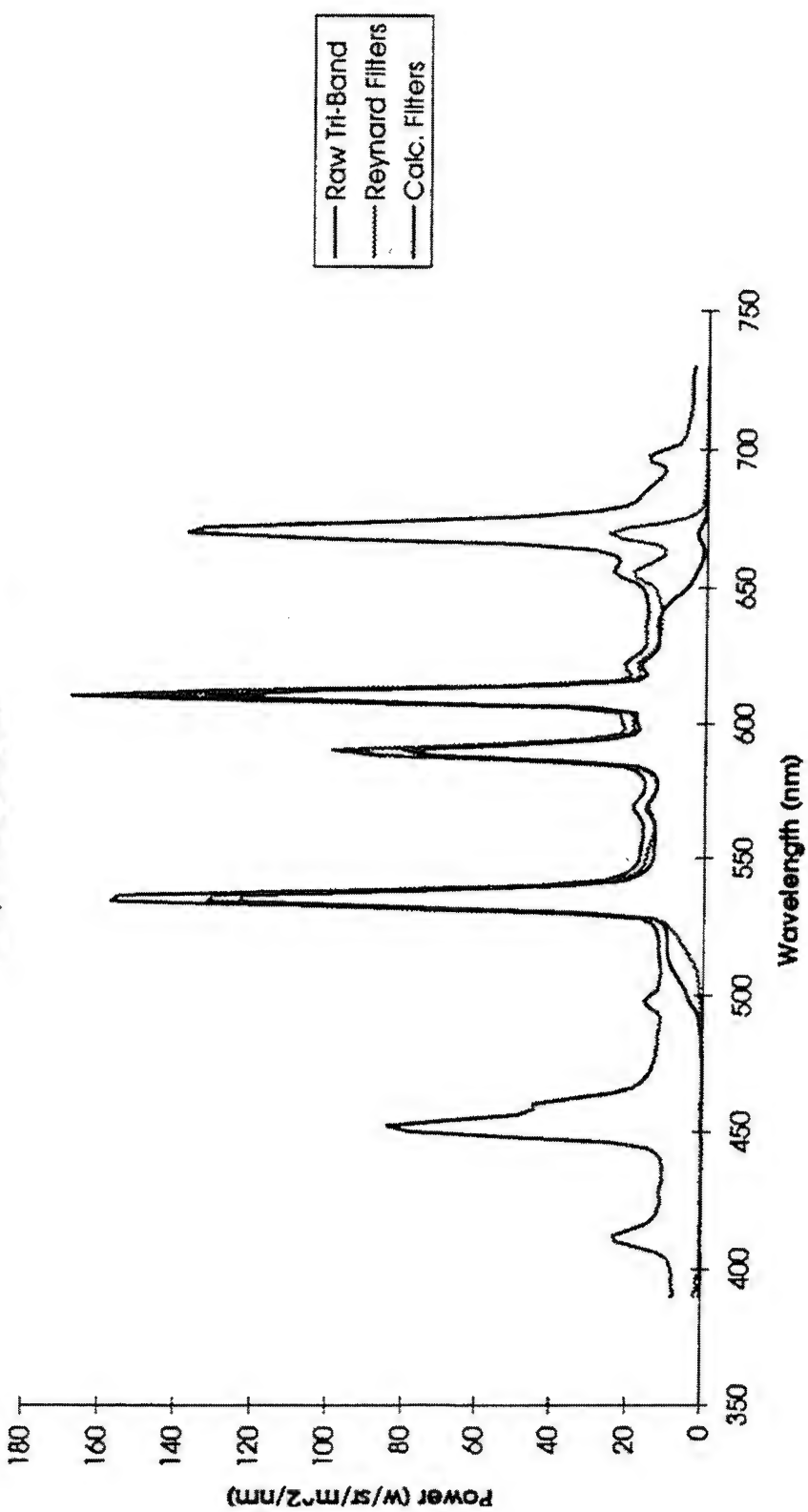


Figure 3-93. Tri-band Lamp Characteristics - Power vs. Wavelength.

3.10 Summary of Stack Test Data

The following tables summarize the stack test data, showing the results of all six two-primary color stacks.

Table 3-14. Stack Test Data Summary, Xenon Lamp and Reynard Filters

Directional illumination Xenon Lamp and Reynard Filters						
MCD Stack	Lamp	Hybrid #1	Lamp	Hybrid #2	Lamp	Hybrid #3
MCD Stack:						
Yellow	8504000	1L	U	Y	9585000	1L
Red	519200	0.2197	0.5638	Yellow	6189000	0.2300
Green	130600	0.4086	0.5374	Red	839360	0.4704
Black	128100	0.1239	0.5749	Green	172500	0.1066
	224900	0.1819	0.5634	Black	1349	0.5556
Transmission:						
Contrast Ratio:	0.11%					
	23.09					
Noich Polarizer:						
Transmission:						
Contrast Ratio:	6.48%					
	459.53					
Hybrid #2						
Transmission:						
Contrast Ratio:						
	9493000	1L	U	Y	8806000	0.2305
Yellow	1069000	0.2226	0.5638	Red	2209800	0.4234
Red	216100	0.3946	0.5393	Green	421800	0.1245
Green	552300	0.1303	0.5261	Black	11680	0.5545
Black	46690	0.1378	0.5731			
Transmission:						
Contrast Ratio:	10.86%					
	22.90					
Sony Stack						
Transmission:						
Contrast Ratio:						
	9311000	1L	U	Y	9957000	0.2176
Yellow	1279000	1L	U	Y	488100	0.3259
Red	18810	0.2231	0.5638	Red	524300	0.1262
Green	2430	0.4567	0.5310	Green	141600	0.2179
Black	4089	0.0977	0.5792	Black		0.5641
	45.11	0.2168	0.5630			
Transmission:						
Contrast Ratio:	1.47%					
	418.98					

Transmission is the ratio of the yellow luminance to the white background luminance, and includes the attenuation of the Reynard filters as well as the LCD stack absorption. Contrast ratio is the ratio of yellow to black luminance.

Table 3-15. Stack Test Data Summary, Xenon Lamp and Calculated Filters

		Directional Illumination							
		Xenon Lamp and Calculated Filters:							
MCD Stack:		Hybrid #1:			Hybrid #2:				
Lamp =	6894000 IL	IL	u'	v'	Lamp =	7108000 IL	u'	v'	
Yellow	570400	0.1943	0.5636		Yellow	663000	0.2086	0.5631	
Red	127300	0.3860	0.5373		Red	75950	0.4654	0.5298	
Green	159300	0.1023	0.5695		Green	204700	0.0913	0.5741	
Black	32070	0.1314	0.5517		Black	1425	0.2483	0.5502	
Transmission:	9.06%				Transmission:	9.33%			
Contrast Ratio:	17.79				Contrast Ratio:	465.26			
Notch Polarizer:		Hybrid #1:			Hybrid #2:				
Lamp =	7252000 IL	IL	u'	v'	Lamp =	7052000 IL	u'	v'	
Yellow	1130000	0.2039	0.5638		Yellow	943000	0.2088	0.5630	
Red	286200	0.3815	0.5353		Red	179400	0.1200	0.5369	
Green	622500	0.1173	0.5734		Green	492800	0.1117	0.5738	
Black	46890	0.1296	0.5528		Black	12730	0.2822	0.5548	
Transmission:	16.58%				Transmission:	13.37%			
Contrast Ratio:	23.07				Contrast Ratio:	74.08			
Sony Stack:		Double Narrow Band Design:			Lamp =				
Lamp =	945500 IL	IL	u'	v'	Lamp =	6804000 IL	IL	u'	v'
Yellow	20650	0.2028	0.5640		Yellow	1088000	0.1954	0.5317	
Red	2469	0.4340	0.5339		Red	501600	0.3052	0.5496	
Green	5160	0.0834	0.5745		Green	620700	0.1111	0.5738	
Black	8812	0.1438	0.5640		Black	186500	0.1888	0.5592	
Transmission:	2.18%				Transmission:	15.76%			
Contrast Ratio:	208.33				Contrast Ratio:	6.53			

TRANSMISSION IS THE RATIO OF THE XENON LUMINANCE TO THE BULB POWER DENSITY. CONTRAST IS THE RATIO OF THE CALCULATED YELLOW LUMINANCE AS WELL AS THE LCD STACK ABSORPTION. CONTRAST RATIO IS THE RATIO OF YELLOW TO BLACK LUMINANCE.

4 DISPLAY ANALYSIS

4.1 Electronic System Analysis

In this section, we present the results of examining and developing gray scale driver approaches. Two years ago, when this project was proposed, the assembled design team envisioned an examination of alternative gray scale approaches. The objective of this effort was to achieve the lowest possible cost and the highest possible image quality. Team members saw two major pathways for reaching the proposed goal: (1) distribute the limited number of gray shades of low-cost drivers to better match the psychophysical requirements of the human visual system and thus achieve higher levels of image quality; (2) develop alternative gray scale driver approaches that took advantage of the spatiotemporal characteristics of the liquid crystal medium. This latter path was set to improve on work in progress, state-of-the art methods that already held a high degree of promise for achieving the cost/performance goals. It was also expected that as worked developed along each of these three pathways, optimal blending of the results of these pathways would also be done.

The first strategy relied on tactics like distributing noise throughout the image, or distributing the luminance in accordance with the known power-law relationship in human vision (see Section 1.2.2 of this report). The motivation for this effort was underpinned by promising results demonstrated in lab tests in several low-cost and cost-reduction liquid crystal display product efforts throughout Honeywell. A combination of noise insertion and nonlinear gray scale distributions was found to be effective in meeting the target performance level of one product area. Nonlinear gray scale distribution was found to be *lacking* in reaching the goals of another product area, which demanded absence of iso-luminance contours. Another product area was satisfied by using a combination of halftone gray scale error distribution and temporal multiplexing of gray scale. *In all cases, the image quality fell short* of achieving the level of performance often associated with medium- and high quality CRTs.

The second strategy relied on tactics like extending the gray level performance of active addressing techniques by using temporal pulse width modulation. This held a strong pull for the team because it had the potential of eliminating the TFT from the panel. This held strong cost

implications without sacrificing active matrix gray scale performance. Preliminary work was done in this area. This work suggested no show stoppers lay in the path of the approach. Another tactic was to advance the state of the art of “zero power analog drive.” Honeywell and others had done work in this area, too. Early results suggested a vigorous pursuit in this and the active addressing design directions.

In the first stages of this project, we scheduled and performed experimental studies on the nonlinear gray scale distribution. What we found was that regardless of the power law used and regardless of how it was adjusted for optimum image quality for a given test image, the distribution selected was not optimal for all of any image and certainly not optimal for all images tried subsequently. It became apparent to the design team that for managing all manner of images, the gray scale redistribution strategy held significant risk. The algorithm for doing the redistribution in the experimental studies was passed on to the human factors evaluation portion of this project for more formal review. In this preliminary design work, we concluded that nonlinear gray shade distribution held little promise for meeting the performance goals.

As we set out to advance the state of the art of alternative gray scale drive mechanisms like those discussed above, we earmarked a particular task as the first in the critical path. That task was to validate whether or not existing gray scale drivers were or were not suitable for meeting objectives. As previously discussed, integrated analog drive circuits having the cost performance characteristics we sought do exist and appear to be coming into ready supply. Thus, at this point we saw exit criteria for any further pursuit into the alternative gray scale research and development portion of this program. All work in this area was stopped. The funds for the planned later stages of this effort were freed to other portions of the project.

4.1.1 Cost Reduction Through Electronic Alignment of the Subtractive Layers

Serendipitously, during the assembly of the two primary display deliverable, we found mechanical alignment of the two layers to be problematic. Though due diligence was exercised, the pixels of the red and green layers are offset with respect to each other. This resulted in an image source that does not synthesize colors well and, worse, presents an annoying dual image. This mechanical alignment problem may be specific to the resource we have on hand and so the result may not be completely general. But it does highlight the potential for a problem and an opportunity for lowering assembly difficulty. The opportunity is embedded in the following question:

Is it possible to electronically align the layers and circumvent a potential cost factor in the assembly process?

The answer is yes, and the result is shown in the display deliverable. The alignment compensation circuitry is expected to be best placed in the local control unit. The remote unit is a candidate home, too, but the goal of the design team has been to keep the remote control unit as generic as possible. The local control unit is to have the display specifics encoded in it and is expected to travel with the display or be an inherent part of the display. In it will reside in the custom characterization PROMS that store the idiosyncrasies of each particular image source and compensate for those imperfections.

Cost benefits are expected but will depend on the ultimate manufacturer(s) selected. A primary reason for expecting the cost benefit is that this approach places the two primary implementation that much closer to the standard assembly process, freeing the manufacturer(s) from one more custom precision step. It also frees the assembly process to be done in two stages: (1) use standard LC manufacturing; (2) use a lower cost custom manufacturing facility to do the custom and final assembly steps.

4.1.2 Electronic Compensation for Idiosyncratic Image Source Performance

Taking a systems approach to the Two-Primary Color project implies finding the balance among a multitude of variables. LCD products experience indicates manufacturing costs can be alleviated substantially by using electronics to compensate for part-to-part variations over temperature, time, voltage, etc. No matter how tightly the manufacturing processes are controlled, variations in performance are typical. These variations are effectively managed by measuring the image source performance, characterizing the attributes of each over the range of critical driving variables. The measurements can be done one time at assembly or through a feedback process on a continual basis. Most commonly, a combination of the two types of measurements are done. The initial and real-time characterizations result in functional relationships. Inverse functions are constructed by the designer and embedded into compensation circuitry. As stated in the paragraph above, we envision the compensation circuitry to be located in the local control unit. Look-up tables in combination with D/A converters are the means for achieving the compensation.

Regarding the pursuit for achieving the highest performance at the lowest possible cost, a systems approach strongly favors using electronic compensation under the following philosophy:

Use standard manufacturing facilities wherever possible and use electronic compensation as much as practical to reach the custom high-performance levels.

This philosophy has been used in products like the Boeing 777 display and the Multifunction Electronic Display System (MEDS) Space Shuttle display product lines. It has become even more prevalent lately throughout the industry in the pursuit to use commercially available parts as much as possible. The prevailing wisdom is that the mass market provides the lowest possible cost components. The two-primary color display product will be of the lowest possible cost the more it capitalizes on standard processes and components.

4.1.3 Conclusion of the Alternative Gray Scale Driver Pursuit

As stated in Section 2.3, what we found was that integrated analog drive systems of trivial cost (dollars, size and weight) and excellent performance are ideal for the two-primary color derivative products.

Electronic Alignment of the Subtractive Layers offers a very promising method for reducing the cost of the two-primary subtractive display and derivative products.

Electronic compensation for each image source will relax the requirements and thus also provide avenues for reducing the cost of the two-primary subtractive display and derivative products. This latter conclusion is the result of work funded under the MCD project in which subtractive color synthesis was a key question. This conclusion also follows from extensive IR&D in LCD product areas, including the Boeing 777 Display and the MEDS Space Shuttle Display.

4.2 Analysis of Display Manufacturability

The objective of this analysis involves comparing the cost of manufacturing two-primary color image sources with three-primary color image sources. Particular applications may require two-primary color image sources, while other applications require three image sources. Product cost numbers combine with optical performance metrics to provide a framework for selecting two or three image sources for a given application.

4.2.1 Overview

This section details background information required to frame the ensuing discussion. To understand the issues surrounding manufacturability, we begin with an analysis of manufacturing cost drivers. With this background in place, the specific methodology utilized in this analysis emerges. Finally, the costs and specific methodology combine to present a cost comparison between product design and manufacturing options.

Fabrication of small area AMLCD substrates involve essentially the same technology as fabricating a large area integrated circuit. The semiconductor industry provides the basis for this analysis including;

- Yield models
- Cost models

The starting point for this overview is the fabrication of integrated circuits.

A. Cost Drivers in Semiconductor Processing

Integrated circuit substrate production costs involve three elements, specifically, the following cost drivers;

- Throughput yield
- Product yield

- Cost of operations

This section provides a closer look at each cost driver.

1. Throughput Yield

Throughput yield represents the number the probability that a substrate will successfully survive the particular fabrication operation. Specific causes of substrate loss through fabrication equipment include:

- Substrate breakage
- Executing the incorrect process recipe
- Premature equipment shutdown
- Processing the incorrect side of the substrate

These losses cover the spectrum from individual substrate losses (caused by breakage) to entire lots of material being lost (caused by using incorrect process recipe). In a mature manufacturing process, these yields are quite high, typically greater than 95%.

2. Product Yield

Product yield represents the probability that the electrical devices within the AMLCD operate to achieve their desired impact. Typically this consists of answering two questions:

Do the electrical devices work at all? (Functional yield)

Do the electrical devices perform to specifications? (Final test yield)

The experience from the semiconductor industry indicates that the relative numerical significance of these two yields depends upon the fabrication process maturity and the product design maturity. The following table summarizes this situation.

Product Design Maturity

Process Maturity	<u>Low</u>	<u>High</u>
	Neither Yield Dominates	Functional Yield Dominates
<u>Low</u>	Final Test Yield Dominates	Neither Yield Dominates
<u>High</u>	Neither Yield Dominates	Functional Yield Dominates

The substrate yield measures the probability that a started substrate is processed into a functional performing platform for AMILCD assembly. The following equation summarizes the relationship between substrate yield and its components.

$$\text{Substrate Yield} = \text{Throughput Yield} * \text{Functional Yield} * \text{Final Test Yield}$$

3. Cost of Operations

In the semiconductor industry, operations costs are defined by the number of photolithographic masking levels. There is typically a fixed cost per masking level. The total cost becomes:

$$\text{Total Cost} = \text{Cost of operations per masking level} * \text{Number of mask levels}$$

Current industry estimates put the cost of operations per masking level at \$50.00.

B. Analysis Methodology

This section describes the methodology utilized in the manufacturing analysis. Analysis involves multiple scenarios involving product design concepts and substrate fabrication technologies. The following table summarizes the substrate design strawman.

<u>Design Parameter</u>	<u>Value</u>
Horizontal Resolution	640 pixels
Vertical Resolution	480 pixels
Pixel Pitch	.24 microns
Data Scanners	Interlaced design (top and bottom)
Glass Substrate Size	4 inch round
Number of Candidates	4
Defect density	.2 per cm ²
Chip area	

The analysis methodology involves determination of the cost per (yielded operational) panel for each. This combines with the cost to stack image sources resulting in the total cost.

Scenario #1: This approach involves connecting yielded active matrix substrates with yielded driver circuitry using flip chip technology. The following table summarizes the particulars.

AMLCD substrate	a:Si or p:Si requires 8 masks to fabricate
Data drivers	x:Si fabricated at foundry cost \$.30 per output two per functional display
Flip chip bonding	equipment is Suss FC-150 UV epoxy used to bond cost determined from NCALCM cost of ownership model

Figure 4-1 summarizes the manufacturing flow for this scenario.

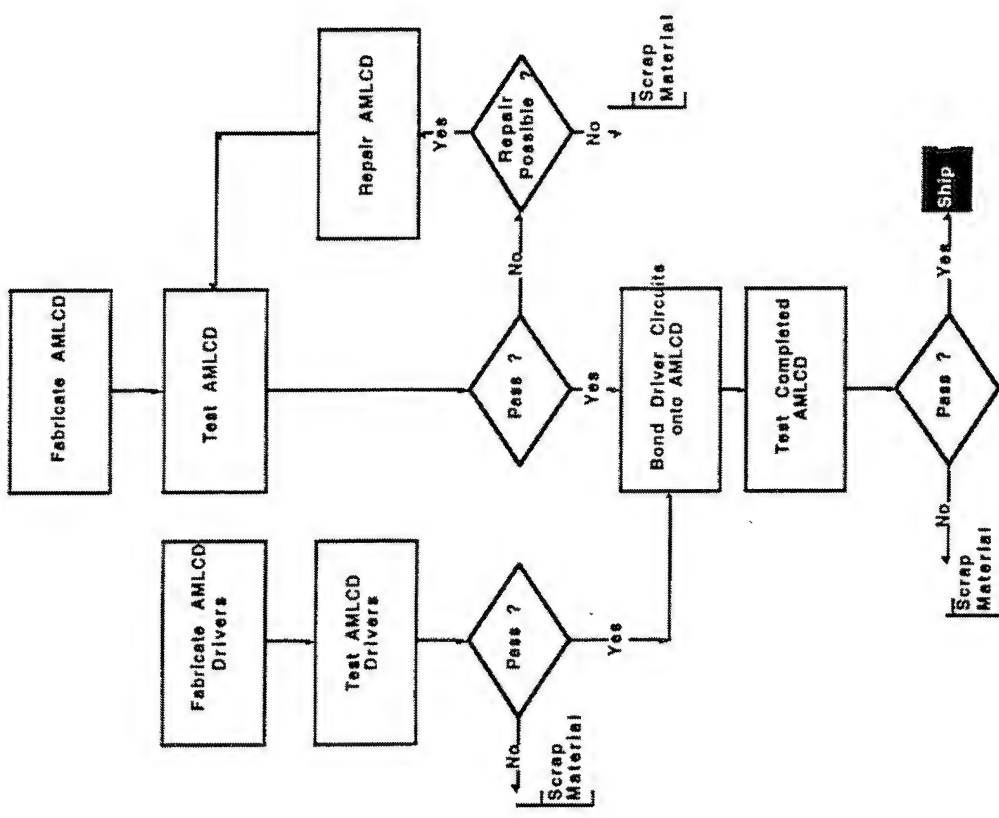


Figure 4-1. AMLCD Manufacturing System Flowchart for Scenario #1

Scenario #2: This approach involves fabricating the AMLCD drivers commensurate with array processing, and is referred to as integrated drivers. In this case there is no redundancy or repair. The following table summarizes the particulars.

AMLCD substrate	a:Si or p:Si requires 23 masks to fabricate
Data drivers	a:Si or p:Si fabricated during array processing data drivers reside on both sides of the display

Figure 4-2 summarizes the manufacturing flow for this scenario.

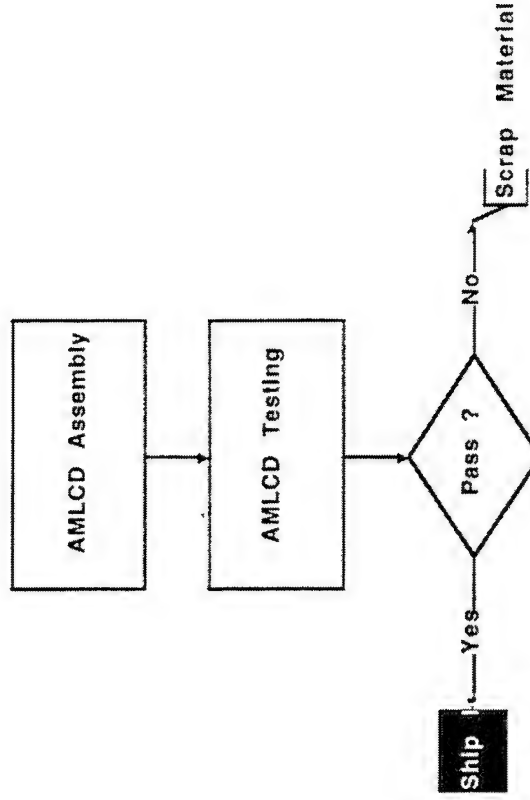


Figure 4-2. AMLCD Manufacturing System Flowchart for Scenario #2

Scenario #3: This approach involves fabricating the AMLCD drivers commensurate with array processing. In this case there is redundancy but no repair. The following table summarizes the particulars.

AMLCD substrate	a:Si or p:Si requires 23 masks to fabricate
Data drivers	a:Si or p:Si fabricated during array processing data drivers reside on both sides of the display

Scenario #4: This approach involves fabricating the AMLCD drivers commensurate with array processing. In this case there is both driver redundancy and repair. The following table summarizes the particulars.

AMLCD substrate	a:Si or p:Si requires 23 masks to fabricate
Data drivers	a:Si or p:Si fabricated during array processing data drivers reside on both sides of the display

Figure 4-3 summarizes the manufacturing flow for this scenario.

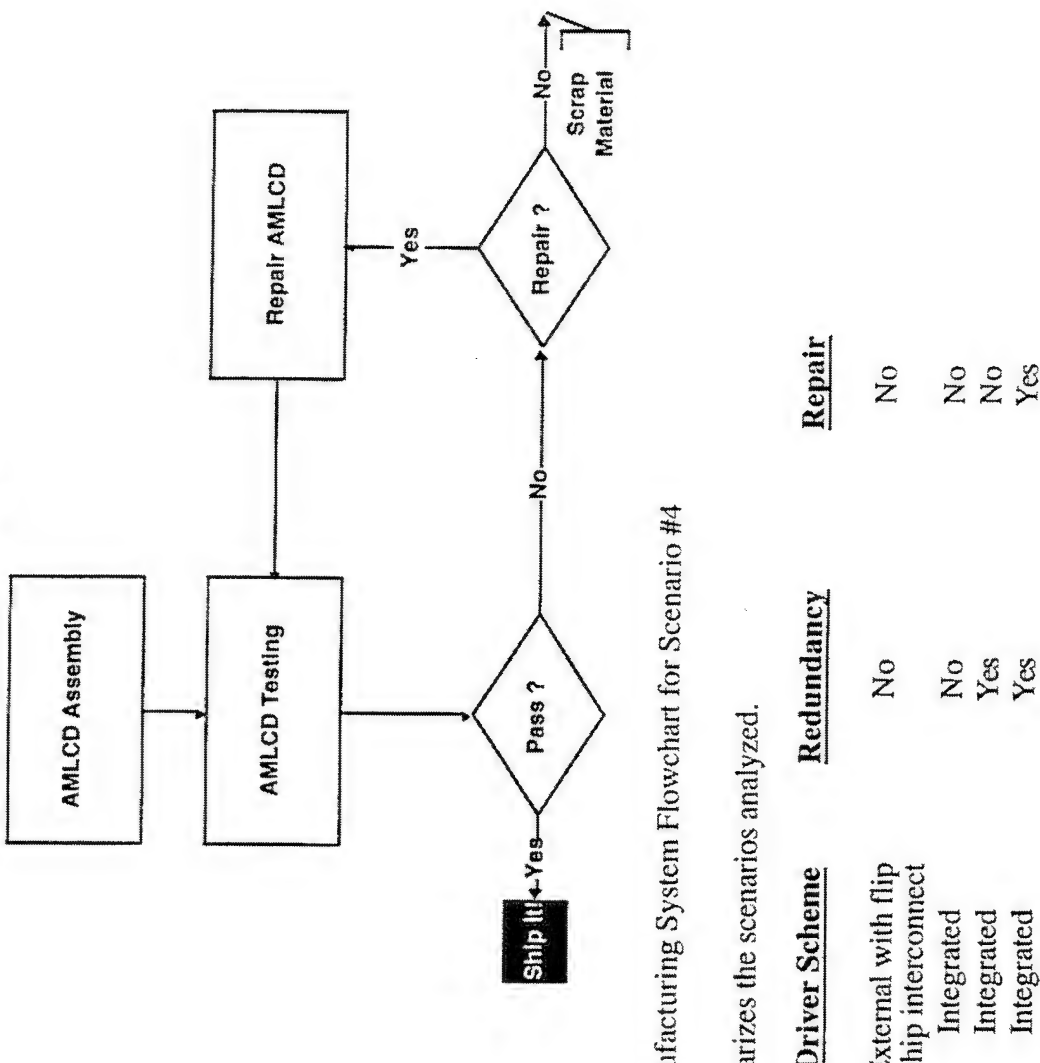


Figure 4-3. AMLCD Manufacturing System Flowchart for Scenario #4

The following table summarizes the scenarios analyzed.

<u>Scenario</u>	<u>Driver Scheme</u>	<u>Redundancy</u>	<u>Repair</u>
1	External with flip chip interconnect	No	No
2	Integrated	No	No
3	Integrated	Yes	No
4	Integrated	Yes	Yes

Cost of Operations

This section describes the general basic cost of display fabrication and assembly operations. These general cost assumptions form the basis of analyzing the four manufacturing scenarios detailed above. Specific information emerges on substrate costs, LC assembly costs, and cell stacking costs. Let's look closer at each cost element.

A. Substrate

Actual knowledge of substrate processing costs is the most carefully guarded secret in the semiconductor industry, however, semiconductor industry costing models exist.

The number of photo masking layers determines the overall cost of substrate fabrication. The industry accepted costing figure, utilized in this analysis, is \$50 per photo lithographic layer per substrate. Determining the relative costing differences among the four scenarios analyzed under the industry benchmark assumption yields valid results.

B. LC Assembly

Once again, specific detailed costing information is closely guarded in the AMLCD industry. Considering the work completed at Honeywell, we have assumed that it costs \$75 to assemble and evaluate one AMLCD panel. This is a reasonable assumption that results in no significant impact to the results of this analysis. All scenarios analyzed used the same AMLCD assembly costs and yield assumptions. Therefore, while the modeled costs may differ from actual costs, the cost comparison between the scenarios yields valid results.

C. Cell Stacking

Stacking AMLCD panels is unique to forming subtractive color image sources. Considering the work completed at Honeywell, the cost of stacking two panels is set at \$50. All four scenarios utilized the same assumptions regarding stacking costs. Whereas the absolute cost may differ, the relative difference among the four scenarios yields valid costing insights.

Yielded Substrate Cost

This section combines the cost of operations with product yield estimates to arrive at the cost of a yielded substrate. Determining this parameter requires estimating product yields, totaling the costs, and standardizing on a per yielded substrate. Each scenario described above undergoes a separate analysis.

A. Scenario #1

Yield estimates require knowledge of the area of the display matrix and a defect density. The basis for this approach arises from the semiconductor industry. In this approach, a random distribution of defects that result in catastrophic display performance determines yield. The following table summarizes the critical assumptions in the yield determination for this scenario.

Defect Density	0.3 defects/cm ²
Active Area	1.8 cm ²
(Exclude drivers since they are fabricated separately)	
Number of Masking Levels	8

On the basis of these assumptions, the substrate yield is estimated to be 98% following Takafuji. The following table summarizes the cost analysis results for this scenario.

Array Processing Cost (8 layers @ \$50 per)	\$400
Array Yield	98%
Number of Good Substrates	3.92
Yielded Array Cost	\$102

The next table summarizes the data driver costs.

Rows (2 drivers)	640
Cost	
(\$0.30 per row)	\$192

The next cost element is the chip on glass interconnection. In order to accurately estimate this cost, the NCAICM cost of ownership model was employed. The equipment selected is the Karl Suss FC-150. Detailed summary of this analysis is found in the appendix. The following table summarizes the salient results.

<u>Equipment</u>	<u>Calculated Cost</u>	<u>Unit Cost</u>
Original Capital Cost	\$350,000	\$4.12
Raw Throughput	30 per hour	
Max. Starts per Week	2249	
Equipment Utilization (24 hr day)	13%	
Equipment Utilization Factory	27%	
Headcount Per Shift		
Direct	0.4	\$1.60
Maintenance	0.0	\$0.51
Indirect	0.2	\$1.27
Total		\$3.39
Top Three Cost Drivers		
Equipment (Depreciation, etc.)	26%	\$4.12
Rework	24%	\$3.74
Material	15%	\$2.37
All Others	35%	\$5.51
Cost Per Good Unit Out From This Operation		<u>\$15.74</u>

It costs \$15.74 to connect one driver chip to the display glass. Connecting drivers to the entire display costs \$31.

The following table summarizes the cost of fabricating a yielded substrate under scenario #1.

<u>Item</u>	<u>Cost</u>	<u>% Total</u>
Yielded Pixel Array	\$102	25%
Display Driver Cost	\$192	59%
Driver Interconnect	\$31	10%
Total	\$299	

B. Integrated Driver Option

The next scenarios analyzed involved variations of integrated driving schemes. One scheme involves no redundancy and no repair, a second scheme involves redundancy with no repair, and the last scheme involves both redundancy and repair. Each scheme deserves closer analysis.

I. Scenario #2

This scenario involves display drivers fabricated without the benefit of redundancy or repair. The following table summarizes the critical assumptions in the yield determination for this scenario.

Defect Density	0.3 defects/cm ²
Active Area	3 cm ²
(Exclude drivers since they are fabricated separately)	
Number of Masking Levels	23

On the basis of these assumptions, the substrate yield is estimated to be 41% following Takafuji. The following table summarizes the cost analysis results for this scenario.

Array Processing Cost (23 layers @ \$50 per)	\$1,150
Array Yield	41%
Number of Good Arrays per Substrate	1.64
Yielded Array Cost	\$701

The following table summarizes the cost of fabricating a yielded substrate under scenario #2.

<u>Item</u>	<u>Cost</u>	<u>% Total</u>
Yielded Pixel Array	\$102	15%
Display Driver Cost	\$599	85%
Total	\$701	

2. Scenario #3

This scenario involves display drivers fabricated without the benefit of redundancy but without repair. The following table summarizes the critical assumptions in the yield determination for this scenario.

Defect Density	0.3 defects/cm ²
Active Area	
(Includes driver area)	3 cm ²
Number of Masking Levels	23

On the basis of these assumptions, the substrate yield is estimated to be 70% following Takafuji. The following table summarizes the cost analysis results for this scenario.

Array Processing Cost (23 layers @ \$50 per)	\$1,150
Array Yield	70%
Number of Good Arrays per Substrate	2.8
Yielded Array Cost	\$411

The following table summarizes the cost of fabricating a yielded substrate under scenario #3.

<u>Item</u>	<u>Cost</u>	<u>% Total</u>
Yielded Pixel Array	\$102	25%
Display Driver Cost	\$309	75%
Total	<u>\$411</u>	

3. Scenario #4

This scenario involves display drivers fabricated with the benefit of redundancy and repair. The following table summarizes the critical assumptions in the yield determination for this scenario.

Defect Density	0.3 defects/cm ²
Active Area	3 cm ²
(Includes driver area)	
Number of Masking Levels	23
Cost of Repair	\$75 per glass substrate

On the basis of these assumptions, the substrate yield is estimated to be 90% following Takafuji. The following table summarizes the cost analysis results for this scenario.

Array Processing Cost (23 layers @ \$50 per)	\$1,225
Array Yield	90%
Number of Good Arrays per Substrate	3.60
Yielded Array Cost	\$340

The following table summarizes the cost of fabricating a yielded substrate under scenario #4. In this scenario, the array yield is effectively 100%.

<u>Item</u>	<u>Cost</u>	<u>% Total</u>
Yielded Pixel Array	\$111	29%
Display Driver Cost	\$244	71%
Total	\$355	

Image Source Cost

This section summarizes the cost of fabricating one yielded two-primary color image source for each of the design and manufacturing scenarios described above. After determining the yielded panel cost, the cost of completing the two-primary color image source follows.

Yielded Panel Cost

In order to determine yielded panel cost, the following assumptions were used:

Panel Assembly Cost	\$75
Panel Assembly Yield	75%

The following table summarizes the yielded panel cost.

	<u>Scenario #1</u>	<u>Scenario #2</u>	<u>Scenario #3</u>	<u>Scenario #4</u>
Substrate Cost	\$325	\$701	\$411	\$340
Panel Cost	\$75	\$75	\$75	\$75
Yield	75%	75%	75%	75%
Cost of Yielded Panel	\$533	\$1,035	\$648	\$553

The cost differences reflect the high cost of scrap under scenarios #2 and #3.

Two-Primary Color Cost

In order to determine yielded two-primary color image source cost, the following assumptions were used:

Stack Assembly Cost	\$50
Panel Assembly Yield	90%

The following table summarizes the yielded two-primary image source cost.

	<u>Scenario #1</u>	<u>Scenario #2</u>	<u>Scenario #3</u>	<u>Scenario #4</u>
Panel Cost (Two panels)	\$1,066	\$2,070	\$1,296	\$1,106
Stacking Cost	\$50	\$50	\$50	\$50
Yield	90%	90%	90%	90%
Cost of Yielded Image Source	\$1,240	\$2,356	\$1,496	\$1,284

The cost differences reflect the high cost of scrap under scenarios #2 and #3.

Three-Primary Color Cost

In order to determine yielded two primary color image source cost, the following assumptions were used:

Stack Assembly Cost	\$50
Panel Assembly Yield	90%

The following table summarizes the yielded two primary image source cost.

	<u>Scenario #1</u>	<u>Scenario #2</u>	<u>Scenario #3</u>	<u>Scenario #4</u>
Panel Cost (Three panels)	\$1,773	\$3,391	\$2,144	\$1,837
Stacking Cost	\$50	\$50	\$50	\$50
Yield	90%	90%	90%	90%
Cost of Yielded Image Source	\$2,026	\$3,823	\$2,438	\$2,097

Summary

A manufacturing cost analysis for two-primary color image sources leads to the following results.

	<u>Scenario #1</u>	<u>Scenario #2</u>	<u>Scenario #3</u>	<u>Scenario #4</u>
Monochrome Panel Cost	\$533	\$1,035	\$648	\$553
Two Primary Color Image Source	\$1,240	\$2,356	\$1,496	\$1,284
Three Primary Color Image Source	\$2,026	\$3,823	\$2,438	\$2,097

The most cost-effective solution is described in scenario #1. This combines drivers fabricated at silicon foundries with pixel arrays fabricated separately. These tested, yielded components are connected using flip chip on glass bonding methodologies.

Silicon foundry driver costs are expected to drop in the future from the current \$0.30 per output to \$0.03 per output. This results in significant downside cost potential for this approach.

Scenario #4 is a second possibility for cost-effective subtractive color applications. This approach utilizes integrated drivers designed with redundancy and repair capability.

Scenarios #2 and #3 are cost prohibitive in light of the other options.

The semiconductor industry discovered that economy of scale significantly impacted production costs. Most of the costs associated with semiconductor processing are fixed costs associated with plant and equipment. To reduce unit cost, the strategy utilized in the semiconductor

industry is to increase the number of available parts per wafer. This is accomplished by increasing wafer size and decreasing minimum design tolerances.

In the display industry, cost reduction is typically achieved by fabricating on fully depreciated processing lines. However, as the industry matures, a transition to increasing the number of available parts occurs. Figure 4-4 summarizes the relative tradeoff between increasing substrate size versus reducing minimum processing tolerances in the total available displays per substrate.

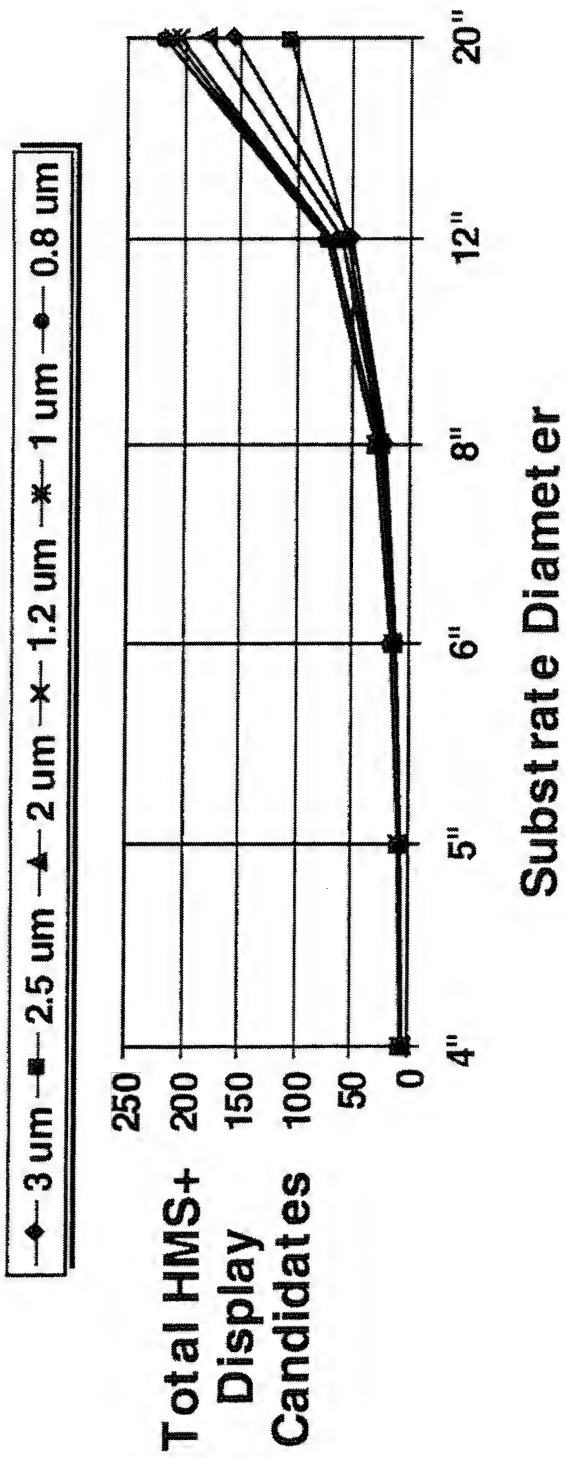


Figure 4-4. Substrate size versus processing tolerance.

As seen, the greatest impact on increasing the number of displays available is to increase the size of the substrate.

From a customer's perspective the two best scenarios are;

Scenario #1: Utilizing silicon foundry fabricated display drivers bonded onto active matrix glass substrates

Scenario #4: Utilizing drivers fabricated commensurate with the active matrix glass substrate exploiting redundancy in design and repair capabilities.

The following table compares some important features for each option.

<u>Feature</u>	<u>Scenario #1 Drivers Bonded to Glass</u>	<u>Scenario #4 Integrated Drivers with Redundancy and Repair</u>
Overall Display Size	Larger	Much Smaller
Design Cost	Lower	Higher
Design Cycle Time	Shorter	Longer
Product Development Cycle	Shorter	Longer
Capability to Increase Display Functionality	Easier	Hard
Driver Reliability	>10 Years	Unknown at this Point
Power Requirements	Higher	Lower

Deciding which scenario to use fundamentally resides in the display's application. Small, low-power applications favor using integrated drivers designed with redundancy and repair capabilities. Applications where small size and low power are not strict requirements favor use of drivers bonded onto the display glass.

4.3 Luminance Capability Analysis

Of key interest to the present analysis is the luminance capability of the two primary color, subtractive color light valve approach. The stated luminance objectives of 7500 fL in each of the red and green primaries (for a total of 15000 fL) are quite high in comparison with conventional display requirements, and are beyond the capability of most display technologies.

The light valve approach, however, allows considerable flexibility in the backlight design. Conceptually, it is possible to deliver far more light to an HMD than would be needed. In practice, however, there are a variety of constraints, each of which must be weighed (in terms of cost, complexity, size, weight, power, etc.) against the desired performance goals. The optical portions of the display system can be described in terms of the following subsystems, each of which affects the efficiency and can introduce performance limitations:

- Collimation and combining optics
- Light valve device(s)
- Backlight optics
- Optical coupling mechanism (e.g., fiber bundle, if used)
- Lamp collection optics
- Light source

4.3.1 Luminance Using a Broadband Arc Lamp

As demonstrated in Section 3, luminances well beyond the 15000 fL target can be achieved. For example, using stack #4 and the filtered, broadband Xenon arc lamp configuration, 880600 fL was measured normal to the light valve. Before using this as a final estimate, though, the other requirements for HMD use must be identified and checked. There are several important parameters to review, one being the angle of illumination required to fill the exit pupil at the desired field of view. For the present analysis we narrow the scope of the problem by using the following representative parameter values as a guideline:

Field of View (FOV)	32 degrees (32 x 24, with clipped corners)
Exit pupil	18 mm diameter
Luminance	7500 fL red, 7500 fL green, 15000 fL yellow
Pixel density	20 pixels/degree
Pixel pitch	24 microns (on light valve)
Aperture ratio	73%
Fiber bundle diameter	4 mm (optical aperture)

Using the simplified optical arrangement depicted in Figure 4-5, we then estimate the values of additional meaningful parameters. Figure 4-5 shows a conceptual collimating system in which the backlight provides illumination over a limited solid angle. The illuminated light valve is collimated by the lens in a telecentric manner, forming an external pupil as shown.

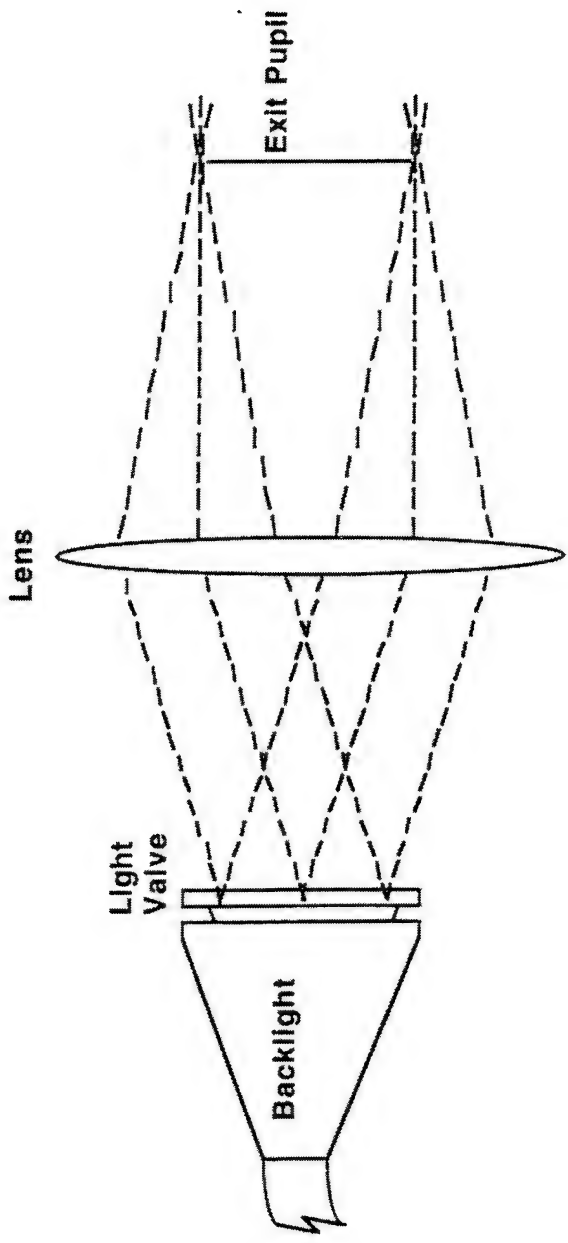


Figure 4-5. Simplified optical collimating configuration.

Using this and the parameters above, we obtain:

Angular resolution	3 arcminutes/pixel
Source size	19.2 mm (0.76") diagonal
Focal length	22.9 mm
Illumination half-angle	21.5 degrees
Pixel count	640 (H) x 480 (V)

To compare with the measurements of Section 3, we note that the pixel count and pitch are the same as were used. The primary difference with the measured luminance is that the illumination half-angle was quite different. Based upon the sketch in Figure 3-1, we can estimate the half-angle in that case as being approximately 3.4 degrees, far less than required to fill the pupil in our example here. Assuming that the half-angle were increased by a factor of $21.5/3.4$, the measured luminances would scale by approximately the inverse square of that, or about .025. Thus the measured luminances, for the filtered Xenon lamp and Stack #4, would be reduced to approximately 10500 fL green, 5600 fL red, and 22000 fL yellow.

We can see that the green and yellow targets are met in this case. While the red luminance is somewhat lower than desired, it is close. The test arrangement of Figure 3-1 was not optimized for efficiency, however. The backlight arrangement was overfilled to provide reasonable uniformity across the simulated light valve. By utilizing the light from the bundle more effectively, it should be possible to boost the red luminance for this example by 50% or more, beyond the 7500 fL level. Of course, the relative balance between green and red can be readily adjusted with suitable filtration in the optical path.

There remains room for considerable improvement in this area. A standard laboratory Xenon light source was used. The collection optics in this unit are generalized in nature and not specifically designed for the fiber cable used in the tests. Numerous air/glass interfaces could be optimized, as could the filters used to remove the blue and deep red bands. Overall, it may be possible to increase the coupling efficiency to the lamp several-fold.

There is also ample opportunity for tradeoffs involving the luminance. Given excess luminance over the targeted level, the broadband colors (Xenon lamp) could be narrowed, which increases the color saturation and potentially simplifies the optical configuration. Lower transmission light valves could be supported, including lower aperture ratios unless precluded for other reasons. Contrast of the light valves can be improved, such as in the configuration of Stack #3. Spectral crosstalk between the layers could also be reduced, such that the yellow output more closely matches the sum of the independently modulated red and green outputs.

As we have seen, luminance capability is closely related to other requirements, especially the exit pupil diameter and the FOV. Reductions in these parameters, or allowances for some reduction near the edges (if allowed by the application) would strongly impact luminance considerations.

4.3.2 Narrow Band Arc Lamp Illumination

A benefit of using narrow band illumination in each of the red and green spectral bands is that it simplifies certain optical methods and enhances overall performance. While narrow band illumination can come from a variety of sources, the high luminance targets discussed here suggest that arc lamps, lasers or other high brightness technologies be used. The analysis in Section 3 includes measured results from an early prototype tri-band metal halide lamp currently under development. It must be noted that these results are very preliminary, since neither the lamp development nor the optical coupling to the lamps are completed or optimized. Still, we can review the results for a benchmark of progress to date.

Stack #5 was specifically tuned to match the primary red and green narrow-band peaks of the lamp tested, and assumes that the remaining spectral components will be removed by another means (filters, combiner, etc.). The bundle luminance and Stack #5 transmittance associated with each of the peaks (± 10 nm) is

Color band (20 nm wide)	Bundle luminance	Stack #5 transmittance	Anticipated luminance
green	236600 fL	13.8%	32650 fL
red	102900 fL	14.4%	14800 fL
yellow (r+g)	339500 fL	...	47450 fL

By designing for just these spectral bands, a higher transmittance was achieved than for broader bands while still maintaining contrast ratios in the range of 100:1. These numbers also need to be scaled down, as was done above in the broadband case, if the light from the bundle does not provide sufficient angular spread to fill the pupil at the required FOV. Data on the anticipated angular spread of the light leaving the bundle is not yet available for this preliminary lamp and its fixture, hence it would be premature to estimate the luminance to be available. It is likely, however, that additional development of the collection optics, the lamp or both may be needed to meet the stated high luminance objectives for a two-primary color display.

4.3.3 Other Illumination Options

The suitability of lasers for providing the backlight illumination is primarily limited by the cost, size and weight of the laser and optical coupling systems. Adequate light output is readily achieved by combining parallel systems, and the fiber optic cable can be even more compact than with arc lamps. Some additional attention would be necessary in the system design and evaluation to minimize undesired coherence and polarization effects, but these should present no major obstacle in this application. While this program has not specifically addressed lasers as a candidate light source, possible types include semiconductor lasers for the red component and diode-pumped solid state lasers (or even gas lasers) for the green component. The availability, practicality and number of lasers required would need to be determined.

LEDs might provide yet another option, although the optical coupling is much less straightforward than with lasers. Further study would be required to confirm the viability of an LED approach.

4.3.4 Fiber Bundle Considerations

The laboratory tests were performed using a standard incoherent fiber optic bundle. The cable was approximately 5 feet long and the diameter of the ends (optical aperture) was 0.25 inch. Additional, protective shielding on the bundle increased the actual package diameter beyond this size.

In an aircraft installation, it is likely that a significantly longer cable might be used. This would reduce the throughput of the cable, and would require the coupling and collection efficiency to be improved to compensate. The other likely change is that of reducing the diameter of the fiber bundle. Reducing the diameter does not necessarily require a decrease in luminance capability (to a point), since the angular capacity (Numerical Aperture, N.A.) of the conventional bundle was not filled by the test configuration in Section 3. By increasing the angular spread of the light in the cable without decreasing the forward luminance, the same amount of light can be transferred through a much smaller diameter. Additional complexity may be required in the coupling to and from the fiber bundle to achieve this.

Optical disconnects for safety reasons should pose no problems beyond a coupling loss. This loss could be significant, so the number of connection points should be kept to a minimum.

4.3.5 Other Considerations

To be useful at very high luminances, the AMLCD must have adequate light shielding over its TFT switching elements. Inadequate light shielding can lead to loss of contrast or other nonconformance with requirements. Appropriate design of the illumination and optical system can minimize the impact by allowing only the required light to reach the rear panel (especially the rear panel). Contrast ratio will of course be limited by the intrinsic contrast of the light valves used, so high contrast devices are preferred.

Dimming capability can perhaps best be provided in the lamp collection optical path, as is commonly done with commercial arc lamp sources, although other options exist if desired. Redundancy or extra luminance can be provided through the use of multiple lamps with a common fiberoptic bundle in a variety of configurations.

4.3.6 Luminance Capability Conclusions

Based upon the test results and the assumptions in this section, two-primary subtractive color should meet the stated luminance objectives of 7500 fL in each of the green and red color bands, and 15000 fL total for a yellow state. While this conclusion relies upon data from a broad band (Xenon arc) lamp, preliminary results for narrow band emitting metal halide lamps are also encouraging. In either case, further optimization of the optical coupling configuration has significant benefits in meeting requirements or allowing enhancements in other areas.

5 SIMULATION DEVELOPMENT AND EVALUATION

5.1 Overview

The simulations described here were conducted to assess the impact of image source design on the quality of HMS+ imagery. The general approach (Figure 5-1, p. 225) was to produce a series of static representations of HMS+ images such that observers could evaluate image quality in comparing various image sources. The general simulation method was to digitally overlay imagery onto LCD image source models using a high-performance graphics workstation. The modified images were then output to a high resolution CRT and viewed at an appropriate distance such that the angular subtense of the simulated LCD pixels was controlled.

This overview describes the general methodology used to establish the display simulations and to conduct ten discrete subjective evaluations of these simulations. The overview describes the simulation software used, simulation images, the designs of simulation evaluations, the general procedures used to collect evaluation data, and the analysis approach used to interpret subjective rating data collected during the evaluations.

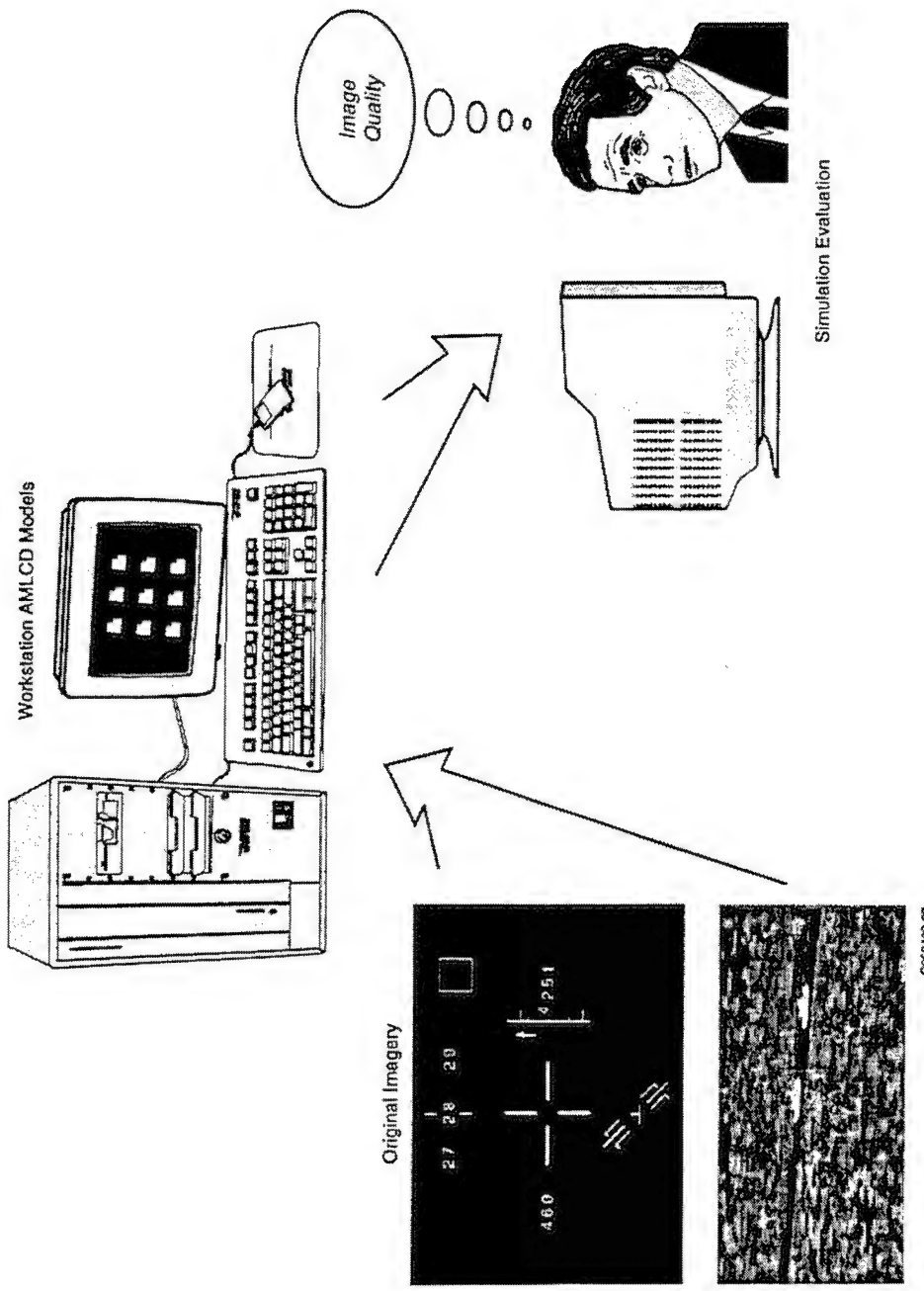


Figure 5-1. General AMLCD Simulation and Evaluation Process.

Symbology and LANTIRN FLIR images were submitted to AMLCD simulation models on a Silicon Graphics workstation. The simulated AMLCD images were viewed on a high-resolution CRT at a viewing distance calculated to control angular resolution of the AMLCD pixels. Systematic image evaluations were conducted to establish AMLCD design trades in terms of subjective quality.

5.1.1 Simulation Software

The simulation models were embodied in 'C' code on a Silicon Graphics workstation. This software is schematically illustrated in Figure 5-2, p. 228. Images were prepared using this software and stored for later use by evaluation/image presentation software. The image processing software, developed at Honeywell, includes a pull-down menu to configure model parameters. The software includes convolution modules for symbol anti-aliasing and simulation of subtractive color layer diffraction effects. Other optional modules include the selective elimination of color channels, blending of AMLCD images with background images (image transparency), and luminance matching as a function of aperture ratio. Image gamma correction is selectable to a variety of image output devices.

The heart of the image processing software is gamma correction, the assignment of grayscale values, and the application of the pixel mask. For most output devices, the nonlinearity of the relationship between image RGB DAC (Digital-to-Analog Converter) values and the luminance of the display necessitates first converting DAC values into luminance values using the measured gamma function of the display. The same process is reversed prior to saving the image to disk. Once image values are converted to luminance, gray scale thresholding is applied. The general equation used to perform gray scale thresholding is:

$$\text{Luminance}(i) = [(L_{\max}^P - L_{\min}^P)(i / (n - 1)) + L_{\min}]^{1/p} \quad (1)$$

where $\text{Luminance}(i)$ is the luminance of any given step in the gray scale distribution for a given color primary from 0 to n , n is the number of discretely addressable steps in the gray scale distribution for that primary, L_{\max} is the maximum luminance of the primary, L_{\min} is the minimum luminance of the primary, and P is an exponent ranging from 1.0 (linear distribution) to 0.33. In the simulations reported here, nonlinearities of the original CRT gammas produced some loss of addressable gray scale levels when applying equation 1, with the loss most likely occurring as n approached 256.

Subsequent to gray scale thresholding, each pixel in the original image is mapped to a matrix of pixels in image memory to simulate a single LCD pixel (Figure 5-3 through Figure 5-8). This transformation is accomplished by multiplying the luminance value of the kernel pixel in the

original image by an array of coefficients representing the overall luminance profile of the LCD pixel. The coefficients for the current simulations were calculated to provide aperture ratios ranging from 40% to 80% (aperture ratio is operationally defined here as the average percentage of the luminance of the simulated LCD pixel relative to the luminance of the kernel pixel). The luminance profile for AMLCD masks includes a thin-film transistor (TFT) structure in the upper right corner of the pixel. Note that the coefficients depicted in the illustrations in this report are approximations used for illustration. The actual values used in the simulation code are given in Table 5-1 (p. 235).

The simulated AMLCD pixels modeled in this way had a square pixel shape when displayed on the output CRT (the CRT had an equivalent horizontal and vertical pixel pitch).

Completed simulation images were presented to evaluation participants using the evaluation software illustrated in Figure 5-9 (p. 236). The evaluation software controlled randomization and blocking of image order and location, presentation of images, and recording of data files for tracking the history of image presentation.

Silicon Graphics Workstation

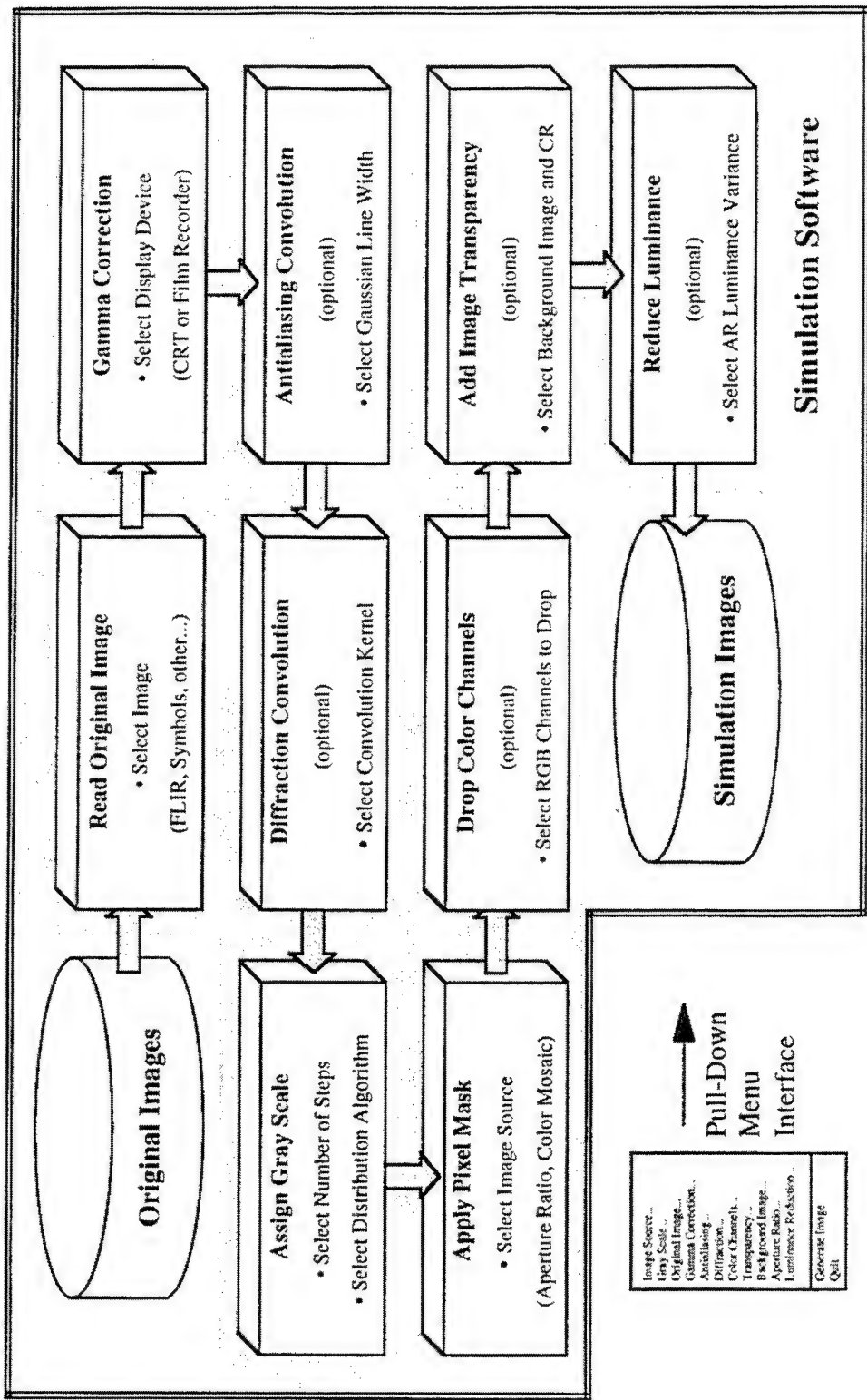


Figure 5-2. Image Processing Steps Incorporated in Simulation Software.

The simulation image files produced by the simulation software were presented to observers via the evaluation software (Figure 5-9).

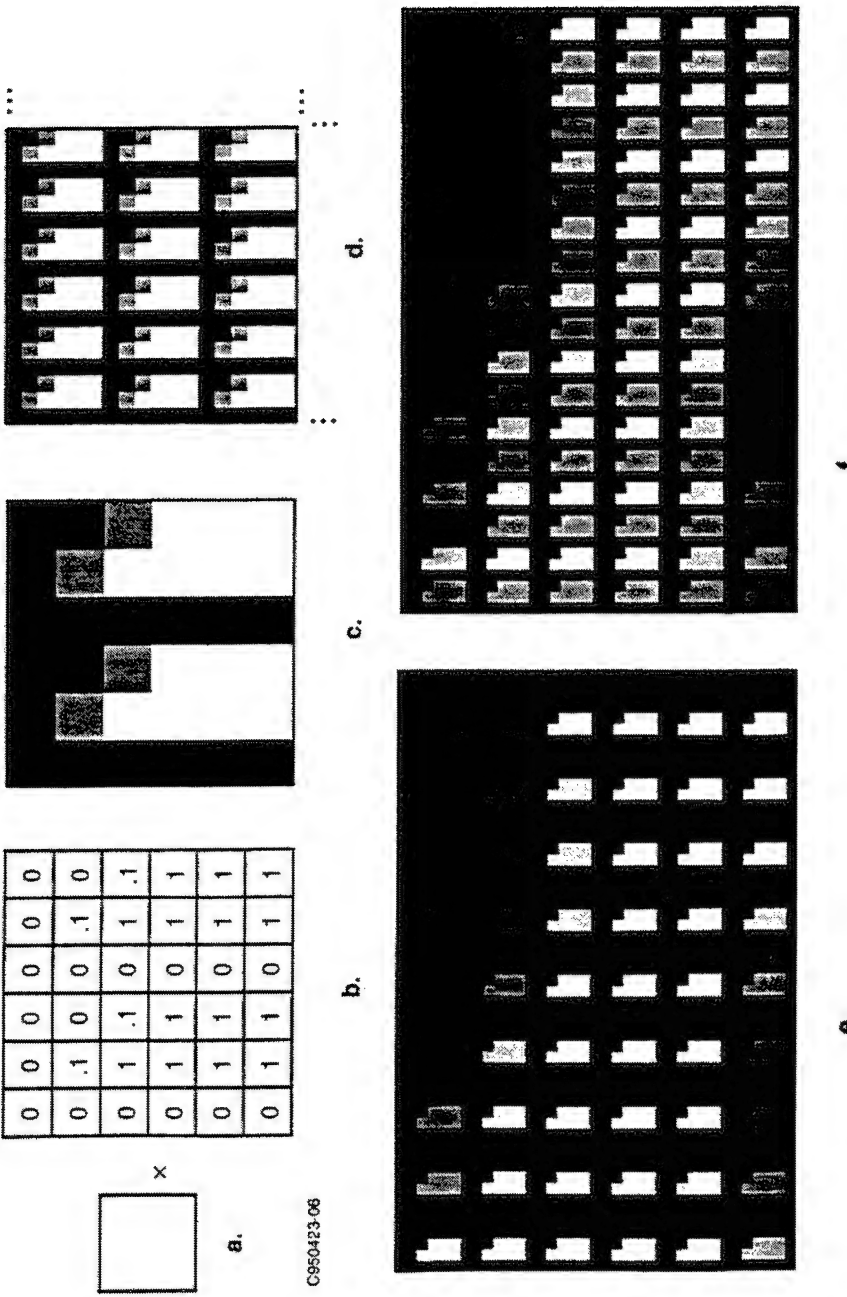


Figure 5-3. Simulation Model of Additive Color AMLCD (40%).

Each pixel in the original image (a) was replicated in a 6x6 matrix. The luminance of the original pixel was multiplied by the coefficients in the matrix (b) to form the luminance profile of an AMLCD pixel (c), including a TFT bite in the upper-right corner of each color element. The displayed image (d) was made up of many such pixel matrices tiled together. The left color element of each pixel was red, while the right color element was green. No row or column offset was modeled for the additive color image source. Images (e) and (f) show the relative difference between red (e) and yellow (f) images modeled with the additive color image source. Note that evaluation images were actually presented in color on a high-resolution CRT. Also, these printed gray scale images are not gamma-corrected for printing. In addition, their size as printed is not intended to simulate the angular resolutions tested in the evaluations.

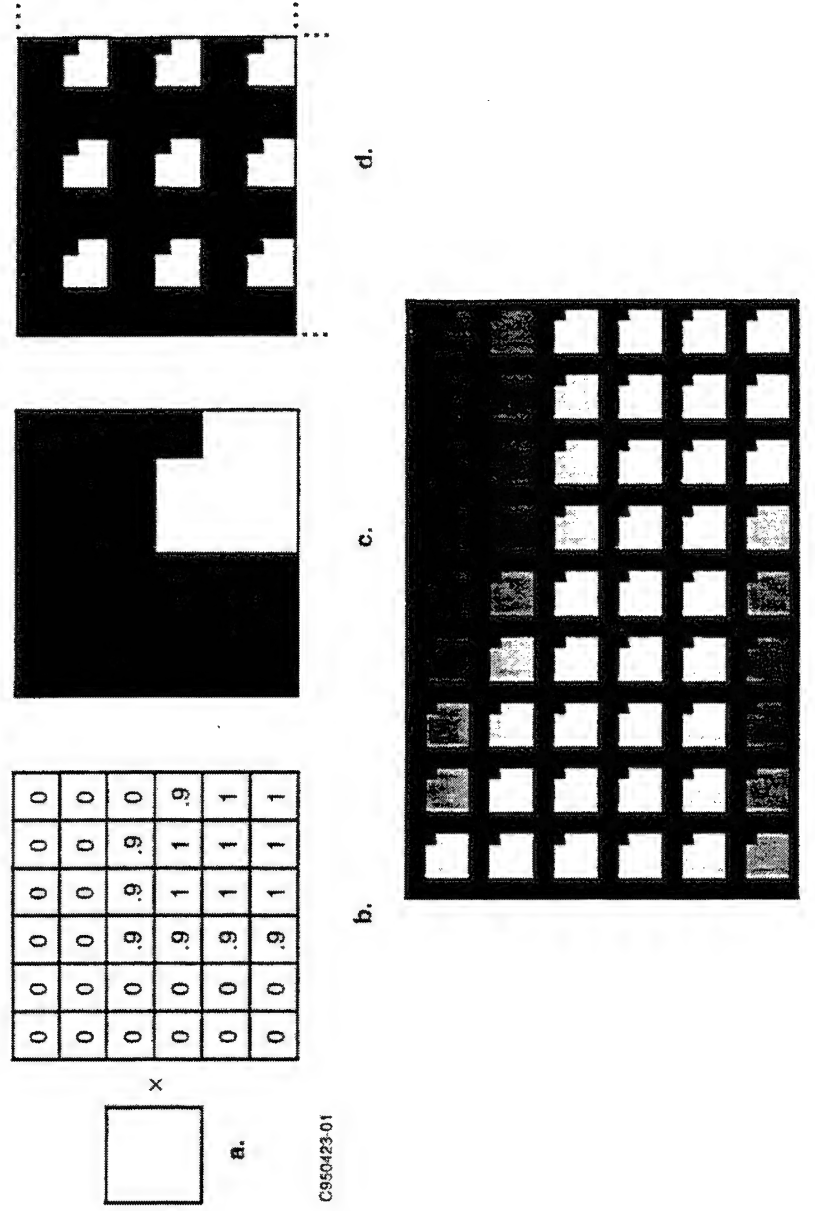


Figure 5-4. Simulation Model of Subtractive Color AMLCD (40%).

Each pixel in the original image (a) was replicated in a 6x6 matrix. The luminance of the original pixel was multiplied by the coefficients in the matrix (b) to form the luminance profile of an AMLCD pixel (c), including a TFT bite in the upper-right corner of the pixel. The displayed image (d) was made up of many such pixel matrices tiled together. Each color element of the subtractive color image source was equivalent to a color pixel. Image (e) shows a bitmap from an actual simulation image using this image source model. Note that evaluation images were actually presented in color on a high-resolution CRT. Also, these printed gray scale images are not gamma-corrected for printing. In addition, their size as printed is not intended to simulate the angular resolutions tested in the evaluations.

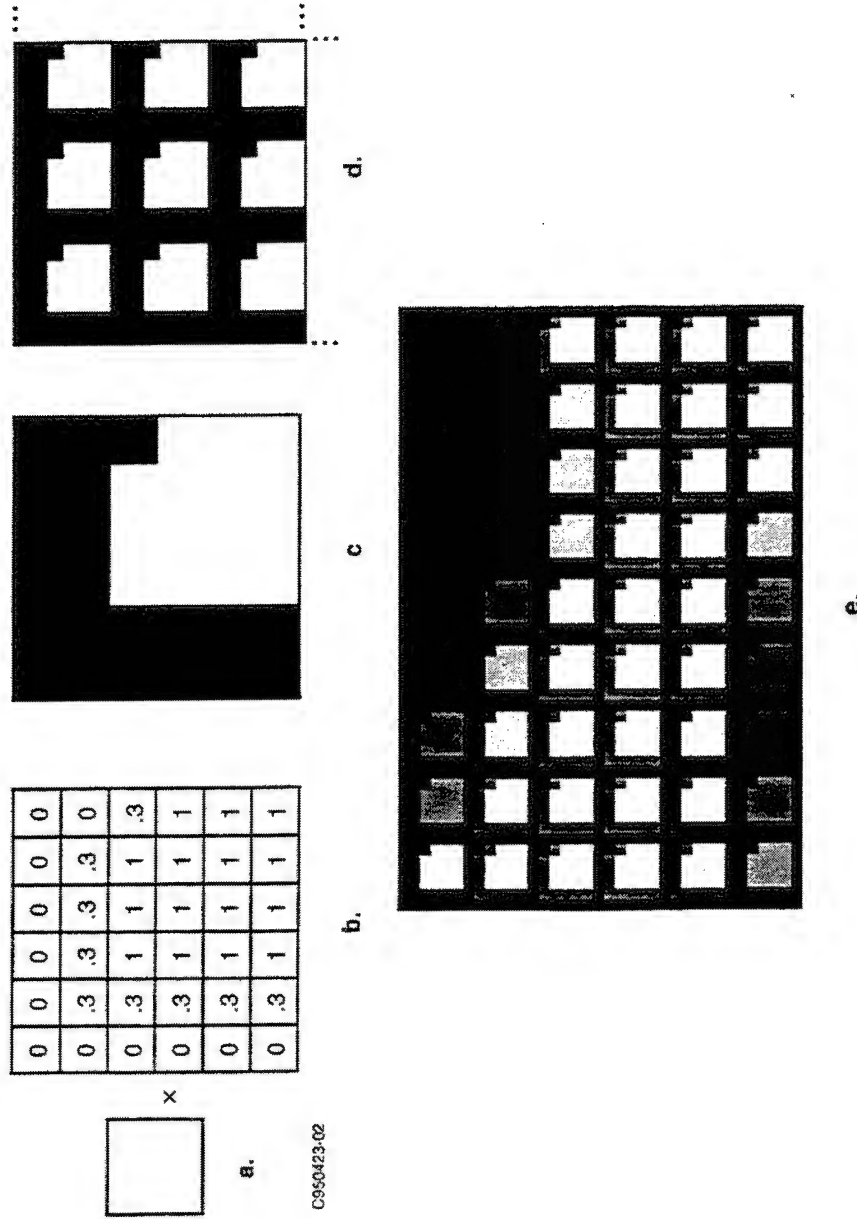


Figure 5-5. Simulation Model of Subtractive Color AMLCD (50%).

Each pixel in the original image (a) was replicated in a 6x6 matrix. The luminance of the original pixel was multiplied by the coefficients in the matrix (b) to form the luminance profile of an AMLCD pixel (c), including a TFT bite in the upper-right corner of the pixel. The displayed image (d) was made up of many such pixel matrices tiled together. Each color element of the subtractive color image source was equivalent to a color pixel. Image (e) shows a bitmap from an actual simulation image using this image source model. Note that evaluation images were actually presented in color on a high-resolution CRT. Also, these printed gray scale images are not gamma-corrected for printing. In addition, their size as printed is not intended to simulate the angular resolutions tested in the evaluations.

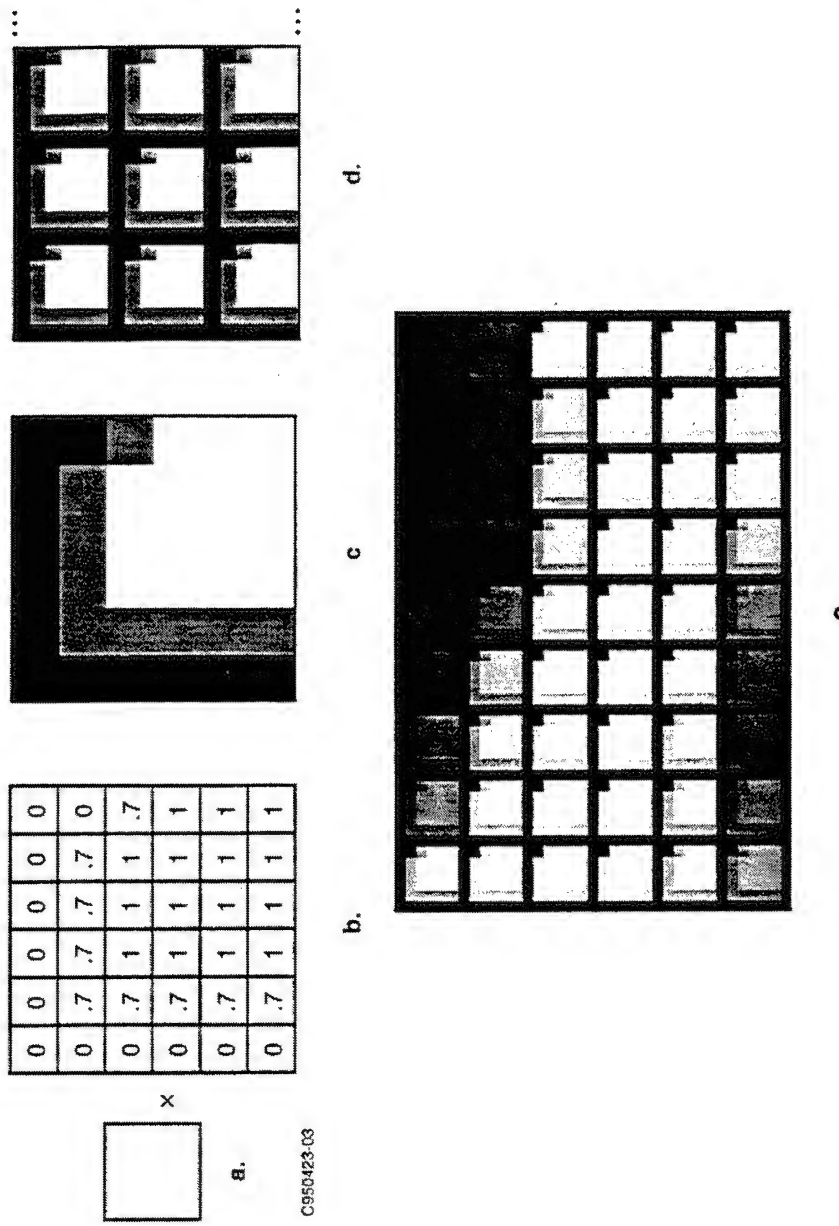


Figure 5-6. Simulation Model of Subtractive Color AMLCD (60%).

Each pixel in the original image (a) was replicated in a 6x6 matrix. The luminance of the original pixel was multiplied by the coefficients in the matrix (b) to form the luminance profile of an AMLCD pixel (c), including a TFT bite in the upper-right corner of the pixel. The displayed image (d) was made up of many such pixel matrices tiled together. Each color element of the subtractive color image source was equivalent to a color pixel. Image (e) shows a bitmap from an actual simulation image using this image source model. Note that evaluation images were actually presented in color on a high-resolution CRT. Also, these printed gray scale images are not gamma-corrected for printing. In addition, their size as printed is not intended to simulate the angular resolutions tested in the evaluations.

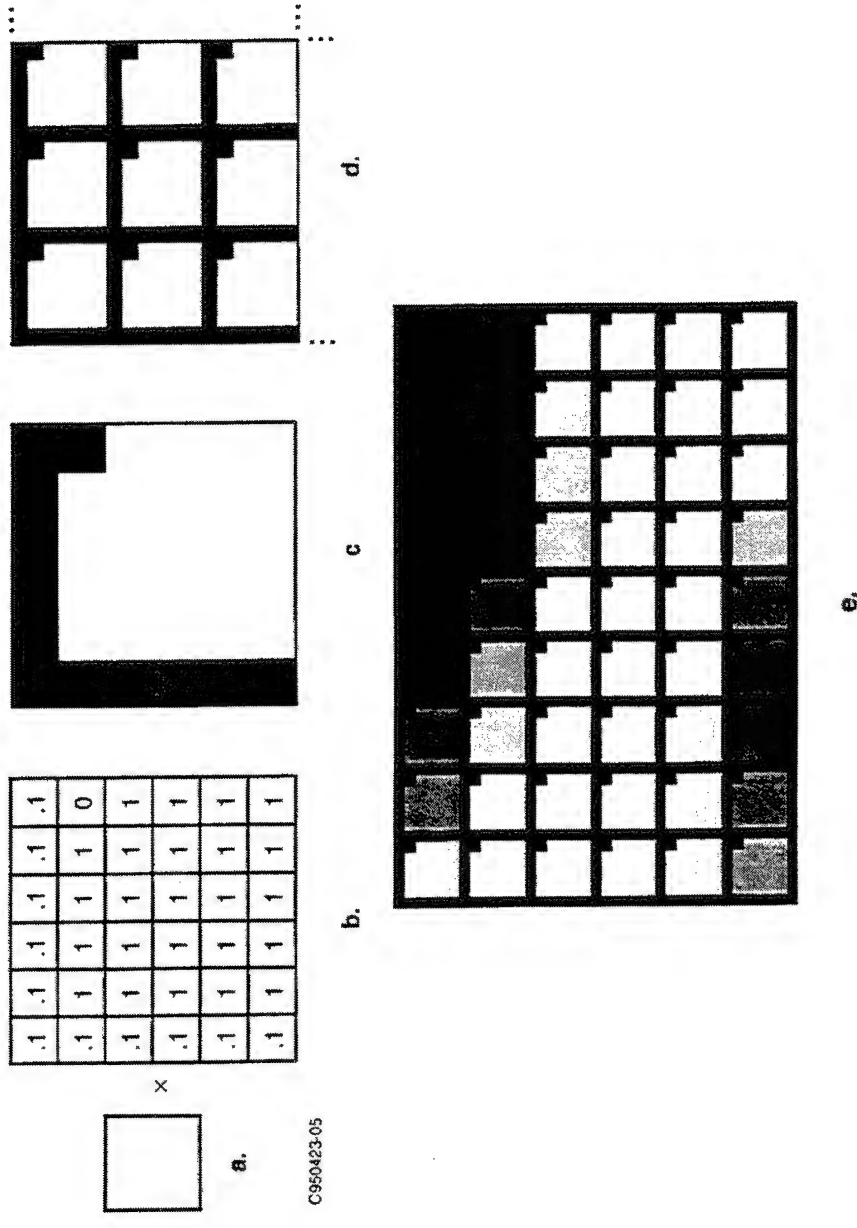


Figure 5-7. Simulation Model of Subtractive Color AMLCD (70%).

Each pixel in the original image (a) was replicated in a 6x6 matrix. The luminance of the original pixel was multiplied by the coefficients in the matrix (b) to form the luminance profile of an AMLCD pixel (c), including a TFT bite in the upper-right corner of the pixel. The displayed image (d) was made up of many such pixel matrices tiled together. Each color element of the subtractive color image source was equivalent to a color pixel. Image (e) shows a bitmap from an actual simulation image using this image source model. Note that evaluation images were actually presented in color on a high-resolution CRT. Also, these printed gray scale images are not gamma-corrected for printing. In addition, their size as printed is not intended to simulate the angular resolutions tested in the evaluations.

Directional Illumination

Xenon Lamp and Calculated Filters:

MCD Style:	Lamp =	6294000 fL	fL	u'	v'
Yellow	570400	0.1943	0.5636		
Red	127300	0.3860	0.5373		
Green	159300	0.1023	0.5695		
Black	32070	0.1314	0.5517		
Transmission:	9.06%				
Contrast Ratio:	17.79				

Sony Stack:

	Lamp =	945500 fL	fL	u'	v'
Yellow	20650	0.2028	0.5640		
Red	2469	0.4340	0.5339		
Green	5160	0.0834	0.5745		
Black	99.12	0.1439	0.5640		
Transmission:	2.18%				
Contrast Ratio:	208.33				

SONY Stack:

	Lamp =	7109000 fL	fL	u'	v'
Yellow	663000	0.2086	0.5631		
Red	75960	0.4654	0.5298		
Green	204700	0.0913	0.5741		
Black	1425	0.2493	0.5502		
Transmission:	9.33%				
Contrast Ratio:	465.26				

	Lamp =	7052000 fL	fL	u'	v'
Yellow	943000	0.2088	0.5630		
Red	179400	0.4200	0.5369		
Green	492900	0.1117	0.5738		
Black	12730	0.2822	0.5548		
Transmission:	13.37%				
Contrast Ratio:	74.08				

Double Narrow Band Design:

	Lamp =	6904000 fL	fL	u'	v'
Yellow	1088000	0.1954	0.5647		
Red	501600	0.3052	0.5496		
Green	620700	0.1111	0.5738		
Black	168500	0.1868	0.5592		
Transmission:	15.76%				
Contrast Ratio:	6.53				

Transmission is the ratio of the yellow luminance to the white backlight luminance, and includes the attenuation of the calculated yellow and IR filters as well as the LCD stack absorption. Contrast ratio is the ratio of yellow to black luminance.

Directional Illumination

Xenon Lamp and Reynard Filters:

LCD Style:		Lamp = 8504000 fL	fl	u'	v'	
Yellow	519200	0.2197	0.5638			
Red	130600	0.4086	0.5374			
Green	128100	0.1239	0.5749			
Black	22490	0.1619	0.5634			
Transmission:	6.11%					
Contrast Ratio:	23.09					

Notch Polarizer:

LCD Style:		Lamp = 9757000 fL	fl	u'	v'	
Yellow	1069000	0.2226	0.5638			
Red	216100	0.3946	0.5393			
Green	552300	0.1303	0.5761			
Black	46690	0.1378	0.5731			
Transmission:	10.96%					
Contrast Ratio:	22.90					

Hybrid #1:

LCD Style:		Lamp = 9565000 fL	fl	u'	v'	
Yellow	619900	0.2300	0.5628			
Red	83560	0.4704	0.5289			
Green	172500	0.1066	0.5782			
Black	1349	0.2740	0.5556			
Transmission:	6.48%					
Contrast Ratio:	459.53					

Hybrid #2:

LCD Style:		Lamp = 9493000 fL	fl	u'	v'	
Yellow	880600	0.2305	0.5628			
Red	226800	0.4234	0.5360			
Green	421800	0.1245	0.5767			
Black	11680	0.2938	0.5545			
Transmission:	9.28%					
Contrast Ratio:	75.39					

Double Narrow Band Design

LCD Style:		Lamp = 9311000 fL	fl	u'	v'	
Yellow	995700	0.2175	0.5644			
Red	488100	0.3259	0.5498			
Green	524300	0.1262	0.5764			
Black	141600	0.2179	0.5641			
Transmission:	10.69%					
Contrast Ratio:	7.03					

Transmission is the ratio of the yellow lumiance to the white background lumiance, and includes the attenuation of the Reynard filters as well as the LCD stack absorption. Contrast ratio is the ratio of yellow to black lumiance.

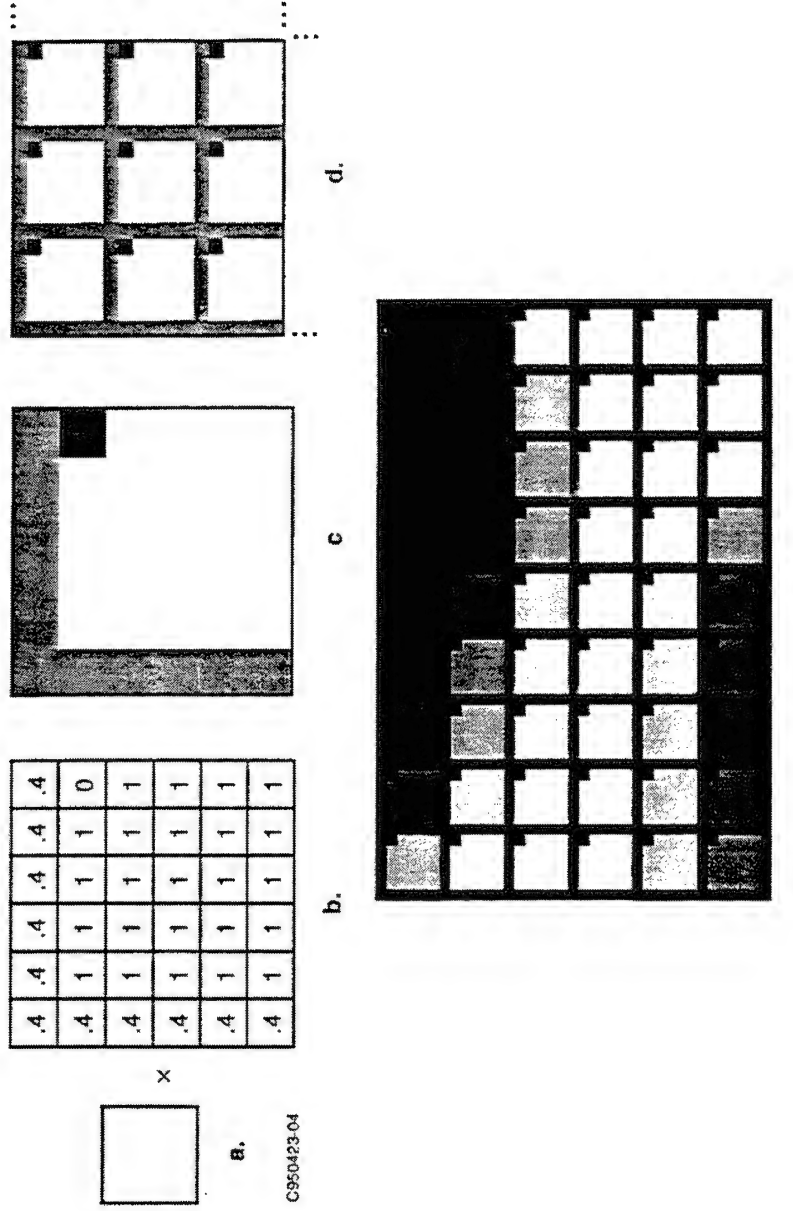


Figure 5-8. Simulation Model of Subtractive Color AMLCD (80%).

Each pixel in the original image (a) was replicated in a 6x6 matrix. The luminance of the original pixel was multiplied by the coefficients in the matrix (b) to form the luminance profile of an AMLCD pixel (c), including a TFT bite in the upper-right corner of the pixel. The displayed image (d) was made up of many such pixel matrices tiled together. Each color element of the subtractive color image source was equivalent to a color pixel. Image (e) shows a bitmap from an actual simulation image using this image source model. Note that evaluation images were actually presented in color on a high-resolution CRT. Also, these printed gray scale images are not gamma-corrected for printing. In addition, their size as printed is not intended to simulate the angular resolutions tested in the evaluations.

Table 5-1. Illustrated and actual pixel mask luminance coefficients.

AR	Subtractive Color			Additive Color	
	40%	50%	60%	70%	80%
Illustrated	0.9	0.3	0.7	0.1	0.4
Actual	0.9143	0.3333	0.7333	0.1091	0.4364

Silicon Graphics Workstation

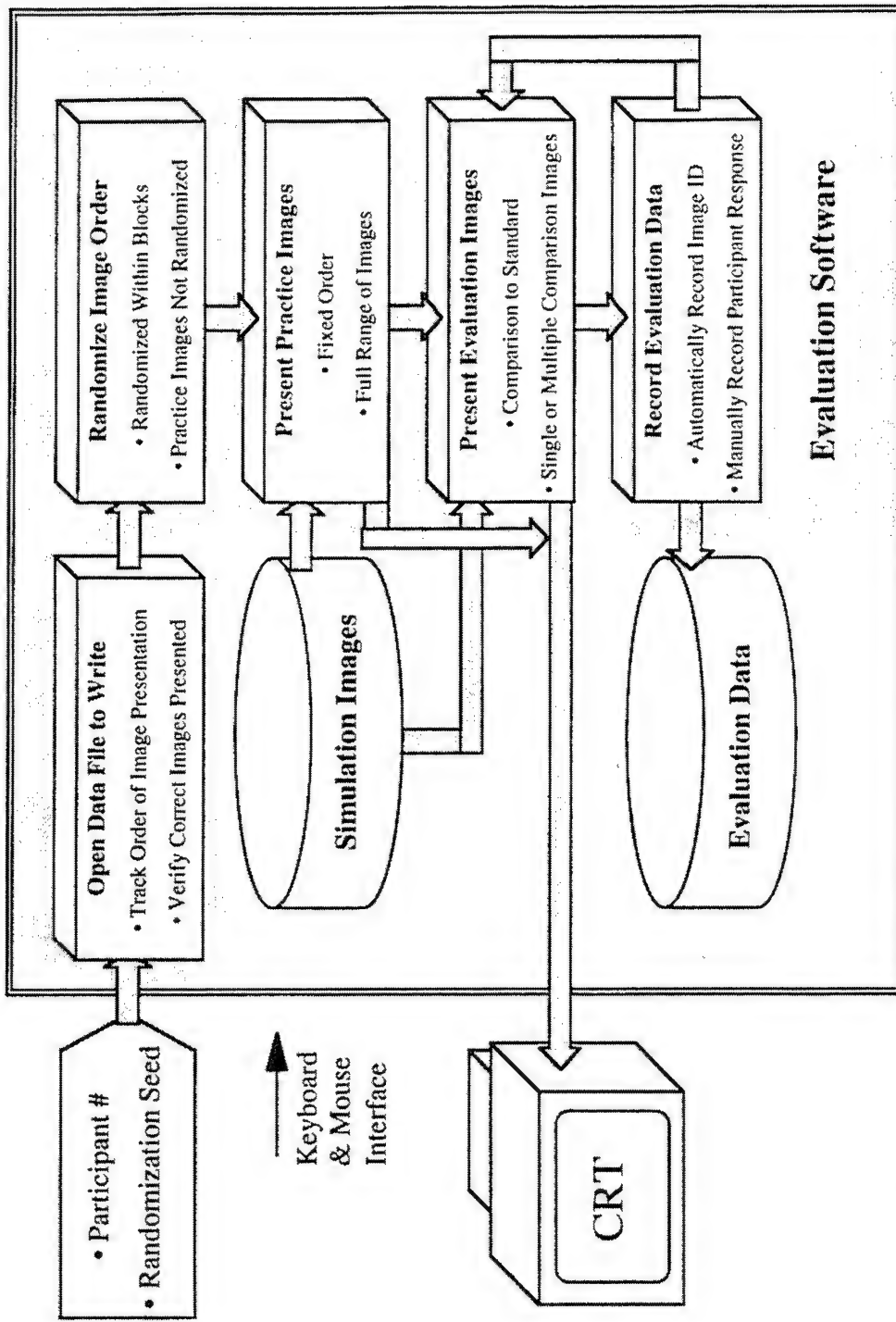


Figure 5-9. Evaluation Software Used to Control Simulation Image Presentation.

Image identification data files were automatically recorded for subsequent correlation with manually recorded subjective image ratings.

5.1.2 Simulator Imagery

The display simulations incorporated two classes of imagery: flight reference, guidance, and targeting symbology (Figure 5-10, p. 239) and LANTIRN FLIR (Figure 5-11 and Figure 5-12, p. 240). The flight symbology was created on a 640 x 480 pixel matrix at Honeywell and is hypothetical only, but intended to be representative of HMS+ symbology. The original symbology image was created as a binary image with green and red lines. The FLIR imagery (720 x 356) came from the Fractil program (U.S. Air Force, Night Vision Lab) and was provided by Boeing. The FLIR was captured with a production grade LANTIRN FLIR targeting pod, and included only narrow FOV images (wide FOV imagery was unavailable, except on NTSC-sampled tape). The FLIR used 8 bits of monochrome gray scale resolution. The FLIR was captured during night flyovers at Edwards AFB and was digitally captured directly from the FLIR sensor. Over 100 FLIR images were reviewed from the Fractil data. The images selected were captured from a range of approximately 3 km. Two images were selected for use: a side profile of a tank on a road, representing a light target against a dark background; and what appears to be an overhead view of a heavy truck (although the identity of the target in this image is uncertain), also on a road, representing a dark target against a light background.

The display simulation approach used required a 6 x 6 matrix of CRT pixels to simulate each LCD pixel. Consequently, it was not possible to simulate the full 640 x 480 HMS+ FOV simultaneously. In addition, the need to allow simultaneous presentation of multiple images to allow visual comparison also limited the size of simulation images. Consequently, limited portions of the original images were selected for use in the simulations. For the Symbol images, numeric characters with curves were selected as worst case examples of aliasing. For the FLIR images, the portion of the image containing the target (i.e., Tank or Truck) was selected. While the full FOV was not shown to participants in the evaluations, the parameters most critical to image quality (i.e., contrast, resolution, aperture ratio) were faithfully simulated.

At the intermediate resolution of 22 pix/deg, each simulated LCD subtended approximately 2.73 arcminutes of visual angle. Symbols presented without antialiasing had a height of approximately 57 arcminutes (21 LCD pixels) and a stroke width of approximately 6.5 arcminutes (between 2 and 3 LCD pixels). Symbols were centered in a background of approximately 4 deg in width (88 LCD pixels) nad 2.55 degrees in height (56 LCD pixels). FLIR image sizes matched the size of the symbol backgrounds, with FLIR targets (tank, truck) largely filling the background area.

Tanks subtended approximately 3.8 deg horizontally and 1 deg vertically within the larger image frame. Trucks, which ran diagonally through the image frame, subtended approximately 2.9 deg in a horizontal line perpendicular to the vertical, and 2 deg vertically.

High-quality standard images were constructed to serve as benchmarks for subjective image ratings. For the Symbol images, the standard was formed by redrawing the symbology at a higher resolution than the original (Figure 5-13, p. 242). The luminance and luminance contrast of the standard was increased as high as could be comfortably viewed in the darkened room. For the FLIR images (Figure 5-14, p. 243, and Figure 5-15, p. 244) it was not possible to enhance the resolution of the original images. Therefore, only luminance/contrast enhancement was used to improve the appearance of the FLIR standards. Standard images were further differentiated in appearance from evaluation comparison images by the lack of any TFT or row and column lines (AMLCD models were not used to create standard images). Standard images were always presented in the same color as comparison images.

Note that simulation images reproduced in this document vary significantly from their appearance as presented in the simulation evaluations. The images are reproduced here only to convey the approximate appearance of the simulation images. Anomalies appearing in the images are likely to be artifacts associated with their reproduction. In particular, please note that:

1. Images were presented on a color CRT during the evaluation. The images were converted to gray-scale images for inclusion in this report.
2. No attempt has been made to correct the images for the gamma of the printing process.
3. The image file conversion process has limited the resolution with which subpixel structures are represented.
4. Paper reproduction (xerography) has further exacerbated the differences noted above.

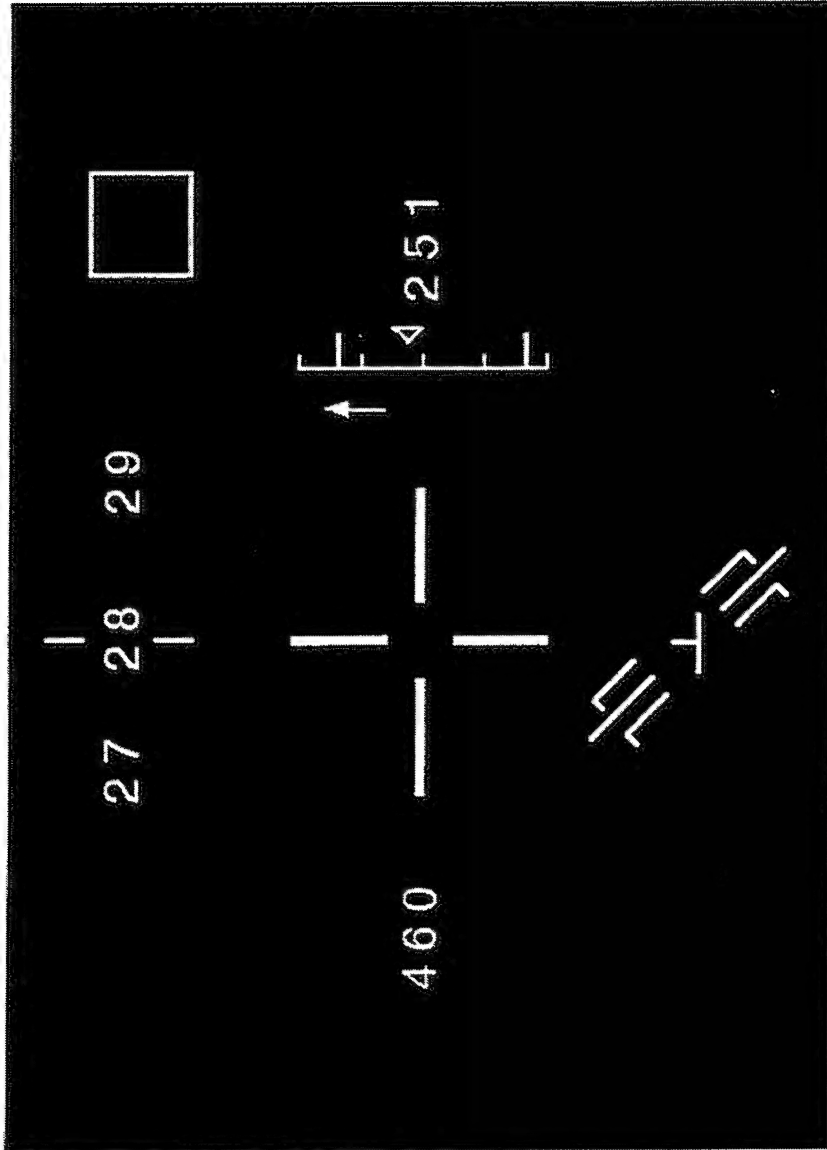


Figure 5-10. Original Image of Flight Guidance, Reference, and Targeting Symbols.

A limited portion of this image was used in the simulations (see Figure 5-13, p 242). Note that evaluation images were actually presented in color on a high-resolution CRT. Also, these printed gray scale images are not gamma-corrected for printing.



Figure 5-11. Original FLIR Truck Image.

A limited portion of this image was used in the simulations (see Figure 5-14, p. 243). Note that evaluation images were actually presented in color on a high-resolution CRT. Also, these printed gray scale images are not gamma-corrected for printing.

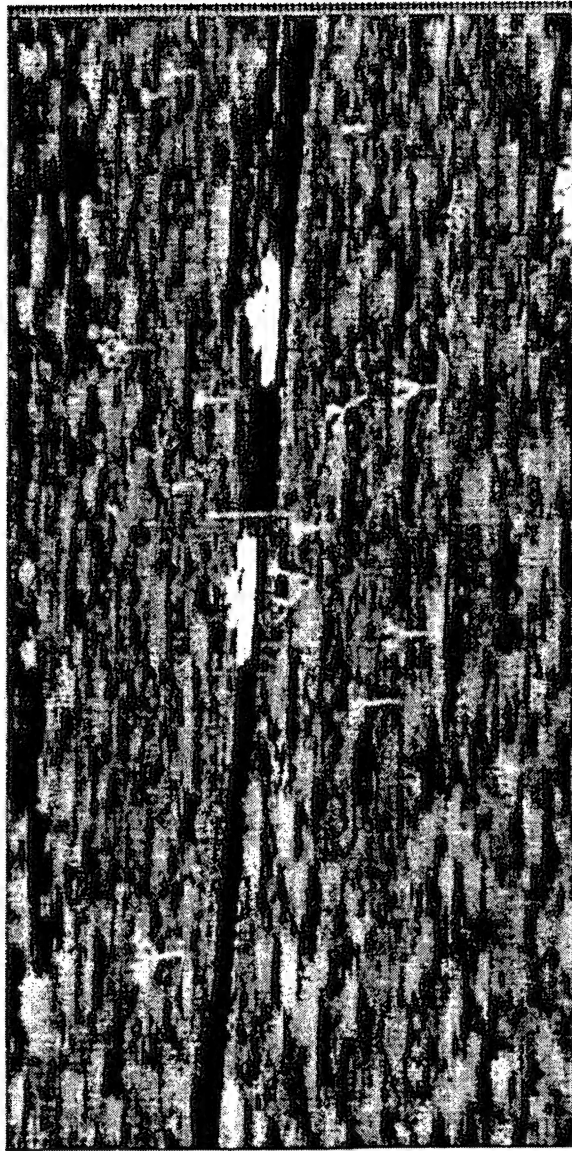
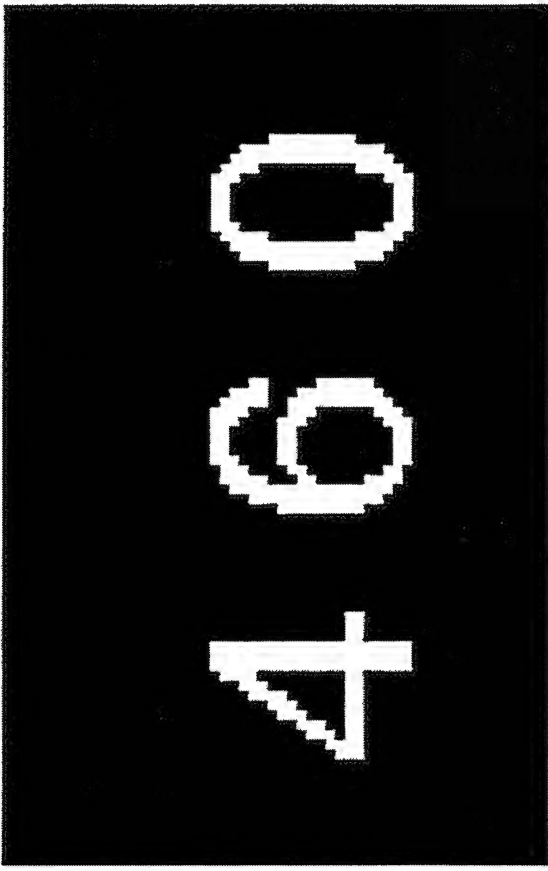
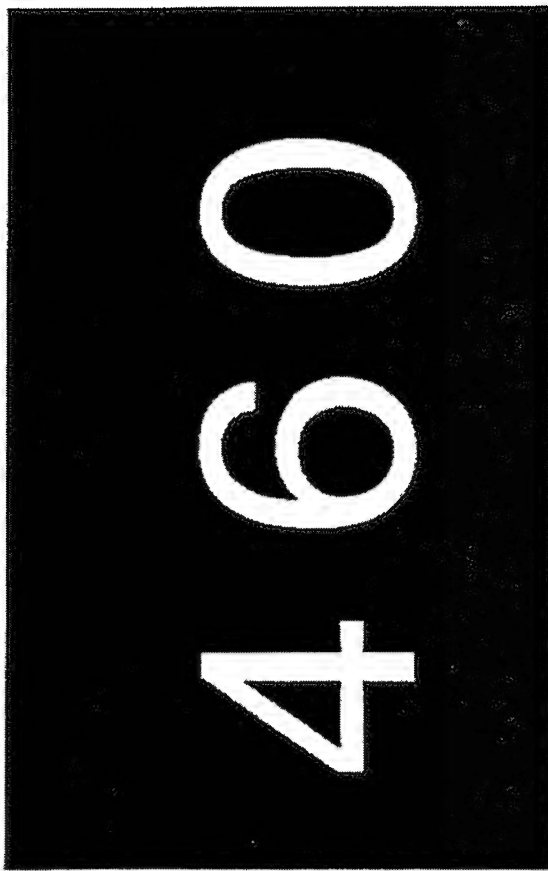


Figure 5-12. Original FLIR Tank Image.

A limited portion of this image was used in the simulations (see Figure 5-15, p. 244). Note that evaluation images were actually presented in color on a high-resolution CRT. Also, these printed gray scale images are not gamma-corrected for printing.



(a)



(b)

Figure 5-13. Construction of Standard Image for Symbol Images Used in Evaluations 1, 7, 8 and 10.

The standard image with contrast enhancement but without resolution enhancement (a) and with resolution enhancement (b). Note that evaluation images were actually presented in color on a high-resolution CRT. Also, these printed gray scale images are not gamma-corrected for printing. In addition, their size as printed is not intended to simulate the angular resolutions tested in the evaluations.

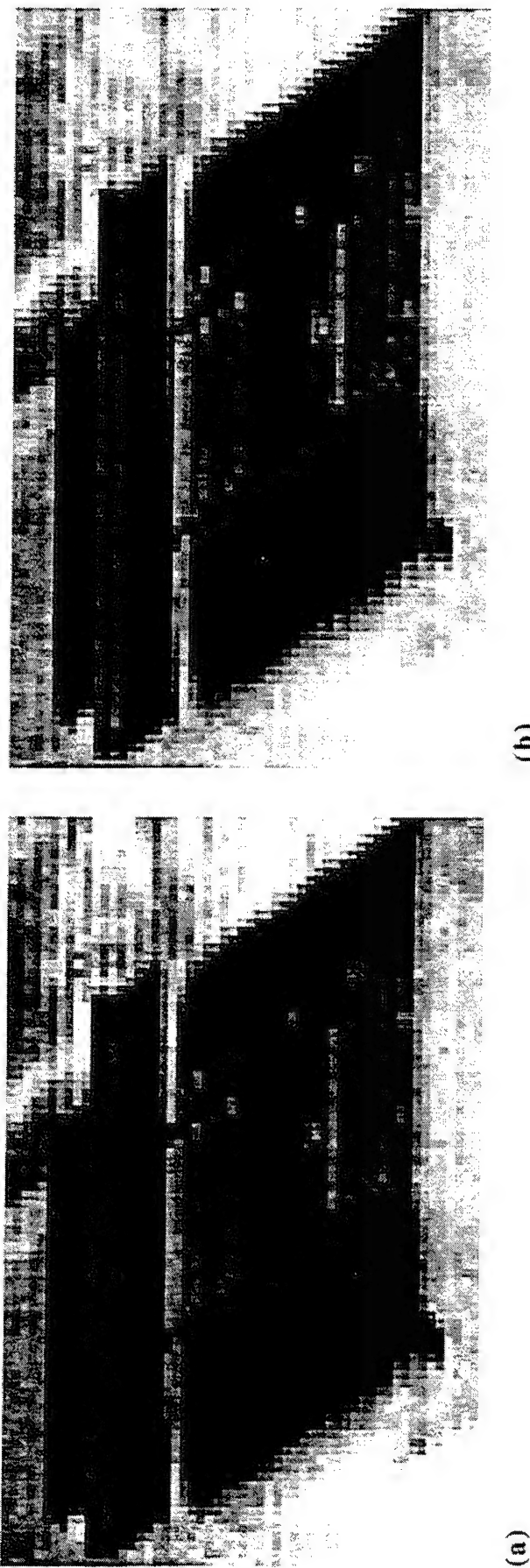
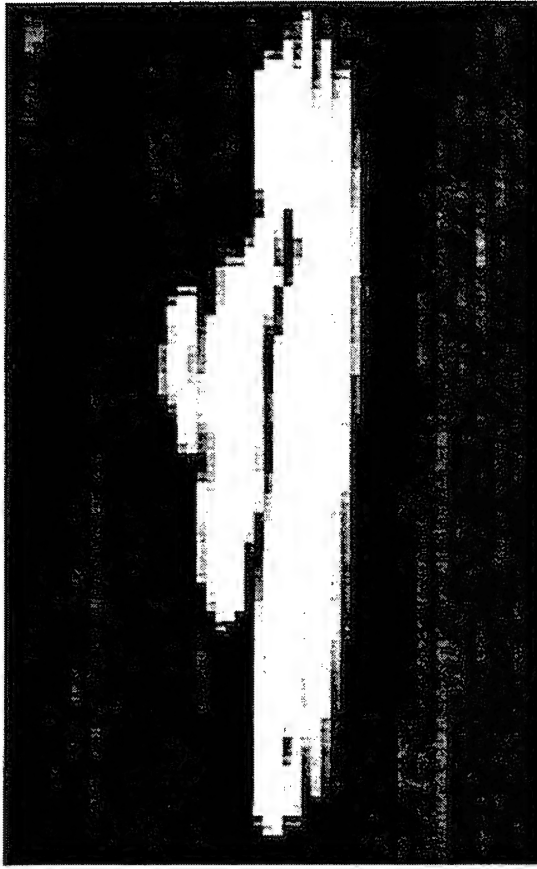
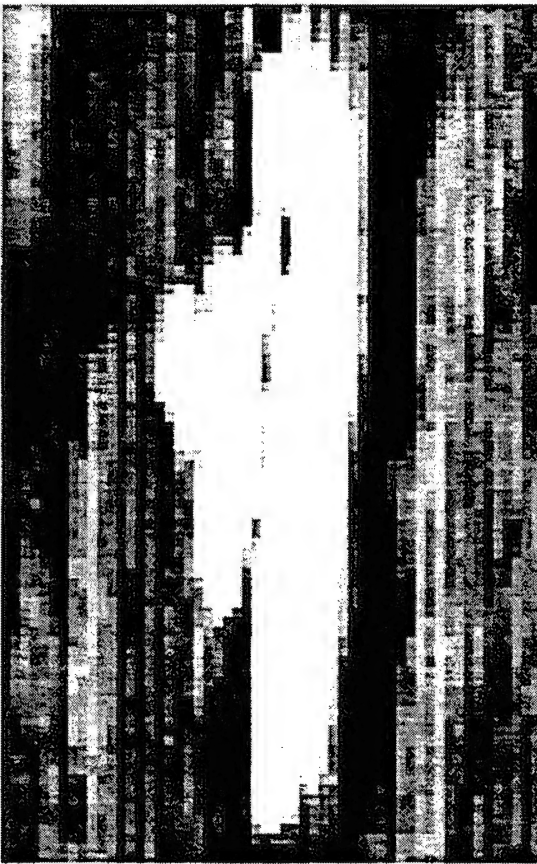


Figure 5-14. Construction of Standard Image for FLIR Truck Images Used in Evaluations 2 through 6 and 9.

The standard image without contrast enhancement (a) and with contrast enhancement (b). Note that evaluation images were actually presented in color on a high-resolution CRT. Also, these printed gray scale images are not gamma-corrected for printing. In addition, their size as printed is not intended to simulate the angular resolutions tested in the evaluations.



(a)



(b)

Figure 5-15. Construction of Standard Image for FLIR Tank Images Used in Evaluations 2 through 6.

The standard image without contrast enhancement (a) and with contrast enhancement (b). Note that evaluation images were actually presented in color on a high-resolution CRT. Also, these printed gray scale images are not gamma-corrected for printing. In addition, their size as printed is not intended to simulate the angular resolutions tested in the evaluations.

5.1.3 Evaluation Design Overview

While detailed descriptions of evaluation designs are provided in subsequent portions of this report, an overview of the ten evaluation designs is provided here to convey the overall scope and direction of the simulation activities. The evaluation designs may be differentiated on the basis of the test procedures, test imagery, subjective rating scales, design variables, and number of trials and participants (Table 5-2, p. 247). In the table, shaded cells in the top half of the table indicate inclusion of that characteristic in the corresponding evaluation. For example, the serial comparison procedure was used in Evaluations 1 through 4. Cells associated with design variables contain either the specific values included in the evaluation or the range of that variable tested with the number of levels tested indicated in parentheses.

Evaluation 1. The first evaluation was conducted to examine the effects of luminance contrast, number of gray scale levels, and gray scale distribution linearity on aliasing and image contrast judgments in the context of anti-aliased symbology presented via a subtractive color image source in a see-through display. The evaluation results address gray scale level asymptotes, relative advantages and disadvantages of nonlinear gray scale distribution, and the impact which luminance contrast reduction, through combination of the AMLCD image with a forward scene, has on each of these.

Evaluation 2. Evaluation 2 was conducted to extend the results of Evaluation 1 to include FLIR imagery.

Evaluation 3. The third evaluation was conducted to extend the results of Evaluation 2 to include a range of subtractive color image source aperture ratios. Image luminance was not allowed to covary with aperture ratio in this evaluation. The evaluation results go beyond those of Evaluations 1 and 2 to address the subjective consequences of subtractive color image source aperture ratio changes both below and above the 70% level tested previously. The evaluation results also provide data for two additional subjective rating dimensions (line visibility and image quality).

Evaluation 4. Evaluation 4 was conducted to replicate the procedure of Evaluation 3 while allowing image luminance to covary with aperture ratio (images with higher aperture ratios had higher luminances).

Evaluation 5. The fifth evaluation was conducted to compare the subjective quality of subtractive and additive color image sources. New to this evaluation was an additive color image source model (40% aperture ratio) as well as two subtractive color image source models which included diffractive pixel broadening of the red layer. The simulation scope was also expanded to include two additional resolutions as well as both red and yellow images. Image luminance was held constant among the various image sources modeled. A new rating scale was added to capture differences in image sharpness associated with the diffraction effects. The evaluation results illustrate the relative subjective value of subtractive and additive image sources in light of resolution, image color, and diffraction effects.

Evaluation 6. Evaluation 6 was a replication of Evaluation 5. Image luminance was allowed to vary among image sources modeled.

Evaluation 7. The seventh evaluation was conducted to extend the results of Evaluation 5 to include Symbol imagery. Binary symbols (no anti-aliasing) were used to examine possible anti-aliasing properties of subtractive color red diffraction. Luminance was held constant among various image sources modeled.

Evaluation 8. Evaluation 8 was a replication of Evaluation 7. Image luminance was allowed to vary among the various image sources modeled.

Evaluation 9. The ninth evaluation was conducted to examine the relative impact of enhancement of the standard FLIR images. While previous FLIR evaluations all used contrast/luminance enhanced standard images, standard images in Evaluation 9 were closely matched in these properties with comparison images while allowing other image source model variables such as aperture ratio to vary (standard images had effective aperture ratios of 100%). The evaluation replicated a portion of the design found in Evaluation 5, while using matched rather than enhanced standard images. The results of the evaluation provide a benchmark for better interpretation of the relative acceptability of images presented in this program.

Evaluation 10. Evaluation 10 was conducted to extend the results of Evaluation 9 to include numeric symbol imagery. The evaluation replicated a portion of the design found in Evaluation 7, while using standard images matched in resolution, luminance, and contrast.

Table 5-2. Summary of Evaluation Designs (Evaluations 1 - 10).

Evaluation Characteristic	Evaluation									
	1	2	3	4	5	6	7	8	9	10
Test Procedures										
Serial Comparison										
Simultaneous Comparison										
Test Imagery										
Symbology										
FLIR (Tank and Truck)										
Subjective Rating Scales										
Aliasing										
Contrast										
Line Visibility										
Image Quality										
Sharpness										
Design Variables										
Background Image	Clouds, blue	Clouds	None	None	None	None	None	None	None	None
Luminance Contrast	1.3-50 (6)	1.3-10 (5)	10:1, 5:1	10:1, 5:1	10:1, 5:1	10:1, 5:1	50:1	50:1	10:1, 5:1	50:1
Gray Scale Levels	4-32 (4)	8-64 (5)	8-64 (5)	8-64 (5)	64	64	2	2	2	2
Gray Scale Distribution	3 tested	3 tested	3 tested	3 tested	Linear	Linear	Linear	Linear	Linear	Linear
Aperture Ratio	70%	70%	40%-80% (5)	5 tested	40% /70%	40% /70%	40% /70%	40% /70%	40% /70%	40% /70%
Color Approach	Subtractive	Subtractive	Subtractive	Subtractive	Subtractive, Additive					
Subtractive Diffraction	No	No	No	No	Yes	Yes	Yes	Yes	Yes	Yes
Image Color	green	green	green	red, yellow	red, yellow	red, yellow	red, yellow	red, yellow	red, yellow	red, yellow
Resolution (pix/deg)	22 pix/deg	22 pix/deg	22 pix/deg	11, 22, 33	11, 22, 33	11, 22, 33	11, 22, 33	11, 22, 33	11, 22, 33	11, 22, 33
Luminance (AR/Color Approach)	n/a	n/a	Equal	Variable	Equal	Variable	Equal	Variable	Equal	Equal
Standard Image	Enhanced	Enhanced	Enhanced	Enhanced	Enhanced	Enhanced	Enhanced	Enhanced	Matched	Matched
Trials and Participants										
Trials per Replicate	72	75	75	75	60	60	60	60	15	15
Replicates	2	2	2	2	2	2	1	1	2	1
Total Trials/Participant	144	150	150	150	120	120	60	60	30	15
Rating Scale Participants	8	8	8	8	8	8	8	8	4	4

5.1.4 General Evaluation Procedure

Twenty-five Honeywell employees participated in the ten simulation evaluations, with eight participants included in each of all but the last two evaluations (most participants took part in more than one evaluation). The age range of participants was approximately 18 to 35 years old. For any given evaluation, 50% to 88% of participants were male.

The vision of all participants was measured for color vision as well as binocular near and far Snellen acuity using a Bausch and Lomb Master Ortho-Rater. All participants had normal color vision. The modal Snellen acuity of participants was 20/18 (far) and 20/20 (near), with one participant scoring as low as 20/25 (Figure 5-16, p. 249).

Participants were seated in front of the CRT at a distance calibrated to yield the desired angular subtense of simulation pixels. The chair was fixed in place and participants were instructed not to shift their position or lean forward. The evaluations were conducted in a darkened room, and all instructions were read aloud to participants as their eyes adapted.

Participants rated screen images on a variety of subjective rating scales (specific rating scales used are presented in detail in subsequent sections associated with each evaluation). A trained observer recorded participant's ratings on response sheets for subsequent analysis. The same observer manually advanced images via a computer mouse. Prior to data collection, participants viewed images which were representative of the evaluation images to be rated and they received instruction on image features to rate. Participants always completed practice ratings and were given the opportunity to ask procedural questions prior to data collection.

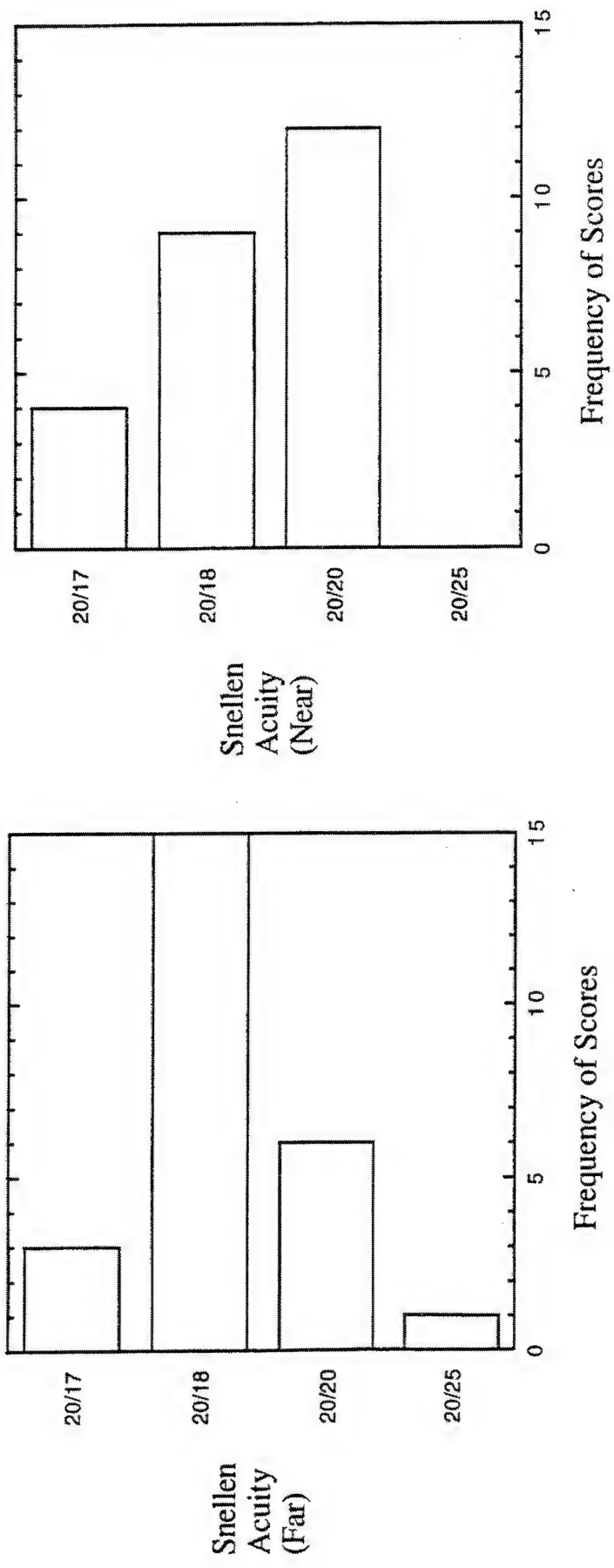


Figure 5-16. Binocular Visual Acuity of Evaluation Participants.

Image ratings were always made relative to the standard image. Comparison images were presented either serially (Figure 5-17) or simultaneously (Figure 5-18). The standard image was always presented in a fixed location. In the simultaneous image procedure, the position of comparison images was randomly assigned among the five screen positions. Practice images in all evaluations were always presented using the simultaneous presentation procedure. Data collection sessions generally lasted between 30 and 60 minutes.

Additional procedural details are provided in the report text associated with each evaluation.

5.1.5 General Analysis Procedure

Analysis of variance (ANOVA) models were developed using SuperAnova analysis software on a Macintosh IIfx computer. Separate ANOVAs were conducted for each dependent variable. All ANOVAs used a completely within-subjects (repeated measures) design. Therefore, ANOVA error terms used were calculated for each effect as the interaction of that effect with Subjects. Data were collapsed on replicates prior to analysis. Where missing observations occurred, mean ratings were calculated using the remaining replicates corresponding to the design cell of the missing observation. Post-hoc analyses were accomplished through simultaneous means contrasts with probability values weighted against the number of comparisons.

Abbreviated ANOVA summary tables are included with the results for each evaluation to provide an overview of the significant data trends. Each table summarizes data from multiple ANOVA models (i.e., multiple dependent variables). ANOVA probability values given are Greenhouse-Geisser values. Values reported in these tables for R^2 were calculated by dividing the sums of squares (SS) for each effect by the total SS for that node. These R^2 values reflect the proportion of variance in the data accounted for by each effect. Values reported for R^2 were calculated by dividing the total SS for all effects in the ANOVA model by the total SS for that model. These R^2 values reflect the proportion of variance in the data accounted for by the sum of all effects in the ANOVA model.

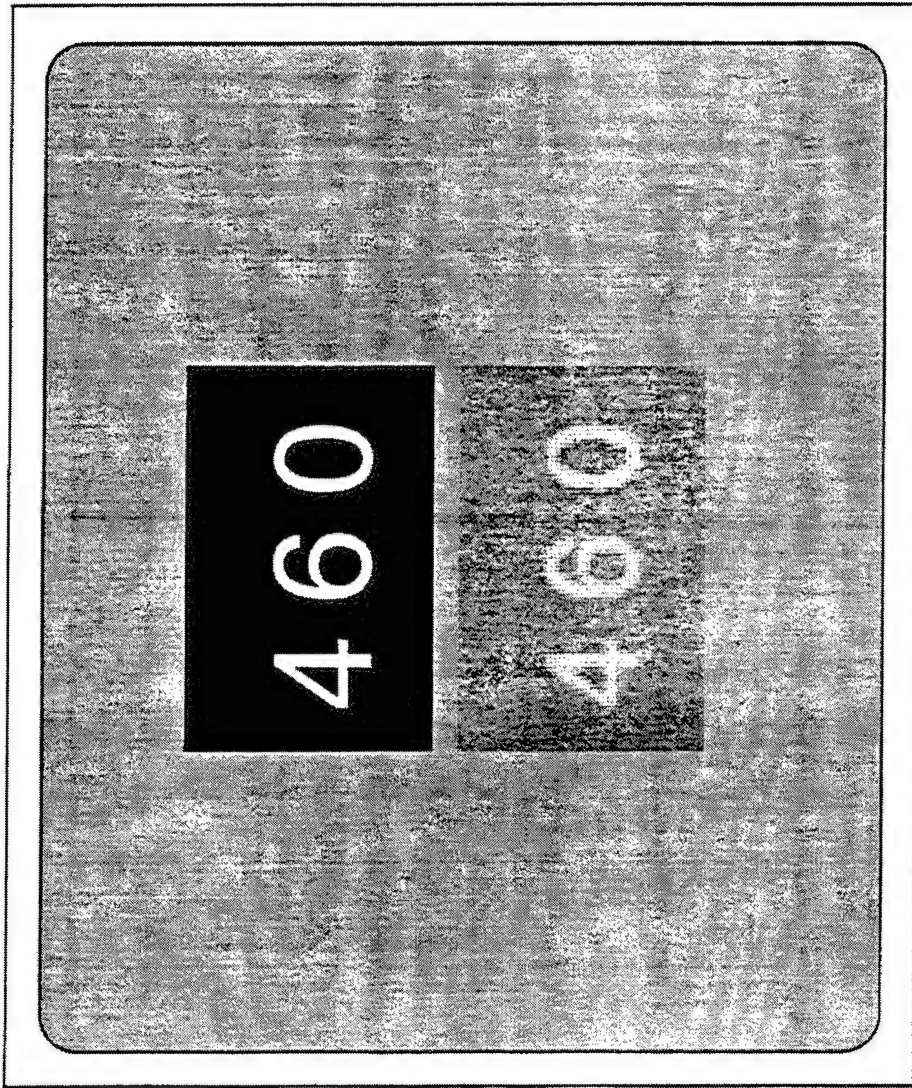


Figure 5-17. Serial Image Comparison Procedure Used in Evaluations 1 through 4.

Simulated AMI-CD images (bottom) were rated relative to high-resolution/high contrast standard images (top). Note that evaluation images were actually presented in color on a high-resolution CRT. Also, these printed gray scale images are not gamma-corrected for printing. In addition, their size as printed is not intended to simulate the angular resolutions tested in the evaluations.

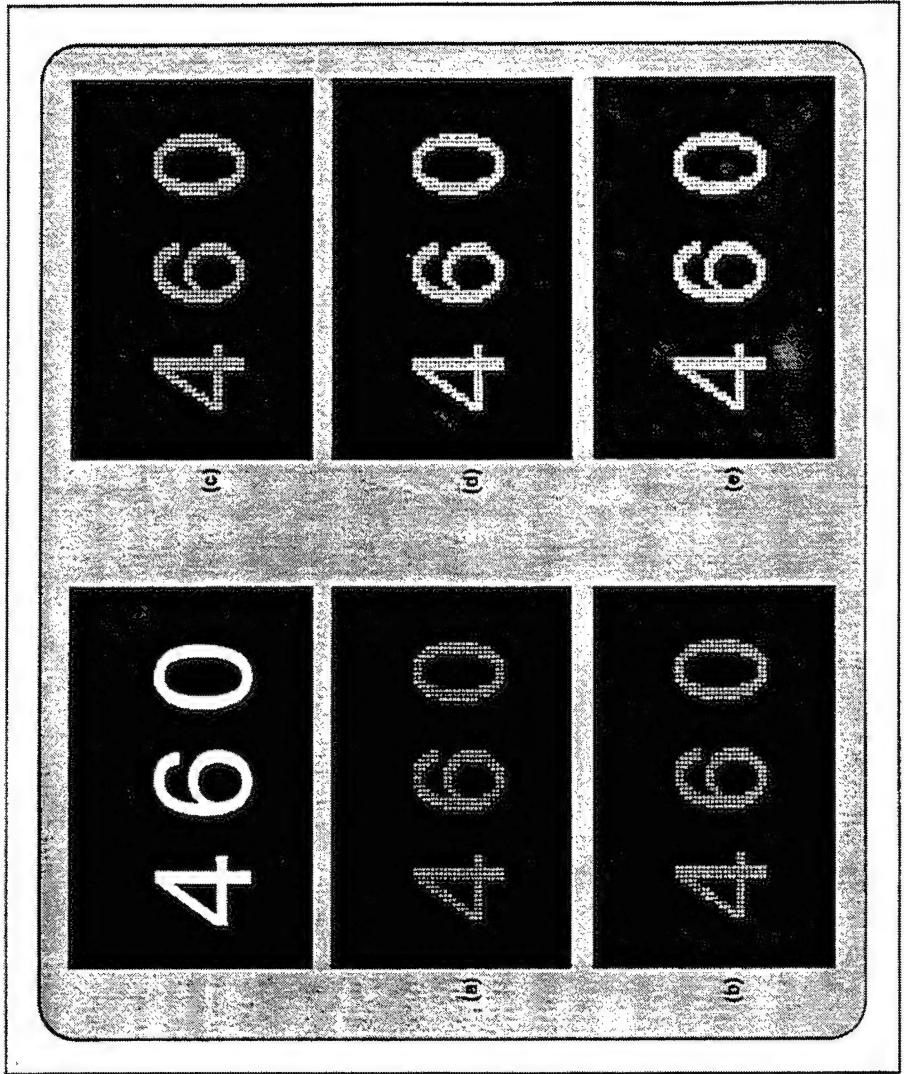


Figure 5-18. Simultaneous Image Comparison Procedure Used in Evaluations 5 Through 10.

Simulated AMLCD images (a - e) were rated relative to high-resolution/high-contrast standard images (upper left). Note that evaluation images were actually presented in color on a high-resolution CRT. Also, these printed gray scale images are not gamma-corrected for printing. In addition, their size as printed is not intended to simulate the angular resolutions tested in the evaluations.

5.2 Evaluation 1

5.2.1 Objectives

Evaluation 1 was conducted to examine the effects of luminance contrast, number of gray scale levels, and gray scale distribution linearity on aliasing and image contrast judgments in the context of anti-aliased symbology presented via a subtractive color image source. The specific objectives of Evaluation 1 were:

1. Assess the relative impact of symbol transparency on perception of image contrast and aliasing using representative background imagery.
2. Document the perceptual consequences of using nonlinear gray scale distribution for symbol anti-aliasing.
3. Confirm the gray scale level asymptote for perception of symbol aliasing.

5.2.2 Design

Evaluation 1 images were modeled using the 70% AR subtractive color image source and the symbol imagery described previously. Images were presented at a resolution of 22 simulated AMLCD pixels per degree. Binary symbols were subjected to an anti-aliasing convolution procedure using varied degrees of gray scale distribution linearity and number of gray scale levels as previously described under *Simulation Software*. Symbols were presented in monochrome green. In addition, a third class of imagery was introduced for Evaluations 1 and 2: background imagery. To assess the impact of image transparency on image contrast and aliasing, net image luminance contrast was varied in Evaluation 1 by blending simulation images with one of two color background images. Background images constituted a full-color segment of blue sky or a segment of cloudy sky, and were extracted from a large (4096 x 3072) 24-bit color image captured from a color photograph via a drum scanner. The two background images were included to represent typical background scenes for daylight flight. Background image was included as a design replicate with no intention of including background image as an analysis variable.

The simulation design levels included in Evaluation 1 are summarized in Table 5-3. For each variable, a figure illustrating the variable is referenced in the table.

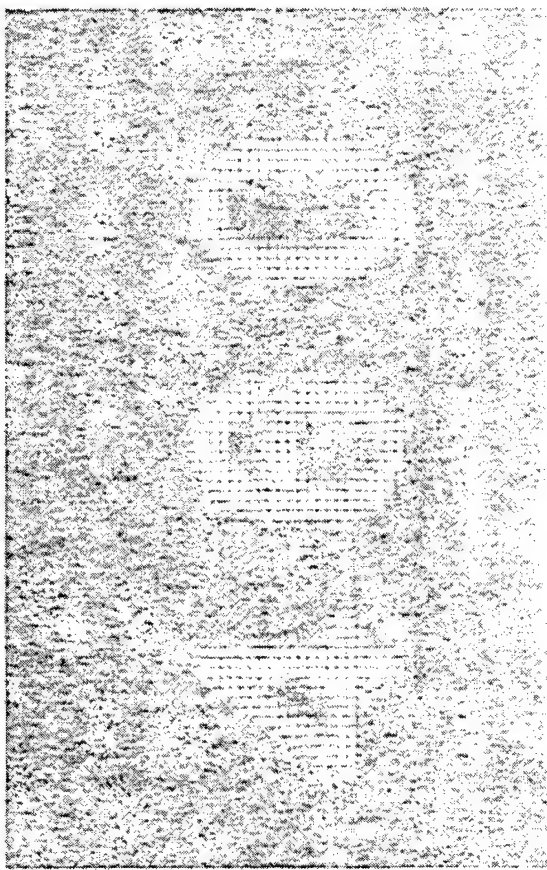
Table 5-3. Design variables for Evaluation 1.

Variable	Levels	Figure	Page
Background Image	Blue Sky, Cloudy Sky	Figure 5-19	255
Luminance Contrast	1.3, 1.5, 2, 3, 10, 50	Figure 5-20	256
Gray Scale Levels	4, 8, 16, 32	Figure 5-21	257
Gray Scale Distribution Exponent	1.0, 0.5, 0.33	Figure 5-22	258

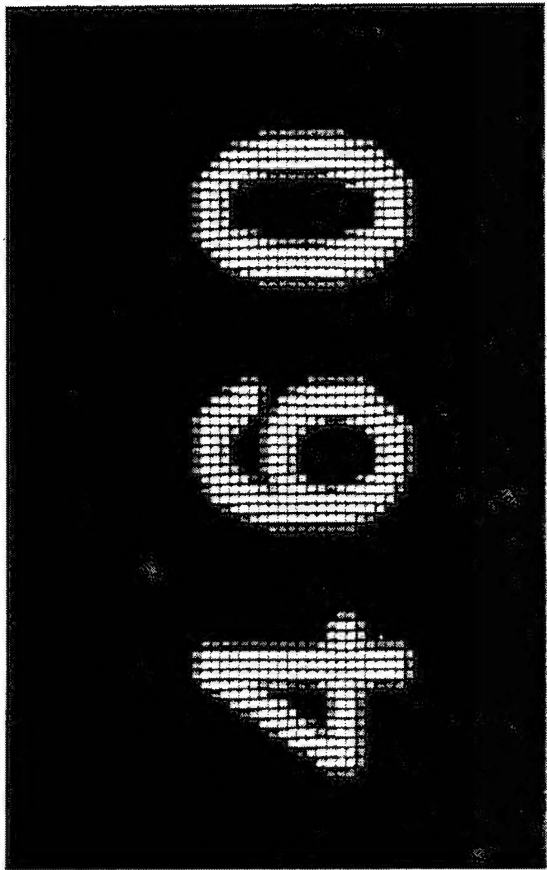


Figure 5-19. Original Image from which Cloud and Blue Sky Backgrounds Were Extracted in Evaluations 1, 2, and 3.

Only small portions of this image were used as background (see Figure 5-20). Note that evaluation images were actually presented in color on a high-resolution CRT. Also, these printed gray scale images are not gamma-corrected for printing.



(a)



(b)

Figure 5-20. Luminance Contrast for Symbol Images in Evaluation 1, Ranging from 1.3 (a) to 50 (b).

This figure shows the "Blue Sky" background in (a). Note that evaluation images were actually presented in color on a high-resolution CRT. Also, these printed gray scale images are not gamma-corrected for printing. In addition, their size as printed is not intended to simulate the angular resolutions tested in the evaluations.

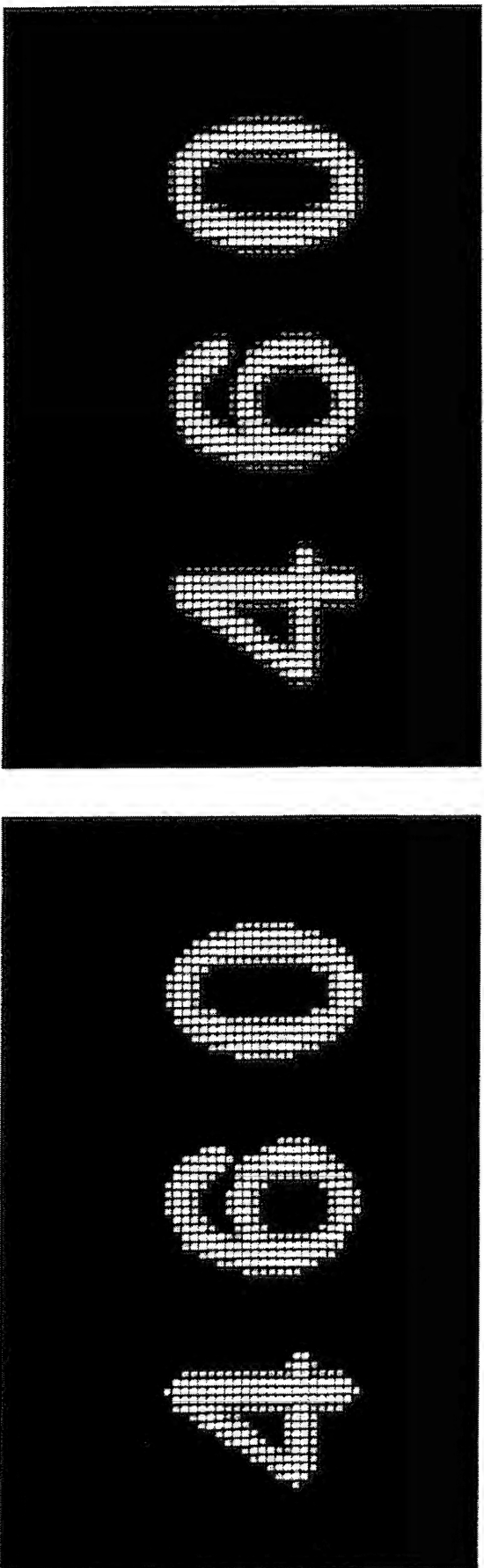
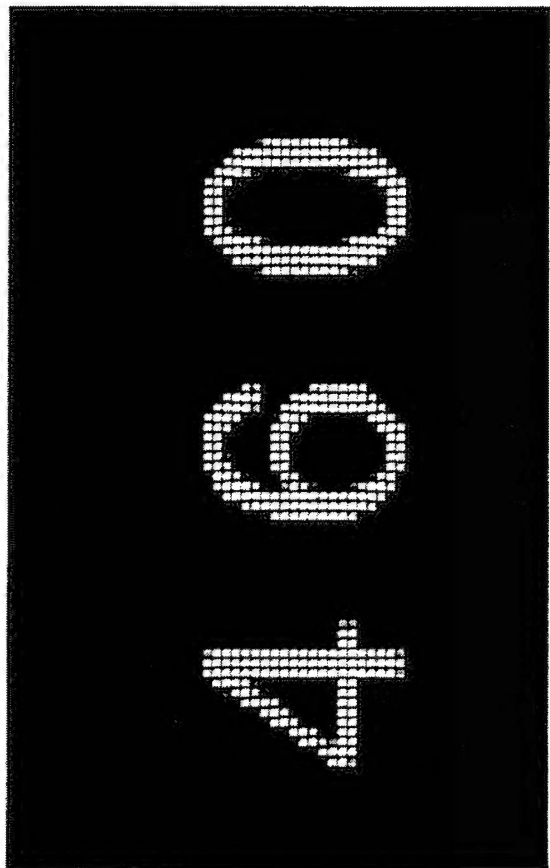
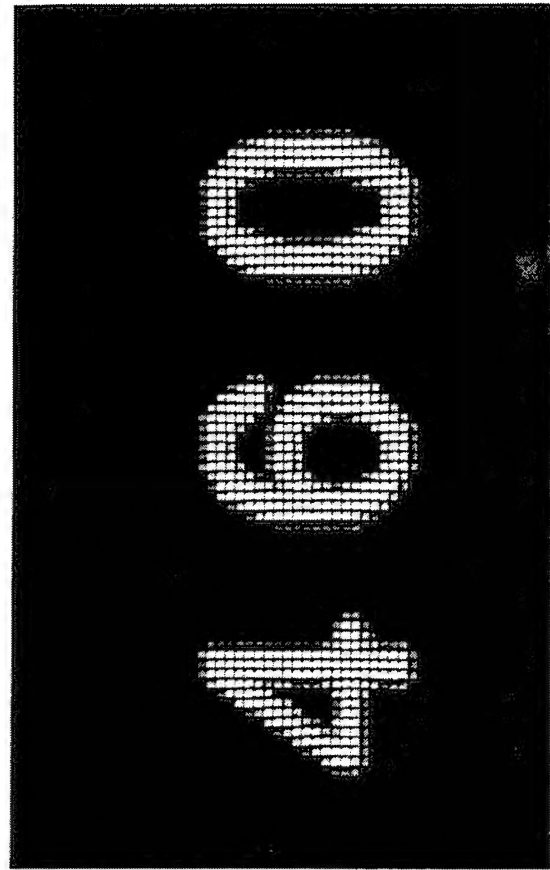


Figure 5-21. Gray Scale Levels for Symbol Images in Evaluation 1, Ranging from 4 levels (a) to 32 levels (b).

Note that evaluation images were actually presented in color on a high-resolution CRT. Also, these printed gray scale images are not gamma-corrected for printing. In addition, their size as printed is not intended to simulate the angular resolutions tested in the evaluations.



(a)



(b)

Figure 5-22. Gray Scale Distribution Exponents for Symbol Images in Evaluation 1, Ranging from 0.3 (a) to 1.0 (b).

Note that evaluation images were actually presented in color on a high-resolution CRT. Also, these printed gray scale images are not gamma-corrected for printing. In addition, their size as printed is not intended to simulate the angular resolutions tested in the evaluations.

5.2.3 Procedure

Two subjective rating scales were used to evaluate imagery in Evaluation 1 (Figure 5-23, p. 260). The contrast scale was used to capture subjective contrast of images as image transparency (net contrast) was varied. The aliasing scale was used to measure the visibility of image artifacts associated with reduced image quality. For each evaluation trial, a separate rating was made on each scale. Participants were instructed to make their image ratings relative to the standard image. Eight participants followed the general evaluation procedure described previously, using the serial comparison procedure and rating 8 practice images and 144 evaluation trials during a 60 minute period. The order of image presentation was completely randomized for each observer.

Contrast (Evaluations 1 and 2):

The degree to which foreground (numbers or FLIR target) stands out from the background in the comparison image relative to the standard image.

10%	Foreground is virtually indistinct from the background
20%	
30%	
40%	
50%	Foreground stands out half as much as in the standard image
60%	
70%	
80%	
90%	
100%	Foreground stands out the same as in the standard image

Aliasing (Evaluations 1 and 2):

The smoothness of number edges (or FLIR image) in the comparison image relative to the standard image.

10%	Number edges are (or FLIR image is) about as jagged as I can imagine
20%	
30%	
40%	
50%	Numbers are (or FLIR image is) about half as smooth as in the standard image
60%	
70%	
80%	
90%	
100%	Numbers are (or FLIR image is) as smooth as in the standard image

Figure 5-23. Contrast and Aliasing Rating Scales Used in Evaluations 1 and 2.

5.2.4 Results

Data were collapsed on replicates (background image) prior to analysis. Table 5-4 provides an overview of the significant data trends. The effects summarized in the table are discussed in the text following the table.

Table 5-4. ANOVA summary table for Evaluation 1.

Effect	Dependent Variable	Image	Figure	Page	df	MS	F	p	R ²
Luminance Contrast	Contrast	Symbols	Figure 5-24	264	5,35	58058.194	124.89	<.0001	.86
	Aliasing	Symbols	Figure 5-25	265	5,35	4100.411	10.21	.0027	.12
Gray Scale Levels	Aliasing	Symbols	Figure 5-26	266	3,21	3682.770	28.69	<.0001	.06
Luminance Contrast x Gray Scale Distribution	Aliasing	Symbols	Figure 5-27	267	10,70	262.932	4.32	.0097	.01

Luminance Contrast. Symbol contrast ratings increased monotonically as a function of increasing symbol luminance contrast (Figure 5-24), with each increase in luminance contrast associated with a significant increase in contrast rating ($p < .05$).

Conversely, symbol aliasing ratings decreased (i.e., aliasing was more apparent) with increased luminance contrast (Figure 5-25), although not all consecutive increases in contrast produced significant decreases in aliasing ratings at the $p < .05$ level. Most notably, there was no reliable difference between aliasing ratings given at the CR 10 and CR 50 levels.

Gray Scale Levels. Symbol aliasing ratings were significantly higher (i.e., aliasing was less apparent) when symbols were presented with 8 or more anti-aliasing gray scale levels (Figure 5-26). There were no differences among aliasing ratings for images presented with 8, 16, and 32 gray scale levels.

Luminance Contrast x Gray Scale Distribution Interaction. Symbol aliasing ratings varied as an interaction of luminance contrast and gray scale distribution exponent (Figure 5-27). Specifically, while aliasing ratings were generally superior for images presented with either of the two nonlinear gray scale distribution exponents, the nonlinear gray scale distribution advantage was not demonstrated at CR values of 1.3 and 1.5, where image aliasing ratings were not significantly different ($p>.05$).

5.2.5 Summary

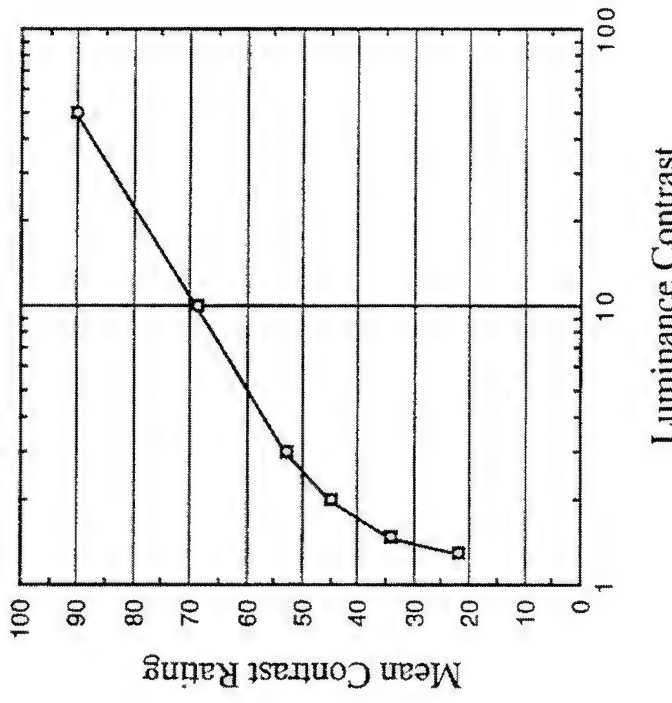
The results from Evaluation 1 are summarized in Table 5-5 and the following summary statements:

Table 5-5. Preliminary conclusions based on Evaluation 1 results.

Variable	Image Type	Rating Asymptote	Notes
Luminance Contrast	Symbols	>50:1	Increased aliasing visibility at up to 10:1
Gray Scale Levels	Symbols	8 Levels of Gray	Gray scale anti-aliasing of binary symbols
Gray Scale Distribution	Symbols	Nonlinear	Distribution exponent of 0.5 to 0.33

1. Subjective image contrast was expected to and did increase monotonically with increases in luminance contrast. These data confirm that the luminance contrast manipulation produced the anticipated direction and magnitude of changes in subjective image contrast. They also indicate that changes in luminance contrast will be visible to levels at least as high as 50:1. The increased prominence of symbol aliasing with increased luminance contrast documents one of the image quality tradeoffs inherent in presenting low-resolution symbols with high luminance contrast.
2. The identification of 8 gray scale levels as an asymptote for symbol anti-aliasing benefit is consistent with prior Honeywell simulation programs addressing similar imagery.
3. Neither gray scale levels nor gray scale distribution affected ratings of image contrast. While the gray scale distribution exponent might reasonably be expected to impact contrast ratings of video imagery, such an effect would seem unlikely for binary symbols where the gray scale component is limited to anti-aliased edges.

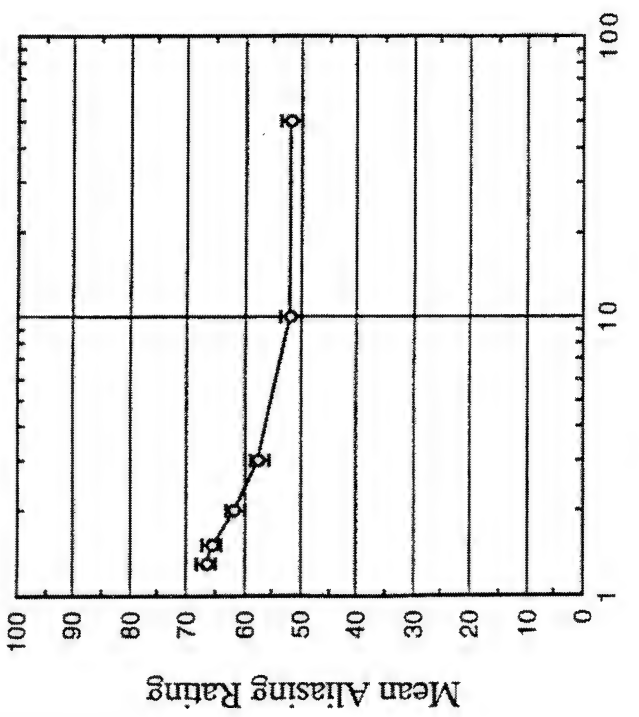
4. The importance of the interaction of gray scale distribution and luminance contrast in subjective aliasing lies less in the interaction, which simply corroborates the diminishing visibility of aliasing (and the symbols themselves) at low contrasts, and more in the relative advantage of the nonlinear gray scale anti-aliasing.



Luminance Contrast	Mean Rating	Standard Error
1.3	21.979	0.809
1.5	34.167	0.924
2.0	45.052	0.899
3.0	52.812	0.930
10.0	68.854	1.124
50.0	90.365	0.845

Figure 5-24. Mean Contrast Rating as a Function of Luminance Contrast (Evaluation 1, Symbols).

High contrast ratings indicate high subjective similarity of comparison images to the standard image (i.e., high brightness contrast). Error bars show standard error of the mean.



Luminance Contrast	Mean Rating	Standard Error
1.3	66.510	1.487
1.5	65.625	1.485
2.0	61.531	1.558
3.0	57.448	1.634
10.0	51.771	1.908
50.0	51.771	1.974

Figure 5-25. Mean Aliasing Rating as a Function of Luminance Contrast (Evaluation 1, Symbols).

High aliasing ratings indicate high subjective similarity of comparison images to the standard image (i.e., relatively little visible aliasing). Error bars show standard error of the mean.

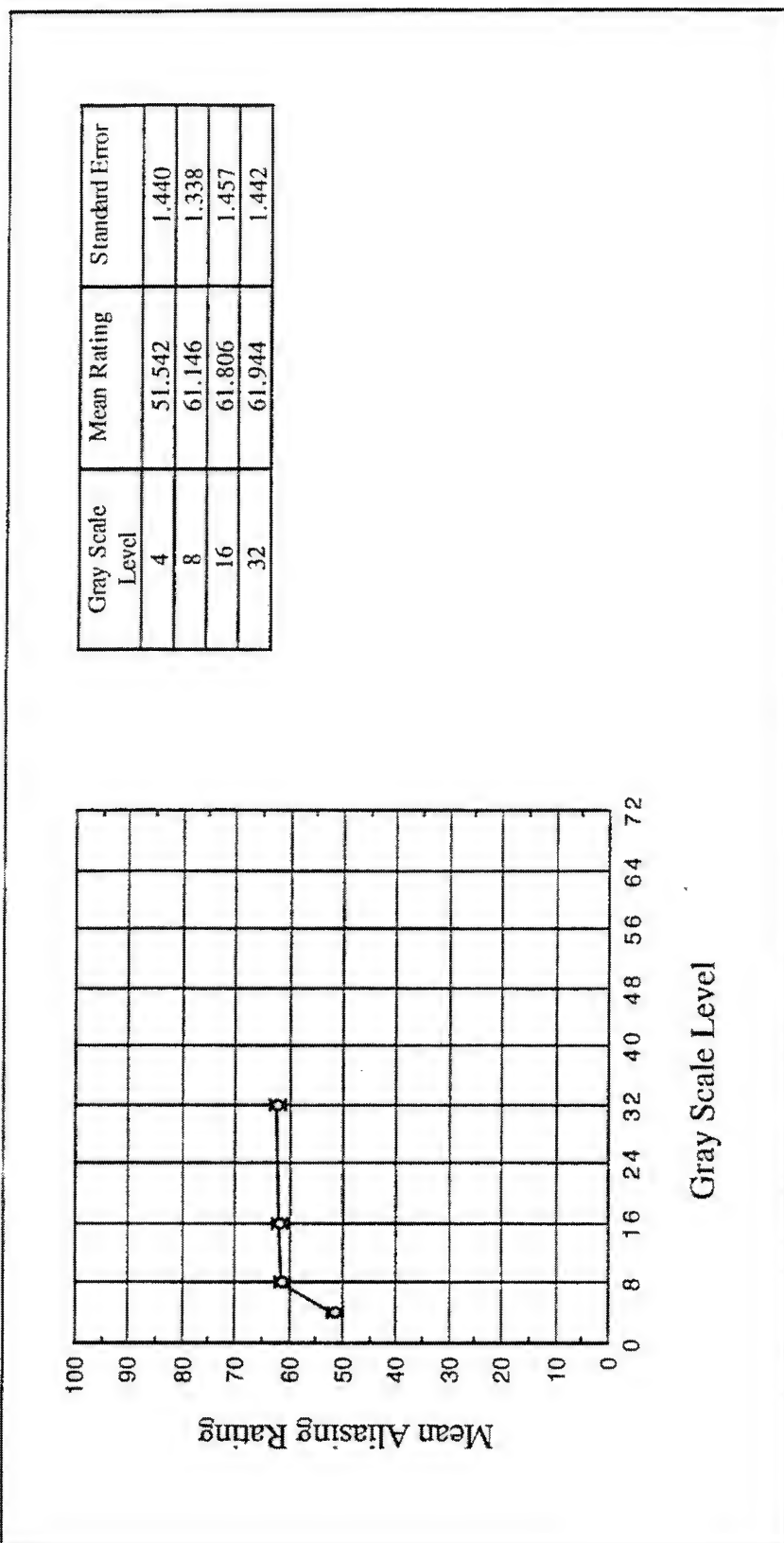


Figure 5-26. Mean Aliasing Rating as a Function of Gray Scale Level (Evaluation 1, Symbols).

High aliasing ratings indicate high subjective similarity of comparison images to the standard image (i.e., relatively little visible aliasing). Error bars show standard error of the mean.

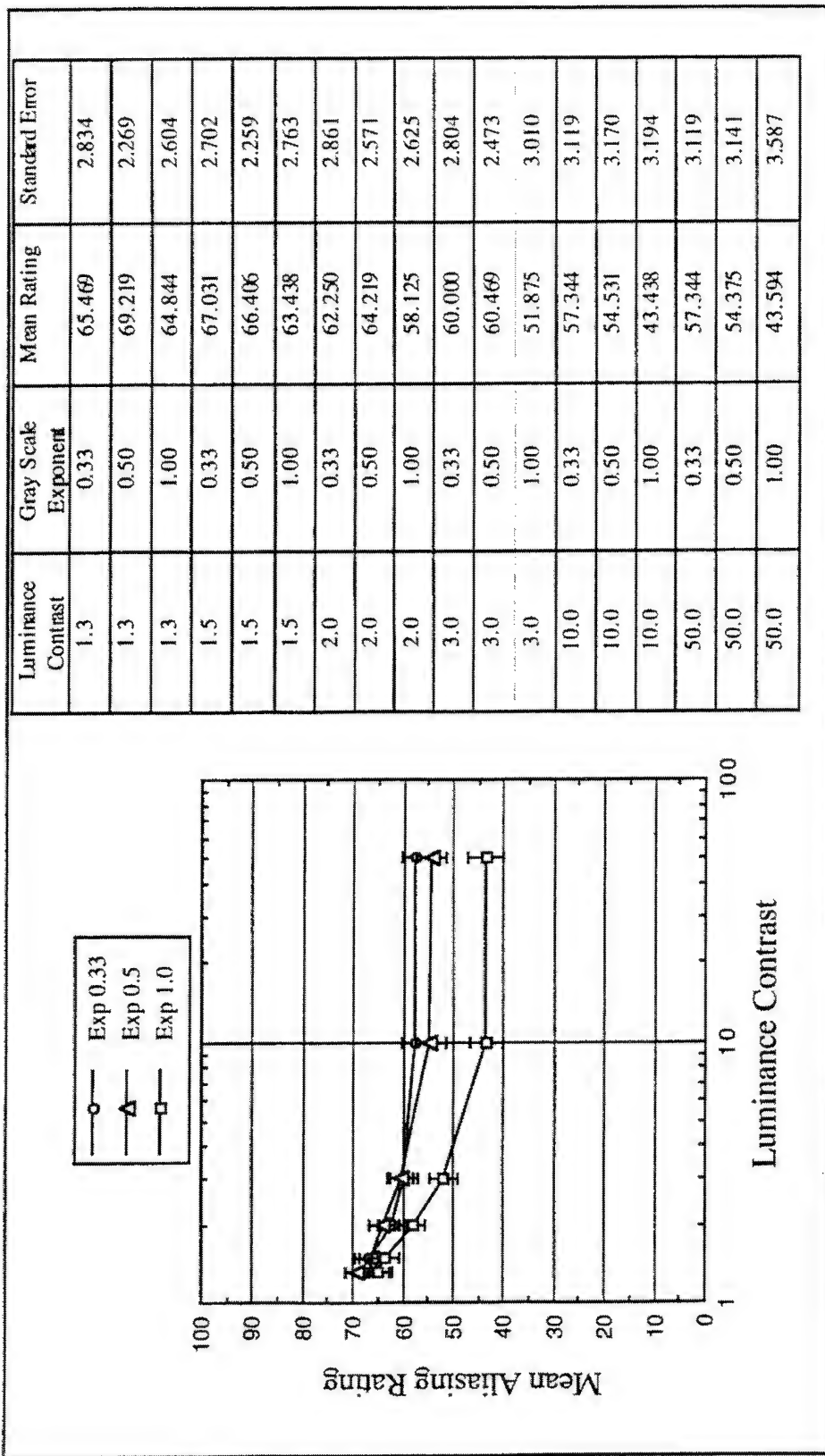


Figure 5-27. Mean Aliasing Rating as a Function of Luminance Contrast by Gray Scale Exponent (Evaluation 1, Symbols).

High aliasing ratings indicate high subjective similarity of comparison images to the standard image (i.e., relatively little visible aliasing). Error bars show standard error of the mean.

5.3 Evaluation 2

5.3.1 Objectives

Evaluation 2 was conducted to extend the results of Evaluation 1 to include FLIR imagery; That is, to examine the effects of luminance contrast, number of gray scale levels, and gray scale distribution linearity on aliasing and image contrast judgments in the context of FLIR imagery presented via a subtractive color image source. The specific objectives of Evaluation 2 were:

1. Assess the relative impact of FLIR transparency on the perception of image contrast and aliasing using representative background imagery.
2. Document the perceptual consequences of using nonlinear gray scale distribution for FLIR imagery.
3. Determine the gray scale level asymptote for perception of FLIR aliasing.

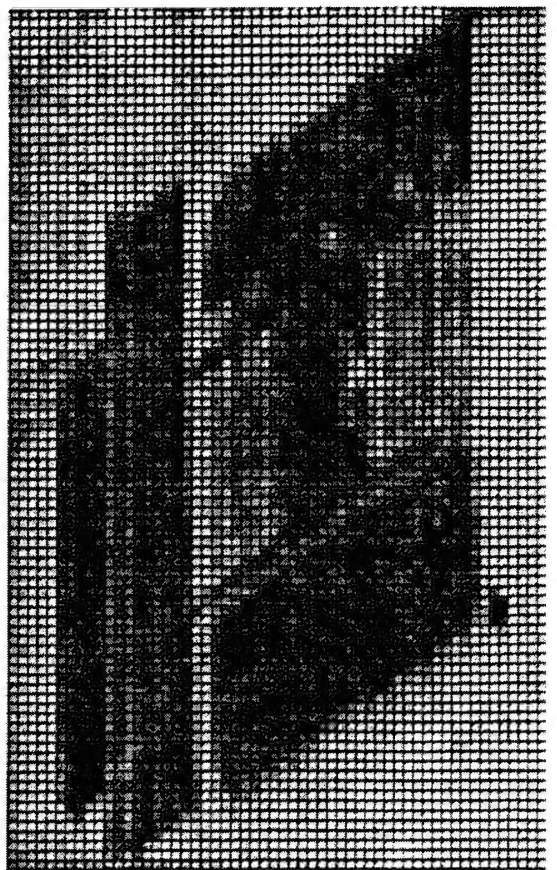
5.3.2 Design

Evaluation 2 images were modeled using the 70% AR subtractive color image source and the two original FLIR images described previously. Images were presented at a resolution of 22 simulated AMLCD pixels per degree. FLIR images were subjected to gray scale level clipping and distribution as previously described under *Simulation Software*. FLIR images were presented in monochrome green. In addition, the "Cloudy Sky" background image was used for luminance contrast reduction blending as previously described in Evaluation 1. The "Blue Sky" image was excluded from Evaluation 2 because it was not meaningful to present ground target imagery against a blue sky (however, cloud cover could easily be interposed between the aircraft and the ground and therefore the "Cloudy Sky" background was included). It was not possible to test the contrast variable as high as 50:1 (as per Evaluation 1) due to the limited contrast of the original FLIR images.

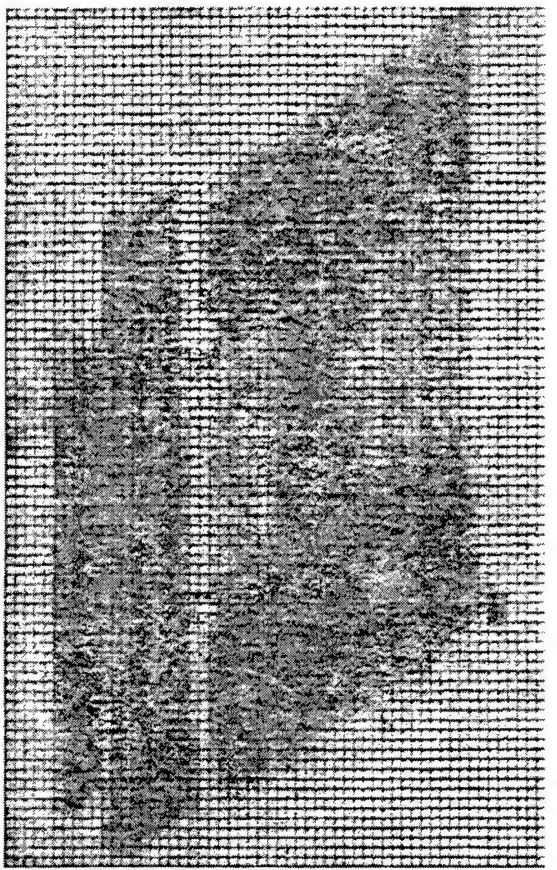
The simulation design levels included in Evaluation 2 are summarized in Table 5-6. For each variable, a figure illustrating the variable is referenced in the table.

Table 5-6. Design variables for Evaluation 2.

Variable	Levels	Figure	Page
Background Image	Cloudy Sky	(see <i>Evaluation 1</i>)	Figure 5-19 (p. 255)
FLIR Image	Truck, Tank	(see <i>Software Imagery</i>)	Figure 5-11 (p. 240)
Luminance Contrast	1.3, 1.5, 2, 3, 5/10	Figure 5-28, Figure 5-29	270
Gray Scale Levels	8, 16, 24, 32, 64	Figure 5-30, Figure 5-31	272
Gray Scale Distribution Exponent	1.0, 0.5, 0.33	Figure 5-32, Figure 5-33	274



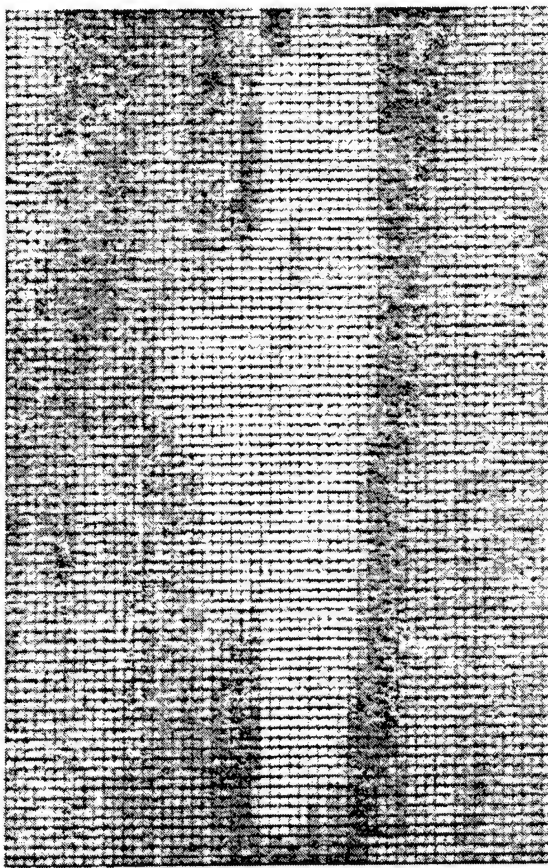
(a)



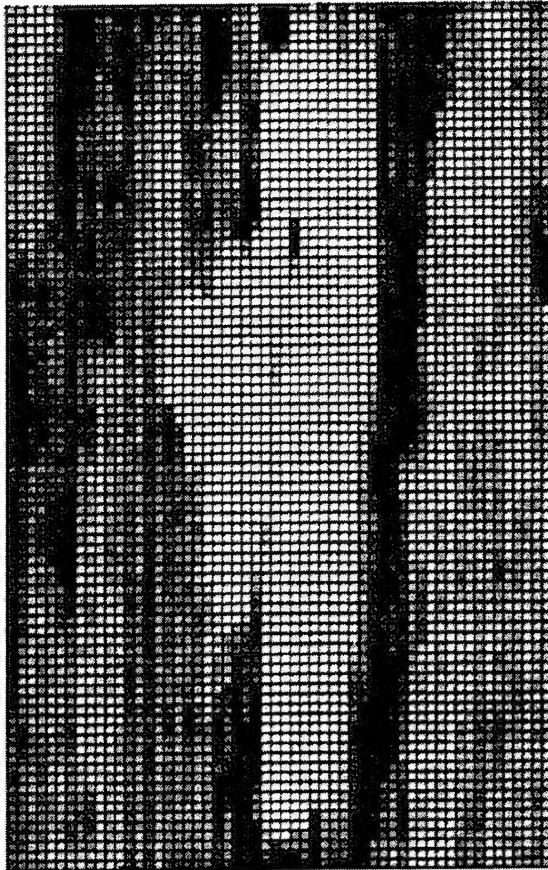
(b)

Figure 5-28 Luminance Contrast for FLIR Truck Images in Evaluation 2, Ranging from 1.3 (a) to 10 (b).

Note that evaluation images were actually presented in color on a high-resolution CRT. Also, these printed gray scale images are not gamma-corrected for printing. In addition, their size as printed is not intended to simulate the angular resolutions tested in the evaluations.



(a)



(b)

Figure 5-29. Luminance Contrast for FLIR Tank Images in Evaluation 2, Ranging from 1.3 (a) to 5 (b).

Note that evaluation images were actually presented in color on a high-resolution CRT. Also, these printed gray scale images are not gamma-corrected for printing. In addition, their size as printed is not intended to simulate the angular resolutions tested in the evaluations.

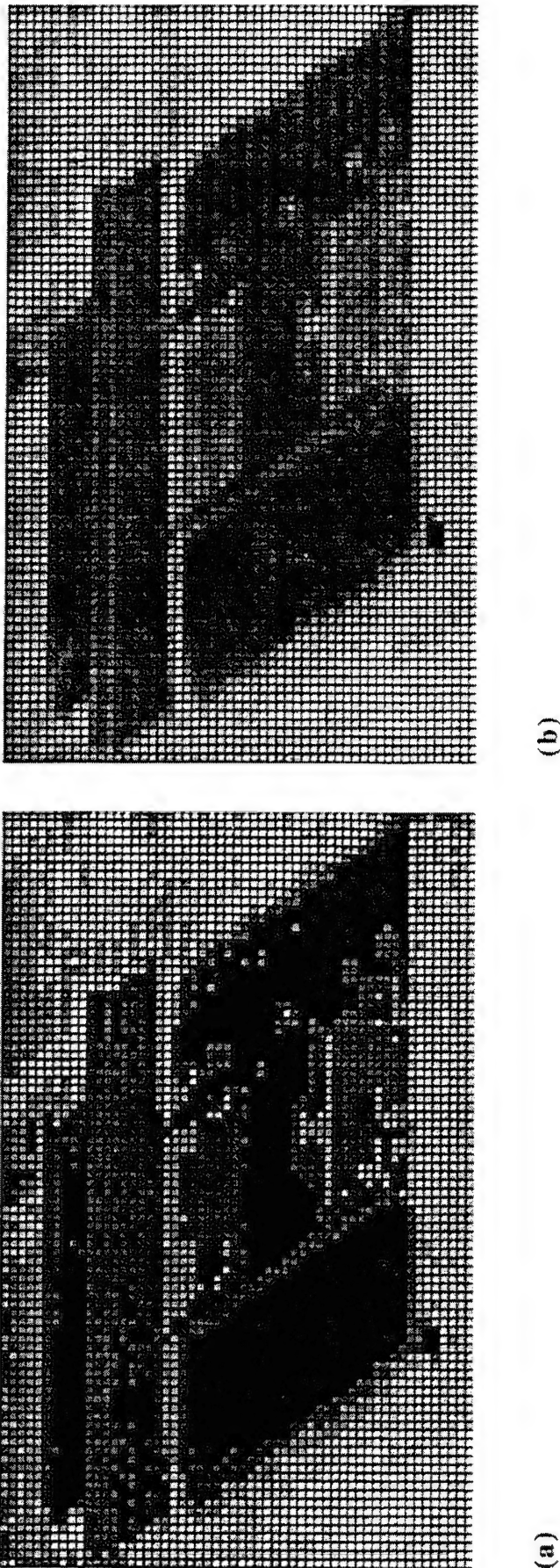


Figure 5-30. Gray Scale Levels for FLIR Truck Images in Evaluations 2, 3, and 4, Ranging from 8 (a) to 64 Levels (b).

Note that evaluation images were actually presented in color on a high-resolution CRT. Also, these printed gray scale images are not gamma-corrected for printing. In addition, their size as printed is not intended to simulate the angular resolutions tested in the evaluations.

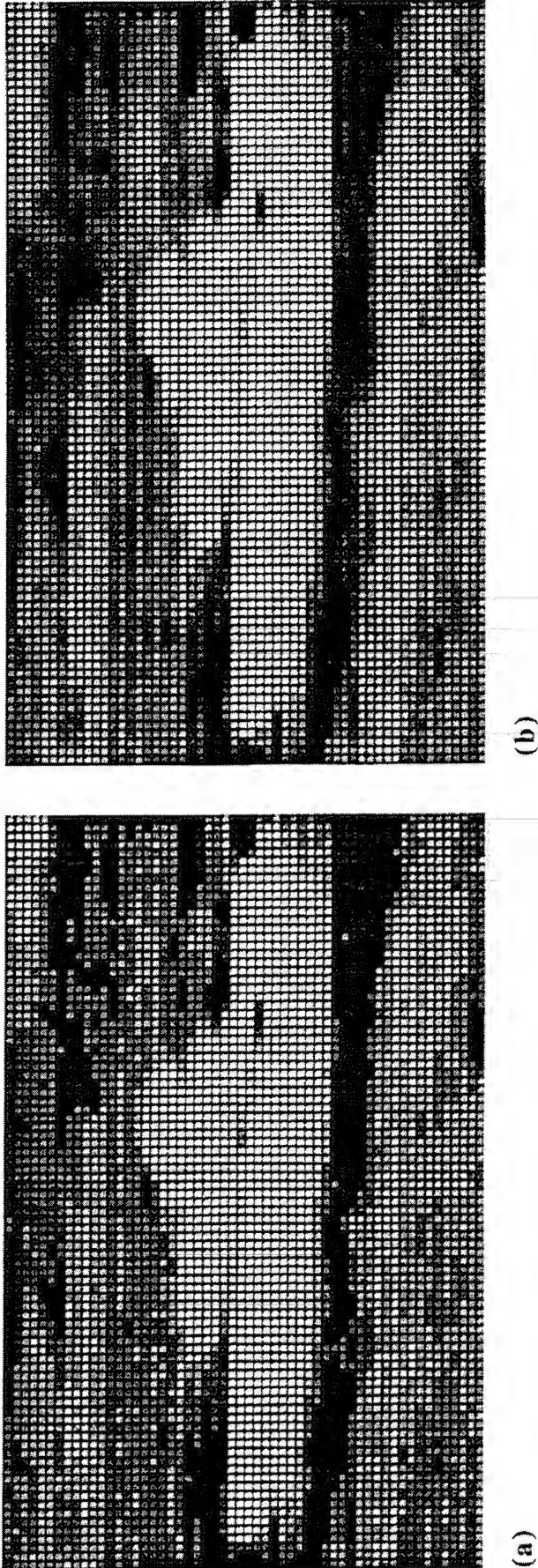
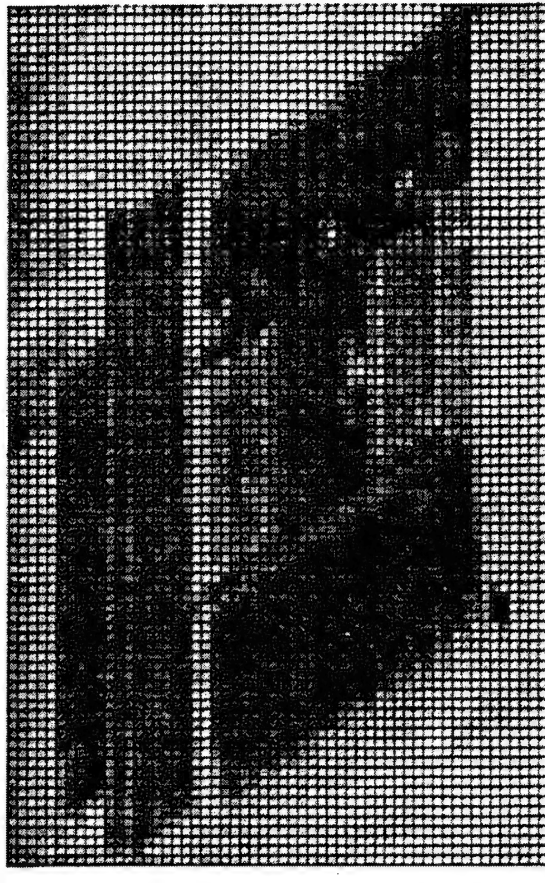


Figure 5-31. Gray Scale Levels for FLIR Tank Images in Evaluations 2, 3, and 4, Ranging from 8 (a) to 64 Levels (b).

Note that evaluation images were actually presented in color on a high-resolution CRT. Also, these printed gray scale images are not gamma-corrected for printing. In addition, their size as printed is not intended to simulate the angular resolutions tested in the evaluations.



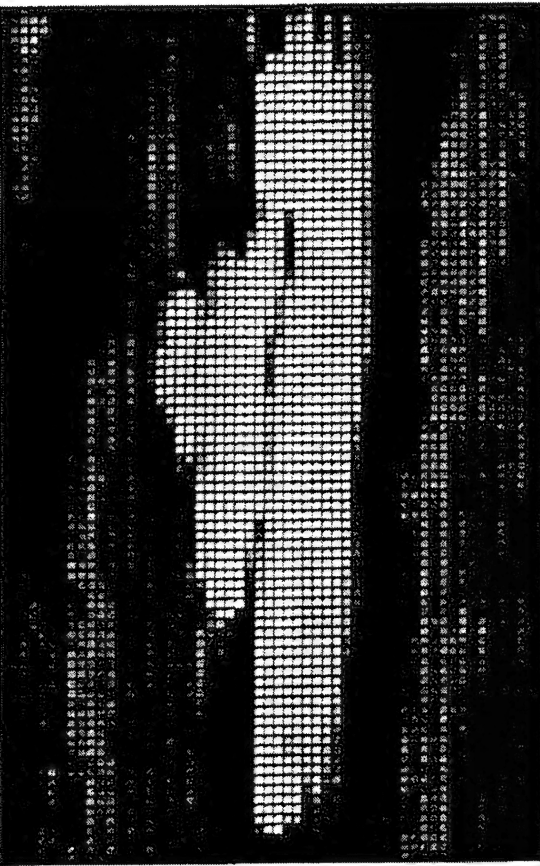
(b)



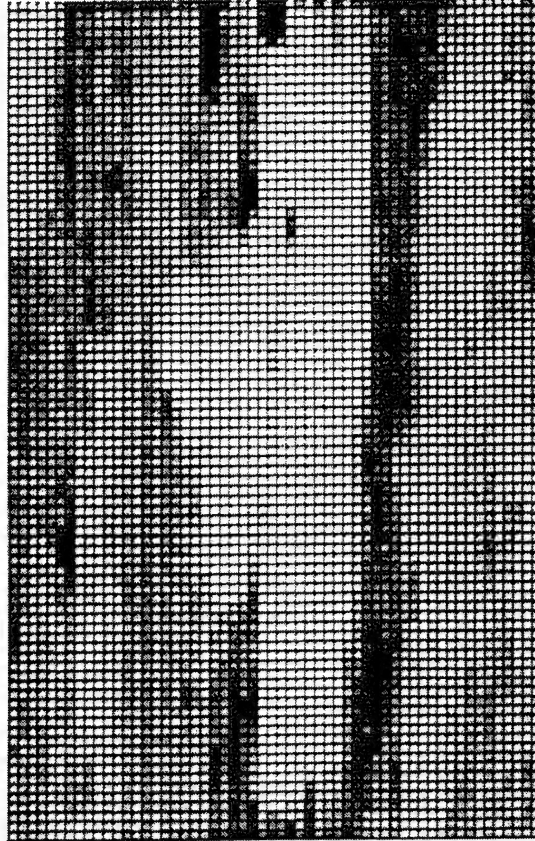
(a)

Figure 5-32. Gray Scale Distribution Exponents for FLIR Truck Images in Evaluations 2, 3, and 4, Ranging from 0.3 (a) to 1.0 (b).

Note that evaluation images were actually presented in color on a high-resolution CRT. Also, these printed gray scale images are not gamma-corrected for printing. In addition, their size as printed is not intended to simulate the angular resolutions tested in the evaluations.



(a)



(b)

Figure 5-33. Gray Scale Distribution Exponents for FLIR Tank Images in Evaluations 2, 3, and 4, Ranging from 0.3 (a) to 1.0 (b).

Note that evaluation images were actually presented in color on a high-resolution CRT. Also, these printed gray scale images are not gamma-corrected for printing. In addition, their size as printed is not intended to simulate the angular resolutions tested in the evaluations.

5.3.3 Procedure

The same two subjective rating scales used in Evaluation 1 (contrast and aliasing) were used to evaluate imagery in Evaluation 2. For each evaluation trial, a separate rating was made on each scale. Participants were instructed to make their image ratings relative to the standard image. Eight participants followed the general evaluation procedure described previously, using the serial comparison procedure and rating eight practice images and 150 evaluation trials during a 60 minute period. The order of image presentation was randomized within blocks of FLIR image (Truck or Tank) for each observer. The order of block presentation was counterbalanced, with 50% of participants rating Tank images first.

5.3.4 Results

Table 5-7 provides an overview of the significant data trends. Separate ANOVA procedures were run for the types of FLIR images. The effects summarized in the table are discussed in the text following the table.

Table 5-7. ANOVA summary table for Evaluation 2.

Effect	Dependent Variable	Image	Figure	Page	df	MS	F	p	R^2
Luminance Contrast	Contrast	Truck	Figure 5-34	281	4, 28	51103.917	47.81	<.0001	.65
	Contrast	Tank	Figure 5-35	282	4, 28	33769.000	29.90	<.0001	.47
Gray Scale Levels	Aliasing	Truck	Figure 5-36	283	4, 28	9273.917	23.41	.0002	.08
	Aliasing	Tank	Figure 5-37	284	4, 28	2038.083	6.92	.0045	.02
Gray Scale Distribution	Contrast	Truck	Figure 5-38	285	2, 14	3792.667	40.84	<.0001	.02
	Contrast	Tank	Figure 5-39	286	2, 14	2486.167	20.84	.0005	.01
Luminance Contrast x Gray Scale Distribution	Contrast	Truck	Figure 5-40	287	8, 56	419.542	4.69	.0121	.01
Luminance Contrast x Gray Scale Levels	Aliasing	Truck	Figure 5-41	288	8, 56	1248.917	3.37	.0418	.02
	Aliasing	Tank	Figure 5-42	289	16, 112	1199.646	8.22	<.0001	.04
Gray Scale Levels x Gray Scale Distribution	Aliasing	Truck	Figure 5-43	290	8, 56	722.042	5.31	.0027	.01
	Aliasing	Tank							.22

Luminance Contrast. FLIR contrast ratings increased monotonically as a function of increasing luminance contrast (Figure 5-34 and Figure 5-35), with each increase in luminance contrast above CR 1.5 associated with a significant increase in contrast ratings ($p < .05$).

Gray Scale Levels. FLIR aliasing ratings were significantly higher (i.e., aliasing was less apparent) when FLIR Truck images were presented with 24 or more gray scale levels (Figure 5-36) and when FLIR Tank images were presented with 16 or more gray scale levels (Figure 5-37).

Gray Scale Distribution. FLIR contrast ratings increased significantly as the gray scale distribution exponent for the Truck image became more linear (Figure 5-38). Conversely, the FLIR Tank image received higher contrast ratings with either of the nonlinear gray scale distribution exponents (Figure 5-39).

Luminance Contrast x Gray Scale Distribution Interaction. FLIR Truck contrast ratings varied as an interaction of luminance contrast and gray scale distribution exponent (Figure 5-40). Specifically, while contrast ratings were generally highest for the Truck image when presented with linear grayscale, at the highest luminance contrast level (CR 10) the mostly highly rated images were those presented with a nonlinear (0.5) gray scale distribution.

FLIR Truck aliasing ratings also varied as an interaction of luminance contrast and gray scale distribution exponent (Figure 5-41). Truck images presented with linear gray scale were rated more favorably than those with nonlinear gray scale at lower contrast levels ($CR \leq 2.0$, $p < .05$). However, at contrast levels of 3.0, images presented with linear gray scale were rated no differently than those presented with gray scale distribution exponents of 0.5, and at the highest contrast level the linear gray scale presentation was rated as having more visible aliasing than either nonlinear presentation ($p < .05$).

Luminance Contrast x Gray Scale Levels Interaction. FLIR Truck aliasing ratings varied as an interaction of luminance contrast and number of gray scale levels (Figure 5-42). Aliasing ratings for the Truck image showed no increase with increasing gray scale levels at luminance contrast levels of CR 1.5 and 1.3, while the gray scale asymptote was 16 levels for CR 2, 24 levels for CR 3, and 32 levels for CR 10 ($p < .05$).

Gray Scale Levels x Gray Scale Distribution Interaction. FLIR aliasing ratings for the Truck image varied as an interaction of gray scale distribution and number of gray scale levels (Figure 5-43). While aliasing ratings were generally highest for linear gray scale presentations, images presented with either of the two nonlinear gray scale distributions received the highest aliasing ratings at gray scale levels of 8 or 16 ($p < .05$).

5.3.5 Summary

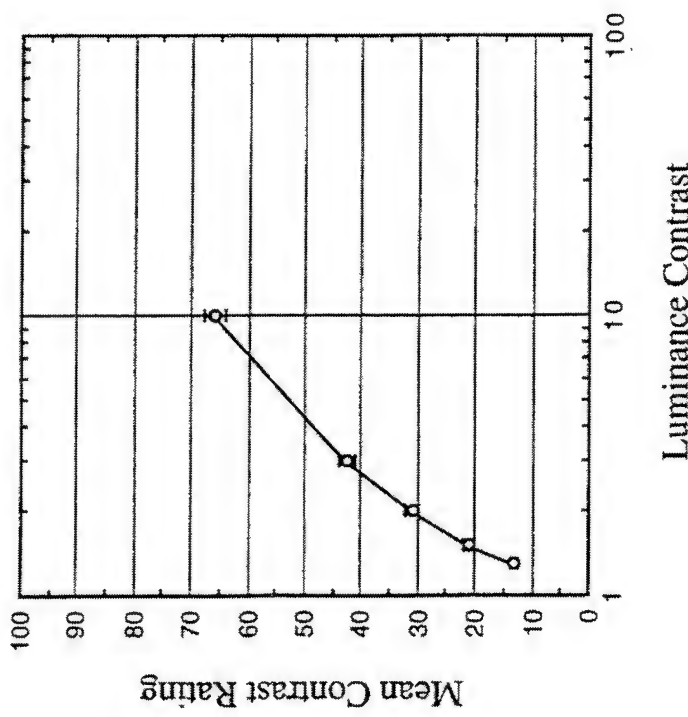
The results from Evaluation 2 are summarized in Table 5-8 and the following summary statements:

Table 5-8. Preliminary conclusions based on Evaluation 2 results.

Variable	Image Type	Rating Asymptote	Notes
Luminance Contrast	FLIR	>10:1	Contrast limited by original image Increased aliasing visibility with high CR
Gray Scale Levels	FLIR	24 Levels of Gray	
Gray Scale Distribution	FLIR	Nonlinear for light target (Tank) Linear for dark target (Truck)	Interacts with luminance contrast: Nonlinear may be preferred in either case at high CR levels.

1. Subjective image contrast was expected to and did increase monotonically with increases in luminance contrast. These data confirm that the luminance contrast manipulation produced the anticipated direction and magnitude of changes in subjective image contrast. They also indicate that changes in luminance contrast will be visible to levels at least as high as 10:1. This result is consistent with a similar finding for symbol images in Evaluation 1.
2. FLIR aliasing was reduced with 24 or more gray scale levels for the Truck image and 16 steps for the Tank image, beyond which there was no reliable improvement. The higher asymptote for the Truck image reflects rating sensitivity to gray scale detail presented in the dark shades in the Truck itself. These asymptotes are considerably lower than those reported for other classes of video imagery, and are likely due in part to the poor resolution and contrast of the images. The visibility of FLIR aliasing was highest for Truck images presented with the highest luminance contrast and only 8 gray scale levels. A similar trend was evident in the data for the Tank image, but the effect was not as robust ($p=.0653$). These results are generally consistent with the results of Evaluation 1, and again demonstrate the relatively higher sensitivity of participants to aliasing noise at higher luminance contrast values.
3. Images presented with either of the two nonlinear gray scale distributions received the highest aliasing ratings at gray scale levels of 8 or 16 and at high luminance contrast levels. Subjective image contrast for the tank image (bright target on a dark background) was highest in either of the nonlinear gray scale conditions relative to the linear gray scale condition. However, subjective image contrast for the Truck image (dark target on a light background) was generally higher for linear gray scale, although at the highest luminance contrast level (CR 10) the mostly highly rated gray scale distribution exponent for Truck images was nonlinear. One consequence of the nonlinear gray scale

distribution algorithm used was a general reduction in overall image brightness. For the Tank image, which portrayed a light target with well-defined contrast borders with the background, a disproportionate darkening of the background areas produced an apparent foreground to background contrast improvement. For the Truck image, however, target borders were less abrupt and the nonlinear gray scale distribution appeared to generally darken both target and background features. This image dependence is consistent with earlier observations made in informal examination of nonlinear gray scale.



Luminance Contrast	Mean Rating	Standard Error
1.3	75.000	0.496
1.5	70.917	0.961
2.0	65.000	1.162
3.0	42.750	1.400
10.0	15.750	1.813

Figure 5-34. Mean Contrast Rating as a Function of Luminance Contrast (Evaluation 2, Truck).

High contrast ratings indicate high subjective similarity of comparison images to the standard image (i.e., high brightness contrast). Error bars show standard error of the mean.

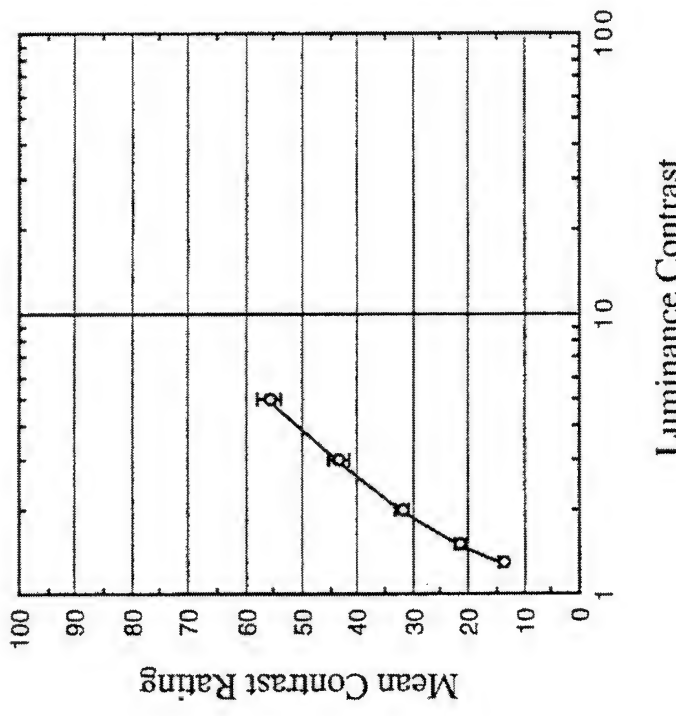


Figure 5-35. Mean Contrast Rating as a Function of Luminance Contrast (Evaluation 2, Tank).

High contrast ratings indicate high subjective similarity of comparison images to the standard image (i.e., high brightness contrast). Error bars show standard error of the mean.

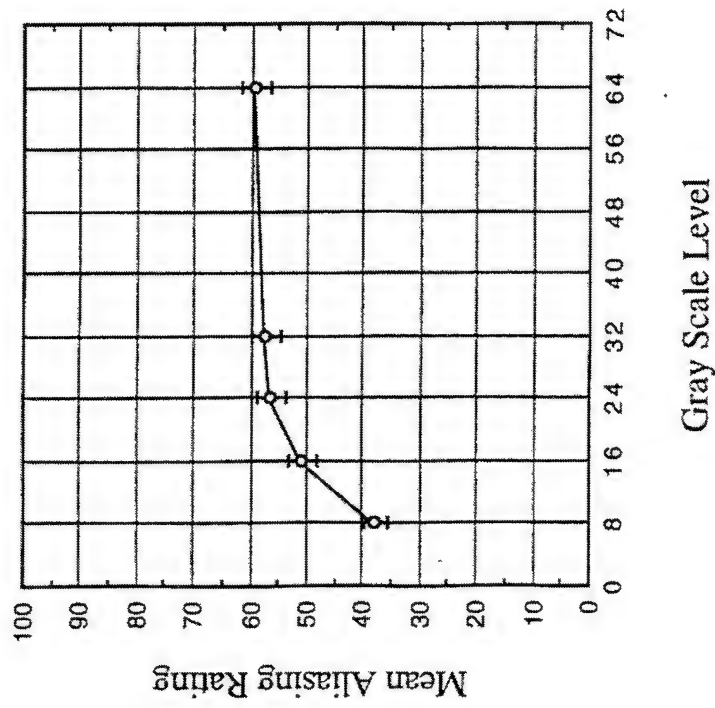


Figure 5-36. Mean Aliasing Rating as a Function of Gray Scale Level (Evaluation 2, Truck).

High aliasing ratings indicate high subjective similarity of comparison images to the standard image (i.e., relatively little visible aliasing). Error bars show standard error of the mean.

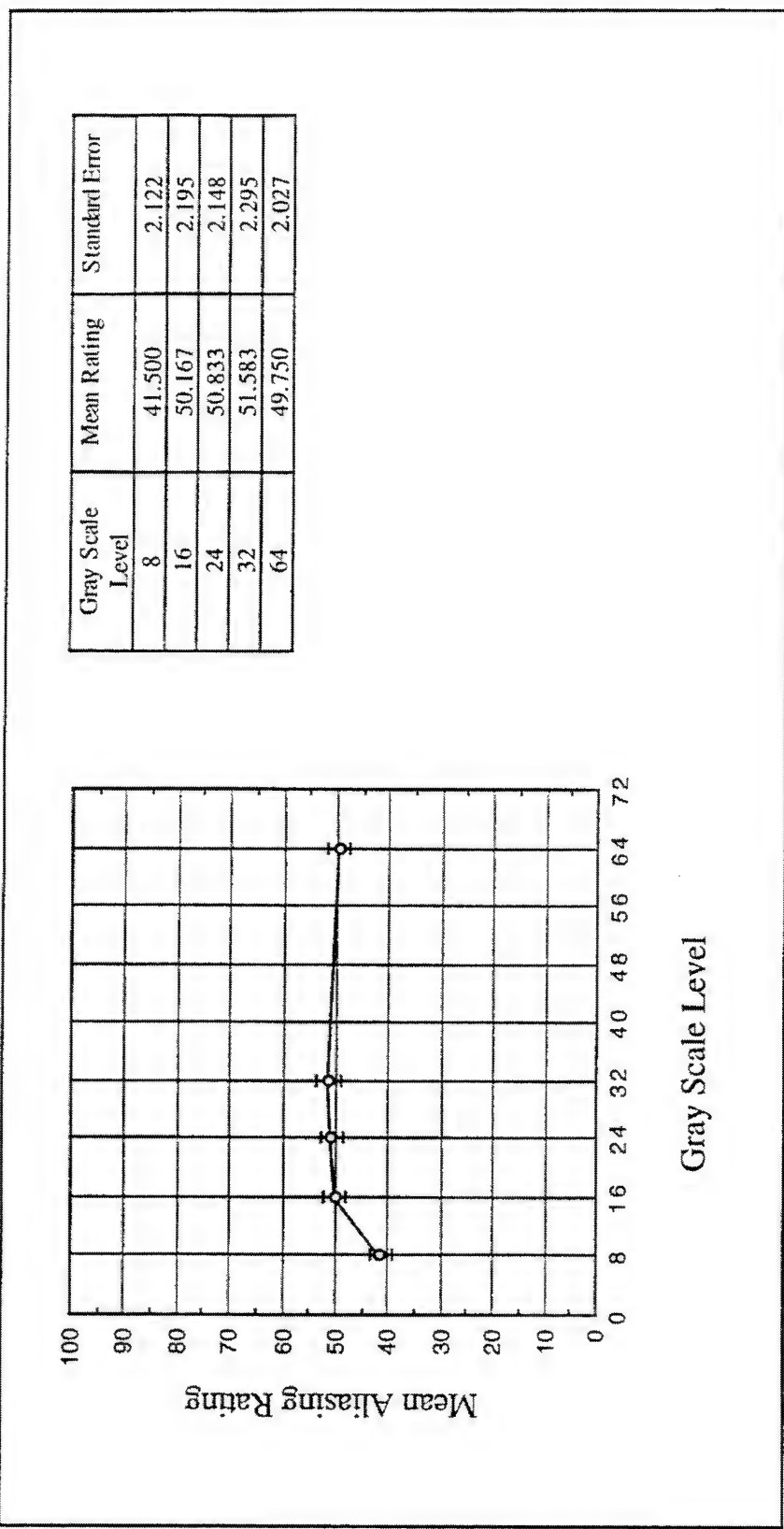


Figure 5-37. Mean Aliasing Rating as a Function of Gray Scale Level (Evaluation 2, Tank).

High aliasing ratings indicate high subjective similarity of comparison images to the standard image (*i.e.*, relatively little visible aliasing). Error bars show standard error of the mean.

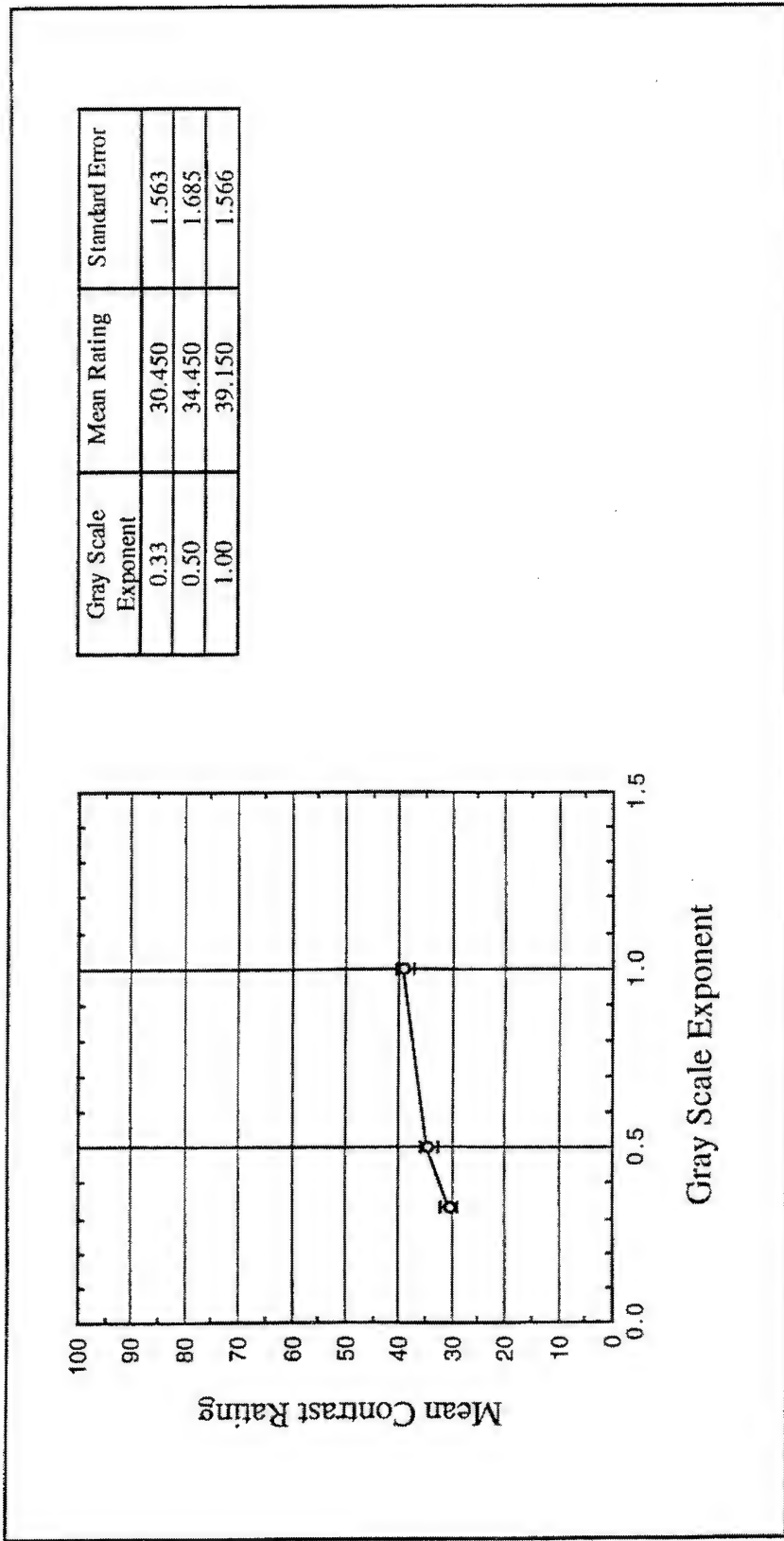


Figure 5-38. Mean Contrast Rating as a Function of Gray Scale Exponent (Evaluation 2, Truck). High contrast ratings indicate high subjective similarity of comparison images to the standard image (i.e., high brightness contrast). Error bars show standard error of the mean.

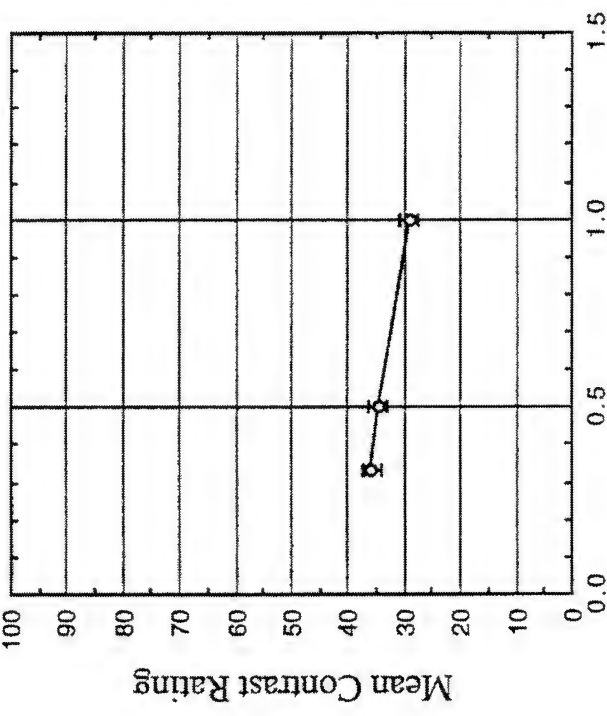


Figure 5-39. Mean Contrast Rating as a Function of Gray Scale Exponent (Evaluation 2, Tank).

High contrast ratings indicate high subjective similarity of comparison images to the standard image (i.e., high brightness contrast). Error bars show standard error of the mean.

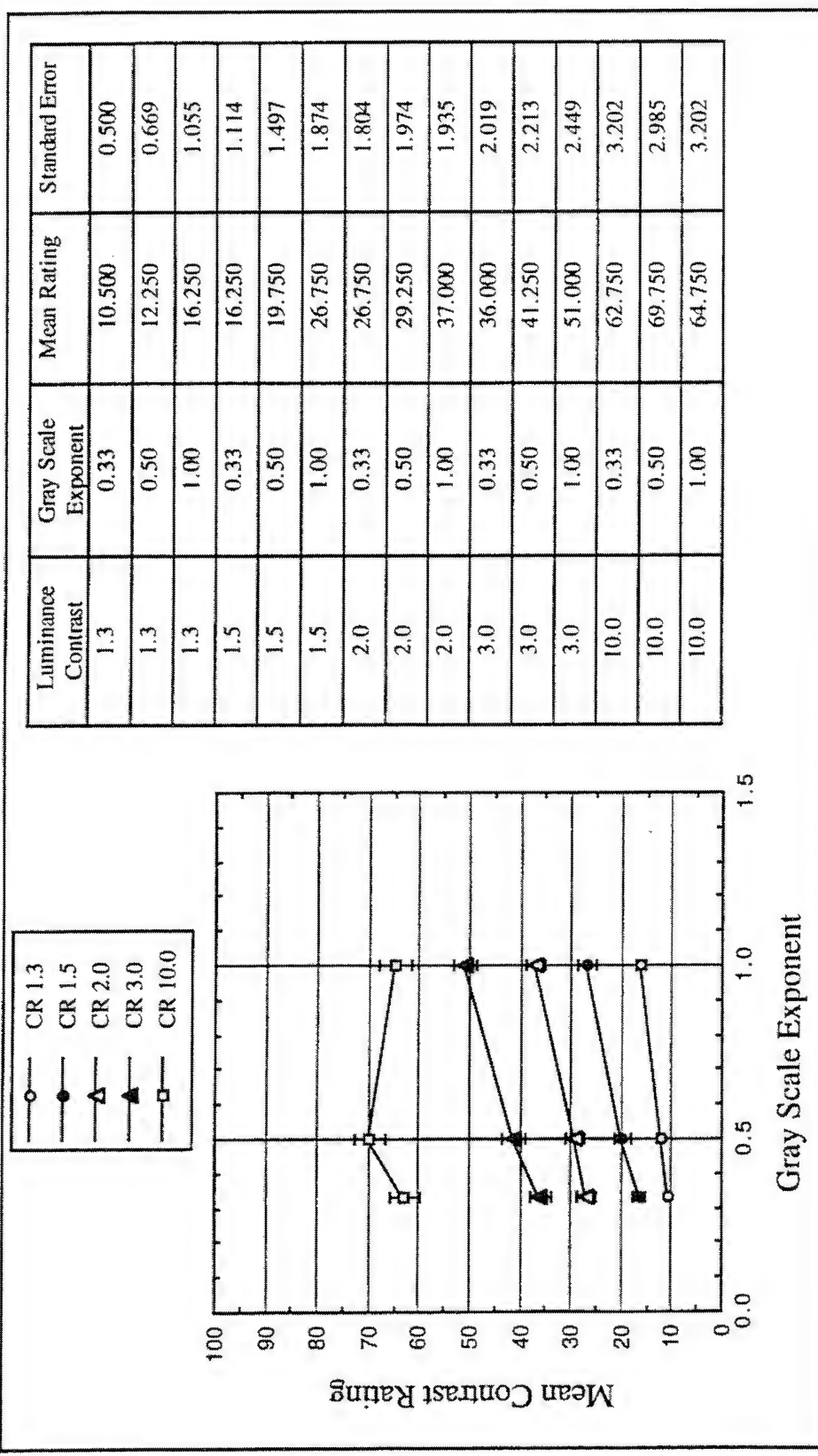


Figure 5-40. Mean Contrast Rating as a Function of Gray Scale Exponent by Luminance Contrast (Evaluation 2, Truck).

High contrast ratings indicate high subjective similarity of comparison images to the standard image (i.e., high brightness contrast). Error bars show standard error of the mean.

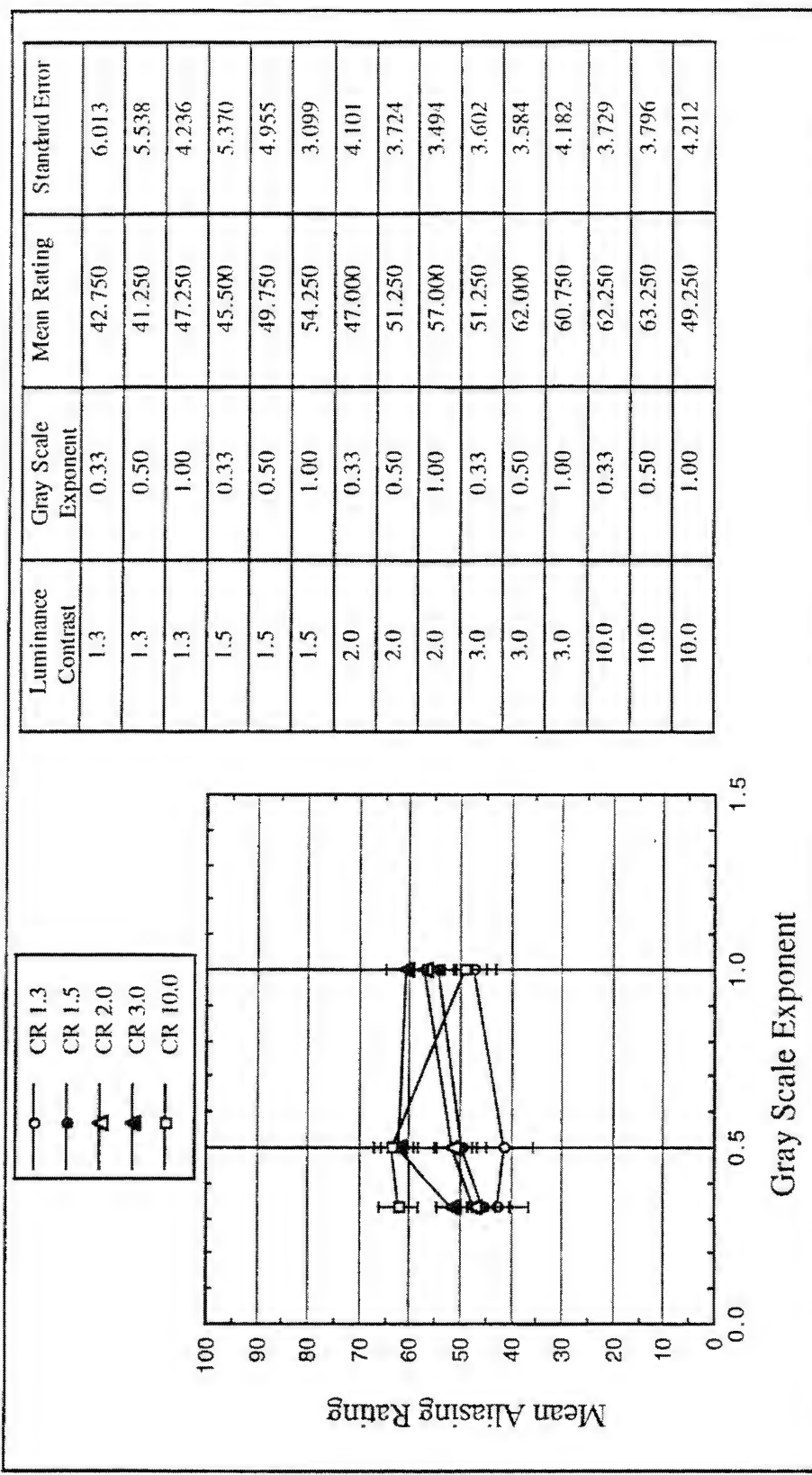


Figure 5-41. Mean Aliasing Rating as a Function of Gray Scale Exponent by Luminance Contrast (Evaluation 2, Truck).

High aliasing ratings indicate high subjective similarity of comparison images to the standard image (i.e., relatively little visible aliasing). Error bars show standard error of the mean.

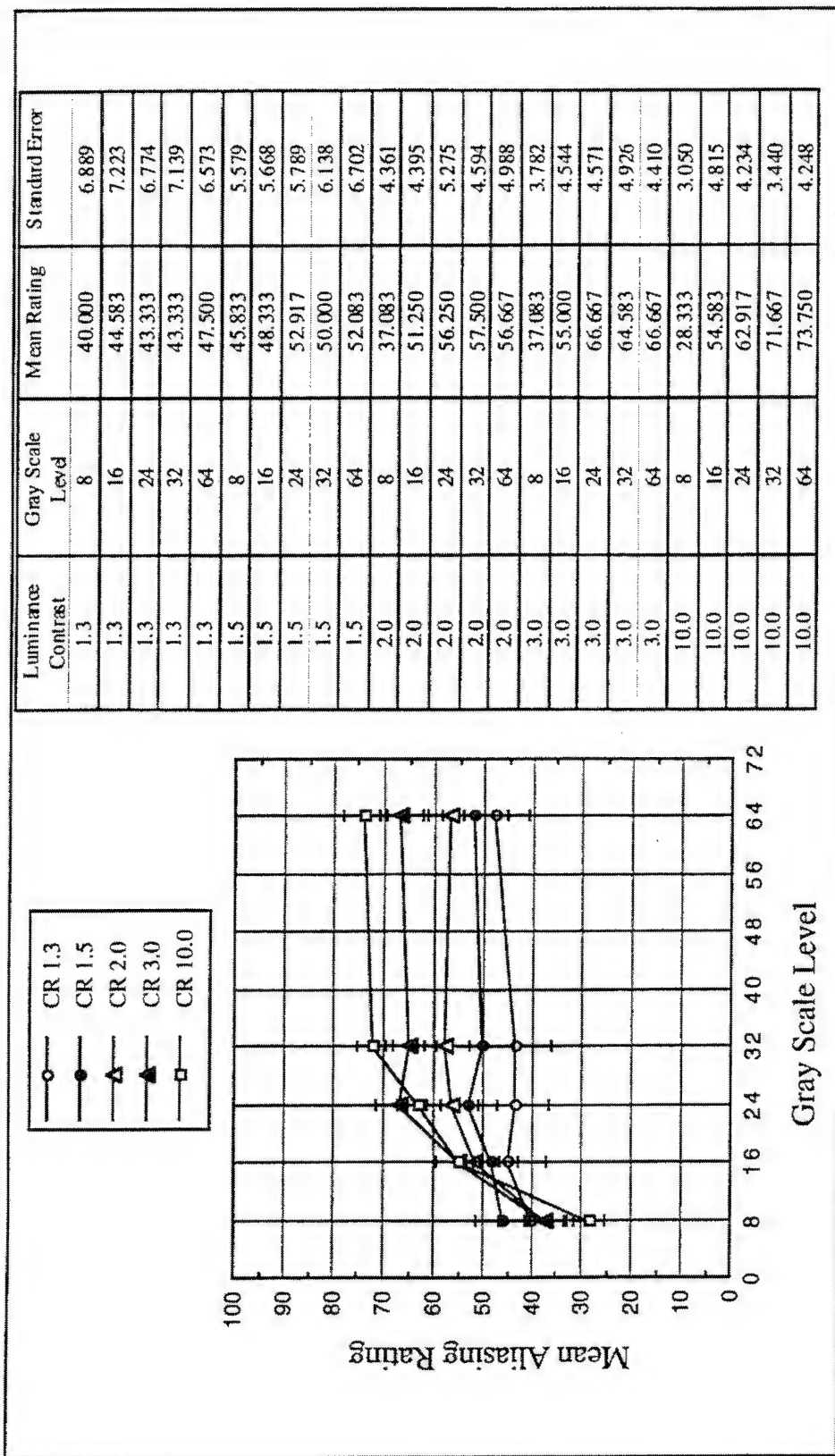


Figure 5-42. Mean Aliasing Rating as a Function of Gray Scale Level by Luminance Contrast (Evaluation 2, Truck).

High aliasing ratings indicate high subjective similarity of comparison images to the standard image (i.e., relatively little visible aliasing). Error bars show standard error of the mean.

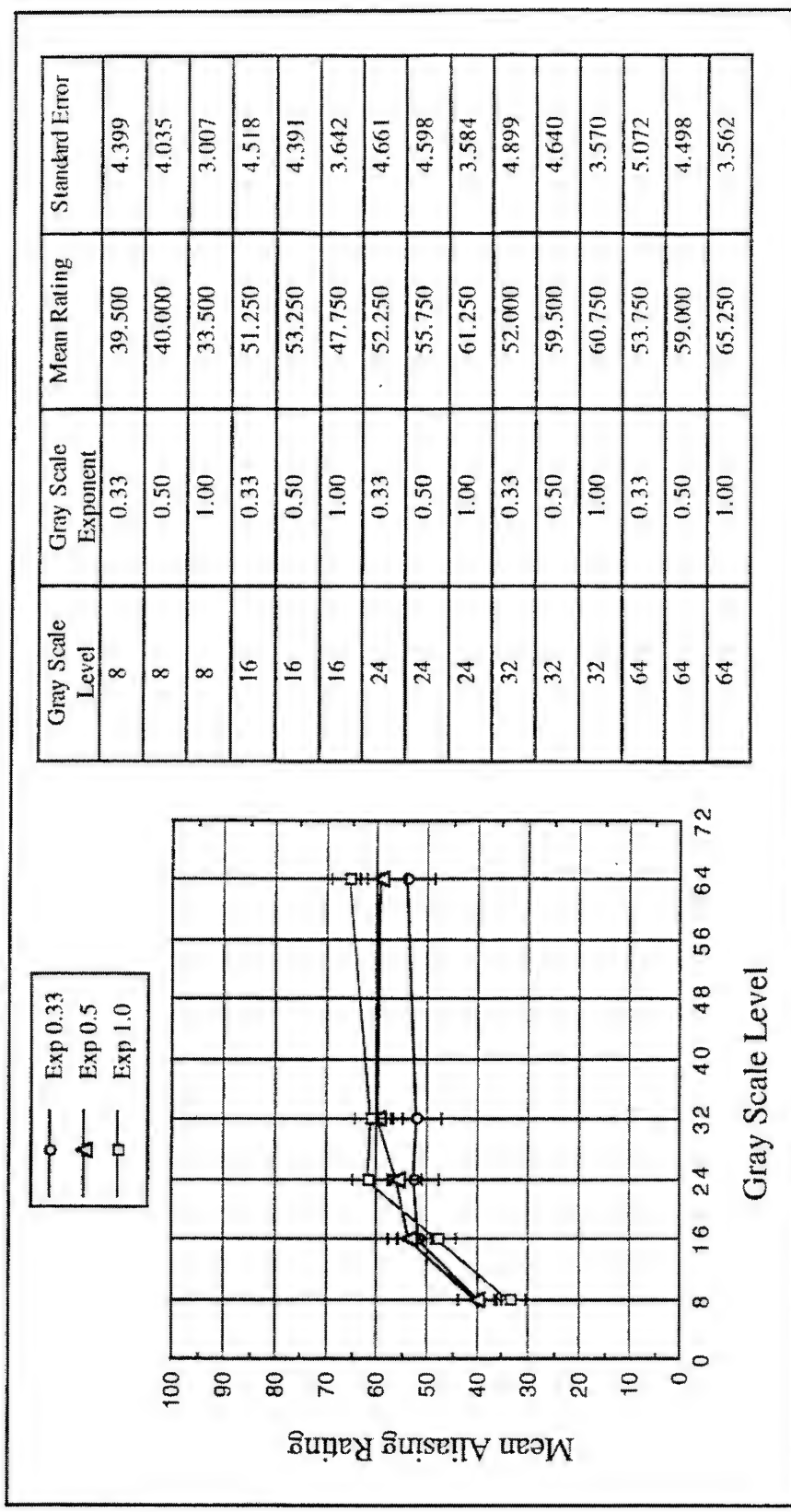


Figure 5-43. Mean Aliasing Rating as a Function of Gray Scale Level by Gray Scale Exponent (Evaluation 2, Truck).

High aliasing ratings indicate high subjective similarity of comparison images to the standard image (i.e., relatively little visible aliasing). Error bars show standard error of the mean.

5.4 Evaluation 3

5.4.1 Objectives

Evaluation 3 was conducted to extend the results of Evaluation 2 to include a range of subtractive color image source aperture ratios, while controlling image luminance at a constant value. The specific objectives of Evaluation 3 were:

1. Assess the relative impact of aperture ratio on perception of FLIR line visibility and image quality.
2. Further document the perceptual consequences of using nonlinear gray scale distribution for FLIR imagery.
3. Determine the gray scale level asymptote for FLIR image quality and compare this result to those of Evaluation 2.

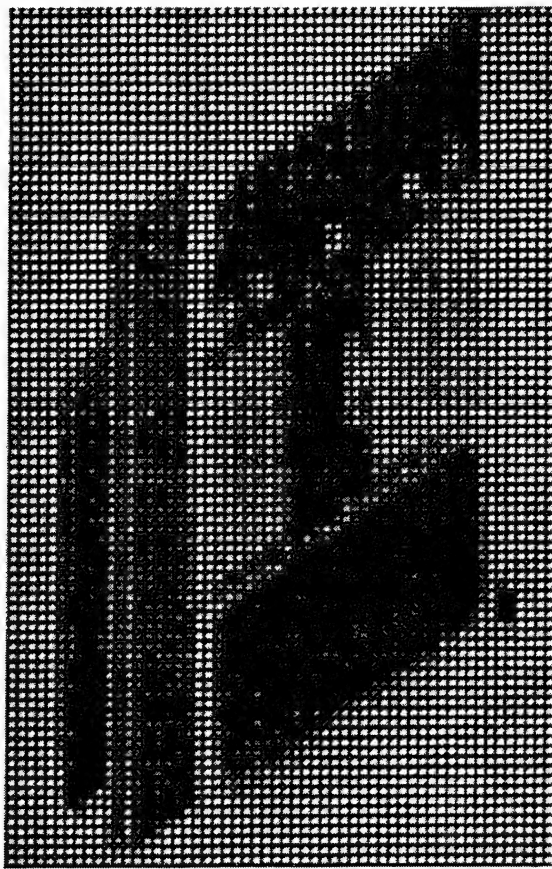
5.4.2 Design

Evaluation 3 images were modeled using subtractive color image source models with varied aperture ratios and the two original FLIR images described previously. Comparison image luminance was held constant among aperture ratios by reducing the luminance range of images with aperture ratios greater than 40% (the luminance of standard images was not reduced). Luminance reduction produced pixels with lower luminance levels at higher aperture ratios but images with equivalent space-averaged luminance (images with higher aperture ratios had a greater percentage of the pixel area contributing to the space-averaged luminance). Images were presented at a resolution of 22 simulated AMLCD pixels per degree. FLIR images were subjected to gray scale level clipping and distribution as previously described under *Simulation Software*. FLIR images were presented in monochrome green. Image transparency was not evaluated in Evaluation 3; therefore, no background images were merged with the AMLCD images.

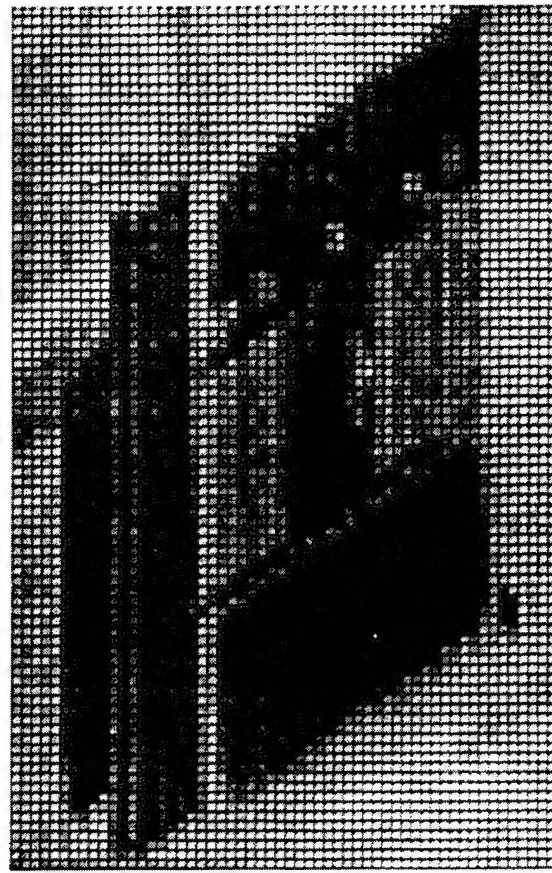
The simulation design levels included in Evaluation 3 are summarized in Table 5-9.

Table 5-9. Design variables for Evaluation 3.

Variable	Levels	Figure	Page
HILR Image	Truck, Tank	(see Software Imagery)	Figure 5-11 (p. 240)
Aperture Ratio	40%, 50%, 60%, 70%, 80%	Figure 5-44, Figure 5-45	Figure 5-11 (p. 240) 293
Gray Scale Levels	8, 16, 24, 32, 64	(see Evaluation 2)	Figure 5-30 (p. 272)
Gray Scale Distribution Exponent	1.0, 0.5, 0.33	(see Evaluation 2)	Figure 5-32 (p. 274)



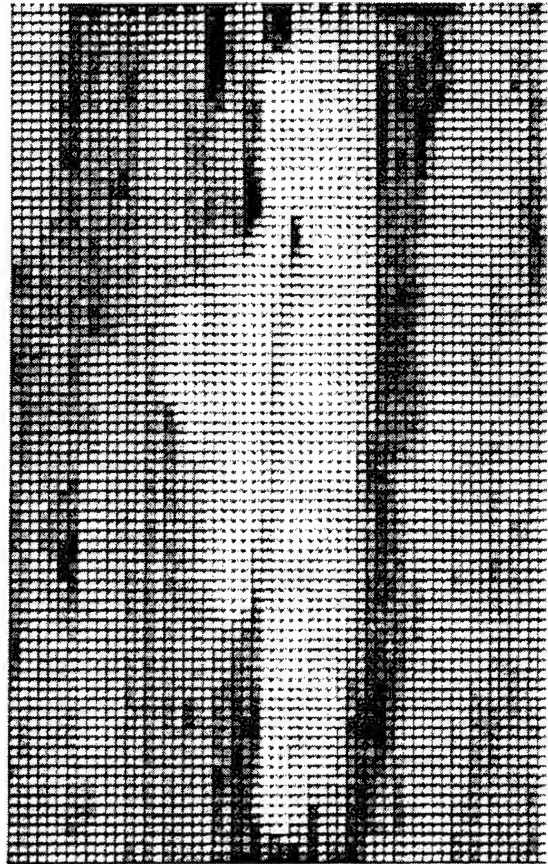
(a)



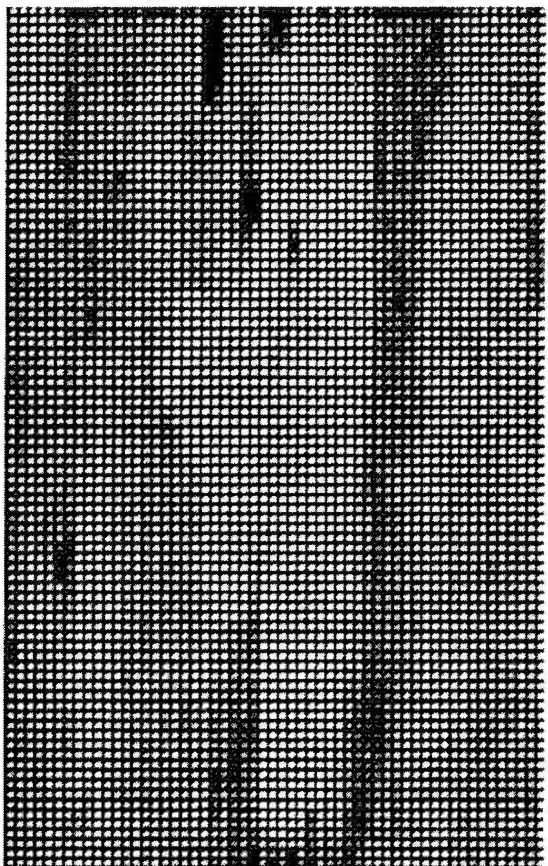
(b)

Figure 5-44. Aperture Ratio Variable for FLIR Truck Images in Evaluations 3 and 4.

Aperture ratio ranged from 40% (a) to 80% (b). Images shown here are from Evaluation 4 (luminance covaried with aperture ratio). Luminance was not allowed to covary with aperture ratio in Evaluation 3. Note that evaluation images were actually presented in color on a high-resolution CRT. Also, these printed gray scale images are not gamma-corrected for printing. In addition, their size as printed is not intended to simulate the angular resolutions tested in the evaluations.



(a)



(b)

Figure 5-45. Aperture Ratio for FLIR Tank Images in Evaluations 3 and 4.

Aperture ratio ranged from 40% (a) to 80% (b). Images shown are from Evaluation 4 (luminance covaried with aperture ratio.) Luminance was not allowed to covary with aperture ratio in Evaluation 3. Note that evaluation images were actually presented in color on a high-resolution CRT. Also, these printed gray scale images are not gamma-corrected for printing. In addition, their size as printed is not intended to simulate the angular resolutions tested in the evaluations.

5.4.3 Procedure

Two new subjective rating scales were used to evaluate imagery in Evaluation 3 (Figure 5-46, p. 296). The line visibility scale was used to capture subjective visibility of row and column lines as aperture ratio was varied. The image quality scale supplanted the aliasing scale to include other factors beyond aliasing that participants may include in their overall assessment of image quality. Note that participants were asked to include any image features in their assessment of quality that they believed impacted the overall quality of the image appearance, including line visibility. For each evaluation trial, a separate rating was made on each scale. Participants were instructed to make their image ratings relative to the standard image. Eight participants followed the general evaluation procedure described previously, using the serial comparison procedure and rating 8 practice images and 150 evaluation trials during a 60 minute period. The order of image presentation was randomized within blocks of FLIR image (Truck or Tank) for each observer. The order of block presentation was counterbalanced, with 50% of participants rating Tank images first.

Line Visibility (Evaluations 3 through 10):
The degree to which the comparison image is free from visible grid lines (thin horizontal and vertical lines) relative to the standard image.

- | | |
|------|--|
| 10% | Grid lines are as visible as possible |
| 20% | |
| 30% | |
| 40% | |
| 50% | Grid lines are about twice as visible as in the standard image |
| 60% | |
| 70% | |
| 80% | |
| 90% | |
| 100% | Grid lines are no more visible than in the standard image |

Image Quality (Evaluations 3 through 10):

The overall quality of the comparison image relative to the standard image.

- | | |
|------|---|
| 10% | Image is of very poor quality |
| 20% | |
| 30% | |
| 40% | |
| 50% | Image is about half as good looking as the standard image |
| 60% | |
| 70% | |
| 80% | |
| 90% | |
| 100% | Image is as good looking as the standard image |

Figure 5-46 Line Visibility and Image Quality Rating Scales Used in Evaluations 3 Through 10.

5.4.4 Results

Table 5-10 provides an overview of the significant data trends. Separate ANOVA procedures were run for the two types of FLIR images. The effects summarized in the table are discussed in the text following the table.

Table 5-10. ANOVA Summary Table for Evaluation 3.

Effect	Dependent Variable	Image	Figure	Page	df	MS	F	p	R ²
Aperture Ratio	Line Visibility	Truck	Figure 5-47	300	4, 28	21436.083	50.46	<.0001	.45
	Line Visibility	Tank	Figure 5-48	301	4, 28	22785.167	52.41	<.0001	.38
Gray Scale Levels	Image Quality	Truck	Figure 5-49	302	4, 28	17094.833	70.73	<.0001	.34
	Image Quality	Tank	Figure 5-50	303	4, 28	11656.292	42.60	<.0001	.23
Gray Scale Distribution	Image Quality	Truck	Figure 5-51	304	2, 14	9158.000	16.40	.0034	.09
	Image Quality	Tank	Figure 5-52	305	2, 14	14723.792	38.46	<.0001	.14
Gray Scale Levels x Gray Scale Distribution	Image Quality	Truck	Figure 5-53	306	8, 56	1970.708	15.34	<.0001	.08
	Image Quality	Tank	Figure 5-54	307	8, 56	575.042	5.56	.0013	.02

Aperture Ratio. FLIR line visibility ratings increased (i.e., lines became less apparent) monotonically as a function of increasing aperture ratio (Figure 5-47 and Figure 5-48), with each increase in aperture ratio associated with a significant increase in line visibility ratings ($p < .05$).

Gray Scale Levels. FLIR image quality ratings were significantly higher when images were presented with 64 gray scale levels (Figure 5-49 and Figure 5-50), although the relative improvement in image quality was small beyond 24 levels for the FLIR Truck and 16 levels for the FLIR Tank. Specifically, the differences between ratings at 24 and 32 levels and between ratings at 32 and 64 levels were not statistically significant for either image ($p > .05$), and the difference between ratings at 16 and 24 levels was not statistically significant for the Tank image ($p > .05$).

Gray Scale Exponent. FLIR image quality ratings were significantly greater for the Truck image when presented with linear gray scale or using the intermediate gray scale exponent (Figure 5-51). Conversely, the FLIR Tank image received higher image quality ratings with either of the nonlinear gray scale distribution exponents (Figure 5-52).

Gray Scale Distribution x Gray Scale Levels Interaction. FLIR image quality ratings varied as an interaction of gray scale distribution and number of gray scale levels (Figure 5-53 and Figure 5-54). While FLIR Truck image quality ratings were highest for linear gray scale presentations at 32 and 64 gray levels, images presented with the intermediate gray scale distribution exponent received equally high ratings to linear presentations at 24 gray levels and higher ratings at 16 gray levels ($p < .05$). At 8 gray levels there were no significant differences in ratings as a function of gray scale exponents ($p > .05$). While FLIR Tank image quality ratings were highest for the most nonlinear gray scale presentations at 32 and 64 gray levels gray levels, images presented with the intermediate gray scale distribution exponent received equally high ratings to the most nonlinear images at 8 to 24 gray levels ($p < .05$).

5.4.5 Summary

The results from Evaluation 3 are summarized in Table 5-11 and the following summary statements:

Table 5-11. Preliminary conclusions based on Evaluation 3 results.

Variable	Image Type	Rating Asymptote	Notes
Aperture Ratio	FLIR	≥80%	Line visibility
Gray Scale Levels	FLIR	64 Levels of Gray	Reduced advantage beyond 24 levels
Gray Scale Distribution	FLIR	Nonlinear for light target Linear for dark target	Differences greatest at larger number of gray scale levels

1. Visibility of row and column lines decreased monotonically (and almost linearly) with increases in aperture ratio across the full range of aperture ratios simulated (40% to 80%). Aperture ratio did not have a reliable effect on overall image quality ratings (even though the differences were clearly visible, as indicated by the line visibility data).

2. FLIR image quality improved with as many as 64 gray scale levels, although the relative improvement in image quality was generally small beyond 24 levels. This result is generally consistent with the earlier aliasing findings of Evaluation 2, although the aliasing results of Evaluation 2 failed to capture the same small gains realized at 64 gray scale levels.
3. Subjective ratings of image quality for the tank image were highest in either of the nonlinear gray scale conditions while ratings of image quality for the Truck image were generally higher as gray scale became more linear. This direction of this image dependence is consistent with the contrast and aliasing results of Evaluation 2. Gray scale distribution differences in image quality ratings (above) were greatest for images with the highest number of gray scale levels.

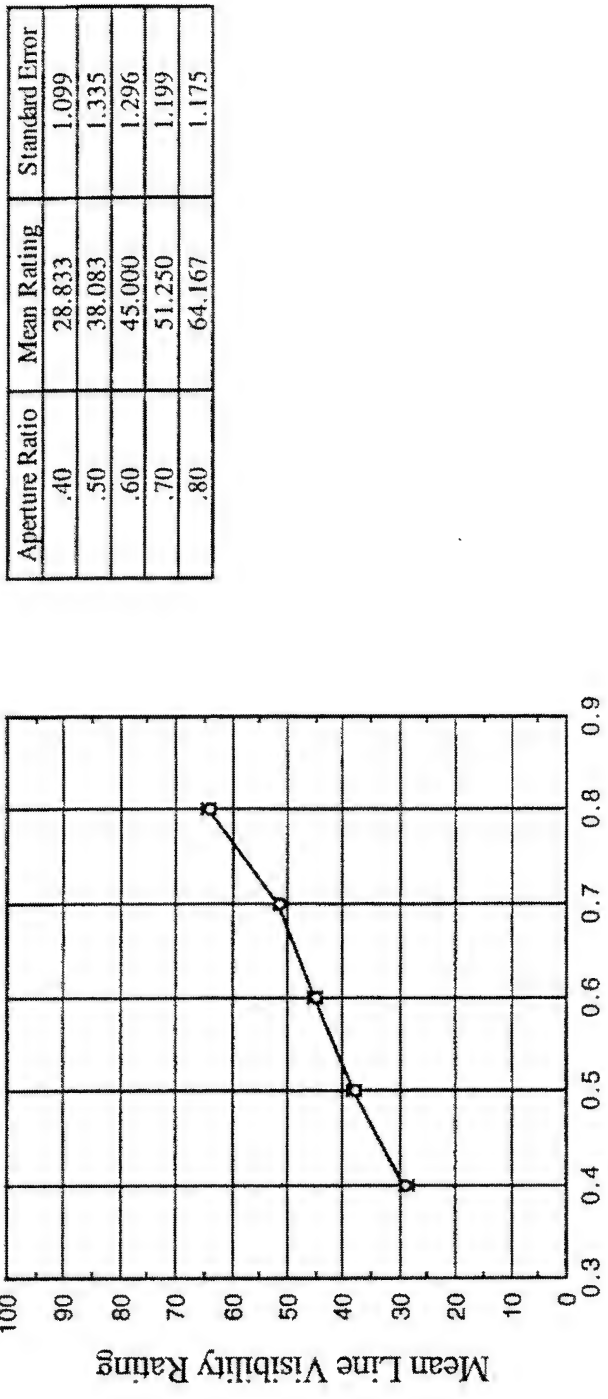


Figure 5-47. Mean Line Visibility Rating as a Function of Aperture Ratio (Evaluation 3, Truck).

High line visibility ratings indicate high subjective similarity of comparison images to the standard image (i.e., low visibility of row and column lines). Error bars show standard error of the mean.

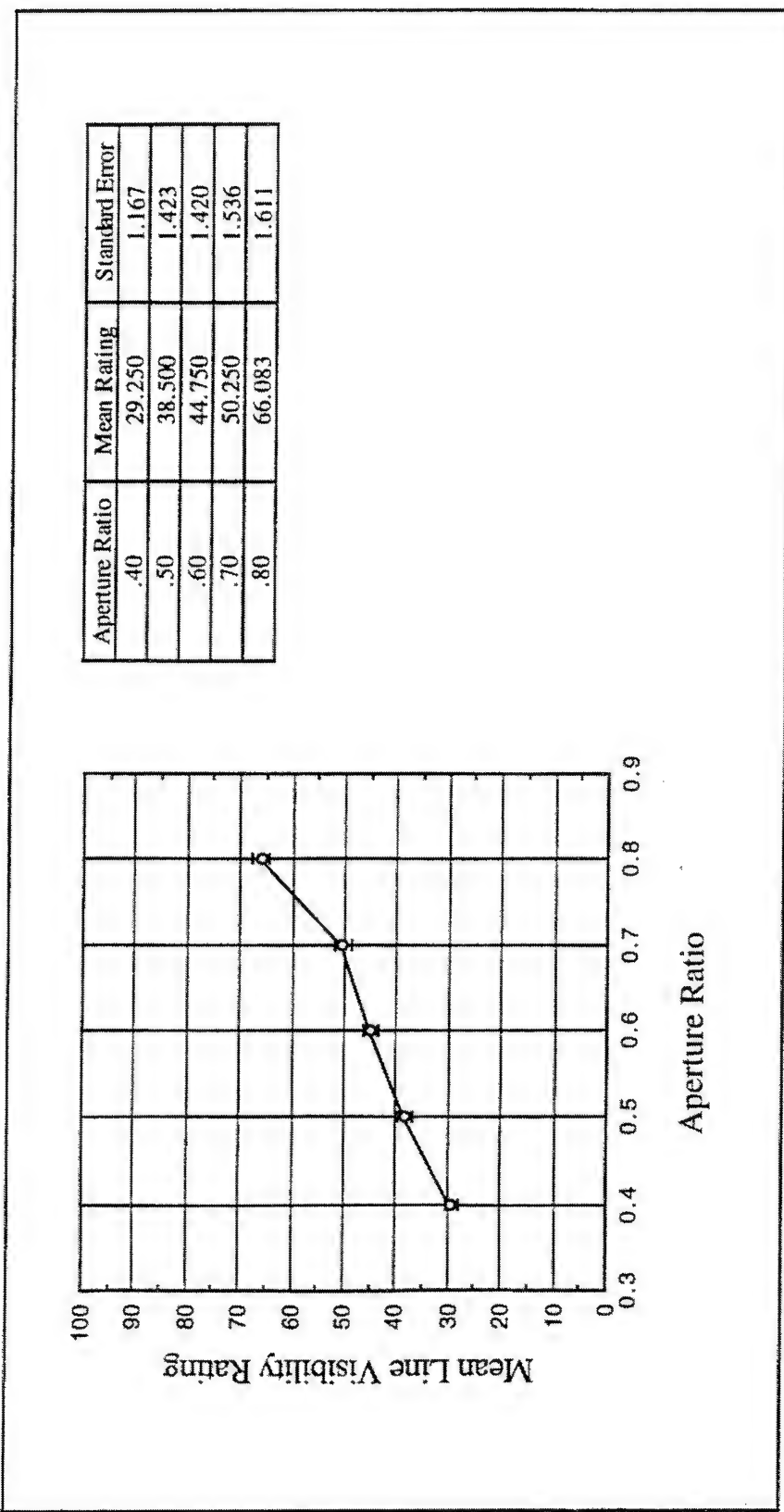


Figure 5-48. Mean Line Visibility Rating as a Function of Aperture Ratio (Evaluation 3, Tank).

High line visibility ratings indicate high subjective similarity of comparison images to the standard image (i.e., low visibility of row and column lines). Error bars show standard error of the mean.

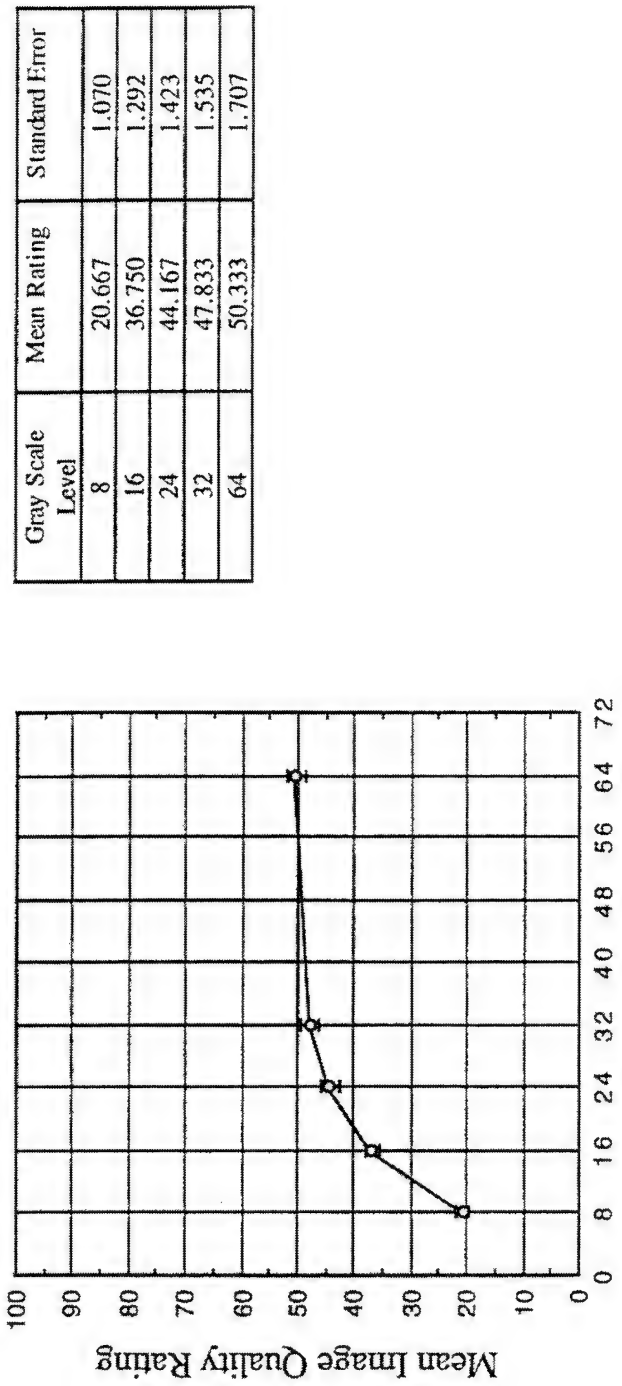


Figure 5-49. Mean Image Quality Rating as a Function of Gray Scale Level (Evaluation 3, Truck).

High image quality ratings indicate high subjective similarity of comparison images to the standard image (i.e., relatively high image quality). Error bars show standard error of the mean.

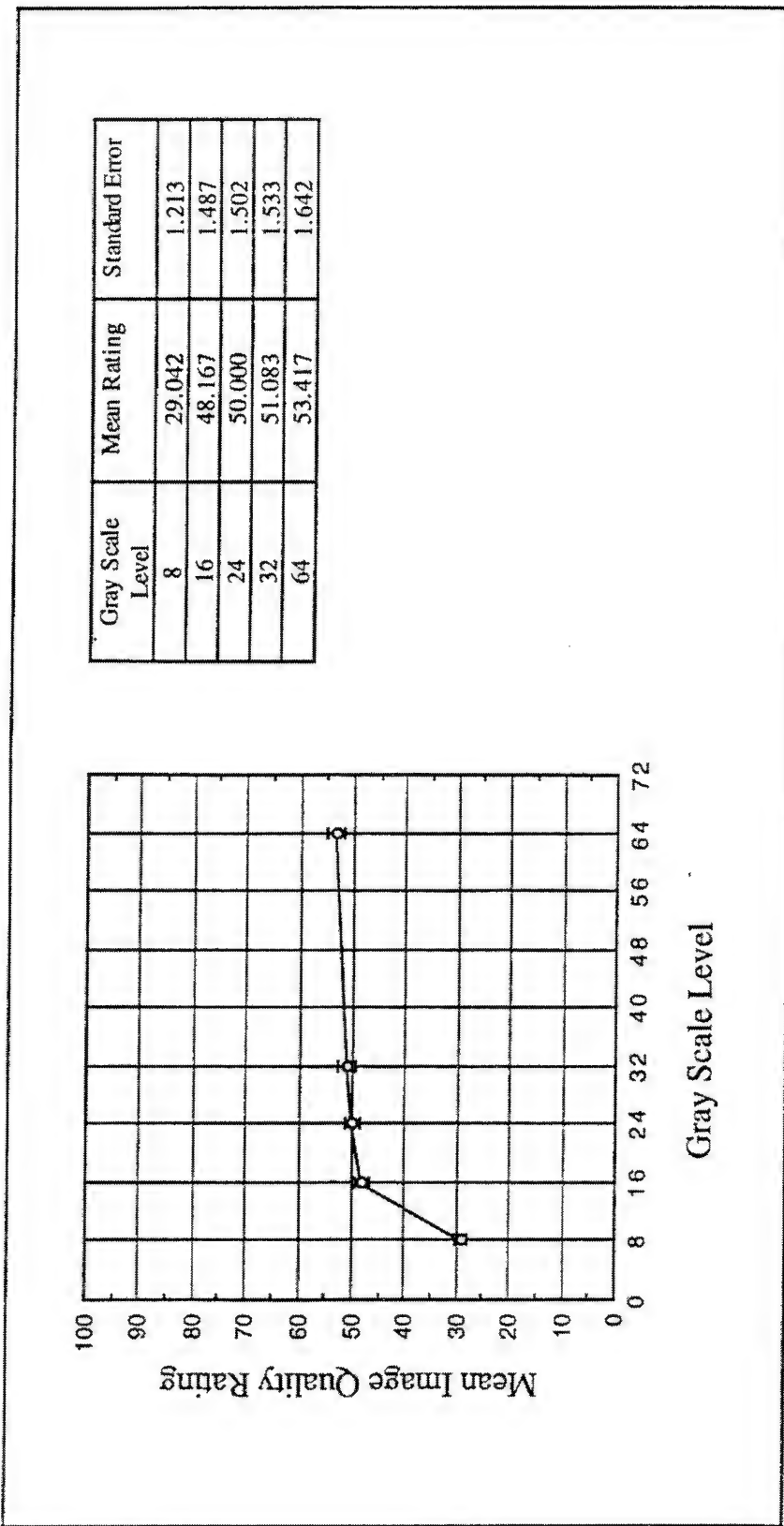


Figure 5-50. Mean Image Quality Rating as a Function of Gray Scale Level (Evaluation 3, Tank).

High image quality ratings indicate high subjective similarity of comparison images to the standard image (i.e., relatively high image quality). Error bars show standard error of the mean.

Gray Scale Exponent	Mean Rating	Standard Error
0.33	32.150	1.065
0.50	43.450	1.245
1.00	44.250	1.483

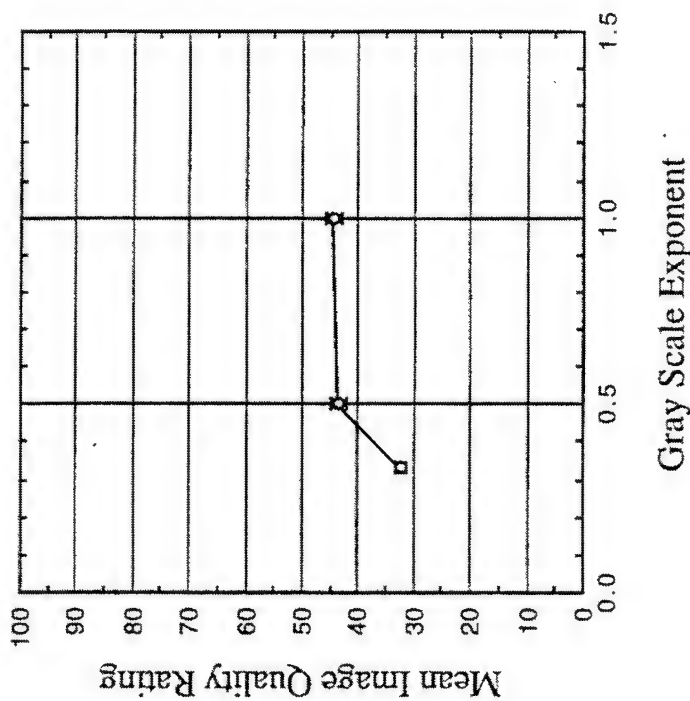


Figure 5-51. Mean Image Quality Rating as a Function of Gray Scale Exponent (Evaluation 3, Truck).

High image quality ratings indicate high subjective similarity of comparison images to the standard image (i.e., relatively high image quality). Error bars show standard error of the mean.

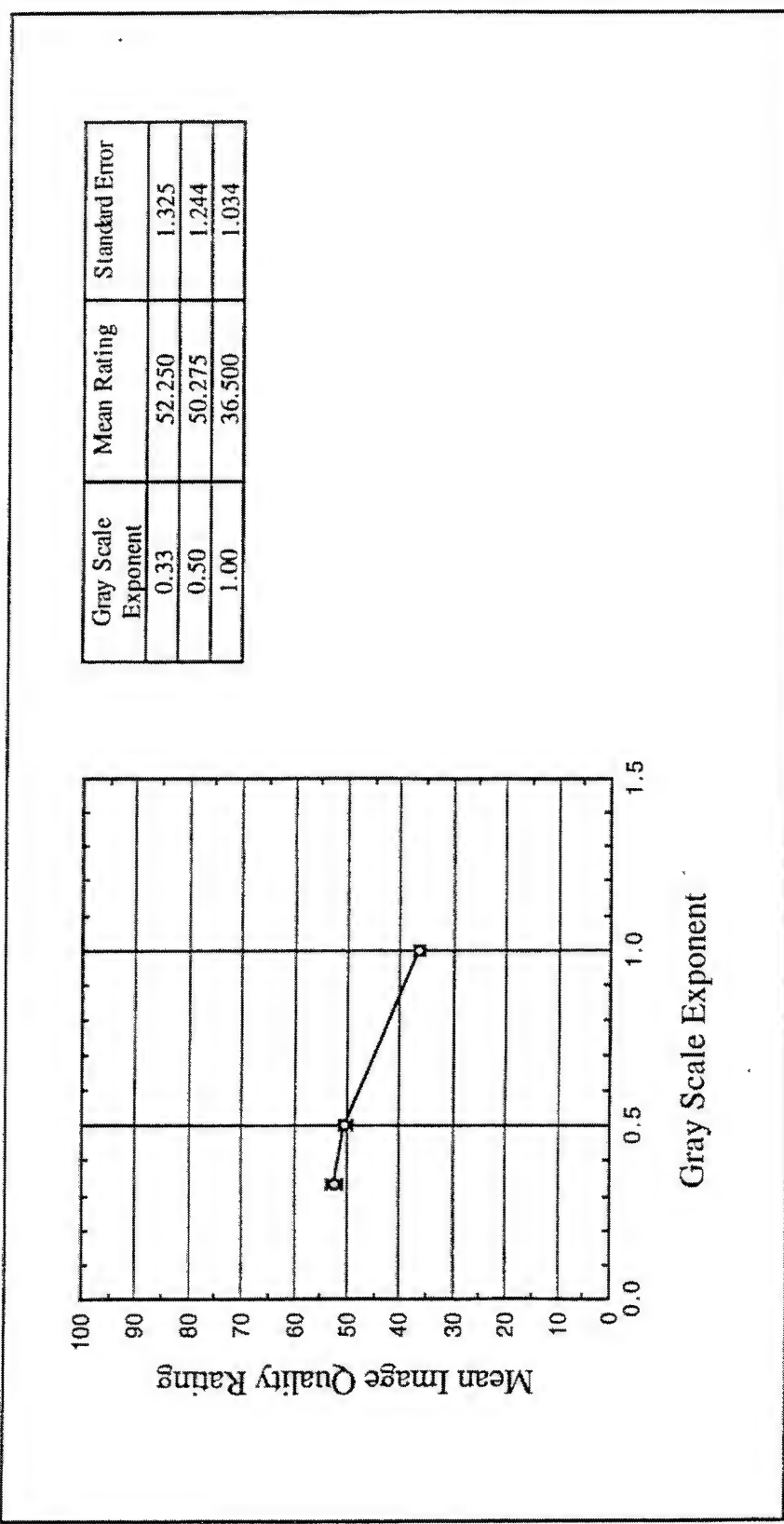


Figure 5-52. Mean Image Quality Rating as a Function of Gray Scale Exponent (Evaluation 3, Tank).

High image quality ratings indicate high subjective similarity of comparison images to the standard image (i.e., relatively high image quality). Error bars show standard error of the mean.

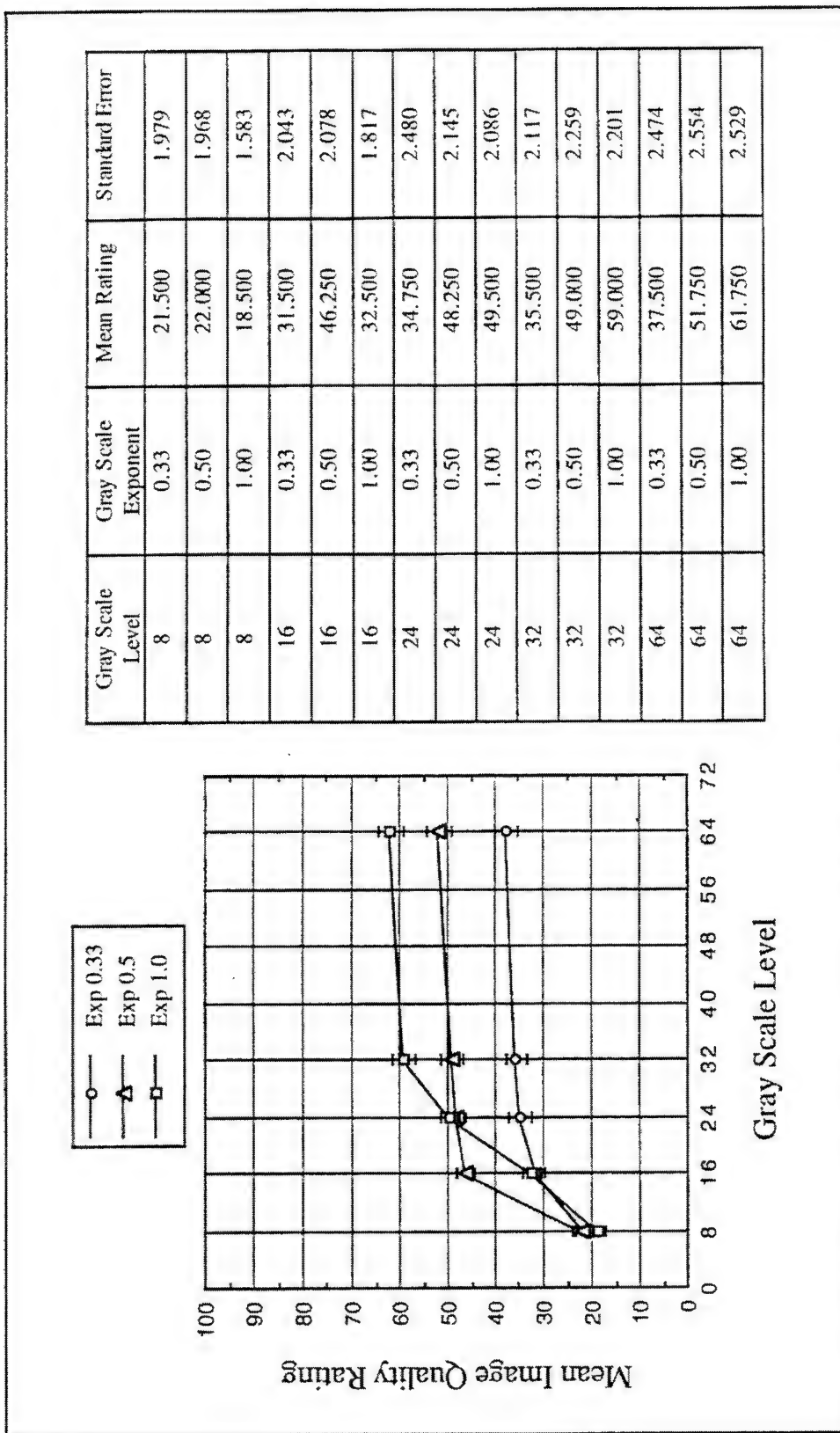


Figure 5-53. Mean Image Quality Rating as a Function of Gray Scale Level by Gray Scale Exponent (Evaluation 3, Truck).

High image quality ratings indicate high subjective similarity of comparison images to the standard image (i.e., relatively high image quality). Error bars show standard error of the mean.

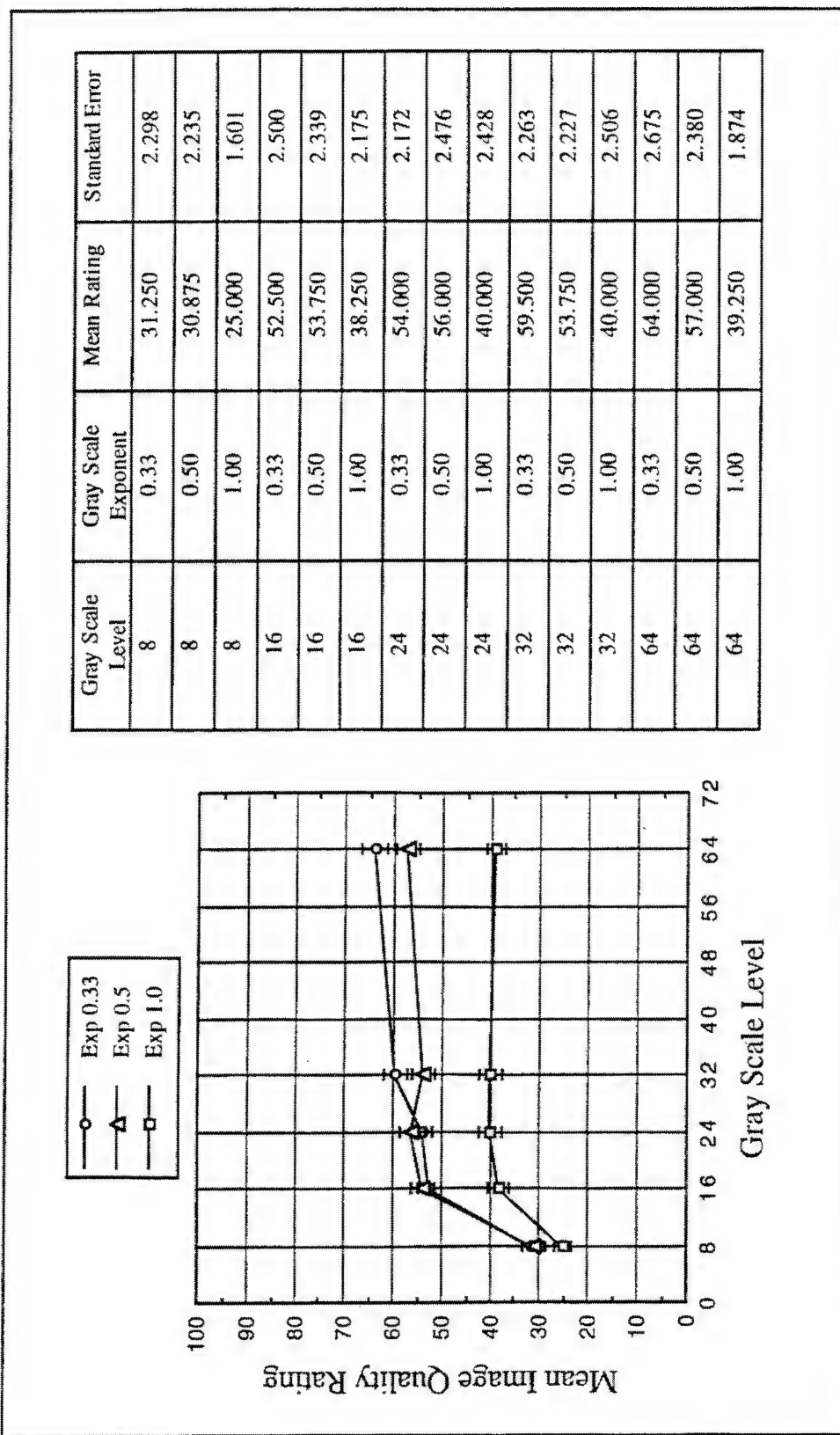


Figure 5-54. Mean Image Quality Rating as a Function of Gray Scale Level by Gray Scale Exponent (Evaluation 3, Tank).

High image quality ratings indicate high subjective similarity of comparison images to the standard image (i.e., relatively high image quality). Error bars show standard error of the mean.

5.5 Evaluation 4

5.5.1 Objectives

Evaluation 4 was conducted to replicate the procedure of Evaluation 3 while allowing image luminance to covary with aperture ratio (images modeled with higher aperture ratios had higher luminances). The specific objectives of Evaluation 4 were:

1. Assess the relative impact of aperture ratio on perception of image line visibility and image quality.
2. Further document the perceptual consequences of using nonlinear gray scale distribution for FLIR imagery.
3. Determine the gray scale level asymptote for FLIR image quality and compare this result to that found for FLIR aliasing.
4. Determine the effect of allowing image luminance to covary with aperture ratio on 1-3 above.

5.5.2 Design

Evaluation 4 images were modeled using subtractive color image source models with varied aperture ratios and the two original FLIR images described previously. Comparison image luminance was allowed to vary among aperture ratios, such that images with greater aperture ratios had greater luminances (the luminance of the standard image remained the same as in Evaluation 3). Images were presented at a resolution of 22 simulated AMLCD pixels per degree. FLIR images were subjected to gray scale level clipping and distribution as previously described under *Simulation Software*. FLIR images were presented in monochrome green.

The simulation design levels included in Evaluation 4 are summarized in Table 5-12.

Table 5-12. Design variables for Evaluation 4.

Variable	Levels	Figure (see Software Imagery)	Page
FLIR Image	Truck, Tank	Figure 5-11 (p. 240)	
Aperture Ratio	40%, 50%, 60%, 70%, 80%	Figure 5-44 (p. 293)	
Gray Scale Levels	8, 16, 24, 32, 64	Figure 5-30 (p. 272)	
Gray Scale Distribution Exponent	1.0, 0.5, 0.33	Figure 5-32 (p. 274)	

5.5.3 Procedure

The same rating scales (line visibility and image quality) and procedure that were used in Evaluation 3 were also used in Evaluation 4. For each evaluation trial, a separate rating was made on each scale. Participants were instructed to make their image ratings relative to the standard image. Eight participants followed the general evaluation procedure described previously, using the serial comparison procedure and rating 8 practice images and 150 evaluation trials during a 60 minute period. The order of image presentation was randomized within blocks of FLIR image (Truck or Tank) for each observer. The order of block presentation was counterbalanced, with 50% of participants rating Tank images first.

5.5.4 Results

Table 5-13 provides an overview of the significant data trends. Separate ANOVA procedures were run for the types of FLIR images. The effects summarized in the table are discussed in the text following the table.

Table 5-13. ANOVA summary table for Evaluation 4.

Effect	Dependent Variable	Image	Figure	Page	df	MS	F	p	R ²
Aperture Ratio	Line Visibility	Truck	Figure 5-55	314	4, 28	26016.917	134.01	<.0001	.54
	Line Visibility	Tank	Figure 5-56	315	4, 28	25003.583	114.41	<.0001	.49
Gray Scale Levels	Image Quality	Truck	Figure 5-57	316	4, 28	20839.750	76.71	<.0001	.43
	Image Quality	Tank	Figure 5-58	317	4, 28	9704.333	24.03	.0003	.22
Gray Scale Distribution	Image Quality	Truck	Figure 5-59	318	2, 14	3313.500	4.88	.0496	.03
	Image Quality	Tank	Figure 5-60	319	2, 14	8720.667	15.62	.0035	.10
Gray Scale Levels x Gray Scale Distribution	Image Quality	Truck	Figure 5-61	320	8, 56	940.375	8.16	.0003	.04
	Image Quality	Tank	Figure 5-62	321	8, 56	258.583	2.93	.0479	.01

Aperture Ratio. FLIR line visibility ratings increased (i.e., lines became less apparent) monotonically as a function of increasing aperture ratio. Figure 5-56 and Figure 5-56), with each increase in aperture ratio associated with a significant increase in line visibility ratings ($p < .05$).

Gray Scale Levels. FLIR image quality ratings were significantly higher when the Truck image was presented with 64 gray scale levels (Figure 5-57), although the relative improvement in image quality was small beyond 24 levels. Specifically, the differences between ratings at 24 and 32 levels and between ratings at 32 and 64 levels were not statistically significant ($p > .05$). FLIR image quality ratings were significantly higher when the Tank image was presented with 16 gray scale levels (Figure 5-58).

Gray Scale Exponent. FLIR image quality ratings were significantly greater for the Truck image when presented with the intermediate gray scale distribution exponent (Figure 5-59). The FLIR Tank image received higher contrast ratings with either of the nonlinear gray scale distribution exponents (Figure 5-60).

Gray Scale Distribution x Gray Scale Levels Interaction. FLIR image quality ratings varied as an interaction of gray scale distribution and number of gray scale levels (Figure 5-61 and Figure 5-62). FLIR Truck image quality ratings were highest for linear or intermediate nonlinear gray scale presentations at 32 and 64 gray levels ($p < .05$). The Truck image presented with linear gray scale received low ratings equal to those given to the most nonlinear images at 24 gray levels and the lowest ratings at 16 gray levels ($p < .05$). At 8 gray levels there were no significant differences in ratings as a function of gray scale exponents ($p > .05$). FLIR Tank image quality ratings were lowest for all linear gray scale presentations, while images presented with the most nonlinear gray scale distribution generally received the highest ratings ($p < .05$). At 16 and 32 gray levels, images with the two nonlinear gray scale distributions were rated equally high ($p < .05$).

5.5.5 Summary

The results from Evaluation 4 are summarized in Table 5-14 and the following summary statements:

Table 5-14. Preliminary conclusions based on Evaluation 4 results.

Variable	Image Type	Rating Asymptote	Notes
Aperture Ratio	FLIR	>80%	Line visibility
Gray Scale Levels	FLIR	64 Levels of Gray	Diminishing returns beyond 24 levels
Gray Scale Distribution	FLIR	Nonlinear for light target Linear for dark target	Differences greatest at larger number of gray scale levels

1. The results of Evaluation 4 are highly consistent with those of Evaluation 3. Allowing luminance to covary with aperture ratio appears to have made little difference in line visibility or image quality ratings, with the possible exception that there was a less than two-point average increase in image ratings in Evaluation 4 relative to Evaluation 3 (Table 5-15). Otherwise, the following conclusions mirror those from Evaluation 3.

2. Visibility of row and column lines decreased monotonically (and almost linearly) with increases in aperture ratio across the full range of aperture ratios simulated (40% to 80%). None of the other simulation parameters reliably influenced ratings of line visibility. Aperture ratio did not have a reliable effect on overall image quality ratings (even though the differences were clearly visible, as indicated in the above conclusion). These conclusions are consistent with the results of Evaluation 3.
3. FLIR image quality improved with as many as 64 gray scale levels, although the relative improvement in image quality was generally small beyond 24 levels. This result is consistent with the results of Evaluation 3, and generally consistent with the earlier aliasing findings of Evaluation 2, although the aliasing results of Evaluation 2 failed to capture the same small gains realized at 64 gray scale levels.
4. Subjective ratings of image quality for the tank image were highest in either of the nonlinear gray scale conditions while ratings of image quality for the Truck image were generally higher as gray scale became more linear. Gray scale distribution differences in image quality ratings (above) were greatest for images with the highest number of gray scale levels. These conclusions are consistent with the results of Evaluation 3.

Table 5-15. Mean rating differences between Evaluations 3 and 4.

	Rating Scale	Image Type	Evaluation 3	Evaluation 4	Difference
Image Quality	Truck	39.950	42.600	2.650	
	Tank	46.342	47.566	1.224	
Line Visibility	Truck	45.457	47.200	1.743	
	Tank	45.767	47.133	1.366	

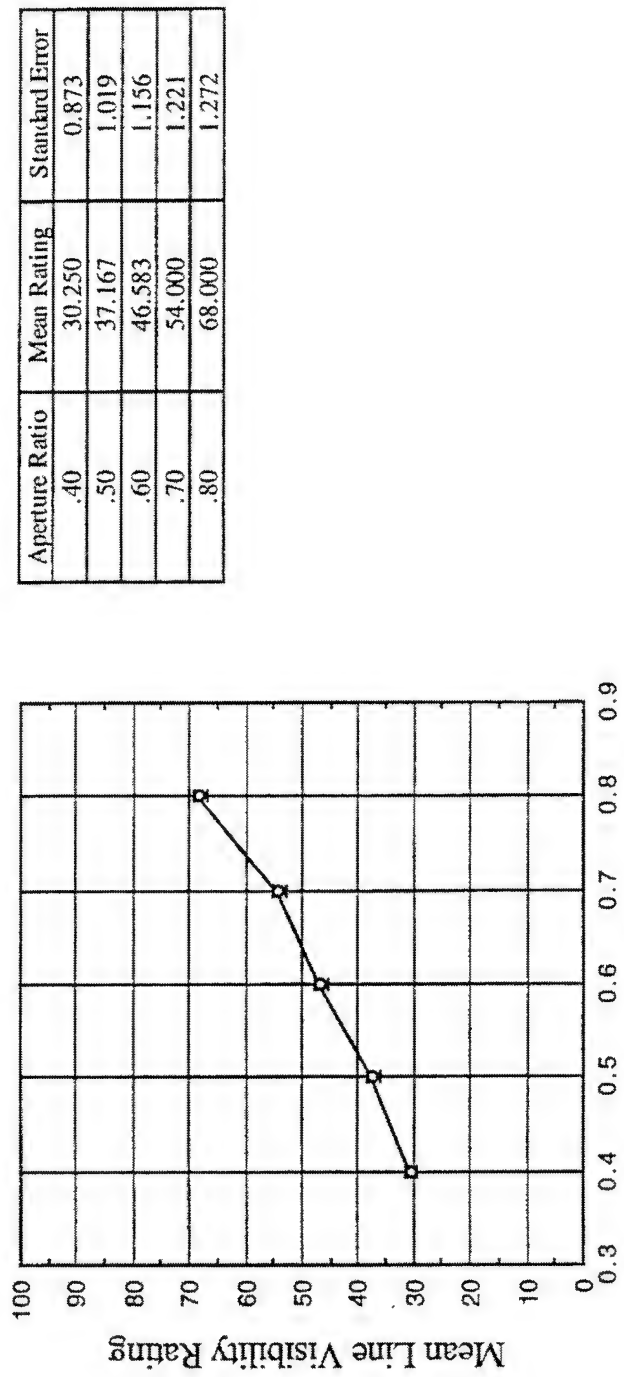


Figure 5-55. Mean Line Visibility Rating as a Function of Aperture Ratio (Evaluation 4, Truck).

High line visibility ratings indicate high subjective similarity of comparison images to the standard image (i.e., low visibility of row and column lines). Error bars show standard error of the mean.

Aperture Ratio	Mean Rating	Standard Error
.40	29.417	1.149
.50	39.750	1.315
.60	45.667	1.170
.70	53.000	1.145
.80	67.833	1.190

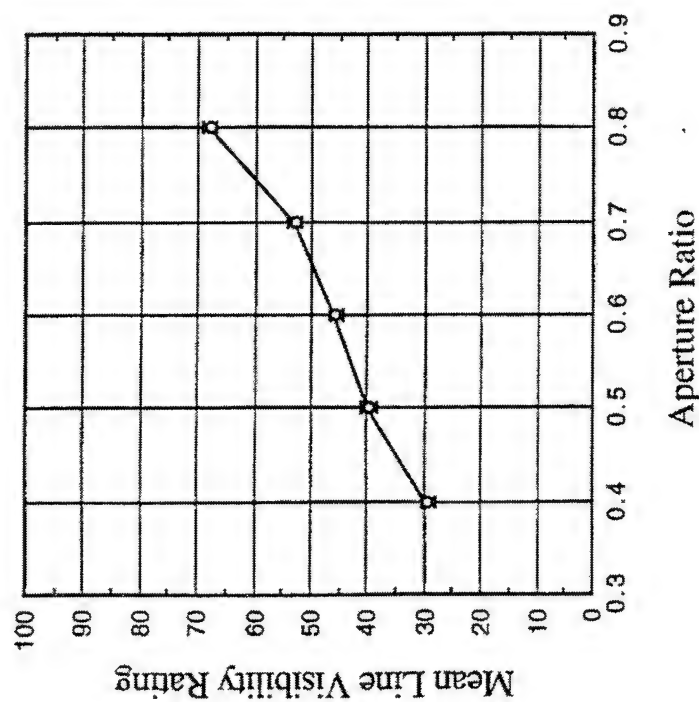


Figure 5-56. Mean Line Visibility Rating as a Function of Aperture Ratio (Evaluation 4, Tank).

High line visibility ratings indicate high subjective similarity of comparison images to the standard image (i.e., low visibility of row and column lines). Error bars show standard error of the mean.

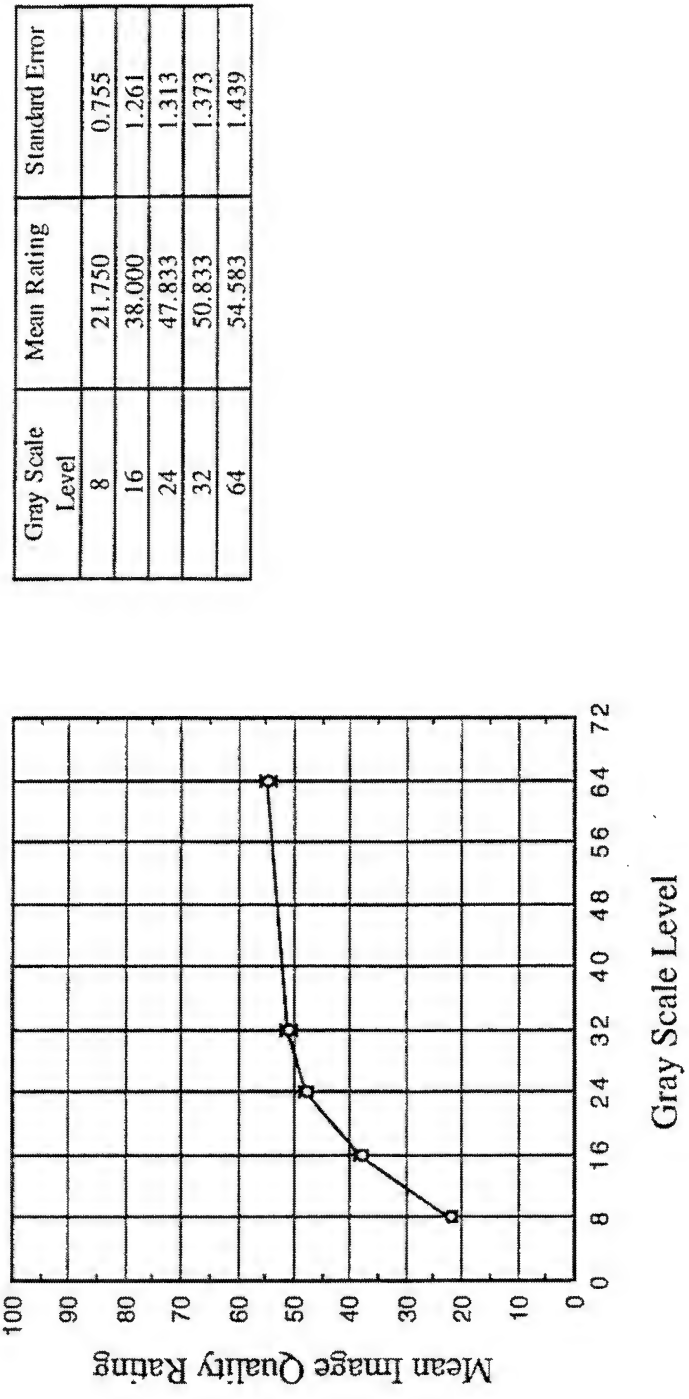


Figure 5-57. Mean Image Quality Rating as a Function of Gray Scale Level (Evaluation 4, Truck).

High image quality ratings indicate high subjective similarity of comparison images to the standard image (i.e., relatively high image quality). Error bars show standard error of the mean.

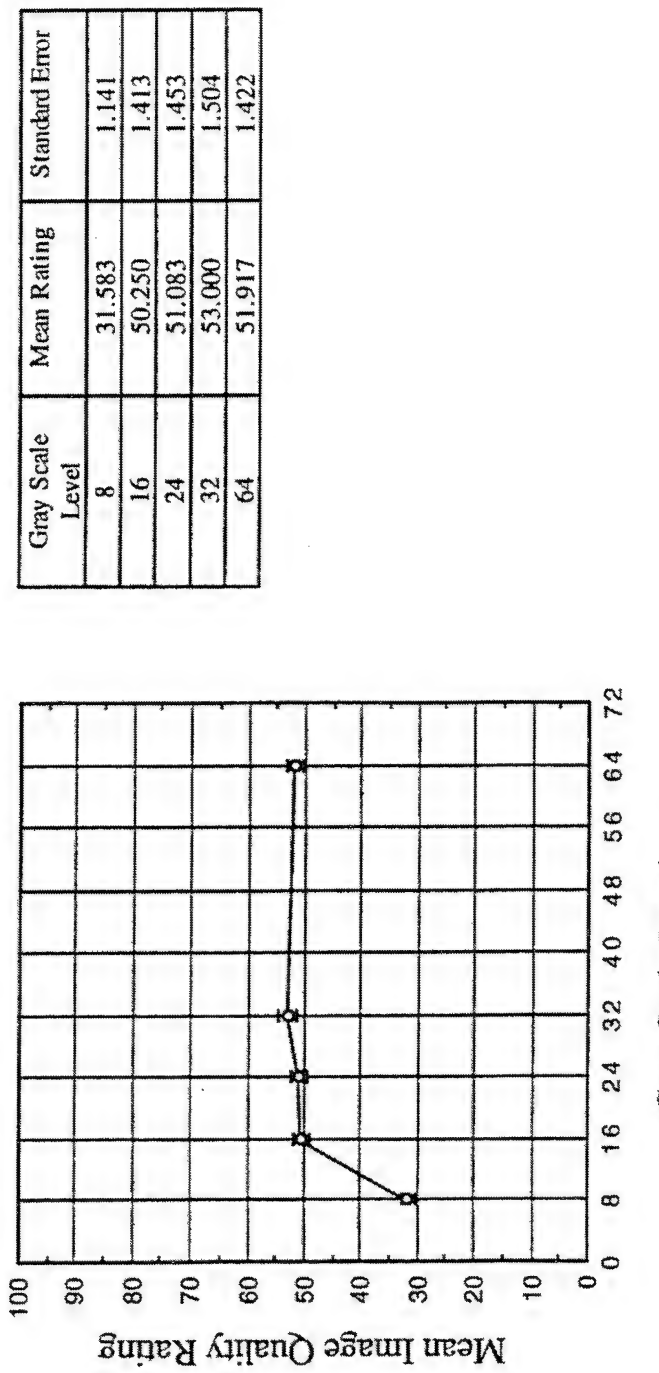


Figure 5-58. Mean Image Quality Rating as a Function of Gray Scale Level (Evaluation 4, Tank).

High image quality ratings indicate high subjective similarity of comparison images to the standard image (i.e., relatively high image quality). Error bars show standard error of the mean.

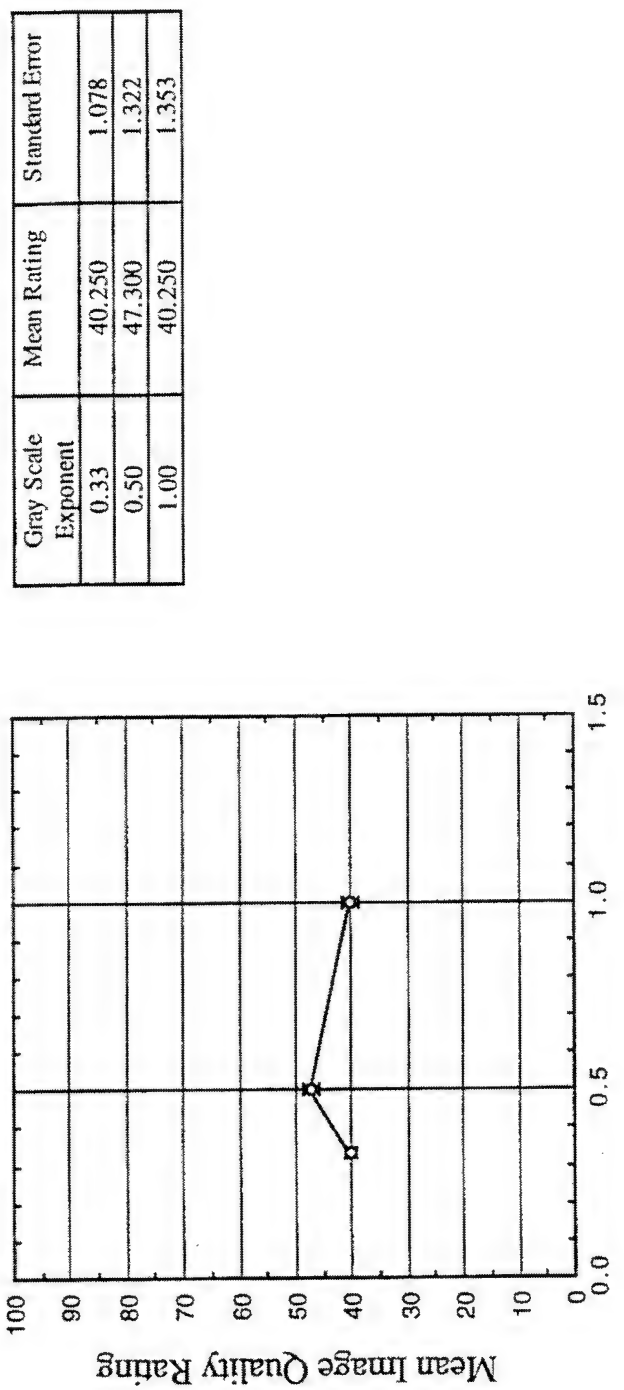


Figure 5-59. Mean Image Quality Rating as a Function of Gray Scale Exponent (Evaluation 4, Truck).

High image quality ratings indicate high subjective similarity of comparison images to the standard image (i.e., relatively high image quality). Error bars show standard error of the mean.

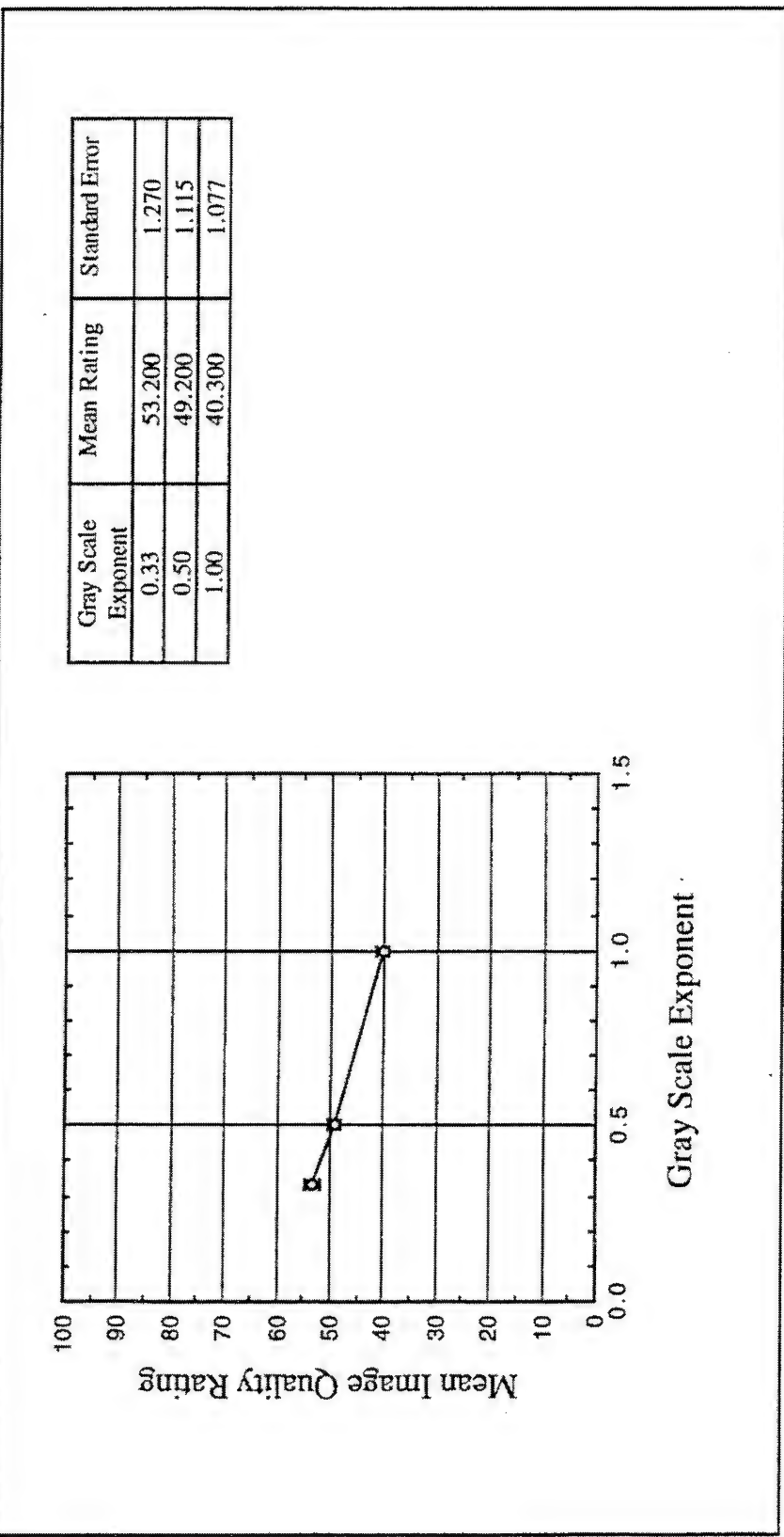


Figure 5-60. Mean Image Quality Rating as a Function of Gray Scale Exponent (Evaluation 4, Tank).

High image quality ratings indicate high subjective similarity of comparison images to the standard image (i.e., relatively high image quality). Error bars show standard error of the mean.

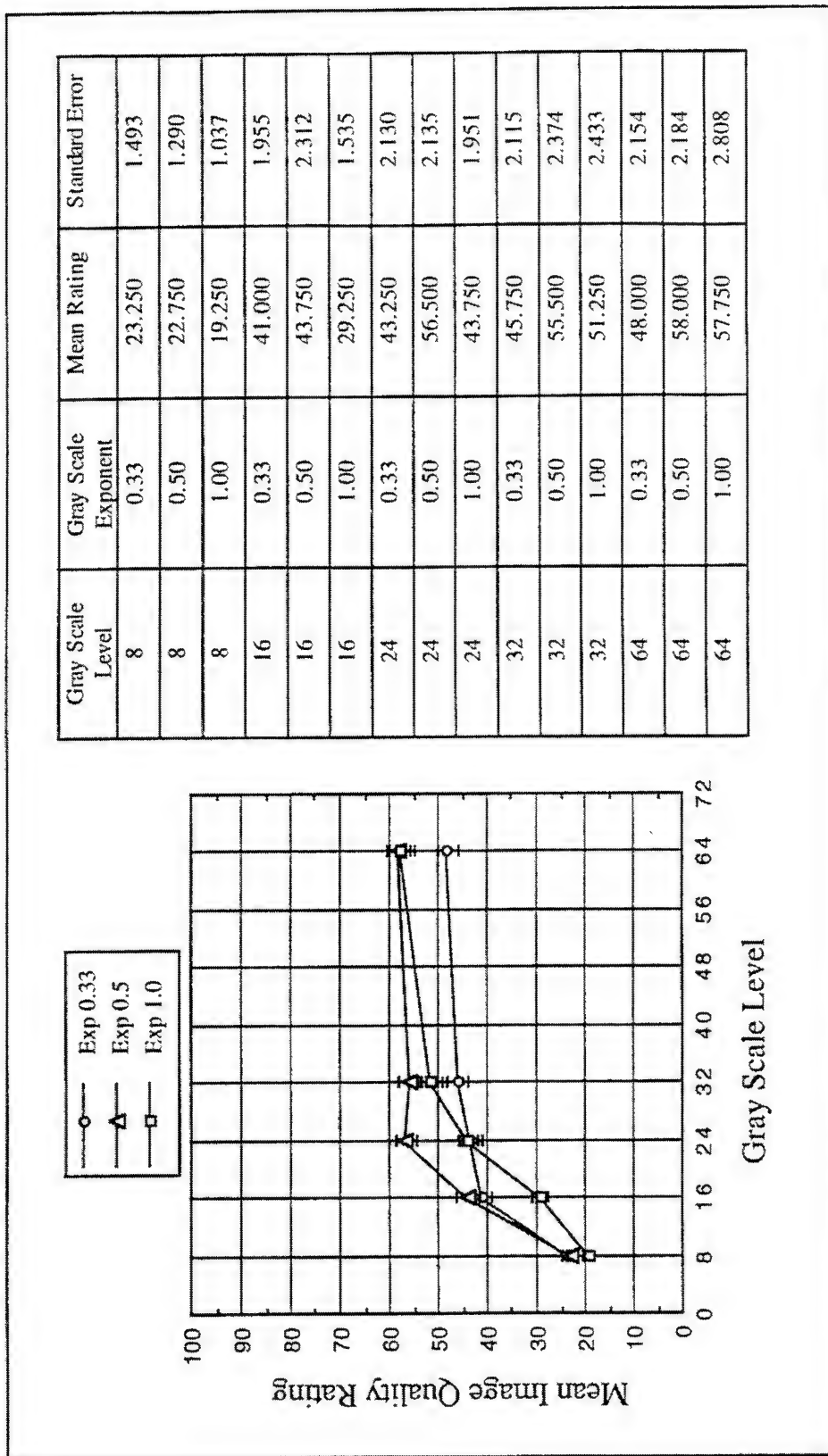


Figure 5-61. Mean Image Quality Rating as a Function of Gray Scale Level by Gray Scale Exponent (Evaluation 4, Truck).

High image quality ratings indicate high subjective similarity of comparison images to the standard image (i.e., relatively high image quality). Error bars show standard error of the mean.

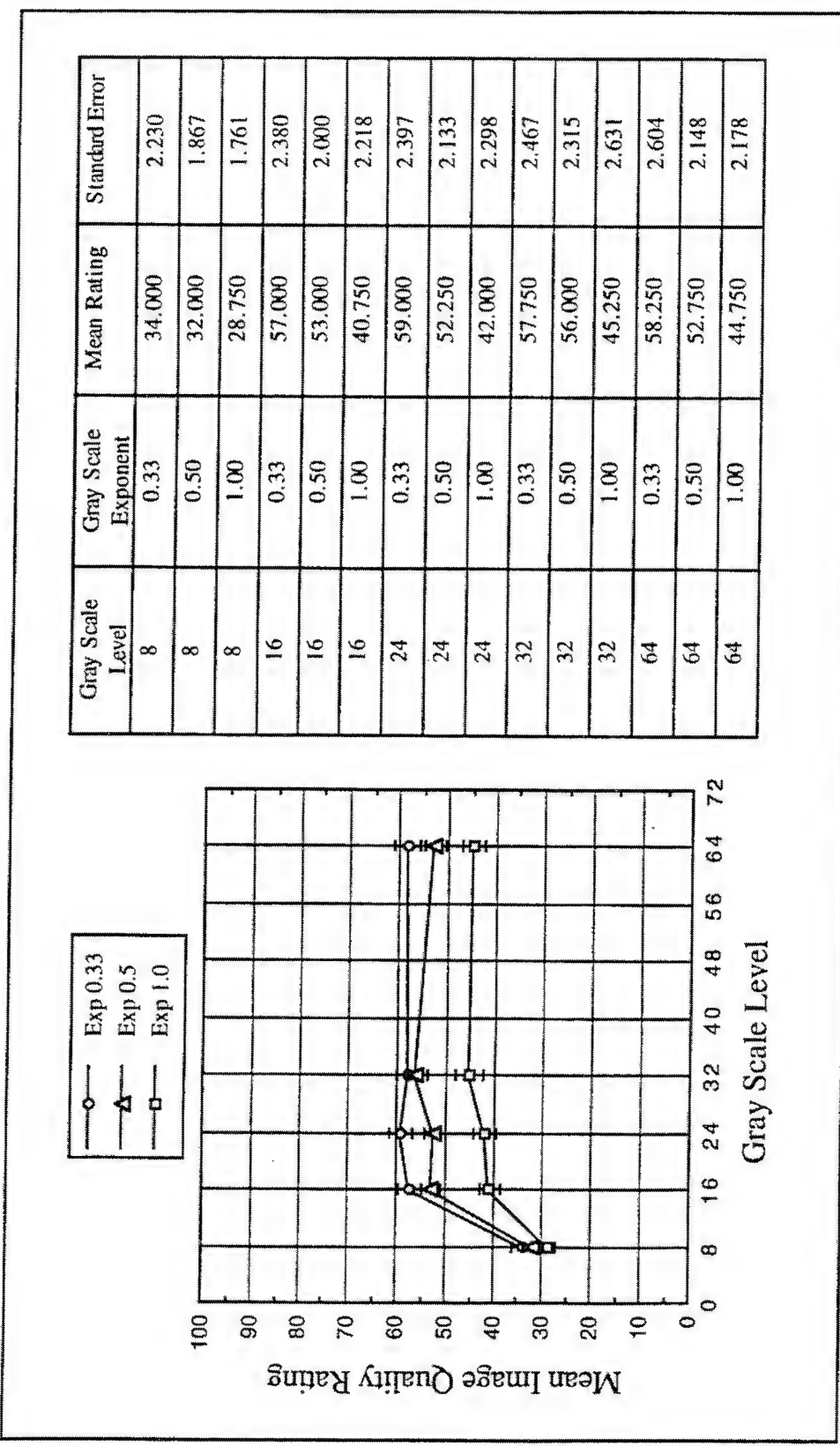


Figure 5-62. Mean Image Quality Rating as a Function of Gray Scale Level by Gray Scale Exponent (Evaluation 4, Tank).
High image quality ratings indicate high subjective similarity of comparison images to the standard image (i.e., relatively high image quality). Error bars show standard error of the mean.

5.6 Evaluation 5

5.6.1 Objectives

Evaluation 5 was conducted to compare the subjective quality of subtractive and additive color image sources of various aperture ratios, colors, and resolutions. The specific objectives of Evaluation 5 were:

1. Further assess the relative impact of aperture ratio on perception of FLIR line visibility and image quality.
2. Evaluate the relative impact of additive vs subtractive color pixel structures on perception of FLIR line visibility and image quality.
3. Determine the perceptual impact of diffraction of the red layer in a subtractive color stack.
4. Evaluate the sensitivity of a new rating scale, sharpness, to image blurring associated with red diffraction.
5. Assess the relative change in impact of red diffraction between red and yellow images.
6. Determine how changes in image source resolution, above and below the baseline HMS+ resolution, impact all of the above.

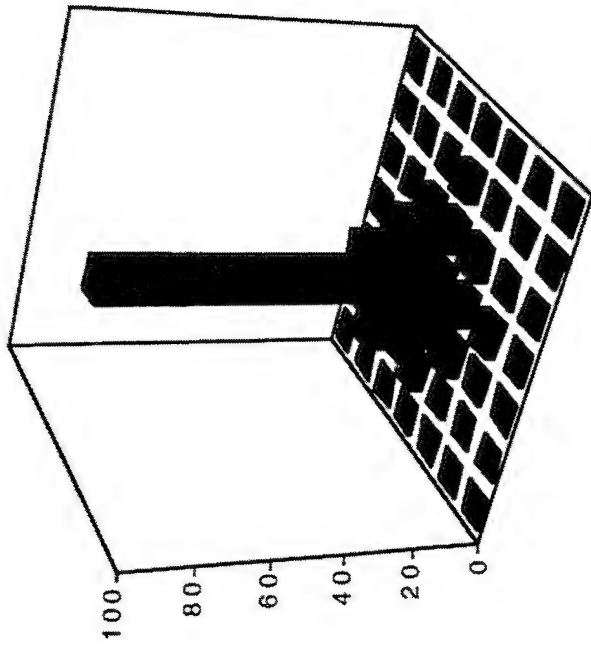
5.6.2 Design

Evaluation 5 images were modeled using subtractive and additive color image source models with varied aperture ratios and colors, using the two original FLIR images described previously. Half of the subtractive color image source models included diffraction of the red layer (Figure 5-63 and Figure 5-64, p. 325). Comparison image luminance was held constant among aperture ratio and color method, such that equivalent images modeled with different image sources were of equal luminance (the luminance of the standard image was not reduced). Images of different colors, however, did vary in luminance (yellow images were of higher luminance than red images). Comparison images were presented at resolutions of between 11 and 33 simulated AMLCD pixels per degree. Resolution was controlled by increasing or decreasing participant viewing distance (image field of view and stimulus size therefore covaried with resolution). FLIR images were subjected to gray scale level clipping and distribution as previously described under *Simulation Software*. Comparison images were presented at 64 gray scale levels with a linear distribution in red or yellow.

The simulation design levels included in Evaluation 5 are summarized in Table 5-16. Figures illustrating variables are referenced in the table where available.

Table 5-16. Design variables for Evaluation 5.

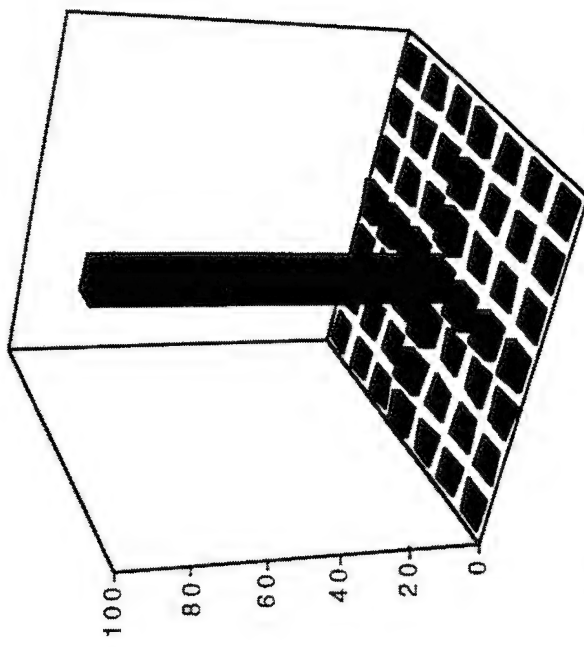
Variable	Levels	Figure	Page
FLIR Image	Truck, Tank	(see <i>Software Imagery</i>)	Figure 5-11 (p. 240)
Resolution	11, 22, 33 pix/deg	(not illustrated)	
Color	Red, Yellow	Figure 5-65, Figure 5-66	327
Image Source	Additive (40% AR), Subtractive (40% AR) (with or without diffraction), Subtractive (70% AR) (with or without diffraction)	Figure 5-65, Figure 5-66 Figure 5-67, Figure 5-68 Figure 5-69, Figure 5-70	327 329 331



	1	2	3	4	5	6	7
1	0.000798	0.009775	0.060000	0.282500	0.060000	0.009775	0.000798
2	0.009775	0.120000	0.733750	3.462500	0.733750	0.120000	0.009775
3	0.060000	0.733750	4.490750	21.19150	4.490750	0.733750	0.060000
4	0.282500	3.462500	21.19150	100.000	21.1915	3.462500	0.282500
5	0.060000	0.733750	4.490750	21.19150	4.490750	0.733750	0.060000
6	0.009775	0.120000	0.733750	3.462500	0.733750	0.120000	0.009775
7	0.000798	0.009775	0.060000	0.282500	0.060000	0.009775	0.000798

Figure 5-63. Convolution Kernel Applied to Red Layer of Subtractive Color Images in Evaluations 5 Through 10 (40% AR).

Values from the original diffraction model, which ranged from 0-40%, were normalized to 100% and convolved with the original image. Convolution occurred prior to application of the 6x6 AMLCD mask.



	1	2	3	4	5	6	7
1	0.025857	0.042571	0.056000	1.606710	0.056000	0.042571	0.025857
2	0.042571	0.070143	0.092429	2.647710	0.092429	0.070143	0.042571
3	0.056000	0.092429	0.121714	3.488430	0.121714	0.092429	0.056000
4	1.606710	2.647710	3.488430	100.0000	3.488430	2.647710	1.606710
5	0.056000	0.092429	0.121714	3.488430	0.121714	0.092429	0.056000
6	0.042571	0.070143	0.092429	2.647710	0.092429	0.070143	0.042571
7	0.025857	0.042571	0.056000	1.606710	0.056000	0.042571	0.025857

Figure 5-64. Convolution Kernel Applied to Red Layer of Subtractive Color Images in Evaluations 5 through 10 (70% AR).

Values from the original diffraction model, which ranged from 0-70%, were normalized to 100% and convolved with the original image. Convolution occurred prior to application of the 6x6 AMLCD mask.

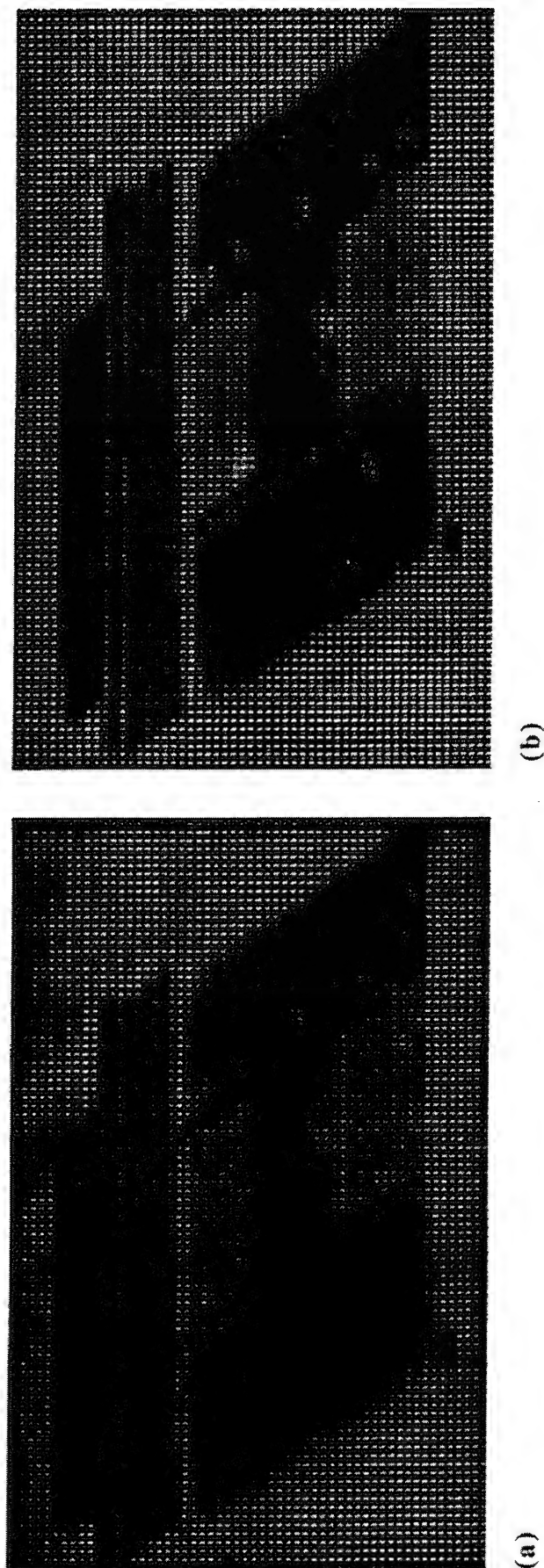


Figure 5-65. Additive Color Image Source (40% AR) Modeled in Evaluations 5, 6, and 9 for FLIR Truck Images

One primary (red, a) and two primaries (yellow, b). Images shown here were used in all three evaluations. Note that evaluation images were actually presented in color on a high-resolution CRT. Also, these printed gray scale images are not gamma-corrected for printing. In addition, their size as printed is not intended to simulate the angular resolutions tested in the evaluations.

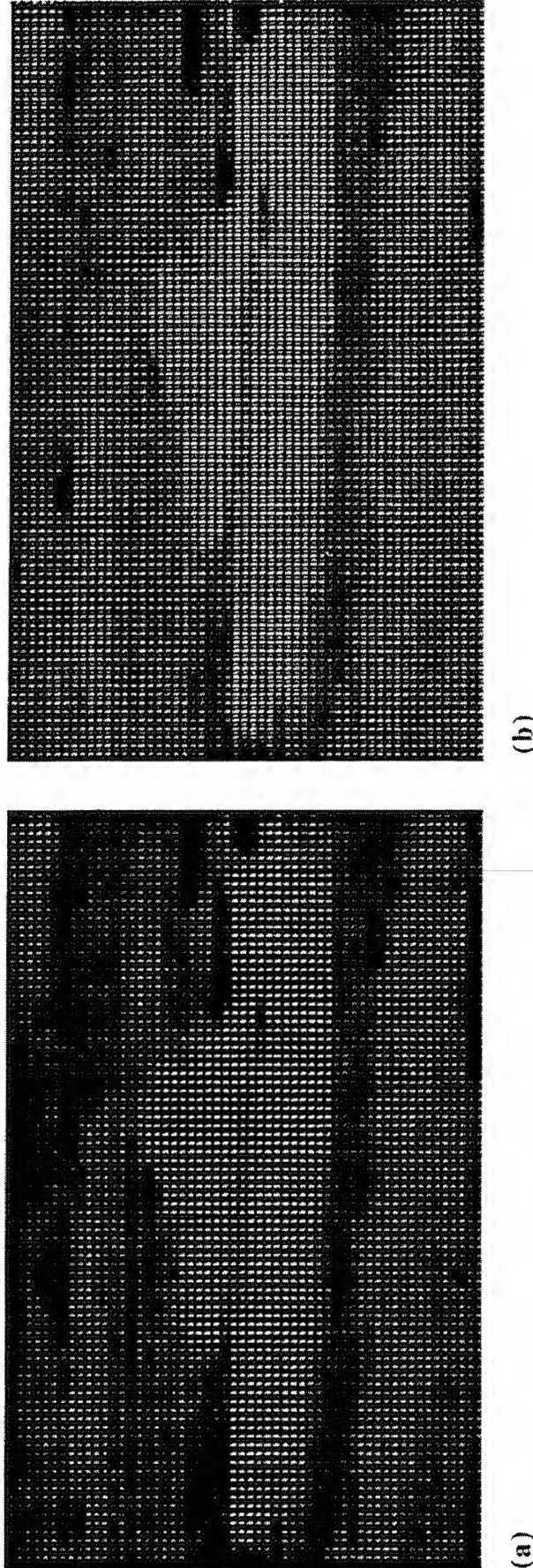


Figure 5-66. Additive Color Image Source (40% AR) Modeled in Evaluations 5, 6, and 9 for FLIR Tank Images.

One primary (red, a) and two primaries (yellow, b). Images shown are from Evaluation 6 (luminance covaried with aperture ratio). Luminance was not allowed to covary with aperture ratio in Evaluations 5 and 9. Note that evaluation images were actually presented in color on a high-resolution CRT. Also, these printed gray scale images are not gamma-corrected for printing. In addition, their size as printed is not intended to simulate the angular resolutions tested in the evaluations.

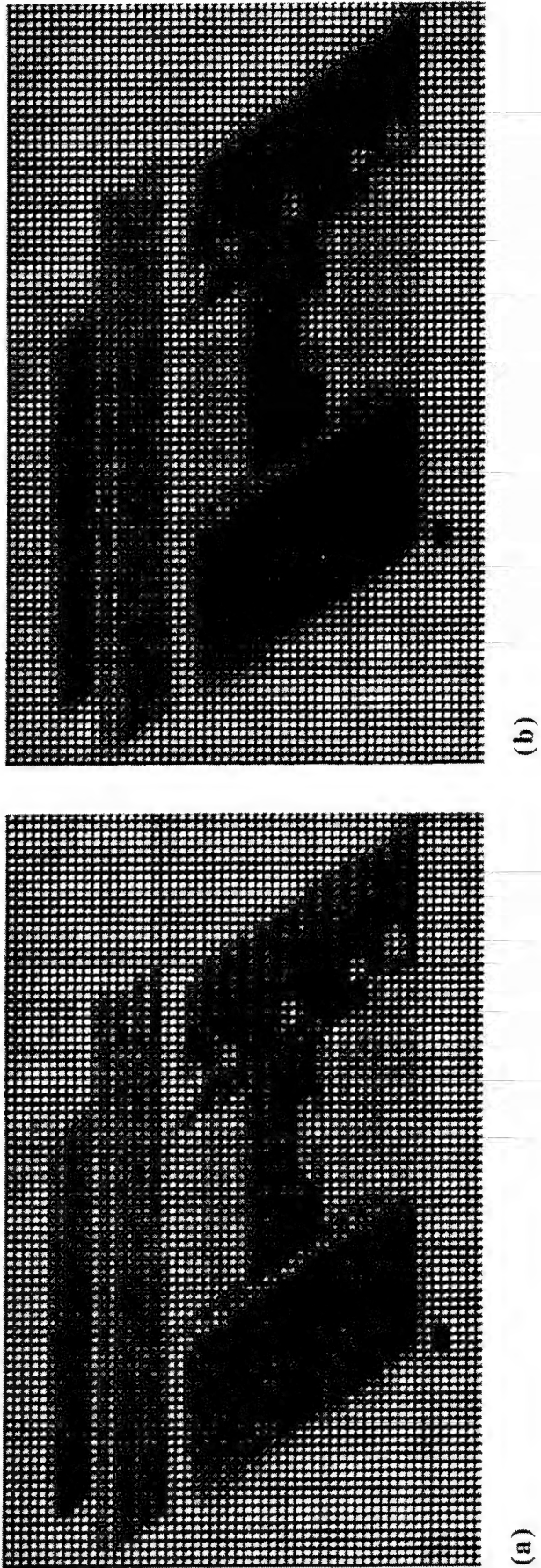
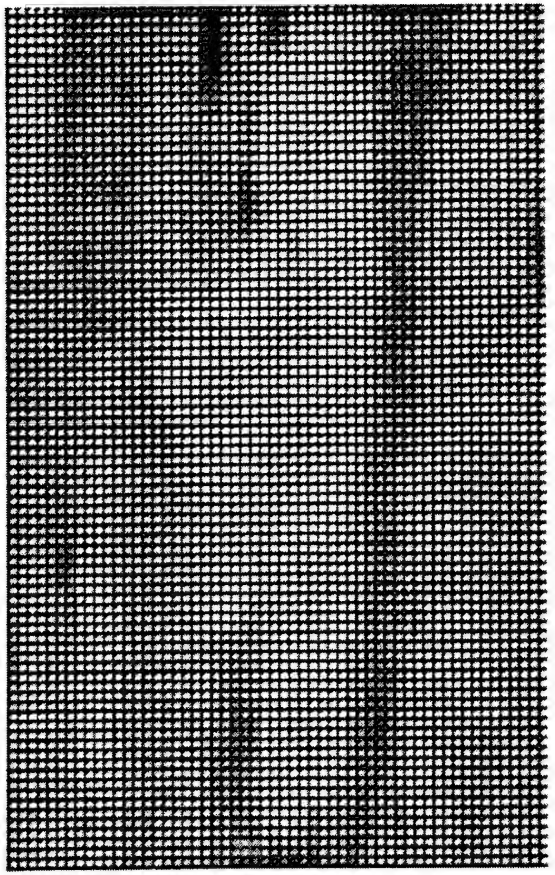
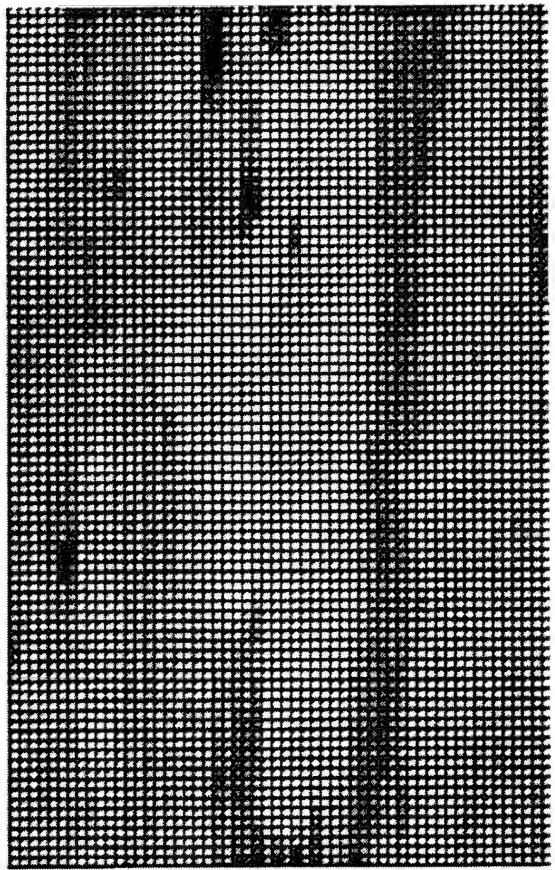


Figure 5.67. Subtractive Color Image Source (40% AR) Modeled in Evaluations 5, 6, and 9 for FLIR Truck Images.

Without (a) and with (b) diffraction of the red layer. Images shown here are from Evaluation 6 (luminance covaried with aperture ratio). Luminance was not allowed to covary with aperture ratio in Evaluations 5 and 9. Note that evaluation images were actually presented in color on a high-resolution CRT. Also, these printed gray scale images are not gamma-corrected for printing. In addition, their size as printed is not intended to simulate the angular resolutions tested in the evaluations.



(a)



(b)

Figure 5-68. Subtractive Color Image Source (40% AR) Modeled in Evaluations 5, 6, and 9 for FLIR Tank Images.

Without (a) and with (b) diffraction of the red layer. Images shown here are from Evaluation 6 (luminance covaried with aperture ratio). Luminance was not allowed to covary with aperture ratio in Evaluations 5 and 9. Note that evaluation images were actually presented in color on a high-resolution CRT. Also, these printed gray scale images are not gamma-corrected for printing. In addition, their size as printed is not intended to simulate the angular resolutions tested in the evaluations.

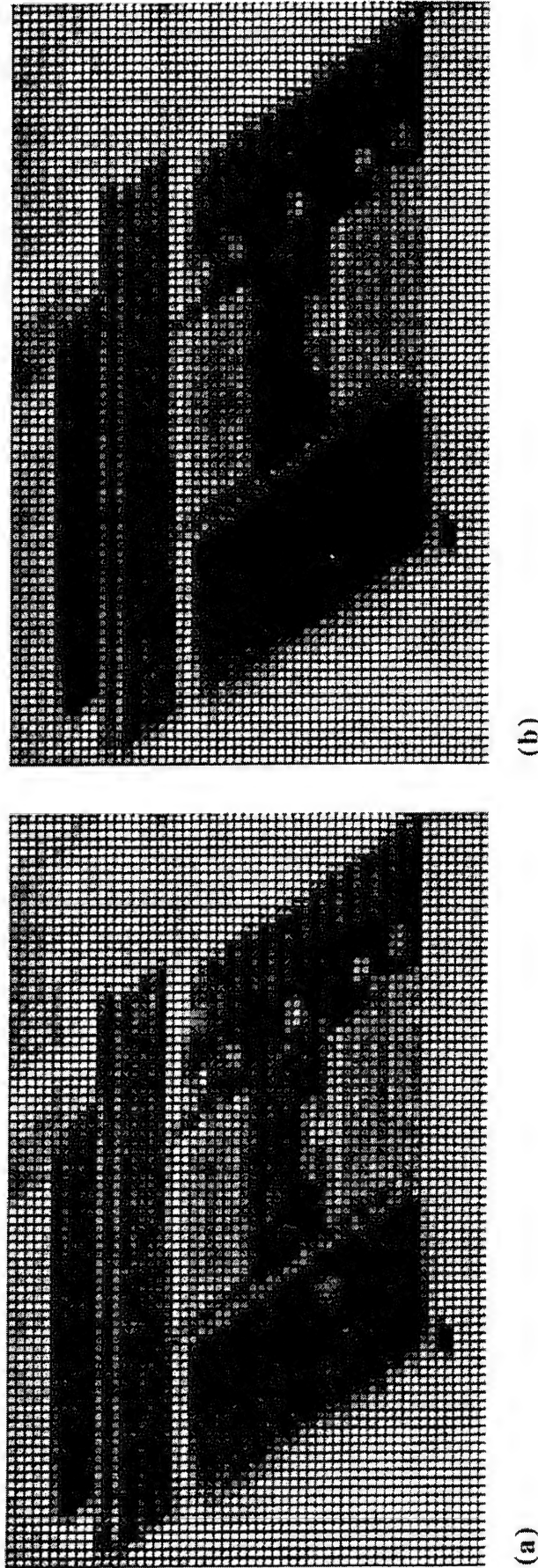
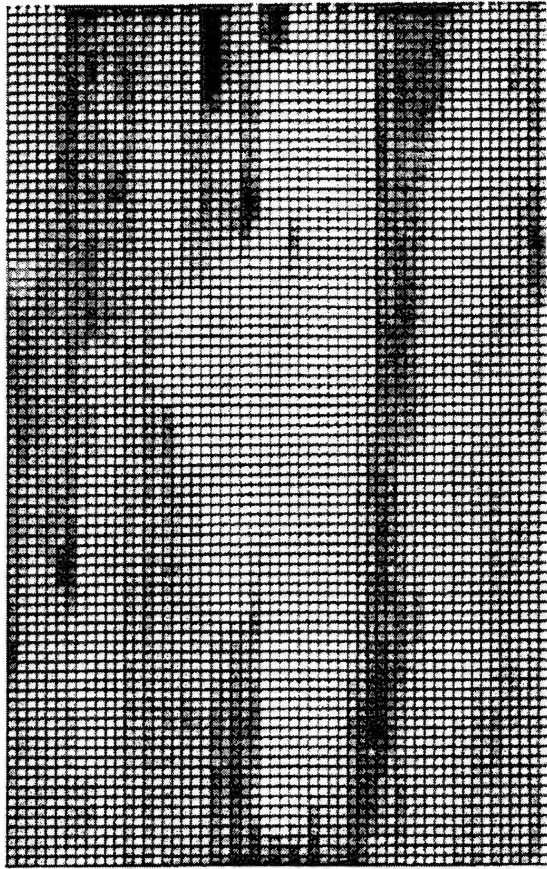


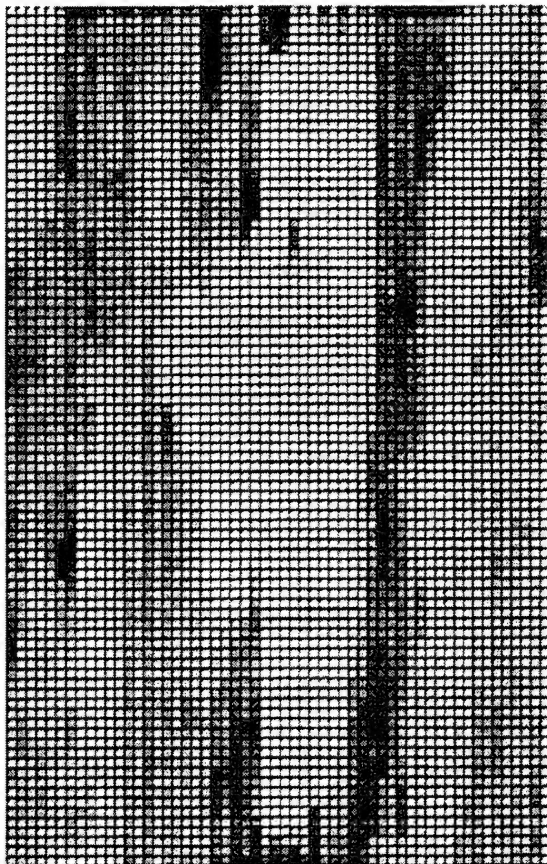
Figure 5-69. Subtractive Color Image Source (70% AR) Modeled in Evaluations 5, 6, and 9 for FLIR Truck Images.

Without (a) and with (b) diffraction of the red layer. Images shown here are from Evaluation 6 (luminance covaried with aperture ratio). Luminance was not allowed to covary with aperture ratio in Evaluations 5 and 9. Note that evaluation images were actually presented in color on a high-resolution CRT.

Also, these printed gray scale images are not gamma-corrected for printing. In addition, their size as printed is not intended to simulate the angular resolutions tested in the evaluations.



(b)



(a)

Figure 5.70. Subtractive Color Image Source (70% AR) Modeled in Evaluations 5, 6, and 9 for FLIR Tank Images.

Without (a) and with (b) diffraction of the red layer. Images shown here are from Evaluation 6 (luminance covaried with aperture ratio). Luminance was not allowed to covary with aperture ratio in Evaluations 5 and 9. Note that evaluation images were actually presented in color on a high-resolution CRT.

Also, these printed gray scale images are not gamma-corrected for printing. In addition, their size as printed is not intended to simulate the angular resolutions tested in the evaluations.

5.6.3 Procedure

The two rating scales (line visibility and image quality) that were used in Evaluation 4 were also used in Evaluation 5. In addition, a new subjective rating scale (sharpness) was used to evaluate imagery in Evaluation 5 (Figure 5-71, p. 334). The sharpness scale was used to capture subjective visibility of image blurring associated with diffraction of the red layer of subtractive color image sources. For each comparison image, a separate rating was made on each scale. Participants were instructed to make their image ratings relative to the standard image. Eight participants followed the general evaluation procedure described previously, using the simultaneous comparison procedure and rating 20 practice images and 120 evaluation trials during a 60 minute period. The order of image presentation was randomized within blocks of FLIR image (Truck or Tank) for each observer. Image order was further blocked within image type by resolution, with order of resolution counterbalanced among participants.

Sharpness (Evaluations 5, 6, and 9):

The degree to which the comparison image appears to present clear detail and is free from a blurry appearance relative to the standard image.

10%	Image is unclear and very blurry
20%	
30%	
40%	
50%	Image is about half as clear and free of blur as the standard
60%	
70%	
80%	
90%	
100%	Image is as sharp and free of blur as the standard image

Figure 5-71. Sharpness Rating Scale Used in Evaluations 5, 6, and 9.

5.6.4 Results

Table 5-17 provides an overview of the significant data trends. Separate ANOVA procedures were run for the types of FLIR images. The effects summarized in the table are discussed in the text following the table.

Table 5-17. ANOVA summary table for Evaluation 5.

Effect	Dependent Variable	Image	Figure	Page	df	MS	F	P	R ²
Resolution	Line Visibility	Truck	Figure 5-72	338	2, 14	13886.250	17.89	.0017	.16
	Line Visibility	Tank	Figure 5-73	339	2, 14	13261.250	14.46	.0017	.16
Color	Image Quality	Truck	Figure 5-74	340	1, 7	3920.417	16.50	.0048	.04
	Line Visibility	Truck	Figure 5-75	341	4, 28	3672.917	18.92	.0012	.08
Image Source	Line Visibility	Tank	Figure 5-76	342	4, 28	5553.542	16.19	.0022	.13
	Sharpness	Truck	Figure 5-77	343	4, 28	446.458	3.89	.0235	.02
Sharpness	Image Quality	Tank	Figure 5-78	344	4, 28	1070.417	8.41	.0027	.05
	Image Quality	Truck	Figure 5-79	345	4, 28	395.833	4.12	.0313	.02
Color x Image Source	Image Quality	Tank	Figure 5-80	346	4, 28	950.417	9.79	.0017	.04
	Sharpness	Tank	Figure 5-81	347	4, 28	639.167	7.82	.0041	.03
Resolution x Image Source	Image Quality	Tank	Figure 5-82	348	4, 28	456.667	5.36	.0096	.02
	Line Visibility	Tank	Figure 5-83	349	8, 56	466.979	3.79	.0186	.02
Image Source									.34

Resolution. FLIR line visibility ratings increased (i.e., lines became less apparent) as a function of increasing resolution (Figure 5-72 and Figure 5-73). While the differences in ratings between 11 and 22 pix/deg followed this trend, they were not statistically robust ($p>.05$).

Color. Yellow FLIR Truck images received higher image quality ratings relative to red Truck images (Figure 5-74).

Image Source. FLIR line visibility ratings were significantly greater (i.e., lines were less apparent) for image sources modeled at 70% AR relative to those modeled at 40% AR, regardless of diffraction effects (Figure 5-75 and Figure 5-76).

FLIR sharpness ratings were lower for the images modeled with the 40% AR subtractive color image source with diffraction relative to the other subtractive color image sources (Figure 5-77 and Figure 5-78). Sharpness ratings at the 70% AR followed this trend (diffracted vs nondiffracted), but the differences were not statistically robust ($p>.05$).

For the Truck image (Figure 5-79) images modeled with the two nondiffracted subtractive color image sources were rated as superior in image quality to images modeled with the additive color or either of the diffracted subtractive color images sources. FLIR image quality ratings were higher for Tank images modeled with the nondiffracted 40% AR subtractive color image source than ratings for either the diffracted 40% AR subtractive color image source or the additive color image source (Figure 5-80). In addition, image quality ratings for Tank images modeled with a 70% aperture ratio were higher than for images modeled with the nondiffracted 40% AR subtractive color image source.

Image Color x Image Source Interaction. FLIR sharpness ratings generally varied as an interaction of image color and image source. For yellow Tank images (Figure 5-81), sharpness ratings did not vary significantly. For red Tank images, sharpness ratings were greater for all image sources relative to the diffracted 40% AR subtractive image source. A similar trend with respect to yellow Truck images was apparent, but the interaction was not statistically robust ($p>.05$).

FLIR image quality ratings varied as an interaction of Tank image color and image source (Figure 5-82). Image quality ratings for yellow Tank images did not vary as a function of image source. For red Tank images, image quality ratings were equally high for images modeled with either of the 70% AR subtractive image sources or the nondiffracted 40% subtractive color image source, with the lowest image quality ratings given to images modeled with the diffracted 40% AR subtractive color image source ($p<.05$).

Resolution x Image Source Interaction. FLIR line visibility ratings varied as an interaction of Tank image resolution and image source (Figure 5-83). Line visibility ratings were generally highest (i.e., lines were less apparent) for images modeled with either subtractive color image source at 70% AR relative to images modeled with the additive color or either 40% AR subtractive color image source. However, the magnitude of these differences diminished with increased resolution.

5.6.5 Summary

The results from Evaluation 5 are summarized in Table 5-18 and the following summary statements:

Table 5-18. Preliminary conclusions based on Evaluation 5 results.

Variable	Image Type	Rating Asymptote	Notes
Resolution	FLIR	$\geq 33 \text{ pix/deg}$	Line visibility
Color	FLIR	Yellow > Red	Minimizes red diffraction effects Higher luminance possible
Subtractive vs Additive	FLIR	Subtractive	Limited additive aperture ratio
Aperture Ratio	FLIR	$\geq 70\%$	Line visibility

1. The visibility of row and column lines generally decreased with increases in resolution.
2. Subjective image quality was higher for yellow FLIR Truck images than for red FLIR Truck images. Luminance was controlled among AR conditions but not between colors, so this difference may largely be attributed to the brightness difference between colors, as well as green masking of the diffraction of the red layer in images modeled with the diffracted subtractive color image source.
3. The visibility of row and column lines was lower for images modeled with the 70% AR subtractive image sources as compared to the 40% AR subtractive and additive image sources, but image source differences in subjective line visibility became less pronounced as resolution increased.
4. Subjective image sharpness was lower for the images modeled with the diffracted 40% AR image source than for other subtractive color image sources. This difference was visible for red images but not yellow images.
5. Subtractive color image diffraction was associated with lower image quality ratings for red images at 40% AR. The impact of diffraction on image quality was less robust at 70% AR, and nonexistent for yellow images, where the green contribution was not diffracted.
6. Images modeled with the additive color image source and the diffracted 40% AR subtractive image source were rated equally low in terms of image quality. Images modeled with the 70% AR image sources generally received the highest image quality ratings.

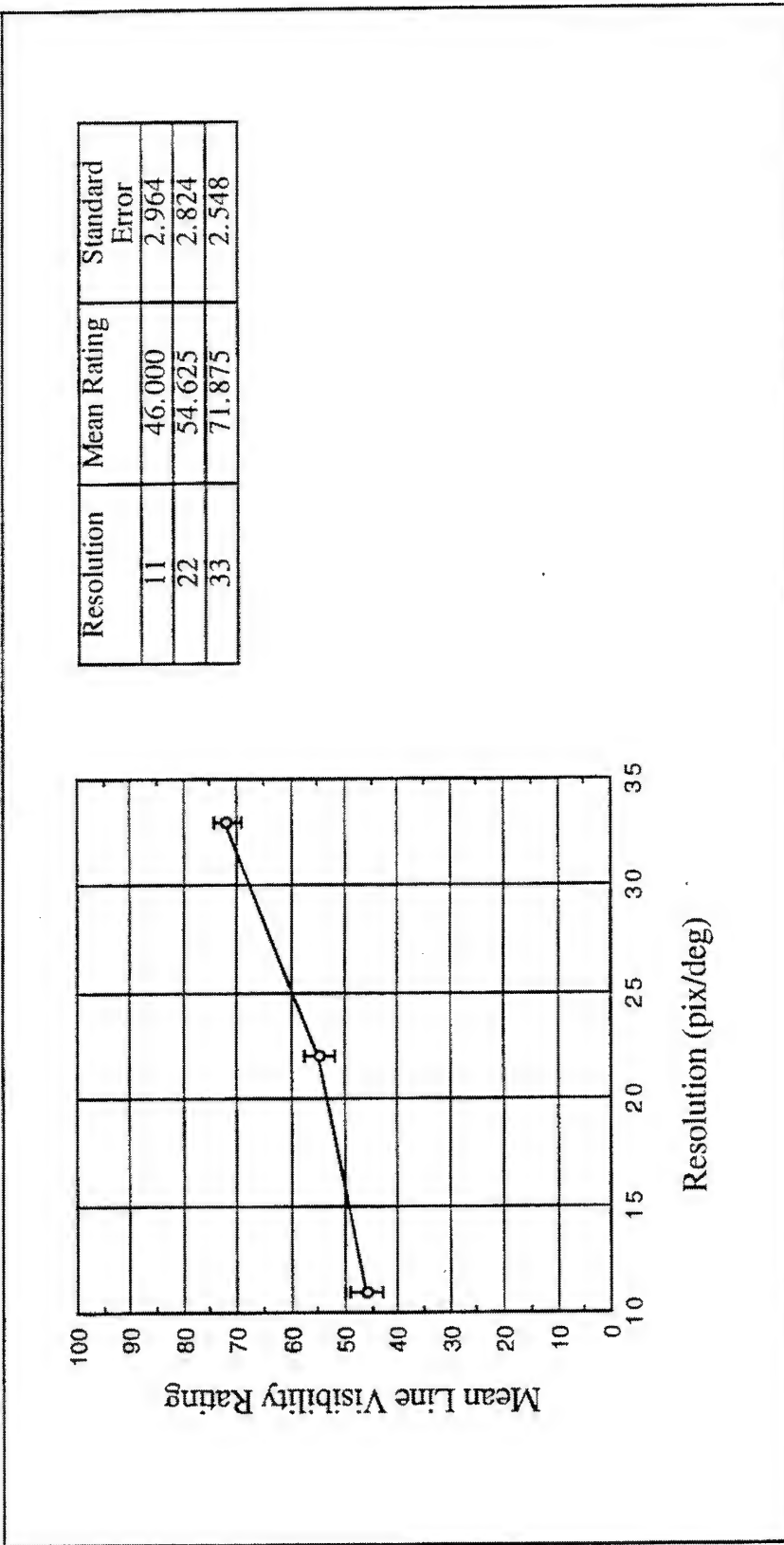


Figure 5-72. Mean Line Visibility Rating as a Function of Resolution (Evaluation 5, Truck).

High line visibility ratings indicate high subjective similarity of comparison images to the standard image (i.e., low visibility of row and column lines). Error bars show standard error of the mean.

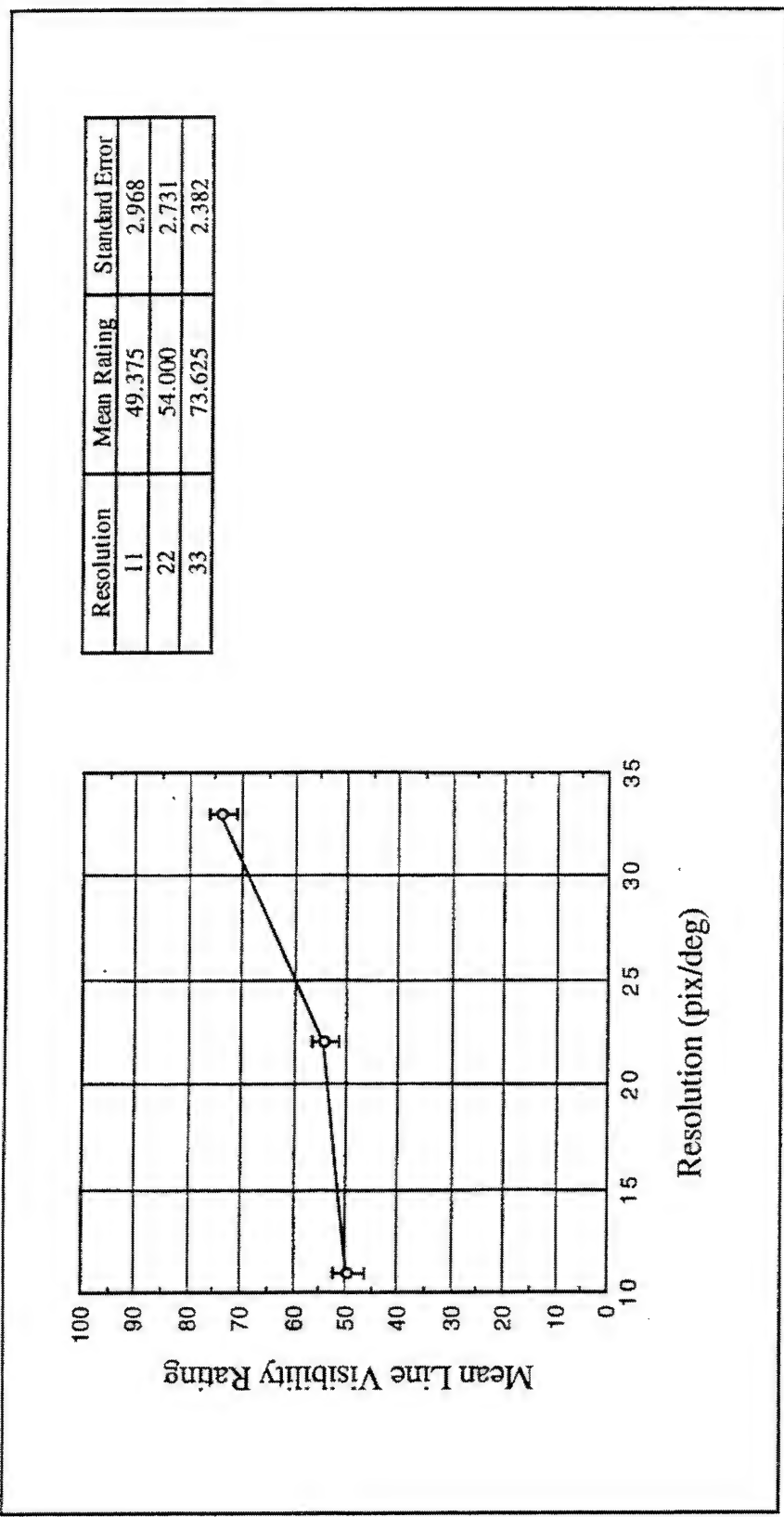


Figure 5-73. Mean Line Visibility Rating as a Function of Resolution (Evaluation 5, Tank).

High line visibility ratings indicate high subjective similarity of comparison images to the standard image (i.e., low visibility of row and column lines). Error bars show standard error of the mean.

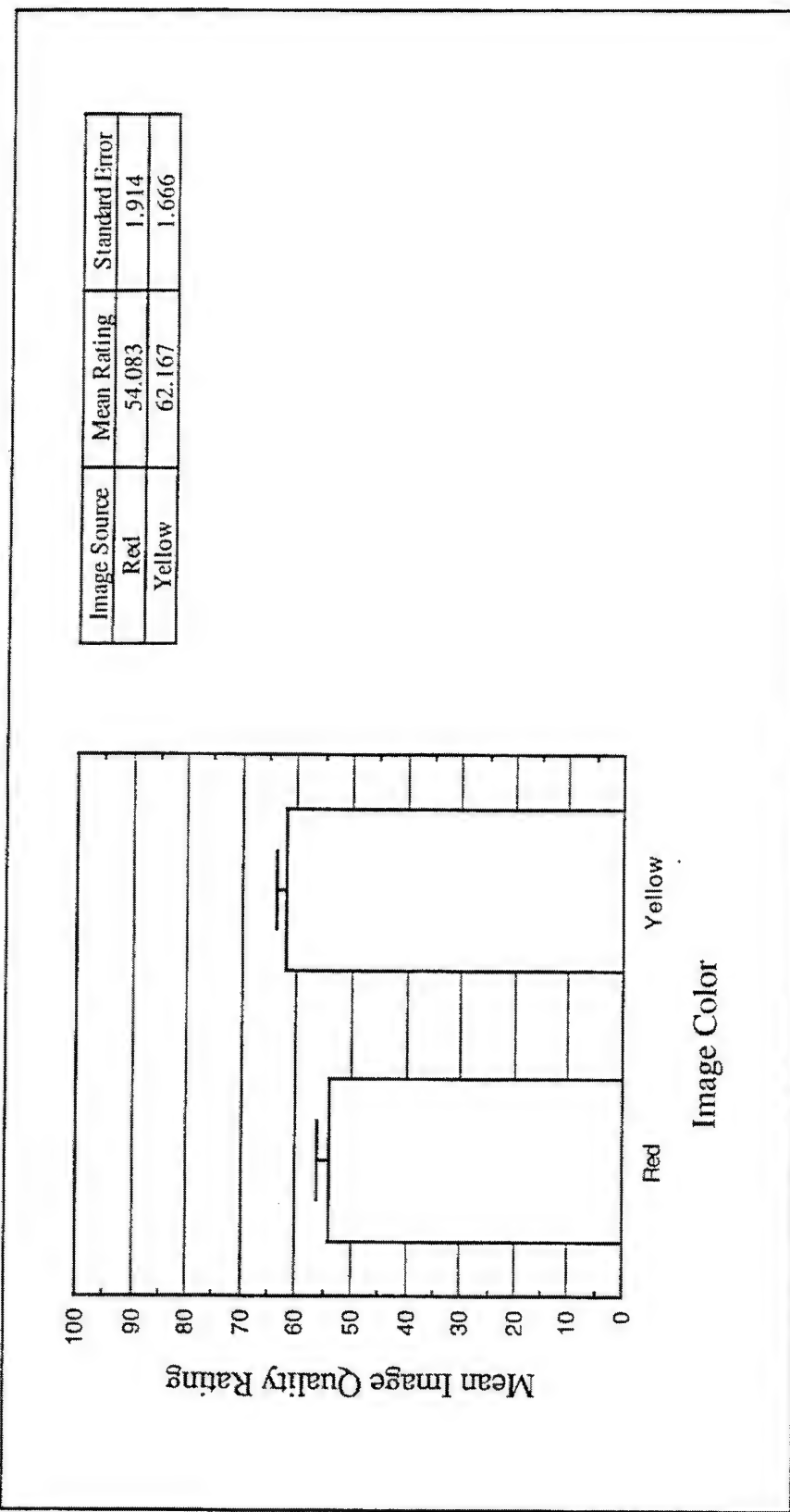


Figure 5-74. Mean Image Quality Rating as a Function of Image Color (Evaluation 5, Truck).

High image quality ratings indicate high subjective similarity of comparison images to the standard image (i.e., relatively high image quality). Error bars show standard error of the mean.

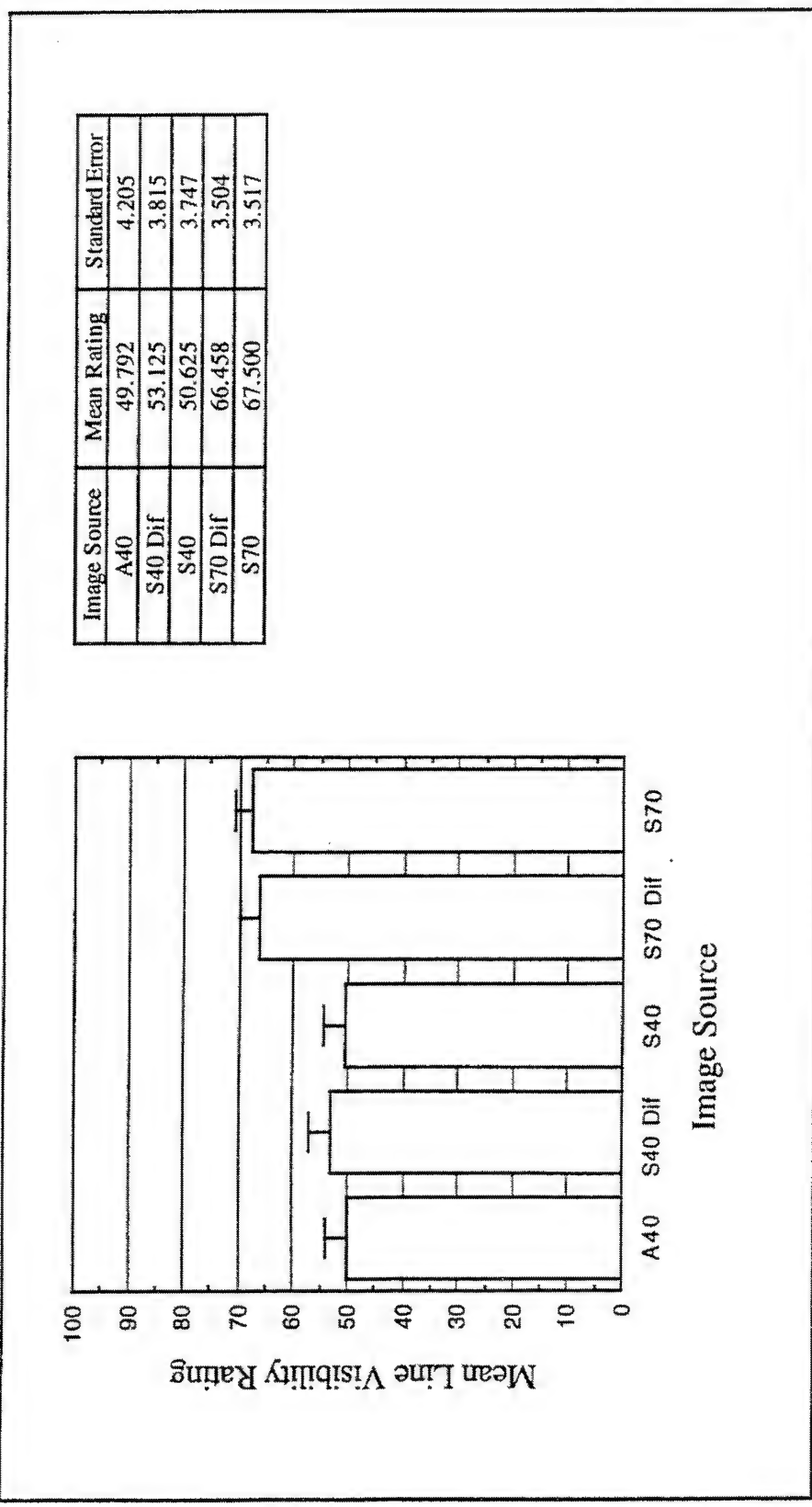


Figure 5-75. Mean Line Visibility Rating as a Function of Image Source (Evaluation 5, Truck).

High line visibility ratings indicate high subjective similarity of comparison images to the standard image (i.e., low visibility of row and column lines). Error bars show standard error of the mean.

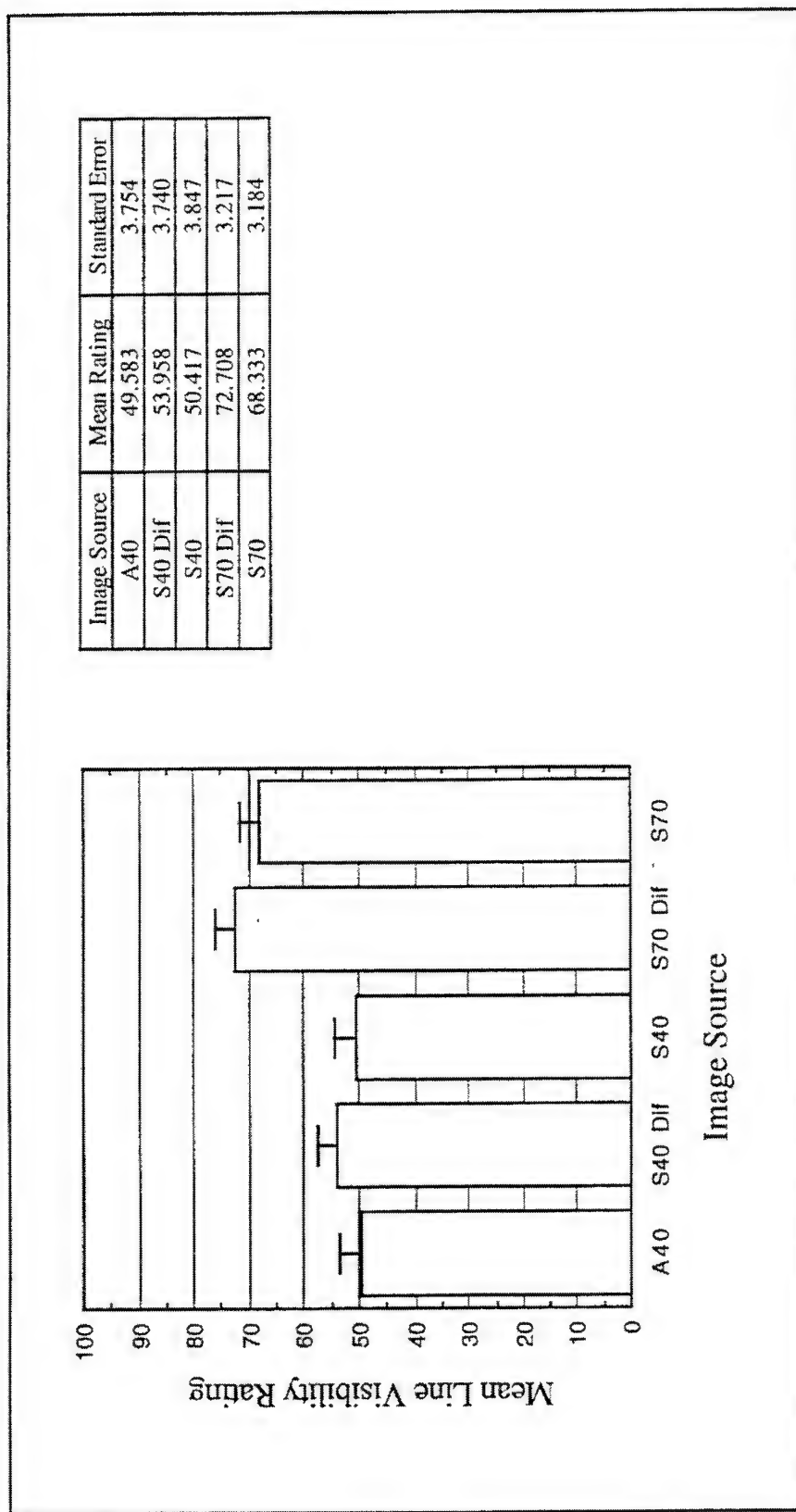


Figure 5-76 Mean Line Visibility Rating as a Function of Image Source (Evaluation 5, Tank).

High line visibility ratings indicate high subjective similarity of comparison images to the standard image (i.e., low visibility of row and column lines).
Error bars show standard error of the mean.

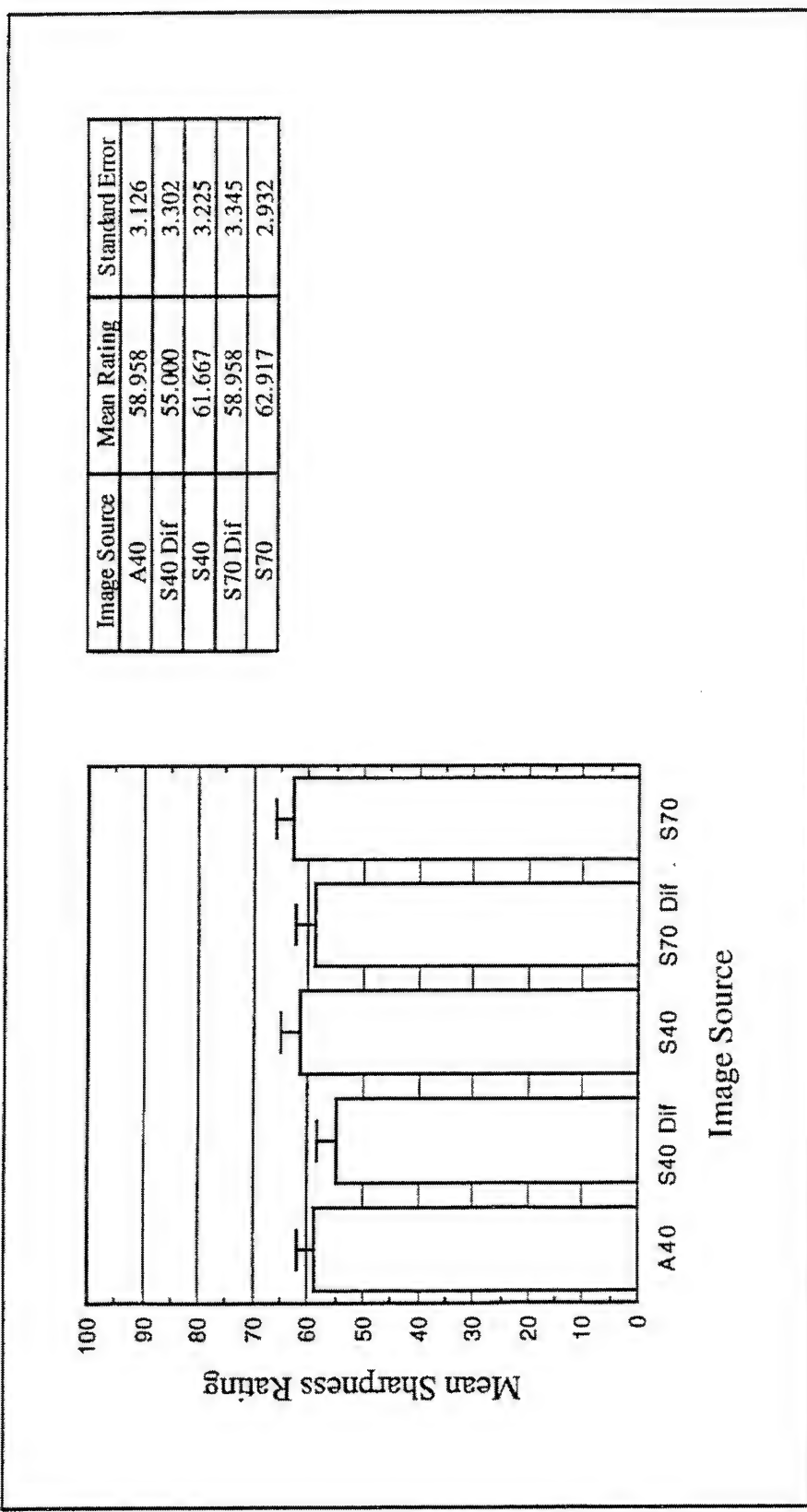


Figure 5-77. Mean Sharpness Rating as a Function of Image Source (Evaluation 5, Truck).

High sharpness ratings indicate high subjective similarity of comparison images to the standard image (i.e., relatively sharp, or nonblurred). Error bars show standard error of the mean.

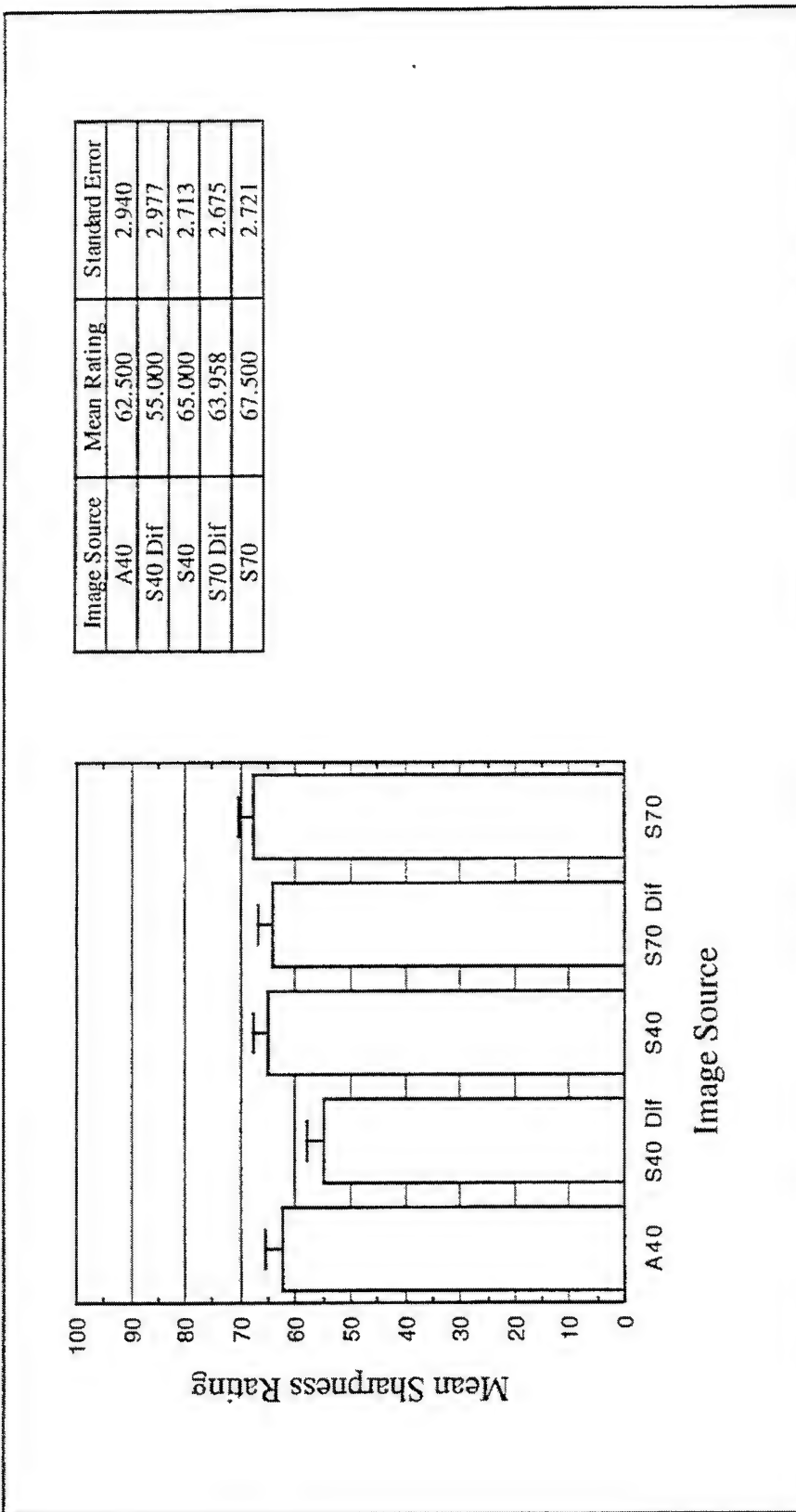


Figure 5.78. Mean Sharpness Rating as a Function of Image Source (Evaluation 5, Tank).

High sharpness ratings indicate high subjective similarity of comparison images to the standard image (i.e., relatively sharp, or nonblurred). Error bars show standard error of the mean.

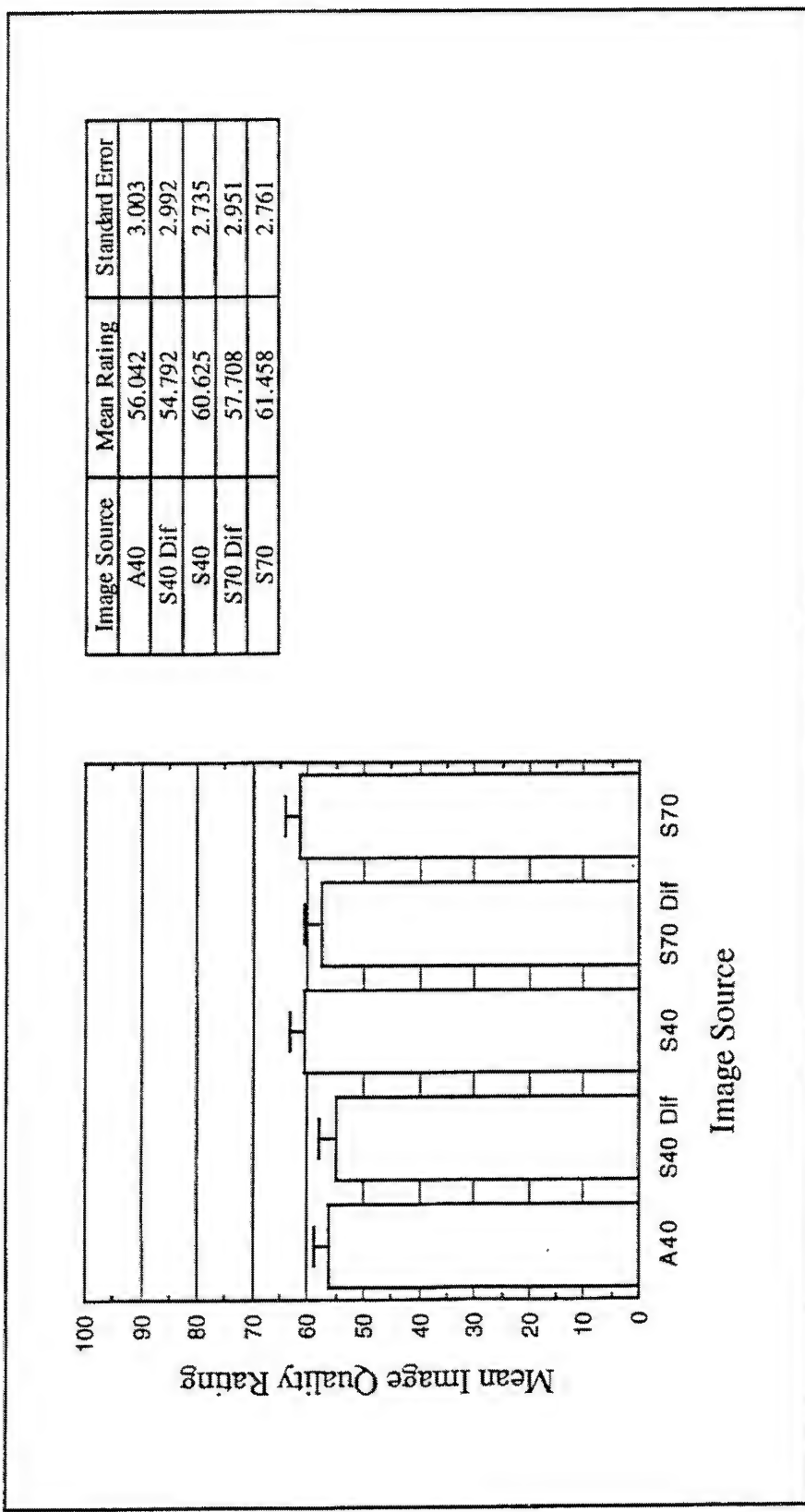


Figure 5-79. Mean Image Quality Rating as a Function of Image Source (Evaluation 5, Truck).

High image quality ratings indicate high subjective similarity of comparison images to the standard image (i.e., relatively high image quality). Error bars show standard error of the mean.

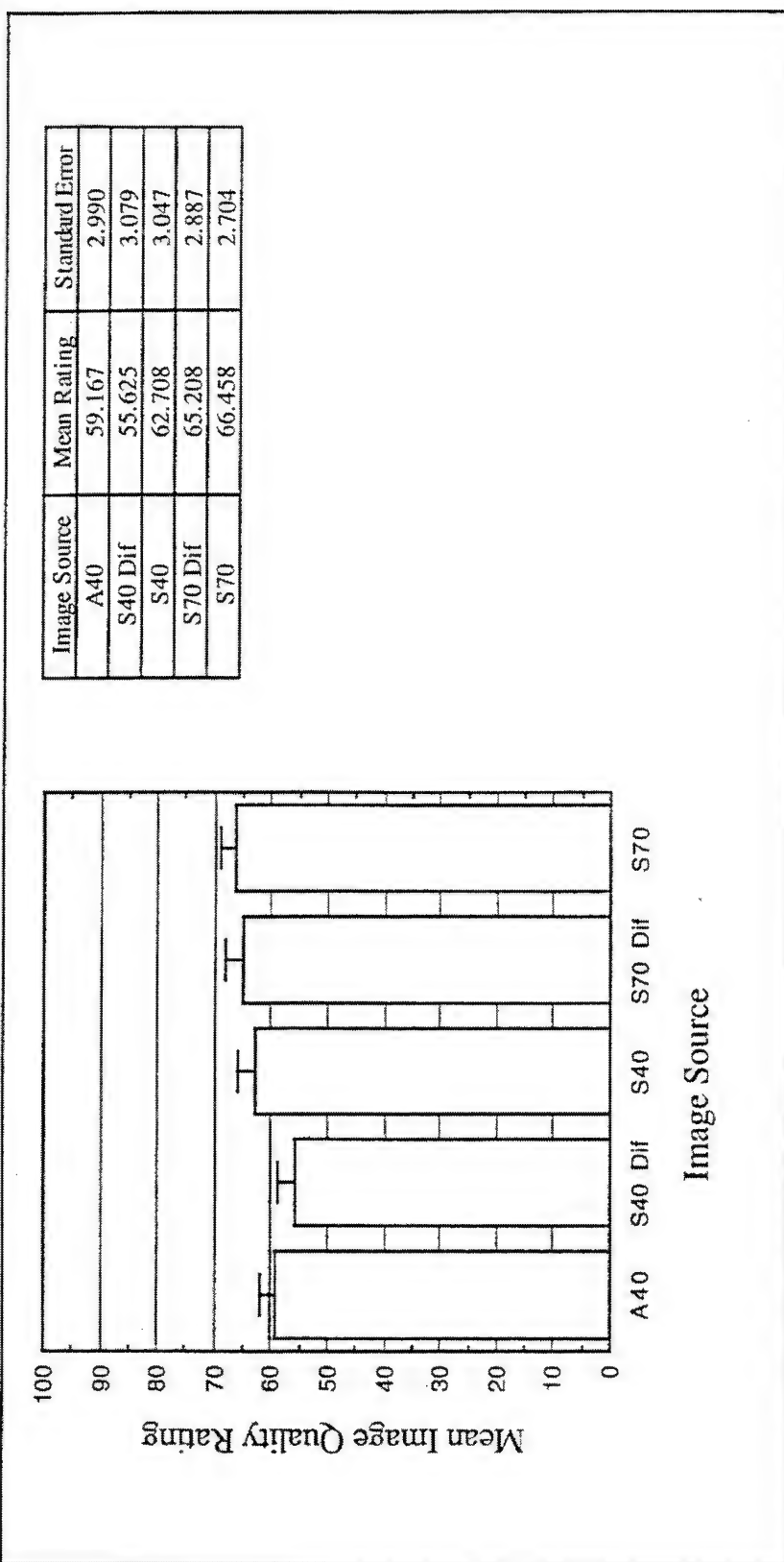


Figure 5-80. Mean Image Quality Rating as a Function of Image Source (Evaluation 5, Tank).

High image quality ratings indicate high subjective similarity of comparison images to the standard image (i.e., relatively high image quality). Error bars show standard error of the mean.

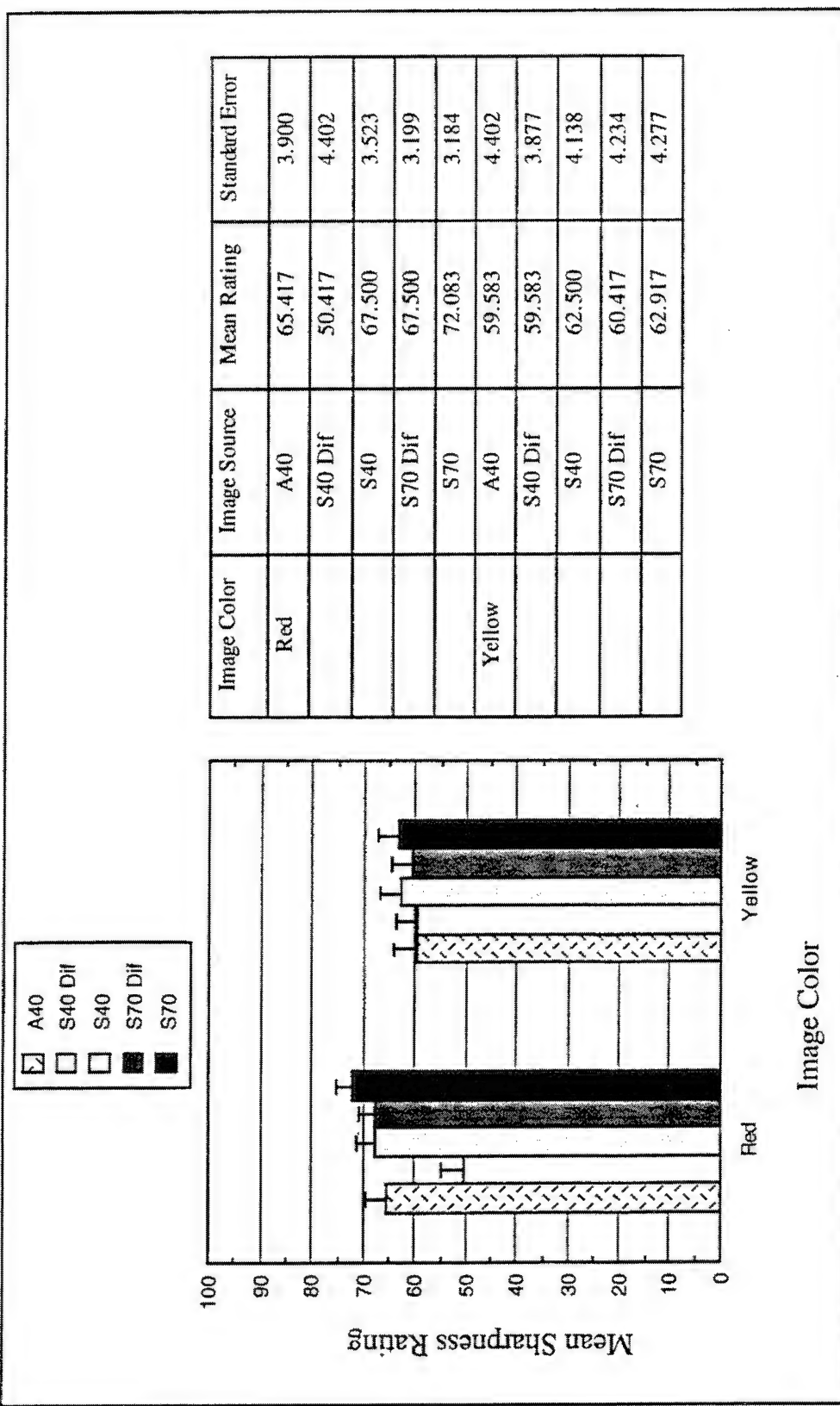


Figure 5-81. Mean Sharpness Rating as a Function of Image Color by Image Source (Evaluation 5, Tank).

High sharpness ratings indicate high subjective similarity of comparison images to the standard image (i.e., relatively sharp, or nonblurred). Error bars show standard error of the mean.

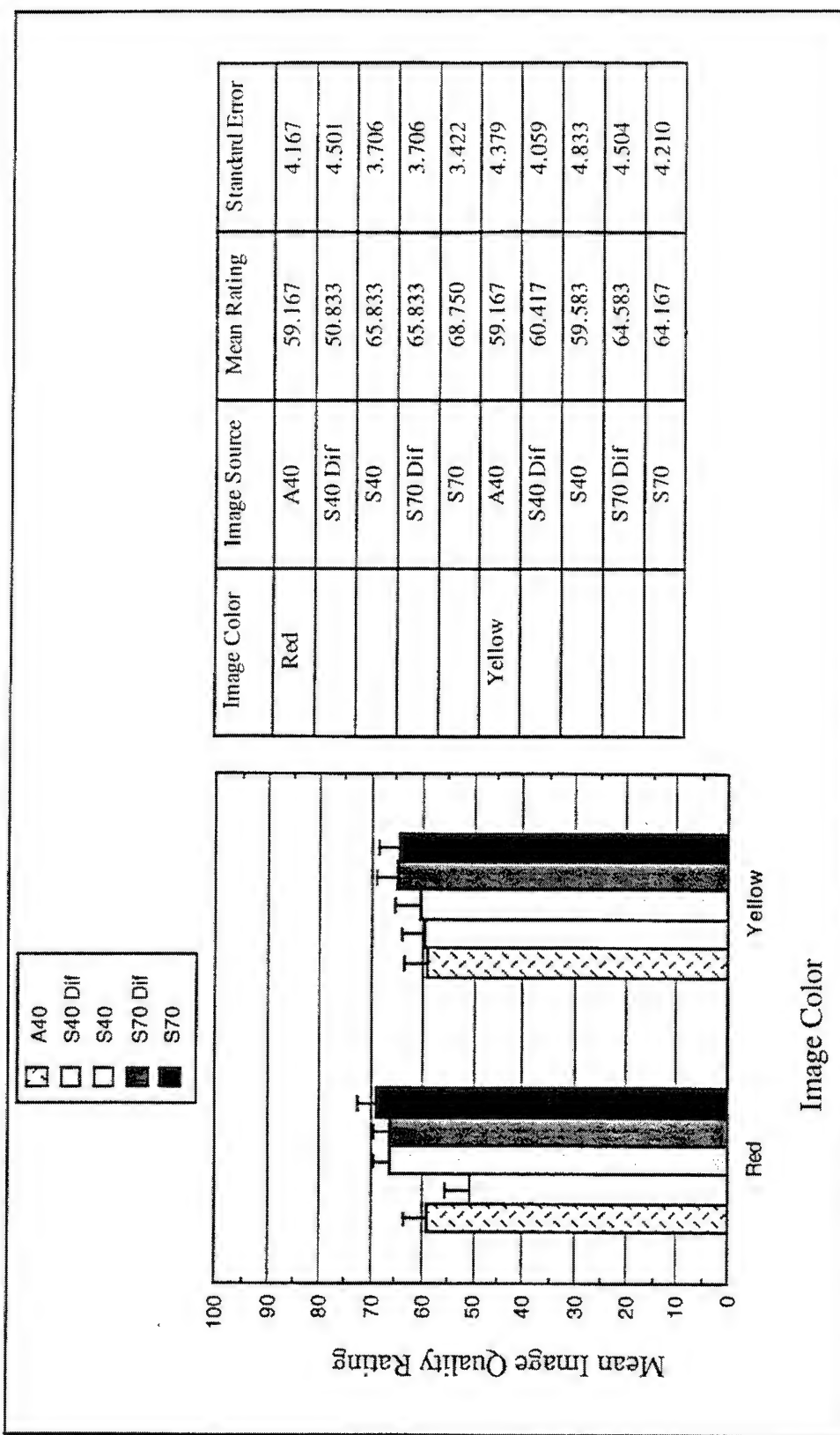


Figure 5-82. Mean Image Quality Rating as a Function of Image Color by Image Source (Evaluation 5, Tank).

High image quality ratings indicate high subjective similarity of comparison images to the standard image (i.e., relatively high image quality). Error bars show standard error of the mean.

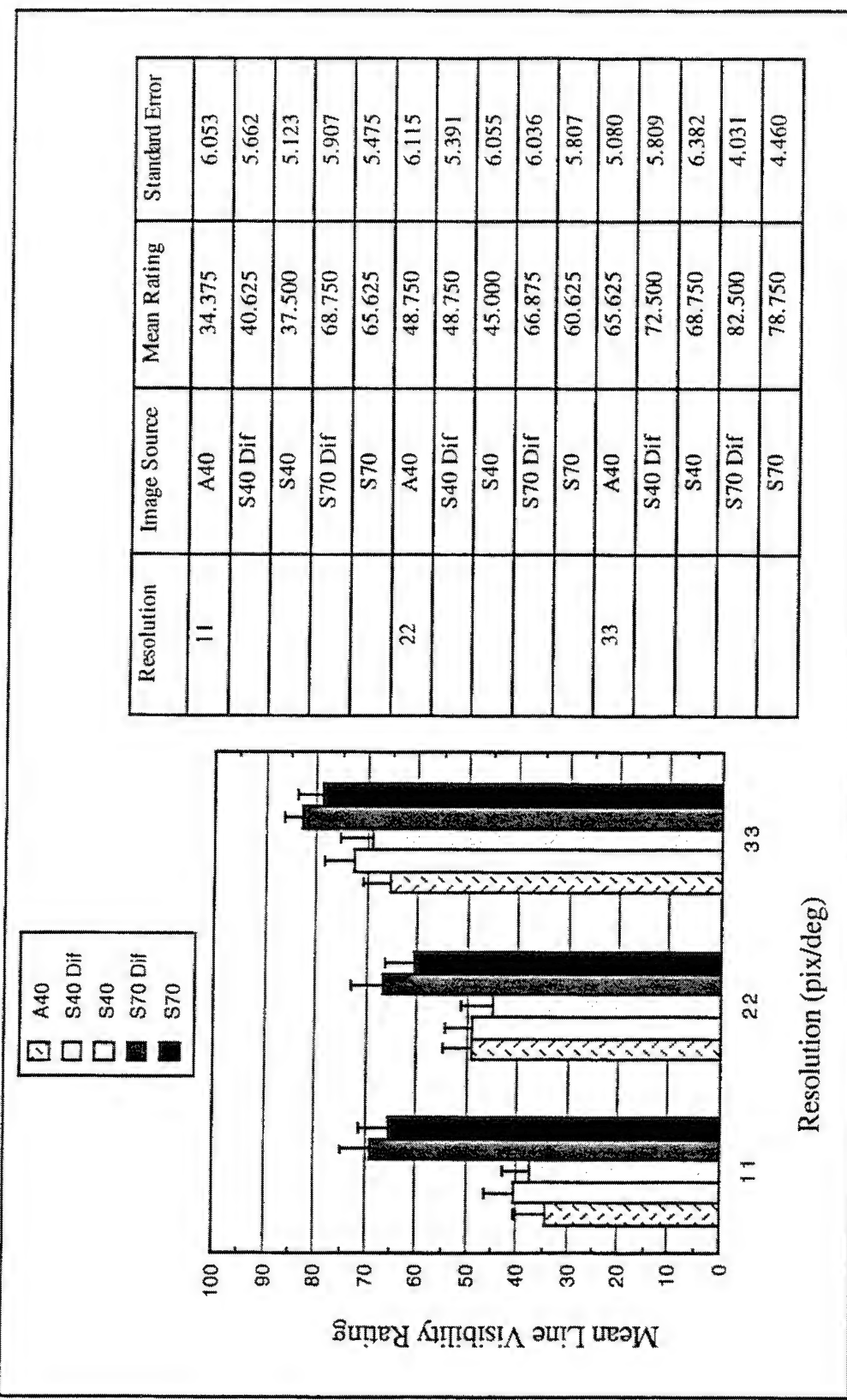


Figure 5-83. Mean Line Visibility Rating as a Function of Resolution by Image Source (Evaluation 5, Tank).

High line visibility ratings indicate high subjective similarity of comparison images to the standard image (i.e., low visibility of row and column lines). Error bars show standard error of the mean.

5.7 Evaluation 6

5.7.1 Objectives

Evaluation 6 was conducted to replicate the procedure of Evaluation 5 while allowing image luminance to covary with aperture ratio and color method (images modeled with higher aperture ratios had higher luminances, and images modeled with subtractive color image sources had higher luminances than those modeled with the additive color image source). The specific objectives of Evaluation 6 were:

1. Further assess the relative impact of aperture ratio on perception of FLIR line visibility and image quality.
2. Evaluate the relative impact of additive vs subtractive color pixel structures on perception of FLIR line visibility and image quality.
3. Determine the perceptual impact of diffraction of the red layer in a subtractive color stack.
4. Evaluate the sensitivity of a new rating scale, sharpness, to image blurring associated with red diffraction.
5. Assess the relative change in impact of red diffraction between red and yellow images.
6. Determine how changes in image source resolution, above and below the baseline HMS+ resolution, impact all of the above.
7. Determine the effect of allowing image luminance to covary with aperture ratio and color method on the above.

5.7.2 Design

Evaluation 6 images were modeled using subtractive and additive color image source models with varied aperture ratios and colors using the two original FLIR images described previously. Representative images from Evaluation 6 are printed in the design description of Evaluation 5. Half of the subtractive color image source models included diffraction of the red layer. Comparison image luminance was allowed to vary among aperture ratio, color method, and image color, such that yellow images modeled with subtractive color image sources of high aperture ratio were of the highest luminance (standard images were of the same luminance as in Evaluation 5). Comparison images were presented at resolutions of between 11 and 33 simulated AMLCD pixels per degree. Resolution was controlled by increasing or decreasing participant viewing distance

(image field of view therefore covaried with resolution). FLIR images were subjected to gray scale level clipping and distribution as previously described under *Simulation Software*. Comparison images were presented at 64 gray scale levels with a linear distribution in red or yellow.

The simulation design levels included in Evaluation 6 are summarized in Table 5-19.

Table 5-19. Design variables for Evaluation 6.

Variable	Levels	Figure	Page
FLIR Image	Truck, Tank	(see <i>Software Imagery</i>)	Figure 5-11 (p. 240)
Resolution	11, 22, 33 pix/deg	(not illustrated)	
Color	Red, Yellow	(see Evaluation 5)	Figure 5-65 (p. 327)
Image Source	Additive (40% AR), Subtractive (40% AR), (with or without diffraction), Subtractive (70% AR) (with or without diffraction)	(see Evaluation 5)	Figure 5-65 (p. 327)

5.7.3 Procedure

The same rating scales (line visibility, image quality, and sharpness) and procedure that were used in Evaluation 5 were used in Evaluation 6. For each comparison image, a separate rating was made on each scale. Participants were instructed to make their image ratings relative to the standard image. Eight participants followed the general evaluation procedure described previously, using the simultaneous comparison procedure and rating 20 practice images and 120 evaluation trials during a 60 minute period. The order of image presentation was randomized within blocks of FLIR image (Truck or Tank) for each observer. Image order was further blocked within image type by resolution, with order of resolution counterbalanced among participants.

5.7.4 Results

Table 5-20 provides an overview of the significant data trends. Separate ANOVA procedures were run for the types of FLIR images. The effects summarized in the table are discussed in the text following the table.

Table 5-20. ANOVA summary table for Evaluation 6.

Effect	Dependent Variable	Image	Figure	Page	df	MS	F	p	R^2	R
Resolution	Line Visibility	Truck	Figure 5-84	358	2, 14	9620.000	10.34	.0092	.12	.30
	Line Visibility	Tank	Figure 5-85	359	2, 14	7835.000	10.34	.0020	.10	.44
Color	Line Visibility	Tank	Figure 5-86	360	1, 7	1126.667	6.68	.0362	.01	.44
	Image Quality	Truck	Figure 5-87	361	1, 7	1653.750	13.31	.0082	.02	.24
Image Source	Line Visibility	Truck	Figure 5-88	362	4, 28	5645.833	29.04	<.0001	.15	.30
	Line Visibility	Tank	Figure 5-89	363	4, 28	11545.417	32.55	<.0001	.29	
Color x Image Source	Image Quality	Truck	Figure 5-90	364	4, 28	4389.167	31.98	<.0001	.17	.24
	Image Quality	Tank	Figure 5-91	365	4, 28	7124.375	20.67	.0002	.23	.29
Image Source	Line Visibility	Tank	Figure 5-92	366	4, 28	587.083	4.35	.0237	.01	.44
	Sharpness	Truck	Figure 5-93	367	4, 28	724.375	6.76	.0087	.03	.10
	Sharpness	Tank	Figure 5-94	368	4, 28	608.958	6.51	.0058	.02	.13
	Image Quality	Truck	Figure 5-95	369	4, 28	568.333	6.07	.0124	.03	.24
	Image Quality	Tank	Figure 5-96	370	4, 28	595.208	6.14	.0034	.02	.29
	Line Visibility	Truck	Figure 5-97	371	8, 56	322.083	3.61	.0256	.02	.30

Resolution. FLIR line visibility ratings increased (i.e., lines became less apparent) as a function of increasing resolution (Figure 5-84 and Figure 5-85). While the differences in ratings between 11 and 22 pix/deg followed this trend, they were not statistically robust ($p>.05$).

Color. There was a small but statistically significant increase in line visibility ratings (i.e., lines became less apparent) for yellow FLIR Tank images relative to red Tank images (Figure 5-86).

Yellow FLIR Truck images received higher image quality ratings relative to red Truck images (Figure 5-87)

Image Source. FLIR line visibility ratings were significantly greater (i.e., lines were less apparent) for image sources modeled at 70% AR relative to those modeled at 40% AR, regardless of diffraction effects (Figure 5-88 and Figure 5-89). For FLIR Tank images, images modeled with the additive color image source received lower line visibility ratings (i.e., lines were more apparent) than the subtractive color image sources of equivalent aperture ratio ($p < .05$). A similar trend was evident in the data for FLIR Truck images, but was not statistically robust ($p > .05$).

FLIR image quality ratings were highest for images modeled with either of the two 70% AR subtractive color image sources (Figure 5-90 and Figure 5-91). The next most highly rated images were those modeled with the nondiffracted 40% AR subtractive color image source, followed by the diffracted 40% AR subtractive color image source ($p < .05$). Images modeled with the additive color image source were assigned lower image quality ratings than images modeled with any of the subtractive color image sources ($p < .05$).

Image Color x Image Source Interaction. FLIR line visibility ratings varied as an interaction of Tank image color and image source (Figure 5-92). Lines were significantly more pronounced for red images modeled with the additive color image source relative to comparable yellow images ($p < .05$). Images modeled with either 70% AR subtractive color image source were rated significantly higher (i.e., lines were less apparent) than all other images, regardless of color ($p < .05$).

FLIR sharpness ratings varied as an interaction of image color and image source (Figure 5-93 and Figure 5-94). Yellow images were rated as least sharp when images were modeled with the additive color image source ($p < .05$), although for the yellow Tank image source, the diffracted 40% AR subtractive color image source was rated as equally sharp to the additive color image source ($p < .05$). Red images modeled with the diffracted 40% AR image source were rated as less sharp than images modeled with the additive color image source ($p > .05$). For the red Tank image, sharpness ratings were lower for the diffracted 70% AR subtractive color image source than the nondiffracted 70% AR subtractive color image source ($p < .05$).

FLIR image quality ratings varied as an interaction of image color and image source (Figure 5-95 and Figure 5-96). Image quality ratings for yellow images were lowest for images modeled with the additive color image source ($p < .05$). Within the red images, image quality ratings were equally high for images modeled with either of the 70% AR subtractive image sources ($p > .05$), followed by those modeled with the nondiffracted 40% AR subtractive color image source, the diffracted 40% AR subtractive color image source, and last, the additive color image source ($p < .05$).

Resolution x Image Source Interaction. FLIR line visibility ratings were generally highest (i.e., lines were less apparent) for Truck images modeled with either subtractive color image source at 70% AR relative to images modeled with the additive color or either 40% AR subtractive color image source (Figure 5-97). However, the magnitude of these differences diminished with increases in resolution. Line visibility ratings for images modeled with the additive color image source were significantly lower than those ratings for images modeled with either 40% AR subtractive color image source at the lowest resolution ($p < .05$).

5.7.5 Summary

The results from Evaluation 6 are summarized in Table 5-21 and the following summary statements:

Table 5-21. Preliminary conclusions based on Evaluation 6 results.

Variable	Image Type	Rating Asymptote	Notes
Resolution	FLIR	$\geq 33 \text{ pix/deg}$	Line visibility
Color	FLIR	Yellow > Red	Minimizes red diffraction effects Higher luminance possible
Subtractive vs Additive	FLIR	Subtractive	Limited additive aperture ratio
Aperture Ratio	FLIR	$\geq 70\%$	Line visibility

1. The results of Evaluation 6 are generally consistent with those of Evaluation 5. There was a less than three-point average difference in image ratings between Evaluation 6 and Evaluation 5, with some ratings in Evaluation 6 being lower than comparable ratings from Evaluation 5 (Table 5-22). However, allowing luminance to covary with aperture ratio and color method appears to have modified image quality ratings. In particular, image quality advantages for images modeled with the 70% AR subtractive color image source were much greater in Evaluation 6

(Figure 5-90 and Figure 5-91) as compared to Evaluation 5 (Figure 5-79 and Figure 5-80), in particular in reference to images modeled with the additive color image source.

2. The visibility of row and column lines generally decreased with increases in resolution. This conclusion is consistent with the results of Evaluation 5.
3. Row and column lines were also less apparent for yellow FLIR tank images than red images. This specific result was not found in Evaluation 5, but is generally consistent with other results indicating a two-primary (yellow) advantage in image appearance. Luminance was controlled among AR conditions but not between colors, so this class of difference may be attributable to the brightness difference between colors.
4. Row and column lines were less apparent for images modeled with the 70% AR subtractive color image sources as compared to the 40% AR subtractive and additive image sources, but image source differences in subjective line visibility became less pronounced as resolution increased. This conclusion is largely consistent with the results of Evaluation 5. In addition, images modeled with the additive color image source were sometimes rated in Evaluation 7 as having the most apparent line structure.
5. Lines were significantly more pronounced for red images modeled with the additive color image source relative to comparable yellow images. Images modeled with either 70% AR subtractive color image source were rated significantly higher (i.e., lines were less apparent) than all other images, regardless of color.
6. Yellow images were rated as least sharp when images were modeled with the additive color image source, although for the yellow Tank image source, the diffracted 40% AR subtractive color image source was rated as equally sharp to the additive color image source. Red images modeled with the diffracted 40% AR image source were rated as less sharp than images modeled with the additive color image source. For the red Tank image, sharpness ratings were lower for the diffracted 70% AR subtractive color image source than the nondiffracted 70% AR subtractive color image source.
7. Image quality ratings for yellow images were lower for images modeled with the additive color image source than for yellow images modeled with any of the subtractive color image sources. Within the red images, image quality ratings were equally high for images modeled with either of the 70% AR subtractive image sources, followed by those modeled with the nondiffracted 40% AR subtractive color image source, the diffracted 40% AR subtractive color image source, and last, the additive color image source.

8. Subjective image quality was higher for yellow FLIR Truck images than for red FLIR Truck images. This result is consistent with the results of Evaluation 5.
9. Images modeled with the 70% AR image sources generally received the highest image quality ratings. Unlike the results of Evaluation 5, there was greater differentiation in image quality among the 40% AR image sources in Evaluation 6. Of these three image sources, images modeled with the nondiffracted 40% AR subtractive color image source were rated most high, followed by the diffracted 40% AR subtractive color image source, and then the additive color image source.

Table 5-22. Mean rating differences between Evaluations 5 and 6.

Rating Scale	Image Type	Evaluation 5	Evaluation 6	Difference
Image Quality	Truck	58.125	60.542	-2.417
	Tank	61.833	58.167	3.666
Sharpness	Truck	59.500	62.250	-2.750
	Tank	62.792	62.917	-0.125
Line Visibility	Truck	57.500	55.000	2.500
	Tank	59.000	55.750	3.250

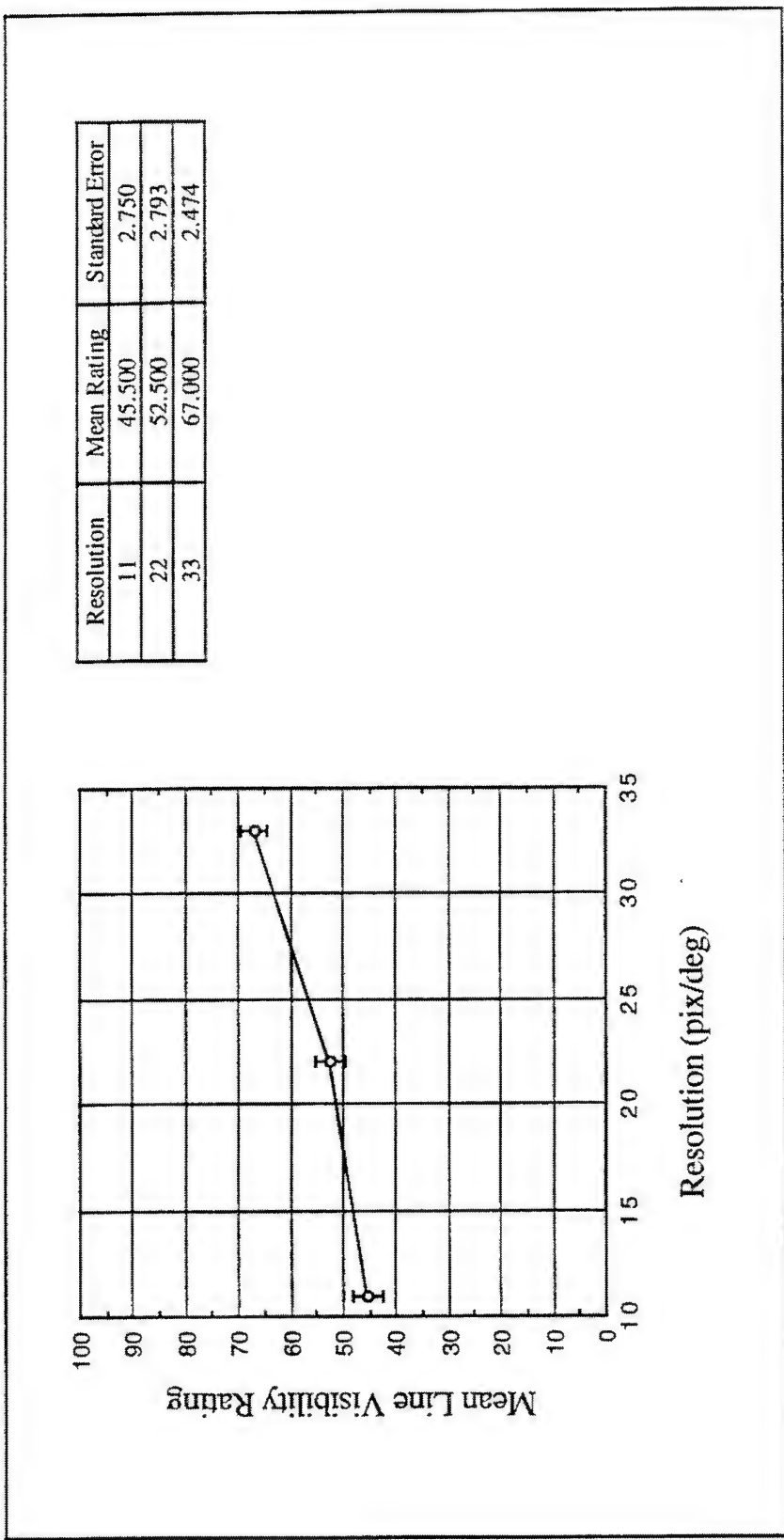


Figure 5-84. Mean Line Visibility Rating as a Function of Resolution (Evaluation 6, Truck).
 High line visibility ratings indicate high subjective similarity of comparison images to the standard image (i.e., low visibility of row and column lines).
 Error bars show standard error of the mean.

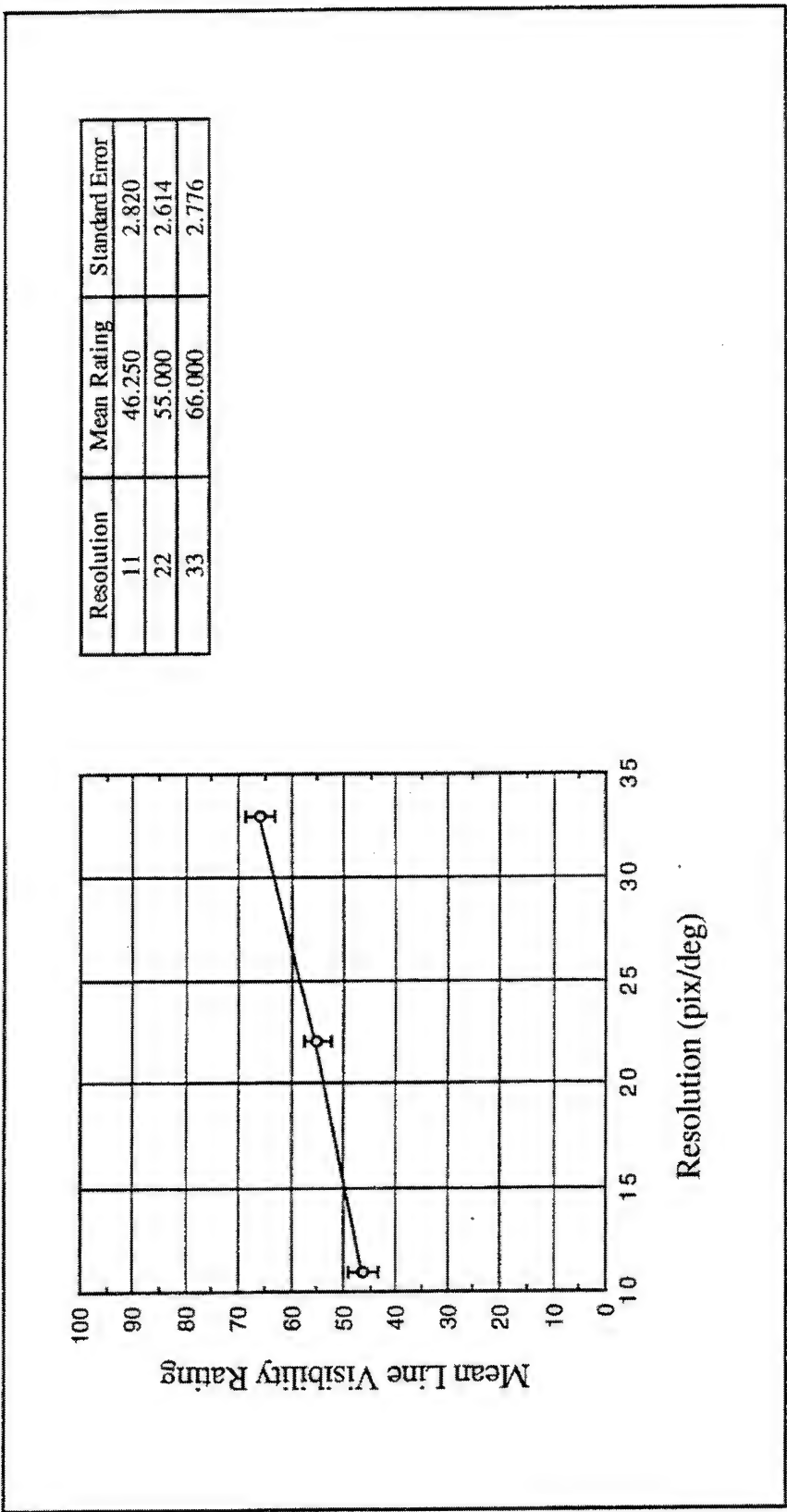


Figure 5-85 Mean Line Visibility Rating as a Function of Resolution (Evaluation 6, Tank).

High line ratings indicate high subjective similarity of comparison images to the standard image (i.e., low visibility of row and column lines). Error bars show standard error of the mean.

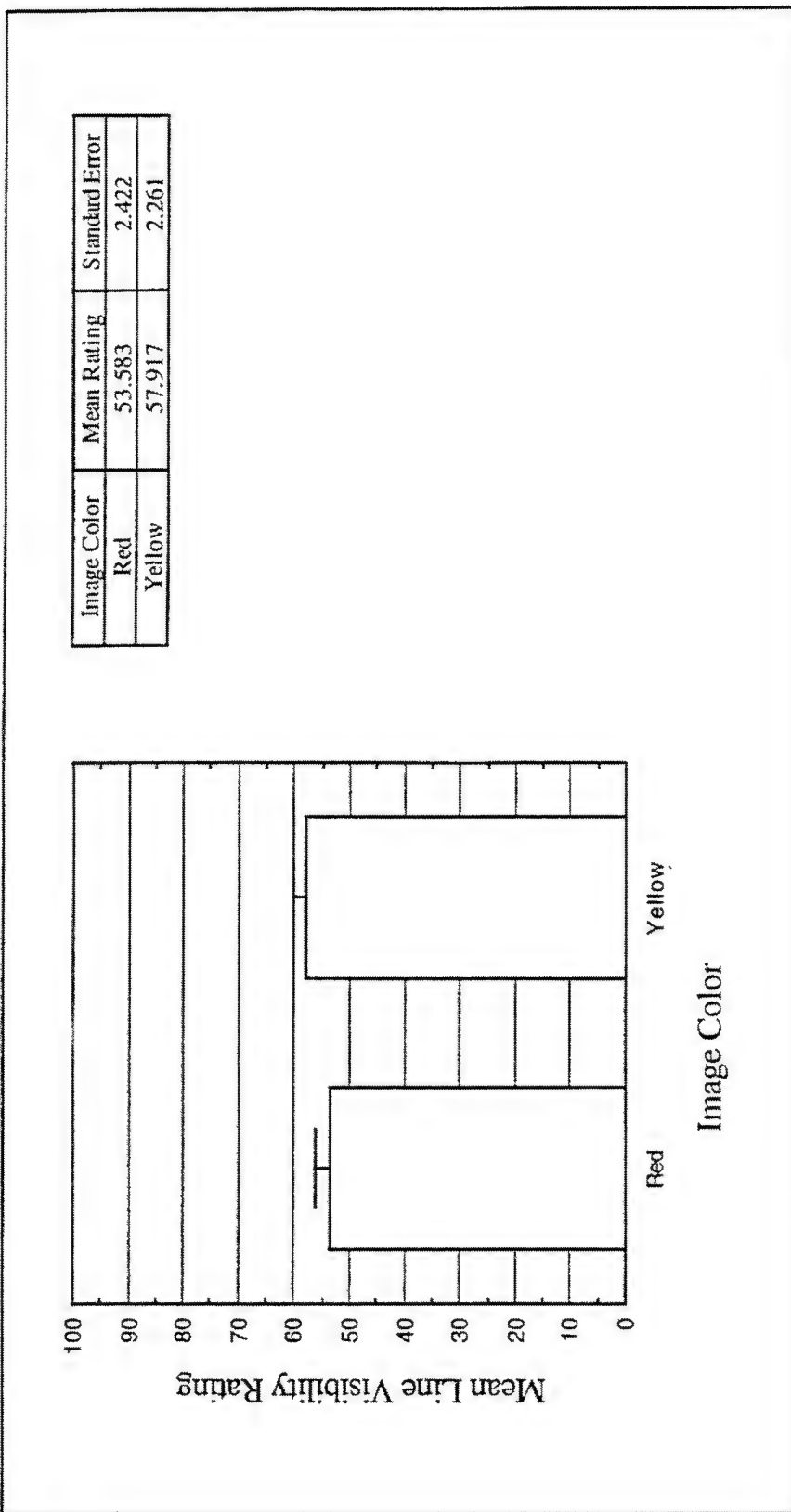


Figure 5-86. Mean Line Visibility Rating as a Function of Image Color (Evaluation 6, Tank).

High line visibility ratings indicate high subjective similarity of comparison images to the standard image (i.e., low visibility of row and column lines). Error bars show standard error of the mean.

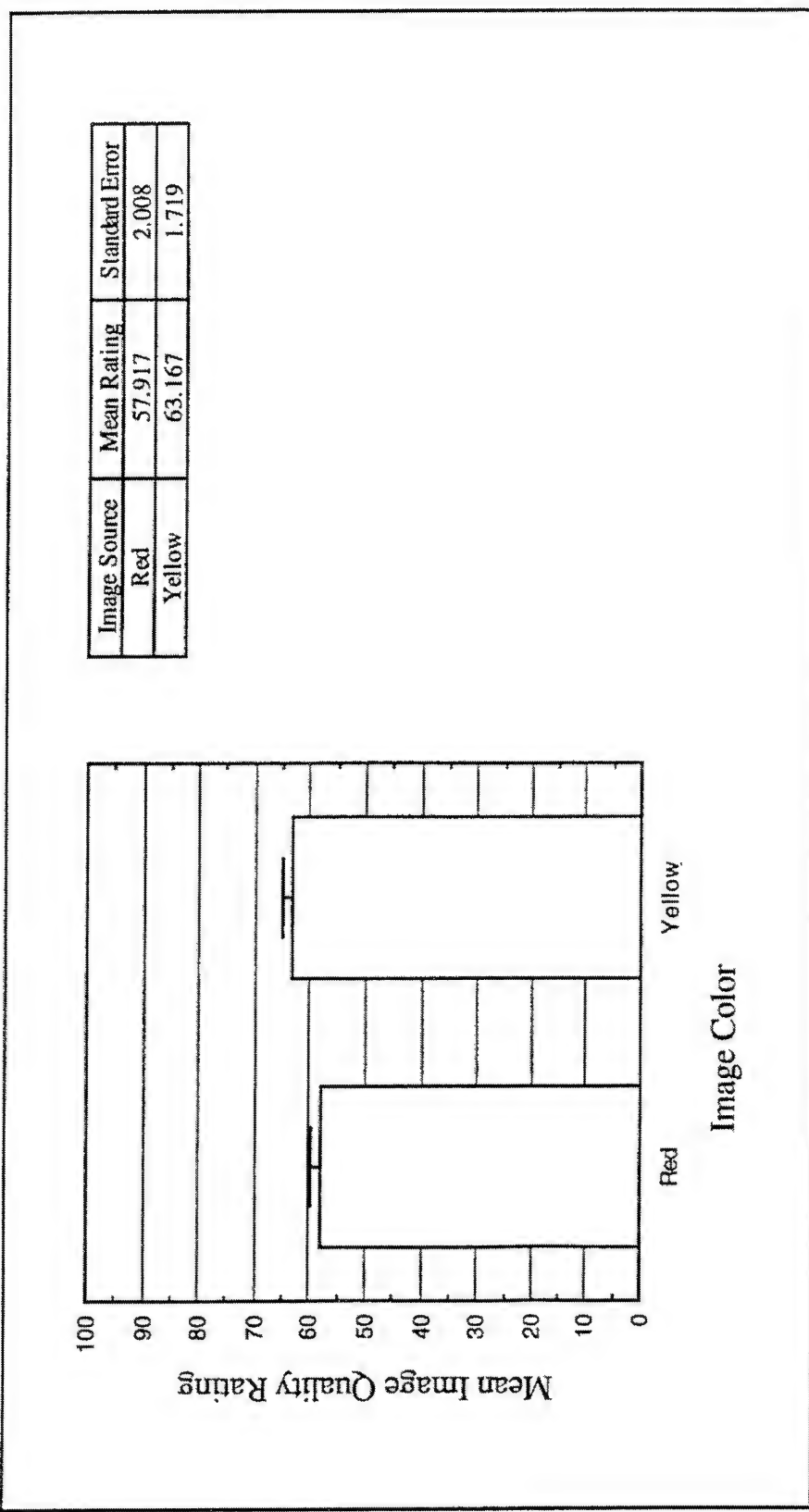


Figure 5-87. Mean Image Quality Rating as a Function of Image Color (Evaluation 6, Truck).

High image quality ratings indicate high subjective similarity of comparison images to the standard image (i.e., relatively high image quality). Error bars show standard error of the mean.

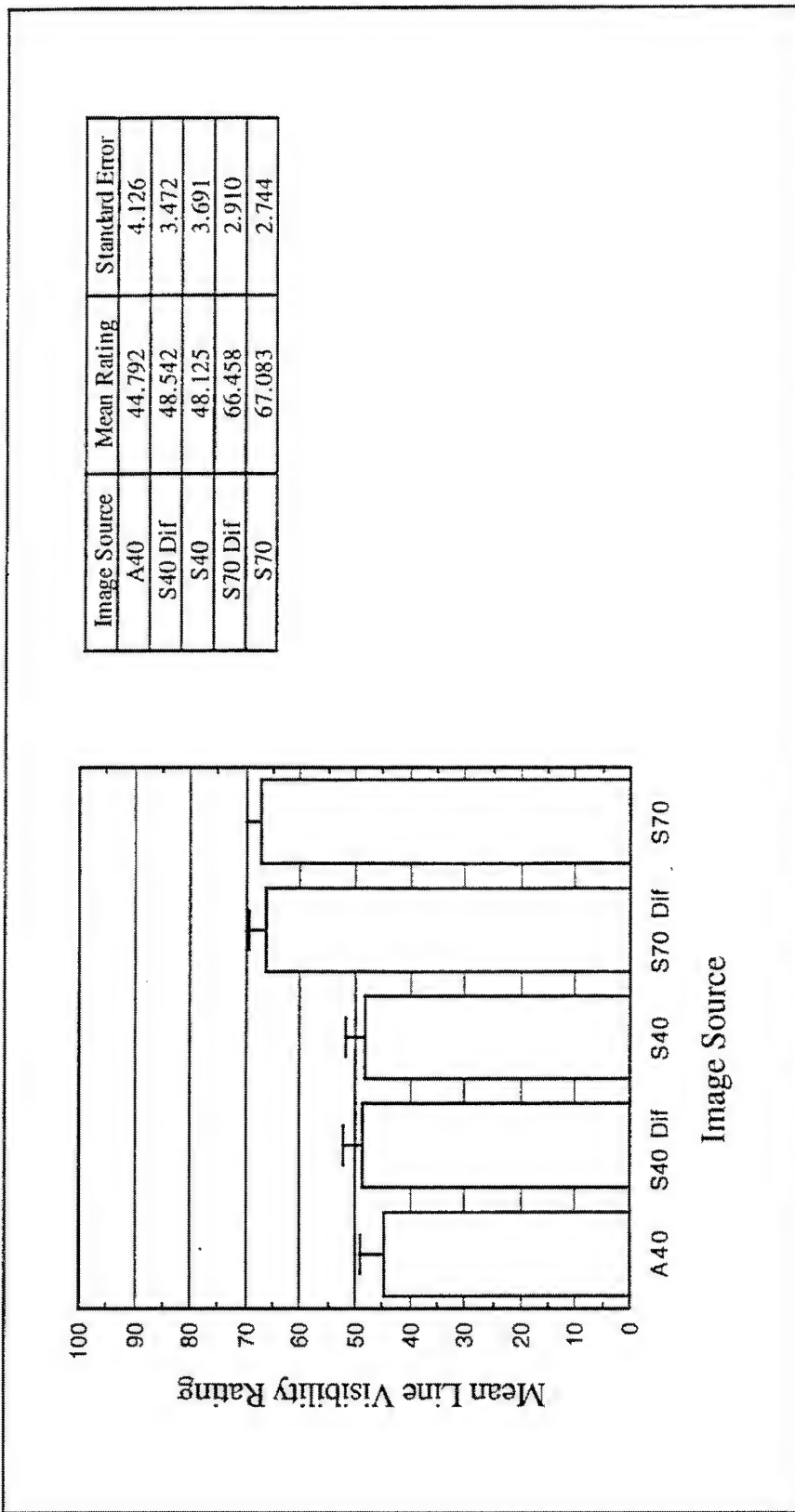


Figure 5-88. Mean Line Visibility Rating as a Function of Image Source (Evaluation 6, Truck).

High line visibility ratings indicate high subjective similarity of comparison images to the standard image (i.e., low visibility of row and column lines).
Error bars show standard error of the mean.

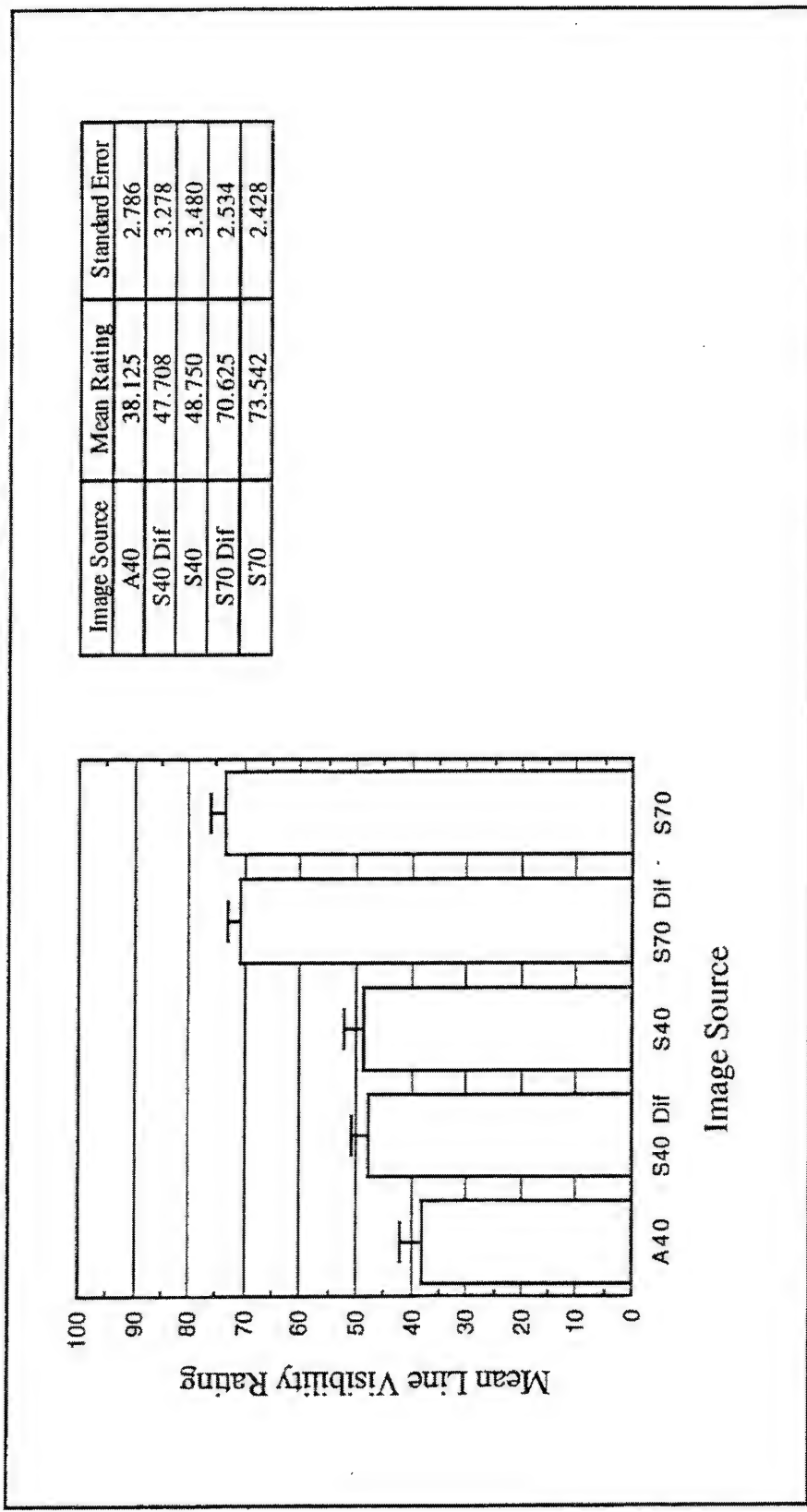


Figure 5-89. Mean Line Visibility Rating as a Function of Image Source (Evaluation 6, Tank).

High line visibility ratings indicate high subjective similarity of comparison images to the standard image (i.e., low visibility of row and column lines). Error bars show standard error of the mean.

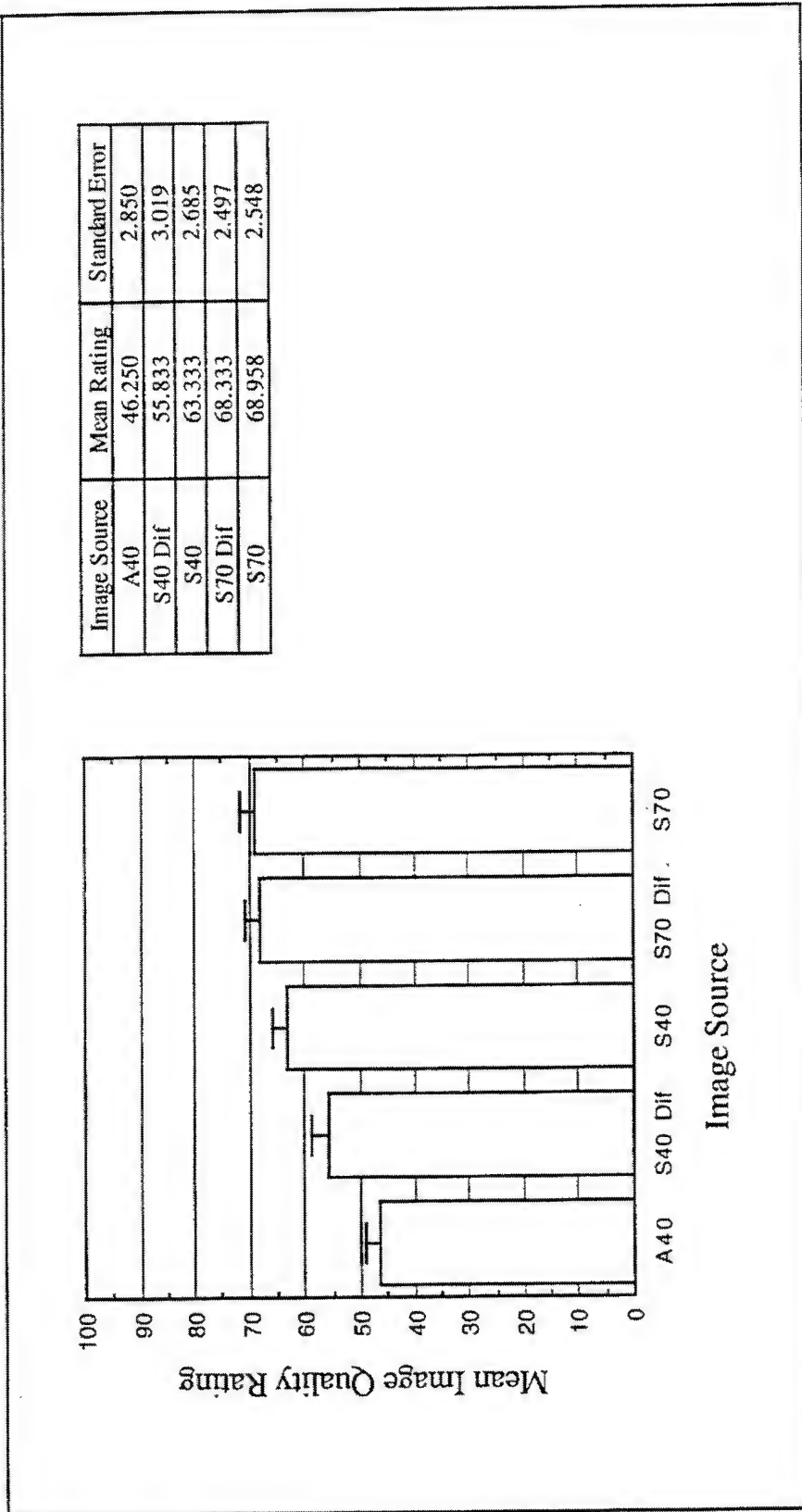


Figure 5-90. Mean Image Quality Rating as a Function of Image Source (Evaluation 6, Truck).

High image quality ratings indicate high subjective similarity of comparison images to the standard image (i.e., relatively high image quality). Error bars show standard error of the mean.

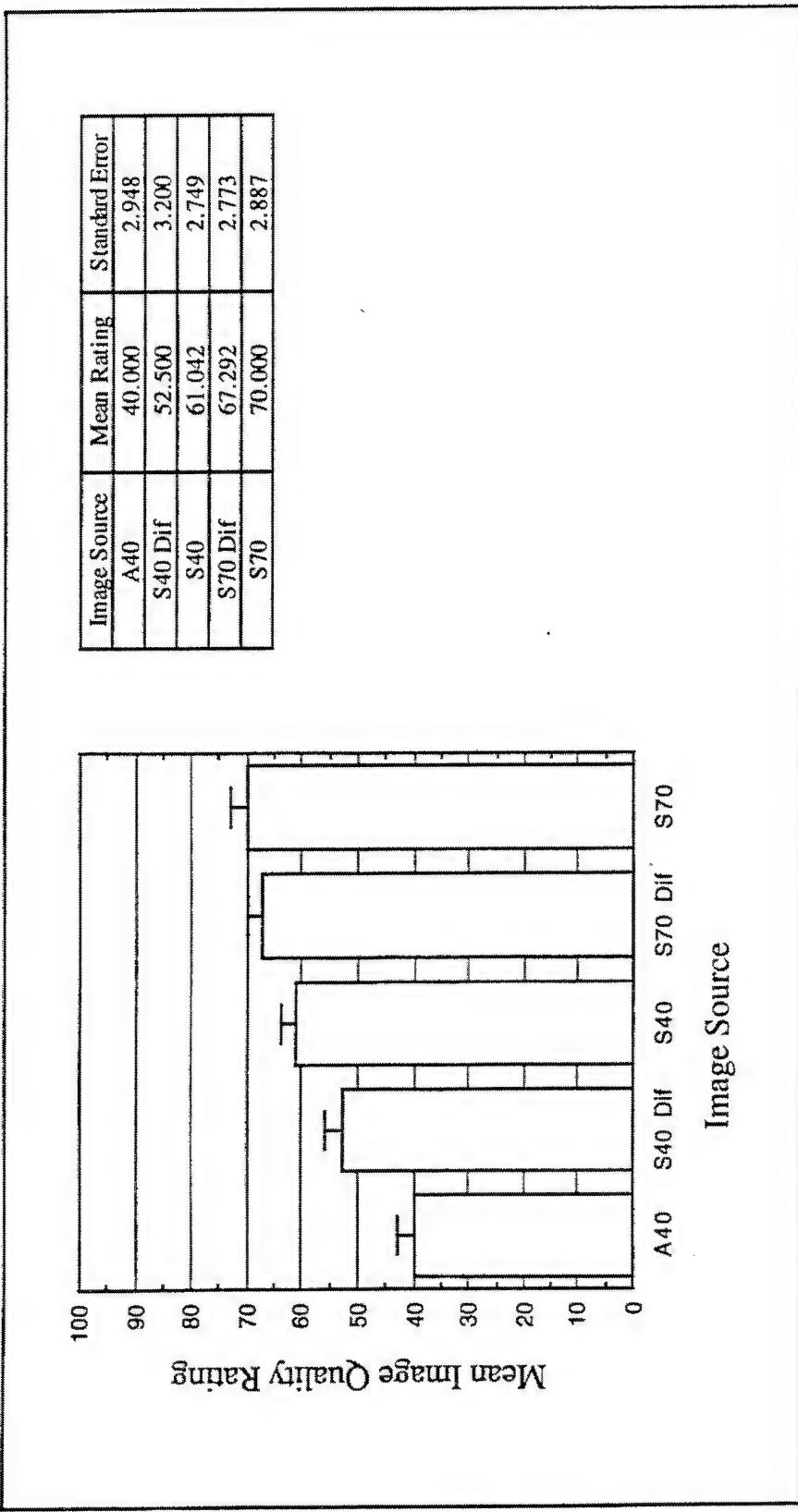


Figure 5-91. Mean Image Quality Rating as a Function of Image Source (Evaluation 6, Tank).

High image quality ratings indicate high subjective similarity of comparison images to the standard image (i.e., relatively high image quality). Error bars show standard error of the mean.

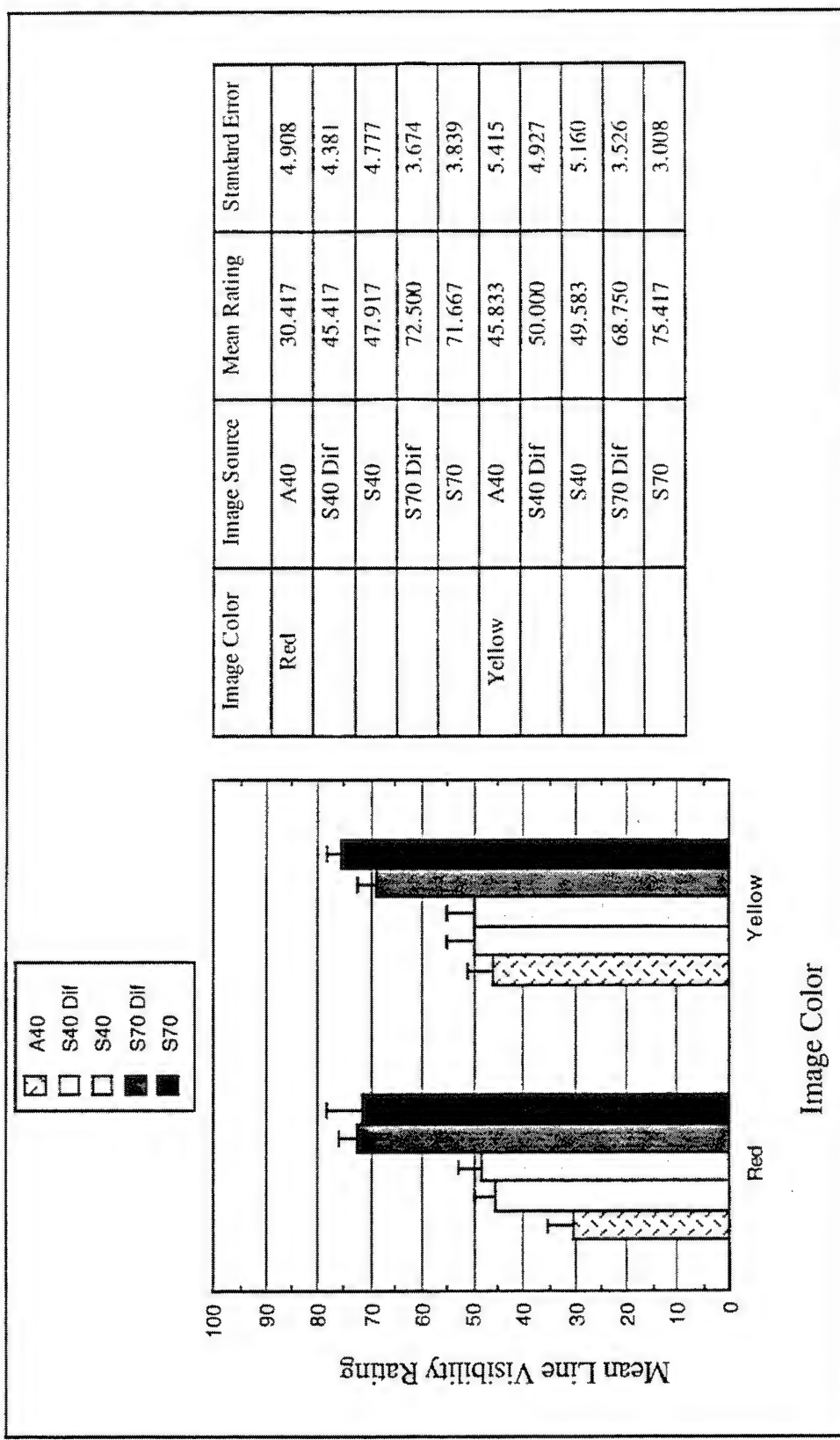


Figure 5-92. Mean Line Visibility Rating as a Function of Image Color by Image Source (Evaluation 6, Tank).

High line visibility ratings indicate high subjective similarity of comparison images to the standard image (i.e., low visibility of row and column lines). Error bars show standard error of the mean.

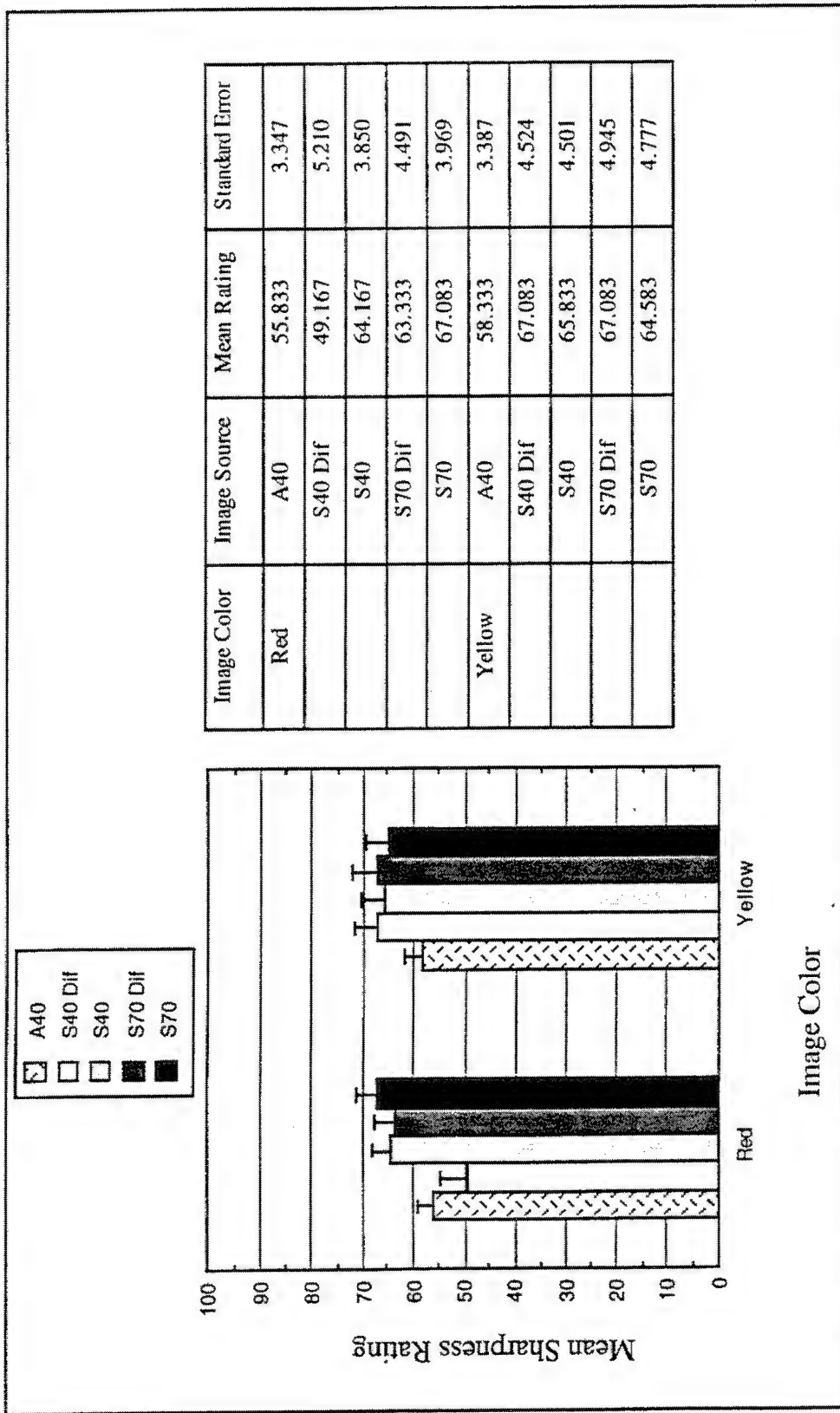


Figure 5-93. Mean Sharpness Rating as a Function of Image Color by Image Source (Evaluation 6, Truck).

High sharpness ratings indicate high subjective similarity of comparison images to the standard image (i.e., relatively sharp, or nonblurred). Error bars show standard error of the mean.

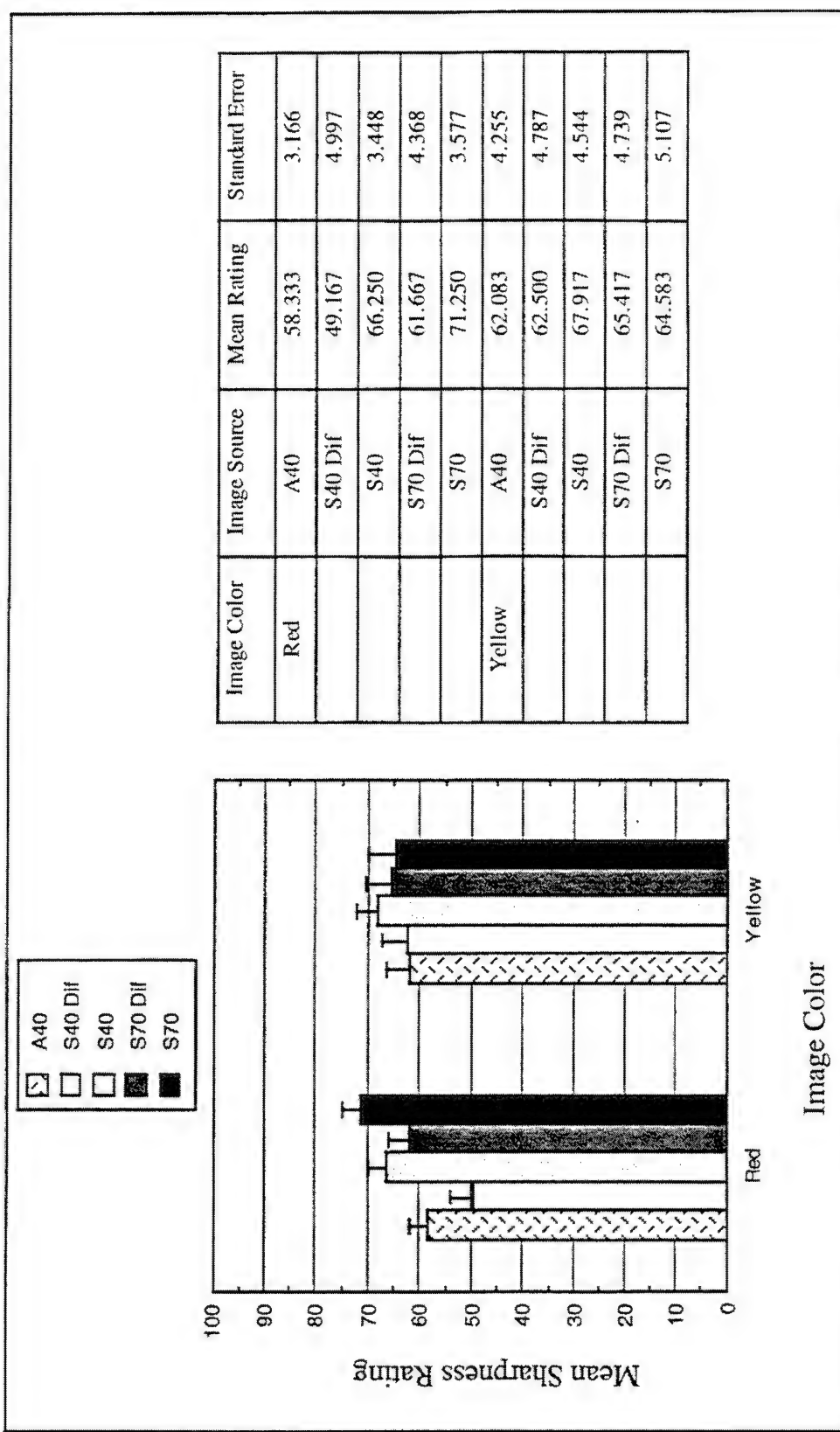


Figure 5-94. Mean Sharpness Rating as a Function of Image Color by Image Source (Evaluation 6, Tank).

High sharpness ratings indicate high subjective similarity of comparison images to the standard image (i.e., relatively sharp, or nonblurred). Error bars show standard error of the mean.

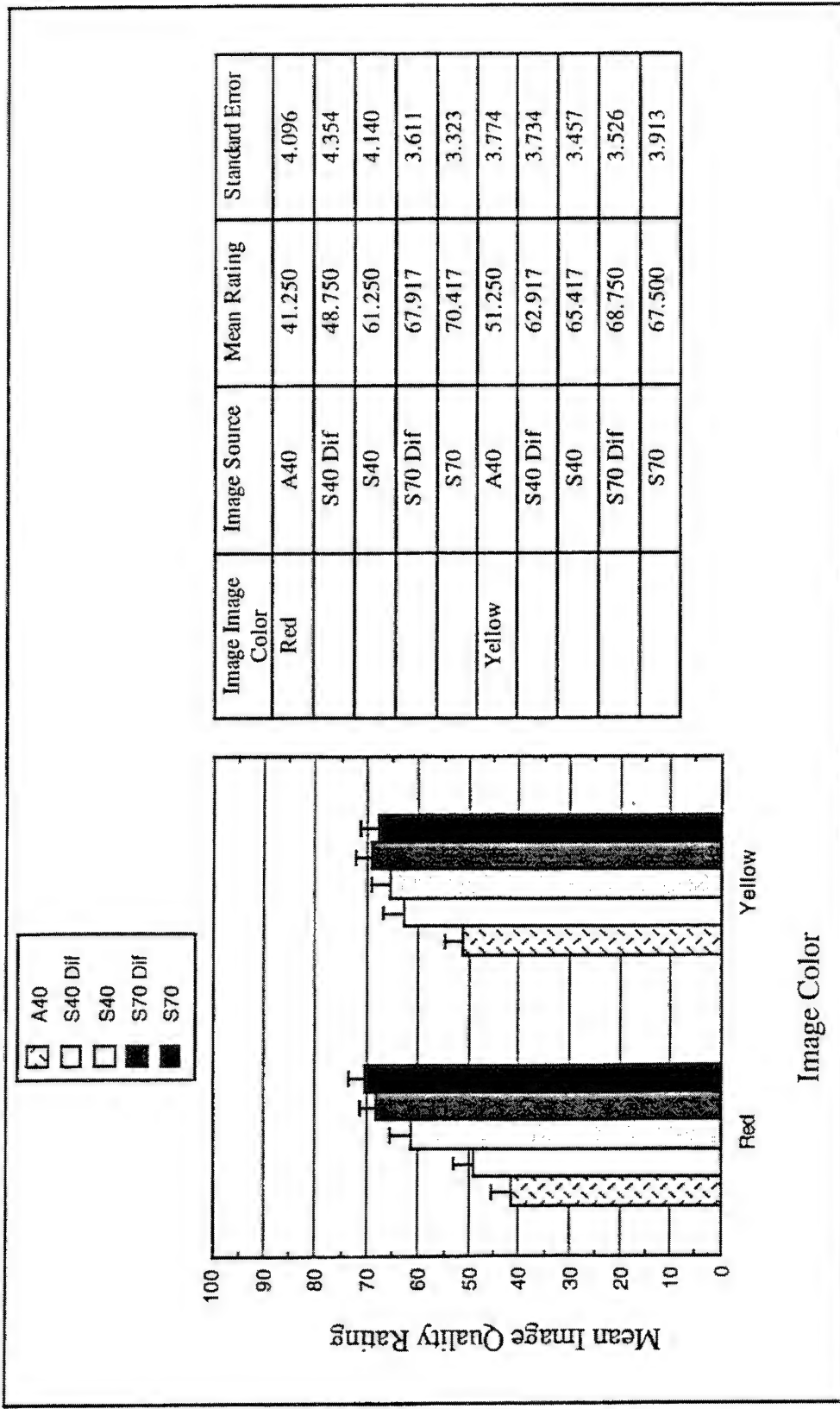


Figure 5-95. Mean Image Quality Rating as a Function of Image Color by Image Source (Evaluation 6, Truck).

High image quality ratings indicate high subjective similarity of comparison images to the standard image (i.e., relatively high image quality). Error bars show standard error of the mean.

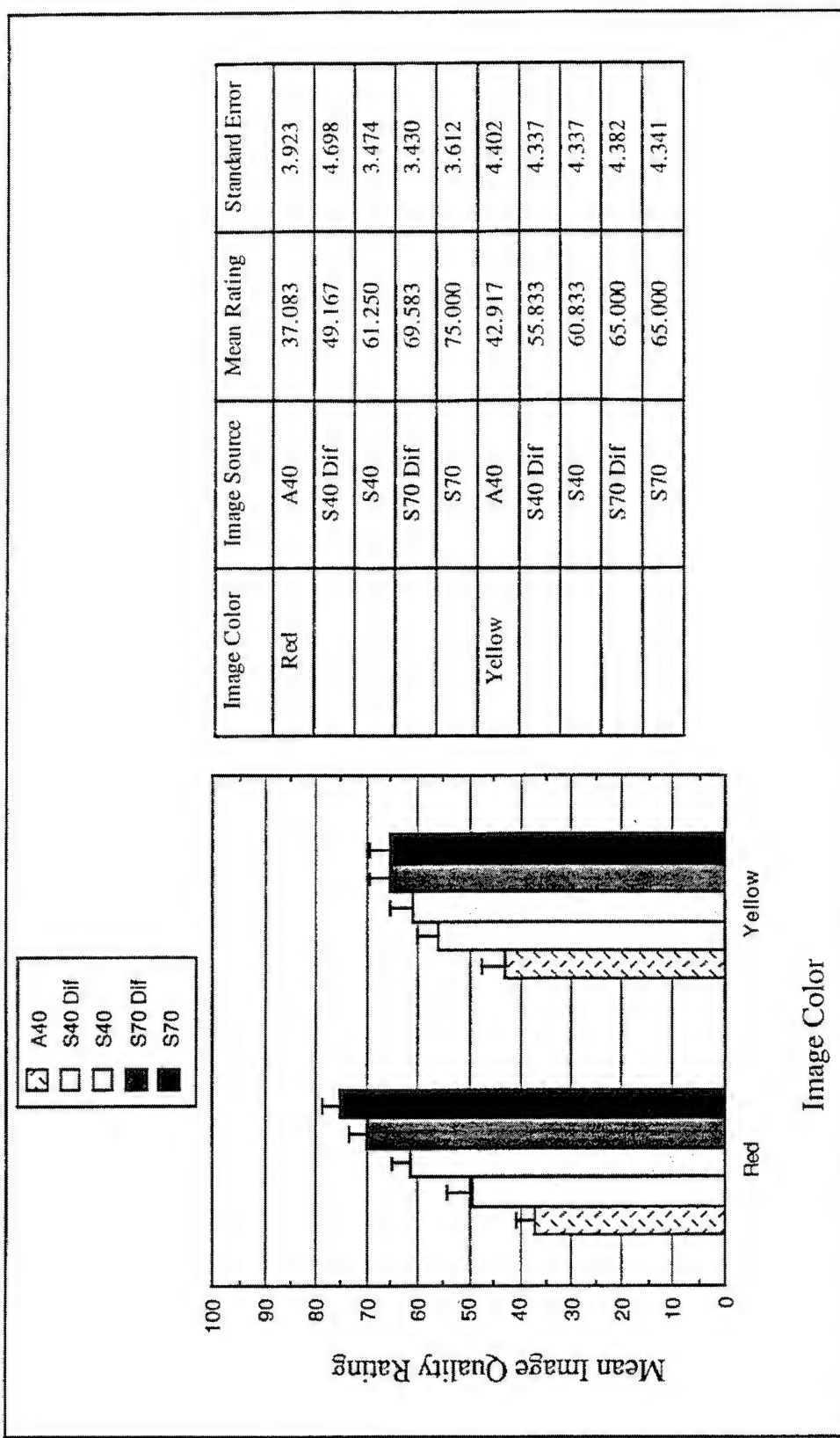


Figure 5-96. Mean Image Quality Rating as a Function of Image Color by Image Source (Evaluation 6, Tank).

High image quality ratings indicate high subjective similarity of comparison images to the standard image (i.e., relatively high image quality). Error bars show standard error of the mean.

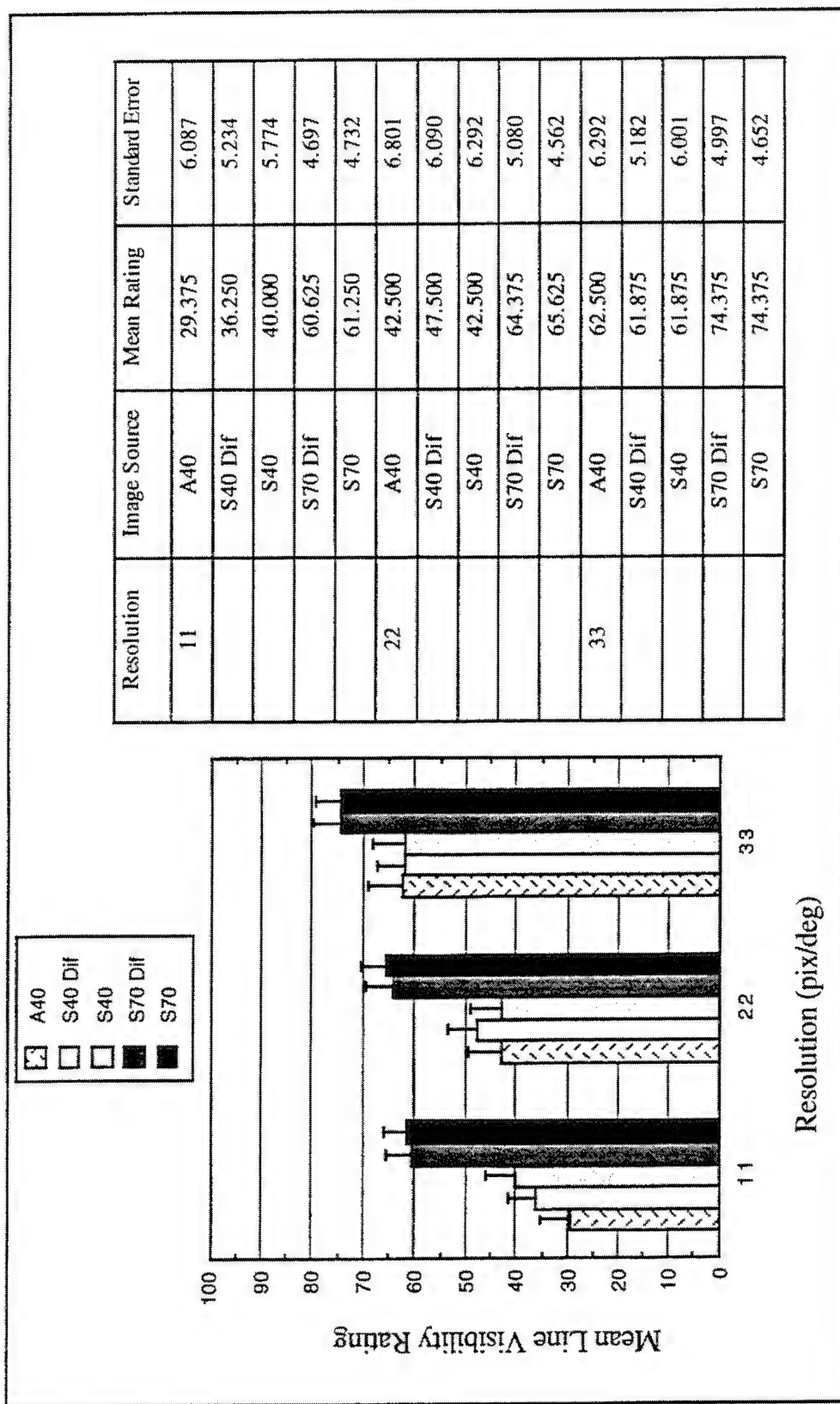


Figure 5-97. Mean Line Visibility Rating as a Function of Resolution by Image Source (Evaluation 6, Truck).

High line visibility ratings indicate high subjective similarity of comparison images to the standard image (i.e., low visibility of row and column lines). Error bars show standard error of the mean.

5.8 Evaluation 7

5.8.1 Objectives

Evaluation 7 was conducted to extend the results of Evaluation 5 to include symbol imagery. Binary symbols (no anti-aliasing) were used to examine possible anti-aliasing properties of subtractive color red diffraction. Luminance was held constant among various image sources modeled. The specific objectives of Evaluation 7 were:

1. Assess the relative impact of aperture ratio on perception of symbol line visibility and image quality.
2. Evaluate the relative impact of additive vs subtractive color pixel structures on perception of symbol line visibility and image quality.
3. Determine the perceptual impact of diffraction of the red layer in a subtractive color stack.
4. Assess the relative change in impact of red diffraction between red and yellow symbols.
5. Determine how changes in image source resolution, above and below the baseline HMS+ resolution, impact all of the above.

5.8.2 Design

Evaluation 7 images were modeled using subtractive and additive color image source models with varied aperture ratios and colors using the original numeric symbols described previously. Half of the subtractive color image source models included diffraction of the red layer (see Evaluation 5). Comparison image luminance was held constant among aperture ratio and color method, such that equivalent images modeled with different image sources were of equal luminance (the luminance of the standard image was not reduced). Images of different colors, however, did vary in luminance (yellow images were of higher luminance than red images). Comparison images were presented at resolutions of between 11 and 33 simulated AMLCD pixels per degree. Resolution was controlled by increasing or decreasing participant viewing distance (image field of view therefore covaried with resolution). Comparison images were presented at 2 gray scale levels (i.e., binary).

The simulation design levels included in Evaluation 7 are summarized in Table 5-16. Figures illustrating variables are referenced in the table where available.

Table 5-23. Design variables for Evaluation 7.

Variable	Levels	Figure	Page
Resolution	11, 22, 33 pix/deg	(not illustrated)	
Color	Red, Yellow	Figure 5-98	374
Image Source	Additive (40% AR), Subtractive (40% AR) (with or without diffraction), Subtractive (70% AR) (with or without diffraction)	Figure 5-98 Figure 5-99 Figure 5-100	374 375 376

5.6 Evaluation 7

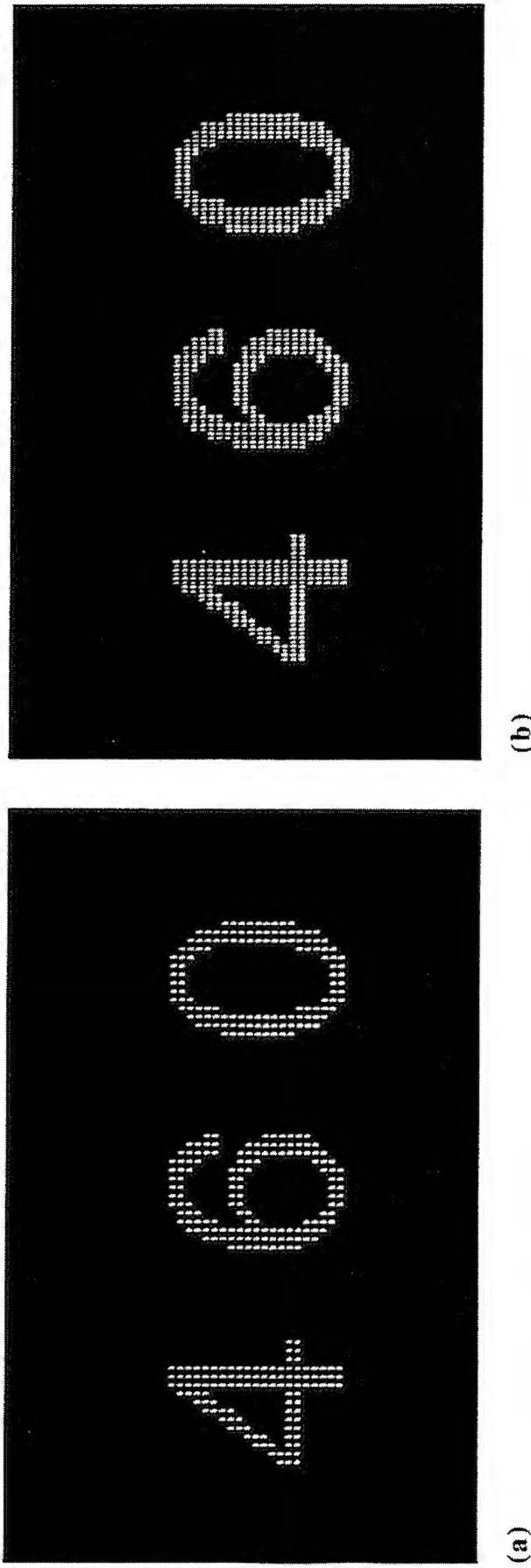


Figure 5-98. Additive Color Image Source (40% AR) Modeled in Evaluations 7, 8, and 10 for Symbol Images.

One primary (red, a) and two primaries (yellow, b). Images shown here were used in all three evaluations. Note that evaluation images were actually presented in color on a high-resolution CRT. Also, these printed gray scale images are not gamma-corrected for printing. In addition, their size as printed is not intended to simulate the angular resolutions tested in the evaluations.

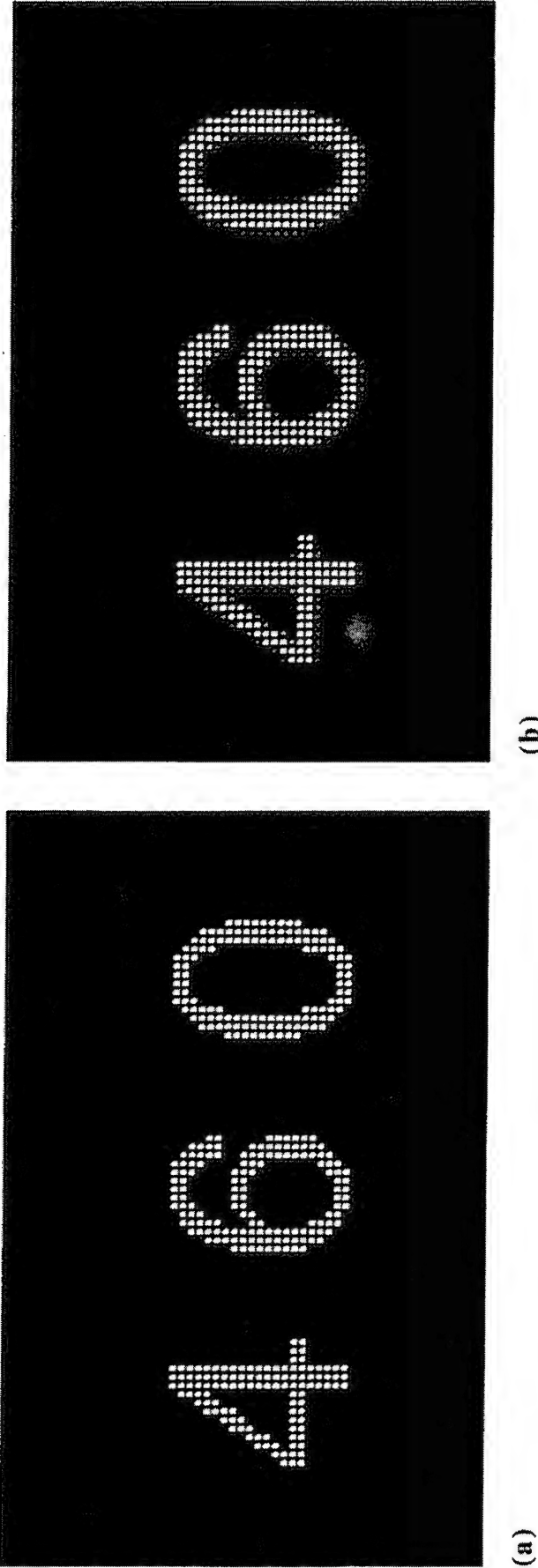
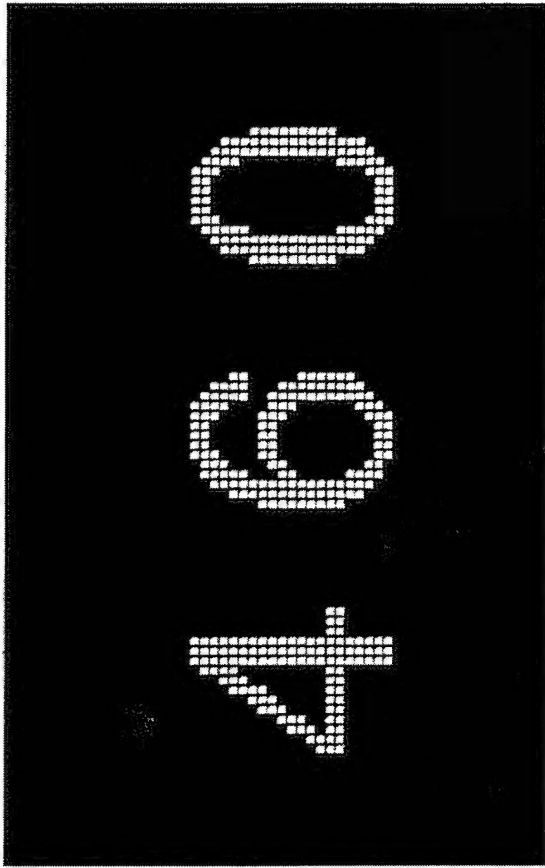


Figure 5-99. Subtractive Color Image Source (40% AR) Modeled in Evaluations 7, 8, and 10 for Symbol Images.

Without (a) and with (b) diffraction of the red layer. Images shown here are from Evaluation 8 (luminance covariated with aperture ratio). Luminance was not allowed to covary with aperture ratio in Evaluations 7 and 10. Note that evaluation images were actually presented in color on a high-resolution CRT. Also, these printed gray scale images are not gamma-corrected for printing. In addition, their size as printed is not intended to simulate the angular resolutions tested in the evaluations.



(a)

(b)

Figure 5-100. Subtractive Color Image Source (70% AR) Modeled in Evaluations 7, 8, and 10 for FLIR Symbol Images.

Without (a) and with (b) diffraction of the red layer. Images shown here are from Evaluation 8 (luminance covaried with aperture ratio). Luminance was not allowed to covary with aperture ratio in Evaluations 7 and 10. Note that evaluation images were actually presented in color on a high-resolution CRT. Also, these printed gray scale images are not gamma-corrected for printing. In addition, their size as printed is not intended to simulate the angular resolutions tested in the evaluations.

5.8.3 Procedure

The line visibility and image quality rating scales were used in Evaluation 7. For each comparison image, a separate rating was made on each scale. Participants were instructed to make their image ratings relative to the standard image. Eight participants followed the general evaluation procedure described previously, using the simultaneous comparison procedure and rating 10 practice images and 60 evaluation trials during a 30 minute period. The order of image presentation was randomized within blocks of resolution, with order of resolution counterbalanced among participants.

5.8.4 Results

Table 5-24 provides an overview of the significant data trends. The effects summarized in the table are discussed in the text following the table.

Table 5-24. ANOVA summary table for Evaluation 7.

Effect	Dependent Variable	Image	Figure	Page	df	MS	F	p	F^2	R ²
Resolution	Line Visibility	Symbols	Figure 5-101	381	2, 14	7671.667	17.28	.0002	.22	.47
	Image Quality	Symbols	Figure 5-102	382	2, 14	1620.417	8.93	.0050	.07	.42
Color	Image Quality	Symbols	Figure 5-103	383	1, 7	3081.667	10.31	.0148	.07	.42
	Line Visibility	Symbols	Figure 5-104	384	4, 28	3379.583	24.38	<.0001	.19	.47
Image Source	Image Quality	Symbols	Figure 5-105	385	4, 28	2466.042	18.92	<.0001	.21	.42
	Color X	Symbols	Figure 5-106	386	4, 28		8.77	.0024	.04	.42
Image Source										

Resolution. Line visibility ratings generally increased (i.e., lines were less apparent) with increased symbol resolution (Figure 5-101), but the difference in ratings between 11 and 22 pix/deg was not statistically robust ($p>.05$).

Image quality ratings generally increased as a function of symbol resolution (Figure 5-102), but the difference in ratings between 11 and 22 pix/deg was not statistically robust ($p>.05$).

Color. Image quality ratings were higher for yellow symbols than red symbols (Figure 5-103).

Image Source. Line visibility ratings were highest (i.e., lines were less apparent) for symbol images modeled with either of the 70% AR subtractive color image sources (Figure 5-104). In addition, line visibility ratings were lowest for symbol images modeled with the additive color image source ($p<.05$).

Image quality ratings also varied as a function of image source (Figure 5-105). Images presented with either of the 70% AR subtractive color image sources or the nondiffracted 40% AR subtractive color image source were assigned higher image quality ratings than images modeled with the diffracted 40% AR subtractive color image source ($p < .05$).

Color x Image Source Interaction. Diffraction reduced the image quality of red images modeled with the 40% AR subtractive color image source, but not yellow images (Figure 5-106).

5.8.5 Summary

The results from Evaluation 7 are summarized in Table 5-25 and the following summary statements:

Table 5-25. Preliminary conclusions based on Evaluation 7 results.

Variable	Image Type	Rating Asymptote	Notes
Resolution	Symbol	$\geq 33 \text{ pix/deg}$	Line visibility Image Quality
Color	Symbol	Yellow > Red	Minimizes red diffraction effects Higher luminance possible
Subtractive vs Additive	Symbol	Subtractive	Limited additive aperture ratio
Aperture Ratio	Symbol	$\geq 70\%$	Line visibility

1. Row and column lines were generally less visible in symbols presented at higher resolutions and higher aperture ratios. Image quality also generally improved with increased symbol resolution.
2. Diffraction effects on symbol image quality were dependent on color, with the addition of a nondiffracted color (green) serving to mask the red blurring in yellow images. Image quality was generally superior for yellow symbol images relative to red symbol images for this reason, as well as a relatively higher luminance of yellow symbol images.
3. Row and column lines were more visible for symbols presented via additive vs subtractive color image sources (given equivalent luminance and aperture ratio).

4. Symbol image quality was influenced by an interaction of diffraction and aperture ratio, such that diffracted image sources provided relatively high symbol image quality only if accompanied by a relatively high aperture ratio (which minimized the magnitude of the diffraction effect).

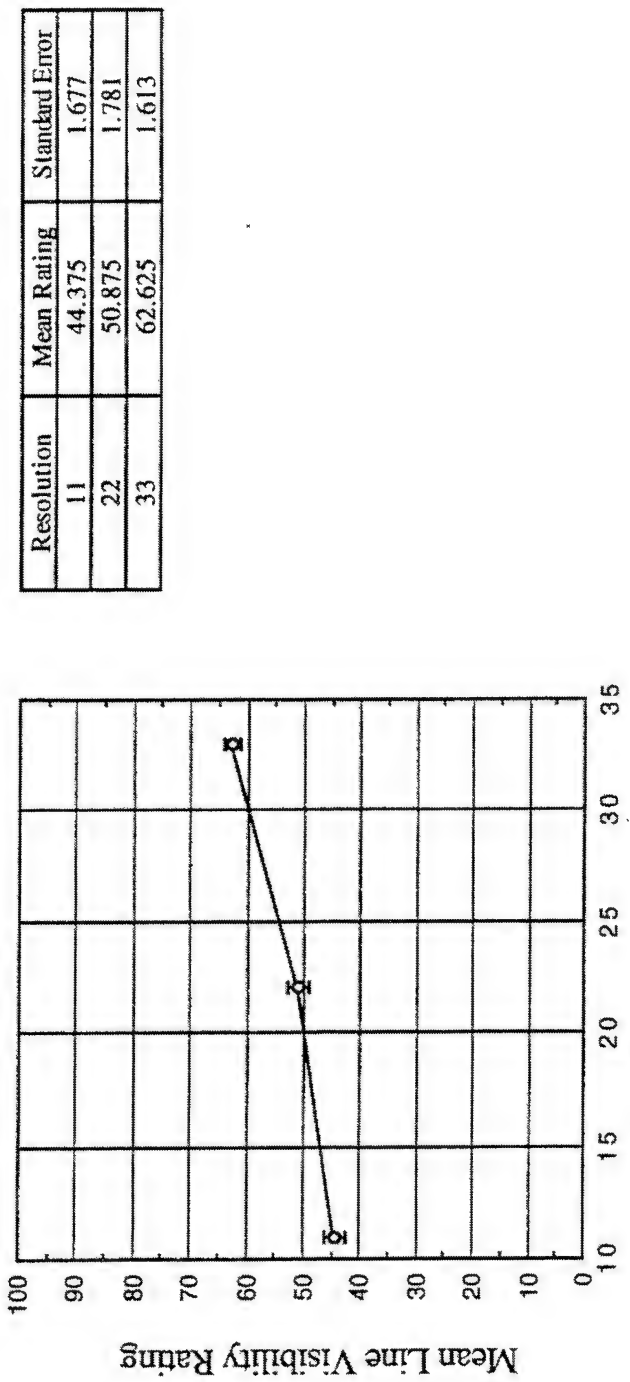


Figure 5-101. Mean Line Visibility Rating as a Function of Resolution (Evaluation 7, Symbol).

High line visibility ratings indicate high subjective similarity of comparison images to the standard image (i.e., low visibility of row and column lines). Error bars show standard error of the mean.

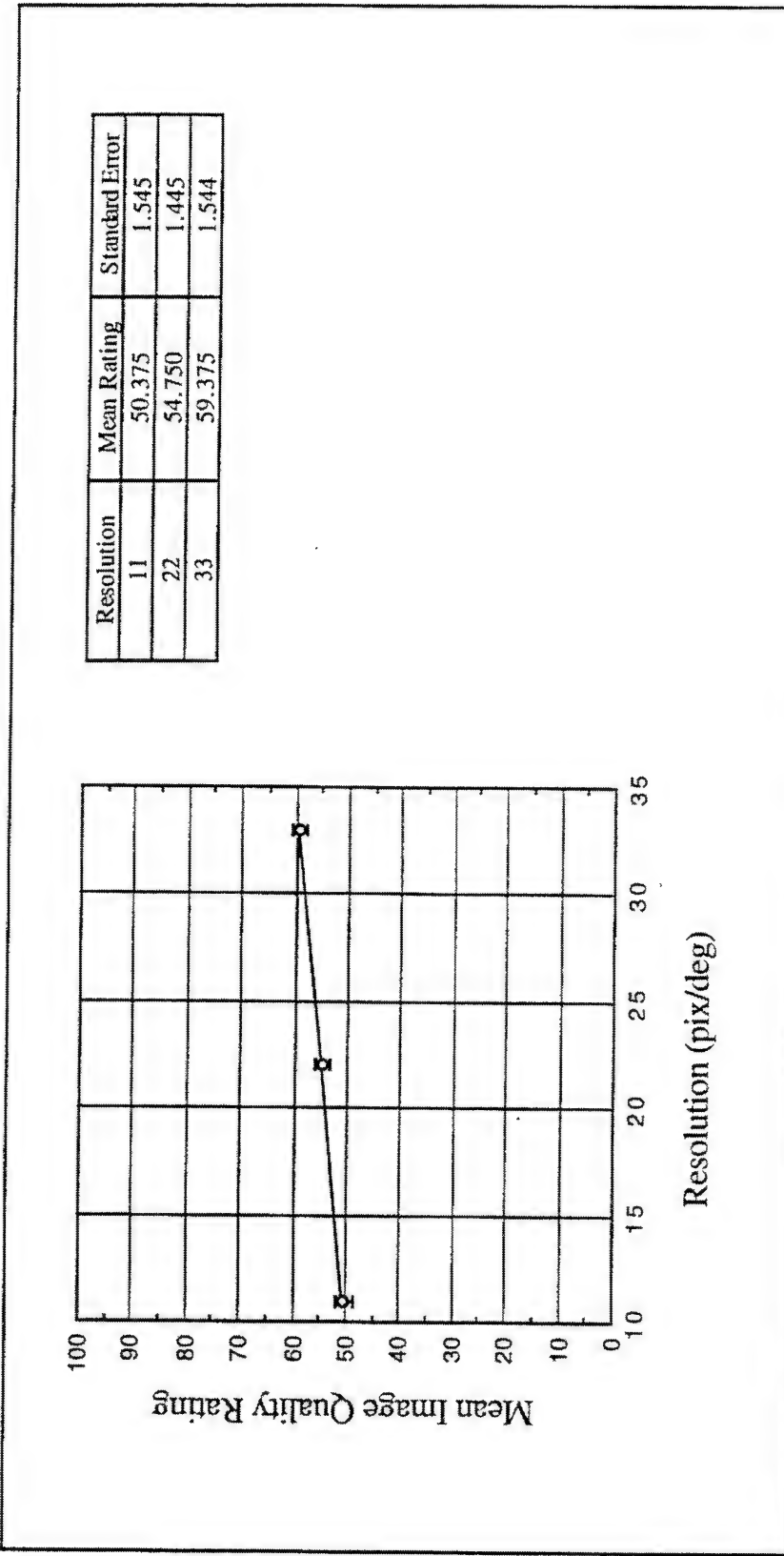


Figure 5-102. Mean Image Quality Rating as a Function of Resolution (Evaluation 7, Symbol).

High image quality ratings indicate high subjective similarity of comparison images to the standard image (i.e., relatively high image quality). Error bars show standard error of the mean.

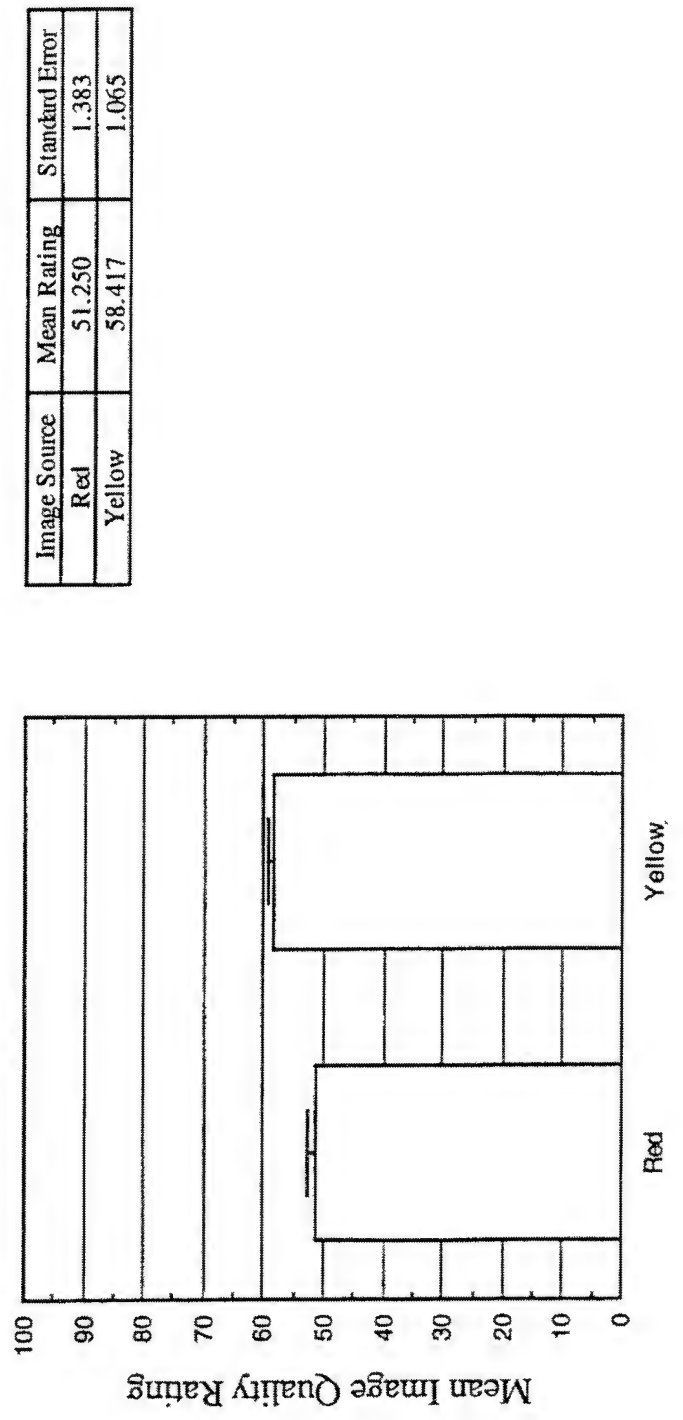


Figure 5-103. Mean Image Quality Rating as a Function of Image Color (Evaluation 7, Symbol).

High image quality ratings indicate high subjective similarity of comparison images to the standard image (i.e., relatively high image quality). Error bars show standard error of the mean.

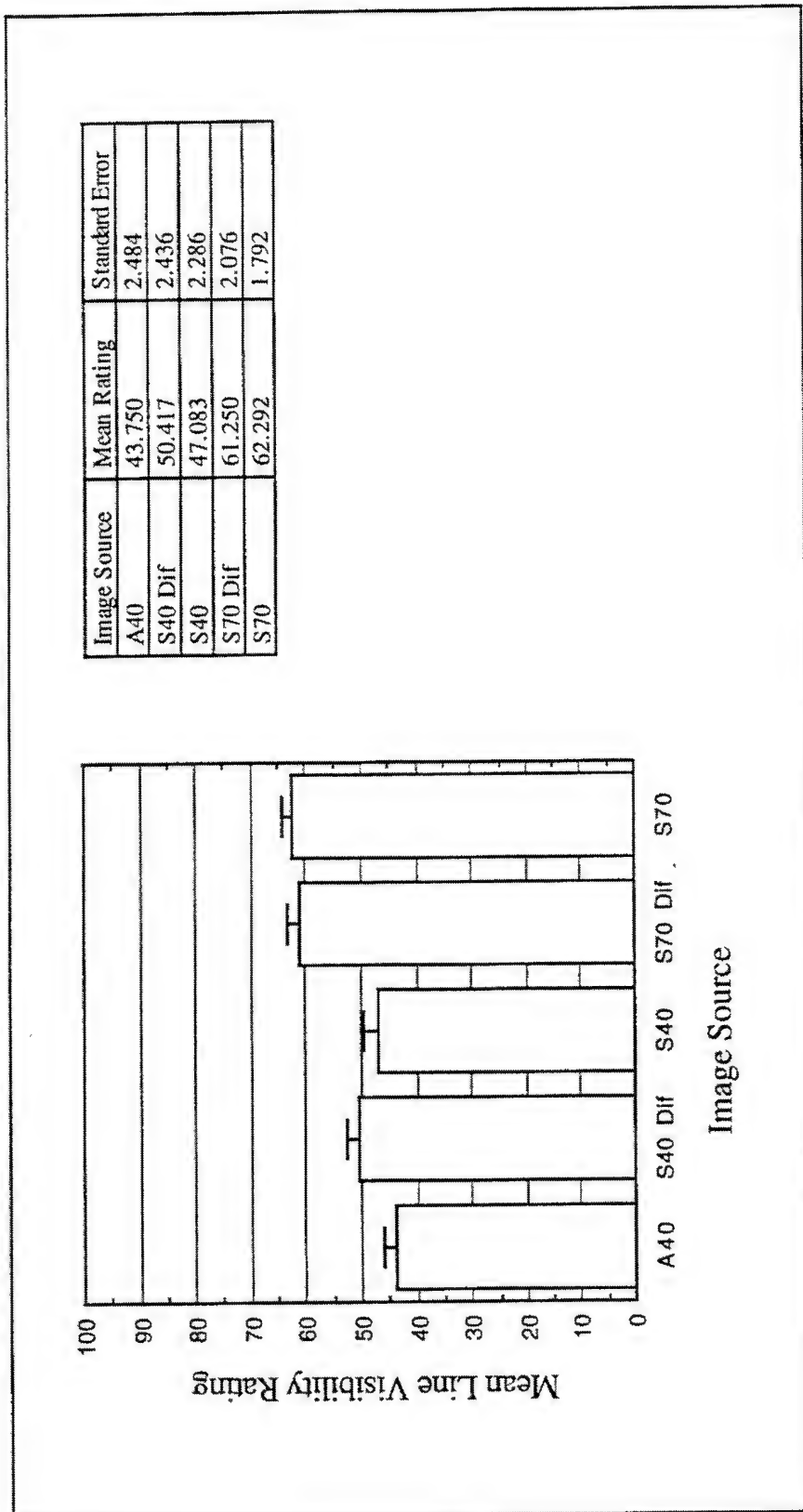


Figure 5-104. Mean Line Visibility Rating as a Function of Image Source (Evaluation 7, Symbol).

High line visibility ratings indicate high subjective similarity of comparison images to the standard image (i.e., low visibility of row and column lines). Error bars show standard error of the mean.

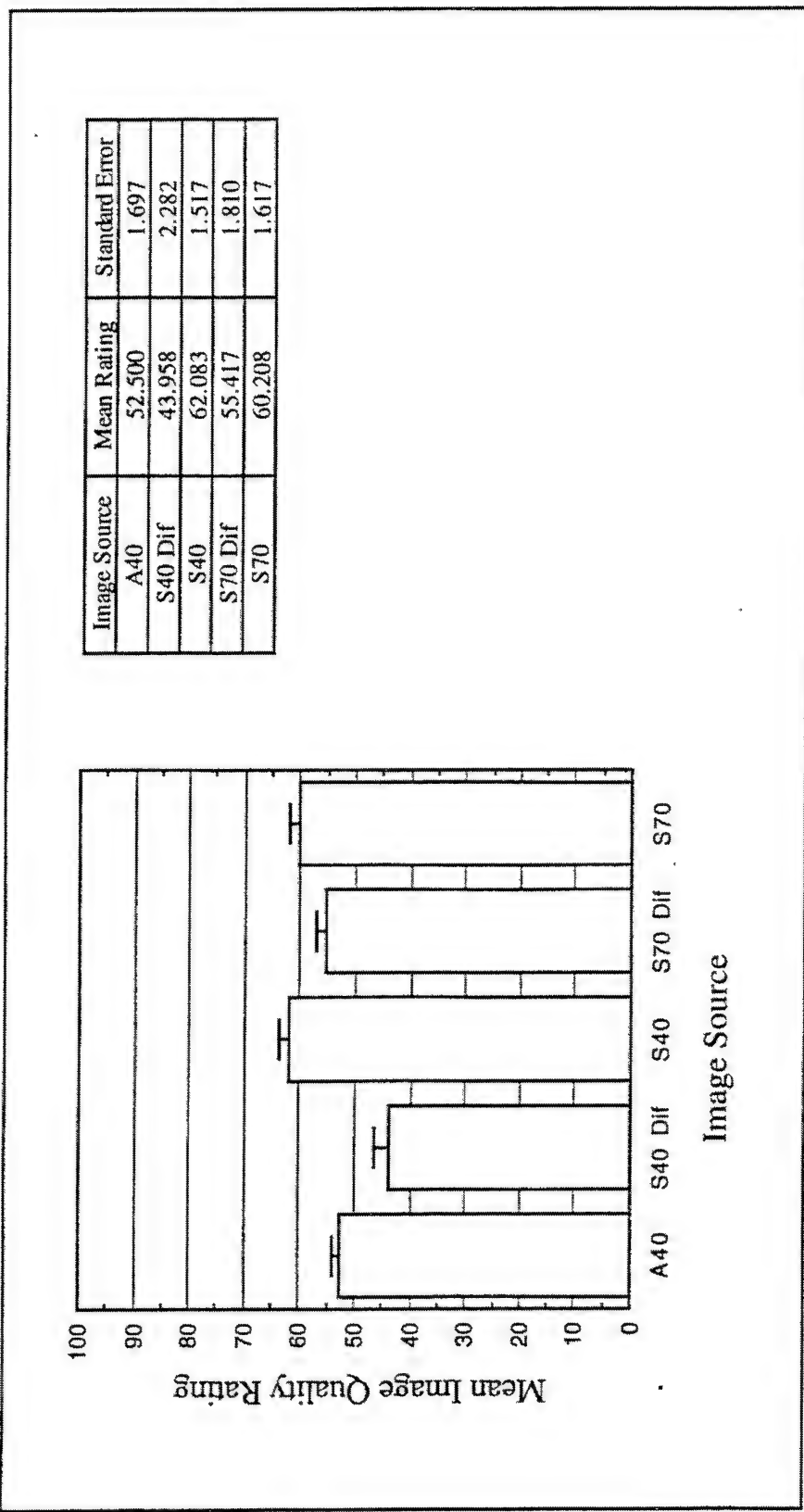


Figure 5-105. Mean Image Quality Rating as a Function of Image Source (Evaluation 7, Symbol).

High image quality ratings indicate high subjective similarity of comparison images to the standard image (i.e., relatively high image quality). Error bars show standard error of the mean.

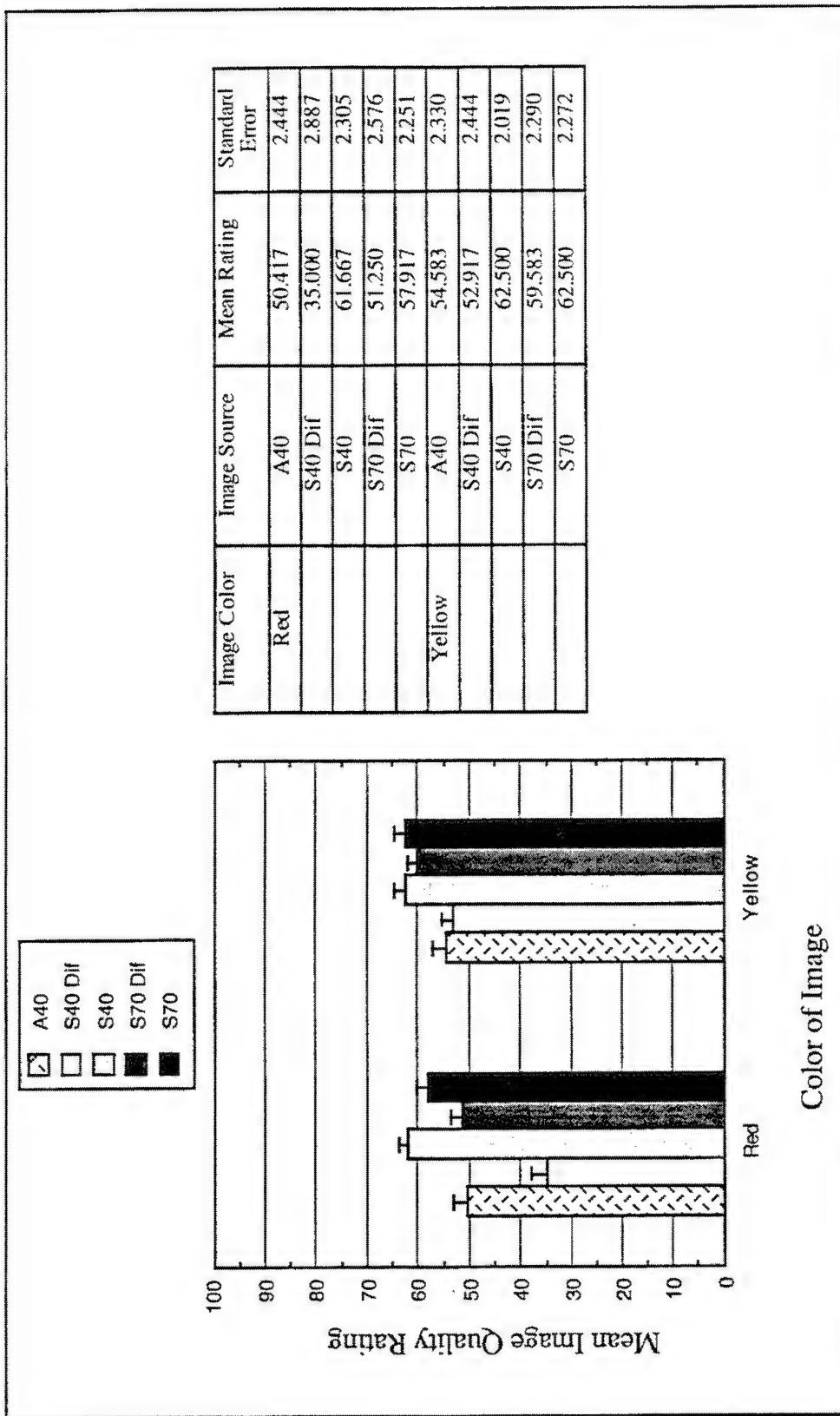


Figure 5-106. Mean Image Quality Rating as a Function of Image Color by Image Source (Evaluation 7, Symbol).

High image quality ratings indicate high subjective similarity of comparison images to the standard image (i.e., relatively high image quality). Error bars show standard error of the mean.

5.9 Evaluation 8

5.9.1 Objectives

Evaluation 8 was conducted to replicate the procedure of Evaluation 7 while allowing image luminance to covary with aperture ratio and color method (images modeled with higher aperture ratios had higher luminances, and images modeled with subtractive color image sources had higher luminances than those modeled with the additive color image source). The specific objectives of Evaluation 8 were:

1. Assess the relative impact of aperture ratio on perception of symbol line visibility and image quality.
2. Evaluate the relative impact of additive vs subtractive color pixel structures on perception of symbol line visibility and image quality.
3. Determine the perceptual impact of diffraction of the red layer in a subtractive color stack.
4. Assess the relative change in impact of red diffraction between red and yellow symbols.
5. Determine how changes in image source resolution, above and below the baseline HMS+ resolution, impact all of the above.
6. Determine the effect of allowing image luminance to covary with aperture ratio and color method on the above.

5.9.2 Design

Evaluation 8 images were modeled using subtractive and additive color image source models with varied aperture ratios and colors using the original numeric symbols described previously. Representative images from Evaluation 8 are printed in the design description of Evaluation 7. Half of the subtractive color image source models included diffraction of the red layer (see Evaluation 5). Comparison image luminance was allowed to vary among aperture ratio, color method, and image color, such that yellow images modeled with subtractive color image sources of high aperture ratio were of the highest luminance (the luminance of the standard image remained the same as in Evaluation 7). Comparison images were presented at resolutions of between 11 and 33 simulated AMLCD pixels per degree. Resolution was controlled by increasing or decreasing participant viewing distance (image field of view therefore covaried with resolution). Comparison images were presented at 2 gray scale levels (i.e., binary).

The simulation design levels included in Evaluation 8 are summarized in Table 5-26.

Table 5-26. Design variables for Evaluation 8.

Variable	Levels	Figure	Page
Resolution	11, 22, 33 pix/deg	(not illustrated)	
Color	Red, Yellow	(see <i>Evaluation 7</i>)	Figure 5-98 (p. 374)
Image Source	Additive (40% AR), Subtractive (40% AR) (with or without diffraction), Subtractive (70% AR) (with or without diffraction)	(see <i>Evaluation 7</i>)	Figure 5-98 (p. 374)

5.9.3 Procedure

The same rating scales used in Evaluation 7 (line visibility and image quality) were also used in Evaluation 8. The procedure was also identical. For each comparison image, a separate rating was made on each scale. Participants were instructed to make their image ratings relative to the standard image. Eight participants followed the general evaluation procedure described previously, using the simultaneous comparison procedure and rating 10 practice images and 60 evaluation trials during a 30 minute period. The order of image presentation was randomized within blocks of resolution, with order of resolution counterbalanced among participants.

5.9.4 Results

Table 5-27 provides an overview of the significant data trends. The effects summarized in the table are discussed in the text following the table.

Table 5-27. ANOVA summary table for Evaluation 8.

Effect	Dependent Variable	Image	Figure	Page	df	MS	F	p	R ²
Resolution	Line Visibility	Symbols	Figure 5-107	393	2, 14	6852.917	7.75	.0172	.55
	Image Quality	Symbols	Figure 5-108	394	2, 14	1448.750	8.15	.0078	.52
Color	Image Quality	Symbols	Figure 5-109	395	1, 7	2100.417	14.47	.0067	.03
	Line Visibility	Symbols	Figure 5-110	396	4, 28	9014.583	32.97	<.0001	.38
Image Source	Image Quality	Symbols	Figure 5-111	397	4, 28	6487.083	20.87	.0004	.37
	Image Quality	Symbols	Figure 5-112	398	4, 28	917.083	10.71	.0012	.52
Color x Image Source									

Resolution. Line visibility ratings generally increased as a function of symbol resolution (Figure 5-107), but the difference in ratings between 22 and 33 pix/deg was not statistically robust ($p>.05$).

Image quality ratings generally increased as a function of symbol resolution (Figure 5-108), but the difference in ratings between 22 and 33 pix/deg was not statistically robust ($p>.05$).

Color. Image quality ratings were higher for yellow symbols than red symbols (Figure 5-109).

Image Source. Line visibility ratings were highest (i.e., lines were less apparent) for symbol images modeled with either of the 70% AR subtractive color image sources (Figure 5-110). In addition, line visibility ratings were lowest for symbol images modeled with the additive color image source ($p<.05$).

Image quality ratings also varied as a function of image source (Figure 5-111). Images presented with either of the 70% AR subtractive color image sources were assigned higher image quality ratings than images modeled with either the diffracted 40% AR subtractive color image source or the additive color image source ($p < .05$).

Color x Image Source Interaction. Diffraction reduced the image quality of red images modeled with the 40% AR subtractive color image source, but not yellow images (Figure 5-112).

5.9.5 Summary

The results from Evaluation 8 are summarized in Table 5-28 and the following summary statements:

Table 5-28. Preliminary conclusions based on Evaluation 8 results.

Variable	Image Type	Rating Asymptote	Notes
Resolution	Symbol	≥ 33 pix/deg	Line visibility Image Quality
Color	Symbol	Yellow > Red	Minimizes red diffraction effects Higher luminance possible
Subtractive vs Additive	Symbol	Subtractive	Limited additive aperture ratio
Aperture Ratio	Symbol	$\geq 70\%$	Line visibility

1. The results of Evaluation 8 are generally consistent with those of Evaluation 7. There was a less than two-point average increase in image ratings in Evaluation 8 relative to Evaluation 7 (Table 5-29). However, allowing luminance to covary with aperture ratio and color method appears to have modified line visibility and image quality ratings. In particular, the line visibility advantages for images modeled with the 70% AR subtractive color image source were much greater in Evaluation 8 (Figure 5-110) than in Evaluation 7 (Figure 5-104), in particular with reference to images modeled with the additive color image source. Similarly, while little image quality advantage was found for images modeled with the subtractive color image sources in Evaluation 7 (Figure 5-105), a clear advantage was demonstrated in Evaluation 8 (Figure 5-111).

2. Row and column lines were generally less visible in symbols presented at higher resolutions and higher aperture ratios. Image quality also generally improved with increased symbol resolution. These conclusions are consistent with the results of Evaluation 7.
3. Diffraction effects on symbol image quality were dependent on color, with the addition of a nondiffracted color (green) serving to mask the red blurring in yellow images. Image quality was generally superior for yellow symbol images relative to red symbol images, due to the diffraction masking effect and a relatively higher luminance of yellow symbol images. These conclusions are consistent with the results of Evaluation 7.
4. Row and column lines were more visible for symbols presented via additive vs subtractive color image sources (given equivalent luminance and aperture ratio). This conclusion is consistent with the results of Evaluation 7.
5. Symbol image quality was influenced by an interaction of diffraction, and aperture ratio, such that diffracted image sources provided relatively high symbol image quality only if accompanied by a relatively high aperture ratio (which minimized the magnitude of the diffraction effect). This conclusion is consistent with the results of Evaluation 7.

Table 5-29. Mean rating differences between Evaluations 7 and 8.

Rating Scale	Evaluation 7	Evaluation 8	Difference
Image Quality	54.833	56.125	1.292
Line Visibility	52.958	53.958	1.000

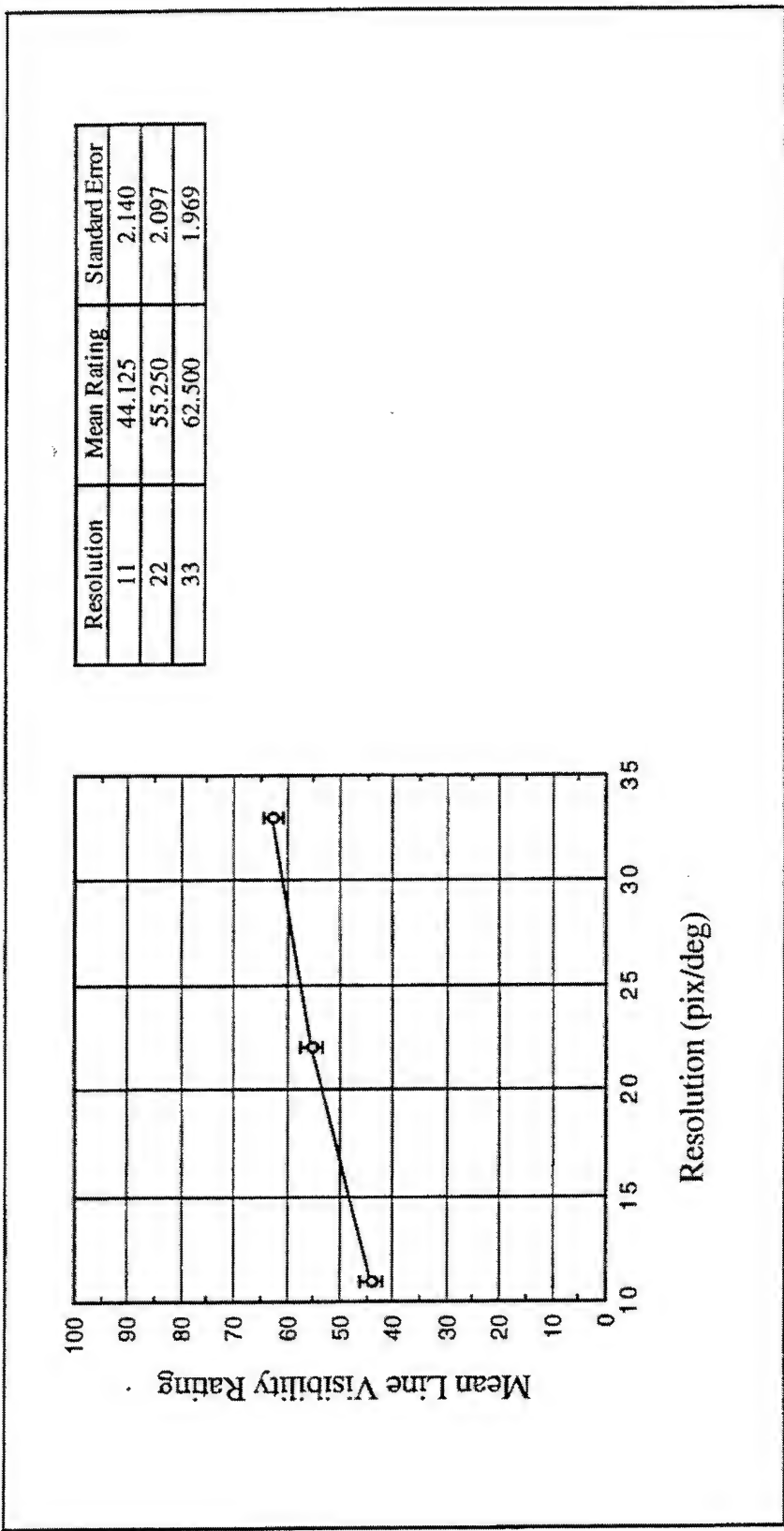


Figure 5-107. Mean Line Visibility Rating as a Function of Resolution (Evaluation 8, Symbol).

High line visibility ratings indicate high subjective similarity of comparison images to the standard image (i.e., low visibility of row and column lines). Error bars show standard error of the mean.

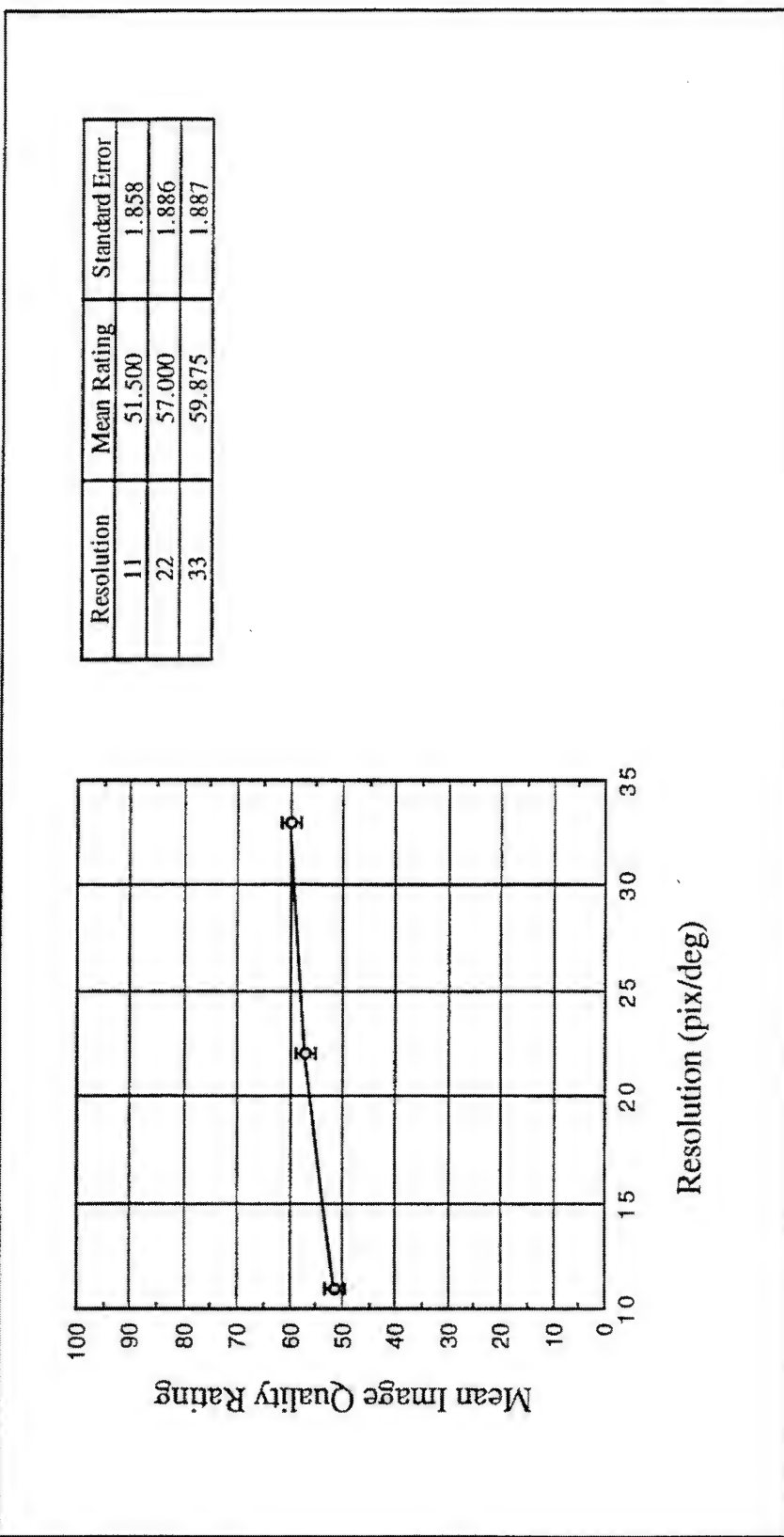


Figure 5-108. Mean Image Quality Rating as a Function of Resolution (Evaluation 8, Symbol).

High image quality ratings indicate high subjective similarity of comparison images to the standard image (i.e., relatively high image quality). Error bars show standard error of the mean.

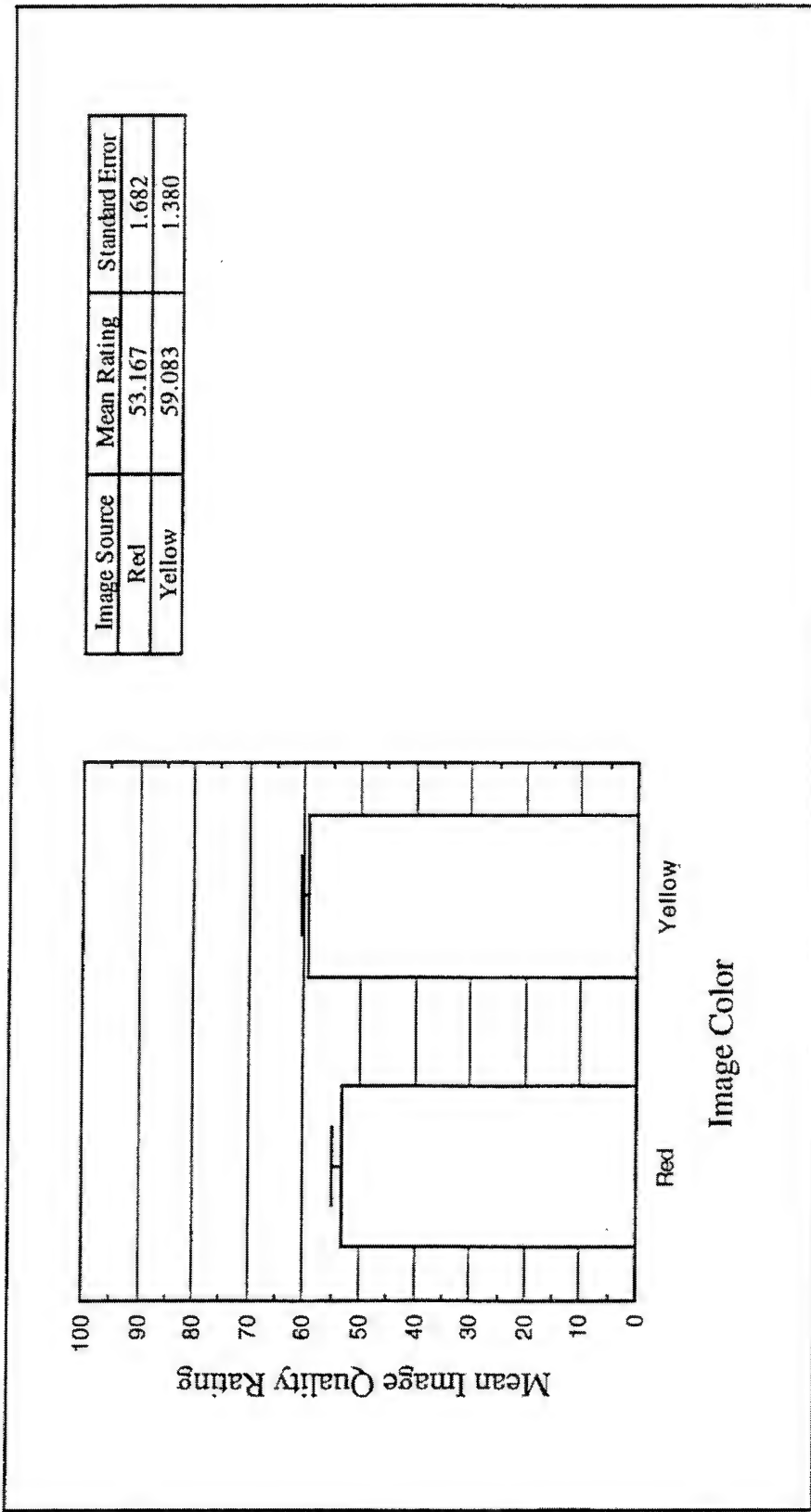


Figure 5-109. Mean Image Quality Rating as a Function of Image Color (Evaluation 8, Symbol).

High image quality ratings indicate high subjective similarity of comparison images to the standard image (*i.e.*, relatively high image quality). Error bars show standard error of the mean.

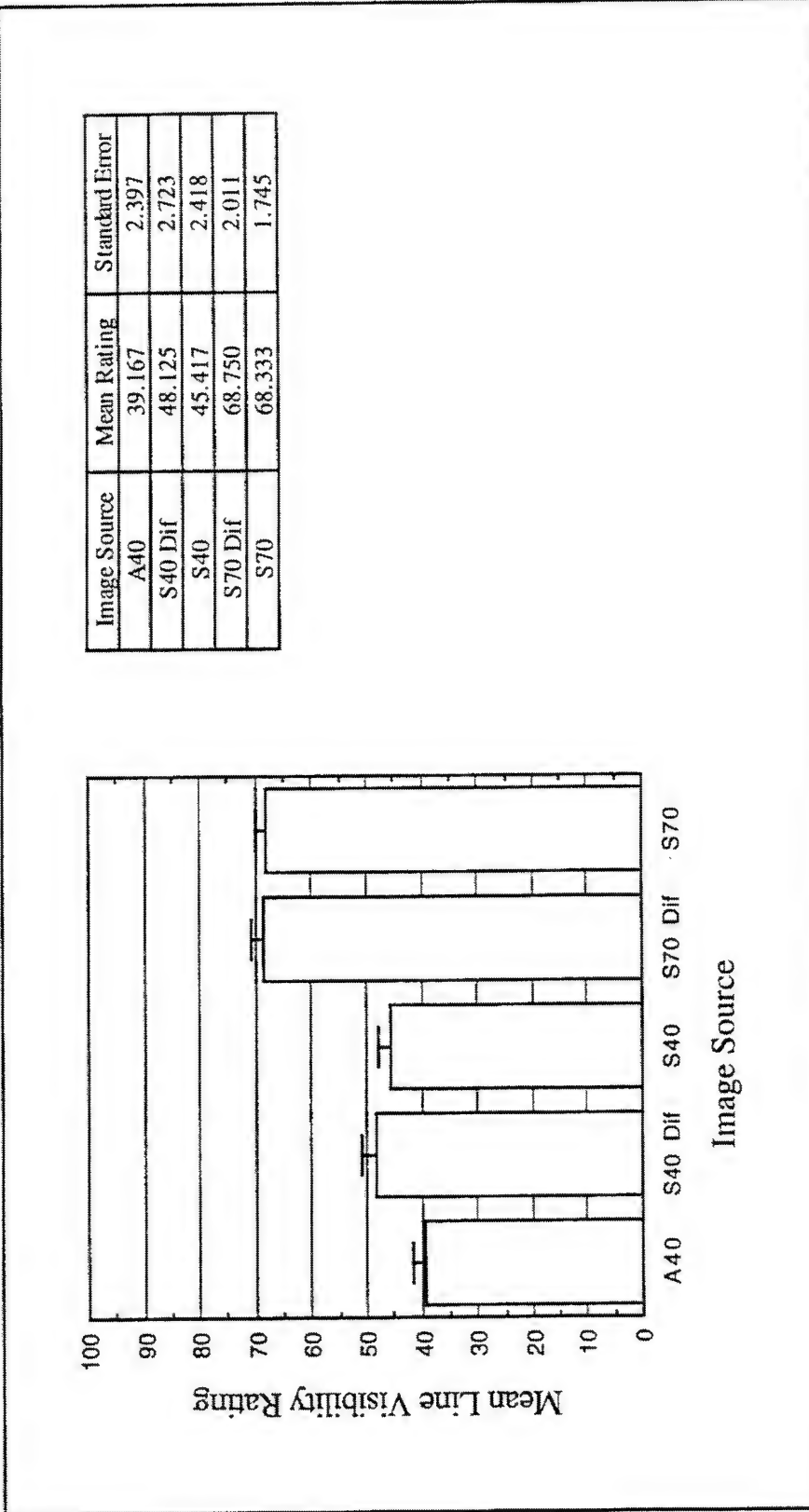


Figure 5-110. Mean Line Visibility Rating as a Function of Image Source (Evaluation 8, Symbol).

High line visibility ratings indicate high subjective similarity of comparison images to the standard image (i.e., low visibility of row and column lines). Error bars show standard error of the mean.

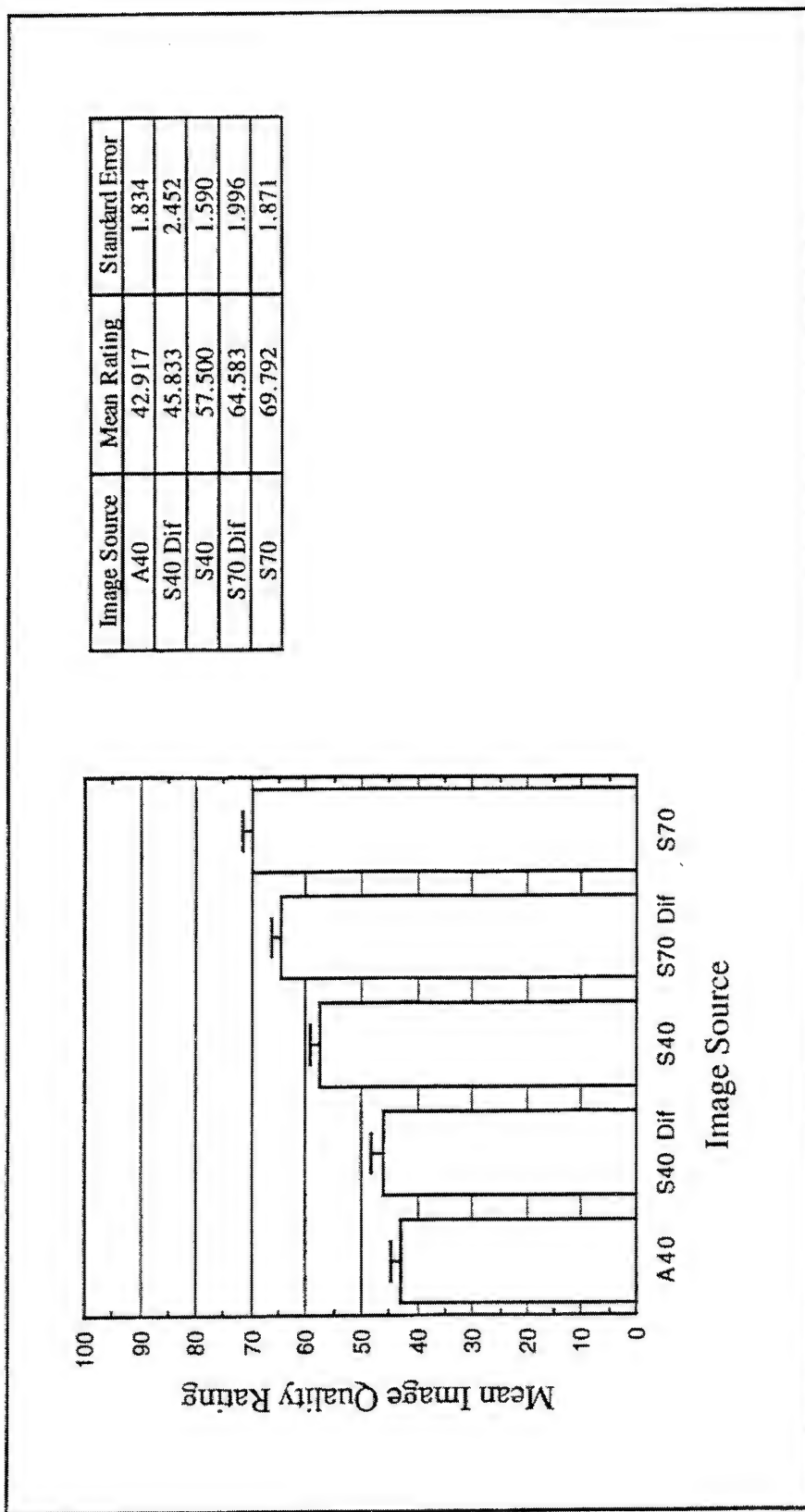


Figure 5-111. Mean Image Quality Rating as a Function of Image Source (Evaluation 8, Symbol).

High image quality ratings indicate high subjective similarity of comparison images to the standard image (i.e., relatively high image quality). Error bars show standard error of the mean.

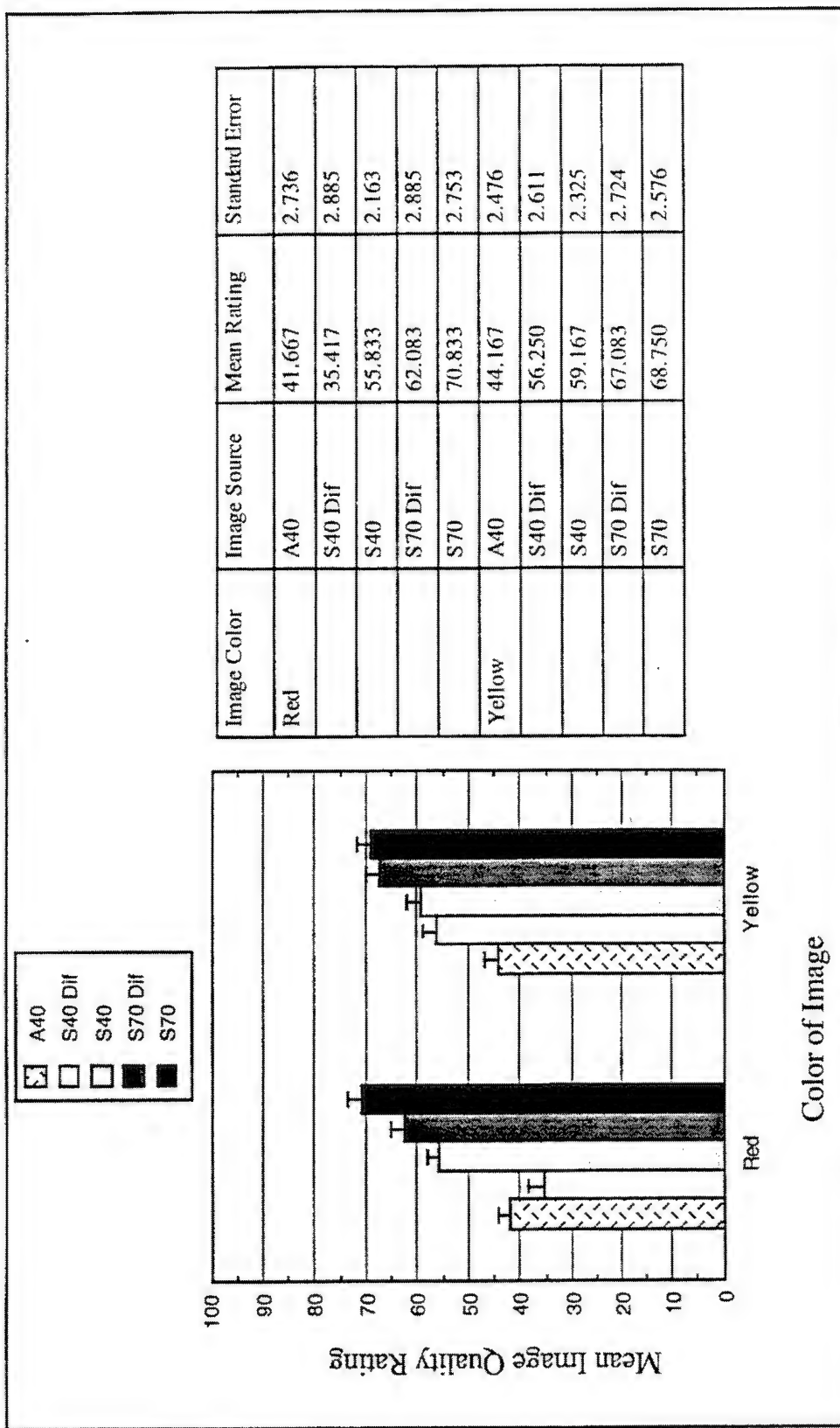


Figure 5-112. Mean Image Quality Rating as a Function of Image Color by Image Source (Evaluation 8, Symbol).

High image quality ratings indicate high subjective similarity of comparison images to the standard image (i.e., relatively high image quality). Error bars show standard error of the mean.

5.10 Evaluation 9

5.10.1 Objectives

Evaluation 9 was conducted to examine the relative impact of enhancement of the standard image used in the simulation evaluations. While previous evaluations incorporating FLIR images all used luminance/contrast enhanced standard images (as previously described), standard images in Evaluation 9 were closely matched in luminance and luminance contrast with comparison images while allowing other image source model variables such as aperture ratio to vary (standard images had effective aperture ratios of 100%). The evaluation replicated a portion of the design found in Evaluation 5, while using matched rather than enhanced standard images. The specific objective of Evaluation 9 was to provide a benchmark for better interpreting the relative acceptability of images simulated in previous evaluations by examining rating shifts between Evaluation 5 and Evaluation 9.

5.10.2 Design

Evaluation 9 comparison images were modeled using subtractive and additive color image source models with varied aperture ratios using the two original FLIR images described previously. Half of the subtractive color image source models included diffraction of the red layer. Image luminance was held constant among aperture ratio and color method, such that equivalent images modeled with different image sources were of equal luminance. Unlike previous evaluations, only red images were simulated in Evaluation 9. Images were presented at resolutions of between 11 and 33 simulated AMLCD pixels per degree. Resolution was controlled by increasing or decreasing participant viewing distance (image field of view therefore covaried with resolution). FLIR images were subjected to gray scale level clipping and distribution as previously described under *Simulation Software*. Images were presented at 64 gray scale levels with a linear distribution.

The simulation design levels included in Evaluation 9 are summarized in Table 5-30.

Table 5-30. Design variables for Evaluation 9.

Variable	Levels	Figure
FLIR Image	Truck, Tank	(see <i>Software Imagery</i>)
Resolution	11, 22, 33 pix/deg	(not illustrated)
Image Source	Additive (40% AR), Subtractive (40% AR) (with or without diffraction), Subtractive (70% AR) (with or without diffraction)	(see <i>Evaluation 5</i>) Figure 5-65 (p. 327)

Standard images used in Evaluation 9 were matched in luminance and luminance contrast with comparison images. The differences between the contrast-enhanced standard images used in Evaluation 5 and the contrast-matched images used in Evaluation 9 are illustrated in Figure 5-113 and Figure 5-114.

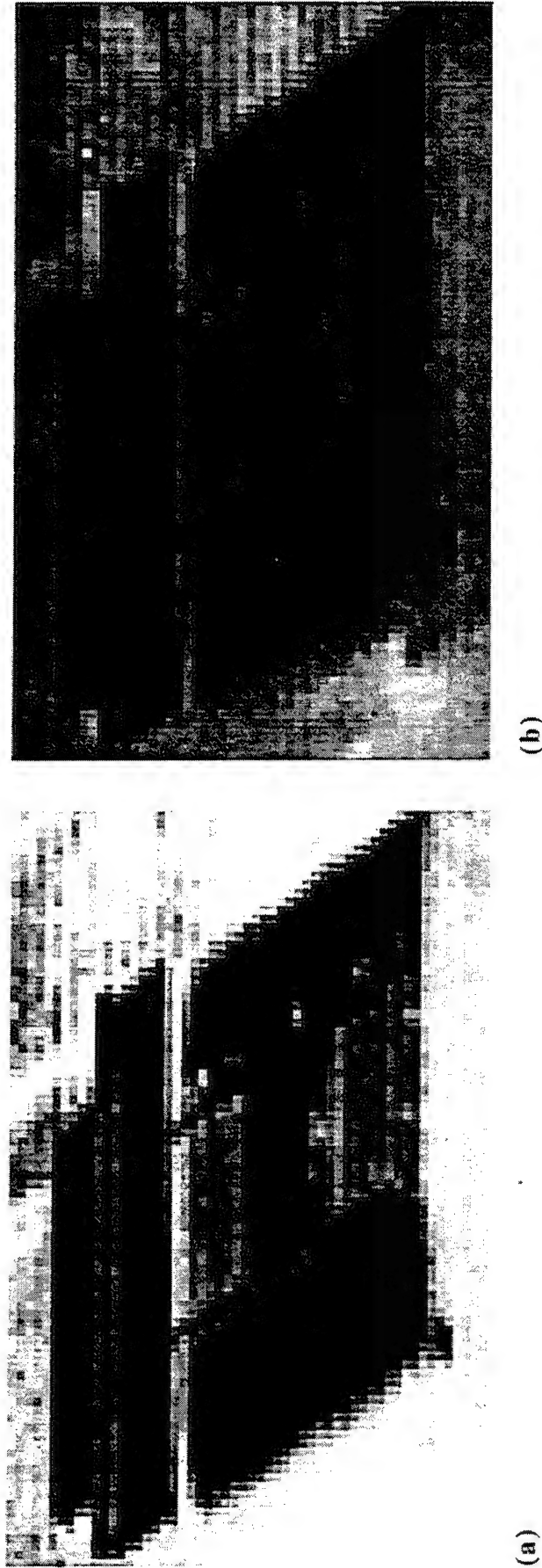
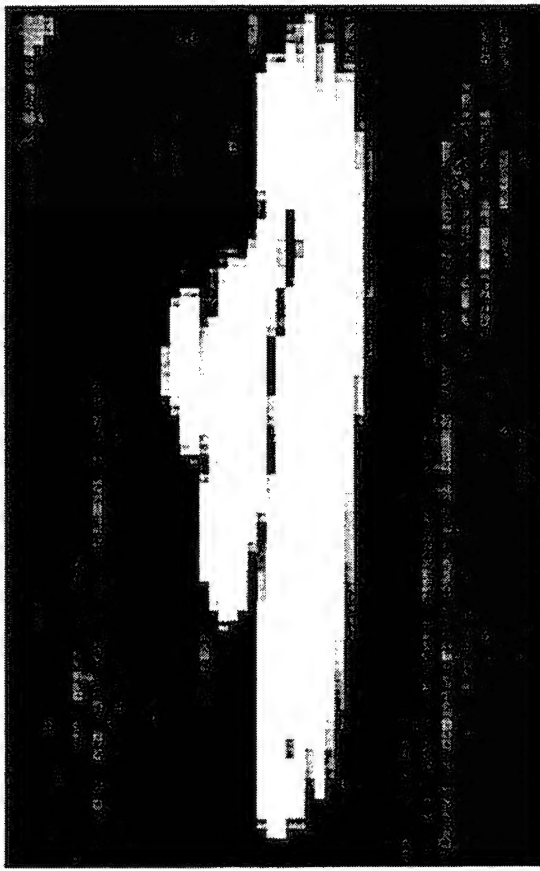


Figure 5-113. Modification of Standard Image in Evaluation 9 for FLIR Truck Images

Enhanced Standard (a) and matched standard (b). Note that evaluation images were actually presented in color on a high-resolution CRT. Also, these printed gray scale images are not gamma-corrected for printing. In addition, their size as printed is not intended to simulate the angular resolutions tested in the evaluations.



(b)



(a)

Figure 5-14. Modification of Standard Image in Evaluation 9 for FLIR Tank Images.

Enhanced Standard (a) and matched standard (b). Note that evaluation images were actually presented in color on a high-resolution CRT. Also, these printed gray scale images are not gamma-corrected for printing. In addition, their size as printed is not intended to simulate the angular resolutions tested in the evaluations.

5.10.3 Procedure

The same rating scales (line visibility, image quality, and sharpness) and procedure that were used in Evaluation 5 were used in Evaluation 9. For each comparison image, a separate rating was made on each scale. Participants were instructed to make their image ratings relative to the standard image. The matched, rather than enhanced, standard image was used. Four participants who previously completed Evaluation 5 followed the general evaluation procedure described previously, using the simultaneous comparison procedure and rating 10 practice images and 30 evaluation trials during a 20 minute period. The order of image presentation was randomized within blocks of FLIR image (Truck or Tank) for each observer. Image order was further blocked within image type by resolution, with order of resolution counterbalanced among participants.

5.10.4 Results

Ratings to the matched standard were paired with the comparable enhanced standard data from Evaluation 5 to examine the net effect of standard enhancement on image ratings. These differences are graphically described in Figure 5-115 to Figure 5-126. The white portions of the graph bars depict the increase in ratings associated with the matched standard relative to the enhanced standard. There was an overall increase of over 13 points in line visibility ratings and over 8 points in image quality ratings to images associated with the matched standard in Evaluation 9 vs images associated with the enhanced standard in Evaluation 5. When decomposed as a function of resolution or image source, mean line visibility ratings increased as little as 5 points and as much as 24.5 points. Mean image quality ratings increased as little as 2.5 points and as much as 16 points.

Although there was an overall increase of 4.5 points in sharpness ratings for images associated with the matched standard, in some instances sharpness ratings were actually lower. When decomposed as a function of resolution or image source, mean sharpness ratings decreased as much as 6 points and increased as much as 18 points.

5.10.5 Summary

The comparison of images in Evaluation 5 to a standard image which was contrast enhanced relative to comparison images produced line visibility and image quality ratings which were relatively low, commensurate with the enhancement of the standard. An alternative index of the relative acceptability of simulation images was provided by comparing images to a standard image which was matched to the comparison images in all respects but the presence of the AMLCD model.

The differences seen in sharpness ratings are relatively small and may represent noise in the data. There was no apriori reason to expect differences in sharpness ratings as a function of FLIR standard image contrast.

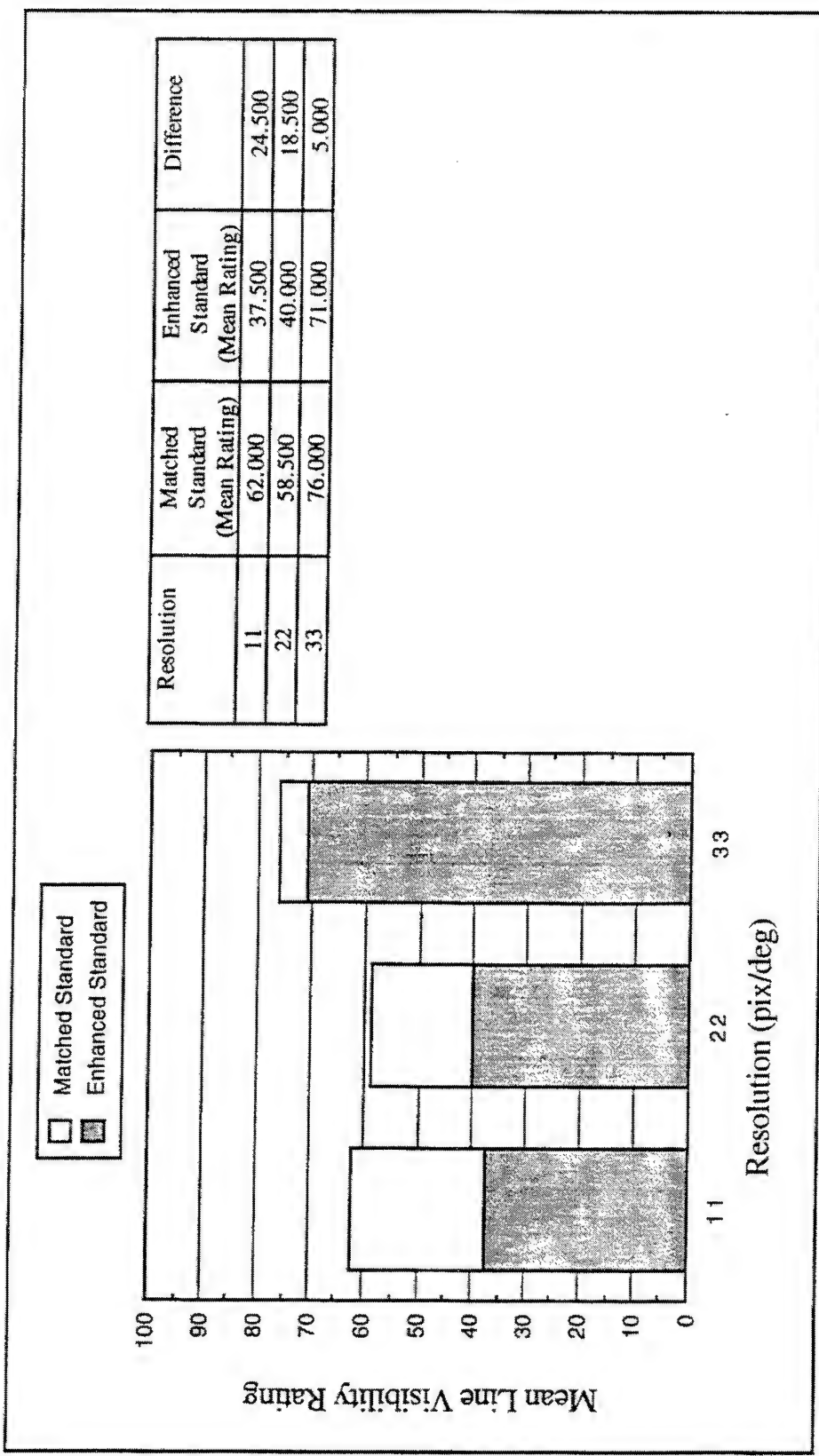


Figure 5-115. Mean Line Visibility Rating as a Function of Resolution and Standard Image (Evaluation 9, Truck). High line visibility ratings indicate high subjective similarity of comparison images to the standard image (i.e., low visibility of row and column lines).

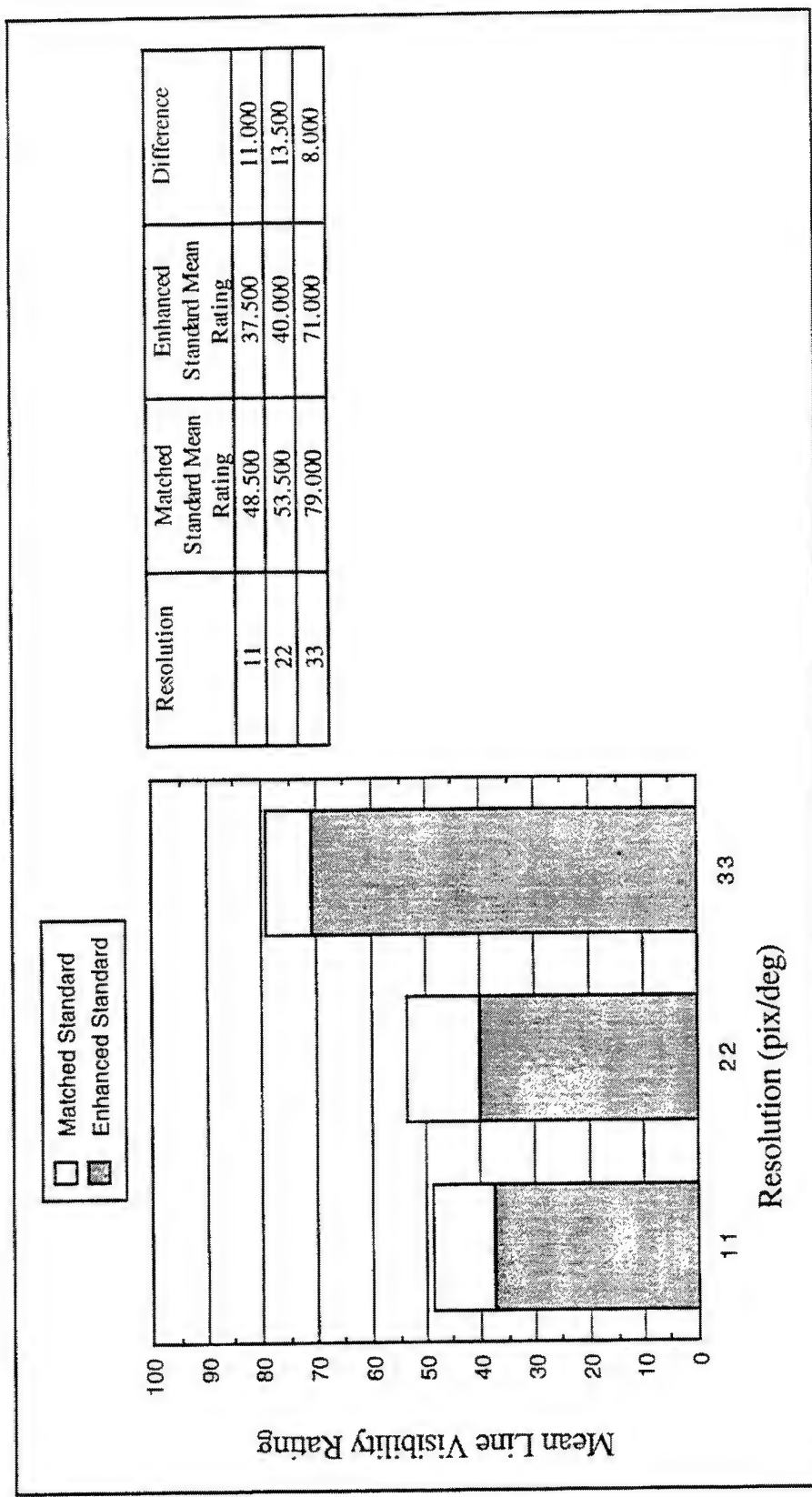


Figure 5-116. Mean Line Visibility Rating as a Function of Resolution and Standard Image (Evaluation 9, Tank).

High line visibility ratings indicate high subjective similarity of comparison images to the standard image (i.e., low visibility of row and column lines).

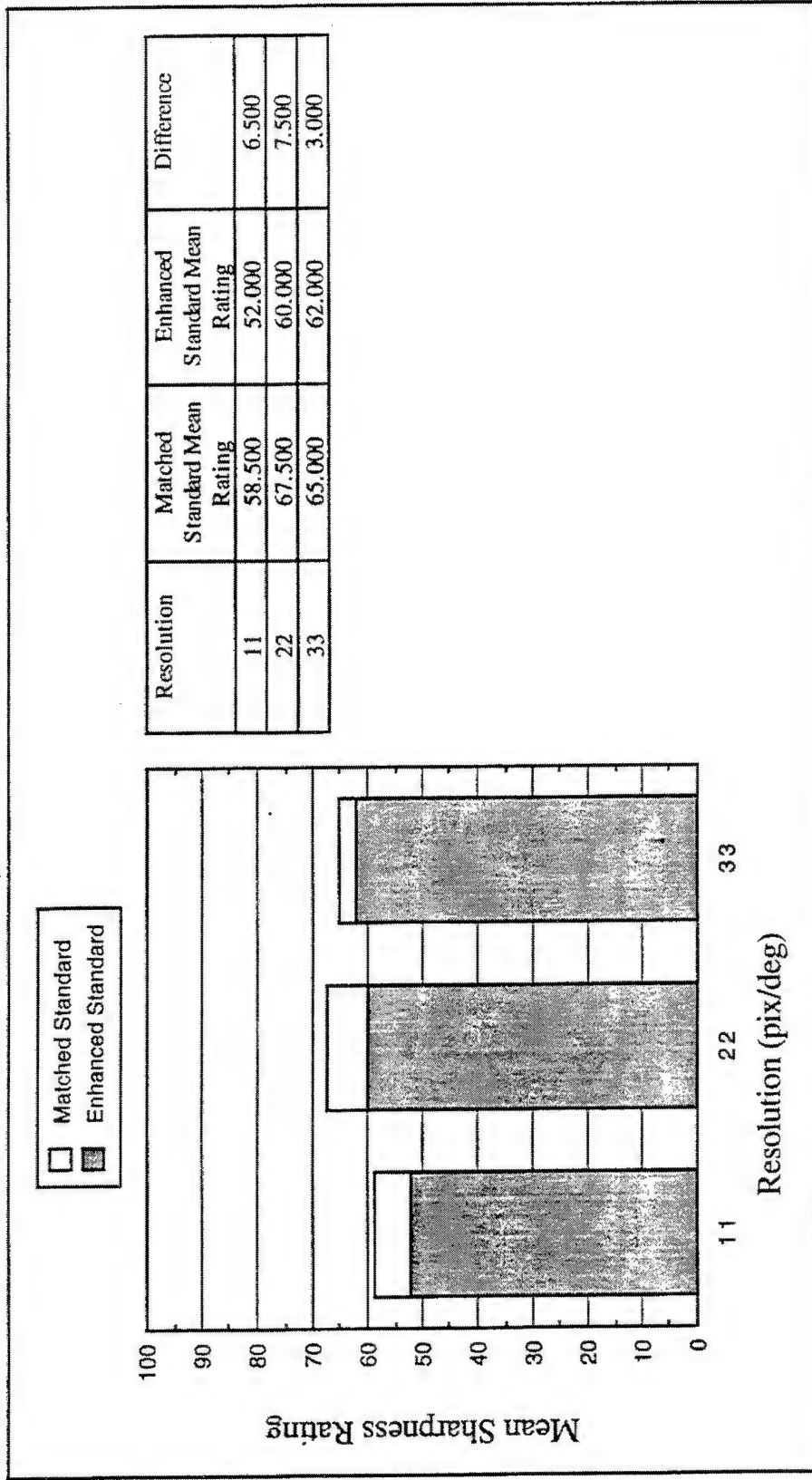


Figure 5-117. Mean Sharpness Rating as a Function of Resolution and Standard Image (Evaluation 9, Truck).

High sharpness ratings indicate high subjective similarity of comparison images to the standard image (i.e., relatively sharp, or non blurred).

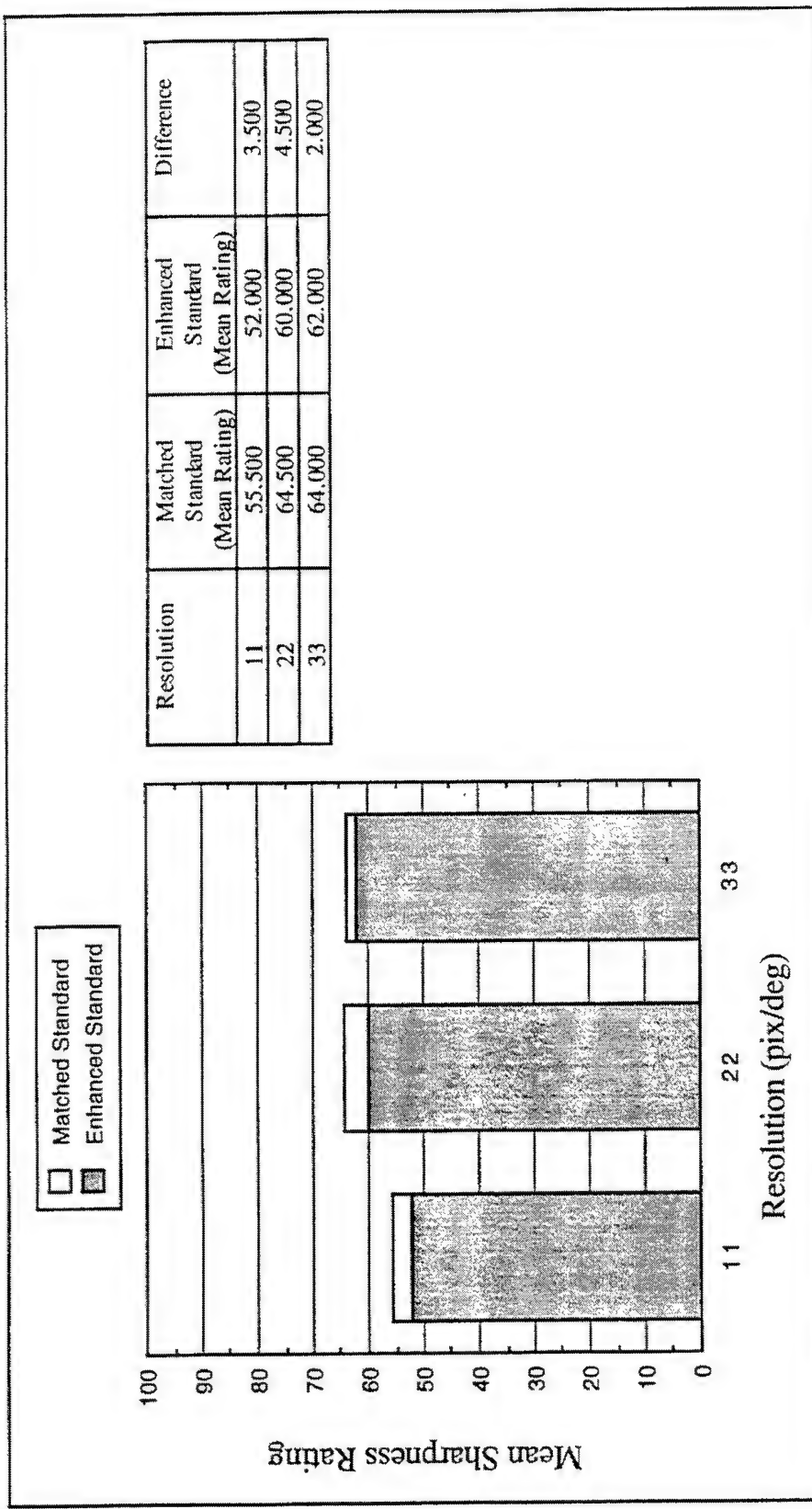


Figure 5-118. Mean Sharpness Rating as a Function of Resolution and Standard Image (Evaluation 9, Tank).
High sharpness ratings indicate high subjective similarity of comparison images to the standard image (i.e., relatively sharp, or non blurred).

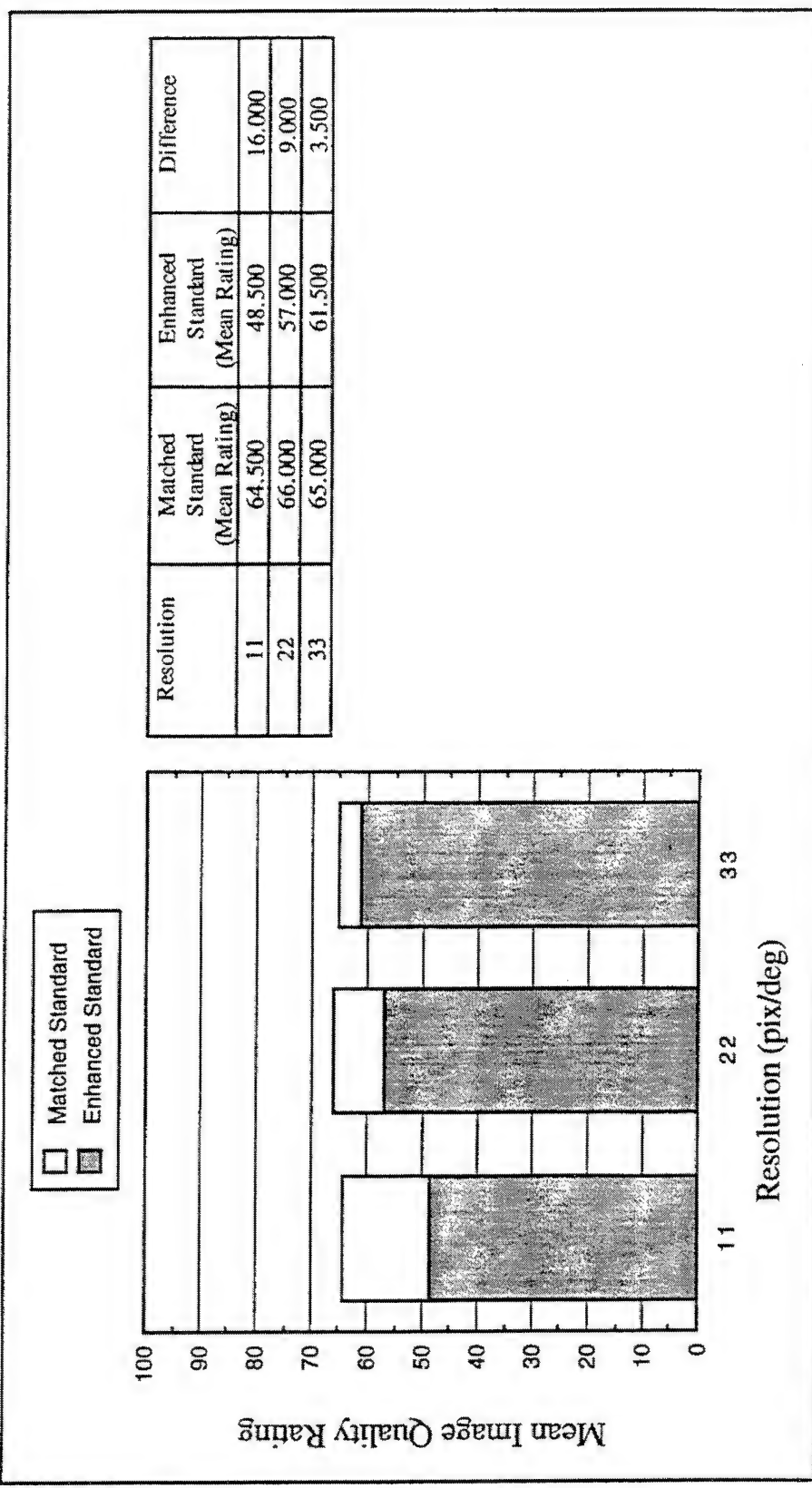


Figure 5-119. Mean Image Quality Rating as a Function of Resolution and Standard Image (Evaluation 9, Truck).

High image quality ratings indicate high subjective similarity of comparison images to the standard image (i.e., relatively high image quality).

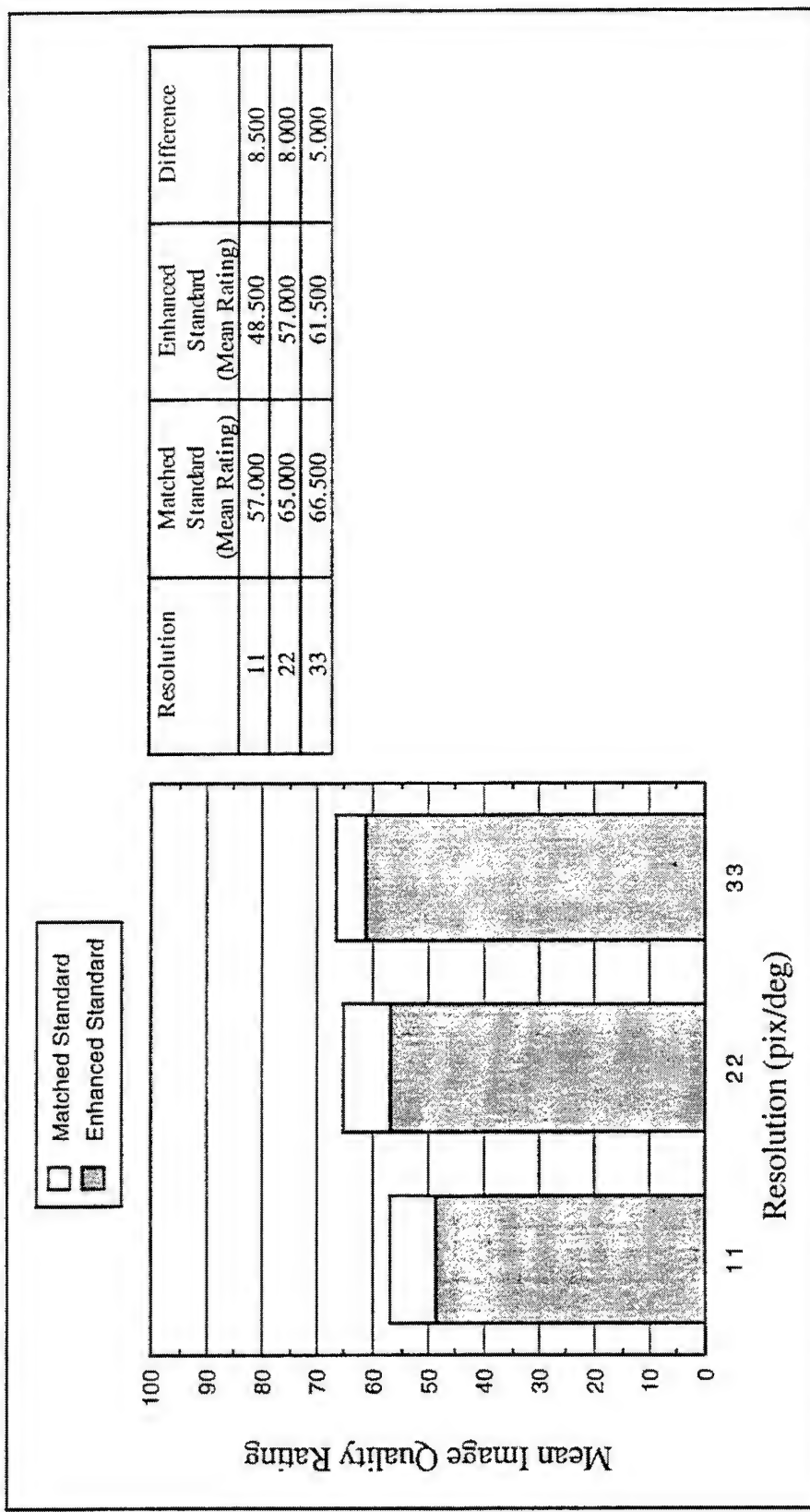


Figure 5-120. Mean Image Quality Rating as a Function of Resolution and Standard Image (Evaluation 9, Tank).

High image quality ratings indicate high subjective similarity of comparison images to the standard image (i.e., relatively high image quality).

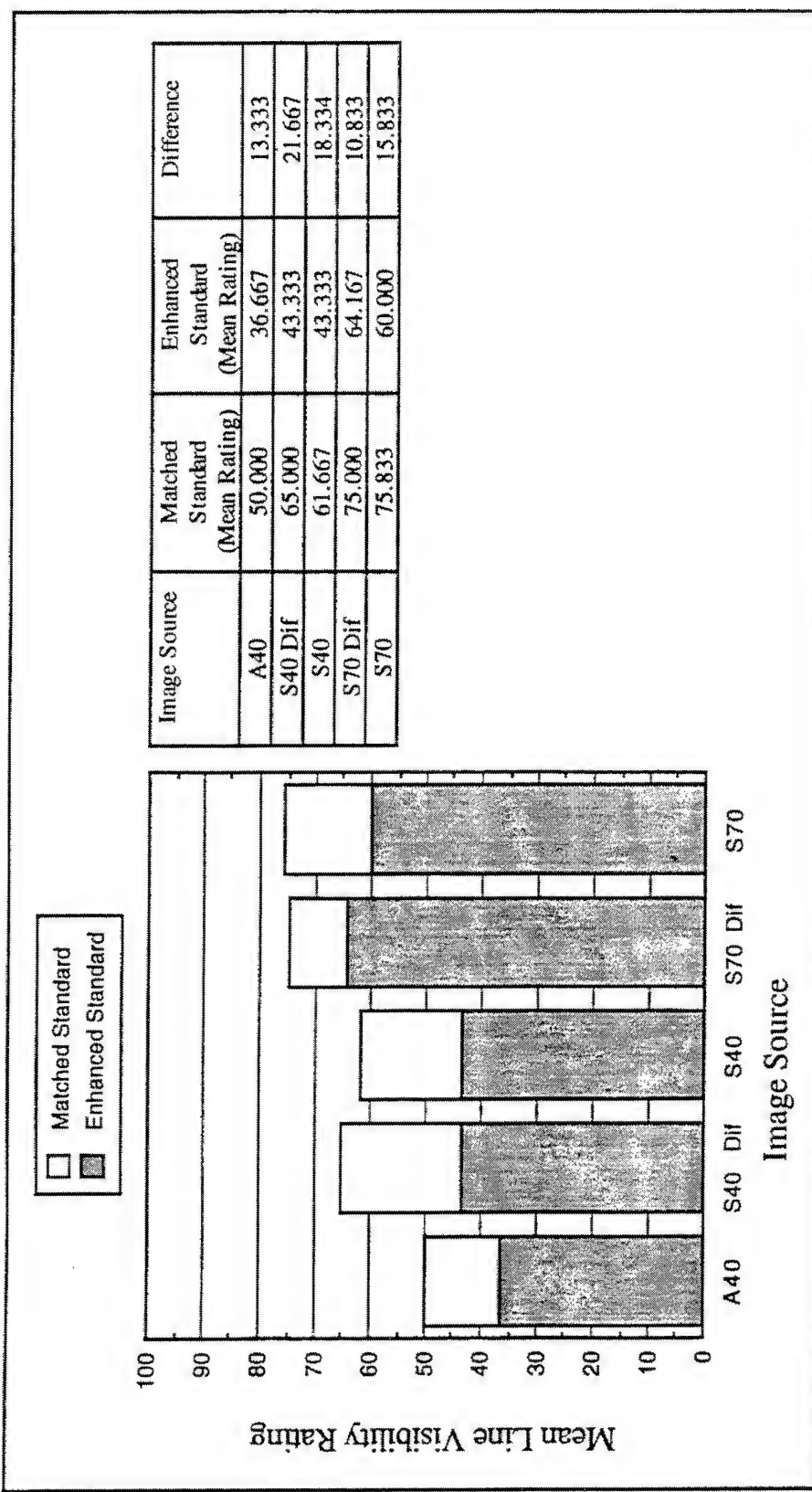


Figure 5-121. Mean Line Visibility Rating as a Function of Image Source and Standard Image (Evaluation 9, Truck). High line visibility ratings indicate high subjective similarity of comparison images to the standard image (i.e., low visibility of row and column lines).

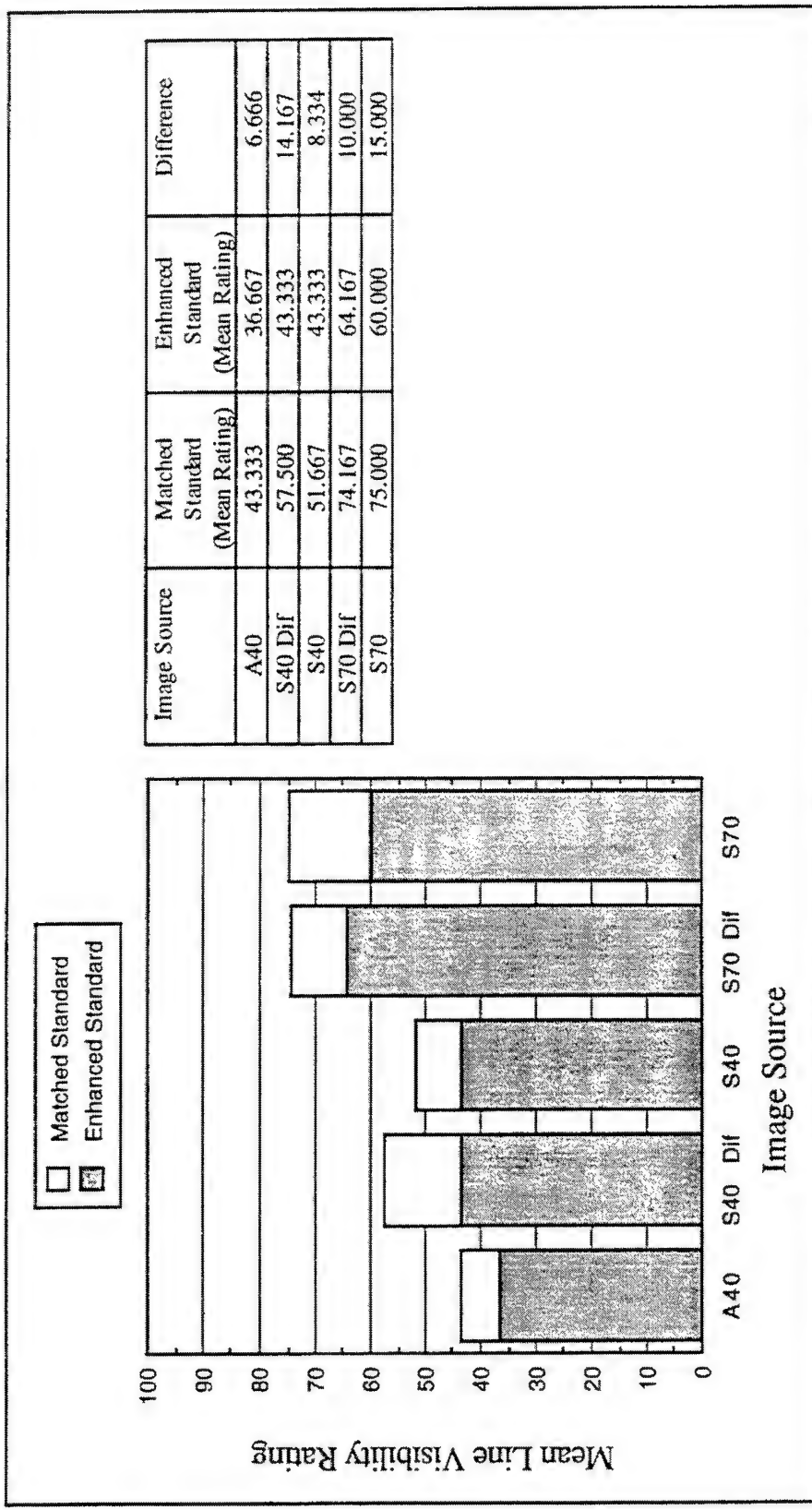


Figure 5-122. Mean Line Visibility Rating as a Function of Image Source and Standard Image (Evaluation 9, Tank). High line visibility ratings indicate high subjective similarity of comparison images to the standard image (i.e., low visibility of row and column lines).

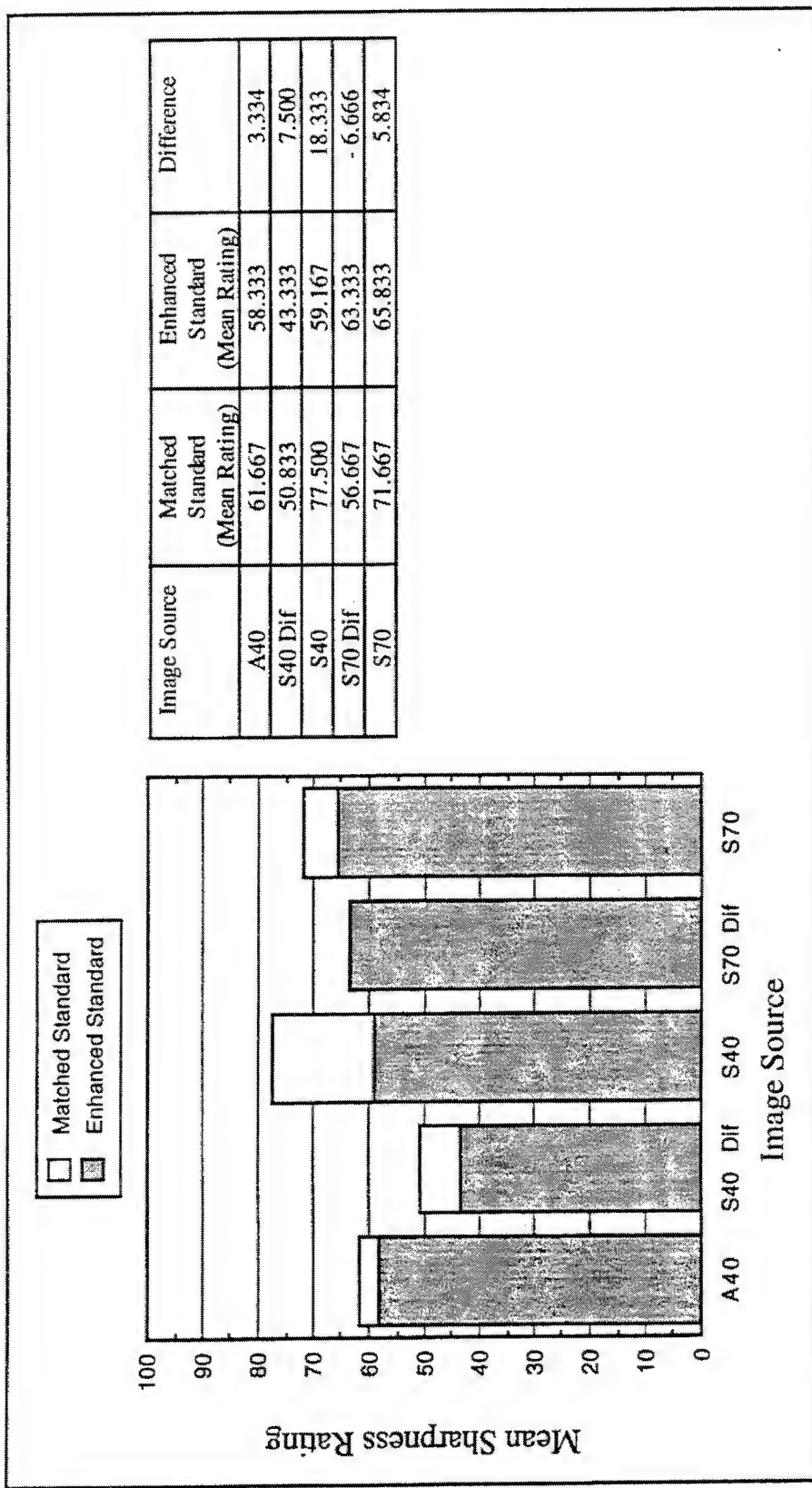


Figure 5-123. Mean Sharpness Rating as a Function of Image Source and Standard Image (Evaluation 9, Truck).

High sharpness ratings indicate high subjective similarity of comparison images to the standard image (i.e., relatively sharp, or non blurred).

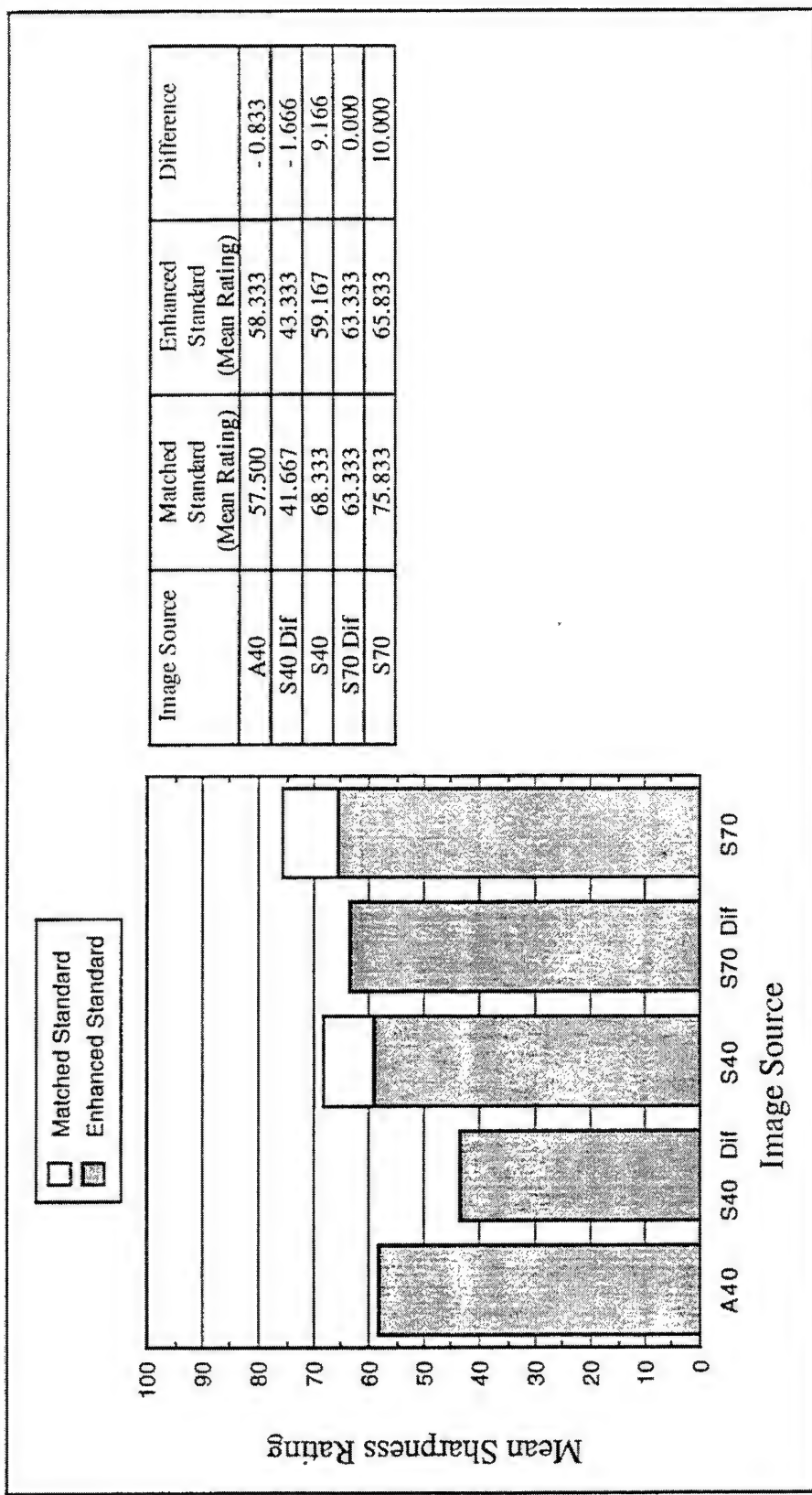


Figure 5-124. Mean Sharpness Rating as a Function of Image Source and Standard Image (Evaluation 9, Tank).

High sharpness ratings indicate high subjective similarity of comparison images to the standard image (i.e., relatively sharp, or non blurred).

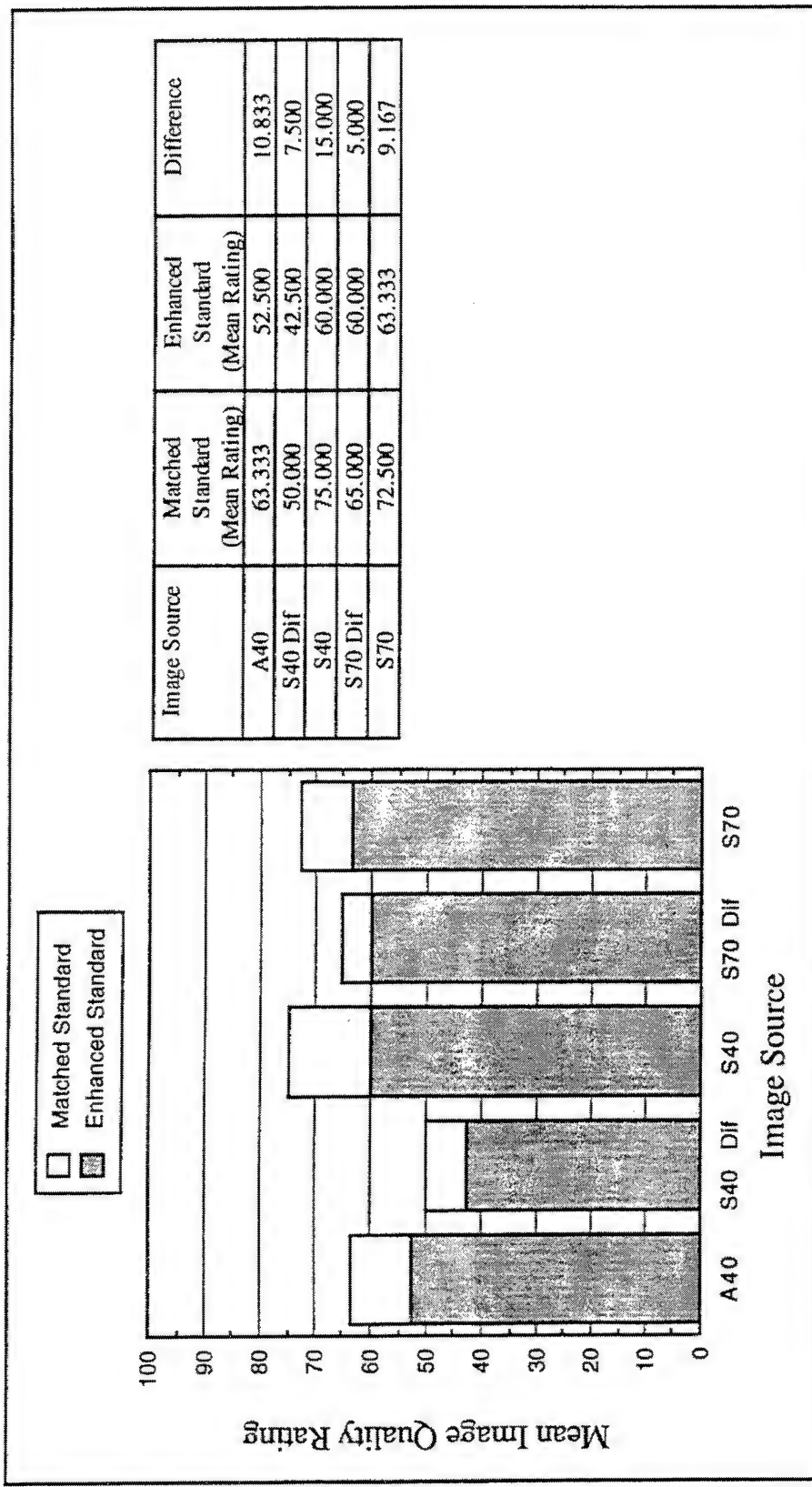


Figure 5-125. Mean Image Quality Rating as a Function of Image Source and Standard Image (Evaluation 9, Truck).

High image quality ratings indicate high subjective similarity of comparison images to the standard image (i.e., relatively high image quality).

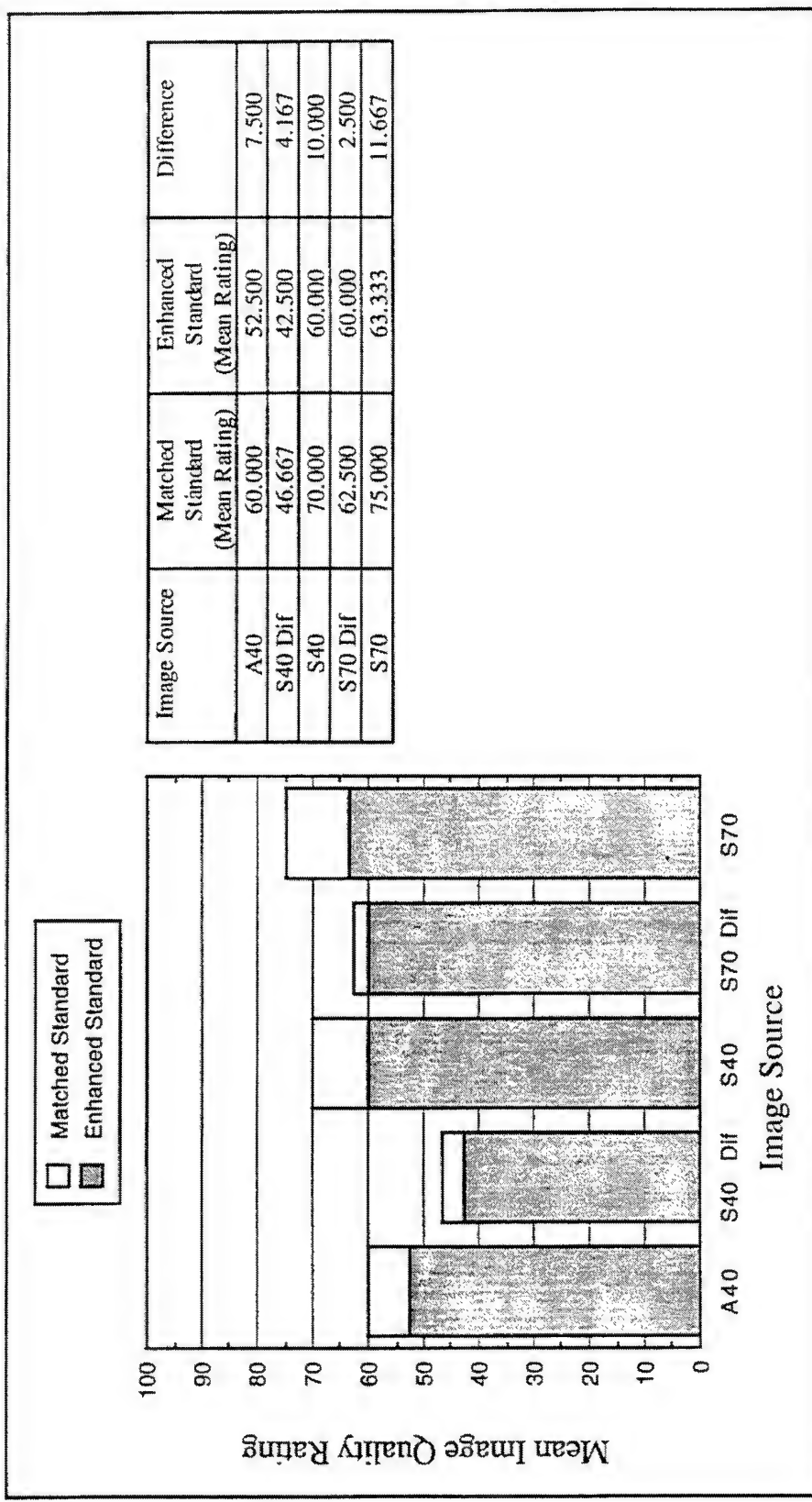


Figure 5-126. Mean Image Quality Rating as a Function of Image Source and Standard Image (Evaluation 9, Tank).
High image quality ratings indicate high subjective similarity of comparison images to the standard image (i.e., relatively high image quality).

5.11 Evaluation 10

5.11.1 Objectives

Evaluation 10 was conducted to extend the results of Evaluation 9 to include numeric symbol imagery. The evaluation replicated a portion of the design found in Evaluation 7, while using matched rather than enhanced standard images. The specific objective of Evaluation 10 was to provide a benchmark for better interpreting the relative acceptability of images simulated in previous evaluations by examining rating shifts between Evaluation 7 and Evaluation 10.

5.11.2 Design

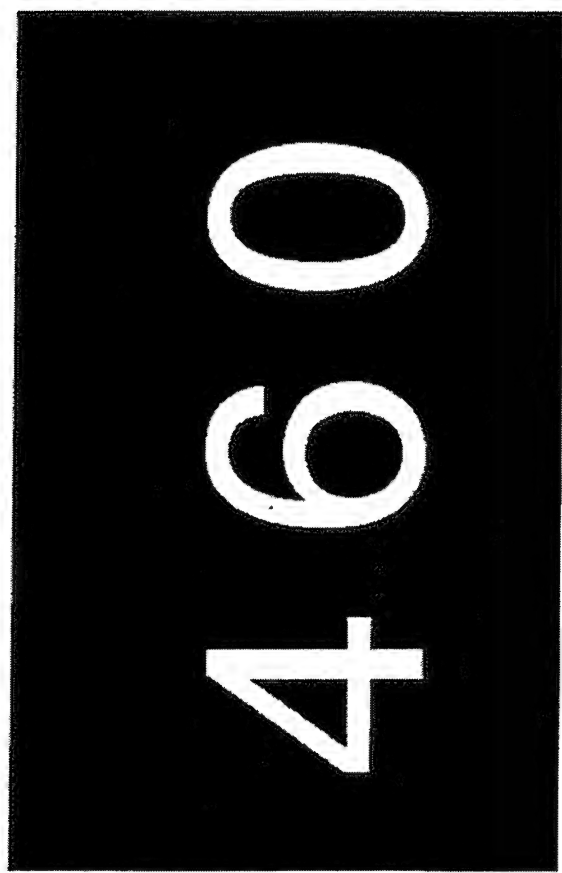
Evaluation 10 comparison images were modeled using subtractive and additive color image source models with varied aperture ratios using the original symbol image described previously. Half of the subtractive color image source models included diffraction of the red layer. Image luminance was held constant among aperture ratio and color method, such that equivalent images modeled with different image sources were of equal luminance. As in Evaluation 9, only red images were simulated in Evaluation 10. Comparison images were presented at resolutions of between 11 and 33 simulated AMLCD pixels per degree. Resolution was controlled by increasing or decreasing participant viewing distance (image field of view therefore covaried with resolution). Symbol images were subjected to gray scale level clipping and distribution as previously described under *Simulation Software*. Comparison images were presented at two gray scale levels (i.e., binary).

The simulation design levels included in Evaluation 10 are summarized in Table 5-31.

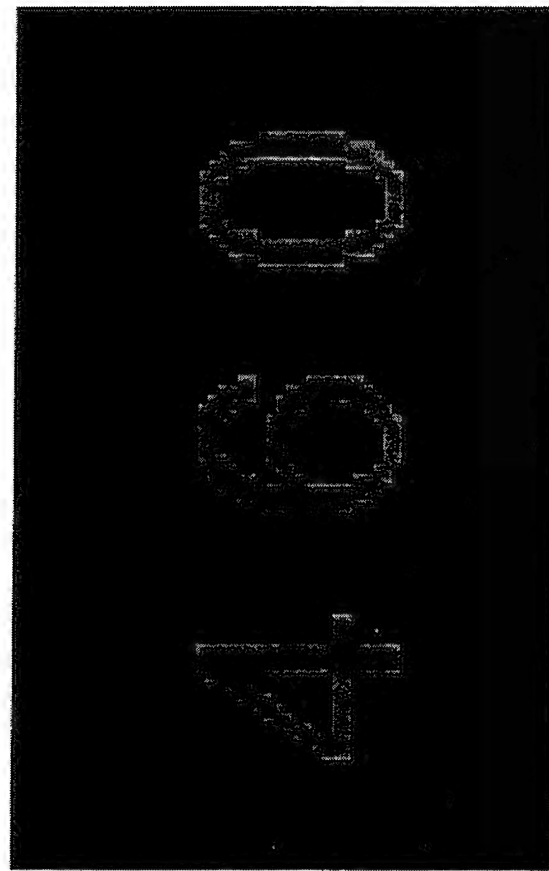
Table 5-31. Design variables for Evaluation 10.

Variable	Levels	Figure
Resolution	11, 22, 33 pix/deg	(not illustrated)
Image Source	Additive (40% AR), Subtractive (40% AR) (with or without diffraction), Subtractive (70% AR) (with or without diffraction)	(see <i>Evaluation 7</i>) Figure 5-98 (p. 374)

Standard images used in Evaluation 10 were matched in luminance/luminance contrast and resolution with comparison images. The differences between the contrast- and resolution-enhanced standard images used in Evaluation 7 and the contrast- and resolution-matched images used in Evaluation 10 are illustrated in Figure 5-127.



(a)



(b)

Figure 5-127. Modification of Standard Image in Evaluation 10 for Symbol Images.

Enhanced Standard (a) and matched standard (b). Note that evaluation images were actually presented in color on a high-resolution CRT. Also, these printed gray scale images are not gamma-corrected for printing. In addition, their size as printed is not intended to simulate the angular resolutions tested in the evaluations.

5.11.3 Procedure

The same rating scales (line visibility and image quality) that were used in Evaluation 7 were used in Evaluation 10. For each comparison image, a separate rating was made on each scale. Participants were instructed to make their image ratings relative to the standard image. The matched, rather than enhanced, standard image was used. Four participants who previously completed Evaluation 7 followed the general evaluation procedure described previously, using the simultaneous comparison procedure and rating 5 practice images and 15 evaluation trials during a 20 minute period. The order of image presentation was randomized within blocks of resolution, with order of resolution counterbalanced among participants.

5.11.4 Results

Ratings to the matched standard were paired with the comparable enhanced standard data from Evaluation 7 to examine the net effect of standard enhancement on image ratings. These differences are graphically described in Figure 5-128 to Figure 5-131. The white portions of the graph bars depict the increase in ratings associated with the matched standard relative to the enhanced standard. There was an overall increase of over 10 points in line visibility ratings and over 19 points in image quality ratings to images associated with the matched standard in Evaluation 10 vs images associated with the enhanced standard in Evaluation 7. When decomposed as a function of resolution or image source, mean line visibility ratings increased as little as 6.5 points and as much as 15 points. Mean image quality ratings increased as little as 13 points and as much as 26.5 points.

5.11.5 Summary

The comparison of images in Evaluation 7 to a standard image which was both contrast and resolution enhanced relative to comparison images produced ratings which were relatively low, commensurate with the enhancement of the standard. An alternative index of the relative acceptability of simulation images was provided by comparing images to a standard image which was matched to the comparison images in all respects but the presence of the AMLCD model.

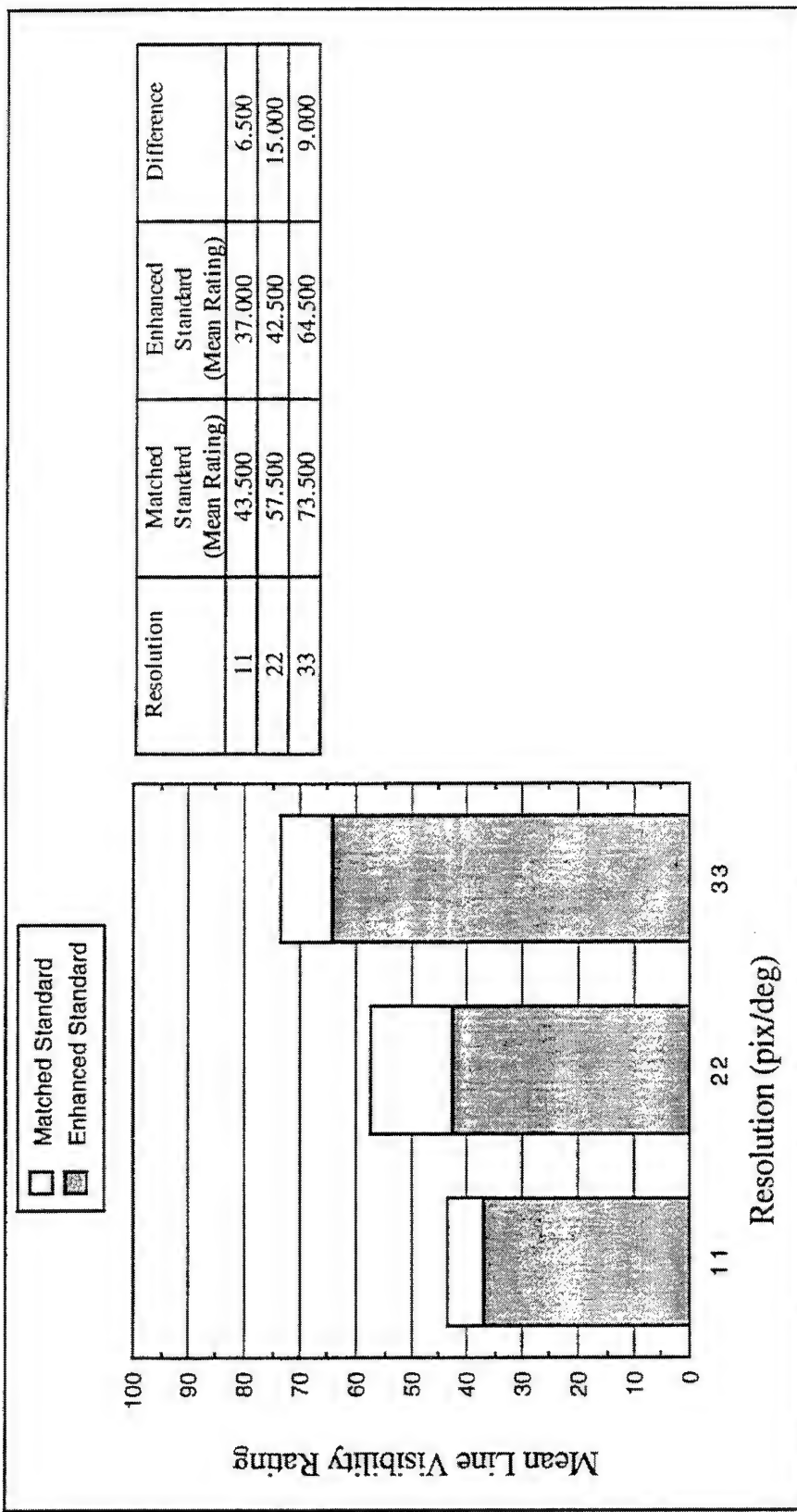


Figure 5-128. Mean Line Visibility Rating as a Function of Resolution and Standard Image (Evaluation 10, Symbol).

High line visibility ratings indicate high subjective similarity of comparison images to the standard image (i.e., low visibility of row and column lines).

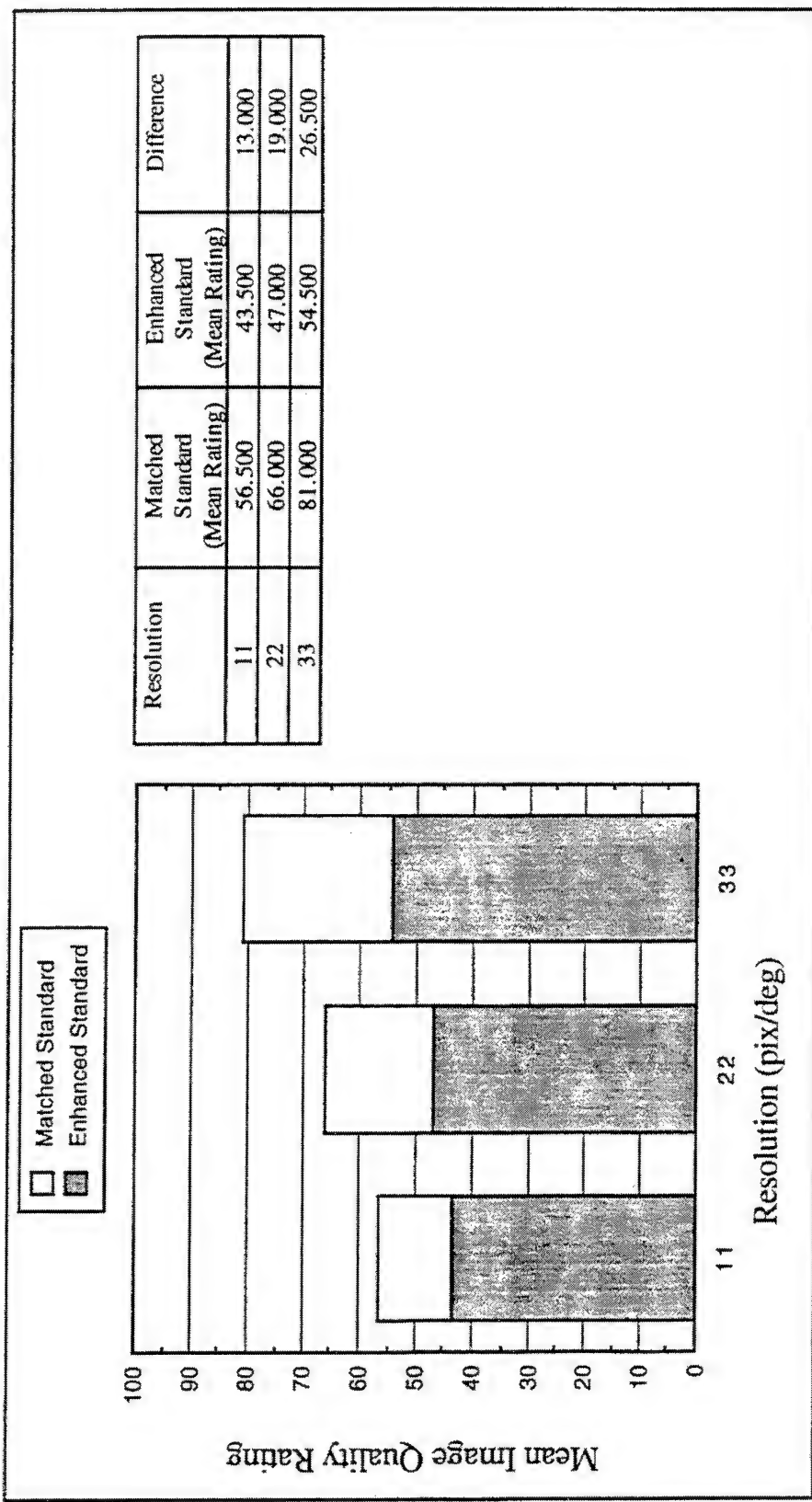


Figure 5-129. Mean Image Quality Rating as a function of Resolution and Standard Image (Evaluation 10, Symbol).

High image quality ratings indicate high subjective similarity of comparison images to the standard image (i.e., relatively high image quality).

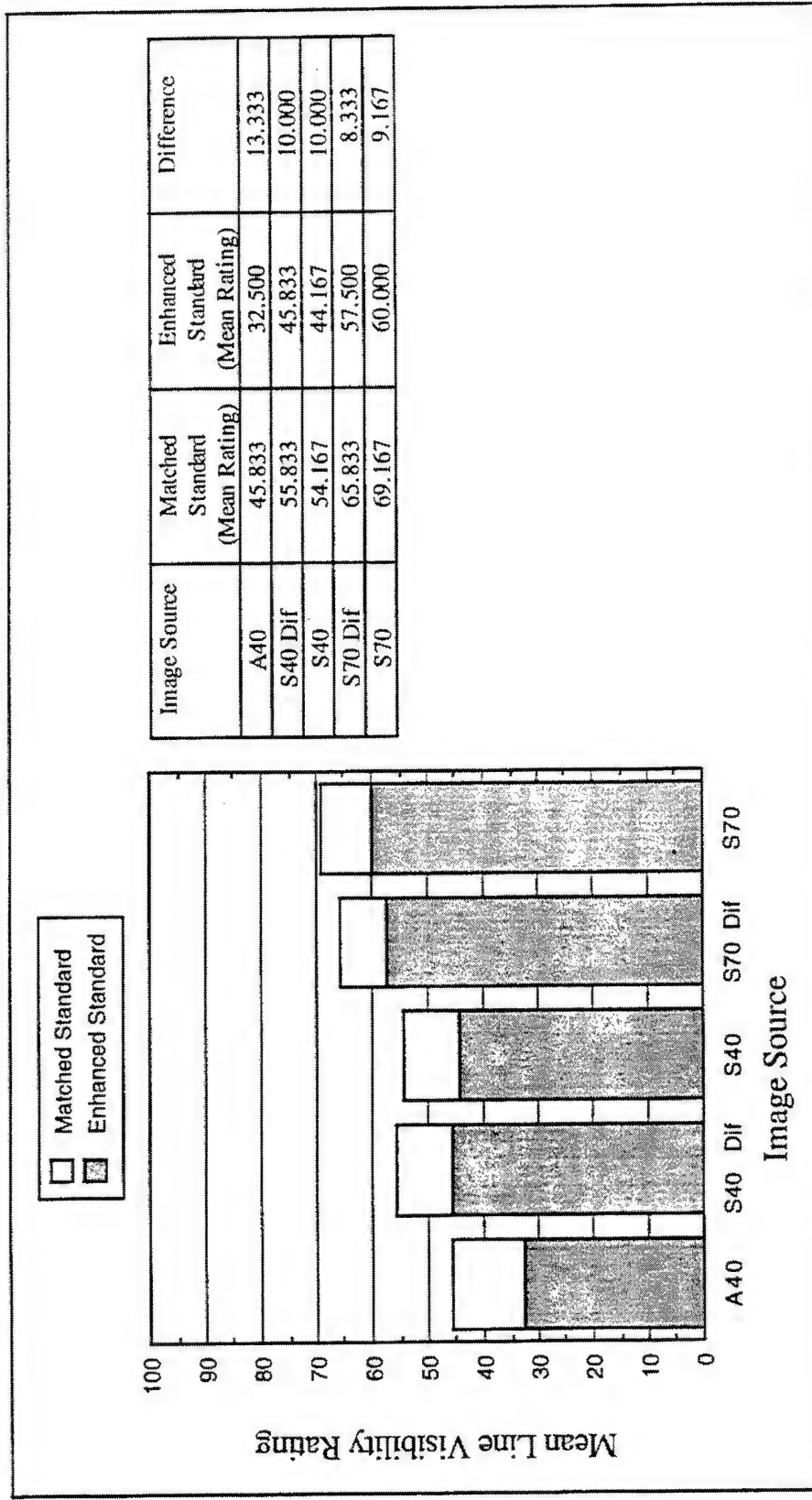


Figure 5-130. Mean Line Visibility Rating as a Function of Image Source and Standard Image (Evaluation 10, Symbol).
High line visibility ratings indicate high subjective similarity of comparison images to the standard image (i.e., low visibility of row and column lines).

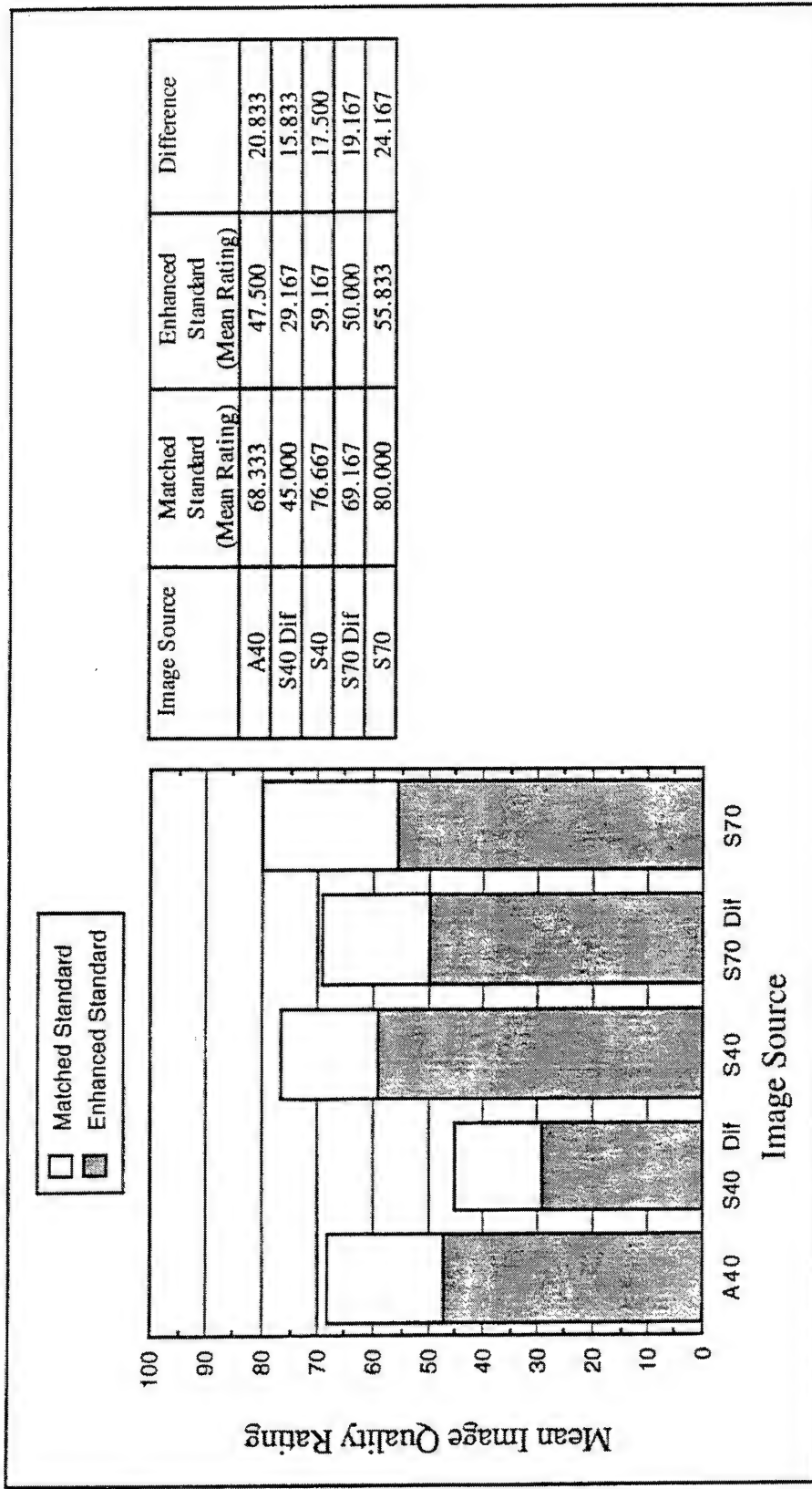


Figure 5-131. Mean Image Quality Rating as a Function of Image Source and Standard Image (Evaluation 10, Symbol).

High image quality ratings indicate high subjective similarity of comparison images to the standard image (i.e., relatively high image quality).

5.12 Simulation Summary (Evaluations 1 Through 10)

5.12.1 Summary and Discussion of Conclusions

The conclusions based on the results of simulation evaluations 1 through 10 are summarized in Table 5-32 and in the following statements.

Table 5-32. Summary of conclusions from Evaluations 1 through 10.

Design Variable	Evaluations	Simulation Evaluation Conclusions	Notes
Luminance Contrast	1 and 2	$\geq 50:1$	Increased aliasing visibility at up to 10:1. May be sensor-limited for FLIR.
Gray Scale Levels	1, 2, 3, and 4	8 Levels of Gray (symbol anti-aliasing) 64 Levels of Gray (FLIR)	Increased aliasing visibility with high CR. Reduced advantage for FLIR quality beyond 24 levels of gray.
Gray Scale Distribution	1, 2, 3, and 4	Nonlinear (symbol anti-aliasing) Nonlinear (light on dark FLIR) Linear (dark on light FLIR)	Strong image dependence. Also interacts with luminance contrast. Differences generally greatest at larger number of gray scale levels.
Aperture Ratio	3 and 4 (5, 6, 7, and 8)	$\geq 80\%$	Visibility of row and column spacing strongly associated with aperture ratio.
Resolution	5, 6, 7, and 8	$\geq 33 \text{ pix}/\text{deg}$	Line visibility as well as image quality improvements.
Color	5, 6, 7, and 8	Yellow preferred to Red	Yellow minimizes visibility of red diffraction effects. Higher luminance possible with two primaries.
Subtractive vs Additive Color	5, 6, 7, and 8	Subtractive	Results largely tied to aperture ratio. Limited additive aperture ratio possible.
Diffraction of the Red Layer	5, 6, 7, and 8	Reduces sharpness and image quality of red subtractive color images at low aperture ratios.	Minimized by use of high (e.g., 70%) aperture ratio. Not an issue for green images.
Covariance of Luminance with Aperture Ratio/Color Method	3 and 4 5, 6, 7, and 8	Image quality and line visibility improvements with increase (covariate) luminance.	Visibility minimized in yellow images. Increased luminance may compensate (in part) for use of low-aperture-ratio additive color approach.
Enhanced vs Matched Image Standard	5 and 9 7 and 10	Ratings of images compared to enhanced standards are relatively deflated due to luminance, contrast, and resolution enhancements of the standard images.	Absolute values of ratings should not be construed as indications of the absolute acceptability of images (attend primarily to relative differences in ratings).

Luminance Contrast. Changes in net image luminance contrast produced predictable changes in ratings of image contrast for both symbol and FLIR images. One consequence of increased image contrast was the increased visibility of image aliasing. The FLIR images used in these evaluations were limited in original contrast to 5 and 10:1, underscoring the likelihood that FLIR sensors will introduce a limiting function in determining net system contrast.

Gray Scale Levels. There was no evidence of a gray-scale symbol anti-aliasing advantage at gray scale levels exceeding 8. For FLIR imagery, improvements were visible at up to 64 levels of gray, but the most noticeable gains were realized by 24 levels. These results are generally consistent with prior Honeywell AMLCD simulation results.

Gray Scale Distribution. Image quality advantages were demonstrated for a nonlinear grayscale distribution algorithm, but these advantages were highly image dependent, with polarity of FLIR image an apparent factor. Other factors demonstrated to impact the preference for gray scale distribution are luminance contrast and number of gray scale levels. Other system factors, such as linearity of sensor image capture, will also play an important role here.

Aperture Ratio. The visibility of row and column spacing was strongly tied to aperture ratio, with line structure visibility improvements demonstrated over the full range of aperture ratios tested (i.e., up to 80%).

Resolution. Line visibility and image quality improved throughout the range of resolutions tested (11 to 33 pix/deg). Although the differences in ratings were not always significant at all levels tested, there was a clear preference for the highest resolution images. This result is consistent with analytical and anecdotal estimates of resolution limits at Honeywell, which suggest that resolutions in the range of 32-48 pix/deg are necessary for high quality video display, and resolutions in excess of 60 pix/deg may be usable in controlled settings.

Color. Yellow images were always preferred to red images. The preference for yellow images can largely be attributed to two sources of difference: yellow images were always of higher luminance than red images; and yellow images modeled with the diffracted subtractive color red layer appeared to have less blur than corresponding red images due to an apparent masking effect of the nondiffracted green layer.

Subtractive vs Additive Color. Aperture ratio emerged as a dominant feature with which to differentiate subtractive and additive color approaches. There was a clear and consistent preference demonstrated for the high-aperture ratio subtractive color image source, although a significant contributor to this preference appears to be the increased luminance associated with the higher aperture ratio. Although diffraction of the red layer often attenuated ratings of images modeled with the subtractive color image source at the 40% aperture ratio level, the diffraction effect was largely unnoticed in subtractive color images modeled with a 70% aperture ratio.

Diffraction of the Red Layer. As noted above, the use of high aperture ratio image source minimized the visibility of the red diffraction effect. Green images, assuming the green layer was on the top of the subtractive color stack, would not present the same problem. Yellow images presented an intermediate visibility of red diffraction, with the nondiffracted green layer apparently serving to mask the diffraction of the red layer.

Covariance of Luminance with Aperture Ratio/Color Method. Allowing image luminance to covary with aperture ratio and/or color method generally increased image quality preferences for the 70% AR subtractive color images relative to the additive color images and, in some cases, also increased comparable line visibility preferences. One implication of this result is that image quality and line visibility deficits associated with low-aperture-ratio additive color image sources may be compensated for, at least in part, by increasing the luminance of the backlight.

Enhanced vs Matched Image Standard. The construction of the standard images with which all other evaluation images were compared had a pronounced effect on image ratings. Image ratings increased by as much as 25% when images were compared with a standard image that was matched to the comparison images in luminance, luminance contrast, and resolution. This result underscores the difficulty in assigning judgments of absolute acceptability to the images modeled in the evaluation and suggests that relative rather than absolute rating differences may be more reliable.

5.12.2 Additional Issues

Gray Scale Nonlinearity. The image dependence of the nonlinear gray scale distribution advantage suggests that a linear gray scale approach may be most appropriate for the HMS+ application. However, the underlying mechanisms of the image dependence should be further examined in order to predict where nonlinear gray scale might be used to consistent advantage. In addition, there appears to be an unavoidable tradeoff in average image brightness for the nonlinear approach, the consequences of which are unclear. These issues should be investigated in a paradigm allowing pilot control of luminance and contrast. Finally, it should be noted that while many attempts were made to characterize the linearity of the LANTIRN FLIR image capture process (e.g., LANTIRN Program Office, Martin Marietta) the degree to which the FLIR images used in the evaluations were captured in a luminance-linear fashion remains unknown to the authors of this report.

Quality of LANTIRN FLIR. FLIR images were presented in these evaluations in absence of NTSC sampling. Because FLIR images presented on the HMS+ will most likely be sampled to NTSC before being displayed on the AMLCD, the effective resolution will be somewhat less than that presented in the simulations. In addition, the FLIR images used in these simulations were captured in a desert setting, and are therefore of relatively high contrast for FLIR. With these two qualifications in mind, the FLIR presented in these evaluations, although of relatively low resolution and contrast, must be considered as best case examples of production grade first-generation LANTIRN FLIR.

Luminance Issues. It was not possible to faithfully simulate both the spatial profile of the AMLCD images and the high luminances required of the HMS+ image source simultaneously. Consequently, most simulated images were presented with average image brightness of less than 10 fL. The degree to which simulation in this lower luminance range limits the generalizability of these results is unknown. Subsequent simulations using a high-luminance image source should be conducted for partial validation of the results, as well as examination of luminance-sensitive issues. Such luminance-related issues include: relative adaptation state of the two eyes between the HMS+, the cockpit interior, and the forward scene; and effects of veiling glare on forward scene visibility associated with the relatively high luminance of the off state of the AMLCD.

Monocular vs Binocular Viewing. Although the HMS+ will be a monocular display, pilot vision will remain binocular, and issues associated with image fusion and binocular rivalry must be considered.

Two-Primary Color Issues. While this program has addressed issues associated with selection of image source color method (additive vs subtractive) and color dependence of the visibility of diffraction blurring, specific chromaticity issues were not investigated. Display formats for the HMS+ should be prototyped under careful control of display chromaticity to ensure safe and acceptable viewing comfort as well as adequate color contrast with the forward scene.

6 RECOMMENDATIONS

6.1 Major Program Findings

6.1.1 Resolution

While simulation results indicated that image quality advantages could be realized by increasing the baseline HMS+ resolution beyond 22 pix/deg, display resolution increases would have to come at the expense of a reduced display FOV, unless next-generation FLIR was available with a higher sensor and transmission (>NTSC) resolution. The baseline HMS+ FOV is currently matched to the wide FOV FLIR mode. It is uncertain what the consequences would be of a FLIR/display FOV mismatch. However, pilots will already be faced with gross mismatches of this nature when operating the FLIR sensor in narrow FOV mode. It is also worth noting that the narrow FOV mode may actually be the most frequently used and most mission-critical FLIR mode used, with the wide FOV FLIR images used primarily for occasional situation orientation.

6.1.2 Color Method/Aperture Ratio

Simulation results indicated a clear preference for a high aperture ratio image source. Given the inherent aperture ratio limitations of the additive color approach, a subtractive color approach should be used, preferably with an aperture ratio in excess of 70%. If an additive color approach is selected, increased backlight luminance can be expected to offset some, but not all, of the quality limitations associated with a limited aperture ratio. While diffractive pixel broadening is a concern for red image sharpness using the subtractive color approach, the issue is largely mitigated through the use of a high aperture ratio image source. Aperture ratio will be especially important in determining the visibility of row and column spacing because of the relatively low resolution baselined for the HMS+ program.

6.1.3 Gray Scale

Simulation results indicate that 8 levels of gray scale symbol anti-aliasing and 64 levels of FLIR gray scale will be sufficient to eliminate visible luminance quantization artifacts for the HMS+. However, it should be noted that the most significant return of image quality comes with the first 24 levels. The simulation results indicated an image dependence of quality advantages for nonlinear gray scale distribution. At this point, a linear (or approximately linear) distribution of gray scale levels across the luminance range should be selected for the HMS+.

6.1.4 Alternative Gray Scale Driver

We found that integrated analog drive systems of low cost and excellent performance are ideal for Two-Primary Color display products.

6.1.5 Color Selection

Although the simulations did not specifically address the selection of color primaries, the simulation results did indicate an advantage for use of yellow in a red/green display rather than primaries only. The use of yellow allows for higher luminance images. Yellow images may also mask blurring of the red layer associated with diffractive pixel broadening in low aperture ratio subtractive color stacks.

6.2 Suggestions for Future Work

6.2.1 Resolution/FOV Trades

The consequences of increasing HMS+ resolution by reducing display FOV should be investigated through simulation. In particular, the consequences of a display/FLIR FOV mismatch should be documented with respect to mission performance and situation awareness.

6.2.2 Luminance Issues

Luminance-related issues such as the relative adaptation state of the two eyes between the HMS+, the cockpit interior, and the forward scene, as well as effects of veiling glare on forward scene visibility associated with the relatively high luminance of the off state of the AMLCD were not

investigated in the current program. Subsequent investigations incorporating high-luminance testbeds should be conducted to address these concerns.

6.2.3 Monocular vs Binocular Viewing

Issues associated with image fusion and binocular rivalry among the HMS+ image, the forward scene, and the alternate eye were not broadly addressed in the current program and should be addressed in subsequent investigations. These issues are closely related to the luminance issues discussed above and are deserving of further attention.

6.2.4 Color Selection

Selection of color primaries and formats for display of colors for HMS+ must provide comfortable long-term use and adequate color contrast with the forward scene. The interaction of color selection with other cockpit displays and transparencies (e.g., combiner, laser-protection visor) should also be empirically demonstrated in carefully controlled color investigations.

6.2.5 Reduced Image Plane Separation

Free-standing thin-layer notch polarizer films may be achieved in the future by fabricating mirror-like flat release layers. Free-standing films are currently not available and require development of the release layers. Once the thin-layer notch polarizers are developed, the support layers can be removed and the image plane separation can be reduced.

6.2.6 Tri-Band Lamp

Two-primary color cells and displays were analyzed using the IL-C developed tri-band lamp with an off-the-shelf elliptical reflector. Optimization of the lamp, reflector (new design) and fiber optic collector will greatly improve the luminance efficiency of the display/optical system.

This document reports research undertaken at the U.S. Army Soldier Systems Command, Natick Research, Development and Engineering Center and has been assigned No. Natick/TR-97/07 in the series of reports approved for publication.

7 APPENDIX

7 APPENDIX. MANUFACTURING COST FOR TWO-PRIMARY COLOR

Management Summary, Version 2.0

Number of Required Systems: 1

For: 2PC Contract
Supplier: Karl Suss
Evaluation Date: 6/16/95
Model: FC-150

Equipment	Calculated Value	\$/Unit
Original Capital Cost per System	\$350,000	\$4,120
Raw Throughput (Throughput at Capacity)	30	
Maximum Unit Starts per Week per System	2249	
Equipment Utilization Capability for 24 hr/day Usage	13.0%	
Equipment Utilization Capability for Factory Schedule	27.2%	

Headcount per Shift

Direct	0.4	\$160
Maintenance	0.0	\$0.51
Indirect	0.2	\$1.27
Total	0.6	\$3.39

Top Three Cost Drivers

Equipment (Depr., Moves, Qual., Space, Training)	25.19%	\$4,120
Scrap	23.74%	\$3.75
Material	15.05%	\$2.37
All Others	35.02%	\$5.51
		\$15.73

Cost per Good Unit Out for This Equipment

5-Year Cost Calculations, CoO Version 2.0		Evaluation Date: 6/15/95		
For: 2pC Contract	Supplier: Karl Stuss	Year 1	Year 2	Year 3
Number of Required Systems: 1				Year 4
Equipment Costs				
Depreciation	\$76,800	\$76,800	\$76,800	\$76,800
Moves and Rearrangements	\$0			
System Prove in Costs	\$4,795			
Floor Space Costs	\$20,000	\$20,600	\$21,218	\$21,865
Training	\$20,012			
Cost/Year	\$121,607	\$121,400	\$98,018	\$98,655
Cumulative Cost	\$121,607	\$219,007	\$317,025	\$415,680
Cost/Good Unit Out	\$4,866	\$3,905	\$3,921	\$3,961
Cum Cost/Good Unit Out	\$4,866	\$4,381	\$4,234	\$4,167
Production Costs				
Utilities	\$6,114	\$6,297	\$6,486	\$6,681
Supplies	\$500	\$315	\$530	\$546
Waste Disposal	\$0	\$0	\$0	\$0
Materials	\$55,734	\$57,406	\$59,128	\$60,902
Maintenance	\$11,949	\$12,307	\$12,676	\$13,057
Personnel				
Operators	\$37,768	\$38,899	\$30,066	\$41,268
Engineering	\$20,000	\$20,600	\$21,218	\$21,856
Supervision	\$10,000	\$10,300	\$10,609	\$10,927
Contract Labor	\$0	\$0	\$0	\$0
Value of Equiv. Units Scrapped	\$87,940	\$90,578	\$93,295	\$96,094

Production Costs				
Cost/Year	\$230,002	\$236,902	\$244,009	\$251,329
Cumulative Cost	\$230,002	\$486,904	\$710,913	\$962,242
Cost/Good Unit Out	\$9.20	\$9.48	\$9.76	\$10.05
Cum Cost/Good Unit Out	\$9.20	\$18.34	\$28.48	\$38.62
Other Support Services				
Employee Related	\$0	\$0	\$0	\$0
Production Related	\$0	\$0	\$0	\$0
Other Support Services				
Cost/Year	\$0	\$0	\$0	\$0
Cumulative Cost	\$0	\$0	\$0	\$0
Cost/Good Unit Out	\$0	\$0	\$0	\$0
Cum Cost/Good Unit Out	\$0	\$0	\$0	\$0
Year 1		Year 2	Year 3	Year 4
Administrative Costs				
Insurance	\$34,560	\$35,880	\$37,200	\$38,520
Taxes	\$13,824	\$10,752	\$7,680	\$4,608
Interest	\$34,560	\$36,880	\$39,200	\$41,520
Cost/Year	\$82,944	\$84,512	\$86,080	\$87,648
Cumulative Cost	\$82,944	\$167,458	\$193,516	\$221,184

5-Year Summary, CoO Version 2.0		For: 2PC Contract			Supplier: Karl Suss
Number of Required Systems: 1		Year 1	Year 2	Year 3	Year 4
Annual Costs (\$K)					
Equipment	\$121.6K	\$97.4K	\$98.0K	\$98.7K	\$99.3K
Consumables	\$6.6K	\$6.8K	\$7.0K	\$7.2K	\$7.4K
Materials	\$55.7K	\$57.4K	\$59.1K	\$60.9K	\$62.7K
Maintenance	\$11.9K	\$12.3K	\$12.7K	\$13.1K	\$13.4K
Labor	\$37.8K	\$38.9K	\$40.1K	\$41.3K	\$42.5K
Support Personnel	\$30.0K	\$30.9K	\$31.8K	\$32.8K	\$33.8K
Scrap	\$87.9K	\$90.6K	\$93.3K	\$96.1K	\$99.0K
Support Services	\$0.0K	\$0.0K	\$0.0K	\$0.0K	\$0.0K
Administrative Costs	\$82.9K	\$64.5K	\$66.1K	\$67.6K	\$69.2K
Total	\$434.6K	\$398.8K	\$388.1K	\$377.6K	\$367.4K
Cumulative Total Cost (\$K)					
Equipment	\$121.6K	\$219.0K	\$317.0K	\$415.7K	\$515.0K
Consumables	\$6.6K	\$13.4K	\$20.4K	\$27.1K	\$35.1K
Materials	\$55.7K	\$113.1K	\$172.3K	\$233.2K	\$295.9K
Maintenance	\$11.9K	\$24.3K	\$36.9K	\$50.0K	\$63.4K
Labor	\$37.8K	\$76.7K	\$116.7K	\$158.0K	\$200.5K
Support Personnel	\$30.0K	\$60.9K	\$92.7K	\$125.5K	\$159.3K
Scrap	\$87.9K	\$178.5K	\$271.8K	\$367.9K	\$466.9K
Support Services	\$0.0K	\$0.0K	\$0.0K	\$0.0K	\$0.0K
Administrative Costs	\$82.9K	\$147.5K	\$193.5K	\$221.2K	\$230.4K
Total	\$434.6K	\$833.4K	\$1221.5K	\$1599.1K	\$1,966.5K
Annual Cost per Good Unit (\$)					
Equipment	\$4.88	\$3.90	\$3.92	\$3.95	\$3.97
Consumables	\$0.26	\$0.27	\$0.28	\$0.29	\$0.30
Materials	\$2.23	\$2.30	\$2.36	\$2.44	\$2.51
Maintenance	\$0.48	\$0.49	\$0.51	\$0.52	\$0.54
Labor	\$1.51	\$1.56	\$1.60	\$1.65	\$1.70
Support Personnel	\$1.20	\$1.24	\$1.27	\$1.31	\$1.35
Scrap	\$3.52	\$3.62	\$3.73	\$3.84	\$3.96
Support Services	\$0.00	\$0.00	\$0.00	\$0.00	\$0.00
Administrative Costs	\$3.32	\$2.58	\$1.84	\$1.11	\$0.37

Total	\$17.38	\$15.95	\$15.52	\$15.11	\$14.70
Cumulative Cost per Good Unit (\$)					
Equipment	\$4.86	\$4.38	\$4.23	\$4.16	\$4.12
Consumables	\$0.26	\$0.27	\$0.27	\$0.28	\$0.28
Materials	\$3.23	\$2.26	\$2.20	\$2.33	\$2.37
Maintenance	\$0.48	\$0.49	\$0.49	\$0.50	\$0.51
Labor	\$1.51	\$1.53	\$1.56	\$1.58	\$1.60
Support Personnel	\$1.20	\$1.22	\$1.24	\$1.26	\$1.27
Scrap	\$3.52	\$3.57	\$3.62	\$3.68	\$3.74
Support Services	\$0.00	\$0.00	\$0.00	\$0.00	\$0.00
Administrative Costs	\$3.32	\$2.95	\$2.58	\$2.21	\$1.84
Total	\$17.38	\$16.67	\$16.29	\$15.99	\$15.73
% of Total Cost - Annual	Year 1	Year 2	Year 3	Year 4	Year 5
Equipment	28.0%	28.0%	28.0%	28.0%	28.0%
Consumables	1.5%	1.7%	1.8%	1.9%	2.0%
Materials	12.8%	14.4%	15.2%	16.1%	17.1%
Maintenance	2.7%	3.1%	3.3%	3.5%	3.7%
Labor	8.7%	8.8%	10.3%	10.9%	11.6%
Support Personnel	6.9%	7.7%	8.2%	8.7%	9.2%
Scrap	20.2%	22.7%	24.0%	25.4%	26.9%
Support Services	0.0%	0.0%	0.0%	0.0%	0.0%
Administrative Costs	19.1%	16.2%	11.9%	7.3%	2.5%
Total	100.0%	100.0%	100.0%	100.0%	100.0%
% of Total Cost - Cumulative					
Equipment	28.0%	26.3%	26.0%	26.0%	26.2%
Consumables	1.5%	1.6%	1.7%	1.7%	1.8%
Materials	12.8%	13.6%	14.1%	14.6%	15.0%
Maintenance	2.7%	2.9%	3.0%	3.1%	3.2%
Labor	8.7%	9.2%	9.6%	9.9%	10.2%
Support Personnel	6.9%	7.3%	7.6%	7.8%	8.1%
Scrap	20.2%	21.4%	22.3%	23.0%	23.7%
Support Services	0.0%	0.0%	0.0%	0.0%	0.0%
Administrative Costs	19.1%	17.7%	15.8%	13.8%	11.7%
Total	100.0%	100.0%	100.0%	100.0%	100.0%

Live of Equipment Cost Calculations & Summary, CoO Version 2.0				Evaluation Date: 6/15/95
For: 2PC Contract	Supplier: Karl Suss	Model FC-150		
Number of Required Systems: 1	Year 1	Uninflated	Inflated	
Equipment Costs				
Depreciation	\$76,800	\$384,000	\$384,000	
Moves and Rearrangements	\$0	\$0	\$0	\$0
System Prove in Costs	\$4,795	\$4,795	\$4,795	
Floor Space Costs	\$20,000	\$100,600	\$106,838	
Training	\$20,012	\$20,012	\$20,012	
Cost/Year	\$121,607	\$508,807	\$514,590	
Cum Cost/Good Unit Out	\$4,861	\$4,071	\$4,112	
Production Costs				
Utilities	\$6,114	\$30,570	\$30,570	\$6,486
Supplies	\$500	\$2,500	\$2,500	\$2,655
Waste Disposal	\$0	\$0	\$0	\$0
Materials	\$55,734	\$278,668	\$295,898	
Maintenance	\$11,949	\$59,744	\$63,438	
Personnel	\$37,768	\$188,829	\$200,504	
Operators	\$20,000	\$100,000	\$106,183	
Engineering	\$10,000	\$50,000	\$53,091	
Supervision	\$0	\$0	\$0	
Contract Labor	\$0	\$0	\$0	
Equivalent Units Scrapped	\$87,940	\$439,698	\$468,884	
Production Costs				
Cost/Year	\$230,002	\$1,150,009	\$1,221,111	
Cum Cost/Good Unit Out	\$9,201	\$9,201	\$9,201	
Other Support Services				
Employee Related	\$0	\$0	\$0	\$0
Production Related	\$0	\$0	\$0	\$0
Cost/Year	\$0	\$0	\$0	\$0
Cum Cost/Good Unit Out	\$0,001	\$0,001	\$0,001	\$0,001

Annual Costs (\$K)		
	Year 1	Uninflated
Equipment	\$121.6K	\$508.8K
Consumables	\$6.6K	\$33.1K
Materials	\$55.7K	\$278.7K
Maintenance	\$11.9K	\$59.7K
Labor	\$37.8K	\$188.8K
Support Personnel	\$30.0K	\$150.0K
Scrap	\$87.9K	\$438.7K
Support Services	\$0.0K	\$0.0K
Administrative Costs	\$82.9K	\$230.4K
Total	\$434.6K	\$1,889.2K
Annual Cost per Good Unit (\$K)		
Equipment	\$4.86	\$4.07
Consumables	\$0.26	\$0.26
Materials	\$2.23	\$2.23
Maintenance	\$0.48	\$0.48
Labor	\$1.51	\$1.51
Support Personnel	\$120	\$120
Scrap	\$3.52	\$3.52
Support Services	\$0.00	\$0.00
Administrative Costs	\$3.32	\$1.84
Total	\$17.38	\$15.11

% of Total Cost - Annual				
Equipment	28.0%	26.9%	26.2%	
Consumables	1.5%	1.8%	1.8%	
Materials	12.8%	14.8%	15.0%	
Maintenance	2.7%	3.2%	3.2%	
Labor	8.7%	10.0%	10.2%	
Support Personnel	6.9%	7.9%	8.1%	
Scrap	20.2%	23.3%	23.7%	
Support Services	0.0%	0.0%	0.0%	
Administrative Costs	19.1%	12.2%	11.7%	
Total	100.0%	100.0%	100.0%	

8 BIBLIOGRAPHY

- ANSI/Human Factors Society (1988). American National Standard for Human Factors Engineering of Visual Display Terminal Workstations. (ANSI/HFS 100-1988). Santa Monica, CA: The Human Factors Society.
- Armstrong Laboratory (1994). Helmet-Mounted Sight + Industry Briefing. Copy of overhead presentation materials.
- Bajura, M., Fuchs, H., and Ohbuchi, R. (1992). Merging virtual objects with the real world: Seeing ultrasound imagery within the patient. *Computer Graphics*, 26 (2), 203-210.
- Boff, K.R. and Lincoln, J.E. (1988). Engineering Data Compendium: Human Perception and Performance. Armstrong Aerospace Medical Research Laboratory, Wright-Patterson AFB, Ohio.
- Bosman, D. (1989). Display Engineering: Conditioning, Technologies, Applications. New York: North-Holland.
- Brahney, J.H. (1985, November). LANTIRN: Turning night into day. *Aerospace Engineering*, pp. 19-22.
- Cahoun, C.S. and Post, D.L. (1990). Heterochromatic brightness matches via Ware and Cowan's luminance correction equation. Society for Information Display International Symposium Digest of Technical Papers (pp. 261-268).
- Carter, R. (1993). Gray scale and achromatic color difference. *Journal of the Optical Society of America*, 10 (6), 1380-1391.
- Decker, J.J., Pigeon, R.D., and Snyder, H.L. (1987). A Literature Review and Experimental Plan for Research on the Display of Information on Matrix-Addressable Displays (Tech Memorandum 4-87). Aberdeen Proving Ground, Maryland: U.S. Army Human Engineering Laboratory.
- Eisen, P.S., Farley, W.W., Snyder, H.L., and Skipper, J.H. (1989). An evaluation of the manipulation of color in alternative color spaces. Society for Information Display International Symposium Digest of Technical Papers (pp. 292-295).
- Farrell, R.J. and Booth, J.M. (1984). Design Handbook for Imagery Interpretation Equipment (D180-19063-1). Boeing Aerospace Company, Seattle, WA.
- Hammer, W. (1989). Occupational Safety Management and Engineering (4th Ed.). New Jersey: Prentice-Hall.
- Hartmann, W., Verhulst, A., van Haaren, J., and Blommaert, F. (1993). The possibilities of ferroelectric liquid crystals for video displays. *Journal of the Society for Information Display*, 1 (3), 255 - 268.

- Hayashi, Y., et al. (1990). A 0.7-in. fully integrated poly-Si CMOS LCD with redundancy. Proc. 10th Display Research Conference (Eurodisplay '90), pp. 60-63, September.
- Hewish, M., Turbe, G., and Wanstall, B. (1991). Towards a fully interactive cockpit environment? International Defense Review, (3), 237-242.
- Hughes, D. (1994). Off-boresight missile test highlights U.S. capabilities. Aviation Week and Space Technology, 140 (23), 66-69.
- Jones, D.K. (1991, July). Practicing forbidden thrills. Aerospace America, pp. 26-29.
- Kelly, D.W. and Spear, M.C. (1986, September). LANTIRN: A technical report. Defense Electronics, pp. 63-68.
- Lerner, E.J. (1985, July). A LANTIRN for seeing in the dark. Aerospace America, pp. 28-29.
- Lindholm, J.M. (1992). Perceptual effects of spatiotemporal sampling. In M.A. Karim (Ed.), Electro-Optical Displays (pp. 787-808). New York: Marcel Dekker.
- Lippert, T.M. (1990). Fundamental monocular/binocular HMD human factors. In Helmet-Mounted Displays II, SPIE Vol. 1290, pp. 185-191. Bellingham, WA: SPIE.
- Lloyd, J.C., Decker, J.J., and Snyder, H.L. (1991). The Effects of Line and Cell Failures on Reading and Search Performance using Matrix-Addressable Displays (Tech Memorandum 7-91). Aberdeen Proving Ground, Maryland: U.S. Army Human Engineering Laboratory.
- McCartney, D. (1992). Application of Discrete Gray Levels to Camera Video. Internal Honeywell Technical Memorandum.
- Melzer, J.E. and Moffitt, K.W. (1992a). Color helmet display for the tactical environment: The pilot's chromatic perspective. In T. Lippert (Ed.), Helmet-Mounted Displays III: Proceedings of the SPIE: Vol. 1695, pp. 47-51. Bellingham, WA: The Society of Photo-Optical Instrumentation Engineers.
- Melzer, J.E. and Moffitt, K.W. (1992b). Color helmet display for the military cockpit. Proceedings of the IEEE/AIAA 11th Digital Avionics Systems Conference, pp. 538-542. New York: IEEE.
- Meyer-Arendt, J.R. (1984). Introduction to Classical and Modern Optics (Second Ed.). New Jersey: Prentice-Hall.
- MIL-STD-1472D (1989). Military Standard: Human Engineering Design Criteria for Military Systems, Equipment and Facilities.
- MIL-STD-850B (1970). Military Standard: Aircrew Station Vision Requirements for Military Aircraft.
- Morozumi, S. (1989). Poly-Si TFTs for large-area applications. Proceedings of 9th International Display Research Conference, pp. 148-51.
- Murch, G.M. (1984). Human factors of displays. Society for Information Display Seminar Lecture Notes (session S-2.1).
- National Aeronautics and Space Administration (1986). Space Station Man-Systems Integration Standards (NASA-STD-3000).

- National Center for Advanced Information Components Manufacturing. (1994). *Cost of Ownership Model for Flat Panel Display Assembly/Fabrication Equipment*, Version 2.0, November.
- Neri, D.F., Jacobsen, A.R., and Luria, S.M. (1986). An evaluation of color sets for CRT displays. Society for Information Display International Symposium Digest of Technical Papers (pp. 82-85).
- Pitt, M. (1991). The effect of defect clustering on yield of AMLCD-TV displays. Proceedings of 9th International Display Research Conference, San Diego, pp. 107-110.
- Post, D., Sarina, K., Trimmier, R., Heinze, W., Rogers, C., Ellis, R., Larson, B., and Franklin, H. (1994). A new color display for head-mounted use. Submitted to Journal of the Society for Information Display, 2(4), pp. 155-163.
- Rash, C.E., Verona, R. W., and Crowley, J.S. (1990). Human factors and safety considerations of night vision systems flight using thermal imaging systems. In R. Lewandowski (Ed.), *Helmet-Mounted Displays II: Proceedings of the SPIE*: Vol. 1290, pp. 142-164. Bellingham, WA: The Society of Photo-Optical Instrumentation Engineers.
- Reinhart, W.F. (1992). Gray-scale requirements for anti-aliasing of stereoscopic imagery. In J. O. Merritt and S.S. Fisher (Eds.), *Stereoscopic Displays and Applications III*, Proceedings of the SPIE: Vol. 1669, pp. 90-100. Bellingham, WA: The Society of Photo-Optical Instrumentation Engineers.
- Sakai, S., et al. (1988). A defect tolerant technology for an active-matrix LCD integrated with peripheral drivers. Society for Information Display International Symposium Digest, pp. 400-3.
- Sauerborn, J.P. (1992). Advances in miniature projection CRTs for helmet displays. In T. Lippert (Ed.), *Helmet-Mounted Displays III: Proceedings of the SPIE*: Vol. 1695, pp. 102-116. Bellingham, WA: The Society of Photo-Optical Instrumentation Engineers.
- Shimada, T., et al. (1991). A study of poly-Si TFT-LCD with very small pixel and high aperture ratio, International Conference SSDM, Ext. Abstract, pp. 641-643, August.
- Silverstein, L.D. and Merrifield, R.M. (1985). The Development and Evaluation of Color Systems for Airborne Applications. Phase 1: Fundamental Visual, Perceptual, and Display System Considerations. DOT/FAA Technical Report PM-85-19, Naval Air Test Center, Patuxent River, MD.
- Silverstein, L.D. et. al. (1989). A psychophysical evaluation of pixel mosaics and gray-scale requirements for color matrix displays. Society for Information Display International Symposium Digest of Technical Papers (pp. 128-131).

- Sweetman, B. (1988a). Combat cockpit of the future: U.S. promotes ambitious cockpit displays. *International Defense Review*, 21 (4), 363-366.
- Sweetman, B. (1988b). Agile falcon and Hornet 2000: The USA's next generation of export fighters. *Interavia*, February, 161-164.
- Takabatake, M., et al. (1991). CMOS circuits for peripheral circuit integrated poly-Si TFT LCD fabricated at low temperature below 600°C. *IEEE Trans. Electron. Devices*, Vol. ED-38, pp. 1303-1308, June.
- Tannas, L.E. (Ed.) (1985). *Flat Panel Displays and CRTs*. New York: Van Nostrand Reinhold.
- Tsurumaki, N., Watanabe, T., and Niire, T. (1991). Multicolor TFEL display panel containing a broad-band phosphor and color filters. *Proceedings of the SID*, 32 (4), 325-329.
- Walraven, J. (1985). Perceptual problems in display imagery. Society for Information Display International Symposium Digest of Technical Papers (pp. 192-195).
- Walraven, J. (1992). Color basics for the display designer. In H. Widdel and D.L. Post (Eds.), *Color in Electronic Displays* (pp. 3-38). New York: Plenum Press.
- Wei, L. and Kalmanash, M. (1989). Design considerations of the sunlight readable night vision image system compatible KROMA color display. *Display System Optics II: Proceedings of the SPIE*: Vol. 1117, pp. 162-167. Bellingham, WA: The Society of Photo-Optical Instrumentation Engineers.
- Wells, M.J. and Haas, M. (1992). The human factors of helmet-mounted displays and sights (pp. 743-785). In M. Karim (Ed), *Electro-Optical Displays* (pp. 337-415). New York: Marcel Dekker.
- Wood, R.B. (1992). *Holographic Head-Up Displays*. In M. Karim (Ed), *Electro-Optical Displays* (pp. 337-415). New York: Marcel Dekker.
- Yutaka, T., et al. (1992). A poly-Si TFT monolithic IC data driver with redundancy. *ISSCC Technical Digest*, pp. 118-120.
- Young, R.A. (1990). Getting more for less: A new opponent color technique for two-channel color displays. *Perceiving, Measuring, and Using Color: Proceedings of the SPIE*: Vol. 1250, pp. 132-143. Bellingham, WA: The Society of Photo-Optical Instrumentation Engineers.

9 DISTRIBUTION LIST

External Distribution

Mr. Robert Buckanin
US Army Aviation & Troop Command
ATTN: AMSAT-R-TI
Ft. Eustis, VA 23604-5577

Mr. James H. Brindle
LME, Inc.
607 Louis Drive
Suite 607A
Warminster, PA 18974

Ms. Monica Glumm
US Army Research Laboratory
Human Research & Engineering
Directorate
ATTN: AMSRL-HR-SB
Aberdeen Proving Ground, MD
21005-5425

Mr. David Osborne
EG&G Dynatrend
VNTSC
55 Broadway
Cambridge, MA 02142-1093

Mr. Mark W. Scerbo
Old Dominion University
Psychology Dept.
Norfolk, VA 23529

Ms. Jennifer B. McGovern
Information Spectrum Inc.
305 Airport Drive
California, MD 20619

Mr. Charles Bradford
Dept. of Army - NVESD
ATTN: AMSEL-RD-NV-SS-SS
10221 Burbeck Road
Suite 430
Ft. Belvoir, VA 22060-5806

Mr. Paul M. Tihansky
Code 4.6.4.2, Bldg. 2187, MS 3
NAWCAD
48110 Shaw Road, Unit 5
Pawtuxent River, MD 20670

Mr. James Walrath
US Army Research Laboratory
Information Science & Technology
Directorate
2800 Powder Mill Road
Adelphi, MD 20783

Mr. Joel S. Warm
University of Cincinnati
Psychology Dept.
Cincinnati, OH 45221

Mr. Thomas Amerson
Vision Dept.
US Naval Submarine Medical Lab
Box 900
Naval Submarine Base
New London, Groton, CT 06349-5900

Ms. Jennie J. Gallimore
Wright State University
3640 Colonel Glenn Highway
Dept. of BHE
Dayton, OH 45435

Internal Distribution

S&TD (Carolyn Bensel)
S&TD (Cynthia Blackwell)
S&TD (George Mastroianni)

S&TD (Herbert Meiselman)
S&TD (James Sampson)